

Noise and sensitivity-measurement theory
for receiving systems and circuits

by

Steve Forrest Russell

A Thesis Submitted to the
Graduate Faculty in Partial Fulfillment of
The Requirements for the Degree of
MASTER OF SCIENCE

Major: Electrical Engineering

Approved:

In Charge of Major Work

For the Major Department

For the Graduate College

Iowa State University
Ames, Iowa

1973

Copyright © Steve Forrest Russell, 1973. All rights reserved.

TABLE OF CONTENTS

	Page
PREFACE	vii
I. INTRODUCTION	1
II. GENERAL ASPECTS OF A COMMUNICATION SYSTEM	11
A. The Ideal System	11
B. The Practical System	11
1. The transmitter	12
2. The propagation path	14
3. Antennas	14
4. The receiver	15
III. RECEIVING SYSTEMS FOR SENSITIVITY STUDIES	17
A. Electromagnetic Transducer (Antenna)	19
B. Feed System	31
C. RF Translator	34
D. IF Amplifier	37
E. Demodulator - Detector	38
F. Sensory Transducers	40
IV. NOISE IN ELECTRONIC CIRCUITS	43
A. Noise as a Physical Phenomenon	44
1. Brownian motion and thermal agitation	44
2. Shot noise	45
3. Statistical properties of noise	45
4. Noise spectrums	57
B. Physical Sources of Noise	71
1. Thermal or Johnson noise	71
2. Shot noise	79
3. Blackbody radiation	82
4. Atmospheric noise	84
5. Extraterrestrial noise	85
6. Man-made noise	87
7. Special noise generation effects	91

C. Noise in Passive Communication Circuits	91
1. Resistive networks	92
2. Tuned circuit, transformer noise	103
3. Filter noise	112
4. Antenna feedline--transmission line noise	118
5. Antenna noise	132
D. Receiving System Noise Temperature	143
E. Noise Theory for Two-Port Networks	153
1. Linear two-port noise model	154
2. Application of model to noise factor studies	163
F. Noise Generation in Electron Devices	172
1. Noise in vacuum tubes	173
2. Noise in semiconductor diodes	187
3. Noise in bipolar transistors	195
4. Noise in field-effect transistors	222
5. Mixer noise	231
V. RF TRANSLATOR NOISE	239
VI. NOISE POWER DETECTORS	248
A. Peak-Reading Voltmeter	253
B. Average-Reading Voltmeter	257
C. Square-Law Detector	261
D. Linear Diode Detector	303
E. Phase-Sensitive Detector (Product Detector)	306
F. Detector Dynamic Range	307
VII. METHODS OF SENSITIVITY COMPARISON	309
A. Complete Receiving Systems	312
B. Two-Port Devices	312
C. Detectors	313

VIII. THEORY OF SENSITIVITY MEASUREMENTS	315
A. A Theorem for Sensitivity Measurements	321
B. Noise Quieting (FM Systems)	324
C. Tangential Noise Sensitivity (PCM Systems)	329
D. Noise Factor and AM Sensitivity	332
1. Noise factor measurement theory	333
2. Test signal sources	341
3. Detectors for noise factor measurements	342
IX. SENSITIVITY MEASURING METHODS	351
A. Using Noise Generators	351
1. Noise sources	352
2. Y-factor method	355
3. Noise diode method (3 db method)	364
4. Gas-discharge noise method	370
B. Using an Unmodulated Sinewave Generator	371
1. Power meter	371
2. Square-law detector	374
3. Linear-diode detector	375
C. Using a Modulated Sinewave Generator	375
1. AM sensitivity	376
2. Tangential noise sensitivity	381
3. FM sensitivity	383
D. Antenna Noise Measurement	388
X. UNCERTAINTIES IN SENSITIVITY MEASUREMENTS	399
A. Sensitivity Measuring System	400
1. Test signal sources	401
2. Device being tested	402
3. Predetection amplifier	404
4. Predetection filter	405
5. Detector device	405
6. Postdetection filter	406
7. Postdetection amplifier	407
8. Sensory transducer (output indicator)	407

B. Test Signal Sources	409
1. Hot-cold noise source	421
2. Noise diode	432
3. Gas-discharge	439
4. Sinewave generator	440
C. Detectors and Output Indicators	447
D. Attenuators	458
E. Measurement Methods	466
1. Y-factor	467
2. Noise diode	478
3. Gas-discharge noise source	488
4. AM sensitivity	488
5. FM sensitivity	492
6. Tangential noise	493
7. Antenna noise temperature	494
F. Gain Variations	500
G. Image Response	501
H. Two-Port Devices	502
XI. INTERRELATIONSHIPS OF MEASUREMENT METHODS	506
A. Noise Factor (Noise Figure)	508
B. Effective Noise Temperature	513
C. AM Sensitivity	514
D. Receiving System Power Sensitivity	514
E. Tangential Noise Sensitivity (Pulse Code Systems)	516
F. Noise Quieting (FM Sensitivity)	519
XII. SUMMARY	521
XIII. BIBLIOGRAPHY	524
XIV. APPENDIX	541
A. Power Spectral Density Function, $\Phi(\omega)$	541
B. Noise Bandwidth	545

C. Available Power	552
D. Insertion Gain (or Loss)	556
E. Equivalent Noise Temperature	562
F. Equivalent Noise Resistance	565
G. Excess Noise Ratio (Excess Noise)	566
H. Noise Factor (Noise Figure)	568
I. Spot and Average Noise Factor	578
J. Friis Equation	580
K. Noise Measure	587
L. Noise Merit	589
M. Noise Matching	595
N. Noise Tuning	597
O. Reference Temperature, T_o	598
P. Sky Temperature	600
Q. "Hard" and "Soft" Microvolts	601
R. Single and Double-Sided Power Spectra	603
S. Error Analysis	608
T. Recommended Reference List	612

PREFACE

The subject of noise theory for electronic circuits and systems is one of those specialized areas which normally cannot receive adequate coverage at the undergraduate level. This is not because the subject level is too advanced but is the natural consequence of the time limitations of such a program. These circumstances make it necessary for the engineer who eventually works in this area to learn the subject on a "do-it-yourself" basis. This approach is time consuming under the best of conditions and frustratingly difficult under the worst. This author has experienced the good fortune of having both the time and the necessary help to accomplish such a task. This work is an attempt at sharing this experience and learning.

As with any text which is basically tutorial, most of the concepts are not original. There are a variety of books and papers that deal with the various aspects of receiver noise theory. Unfortunately, when trying to study these references, the variety of technical levels and notation are difficult to overcome. In addition, the information is scattered throughout many technical publications and study can only be accomplished by access to a large library.

The technical level is suitable for self-study by the new graduate or practicing engineer who finds he must work in this area. The practical aspects of the subject are emphasized and many examples, derivations, tables and graphs are presented. Terminology and definitions are clarified and emphasized so the user may read as much available literature as necessary. It is this author's firm belief that every

article on a subject contributes toward better understanding and it is because of this that a large bibliography is included. An equivalent circuit interpretation is used on most of the problems because it was felt that this would give the best practical insight. It is assumed that the user is fluent in circuit theory, especially two-port theory, and the needed aspects of communication theory. Several other aspects of noise theory such as information theory and propagation have not been included either because of time limitations or because they are adequately treated elsewhere.

For any work of a review nature, the author is greatly indebted to the authors of works already published. To the fullest possible extent, these authors are gratefully acknowledged by the many references. In particular, this author obtained much help from the papers and books published by Bechmann, Bennett, Bracewell, Brown and Nilsson, Davenport and Root, Friis, Haus and Adler, Kraus, Middleton, North, Pappenfus and Bruene and Schoenike, Pastori, Rothe and Dalke, van der Ziel and the many IRE (or IEEE) Standards pertaining to noise.

The author's committee chairman, John Basart, has helped immensely with guidance and suggestions concerning technical content and has cheerfully endured the time consuming task of proofreading. He introduced the author to concepts in Radio Astronomy which were used to solve many noise problems. This work could not have been completed without his continuous encouragement and firm belief in the stated goals.

Sincere thanks are given to the Engineering Division of Collins Radio Company and, in particular, Dave Hallock for the initial

motivation and encouragement in this area. Dave's practical approach and insights into noise measurement problems have greatly influenced the approach taken.

The author's very special thanks go to his wife, Kathy, whose constant encouragement, patience, and understanding made this writing task much easier and to his daughters, Carla and Tracy, who spent many evenings without their father.

The author is indebted to Janice Hufferd for her helpful suggestions concerning text organization and for typing the manuscript.

Although every effort has been made to eliminate errors in the text, tables and figures, some will inevitably occur. The author strongly encourages anyone finding errors to write him so corrections can be made. Also, any suggestions on how to improve the text, tables or figures by any additions, deletions or modifications, will be greatly appreciated.

Ames, Iowa

Steve F. Russell

May, 1973

I. INTRODUCTION

The history of noise theory for electronic circuits and receiving systems should properly begin in 1827 with the discovery of what is now called Brownian Motion. The discovery of random thermal motion by Robert Brown eventually led to the kinetic theory of matter and to Boltzmann statistics. This idea of thermal motion of elementary particles was eventually applied to the motion of free electrons in a conductor (Free Electron Gas Theory). In 1928, J. B. Johnson published a paper on the experimental investigation of thermal noise currents in a conductor. In the same publication, a companion paper by H. Nyquist discussed the results given by Johnson on a theoretical basis. Using arguments from thermodynamics and statistical mechanics, Nyquist derived expressions for the mean-square noise currents and voltages in a conductor. This formulation, which became known as the Nyquist theorem, is used as a basis for deriving many noise equations. Shot noise caused by the flow of electrons under the influence of an electric field was already known at the time and the addition of what we now call thermal or Johnson noise completed the explanation of the physical sources of circuit noise. Much of this text will deal with the phenomena which Johnson referred to as, "that disturbance which is called 'tube noise' in vacuum tube amplifiers".

Many papers concerned with the theoretical and measured properties of noise came after those by Johnson and Nyquist. By 1930, shot noise and thermal noise had been lumped together into a phenomenon called fluctuation noise. Papers by Llewellyn (1930, 1931) and Ballantine (1930)

discussed noise in receiver circuits and a paper by Case (1931) discussed receiver design to minimize 'fluctuation noise'. Landon (1936 and 1941) presented the fundamental ideas on how to describe the statistics of noise. It was during this time that radio static experiments by Karl Jansky (1932) led to the discovery of "a steady hiss type static of unknown origin". What Jansky had discovered was radio noise emission from the galactic plane. This discovery marked the birth of radio astronomy.

As late as 1941 there was still no commonly used technique for specifying the noise characteristics of a radio receiver. Receiver sensitivity specifications depended upon a variety of variables including antenna resistance, bandwidth, modulation and detection characteristic, and measurement method. Two-port noise theory was still in the distant future and there was a pressing need to have a single figure of merit for specifying the absolute sensitivity of a receiving system. The problem of receiver sensitivity comparison was solved in 1942 when D. O. North proposed a figure of merit he called "Noise Factor". The noise factor of a receiver depended upon only the antenna resistance; thus, if two receivers were compared with the same antenna, the one with the lower noise factor would have the better sensitivity. H. T. Friis (1944) used North's idea and expanded on it by rigorously defining "noise factor" in terms of signal-to-noise ratios and applying it to two-port networks in general. Friis defined available signal power, available noise power and effective noise bandwidth. He also suggested that a standard noise temperature of 290°K be adopted. It was also in this paper that Friis derived the equation for the total noise factor of networks in cascade. It is unfortunate, however, that Friis used

the term noise figure instead of noise factor for the same entity described by North. These two competing terms are still used interchangeably in the literature. In an attempt to distinguish between noise factor given as a number and noise factor given in db we will use the following notational convention. When referring to numerical noise factor as defined by North, the symbol, F , will be used. The term noise figure will be used to denote the noise factor in db and the symbol, NF , will be used. This distinction is especially helpful to newcomers to the field because it helps distinguish the numeric and decibel designations for noise factor. Noise figure should always be clearly labeled in db. The numerical values of F and NF are sometimes nearly equal as can be seen from Figure 11A-1 in Chapter XI.

The concept of noise factor (or noise figure) as a means of specifying the absolute sensitivity of a two-port network has increased in popularity until today virtually all specifications and manufacturers literature employ this concept. Around 1950, the idea of an equivalent noise temperature was being used for antennas and diode mixers. The idea of an equivalent or effective noise temperature for specifying absolute sensitivity has had particular appeal to those working in the fields of communication theory and radio astronomy. The effective noise temperature specifies exactly the same information as noise factor and, in fact, they are related by the definition

$$T_e \triangleq (F - 1) T_o$$

where $T_o = 290$ °K is the defined standard temperature of receiver noise theory.

Now that absolute sensitivities were specified, interest turned to the investigation of the effect of detector characteristics on signal-to-noise ratio. Papers by Fubini and Johnson (1948), Middleton (1948) and DeLano (1949) presented theories on the effect of linear detectors on signal-to-noise ratios. The first book devoted entirely to the problem of receiver noise and the detection of low-level signals in noise was written by Lawson and Uhlenbeck in 1950. This work was a summary of noise theory in receiver circuits and detection theory for weak radar signals. The next complete treatment of noise in electronic circuits was written by van der Ziel in 1954. This work covered the entire scope of circuit noise including thermal noise, device noise, statistical methods and the Fourier Analysis method of characterizing fluctuating quantities.

It was during the period following 1954 that solid-state devices began to show serious promise for future electronic applications and interest in two-port noise theory soared. Many papers were written in the latter fifties on noise theory for junction diodes and transistors. The most prominent author in this area was A. van der Ziel who, with different colleagues, published papers on shot noise in junction diodes and transistors (1955, 1957 and 1958), noise theory for junction diodes and transistors (van der Ziel and Becking, 1958) and others (Hanson and van der Ziel, 1957). Uhlir contributed papers on shot noise in junction diodes (1956) and shot noise in junction-diode mixers (1958). This interest in solid-state noise would continue through the sixties.

The Theory of Noisy Fourpoles written by H. Rothe and W. Dahlke (1956) is the classic reference on noise theory for two-port networks.

Their paper showed how to derive the four noise parameters of a two-port network. They also showed, in a rigorous way, how noise factor was related to the noise parameters of a two-port and how the effects of noise matching and noise tuning were explained by the model. This spurred an interest in noise factor theory and several authors started investigating rigorous circuit theory definitions and optimization. Most notable of these were papers by Haus and Adler (1957, 1958a, 1958b, 1959) Adler and Adler and Haus (1958).

The statistical theories of noise were not being ignored during the fifties. In 1954 a collection of papers were published (Wax, 1954) which dealt with noise theory and stochastic processes. The concepts of using statistics, Fourier transforms, and autocorrelation functions to solve noise problems were becoming popular. The classic textbook, which treated the topics of probability and random variables, power spectral density, transform methods, noise processes and statistical detection, was Random Signals and Noise by Davenport and Root (1958). This book introduced the engineer of that period to new techniques which he could use to solve a wide variety of noise problems. It also emphasized the need for knowledge about the theory of random variables and transform methods.

Continued interest in solid-state noise in the sixties was encouraged by the variety of new devices being invented. The field-effect transistor, in particular, seemed to promise newer and better low-noise amplifiers. Noise theory for field-effect transistors was discussed in papers by van der Ziel (1962a), Bruncke (1963 and 1966), Klaassen (1967 and 1969), and Robinson (1969). An engineering text devoted entirely

to the field-effect transistor was published in 1965 (Sevin, 1965). Junction-transistor noise theory was being refined. A letter by Cooke (1961) discussed the phenomenon of an upper-noise-corner frequency and gave a noise factor equation showing frequency dependence. The noise behavior of high-frequency transistors was becoming increasingly important because device technology was on the verge of producing high quality UHF and microwave transistors. An excellent treatment of the noise performance of microwave transistors was given by Fukui in 1966a. He combined two-port noise theory and solid-state device theory with the parasitic effects of transistor packaging. This treatment thoroughly discussed noise factor dependence on source impedance, operating frequency, and device parameters. Other treatments of high-frequency noise in transistors were given by Agouridis and van der Ziel (1967) and by Baechtold and Strutt (1968). The noise generation in transistors used as mixers was given a thorough treatment by Webster (1961).

Interest in the theoretical aspects of noise factor and absolute sensitivity was increased in the early sixties by advances in low-noise device technology and the advent of Masers and Lasers. "Quantum Electronics" was a term being applied to the union of quantum theory and electronics which produced these devices. Fantastically low noise temperatures (only a few degrees Kelvin) made people wonder what theoretical limit of sensitivity existed. Various papers addressing such topics as zero-point energy, thermal and quantum noise and the fundamental noise limit of amplifiers were presented by Siegman (1961), Gordon (1962), Heffner (1962), Buckmaster (1965) and Oliver (1965). To take advantage of the lowest possible noise factor, one must be aware of two-port noise

theory and circuits that will achieve the minimum. A variety of papers and books on how to design low-noise amplifiers have been written. A sample of the available literature includes books by Rheinfelder (1964) and by Jolly (1967) and papers on low-noise amplifier design by Johnson (1966) and Antman (1967). Noise-factor theory was also being updated to include the possibility of negative-conductance amplifiers and to give more explicit definitions (Fisher, 1962; Haus, 1962 and van der Ziel, 1962b). Workers in the area of noise theory were becoming increasingly aware of two-port noise theory (Cooke, 1962) and noise factor problems (Ekiss and Halligan, 1961).

Several excellent books on noise and related theory were written in the sixties. To mention just a few, the most readable book for the self-study beginner was Electrical Noise by William R. Bennett (1960). This book discussed many of the aspects of noise theory encountered in receiving systems. Another book, by D. Middleton (1960), was a very rigorous and thorough treatment of statistical communication theory. Middleton's book discussed detector theory in more detail than any reference known to this author. The important applications of Fourier Transform Theory to noise problems as well as a wide variety of other scientific problems prompted Ron Bracewell (1965) to write an entire text devoted to the Fourier Transform and its applications. Bracewell's book is still the most complete engineering reference on the subject. It may surprise the reader to learn that a book, Radio Astronomy by J. D. Kraus (1966), is an excellent text on receiving system fundamentals. Such topics as radiation laws, wave polarization and propagation

fundamentals, antennas, receivers and noise theory are presented along with radio astronomy fundamentals.

With a proliferation of new theories and new terminology it is necessary to have standards on terms and methods so that newcomers to the field can understand the literature. To keep up with the rapid pace of noise theory the Institute of Radio Engineers (later the IEEE) published several standards on noise theory. These standards covered the topics of noise in electron devices, noise measurements, two-port noise, and noise performance of amplifiers and receiving systems.

Sensitivity measurement theory, noise measurement theory and especially the topic of measurement errors have not received the comprehensive type of treatment that other subjects have received. This can probably be attributed, in part, to the lack of academic interest in the subject as well as the broad spectrum of applications to be encompassed. Although several references dealt with a very specific measurement problem, none were found that covered a broad spectrum. There are three basic categories under which papers concerned with noise measurement may be placed: noise factor measurements, mismatch errors in noise measurements and noise temperature standards. Noise factor measurements were discussed by Hudson (1955), Anouchi (1958), Matthews (1967), and Golding (1968). The problems associated with impedance mismatches in receiving circuits, and how the noise temperature of a source or noise factor of a receiver are affected are treated by, Brady (1964), Harris (1966), Livingston and Bechtold (1968) and Pastori (1968b). Papers on the various types of noise sources and how the equivalent noise temperature is determined are given by, Hart (1962),

Wells et. al. (1964), Eisele (1964), Miller et al. (1967), and Stelzried (1968).

The theories of sensitivity and noise in electronic circuits will continue to be improved and refined. Basic concepts are well established but work will continue in the areas of device noise, detector noise and noise measurement. New microwave devices and the need for better receiving systems in astronomy and space applications will keep the field active. Totally new concepts of communication such as laser communications and laser heterodyne receivers will demand much effort in the area of noise theory analysis and quantum effects. For persons interested in starting major work in this field, a Recommended Reference List is given in Part T of the Appendix.

As stated in the Preface, the goal of this work is to provide a self-study guide for engineers and scientists wanting to learn noise and sensitivity-measurement theory for receiving systems and circuits. Many topics had to be omitted to limit the work to a reasonable scope. Most notable of these were audio noise, flicker noise and quantum noise. The text was written from the viewpoint of a design engineer working with high-frequency receiving systems and circuits. The author used the text to answer many of his own questions about receiver noise. Many fundamental questions were formulated to serve as a basis for writing. Among these were the following:

- a. Why are we interested in the sensitivity of a receiving system?
- b. What are the important functional blocks of a communication link and how is the receiver related to them?

- c. What are the important functional blocks of a receiver and how do they affect sensitivity?
- d. What is meant by an optimum system and what trade-offs are involved?
- e. What is noise, what are its sources, and how is it generated?
- f. What is two-port noise theory?
- g. What are the various methods of specifying receiver sensitivity and how are they interrelated?
- h. What mathematical tools are used to solve noise problems?
- i. How are the various quantities used in noise theory rigorously defined?

It is hoped that the answers to these questions and many others have been provided.

Many of the individual chapters have been made as self-contained as possible so that they can be referred to without reading the entire work. The Appendix contains many derivations and definitions used throughout the field and is written in such a manner as to have reading continuity. It is recommended that the Appendix be read or at least scanned before continuing into the technical part of the text.

II. GENERAL ASPECTS OF A COMMUNICATION SYSTEM

A. The Ideal System

As far as the user is concerned, the ideal communication system is one which allows him to conduct a maximum amount of business at a minimum of cost and maintenance while obtaining a maximum of operational reliability, efficiency and convenience. This ideal system must have a large signal-to-noise ratio with reliable, 24-hour operation. The system must be free from external influences such as man-made static and ionospheric disturbances.

To build such a system would require efficient and reliable transmitters and receivers with large antenna arrays and most likely a satellite link. For all but the most sophisticated levels of communication in government and industry, the ideal system is economically prohibitive and a practical system must be employed which utilizes many design compromises. This chapter is concerned with the compromises made in the signal-to-noise ratio of the system and how to make meaningful measurements of receiver sensitivity. To best analyze this problem it is necessary to examine the four basic system components of a practical communication system.

B. The Practical System

Each practical communications system consists of a transmitter, receiver, associated antennas and the propagation path between communication points. The signal-to-noise ratio of the communication link depends on all four components and the performance of each is

interdependent on the others. For this reason, it is possible to make many tradeoffs among the various components and still maintain an acceptable link. The following discussions of each component are intended to give the reader an overview of the complete system to aid in the understanding of later, more detailed information. Refer to Figure 2-1 for a system diagram.

1. The transmitter

For system sensitivity studies, the transmitter may be considered to be a device which encodes information on an RF signal, amplifies this signal to an appropriately high power level and applies it to an antenna system. The system design engineer need only know the type and content of modulation, RF power level, output impedance, signal-to-noise ratio and harmonic-spurious content to be able to specify the other system components. For the purposes of this study, the transmitter will be represented by an equivalent Thevenin voltage generator having a specified available power output, impedance, modulation, and signal-to-noise ratio (T-SNR)*. The type and content of modulation is important in the fact that the demodulation of low-level signals is dependent upon the type of modulation. The transmitted signal-to-noise ratio is important because it determines the SNR limit that can be achieved with any system. It would be uneconomical, for example, to design a communication link to have a 50 db signal-to-noise ratio when the transmitted ratio was only 30 db. Likewise, the off-channel noise contributed by the transmitter may interfere with other channels or with the primary

*Transmitted signal-to-noise Ratio

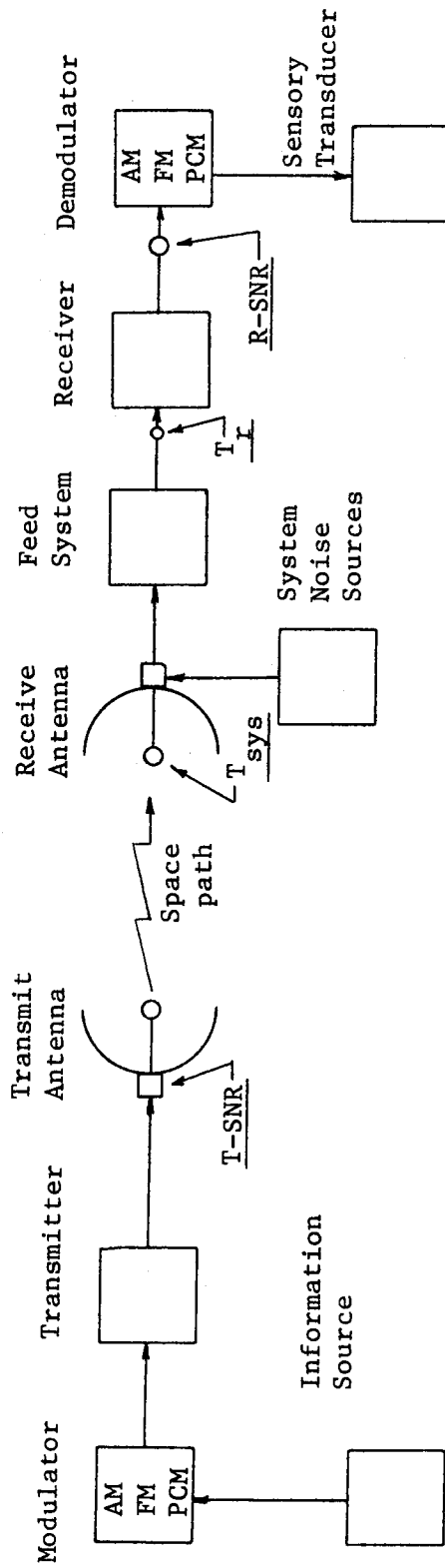


Figure 2-1. System block diagram of a communication system illustrating receiver and system noise temperatures (T_{sys} , T_r) and transmit and receive signal-to-noise ratios ($T-SNR$, $R-SNR$), where for the most economical system, $T-SNR \gg R-SNR$. The common technique of referring all receiving system noise to an equivalent input noise source is illustrated by the system noise sources block input to the antenna

receive channel. The transmitter in a good system must be designed to minimize these undesirable effects.

2. The propagation path

The propagation path of a communication system is that which the desired signals must traverse to get from the transmitter to the receiver. The path of these electromagnetic waves may be short and line-of-sight as in a microwave link, or it may be intercontinental such as with international shortwave broadcasting and ham radio. The path may be extraterrestrial as with communication satellites, planetary probes, solar system radio astronomy, and moon bounce experiments, or it might be cosmic as in galactic and extra galactic radio astronomy.

The physical nature and length of the path has much to do with the reliability and signal-to-noise ratio of the link. Such aspects as power decrease with distance and interspace absorption and background noise must be considered in any design. Because of the complexity of the variables involved in trying to predict space path performance, there is no "best" approach for every case. As a result, there is still a lot of design flexibility in the interface between the space path and the antennas.

3. Antennas

The antenna is the most important component in a high quality communication link. The quality of the transmitter and receiver may be excellent but if they are used with inadequate antennas the complete system will operate poorly. Such concepts as antenna directivity or gain, characteristic impedance and equivalent noise temperature must be

understood before attempting to select the proper antenna design. Especially when determining the system sensitivity, the antenna's equivalent noise temperature must be taken into account. Many antennas have such a high equivalent noise temperature that receiver noise is a minor consideration. This is true most often at frequencies below 30 MHz. Specification of antenna gain alone will not provide a good system because, in addition, one must consider minor lobe response, sidelobe noise pickup, bandwidth and the susceptibility of the antenna to man-made noise. It is worthwhile to examine sky temperature and its effect on antenna noise temperature when designing a system. Once the antenna parameters are determined, it is possible to model the antenna with a Thevinin equivalent circuit using the antenna radiation resistance and the superposition of signal and noise generators. This technique is employed in Chapter III.

4. The receiver

In modern solid-state communication system designs, the receiver is second in importance, and a very close second, to the antenna. The receiver and antenna are intimate partners in the task of providing a usable sensitivity. When the antenna temperature is low (it may be in the 3-20°K range) the system sensitivity is determined strictly by the receiver noise contribution. For this reason, the receiver is a very important component. On the other hand, the state-of-the-art in solid state RF preamplifier design is such that noise figures of 2-4 db (noise temperatures of 170-440°K) are common. In effect, this puts a burden on the system designer to make a compromise between the antenna

and the receiver noise specifications. In spite of this, the author considers the receiver to be the most important contributor to a well designed, low noise, high quality receiving system. This viewpoint is useful in RF circuit designing and testing of low-noise receivers.

The information theory requirement, that the receiver faithfully reproduce the information transmitted, places many restrictions on: 1) the preservation of signal-to-noise ratio, 2) the type of demodulation scheme incorporated, and 3) the presentation of data at the sensory transducer. These requirements are often conflicting and a study of the noise aspects of a receiver aids in choosing among the alternatives. An understanding of the various schemes of measuring receiver sensitivity will help the user choose the appropriate method.

The design of a receiver from antenna to demodulator requires basically that a specific receiver signal-to-noise ratio and bandwidth be provided. The selection of the minimum acceptable SNR and bandwidth is primarily the task of information theory and is not discussed in this report. The approach used here is that the designer has these parameters as boundary conditions and wishes to determine the system circuits and restraints.

These topics and others will be discussed in the next Chapter where the important aspects of a complete receiving system are presented.

III. RECEIVING SYSTEMS FOR SENSITIVITY STUDIES

A thesis on the sensitivity measurements for optimum receiving systems would not be complete without a summary of the theory of receiver operation. After trying to omit this section, it was the feeling of this author that the thesis would lack the unifying effect of a chapter on receiving systems. Much thought has gone into the preparation of Figure 3-1 which contains most of the basic building blocks of a double conversion heterodyne receiver. An attempt has been made to keep it as complete as possible without excessive clutter. There are six main sections to the receiving system illustrated:

1. The electromagnetic transducer
2. The feed system
3. The RF translator
4. The IF amplifier
5. The demodulator-detectors
6. The sensory transducers.

The sections were selected on the basis of their effect on receiver sensitivity measurements.

Elementary theory of operation and functional definitions will now be discussed for each main section. The first section, on antenna theory, is presented from a system engineering standpoint. The opportunity to present the antenna topics necessary to develop equations for signal power did not present itself in any other chapter so they are presented in this one. For this reason, the antenna section will cover much more detail than the others.

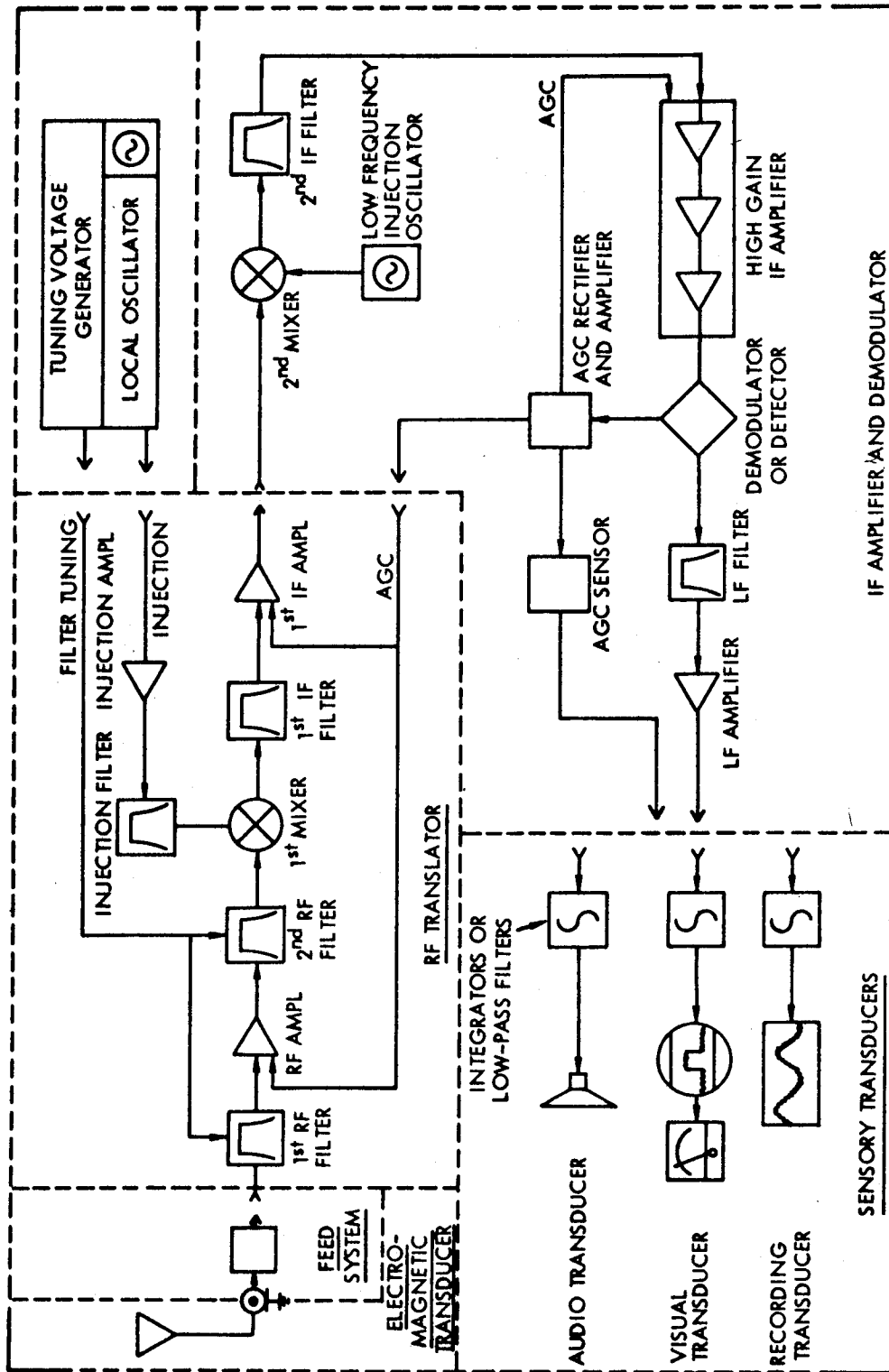


Figure 3-1. Receiving System

A. Electromagnetic Transducer (Antenna)

Wireless communication between two points can only be accomplished if the circuit voltages and currents at the transmitter are transformed into electromagnetic waves that will propagate through space to the receiver where the waves can then be transformed back to voltages and currents to be detected and processed. The devices which accomplish these transformations are electromagnetic transducers which, at radio frequencies, are called antennas. The RF antenna transduces between electromagnetic waves and voltages and currents in the same manner as a loudspeaker does between soundwaves and electrical current or a thermocouple does between heat energy and electrical current. The techniques of analyzing antennas are much the same as those for any transducer. For the antenna, energy transfer equations are used to develop circuitual and field equations. These equations may then be combined to characterize the antenna as a two-port device.

The fields produced by an antenna are not computed directly except in the simplest of cases. For the best accuracy, it is necessary to measure the fields and then characterize the antenna on the basis of its directivity and radiation intensity.

The physical nature of a practical antenna is such that it will not radiate power evenly in all directions. In fact, for many applications it is desirable to radiate power in a narrow beam. The shape of the antenna radiation pattern affects its performance and is usually determined empirically for applications requiring exacting performance. To characterize this, the power output as a function of angular direction

is specified by the radiation intensity $U(\theta, \phi)$ in watts per steradian. Figure 3-2a shows the coordinate definition to be used in this report and Figure 3-2b shows a typical two dimensional radiation intensity pattern (beam power pattern).

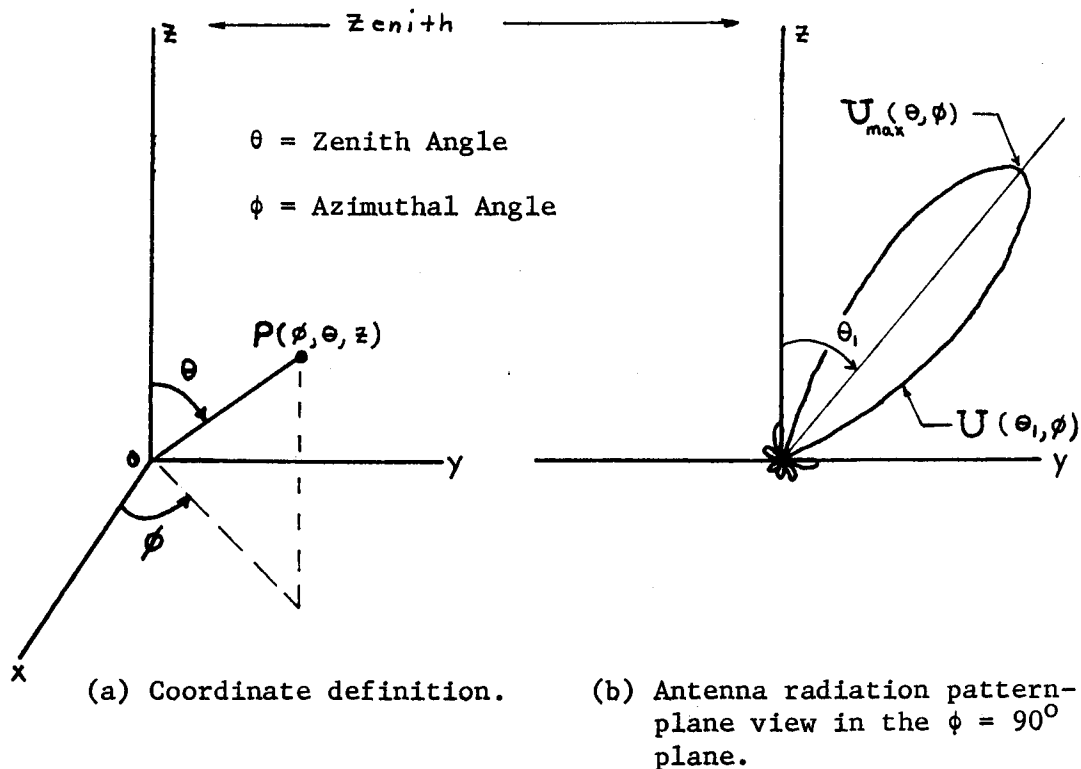


Figure 3-2. Antenna Radiation Pattern

For comparison purposes and for gain reference, it is convenient to define the concept of an isotropic radiator (isotropic antenna). The isotropic radiator acts like a point source of radiation and does not favor a particular direction. The result is an equal flow of radiation in all directions with a radiation intensity of

$$U_{\text{isotropic}}(\theta, \phi) = U_{\text{ave}} = \frac{W_t}{4\pi} \quad (\text{A.1})$$

where W_t is the radiated power. The equivalent power density at a distance r_o from the isotropic radiator is:

$$S_o = \frac{W_t}{4\pi r_o^2} \quad (\text{A.2})$$

For an antenna which is not isotropic, as is the case of the typical beam pattern shown in Figure 3-2, the radiation intensity varies as a function of angular direction as specified by:

$$\text{Antenna Radiation Intensity} = U(\theta, \phi) \quad (\text{A.3})$$

A non-isotropic antenna is usually characterized by the directive gain, $D(\theta, \phi)$, which is the actual radiation intensity normalized by the average intensity:

$$\text{Directive Gain, } D(\theta, \phi) = \frac{U(\theta, \phi)}{U_{\text{ave}}} \quad (\text{A.4})$$

The numerical factor of antenna directivity is the maximum value of directive gain:

$$D = [D(\theta, \phi)]_{\text{max}} = \frac{U_{\text{max}}(\theta, \phi)}{U_{\text{ave}}} \quad (\text{A.5})$$

Antenna directivity can also be specified in decibels:

$$D_{db} = 10 \log_{10} D. \quad (A.6)$$

Directive gain and directivity will specify the performance factors for an antenna but there are other convenient quantities that are used to describe antenna performance which simplify the mathematical discription. These will now be presented and applied to specify the performance of the antennas in a communication system.

The normalized power pattern for an antenna is obtained by normalizing the antenna radiation intensity to its maximum value:

$$\text{Normalized Power Pattern, } P_n(\theta, \phi) = \frac{U(\theta, \phi)}{U_{\max}(\theta, \phi)} \quad (A.7)$$

With this definition, $P_n(\theta, \phi)$ always lies between zero and unity.

Directive gain can now be conveniently defined in terms of the normalized power pattern and antenna directivity:

$$D(\theta, \phi) = D P_n(\theta, \phi) \quad (A.8)$$

We now state the important fundamental relationship which exists between the normalized power pattern, the antenna beam solid angle, and the antenna effective aperture which, by definition, is

$$\Omega_A = \frac{\lambda^2}{A_e} = \iint_{4\pi} P_n(\theta, \phi) d\Omega \quad (A.9)$$

where λ = Wavelength, meters

A_e = Antenna effective aperture, m^2

Ω_A = Beam solid angle, rad^2

$P_n(\theta, \phi)$ = Normalized power pattern.

The last relationship to be developed will relate antenna directivity, effective aperture, and beam solid angle.

Substitute into Equation A.9 an expression for the normalized power pattern obtained by combining Equations A.8 and A.4

$$P_n(\theta, \phi) = \frac{U(\theta, \phi)}{D U_{ave}} \quad (A.10)$$

so that the beam solid angle becomes:

$$\Omega_A = \iint \frac{U(\theta, \phi)}{D U_{ave}} d\Omega \quad (A.11)$$

Using (A.1) this reduces to:

$$\Omega_A = \frac{1}{D} \frac{4\pi}{W_t} \iint U(\theta, \phi) d\Omega \quad (A.12)$$

The integral over a 4π solid angle of the radiation intensity is simply the total radiated power W_t . Using this in (A.12) and combining with (A.9) gives the desired equations:

$$D = \frac{4\pi}{\Omega_A} = 4\pi \frac{A_e}{\lambda^2} \quad (\text{A.13})$$

In the discussion thus far, no mention of antenna losses or reference to antenna geometry has been made. Both directivity and losses depend upon the type and size of the antenna. We will now briefly examine antenna efficiency and physical aperture. Suppose we have a receiving antenna oriented so that the direction of maximum gain is toward a completely polarized point source and that the polarization of the antenna is matched to that of the source. If the antenna were lossless, the signal power available from the antenna, W_r , would simply be the product of the power density incident on the antenna, S_r , and the effective aperture of the antenna:

$$W_r = S_r A_e \quad \text{watts.} \quad (\text{A.14})$$

On the other hand, in a lossy antenna, the available power would be reduced by I^2R losses*. To account for this loss we will define an ohmic loss factor k_r as the ratio of the actual effective receiving aperture of the antenna, A_r , and the effective aperture, A_e , which was determined entirely by the radiation pattern as related in equation A.13. The ohmic loss factor becomes

*Other antenna losses, such as scattering, will not be discussed in this work. For more detail refer to Kraus (1966, Ch. 6).

$$k_r = \frac{A_r}{A_e}, \quad (0 \leq k_r \leq 1) \quad (\text{A.15})$$

and the signal power available is determined from (A.14) by replacing A_e with $k_r A_e$

$$W_r = S_r A_r = S_r k_r A_e \quad (\text{A.16})$$

where W_r = Signal power available from the antenna, watts
 S_r = Power density incident at the antenna, watts/ M^2
 A_e = Effective aperture determined entirely by the radiation pattern, M^2
 A_r = Actual effective receiving aperture, M^2
 k_r = Ohmic loss factor, dimensionless.

A measure of the increase in radiation intensity provided by a directional antenna over that of an isotropic radiator is called the antenna gain. Antenna gain takes into account ohmic losses and is defined as (Kraus, 1966, p. 213):

$$\text{Antenna Gain, } G_r = k_r D_r. \quad (\text{A.17})$$

The antenna gain is always less than antenna directivity because the loss factor is always less than unity.

The physical aperture of an antenna is difficult to define when the antenna is small compared to the operating wavelength but when it is large, its value is comparable to that of the effective aperture.

For a comparison between size and effective area, and as a means of comparing antennas, the aperture efficiency, ϵ_{ap} , is defined as the ratio of the actual effective receiving aperture to the physical aperture:

$$\epsilon_{ap} = \frac{A_r}{A_p} = k_r \frac{A_e}{A_p} . \quad (A.18)$$

For the interested reader, a more extensive discussion of antennas, particularly beam shape and efficiency, can be found in Chapter 6 of Kraus (1966). The essential antenna parameters that have been presented will now be used to demonstrate methods for calculating antenna requirements in a communication system and methods of estimating signal-to-noise ratios.

Consider the simple communication system of Figure 3-3. The power density incident at the receiving antenna, and due to the transmitter, is determined by the product of average power density and the directive gain of the transmitting antenna:

$$S_r = \left(\frac{W_t}{4\pi r_o^2} \right) D_t(\theta_t, \phi_t) \quad \text{watt/M}^2 \quad (A.19)$$

When the transmitter is far away from the receiver so that it looks like a point source, the signal power available at the receiving antenna is found by multiplying the received power density and the actual effective receiving aperture:

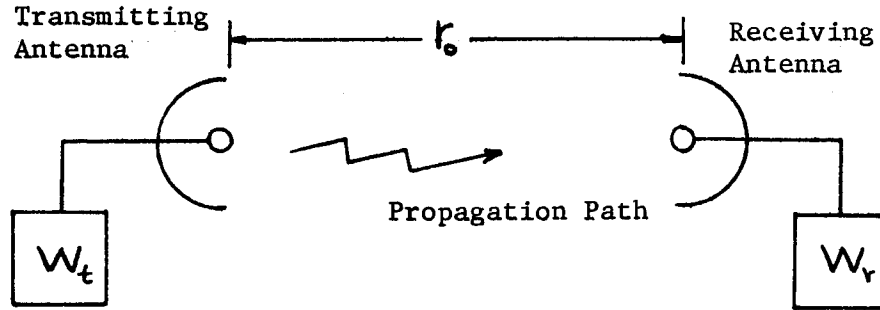


Figure 3-3. Idealized Communication System

$$W_r = S_r A_r = S_r D_r k_r \frac{\lambda^2}{4\pi} = \frac{\lambda^2}{4\pi} S_r G_r \quad (\text{A.20})$$

For the above equation, k_r is the ohmic loss factor for the receiving antenna and the effective area is obtained on the assumption that the receiving antenna is directed toward the transmitter to achieve maximum gain. When the receiver is not directed for maximum gain, and if both transmitting and receiving loss factors are used, the available power at the receiving antenna becomes:

$$W_r = \left(\frac{k_t W_t}{4\pi r_0^2} \right) D_t(\theta_t, \phi_t) D_r(\theta_r, \phi_r) \frac{k_r \lambda^2}{4\pi} \quad (\text{A.21})$$

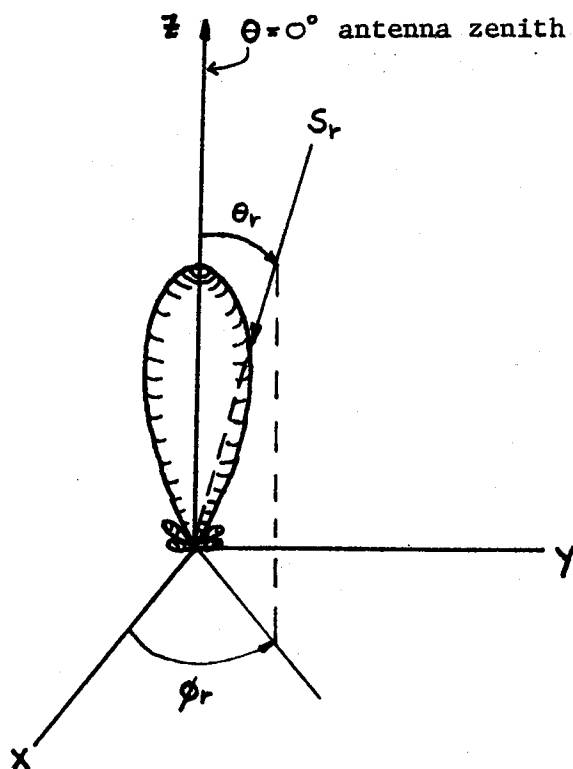


Figure 3-4. Comparison between Antenna Beam Pattern and Incident Flux Direction

where W_r and W_t represent actual received power and transmitted power. Substitution for the directive gains in (A.21) using (A.8) yields the final result:

$$\begin{aligned}
 W_r &= k_t k_r D_t D_r W_t \left(\frac{\lambda}{4\pi r_0} \right)^2 \left[P_t(\theta_t, \phi_t) P_r(\theta_r, \phi_r) \right] \\
 &= W_t G_t G_r \left(\frac{\lambda}{4\pi r_0} \right)^2 \left[P_t(\theta_t, \phi_t) P_r(\theta_r, \phi_r) \right] \quad (A.22)
 \end{aligned}$$

where,

- k_t = Transmitting Antenna ohmic loss factor
- k_r = Receiving Antenna ohmic loss factor
- D_t = Transmitting Antenna directivity
- D_r = Receiving Antenna directivity
- W_t = Transmitter power input to the antenna, watts
- $P_t(\theta_t, \phi_t)$ = Transmitter normalized power pattern
- $P_r(\theta_r, \phi_r)$ = Receiver normalized power pattern.

Equation A.22 shows that, when the transmitting and receiving antennas are not directed for maximum gain, the received power is reduced by the product of the normalized power patterns.

For the general case of receiver operation, the power received is determined by the direction of incident flux and the antenna directive gain. In Figure 3-4, the received flux from a point source is not directed for maximum power. When this happens, the power received is determined from Equation A.22 where all the transmitter terms are replaced by the substitution

$$S_r = \frac{W_t}{4\pi r_o^2} k_t D_t P_t(\theta_t, \phi_t) \quad (A.23)$$

and the power received becomes;

$$W_r = S_r \left(\frac{\lambda^2}{4\pi} D_r \right) k_r P_r(\theta_r, \phi_r) \quad (A.24)$$

The receiver normalized power pattern is always less than or equal to unity and (θ_r, ϕ_r) is the angular direction between the antenna zenith and the point source.

The last aspect of antenna system operation will now be considered—the propagation path loss. In any practical system the received power is always less than that predicted by (A.22). The reason is that the propagation path was assumed to be a vacuum in obtaining Equation A.2 but actually the signal is always attenuated by traveling through a lossy dielectric or ionized media such as the earth's atmosphere or a gas cloud in space. To account for this reduction in signal a space loss factor, k_s , is introduced in Equation A.22. By introducing k_s and examining the system requirement for antenna gain and transmitted power we can assume a value of unity for the normalized power patterns to obtain the following requirement

$$W_r = W_t G_t G_r \left(\frac{\lambda}{4\pi r_0} \right)^2 k_s \quad (\text{A.25})$$

where G_t = Transmitting antenna gain
 G_r = Receiving antenna gain
 k_s = Path loss factor ($0 \leq k_s \leq 1$).

Equations A.22 and A.25 will be used in the antenna noise section to compute signal-to-noise ratio for a communication path.

B. Feed System

The term feed system will be used to refer to the interconnection between antenna and receiver RF translator. The losses in the feed system add directly to the receiver noise figure and cause a reduction in signal-to-noise ratio. Because of this reduction in sensitivity, it is important to consider the noise aspects of the feed system.

A typical feed system may contain elements such as switches, feedline connectors, diplexers, attenuators, filters, baluns, transformers, impedance transforming networks and assorted lengths of feedline. Each of these elements have losses and produce noise which must be accounted for in low-noise designs. As an illustration, consider Figure 3-5 which shows a hypothetical communication center that incorporates several feed system components. In most practical cases, the total insertion loss, in db, of all the feedline elements can be added to the receiver noise figure to obtain the total noise figure as seen by the antenna. To add db loss directly, it is assumed that the feed system components are at standard temperature and the SWR of feed system and antenna is 1:1. Take as an example the following typical feedline installation:

1. Connector losses at 0.1 db each = 0.5 db
2. Balun loss = 0.5 db
3. Antenna switch loss = 0.1 db
4. Feedline loss = 0.8 db

Total feed system loss = 1.9 db.

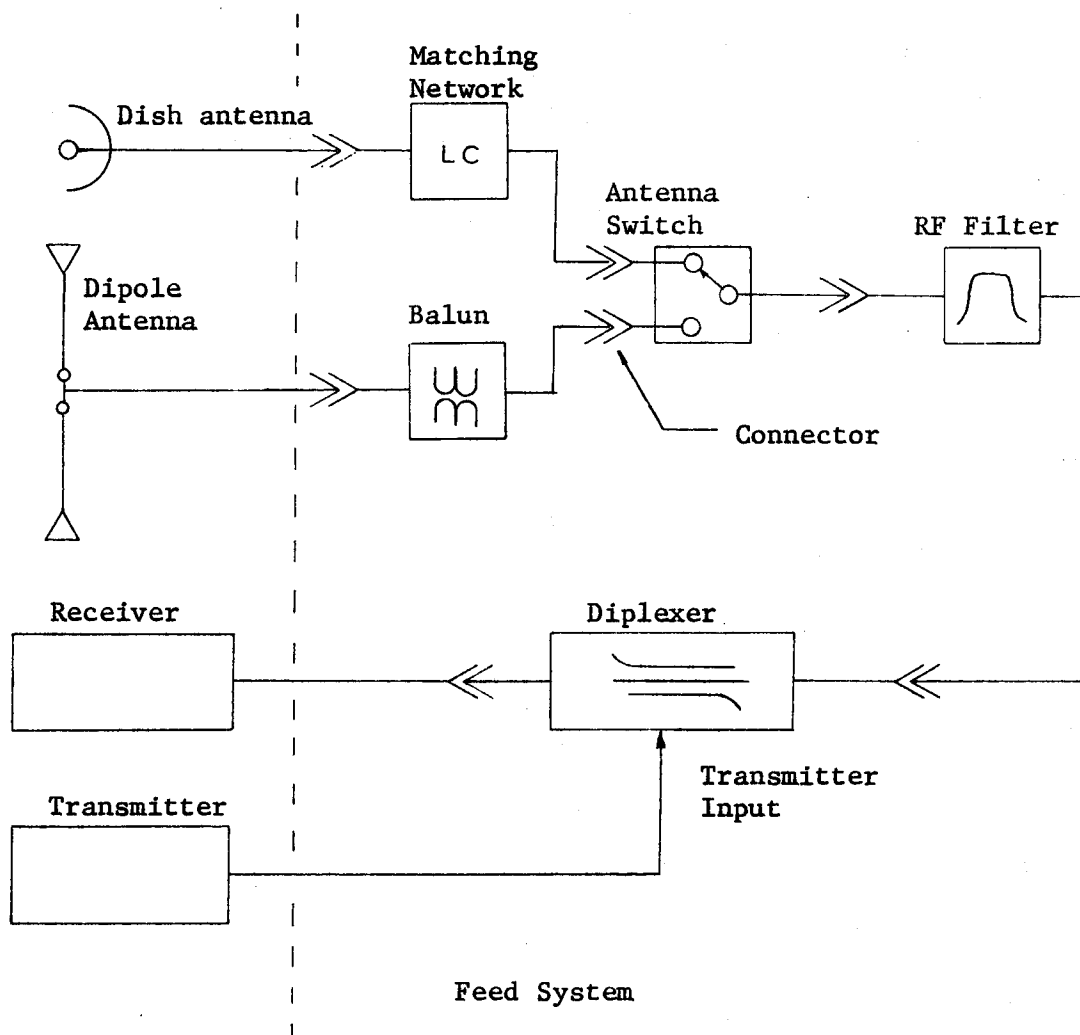


Figure 3-5. Communication System Illustrating Typical Feed System Components

The losses in this typical feed system would add 1.9 db to the receiver noise figure. If the receiver noise figure were originally 3.5 db the total noise figure would be 5.4 db. This represents a doubling in effective noise temperature which is a serious degradation for low-noise systems. A typical feedline contribution to noise figure will be in the range 0.5 to 3.0 db. High-quality low-noise systems will be

considerably less than typical whereas commercial broadcast receivers may have losses of 10-20 db. To help in estimating the effect of the feed system on system noise figure, Table 3-1 has been prepared. This table summarizes the range of losses which might be expected for typical feed-system components.

It is the resistive losses in the feed system that decrease receiver sensitivity and increase the system noise figure by causing signal power losses. Additional receiver sensitivity decreases may occur when noise is injected into the feed system from external sources. Care should be taken to provide adequate shielding to minimize interference from man-made sources.

Table 3-1. Losses for typical feed-system components

Component	Loss--db ^a	
Coax connectors	.01 - 0.2	
Balun	0.2 - 1.0	
Impedance transformers	.05 - 0.3	(0.1)
Antenna switch	.01 - 1.0	
Diplexer	0.5 - 3.0	(1.0)
Feedline	^b	

^aTypical number shown in parenthesis.

^bDepends on length and type of line. Data on transmission-line loss is available in handbooks (International Telephone and Telegraph Corp., 1956, p. 614).

As a typical example of noise being injected into the feed system, consider the case of full duplex operation with a diplexer. The noise sidebands from the transmitter may be large enough to cause an increase in noise on the receive channel. This injected noise would increase the system noise temperature and cause a reduction in signal-to-noise ratio.

The previous discussion of feed system considerations and problems is by no means exhaustive. The noise aspects of the feed system vary so much from one to another that the best recommendation this author can make is that the designer carefully consider all aspects of his individual installation. The effects of transmission lines and attenuators on receiver noise are considered further in section IV-C.

C. RF Translator

The term RF translator has no fixed definition in radio engineering so it will be necessary to define its meaning in this report:

The RF translator is that portion of a heterodyne receiver which selects a band-limited spectrum of high-frequency signals and frequency translates or heterodynes them to a different (usually lower) frequency.

A typical RF translator will include:

1. RF amplifying and filtering
2. A mixer for heterodyning
3. Injection signal filtering and amplifying
4. First IF filtering and amplifying.

The scheme shown in Figure 3-1 is reasonably general and incorporates most of the features found in an RF translator. Many translators are much simpler than that illustrated but it was felt that the basic elements of all designs should be incorporated in the example. It is possible to develop a satisfactory translator with only the first RF filter, first mixer and first IF filter.

The RF translator determines many of the important operating parameters of a heterodyne receiver. The ones we will be most concerned with for noise studies are noise figure and RF selectivity. Almost without exception, the receiver noise figure is determined by the RF translator. The criteria for low-noise operation are that the RF amplifier and first mixer have enough gain to overcome the equivalent noise of succeeding stages while contributing a minimum of their own noise.

In most translator designs, the requirements of good distortion performance and low noise are conflicting. Obtaining good distortion performance means having very selective filtering and high dc power input to the active devices. Both of these conditions degrade low-noise performance. One of the goals of this report is to provide the reader with the information necessary to make good decisions concerning trade-offs between distortion and low noise. A brief description of each element in the RF translator will now follow. Emphasis will be made on those aspects of operation which affect receiver noise performance.

The tuneable RF filters are used to select the desired range of RF spectrum to be received. Filter tuning is made to "track" the local oscillator tuning which, by means of the tuning voltage generator, keeps

the desired signal bandwidth, as determined by the first IF filter, within the passband of the RF filters. The RF filters attenuate signals outside the receiving passband to reduce distortion and interference and also reject the image-frequency response. The important parameters of the RF filter are its bandwidth characteristic and insertion loss. The more important of these two parameters, as far as noise performance is concerned, is the insertion loss. The insertion loss of the first RF filter adds directly to the spot noise figure of the first RF amplifier. For this reason it is desirable to keep the filter passband attenuation as small as possible while still obtaining the desired selectivity. This problem is complicated when the filter has ripple in the passband. Ripple causes the noise figure to be dependent on what portion of the filter passband is being used. Generally speaking, the first RF filter should be used primarily to protect the RF amplifier from the strong signals which cause cross-modulation. The second RF filter is used for cross-modulation and image rejection ahead of the first mixer stage.

The RF amplifier is the first active stage in the receiver and, as such, determines the important operating characteristics of noise figure and cross-modulation. The RF amplifier has four basic functions and responsibilities in the heterodyne receiver:

1. It has gain to boost the amplitude of the received signal
2. It determines the cross-modulation distortion level for the receiver

3. It must have enough gain to overcome the noise figure of the mixer
4. As the first active stage, it has the largest effect on receiver noise performance

The basic requirements of an RF amplifier are that it have a low enough noise figure to meet the total system requirement and have a high enough gain that the noise contribution of the mixer is minimized. Using a device which has a gain much higher than that needed to overcome mixer noise should be avoided because the additional signal amplitude degrades the distortion performance of the mixer. It is the RF amplifier that is the topic of much of the noise theory of this report.

D. IF Amplifier

The IF (intermediate frequency) amplifier in a heterodyne receiver is needed for two primary reasons:

1. to produce the large voltage gain required to amplify the RF translator signal from the low microvolt range to the tenths of volts needed to operate the detectors and demodulators
2. to control the amplitude of the signal voltage input to the demodulator--detectors by means of feedback in an AGC (automatic gain control) circuit.

Sometimes other functions may be performed such as limiting for FM reception and additional bandpass filtering when the first IF filter is inadequate but these will not be discussed.

The IF amplifier typically has 60-100 db of gain and an AGC range of 20-50 db. AGC action helps keep the signal at the demodulator-detector constant for large changes in antenna signal. This feature is needed in applications where a particular operating point must be maintained. The spectrally translated bandwidth of the IF amplifier must be maintained within the RF bandwidth that was initially determined by the RF translator, i.e., the bandwidth of the IF signal must be narrower than the RF filter bandwidth.

This will assume that the signal spectrum at the demodulator-detector is fixed both in bandwidth and in amplitude. Sensitivity problems can occur if the IF bandwidth is much larger than the RF bandwidth as was shown in the derivation of the Friis Equation (Appendix, Part J).

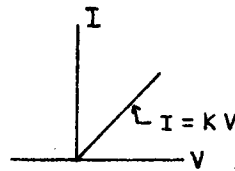
The gain of the IF amplifier is linear in AM and SSB applications but may be logarithmic in the case of radar or other pulse-code modulated systems. For FM, the IF amplifier operates as an amplitude limiter. The gain characteristic of the IF amplifier affects the method used for noise analysis. Because of their definition, noise figure and noise temperature cannot be used to characterize a non-linear receiver and hence can only be applied when the gain characteristic is linear.

E. Demodulator-Detector

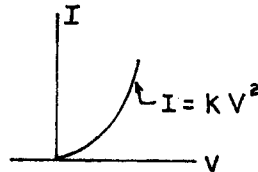
Every receiving system needs a demodulator to recover the information (modulation) on the received signal. An ideal demodulator will

have an output which is the exact replica of the modulation signal at the transmitter. The varying degrees to which practical demodulators accomplish this goal is the predominate factor in their study. Sometimes the output of a demodulator may consist of nearly equal portions of signal and noise while in radio astronomy both signal and noise have the same spectral characteristics. For these cases, it is necessary to analyze the noise performance of the demodulator. Most practical demodulators will fall into four classes as determined by their input-output characteristics:

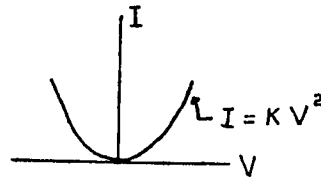
1. Linear



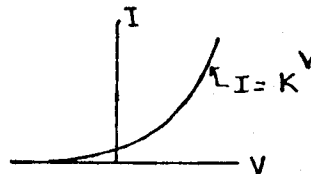
2. Half-wave square law



3. Full-wave square law



4. Exponential



The demodulator is usually used for signals which have a good signal-to-noise ratio (greater than 6db). For low SNR systems, the detection

of the signal in noise must be accomplished by a detection scheme which will improve the SNR. Five such schemes are listed below:

1. Integration and storage
2. Autocorrelation
3. Synchronous detection
4. Matched filtering
5. Statistical detection by threshold sampling.

All of these techniques are used to improve the signal-to-noise ratio of the detected signal and, in theory, are capable of supplying an arbitrarily large signal-to-noise ratio if given enough process time.

For any detection scheme, a tradeoff can be made between the detected SNR and process time. If one is willing to sacrifice process time for SNR, it is possible to detect an arbitrarily low signal level. For "real time" operation, where the signal is demodulated instantly upon reception, it usually takes a SNR of 6db or better.

More information on demodulators and detectors can be found in texts on radio engineering and electronic circuit design.

For more information on detection theory, refer to communication theory texts such as Beckmann (1967, Ch. 7), Papoulis (1965) and Middleton (1960, Ch. 13). A further discussion on demodulator-detectors will be made in Chapter VIII on the theory of sensitivity measurements.

F. Sensory Transducers

An often overlooked subject in technical reports is that of sensory transducers. These devices are very important and yet difficult to

describe. Regardless of the type of information sent over a data link, it must still be comprehended by a human observer. For ease of comprehension, the time scale of presentation must be of the same order of magnitude as the biological integration time of the human observer. This is analogous to high speed and time-lapse photography which is capable of presenting to the human observer a sequence of events either too fast or too slow to comprehend with his biological senses. The task of the sensory transducer in a communication system is to present the demodulated data in a useful and understandable form. To accomplish this, devices such as loudspeakers, meters, lamps, oscilloscopes and stripchart recorders have been used. The type of sensory transducer employed has a major effect on the type of sensitivity measurement to be made. For example, in FM systems it is desirable to specify the quieting ratio as a means of evaluating the quality of a music or voice channel. To obtain quieting ratio, we use a meter to measure signal-to-noise ratio and a loudspeaker to qualitatively determine the minimum ratio that is still pleasing. In pulse code modulated systems, we are concerned with fast risetime pulses usually amplified by a logarithmic IF amplifier. In this case, it is not possible to use linear measurements such as noise figure and one has to utilize a means such as tangential noise sensitivity in which the observer uses an oscilloscope as a sensory transducer and observes the pulse height above the noise level or "grass". As a final example, we look at the strip chart recorder. The best application of this transducer is in systems which require integration times much longer than human biological integration time. For example, in a very low

signal-to-noise ratio receiver as is used in radio astronomy. In many observations, data may be integrated and correlated for minutes or hours. In this long time span the only meaningful display is by means of a chart recorder which can record events occurring over several hours and compress them into visually comprehensible segments.

In all of these systems the critical requirement still remains that the information must be as understandable and as pleasing to the observer as possible. Often the necessary integration time is obtained by the use of a meter, chart recorder, or stage scope. Methods of sensitivity measurement which employ these types of readout devices are presented in Chapter IX.

IV. NOISE IN ELECTRONIC CIRCUITS

The study of noise processes in electronic circuits is a fascinating but almost overwhelming task. It includes determining what kinds of noise physically occur and their statistical properties. Then one must examine the physical sources of noise and determine their effect on both passive and active circuits. Finally the theory of noise in two-port devices must be studied to explain and predict the performance of low-noise amplifiers.

At the outset of this work, it was thought, by the author, that the basic concepts of noise theory for electronic circuits could be concisely presented but after much detailed study it was decided that the subject area is much too broad, and detailed coverage would be beyond the scope of this text. The most difficult task was to separate, out of the large body of probability and random variables theory, the important ideas needed to present the noise theory of receivers. Then it was discovered that it is not practical to try to assimilate the vast number of papers on noise in electronic devices. To solve these problems it was decided that only the most fundamental concepts would be presented and then only those that are used in other parts of the thesis. With this presentation it is hoped that the casual reader will get the basic concepts without overwhelming detail and yet an extensive bibliography is supplied for the reader who wants more detail.

To obtain the best understanding of these topics it is necessary that the reader obtain other viewpoints and methods of presentation. Therefore, for comparative purposes, the reader is encouraged to consult

such widely used texts as Davenport and Root (1958), van der Ziel (1954), and Bennett (1960). For a broader coverage of the topics of probability and noise in communication engineering refer to Beckmann (1967). For a rigorous presentation of the theory of probability, random variables and stochastic processes see Papoulis (1965).

A. Noise as a Physical Phenomenon

1. Brownian motion and thermal agitation

In 1827, a Scotch botanist named Robert Brown observed the irregular zigzag motion of minute particles suspended in a liquid. It was found the smaller the particles, or the higher the temperature of the liquid, the more violent the motion. This phenomenon, known as Brownian Motion, has had a profound effect on science. The existence of Brownian Motion has led to the kinetic theory of matter which states that matter is composed of small particles called molecules which are constantly moving. It is also significant that the motion becomes more violent as the temperature increases. It is the energy of this motion that we use to define a thermal or kinetic temperature.

The term thermal agitation is used to describe the Brownian Motion of atomic particles in materials. The same thermal agitation causes the molecules of a gas to move about just as it does a suspended particle. The postulation of thermal agitation of electrons in a conductor has led to the theory of thermal or Johnson noise. The resulting random voltages and currents caused by this thermal agitation account for many of the noise processes found in a receiver and their study will be an important topic of this report.

2. Shot noise

Shot noise is also caused by a flow of electrons but, in contrast to the lack of an external field which exists for thermal noise, it is caused by the flow of electrons in a dynamic system. The derivation for the noise current of a shot noise source cannot be conducted with the same thermodynamic arguments that are used for thermal noise. This contrast is highlighted by comparing the two types of electronic noise. Shot noise in a vacuum tube is caused by the unidirectional flow of electrons from cathode to plate* while thermal noise is the random thermal motion of elections. Shot noise is encountered in all electronic devices which have current flowing in them and, in particular, the shot noise in diodes, transistors and vacuum tubes is important in receiver noise studies. The flow of electrons in semiconductor devices causes the shot noise which plagues all active devices and causes them to have a noise factor greater than unity. For this reason a noiseless solid state amplifier is impossible because even if the thermal noise sources could be reduced to zero by cryogenic techniques the device will still need electron flow for operation. More information on shot noise will be given in section B of this chapter.

3. Statistical properties of noise

The thermal motion of electrons in a conductor and the flow of electrons in an amplifying device are both examples of random processes and the particular noise voltage or current which results is a sample function of that random process. As such, noise voltages and currents are not deterministic as are noiseless, sinusoidal voltages and currents

* Also referred to as the anode

but are probabilistic i.e., at any instant in time the magnitude and phase cannot be exactly specified but only characterized by a range of values and a probability of occurrence. To study noise processes in communication systems one needs to become familiar with the probabilistic descriptions of noise.

There are two averaging process in noise studies which must be defined. These are the ensemble average (also called the statistical average) and the time average (Davenport and Root, 1958, Ch. 4).

Suppose an ensemble of identical noisy receivers are reproducing, on strip-chart recorders, their output noise fluctuations. Now at a time t_1 the noise voltages of the ensemble are arithmetically averaged. This is the so-called ensemble average. Now suppose the strip-chart record of just one of the receiver outputs is averaged in time. This then is the time average. Mathematically the statistical average is defined in terms of a probability density function, $p(x)$, for a stationary process:

$$\langle X(t) \rangle = \int_{-\infty}^{+\infty} x p(x) dx \quad (4A.1)$$

and the time average is:

$$\overline{X(t)} = \lim_{T \rightarrow \infty} \frac{1}{T} \int_0^T X(t) dt \quad (4A.2)$$

There are two important properties of random processes to be considered before beginning a detailed study of noise processes. These are the properties of stationarity and ergodicity. A random process is stationary if its statistical properties do not change with time. For a strict mathematical definition of stationarity refer to Beckmann

(1967, p. 190). A random process is ergodic if the ensemble average is equal to the time average i.e. if the equality is satisfied with probability one:

$$P [\langle x(t) \rangle = \overline{x(t)}] = 1 \quad (4A.3)$$

It is very desirable to deal with random processes which are both stationary and ergodic as these properties allow many simplifications in the analysis. Fortunately, most random processes studied in communication engineering are both stationary and ergodic.

A measure of the variability of a random process can be determined by another important characteristic called the variance (or dispersion) σ^2 , defined by

$$\sigma_x^2 = \int_{-\infty}^{+\infty} [x - \langle x \rangle]^2 p(x) dx = \langle x^2 \rangle - \langle x \rangle^2 \quad (4A.4)$$

where for a random variable with zero mean ($\langle x \rangle = 0$) the variance equals its mean-square value:

$$\sigma^2 = \langle x^2 \rangle \quad \text{when} \quad \langle x \rangle = 0 \quad (4A.5)$$

The square root of the variance is the standard deviation, σ , and the square root of the mean-square value is the root-mean-square (RMS) value of x as:

$$\text{RMS value of } X, X_{\text{rms}} = \sqrt{\langle x^2 \rangle} \quad (4A.6)$$

The mean-square value of a random variable is determined by the second moment of the distribution:

$$\langle X^2 \rangle = \int_{-\infty}^{+\infty} x^2 p(x) dx \quad (4A.7)$$

The mean-square value of a stationary random variable can also be determined from its time autocorrelation function (Appendix, Part A) and from its power spectral density function. The autocorrelation function is

$$R_x(\tau) = \lim_{T \rightarrow \infty} \frac{1}{T} \int_{-T/2}^{T/2} X(t) X(t-\tau) dt \quad (4A.8)$$

and the mean square value becomes:

$$\langle X^2 \rangle = \overline{X^2} = R_x(0) = \lim_{T \rightarrow \infty} \frac{1}{T} \int_{-T/2}^{T/2} [X(t)]^2 dt \quad (4A.9)$$

The mean square value from the power spectral density function is:

$$\overline{X^2} = \frac{1}{2\pi} \int_{-\infty}^{+\infty} \Phi_x(\omega) d\omega \quad (4A.10)$$

The covariance of two random variables is the mean product of their deviations:

$$\text{Covariance of } X \text{ and } Y = \langle [X - \langle X \rangle] [Y - \langle Y \rangle] \rangle \quad (4A.11)$$

The covariance is a measure of the interdependence of X and Y and is used to determine the correlation between two random variables.

To actually specify the correlation between two random variables, the correlation coefficient is defined by normalizing the covariance with the square root of the variances as

$$\text{Correlation Coefficient, } \gamma_{xy} = \frac{\text{COV}(x,y)}{\sigma_x \sigma_y} \quad (4A.12)$$

where, upon substitution of another form of Equation 4A.11

$$\text{COV}(x,y) = \langle [x - \langle x \rangle] [y - \langle y \rangle] \rangle = \langle xy \rangle - \langle x \rangle \langle y \rangle \quad (4A.13)$$

gives as a final result:

$$\gamma_{xy} = \frac{\langle xy \rangle - \langle x \rangle \langle y \rangle}{\sigma_x \sigma_y} \quad (4A.14)$$

The correlation coefficient is used in the analysis of noise in two-port devices and often has associated with it the units of impedance or admittance. Also, the correlation coefficient is generally complex as expressed by:

$$\gamma_{xy} = |\gamma| e^{j\theta} \quad (4A.15)$$

where

$$0 \leq |\gamma| \leq 1$$

$$-\pi \leq \theta \leq \pi$$

The two most important ways of describing a random variable are by use of the probability distribution function and the probability density function. These functions are defined by the mathematical relationships:

Probability Distribution Function

$$P(x \leq a) = \int_{-\infty}^a p(x) dx \quad (4A.16)$$

Probability Density Function

$$\begin{aligned} p(a) &= \lim_{\Delta a \rightarrow 0} \frac{P[x \leq a] - P[x \leq (a - \Delta a)]}{\Delta a} \\ &= \frac{d}{da} P(x \leq a) \end{aligned} \quad (4A.17)$$

The probability density function $p(x)$ can be interpreted as the probability that a random variable x has a value falling on the interval $[(a - \Delta a) < x \leq a]$. The probability distribution function relates the probability that the random variable will have a value on the interval $[-\infty < x \leq a]$. To conclude the discussion of statistical properties we now summarize the density and distribution functions of the noise distributions commonly encountered in communication systems.

The most important distribution, because it is so often encountered, is the Gaussian Distribution. This distribution adequately describes the distribution of the magnitudes of noise voltage and current for both thermal and shot noise sources. The Gaussian probability density function is given by

$$p(x) = \frac{1}{\sigma_x \sqrt{2\pi}} e^{-\frac{(x - x_0)^2}{2 \sigma_x^2}} \quad (4A.18)$$

and the distribution function as

$$P(x \leq a) = \frac{1}{2} \left[1 + \operatorname{erf} \left(\frac{a - x_0}{\sigma_x \sqrt{2}} \right) \right] \quad (4A.19)$$

where $x_0 = \langle x \rangle$, the mean or average value of x .

σ_x^2 = The variance of x .

$$\langle x^2 \rangle = \sigma_x^2 + x_0^2$$

and the well known error function is defined as:

$$\operatorname{erf}(y) = \frac{2}{\sqrt{\pi}} \int_0^y e^{-t^2} dt \quad (4A.20)$$

When using standard tables one must take care to determine the definition of the cumulative distribution function $F(y)$ actually tabulated.

For example, in the Standard Mathematical Tables published by the Chemical Rubber Co. (1971, p. 575), the error function must be computed in the following manner:

$$\operatorname{erf} \left(\frac{y}{\sqrt{2}} \right) = 2F(y) - 1 \quad (4A.21)$$

where

$$F(y) = \frac{1}{\sqrt{2\pi}} \int_{-\infty}^y e^{-\frac{1}{2}t^2} dt$$

and tables of $F(y)$ are provided. Figure 4A-1 is a plot of density and distribution functions for a Gaussian process.

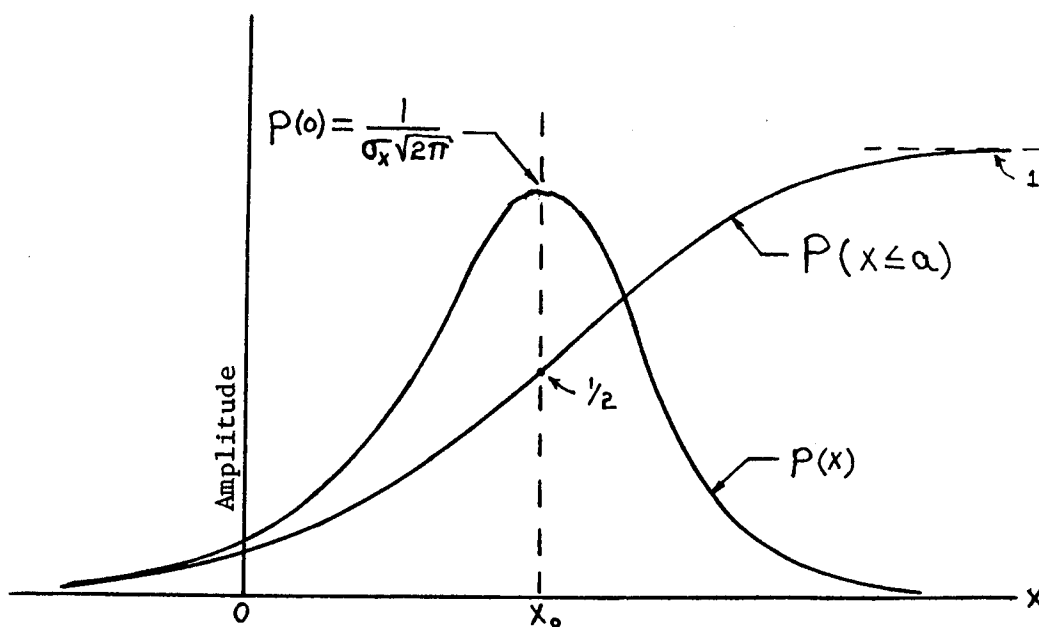


Figure 4A-1. Probability Density and Probability Distribution Functions for a Gaussian Random Process

The Rayleigh distribution characterizes the envelope of a band-limited Gaussian noise voltage. The probability density function for a Rayleigh distribution is

$$p(x) = \frac{x}{\sigma_x^2} e^{-\frac{x^2}{2\sigma_x^2}} \quad x > 0 \quad (4A.22)$$

and the distribution function is:

$$P(x \leq a) = 1 - e^{-\frac{x^2}{2\sigma_x^2}} \quad x > 0 \quad (4A.23)$$

It will be shown later that the noise voltage output of an ideal envelope detector is a random variable with a Rayleigh distribution. Curves for the density and distribution functions are shown in Figure 4A-2.

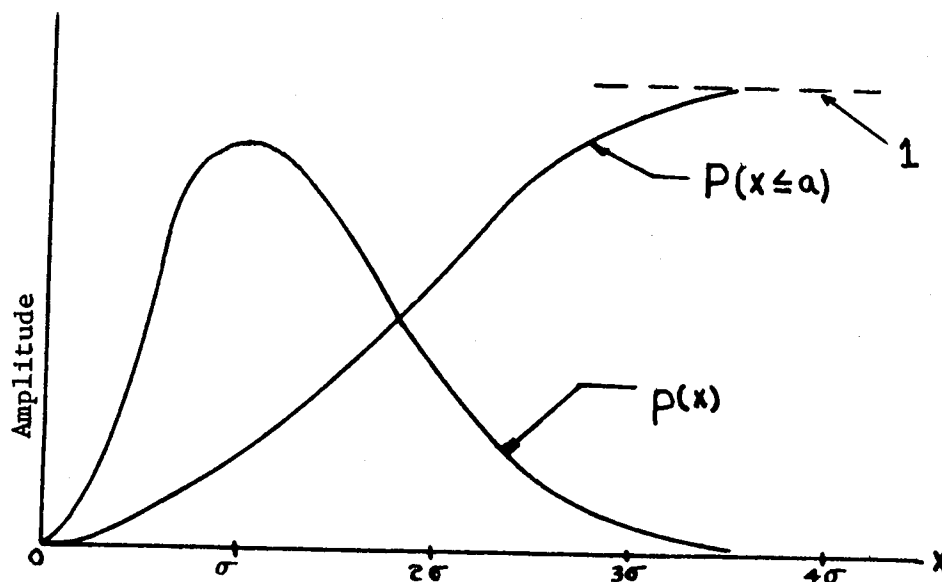


Figure 4A-2. Probability Density and Probability Distribution Functions for a Rayleigh Distribution

The average or mean value and mean-square values for a Rayleigh distribution are:

$$\langle X \rangle = \int_0^{\infty} x p(x) dx = \sqrt{\frac{\pi}{2}} \sigma_x \quad (4A.24)$$

and

$$\langle X^2 \rangle = \int_0^{\infty} x^2 p(x) dx = 2 \sigma_x^2 \quad (4A.25)$$

The variance of the Rayleigh distribution is:

$$\sigma_R^2 = \langle X^2 \rangle - \langle X \rangle^2 = \left(2 - \frac{\pi}{2}\right) \sigma_x^2 \quad (4A.26)$$

It is important to notice that the mean value, mean-square value, and variance for a Rayleigh distribution are all expressed in terms of the variance of the "parent" Gaussian process, σ_x^2 .

Another distribution that is important to receiver noise studies, because it characterizes the noise current distribution at the output of a square-law device, is the chi-squared distribution (International Telephone and Telegraph Corp., 1956, p. 992). The probability density function for this particular chi-squared distribution is ($n = 1$)

$$p(x) = \frac{1}{\sigma_x \sqrt{2\pi x}} e^{-\frac{x}{2\sigma_x^2}} \quad x \geq 0 \quad (4A.27)$$

where σ_x^2 is the variance of the "parent" Gaussian process.

To demonstrate that this is indeed a probability density function we show that

$$\int_0^{\infty} p(x) dx = \frac{1}{\sigma_x \sqrt{2\pi}} \int_0^{\infty} \frac{e^{-\frac{x}{2\sigma_x^2}}}{\sqrt{x}} dx = 1 \quad (4A.28)$$

and from integral 671. of Standard Mathematical Tables (Chemical Rubber Co., 1971, p. 449)

$$\int_0^{\infty} \frac{e^{-nx}}{\sqrt{x}} dx = \sqrt{\frac{\pi}{n}} \quad (4A.29)$$

so upon substitution into Equation 4A.28:

$$\int_0^{\infty} p(x) dx = \frac{1}{\sigma_x \sqrt{2\pi}} \sqrt{2\pi \sigma_x^2} = 1 \quad (4A.30)$$

The curve of the chi-squared density function is shown in Figure 4A-3.

The mean value and mean-square values for the chi-squared distribution are:

$$\langle x \rangle = \int_0^{\infty} x p(x) dx = \sigma_x^2 \quad (4A.31)$$

and (Davenport and Root, 1958, p. 254)

$$\langle x^2 \rangle = \int_0^{\infty} x^2 p(x) dx = 3 \sigma_x^4 \quad (4A.32)$$

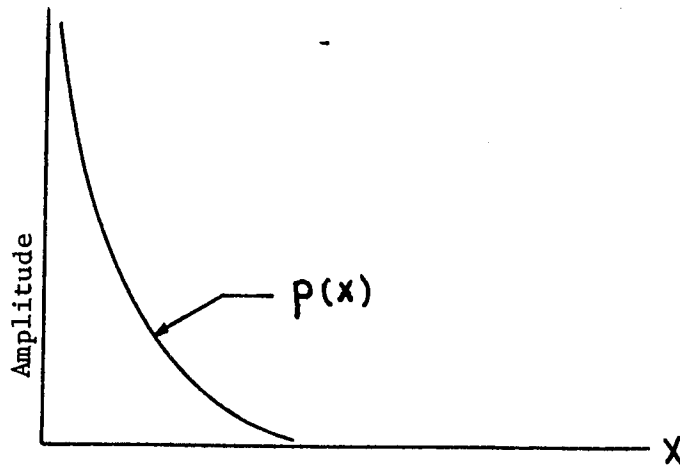


Figure 4A-3. Probability Density Function for a Chi-Squared Distribution

The variance of the chi-squared distribution is:

$$\sigma_c^2 = \langle x^2 \rangle - \langle x \rangle^2 = 2 \sigma_x^2 \quad (4A.33)$$

The exponential density function characterizes the noise output of a low-pass filter following a square-law device. It has the form

$$p(x) = \frac{1}{\sigma_x^2} e^{-\frac{x}{\sigma_x^2}} \quad (4A.34)$$

with mean value, mean-square value, and variance of:

$$\begin{aligned} \langle x \rangle &= \int_0^{\infty} x p(x) dx = \sigma_x^2 \\ \langle x^2 \rangle &= \int_0^{\infty} x^2 p(x) dx = 2 \sigma_x^4 \end{aligned} \quad (4A.35)$$

$$\sigma_c^2 = \langle x^2 \rangle - \langle x \rangle^2 = \sigma_x^4$$

The last distribution we will consider is the Poisson Distribution. This distribution is used for noise processes which are impulsive as for example ignition noise and many types of man-made noise. The Poisson distribution is

$$p(n) = \frac{(\bar{n} \tau)^n}{n!} e^{-\bar{n} \tau} \quad (4A.36)$$

where $p(n)$ is the probability that exactly n pulses will occur in a time interval of duration τ and \bar{n} is the average number of pulses

occurring in a unit of time. When \bar{n} is large, the Poisson distribution tends to a normal or Gaussian distribution (Papoulis, 1965, p. 570). As a matter of fact, shot noise is Poisson distributed but with the average number of electrons flowing usually greater than 6.28×10^9 , (one nanoampere) shot noise is very well represented by a Gaussian distribution.

4. Noise spectrums

Specifying a random variable such as a noise voltage or current by the appropriate probability density function is theoretically adequate but not very useful for receiver noise studies. Three other ways of specifying the character of a random variable are more useful. These are:

- a. The autocorrelation function (Appendix, Part A)

$$R_x(\tau) = \lim_{T \rightarrow \infty} \frac{1}{T} \int_{-T/2}^{T/2} x(t) x(t+\tau) dt \quad (4A.37)$$

- b. The power spectral density function

$$\phi_x(\omega) = \mathcal{F}[R_x(\tau)] = \int_{-\infty}^{\infty} R_x(\tau) e^{-j\omega\tau} d\tau \quad (4A.38)$$

- c. The mean-square value

$$\overline{x^2} = \frac{1}{2\pi} \int_{-\infty}^{\infty} \phi_x(\omega) d\omega \quad (4A.10)$$

$$= R_x(0) \quad (4A.9)$$

$$\text{or} \quad \overline{x^2} = \int_{-\infty}^{\infty} x^2 p(x) dx. \quad (4A.7)$$

Since all physical sources of noise are both band-limited and time limited, the integrations over all frequency and time are never really carried out. At most, in any real system, the functions specified above are only approximated.

We now will examine the spectral characteristics of the types of noise encountered in electronic circuits. In noise analysis it is often convenient to work with either the spectral density or the autocorrelation function. Thus, it is convenient to know that they form a Fourier transform pair i.e., they are reciprocal Fourier transforms (Beckmann, 1967, p. 214):

$$\phi(\omega) = \int_{-\infty}^{+\infty} R(\tau) e^{-j\omega\tau} d\tau \quad (4A.39)$$

$$R(\tau) = \frac{1}{2\pi} \int_{-\infty}^{+\infty} \phi(\omega) e^{j\omega\tau} d\omega \quad (4A.40)$$

If the random process characterized by $R(\tau)$ is real, then $R(\tau)$ is real and even. For this case $\phi(\omega)$ is also even (Papoulis, 1965, p. 338) and the reciprocal transforms become

$$\phi(\omega) = \int_{-\infty}^{+\infty} R(\tau) \cos \omega\tau d\tau \quad (4A.41a)$$

$$R(\tau) = \frac{1}{2\pi} \int_{-\infty}^{+\infty} \phi(\omega) \cos \omega \tau d\omega \quad (4A.41b)$$

where $\phi(\omega)$ is the two-sided or complex Fourier transform i.e., $\phi(\omega)$ is an even function so it has a magnitude in both the positive and negative frequency regions. Since for real physical systems only positive frequencies have meaning, the transforms of Equations 4A.41 can be modified by introducing the single-sided or one-sided power spectral density $S(\omega)$ defined as (Appendix, Part R):

$$S(\omega) = 2 \phi(\omega) \quad \text{for} \quad \omega \geq 0.$$

Now the real-frequency or single-sided transform pair becomes:

$$S(\omega) = 2 \int_0^{\infty} R(\tau) \cos \omega \tau d\tau \quad (4A.42a)$$

$$R(\tau) = \frac{1}{2\pi} \int_0^{\infty} S(\omega) \cos \omega \tau d\omega \quad (4A.42b)$$

Sometimes, however, it may be easier to integrate the complex form as given by (4A.39) and (4A.40).

If this is necessary, the "real world" spectrum represented by $S(\omega)$ must be changed by amplitude scaling and the even function transformation to give:

$$\phi(\omega) = \frac{1}{2} S(\omega) + \frac{1}{2} S(-\omega)$$

When any of the above transforms are carried out, the resulting function must be real. If the function obtained is complex, then the result is not correct. Some examples of how to obtain these transforms will be briefly illustrated in the derivations to follow. Table 4A-1, on page 66, will summarize the results of these examples and other commonly used transform pairs.

First consider band-limited white noise with a spectral intensity of N_0 watts/hz. The autocorrelation function is obtained from the integral (Equation 4A.42b):

$$\begin{aligned} R(\tau) &= \frac{1}{2\pi} \int_{\omega_0 - \frac{\Delta\omega}{2}}^{\omega_0 + \frac{\Delta\omega}{2}} N_0 \cos \omega \tau \, d\omega \\ &= \frac{N_0}{2\pi} \Delta\omega \cos \omega_0 \tau \left[\frac{\sin\left(\frac{\Delta\omega}{2} \tau\right)}{\frac{\Delta\omega}{2} \tau} \right] \end{aligned} \quad (4A.43)$$

Applying the complex transform and extending $\phi(\omega)$ to negative frequencies gives (Equation 4A.40)

$$R(\tau) = \frac{1}{2\pi} \int_{-\omega_0 - \frac{\Delta\omega}{2}}^{-\omega_0 + \frac{\Delta\omega}{2}} \frac{N_0}{2} e^{j\omega\tau} \, d\omega + \frac{1}{2\pi} \int_{\omega_0 - \frac{\Delta\omega}{2}}^{\omega_0 + \frac{\Delta\omega}{2}} \frac{N_0}{2} e^{j\omega\tau} \, d\omega$$

$$R(\tau) = \frac{N_0}{2\pi} \Delta\omega \cos \omega_0 \tau \left[\frac{\sin\left(\frac{\Delta\omega}{2} \tau\right)}{\frac{\Delta\omega}{2} \tau} \right] \quad (4A.44)$$

which is the same result as (4A.43) but requires much more computational effort. For the base-band spectrum, let $\omega_0 = \Delta\omega/2$ and the autocorrelation function becomes:

$$R(\tau) = \frac{2N_0}{2\pi\tau} \sin \frac{\Delta\omega}{2} \tau \cos \frac{\Delta\omega}{2} \tau = \frac{N_0}{2\pi} \Delta\omega \left[\frac{\sin(\Delta\omega \tau)}{\Delta\omega \tau} \right] \quad (4A.45)$$

Observing the limiting relationship

$$\lim_{x \rightarrow 0} \frac{\sin x}{x} = 1$$

leads to the mean-square value

$$R(0) = \frac{N_0}{2\pi} \Delta\omega \quad (4A.46)$$

which shows that the mean-square value is dependant only upon the spectral intensity and the bandwidth. Next we look at the Gauss-Markoff process which characterizes the spectrum obtained from a random telegraph signal. Also, the same integration is valid for the RC low-pass filter if the constants are changed. The autocorrelation function is of the form:

$$R(\tau) = \sigma^2 e^{-b|\tau|} \quad (4A.47)$$

and the power spectral density is:

$$\begin{aligned}\Phi(\omega) &= \int_{-\infty}^{+\infty} \sigma^2 e^{-b|\tau|} e^{-j\omega\tau} d\tau \\ &= \sigma^2 \int_{-\infty}^{+\infty} e^{-b|\tau|} \cos \omega\tau d\tau - j\sigma^2 \int_{-\infty}^{+\infty} e^{-b|\tau|} \sin \omega\tau d\tau\end{aligned}$$

The second term is zero because it is the integral of an odd function so we are left with:

$$\Phi(\omega) = 2\sigma^2 \int_0^{\infty} e^{-b\tau} \cos \omega\tau d\tau = 2\sigma^2 \frac{b}{b^2 + \omega^2} \quad (4A.48)$$

The reciprocal transform of (4A.48) will give (4A.47) so these two equations form the transform pair for a Gauss-Markoff process.

The transform pair for the RC low-pass filter is obtained from those for the Gauss-Markoff process by making the following substitutions:

$$b = \frac{1}{RC} \quad \text{and} \quad \sigma^2 = \frac{1}{4RC}$$

Now let's look at the autocorrelation function for deterministic function such as a single frequency sinewave. For this simple example, the autocorrelation function can be found directly from Equation (4A.37). The sinewave function is:

$$X(t) = \sqrt{N_0} \cos \omega_0 t \quad (4A.49)$$

which gives the following autocorrelation function:

$$\begin{aligned} R_x(\tau) &= \lim_{T \rightarrow \infty} \frac{1}{T} \int_{-T/2}^{T/2} \sqrt{N_0} \cos \omega_0 t \sqrt{N_0} \cos (\omega_0 t - \omega_0 \tau) dt \\ &= \lim_{T \rightarrow \infty} \frac{1}{T} \int_{-T/2}^{T/2} N_0 \cos \omega_0 t [\cos \omega_0 \tau \cos \omega_0 t + \sin \omega_0 t \sin \omega_0 \tau] dt \end{aligned}$$

The integral of the odd part of the integrand over the period is zero so we are left with:

$$\begin{aligned} R_x(\tau) &= \lim_{T \rightarrow \infty} \frac{1}{T} \int_{-T/2}^{T/2} N_0 \cos \omega_0 \tau \cos^2 \omega_0 t dt \\ &= \frac{N_0}{2} \cos \omega_0 \tau \end{aligned} \quad (4A.50)$$

The two-sided power spectral density function for a single frequency sinewave can be shown to be

$$\Phi_x(\omega) = \pi \left(\frac{N_0}{2} \right) [\delta(\omega - \omega_0) + \delta(\omega + \omega_0)] \quad (4A.51)$$

where $\delta(\omega - \omega_0)$ is called the Dirac delta function (also called the unit-impulse function) and is characterized by its sifting (or sampling) property as

$$\int_{\text{all } x} f(x) \delta(x-\tau) dx = f(\tau) \quad (4A.52a)$$

or from the Fourier inversion integral (Davenport and Root, 1958, p. 368) as:

$$\delta(\omega - \omega_0) = \frac{1}{2\pi} \int_{-\infty}^{+\infty} e^{j(\omega - \omega_0)t} dt \quad (4A.52b)$$

The unit impulse function is also an even function.

Taking the complex transform of $\Phi(\omega)$ we get $R(\tau)$ as given by Equation 4A.40

$$\begin{aligned} R(\tau) &= \frac{1}{2\pi} \int_{-\infty}^{+\infty} \frac{\pi N_0}{2} [\delta(\omega - \omega_0) + \delta(\omega + \omega_0)] e^{j\omega \tau} d\omega \\ &= \frac{N_0}{4} [e^{j\omega_0 \tau} + e^{-j\omega_0 \tau}] = \frac{N_0}{2} \cos \omega_0 \tau \end{aligned} \quad (4A.53)$$

which is the same result as (4A.50). Now we consider the important example of working with the single-sided transform pair for a single-frequency sinewave. The power spectral density amplitude must be doubled to keep the mean-square value constant so:

$$S_x(\omega) = \pi N_0 \delta(\omega - \omega_0) \quad (4A.54)$$

The autocorrelation function becomes:

$$R_x(\tau) = \frac{1}{2\pi} \int_0^{\infty} S(\omega) \cos \omega \tau d\omega \quad (4A.55a)$$

$$R_x(\tau) = \frac{N_o}{2} \cos \omega_o \tau \quad (4A.55b)$$

where the integral is for positive frequencies only and the complex part has been dropped (see Equation 4A.42b).

The common requirement for all the results is that the mean-square value remain the same for both the single-sided and double-sided transforms. The following mean square values are computed:

a) From (4A.49)

$$\overline{x^2(t)} = \left(\frac{\text{peak value}}{\sqrt{2}} \right)^2 = \frac{N_o}{2}$$

b) From (4A.50), (4A.53) and (4A.55b)

$$R_x(0) = \frac{N_o}{2} \cos(\omega_o 0) = \frac{N_o}{2}$$

c) From (4A.51)

$$\frac{1}{2\pi} \int_{-\infty}^{\infty} \frac{\pi N_o}{2} [\delta(\omega - \omega_o) + \delta(\omega + \omega_o)] d\omega = \frac{N_o}{2}$$

d) From (4A.54)

$$\frac{1}{2\pi} \int_0^{\infty} \pi N_o \delta(\omega - \omega_o) d\omega = \frac{N_o}{2}$$

These values all check and are a good indication that the transforms used were correct.

Table 4A-1. Fourier transform pairs which have special application to communication noise studies

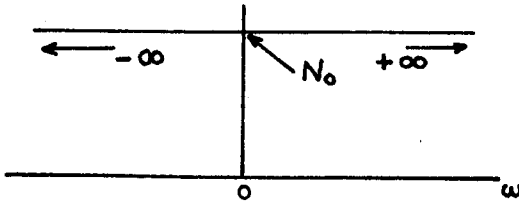
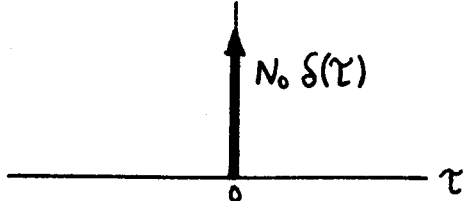
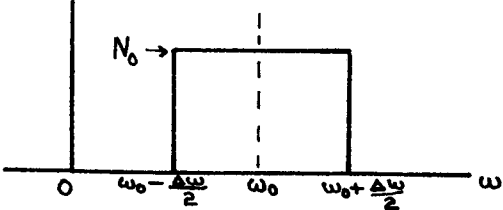
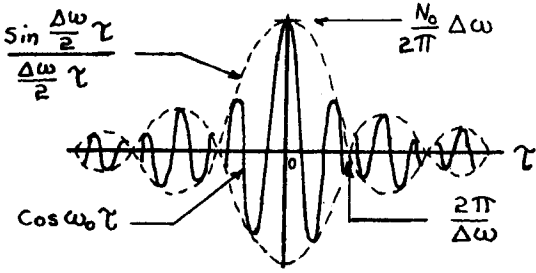
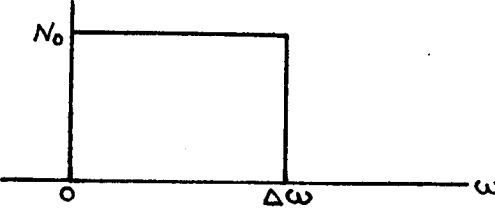
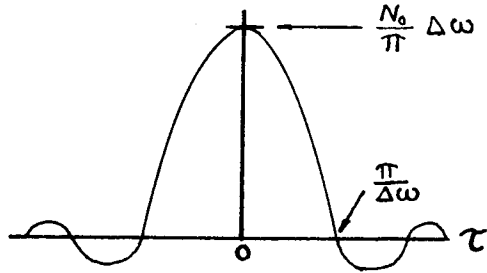
$\Phi(\omega)$ or $S(\omega)$	$R(\tau)$
(a) Pure white noise	
 $= N_0$	 $= N_0 \delta(\tau)$ $R(0) = \infty$
(b) Band-limited white noise	
 $= \begin{cases} N_0 & \text{for } \omega - \omega_0 \leq \frac{\Delta\omega}{2} \\ 0 & \text{otherwise} \end{cases}$	 $= \frac{N_0}{2\pi} \Delta\omega \cos \omega_0 \tau \left[\frac{\sin\left(\frac{\Delta\omega}{2} \tau\right)}{\frac{\Delta\omega}{2} \tau} \right]$ $R(0) = \frac{N_0}{2\pi} \Delta\omega$
(c) Base-band white noise	
 $= \begin{cases} N_0 & \text{for } 0 \leq \omega \leq \Delta\omega \\ 0 & \text{otherwise} \end{cases}$	 $= \frac{N_0}{2\pi} \Delta\omega \left[\frac{\sin(\Delta\omega \tau)}{\Delta\omega \tau} \right]^2$ $R(0) = \frac{N_0}{2\pi} \Delta\omega$

Table 4A-1. (Continued)

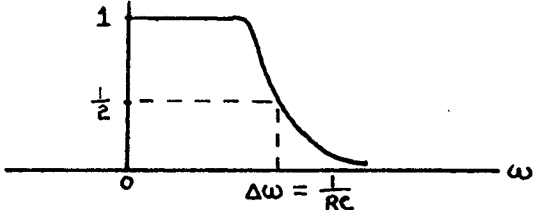
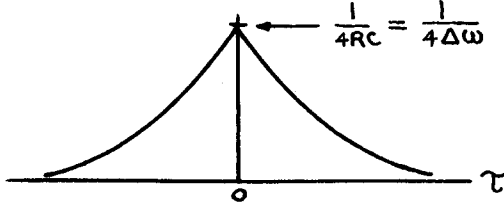
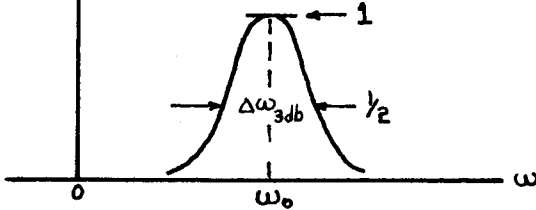
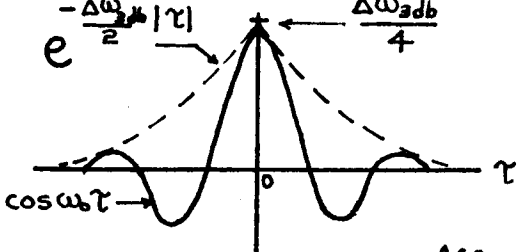
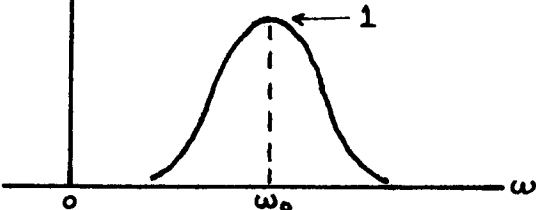
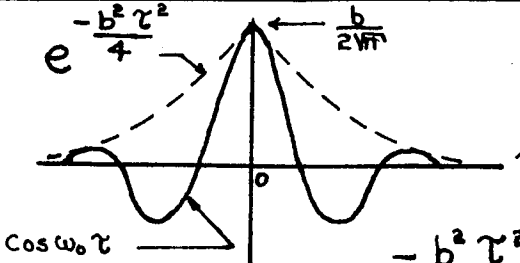
$\Phi(\omega)$ or $S(\omega)$	$R(\tau)$
<p>(d) RC low-pass filter</p>  $= \frac{1}{1 + \omega^2 (RC)^2}$	 $= \frac{1}{4RC} e^{-\frac{ \tau }{RC}}$ $R(0) = \frac{1}{4RC} = \frac{1}{4\Delta\omega}$
<p>(e) High-Q tuned circuit</p>  $= \frac{1}{1 + 4 \left(\frac{\omega - \omega_0}{\Delta\omega_{3db}} \right)^2}$	 $= \frac{\Delta\omega_{3db}}{4} \cos \omega_0 \tau e^{-\frac{\Delta\omega_{3db}}{2} \tau }$ $R(0) = \frac{\Delta\omega_{3db}}{4}$
<p>(f) Gaussian filter</p>  $= e^{-\frac{(\omega - \omega_0)^2}{2b^2}}$ <p style="text-align: right;">$\omega_0 \gg b$</p>	 $= \frac{b}{2\sqrt{2\pi}} \cos \omega_0 \tau e^{-\frac{b^2 \tau^2}{4}}$ $R(0) = \frac{b}{2\sqrt{2\pi}} \quad b = \frac{\Delta\omega_{3db}}{\sqrt{2 \ln 2}}$

Table 4A-1. (Continued)

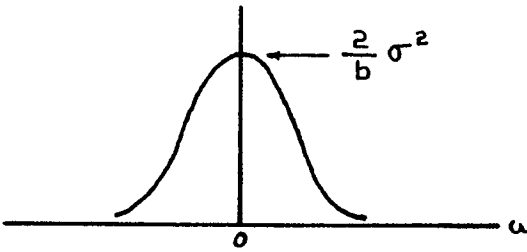
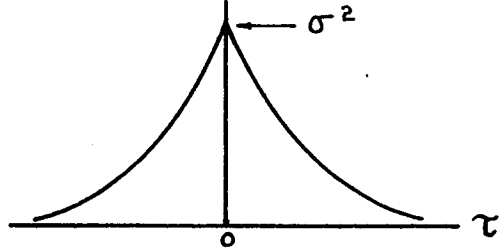
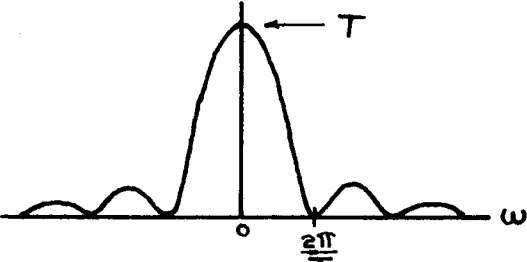
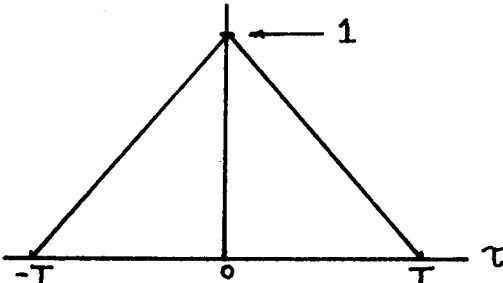
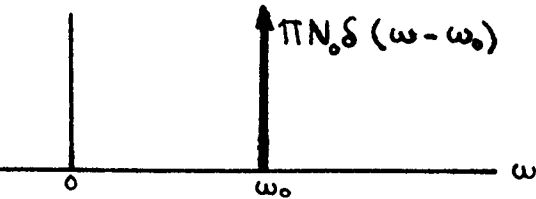
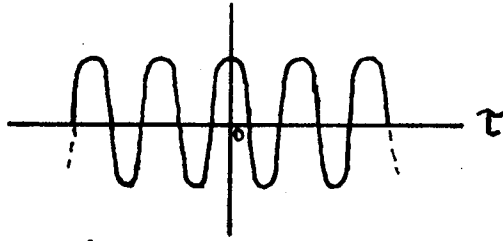
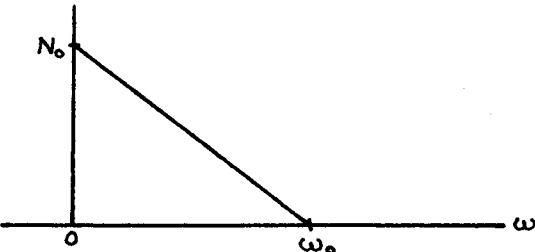
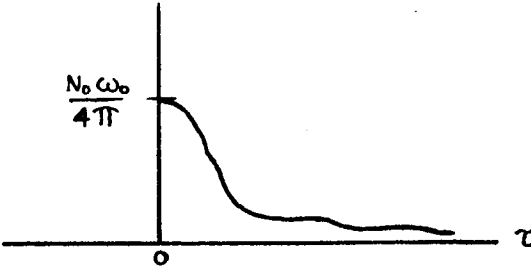
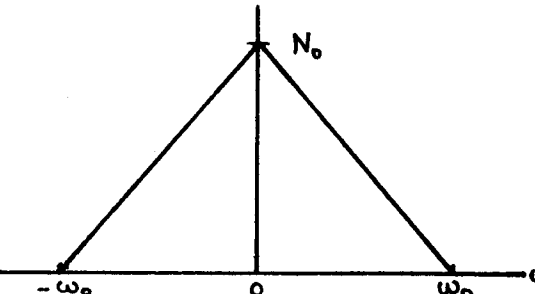
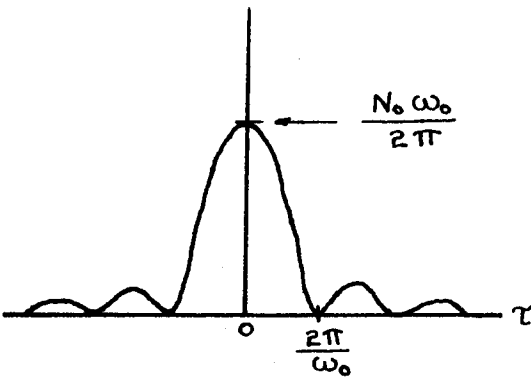
$\Phi(\omega)$ or $S(\omega)$	$R(\tau)$
(g) Gauss-Markoff process	
 $= \frac{2\sigma^2 b}{b^2 + \omega^2}$	 $= \sigma^2 e^{-b \tau }$ $R(0) = \sigma^2$
(h) Binary transmission	
 $= T \left[\frac{\sin(\frac{T}{2}\omega)}{\frac{T}{2}\omega} \right]^2$	 $= \begin{cases} 1 - \frac{ \tau }{T} & \tau < T \\ 0 & \tau > T \end{cases}$ $R(0) = 1$
(i) Single-frequency sinewave	
 $= \pi N_0 \delta(\omega - \omega_0)$	 $= \frac{N_0}{2} \cos \omega_0 \tau$ $R(0) = \frac{N_0}{2}$

Table 4A-1. (Continued)

$\Phi(\omega)$ or $S(\omega)$	$R(\tau)$
(j) Sawtooth spectrum	
 $= \begin{cases} N_0 \left(1 - \frac{\omega}{\omega_0}\right) & 0 \leq \omega \leq \omega_0 \\ 0 & \text{otherwise} \end{cases}$	 $= \frac{N_0}{(2\pi)^2} \frac{j}{\tau} \left[\frac{\sin \pi \omega_0 \tau}{\pi \omega_0 \tau} e^{-j\pi \omega_0 \tau} - 1 \right]$ $R(0) = \frac{N_0}{4\pi} \omega_0$
(k) Triangular spectrum	
 $= \begin{cases} N_0 \left(1 - \frac{ \omega }{\omega_0}\right) & \omega < \omega_0 \\ 0 & \omega > \omega_0 \end{cases}$	 $= \frac{N_0 \omega_0}{2\pi} \left[\frac{\sin\left(\frac{N_0}{2} \tau\right)}{\frac{N_0}{2} \tau} \right]^2$ $R(0) = \frac{N_0 \omega_0}{2\pi}$

The user is not limited to using those transforms given in the table as there are many more transforms that can be applied to electronic systems. Not only can the transforms be used for filters and noise analysis but also for such things as determining the far field pattern of an antenna from its aperture distribution (Kraus, 1966, p. 168). Tables of Fourier transforms are available as well as several examples in Kraus (1966, Sec. 6-8), Beckmann (1967, Ch. 7), Papoulis (1965, Ch. 10), International Telephone and Telegraph Corp. (1956, Ch. 35) and Bracewell (1965).

As a last word on the spectral density of a noise voltage we will discuss the term "white noise". Any noise source which produces a flat noise power spectrum over the bandwidth of concern is termed a white noise source. For practical reasons, many sources are considered white even though they are not perfectly flat. The concept of a pure white noise is abstract because such a random process cannot exist. This can be explained by seeing that such a power spectrum would require infinite power. Still, it is convenient to define pure white noise as a mathematical process so that it can form a basis for looking at other noise spectra. White noise and flat spectrum are synonymous terms.

The majority of noise sources encountered in electronic circuits are both Gaussian and white. Sometimes this leads to a confusion whereby the terms white noise and Gaussian noise are thought to be synonymous. Especially when just beginning to study in this field, it is sometimes difficult to keep the two straight. The differences are now explained. The property of being white characterizes the spectrum of the noise while the property of being Gaussian characterizes the

probability density of the noise voltage amplitudes. For example, the thermal noise from an ideal resistor is both Gaussian and white but after the noise is passed through a tuned circuit it is no longer white although it is still Gaussian. Most of the shot and thermal noise sources used in this report will be considered to be both white and Gaussian.

B. Physical Sources of Noise

1. Thermal or Johnson noise

The experimental and theoretical basis for the theory of thermal noise currents in a resistive conductor was presented in 1928 by J. B. Johnson of Bell Labs* and H. Nyquist of American Telephone and Telegraph. Johnson concluded that the statistical fluctuation of electrical charge in a resistive conductor produced a random voltage between the ends of that conductor. This noise voltage, which appeared to depend upon the resistance as well as the absolute temperature of the resistance, did not depend on the resistive properties of the material from which the resistor was made. To verify this, Johnson measured the apparent noise voltage of resistors made of many different materials such as; platinum and copper wire, India ink, carbon filament, salt (NaCl), copper sulphate, and sulphuric acid in alcohol. The agreement in measured and predicted values of thermal noise voltages for the variety of resistances led to the conclusion that the generation of thermal noise currents in a resistor was independent of the material type, physical shape, and conduction mechanism. Johnson noted, however, that these conclusions

*Bell Telephone Laboratories

may not apply to electronic resistances, that is, resistances which do not obey Ohm's law.

The noise produced by thermal agitation (Brownian motion of electrons) in a conductor is called thermal noise or Johnson noise in honor of Johnson. Nyquist used Johnson's experimental evidence as proof for the validity of his theory of noise generation. He used principles of thermodynamics and statistical mechanics to arrive at an equation for the thermal noise power in a resistor (Nyquist, 1928; Sears, 1953). Statistically, thermal noise is a random process which is Gaussian and, for all practical frequencies, is also white. The average value of the noise voltage produced by a noisy resistor is zero but the mean square value is non-zero i.e.,

$$\overline{V_R(t)} = 0 \qquad \overline{V_R^2(t)} \neq 0 \qquad (4B.1)$$

Nyquist's derivation of the mean-square noise voltage for a noisy resistor produced two equations. The first was based on classical equipartition (Sears, 1953) while the second was based on the quantum view of radiation. It is the first equation, which we now realize is a low-frequency approximation (Appendix, Part A) that is widely used for radio circuits. The second equation although seldom used is thought to be the correct one although there may be some doubt (Lawson and Uhlenbeck, 1950, p. 77).

An important concept that was used by Nyquist in his derivation was that of thermodynamic equilibrium. Without this postulation, which means that the electrons are in a field-free region, derivation of the Nyquist equation is not possible.

The power spectral density function for an ideal physical resistance (ideal meaning no stray reactance and constant resistance over all frequencies) was first published by Nyquist (1928). The power spectral density is given by Planck's factor (Nyquist, 1928; van der Ziel, 1954, p. 9):

$$S_R(\omega) = \frac{hf}{e^{\frac{hf}{kT}} - 1} \quad (4B.2)$$

The available noise power (Appendix, Part C) for a resistor, R_s , is the integral of the power spectral density function over the noise bandwidth, Δf :

$$\frac{\overline{V_n^2}}{4R_s} = \int_{f_0 - \frac{\Delta f}{2}}^{f_0 + \frac{\Delta f}{2}} S_R(\omega) df \quad \text{watts.} \quad (4B.3)$$

The integration over the finite bandwidth, Δf can be carried out after making some approximations for the Planck factor.

At radio frequencies the Rayleigh-Jeans approximation for small frequency-to-temperature ratios is valid. The Planck factor is expanded using a Laurent power series of the following form

$$\frac{1}{e^x - 1} = \frac{1}{x} - \frac{1}{2} + \frac{1}{12}x - \frac{1}{720}x^3 + \dots \quad |x| > 0 \quad (4B.4)$$

which gives for Equation 4B.2 the series

$$\frac{hf}{e^{\frac{hf}{kT}} - 1} = hf \left[\frac{kT}{hf} - \frac{1}{2} + \frac{1}{12} \frac{hf}{kT} \dots \right] \quad (4B.5)$$

where if $\frac{hf}{kT} \ll 1$ we get:

$$\frac{hf}{e^{\frac{hf}{kT}} - 1} \cong kT \left(1 - \frac{1}{2} \frac{hf}{kT} \right) \quad \frac{\text{watts}}{\text{hz}} \quad (4B.6)$$

When $f/T < 400 \text{ MHz}/^\circ\text{K}$, the Rayleigh-Jeans approximation gives less than a one-percent error and we obtain the radio-frequency power spectral density function as:

$$S_R(\omega) = kT \quad \frac{\text{watts}}{\text{hz}} \quad (\text{Rayleigh-Jeans Approximation}) \quad (4B.7)$$

Integrating Equation 4B.3 and solving for the mean-square noise voltage

$$\overline{V_n^2} = 4R_s \int_0^{\Delta f} kT_s df = 4kT_s R_s \Delta f \quad \text{volts.} \quad (4B.8)$$

gives the mean-square noise voltage for a noisy resistor of value R_s at temperature T_s and over a bandwidth Δf . We now summarize with the important conclusion:

The mean-square value of noise voltage produced by the thermal agitation of electrons in a resistor at radio frequencies is given by the famous Nyquist formula,

$$\overline{V_n^2} = 4kT_s R_s \Delta f \quad \text{volts}^2 \quad (4B.9)$$

where k = Boltzmann's constant, 1.38×10^{-23} joules/ $^{\circ}\text{K}$
 T_s = Physical temperature of the resistance, $^{\circ}\text{K}$
 R_s = Ohm's law or dc value of resistance, ohms
 Δf = Effective noise bandwidth, hertz.

It must be remembered that the Nyquist formula is restricted to band-limited white noise at frequencies and temperatures where the Rayleigh-Jeans approximation to Planck's Radiation Law is valid. These criteria are almost always met for practical electronic circuits.

Representation of the mean-square noise voltage by the Nyquist formula (4B.9) can present some mathematical and conceptual difficulties when it is applied to practical circuits. First of all the power available from a noisy resistor is finite (Appendix, Part A) so we must realize that Equation 4B.9 is valid only over bandwidths where the Rayleigh-Jeans approximation is valid. This presents no practical difficulties as all circuits have enough stray reactance to limit the bandwidth. The second difficulty comes about in trying to represent the bandwidth by a single quantity, Δf . Actually, for every circuit we must apply the relationship (Appendix, Part B, Equation B.1) between input and output spectral densities

$$S_o(\omega) = |g(\omega)|^2 S_i(\omega)$$

which is now done for the cascade combination of a noisy resistor and an ideal bandpass filter as shown in Figure 4B-1.

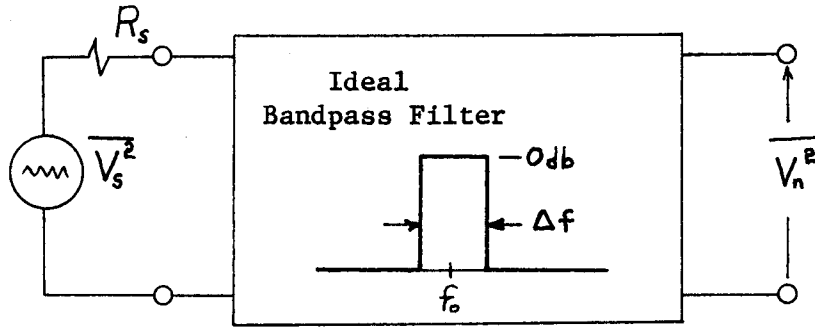


Figure 4B-1. Circuit for Defining the Nyquist Equation

The ideal bandpass filter has no losses and a perfectly rectangular passband of bandwidth Δf . When (B.1) is integrated as done in Part B of the Appendix and the mean-square output voltage $\overline{V_n^2}$ is computed we get

$$\overline{V_n^2} = 4 R_s \int_{\omega_o - \frac{\Delta\omega}{2}}^{\omega_o + \frac{\Delta\omega}{2}} S_s(\omega) |g(\omega)|^2 df = 4 R_s k T_s g_o^2 \Delta f \quad (4B.10)$$

where if the net gain of the filter is unity (lossless) then we get the mean-square output voltage as before (4B.9):

$$\overline{V_n^2} = 4 k T_s R_s \Delta f$$

For ease of representation, the equations used in many papers on noise are written in the Nyquist form of (4B.11) but it must be remembered

that it is only shorthand notation for the process expressed in Equations 4B.10 and B.4 of Part B of the Appendix. When the input is white noise, the simple representation of Equation 4B.8 accounts for the situation of Figure 4B-1.

It has become common practice to represent any noise source which can be represented by Figures 4B-1 or B-1 (Appendix, Part B) by its Nyquist equivalent circuit. Figure 4B-2 illustrates the Thevenin noise generator which is used for this representation.

For notational convenience the bandpass filter is not shown although it is always implied through use of the bandwidth Δf .

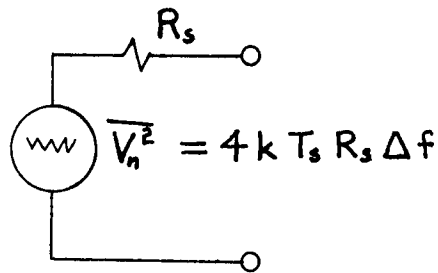


Figure 4B-2. Nyquist Equivalent Noise Source

We see from the figure that any noise source can thus be represented by specifying the three parameters; source resistance R_s , source temperature T_s and effective noise bandwidth Δf . In certain applications, such as noise factor computations, where the bandwidth is a common factor in all expressions it is possible to represent the noise source simply by an equivalent resistance, R_{eq} or by an effective noise temperature T_{eff} . The most common representation is the use of equivalent noise resistance which has nothing to do with the physical source resistance

but merely expresses the noise power available. For this representation, the mean-square noise voltage is written

$$\overline{V_n^2} = 4kT_o R_{eq} \Delta f \quad (4B.11)$$

where

$$T_o R_{eq} \equiv T_s R_s \text{ (see Figure 4B-2)}$$

T_o = Standard temperature, 290 °K

R_{eq} = Nyquist equivalent noise temperature, °K

Δf = Circuit effective noise bandwidth, hz.

This representation is most often used for device noise studies where the noise sources are current generators caused by shot noise and there is no physical resistance R_s , to use for a reference. This concept will be used in the study of two-port noise theory.

The second representation is the use of an equivalent (effective) noise temperature. Effective noise temperature is used in specifying antenna noise and in reflecting all the receiver noise back to the source. The concept of effective noise temperature is also handy for specifying noise sources and excess noise as is done for a source resistance whose noise power has been increased by addition of a shot noise source. In any given application and for a specified bandwidth, the reader may expect to see a noise voltage generator represented by the Nyquist equivalent circuit in one of three ways:

a. Mean-square value, $\overline{V_n^2}$

b. Equivalent noise resistance, $R_{eq} = \frac{\overline{V_n^2}}{4kT_o \Delta f}$

$$c. \text{ Equivalent noise temperature, } T_{eq} = \frac{\overline{V_n^2}}{4kR_s \Delta f}$$

A better idea of the concepts of equivalent noise resistance and noise temperature is obtained by application as will be done in later sections.

2. Shot noise

The noise produced by the flow of electrons under the influence of a net electric field is called shot noise (Papoulis, 1965, Ch. 16). The term "shot noise" is very descriptive because the electron stream is analogous to a stream of small shot. Whereas thermal noise was characterized by thermodynamic equilibrium; shot noise is not. For this reason the statistical nature of shot noise is different because it is Poisson distributed though, practically speaking, the electron current is large enough that shot noise can be very well approximated by a Gaussian distribution. The spectrum of high-density shot noise is white just as is a thermal noise source. For most applications, a narrowband shot noise process is indistinguishable from a narrowband thermal noise process.

Shot noise is present in vacuum tubes, transistors, diodes, and to a lesser and more unpredictable extent in all electrical conductors. It is both the discreteness and randomness of the electrons in an electrical current that determines the characteristics of shot noise.

As an example, Bennett (1960, p. 55) demonstrated that an electron current (discrete changes) which is perfectly uniform would produce a spectrum which consisted of a signal at the pulse rate frequency and its harmonics but nowhere else. If, however, the flow is not uniform

then this randomness of flow will give rise to a uniform noise spectrum and hence, shot noise. The shot noise in electronic devices very often contributes to a degradation in receiving system sensitivity and we tend to think it is totally undesirable when, actually, the shot noise generated in a temperature-limited vacuum diode is very useful as a noise source for measuring sensitivity.

The power spectral density function for a temperature-limited vacuum tube diode is given by (Smullin and Haus, 1959, p. 14) (Lawson and Uhlenbeck, 1950, p. 79) (Bennett, 1960, p. 59)

$$S_s(\omega) = 2qI_o \quad (4B.12)$$

where q = Electronic charge, 1.60×10^{-19} coul

$I_o = \sqrt{\overline{i(t)^2}}$ = average or DC current, Amperes.

Since the noise diode is always used in conjunction with a specified source resistor it is more meaningful to examine the noise power produced by a diode (shot noise) and a resistor (thermal noise) in parallel.

Figure 4B-3 illustrates how a noise diode producing shot noise can be represented by equivalent noise voltage or noise current sources.

The mean square noise current produced by the diode is

$$\overline{I_{ni}^2} = \int_0^{\Delta f} 2qI_o df = 2qI_o \Delta f \quad (4B.13)$$

and that of the noisy resistor is:

$$I_{nr}^2 = 4G_s \int_0^{\Delta f} kT df = 4kTG_s \Delta f \quad (4B.14)$$

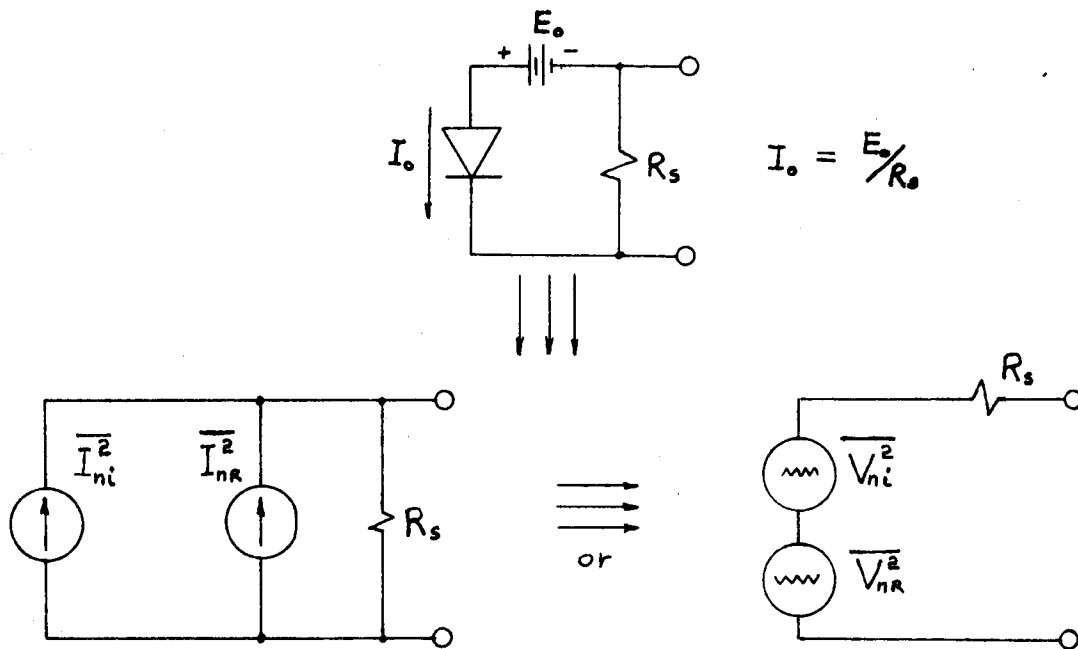


Figure 4B-3. Noise Diode Producing Shot Noise

Likewise, the mean-square voltages of the equivalent noise voltage generators are:

$$\overline{V_{ni}^2} = R_s^2 \int_0^{\Delta f} 2q I_o df = 2q I_o R_s^2 \Delta f \quad (4B.15)$$

$$\overline{V_{nr}^2} = 4R_s \int_0^{\Delta f} k T_s df = 4k T_s R_s \Delta f \quad (4B.16)$$

The available power per-unit-bandwidth from the combination of resistor noise and diode noise can be computed by adding the power contributions from each:

$$\left(\frac{\overline{V_{ni}^2}}{4R_s} + \frac{\overline{V_{nR}^2}}{4R_s} \right) \frac{1}{\Delta f} = \frac{1}{2} q I_0 R_s + k T_s \quad \text{watts/hz} \quad (4B.17)$$

which is also the power spectral density for the diode-resistor combination. This spectral density is important for the calculation of noise measurement equations and will be used later. Rewriting, we express (4B.17) as a power spectral density:

$$S_s(\omega) = \frac{1}{2} q I_0 R_s + k T_s \quad \text{watts/hz} \quad (4B.18)$$

3. Blackbody radiation

Blackbody radiation is important in receiver noise studies because it is this radiation which accounts for most of the antenna noise. All materials at temperatures above absolute zero contain energy in the form of thermal motion (Brownian motion) of elementary particles. This thermal energy causes the material to radiate electromagnetic energy and, by reciprocity, to also absorb it. A material which is a perfect emitter or absorber is referred to as a blackbody radiator and will emit and absorb radiation at all frequencies.

The radiation emitted from a perfect emitter, or blackbody, is characterized by Planck's radiation law which actually formulates the

source brightness, B, as a function of temperature and frequency (Kraus, 1966, Sec. 3-6)

$$B = 2 \left(\frac{f}{c} \right)^2 \left[\frac{hf}{e^{\frac{hf}{kT}} - 1} \right] \frac{\text{watts}}{\text{m}^2 - \text{hz} - \text{rad}^2} \quad (4B.19)$$

where f = Frequency of observation, hz
 c = Velocity of light, 3×10^8 m/sec
 h = Planck's constant, 6.63×10^{-34} j/sec
 T = Source temperature, $^{\circ}\text{K}$
 rad = Solid angle, steradians.

The expression inside the brackets is known as Planck's factor which replaces the kT factor in classical laws and accounts for the quantum aspects of thermal radiation.

There are two special cases of Planck's radiation law which are applicable at high and low frequencies and are used in many practical applications. At high frequencies where $hf \gg kT$, the Planck factor becomes

$$\frac{hf}{e^{\frac{hf}{kT}} - 1} \cong hf e^{-\frac{hf}{kT}} \frac{\text{watts}}{\text{hz}} \quad (4B.20)$$

which upon substitution into Planck's law gives the high frequency approximation known as the Wein Radiation Law:

$$B \cong 2 \left(\frac{f}{c} \right)^2 \left[hf e^{-\frac{hf}{kT}} \right] \frac{\text{watts}}{\text{m}^2 - \text{hz} - \text{rad}^2} \quad (4B.21)$$

which actually is valid for $f/T > 10^5 \text{ Mhz}/^\circ\text{K}$.

At radio frequencies, where $hf \ll kT$, the Planck factor becomes:

$$\frac{hf}{e^{\frac{hf}{kT}} - 1} \cong kT \quad \frac{\text{watts}}{\text{hz}} \quad (4B.22)$$

which upon substitution into Planck's law gives the Rayleigh-Jeans approximation:

$$B = 2 \left(\frac{f}{c} \right)^2 kT \quad \frac{\text{watts}}{\text{m}^2 - \text{hz} - \text{rad}^2} \quad (4B.23)$$

which is valid for $f/T < 400 \text{ mhz}/^\circ\text{K}$.

When the frequency-to-temperature ratio is in the range:

$$400 \text{ Mhz}/^\circ\text{K} < f/T < 10^5 \text{ mhz}/^\circ\text{K}$$

the Wein and Rayleigh-Jeans approximations are no longer valid and Plank's radiation law in the form of Equation 4B.19 must be used.

4. Atmospheric noise

The noise that is produced in the earth's atmosphere is often strong enough to cause interference in a radio receiver. The receiving antenna picks up these atmospheric noise signals which increases the effective noise temperature of the antenna and results in a reduction in the receiving system sensitivity. At high radio frequencies ($> 1 \text{ Ghz}$) the atmospheric noise is caused by atmospheric absorption in water and oxygen molecules. At frequencies below 20 Mhz , noise known as "atmospherics" results in very high noise temperatures. This noise

is the result of atmospheric lightning and ionospheric ionization.

It is estimated that the earth experiences about 200 lightning strokes each second. Ionospheric noise is caused by the solar wind and changes in solar activity affect the amount of noise. Atmospheric noise must be considered in a low-noise receiving system design. For further information consult Kraus (1966, p. 237), Grimm (1959), Jolly (1967, p. 137), Skolnik (1970, p. 39-5) and International Telephone and Telegraph Corp. (1956, p. 763). Quantitative data on antenna noise will be given in Chapter IV-C.

5. Extraterrestrial noise

Noise sources outside the earth^{*} also cause interference to low-noise antenna systems and in the frequency range of 20 to 1000 Mhz are usually dominant factors. The earth receives radio noise energy from the sun, Jupiter, the milky way galaxy and from other galaxies. The characteristics of this noise, its origin and cause are the object of study by radio astronomers. There are thousands of known radio sources in the sky but only a few are strong enough to cause interference in a low noise system.

The radio noise from extraterrestrial sources is caused by two primary mechanisms; thermal emission from hot ionized gasses and synchrotron radiation. Synchrotron radiation is caused by the radial acceleration of charged particles in a magnetic field. The strongest extraterrestrial noise sources are the sun, Jupiter, supernovae remnants, the Cygnus galaxy and hydrogen clouds. All of these sources vary in their temporal and spectral characteristics so that the problems associated with each must be studied as separate phenomenon. The sources

^{*}Discovered by Kark Jansky, 1933

which emit continuously have spectra which may be considered flat over the bandwidth of most practical receivers.

The sun is a strong radiator of energy in the form of thermal noise and solar flares. At radio frequencies the noise emission is higher than that predicted by a blackbody temperature of 6000°K (measured optically) and the excess noise is thought to be due to sunspot activity. For example, at a frequency of 100 Mhz the equivalent blackbody temperature can vary from 5×10^5 to 10^9°K which is calculated on the basis that the sun's angular extent is 0.224 deg^2 . This temperature is not constant with frequency and varies with sunspot activity. Very large solar flares can release large bursts of energy throughout the radio spectrum (Kraus, 1966, Sec. 8-7). These violent bursts can severely disrupt radio communication by causing radio static and also by disturbing the reflective ionospheric layers.

Jupiter bursts, which occur in the frequency spectrum around ten meters, are not very frequent and are usually predictable. The bursts are strong enough to cause interference but, because they are infrequent, are not a serious consideration in designing a communication system. The radio emission from the other planets is too weak to be a factor.

Extraterrestrial noise sources as a whole are generally weak and only a few sources account for most of the potential interference. The strongest sources of emission are due to clouds of ionized hydrogen and supernova remnants which emit by the synchrotron process. The strongest of these sources are Cassiopeia A (3C 461), Cygnus A (3C 405) and the Crab nebula (Taurus A, 3C 144). The ionized clouds of hydrogen

in our own Milky Way galaxy (Cass. A) are the strongest source. It was this noise that was first received by Karl G. Jansky in 1932 at a frequency of 20.5 Mhz to thus begin the science of radio astronomy (Kraus, 1966, p. 6).

6. Man-made noise

Because of increased industrialization and mechanization and the rapid population growth, man-made noise has an ever increasing effect on the sensitivity limit of a communication link. In urban areas, the contribution of man-made noise is such a large part of the total system noise that it very often determines the sensitivity limit. One example of this is the noise created by an automobile in a mobile communication system. A large factor in the success of any mobile system is how effectively automobile noise can be suppressed.

Frequently, the maximum usable sensitivity is governed by man-made noise sources is difficult to determine without field measurements under operating conditions. The usefulness of field measurements can be illustrated by the example of an aircraft flying around the world. When the aircraft is over water or sparsely populated land the noise level external to the aircraft is due mainly to thermal, solar and galactic sources. As the aircraft approaches an urban area, there is a significant increase in the noise level--sometimes several db. With a field intensity measuring system it is possible to plot the noise level as a function of geographic location and frequency. This information is useful in designing reliable communication systems for aircraft. It is hoped that the following discussion of the most common sources will

help the designer to become aware of potential problems due to man-made noise.

a. Power lines The power leakage of high-voltage power lines by discharge, radiation and induction, resulting in noise interference to a communication system, is referred to as "power-line noise". Power-line noise is caused by a multitude of physical defects in a power distribution system, often simply aging. It becomes a serious problem to nearby communications because it is almost impossible to maintain a low-noise system near a power line.

The reader can testify to the seriousness of the problem by remembering the last time he was driving in the country listening to a weak radio station. As the automobile approached a rural power line the noise drowned out the weak station. Only when the car had traveled a considerable distance from the power line did the noise fade. Ham radio operators minimize power-line noise by orienting their dipole antennas 90 degrees to the power line to minimize coupling. Two-way communications employing ground-plane antennas minimize power-line noise by elevating the antenna well above the power line. It is often the most practical solution, however, to separate the antenna sufficiently from the power line because power-line noise decreases rapidly with distance.

b. Automobile ignition The noise generated by the automobile ignition system is referred to as impulse noise because of its frequency and amplitude characteristics. Ignition noise causes the 'popping' sound in an AM receiver when an automobile passes the antenna site. The impulsive nature of ignition noise makes possible the use of an IF noise blanker to reduce or eliminate the annoying popping in voice

communication . This is accomplished by silencing the receiver for the duration of the pulse which a procedure that has little effect on voice intelligibility. For other systems such as data transmission, the effect is more severe. Usually the parity error of the system becomes too large to be practical. A solution for ignition noise is a suppression system on the automobile which eliminates the high-frequency energy from the impulses. This is usually accomplished by shielding and adding series resistance to the high-voltage wires.

c. Thermal radiation from surrounding objects The black-body radiation from objects close to the receiving antenna induces noise and must be accounted for in low-noise systems*. Any source of heat such as electrical power plants, industrial processing plants and chimneys will induce noise in nearby antennas (Lawson and Uhlenbeck, 1950, p. 107).

d. Electrical arcing Severe noise can be generated by any electrical device where arcing occurs. Examples of these devices where arcing is a normal mode of operation are; small universal motors in appliances such as shavers, grinders, table saws, vacuum cleaners, mixers, blenders and a host of other household appliances. Arcing of the commutator in a DC generator is a common source of noise and is often noted as "generator whine" in a mobile receiver.

e. Neon and fluorescent lamps Sources of lighting which employ ionization of gases to generate light will also act as gas discharge noise sources. This effect and the pulsing nature of the AC power source cause the loud buzz heard in a communications receiver operation near neon or fluorescent lamps. Metropolitan areas can contain hundreds of thousands of neon lights which act as a large noise

*Surprisingly, the earth itself is a source of radio noise because its average temperature is nearly 273 Kelvins.

generator with a somewhat flat spectrum which usually results in a severe noise problem.

f. Static discharge The buildup and discharge of large amounts of static electricity causes noise in the radio spectrum. This noise is caused by the acceleration of a large number of charged particles (electrons) much the same as with shot noise. Manifestations of static discharge noise are "wheel static" in mobile systems and electrostatic charge generators such as a Van de Graf generator.

g. Digital switching system In electronic systems employing a large number of switching circuits such as a telephone relay bank or digital frequency synthesizers, the almost random impulses of current generated from a large number of circuits switching causes noise. The noise can usually be reduced by shielding but, because the switching circuits are so intimately associated with the receiving system, enough noise usually leaks through to cause interference.

h. Electrical propulsion devices for space vehicles Ion propulsion engines for space vehicles exhibit a multitude of noise sources due to the acceleration of charged particles in the plasma. Some of these noise generating mechanisms are electron radiation, electron-ion collisions, ion radiation, and black-body radiation (Wanselow, 1963). Wanselow discusses some analytical and experimental studies of RF noise generated by two types of ion propulsion engines. His conclusions are that only two types of propulsion noise are important: electron-radiation from plasma boundary accelerations and a noise-growth mechanism. The noise growth mechanism which theoretically has a noise power spectrum of -100 dbm/mhz is caused by plasma oscillations. This type of noise is

limited to frequencies less than 5% from the plasma frequency (from 200-500 mhz).

7. Special noise generation effects

There are sources of noise which are caused by physical phenomena which are not usually associated with communication noise studies. The source this author is familiar with is the phenomena called Barkhausen noise. It is present in ferromagnetic materials that are subjected to a changing magnetic field. The domain wall motion in the material is impeded by imperfections and impurities in the crystalline structure. The domain wall will "hang up" on one of these and store magnetoelastic energy while the motion is stopped. Suddenly, the domain wall will break free and give up the stored energy with a burst. This sudden energy burst can induce electrical current in the electrical circuit of which the magnetic material is a part and cause the effect called Barkhausen noise.

C. Noise in Passive Communication Circuits

The passive elements of a communication system have an important influence on its performance. A knowledge of the noise behavior of the most important elements can aid in the design of a low-noise system. The development of special analysis techniques and equations makes it desirable to present these topics in a separate section. The noise power equations for generalized resistive networks have been derived and applied to the calculation of the noise contribution of a resistive attenuator. These equations are especially helpful in low-frequency

calculations. Antenna noise is given a comprehensive treatment because it is so important to a low-noise system. Tuned circuit and filter noise are discussed because they affect the noise factor of RF pre-amplifiers. Finally, transmission line noise equations are derived and presented because they are important in computing total system noise temperature and in measuring noise factors.

1. Resistive networks

To effectively derive noise equations for resistive networks it will be helpful to present both the Thevenin and Norton forms of the Nyquist equivalent circuit. Using the Nyquist representation, a noisy resistor R_n at a temperature T_n can be represented by equivalent Thevenin and Norton circuits as shown in Figure C-1.

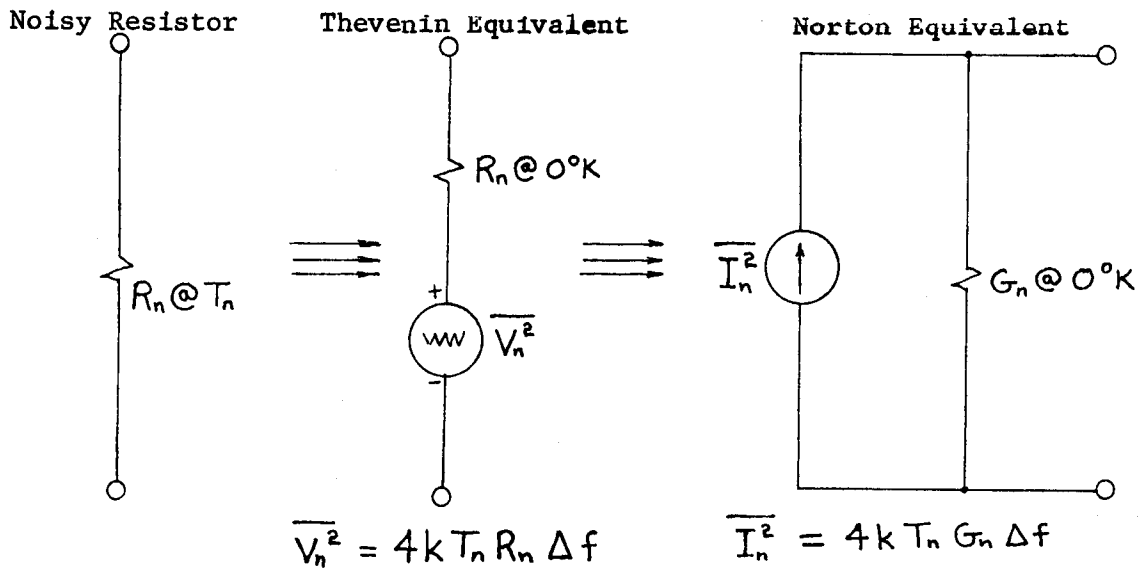


Figure C-1. Circuit Models for Noisy Resistors

Notice that the resistance (or conductance) in the equivalent circuit is at zero degrees Kelvin. The noise of the resistor is always accounted for by the noise generator so it will always be assumed that the resistor in the model is noiseless and its temperature will usually not be illustrated explicitly as it has been in Figure C-1.

a. Noisy resistors in parallel A network consisting of several noisy resistors in parallel can be reduced to a single noisy resistor by considering the proper conditions of power transfer i.e., the single equivalent resistor must deliver the same noise power as the network. Figure C-2 represents the resistive network.

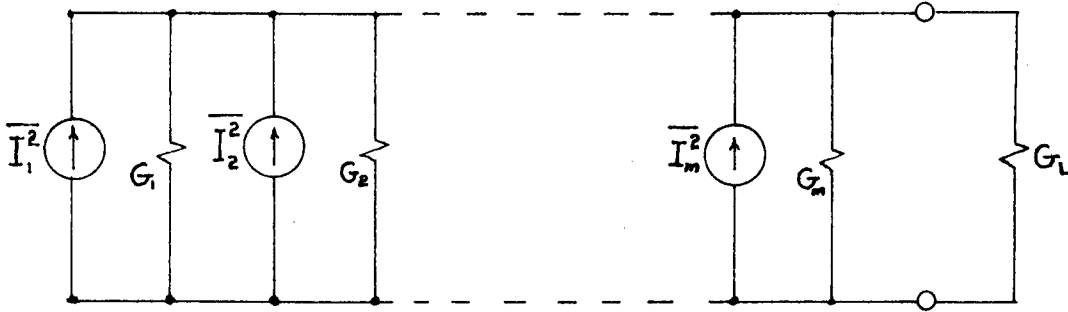


Figure C-2. Noisy resistors in parallel

The current in the load, G_L , due to the i^{th} noise source is:

$$\sqrt{\overline{I}_i^2} = (4kT_i G_i \Delta f)^{1/2} \frac{G_L}{G_L + \sum_{i=1}^m G_i} \quad (4C.1)$$

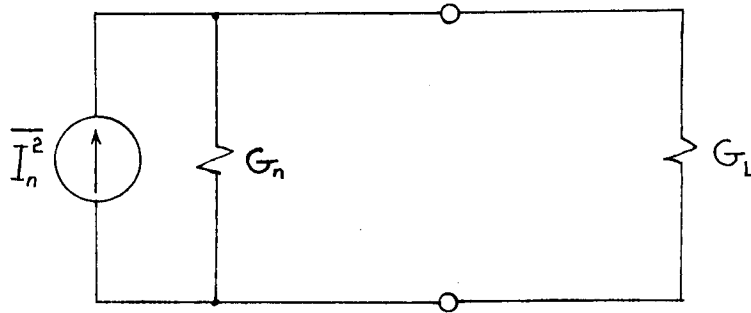
where we consider each resistor to be at a different temperature. The power delivered to G_L due to the i^{th} source is:

$$\frac{\overline{I_i^2}}{G_L} = 4k T_i G_i \Delta f \frac{G_L}{\left(G_L + \sum_{i=1}^m G_i\right)^2} \quad (4C.2)$$

Because the individual noise current generators are totally uncorrelated, the total noise power in the load G_L is the sum of the individual noise powers:

$$\text{Total Noise Power, } P_T = \left[4k \left(\sum_{i=1}^m T_i G_i \right) \Delta f \right] \frac{G_L}{\left(G_L + \sum_{i=1}^m G_i\right)^2} \quad (4C.3)$$

The resistive network can now be reduced to a single resistor whose noise values are given in Figure C-3.



$$\overline{I_n^2} = 4k T_n G_n \Delta f \quad G_n = \sum_{i=1}^m G_i \quad T_n = \sum_{i=1}^m \frac{T_i G_i}{G_n}$$

Figure C-3. Norton's Equivalent for Noisy Resistors in Parallel

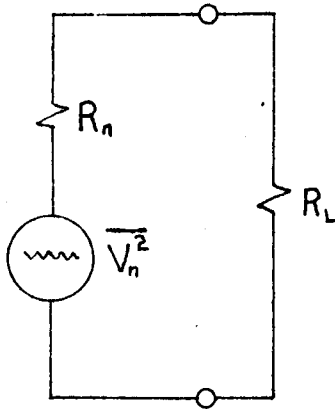
If all of the resistors are at the same temperature, T_r , the noise current generator becomes:

$$\overline{I_n^2} = 4k T_r (G_1 + G_2 + \dots G_m) \Delta f \quad (4C.4)$$

b. Noisy resistors in series In a manner analogous to that for the previous section, it is possible to express the total noise power in a load R_L due to several noisy resistors in series as:

$$\text{Total Noise Power, } P_T = \left[4k \left(\sum_{i=1}^m T_i R_i \right) \Delta f \right] \frac{R_L}{\left(R_L + \sum_{i=1}^m R_i \right)^2} \quad (4C.5)$$

The series of noisy resistors can be reduced to a single resistor whose noise values are given in Figure C-4.



$$\overline{V_n^2} = 4k T_n R_n \Delta f$$

$$R_n = \sum_{i=1}^m R_i$$

$$T_n = \sum_{i=1}^m \frac{T_i R_i}{R_n}$$

Figure C-4. Thevenins Equivalent for Noisy Resistors in Series

If all of the series resistors are at the same temperature, T_r , the noise voltage generator becomes:

$$\overline{V_n^2} = 4k T_r (R_1 + R_2 + \cdots R_m) \Delta f \quad (4C.6)$$

We can now summarize the results for both series and parallel resistive networks for both Thevenins and Nortons equivalent circuits:

Parallel Resistors

$$\overline{I_n^2} = 4k \left[\sum_{i=1}^m T_i G_i \right] \Delta f$$

$$G_n = \sum_{i=1}^m G_i$$

$$\overline{V_n^2} = 4k \left[\frac{\sum_{i=1}^m T_i G_i}{G_n^2} \right] \Delta f$$

Series Resistors

(4C.7)

$$\overline{V_n^2} = 4k \sum_{i=1}^m T_i R_i \Delta f$$

$$R_n = \sum_{i=1}^m R_i$$

$$\overline{I_n^2} = 4k \left[\frac{\sum_{i=1}^m T_i R_i}{R_n^2} \right] \Delta f$$

The simple cases of two resistors in series and in parallel are summarized in Figures C-5 and C-6.

It is appropriate at this point in the development to apply the resistive noise power formulas to a resistive network of significant practical importance--the Resistive Ladder Attenuator. For purposes of illustration, the circuit manipulations will be performed in detail for a Symmetrical-T Attenuator. The methods shown will be applicable, in general, to any resistive network. Figure C-7 shows a Symmetrical-T Attenuator with a noisy resistive source R_s . We now proceed to derive a Thevenin's equivalent circuit for the nodes a-b. Important circuit

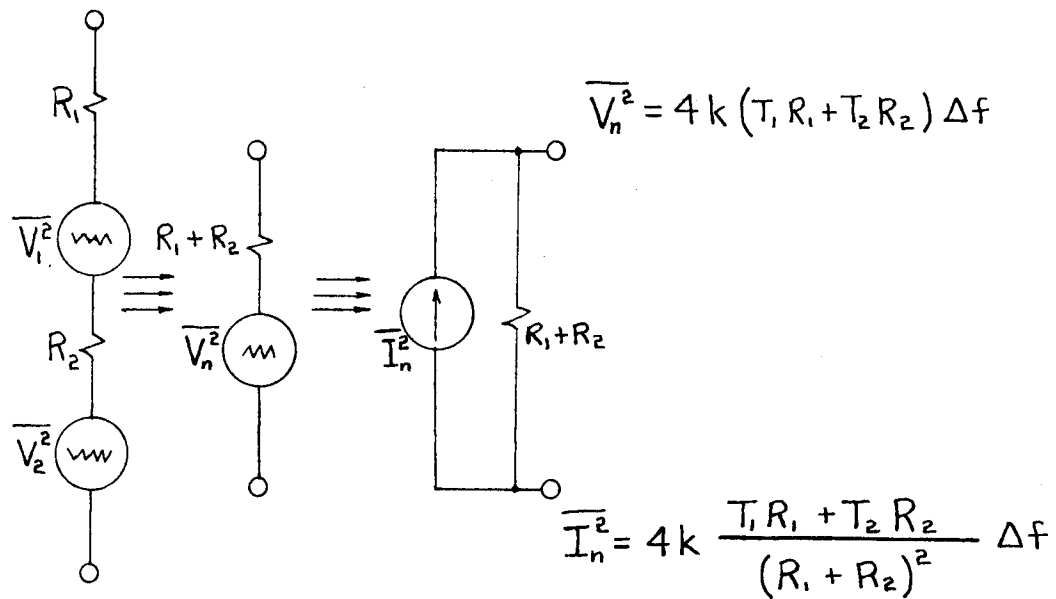


Figure C-5. Two Noisy Resistors in Series

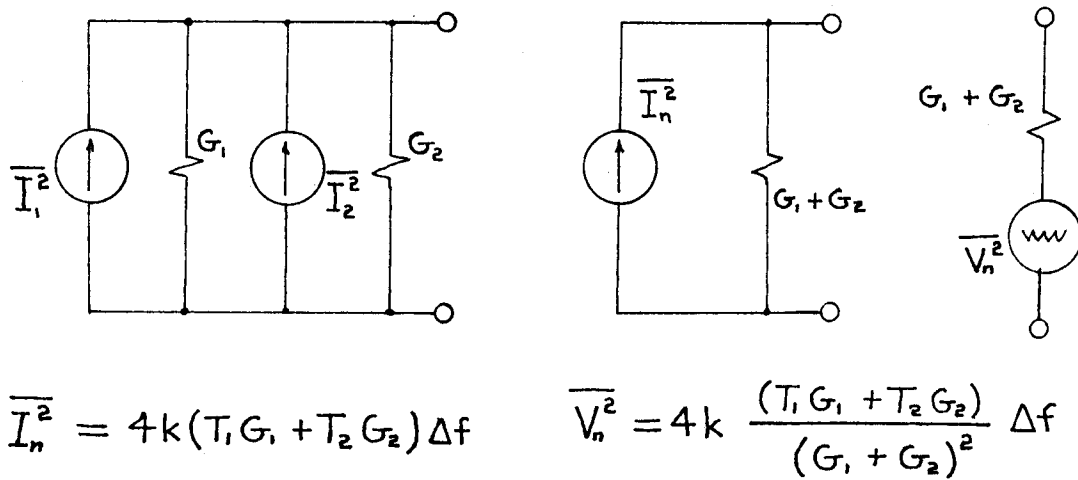


Figure C-6. Two Noisy Resistors in Parallel

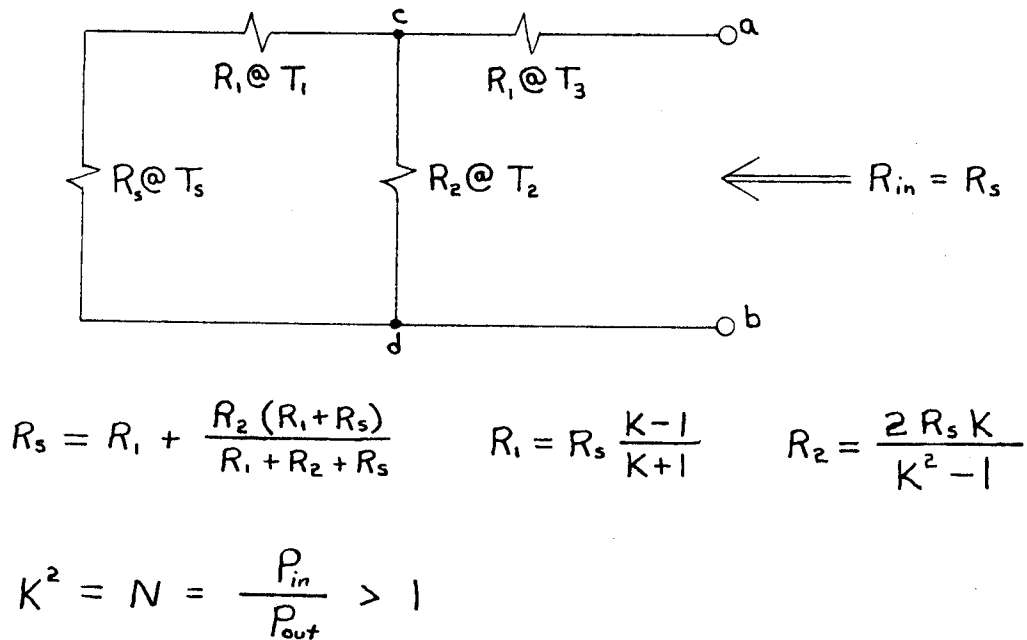
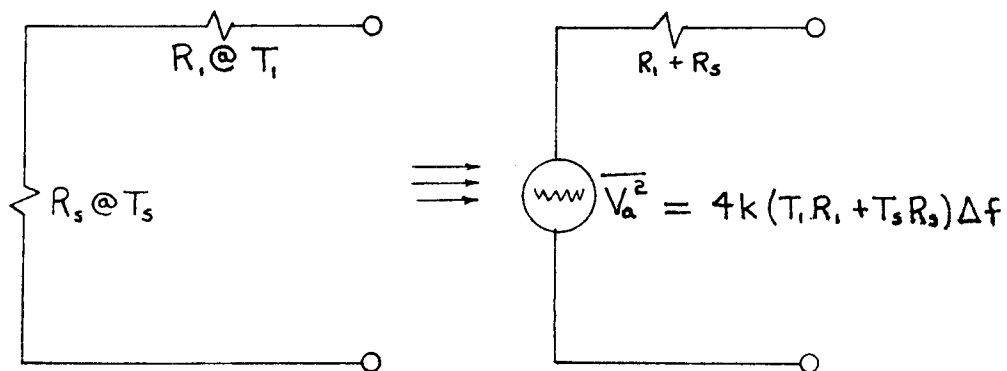
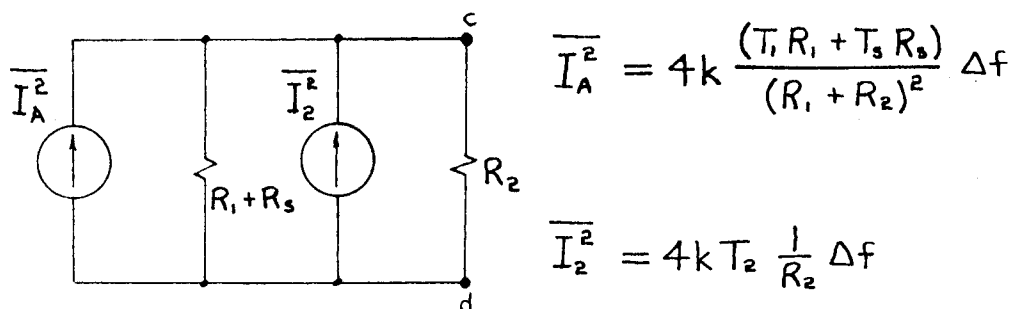


Figure C-7. Symmetrical-T Attenuator

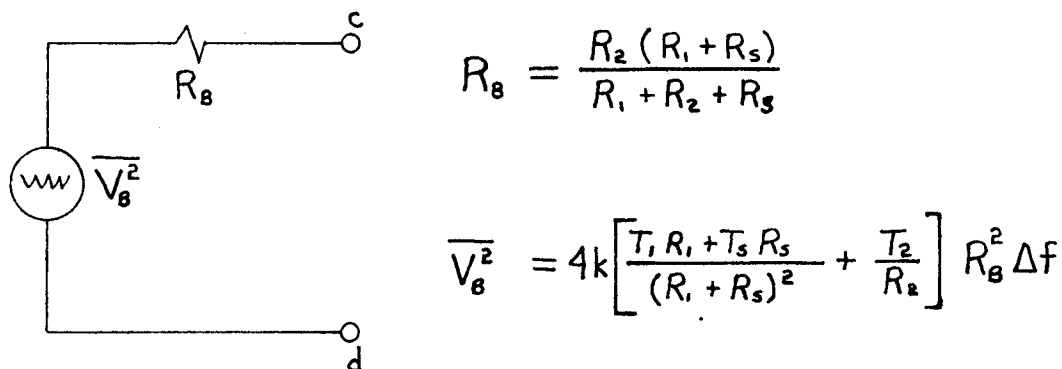
relationships for the attenuator are given with the circuit. We now proceed to obtain the Thevenin's equivalent by a series of Thevenin-Norton conversions. First combine R_3 and R_1 :



Parallel the resultant with R_2 , change both to a Norton's equivalent and combine:



Combine both current generators and convert the resultant to a Thevenin's equivalent:



Finally we combine the above circuit with the final ladder resistor ($R_1 @ T_3$) to obtain the Thevenin's equivalent for nodes a-b.

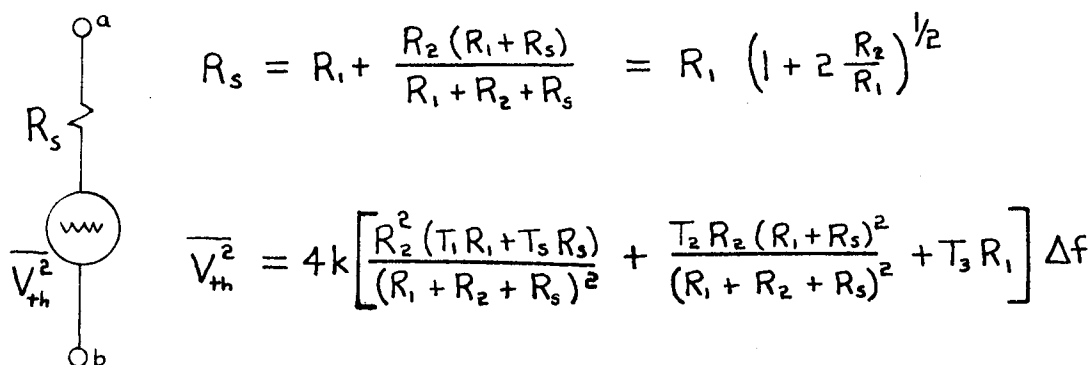


Figure C-8. Thevenin's Equivalent for Noise Output of a Symmetrical-T Attenuator

The Thevenin's equivalent can be further simplified by considering the practical case where the resistive attenuator is at one uniform temperature and the source resistance R_s is at another. Applying these restraints and substituting for R_1 and R_2 in terms of R_s and K , the current ratio from input to output, we can perform the following manipulations (International Telephone and Telegraph Corp., 1956, Ch. 9):

$$\overline{V_{th}^2} = 4kT R_s \Delta f \quad T_1 = T_2 = T_3$$

$$(R_1 + R_2 + R_3)^2 = \left(R_s \frac{K-1}{K+1} + 2R_s \frac{K}{K^2-1} + R_s \right)^2 = R_s^2 \left(\frac{2K^2}{K^2-1} \right)^2$$

$$R_2^2 = 4R_s^2 \left(\frac{K}{K^2-1} \right)^2$$

$$(R_1 + R_2)^2 = \left(R_s \frac{K-1}{K+1} + R_s \right)^2 = R_s^2 \left(\frac{2K}{K+1} \right)^2$$

$$T R_s = \frac{4R_s^2 \left(\frac{K}{K^2-1} \right)^2 \left(T_1 R_s \frac{K-1}{K+1} + T_3 R_s \right)}{R_s^2 \left(\frac{2K^2}{K^2-1} \right)^2} + \frac{T_1 2R_s \frac{K}{K^2-1} R_s^2 \left(\frac{2K}{K+1} \right)^2}{R_s^2 \left(\frac{2K^2}{K^2-1} \right)^2} + T_1 R_s$$

Combining and simplifying,

$$T R_s = \frac{1}{K^2} \left(T_i R_s \frac{K-1}{K+1} + T_s R_s \right) + \frac{T_i 2 R_s}{K} \frac{K-1}{K+1} + T_i R_s \frac{K-1}{K+1}$$

$$= R_s \left[\frac{T_s}{K^2} + T_i \frac{K-1}{K+1} \left(\frac{1}{K^2} + \frac{2}{K} + 1 \right) \right] = R_s \left[\frac{T_s}{K^2} + \frac{T_i (K^2 - 1)}{K^2} \right]$$

$$T = \frac{T_s + T_i (N-1)}{N} \quad N \geq 1$$

A summary of the results of this analysis on a resistive attenuator at uniform temperature is given in Figure C-9.

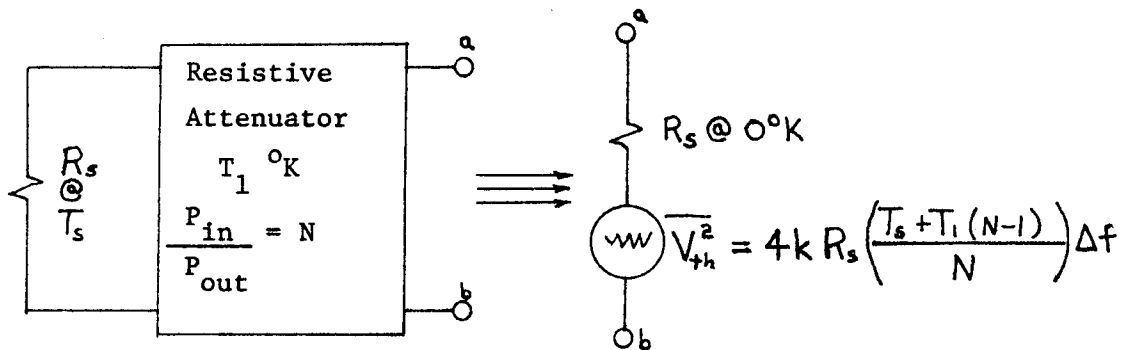


Figure C-9. Thevenin's Equivalent Noise Generator for an Ideal Resistive Attenuator at a Uniform Temperature

Some common examples for standard values of attenuation and the corresponding Thevenin noise generator are given in tabular form below.

Table C-1. Mean-square noise voltage output v.s. attenuation

Attenuation	$N = \frac{P_{in}}{P_{out}}$	$\overline{V_{Th}^2}$
0 db	1	$4 k T_s R_s \Delta f$
3 db	2	$4 k R_s \left(\frac{T_s + T_1}{2} \right) \Delta f$ (mean of T_s and T_1)
6 db	4	$4 k R_s \left(\frac{T_s + 3T_1}{4} \right) \Delta f$
10 db	10	$4 k R_s \left(\frac{T_s + 9T_1}{10} \right) \Delta f$

When the value of attenuation becomes large, the value of Thevenin's noise voltage generator approaches the value:

$$\overline{V_{th}^2} = 4k R_s (T_1 + T_s/N) \Delta f \quad N > 100 \quad (4C.9)$$

The noise voltage generator can also be expressed in terms of the "gain"

of the attenuator $G = \frac{P_o}{P_{in}}$.

$$\overline{V_{th}^2} = 4k R_s \left[T_1 + G (T_s - T_1) \right] \Delta f \quad G = 1/N \quad (4C.10)$$

These results should be compared to the equations for transmission lines which were derived on an entirely different basis.

2. Tuned circuit, transformer noise

The noise analysis of a tuned circuit may be done a variety of ways depending on the desired goal. The analysis presented here will show some applied results of Nyquist's theorem and how the effective noise temperature of the antenna source resistance is increased due to the noise added by the losses in a tuned circuit. Nyquist's theorem (Bennett, 1960, Sec. 2-8; Lawson and Uhlenbeck, 1950, p. 74) states that the noise power available at the nodes of an RLC network at uniform temperature is simply the noise power available from the real part of the driving point impedance (see Appendix, Parts C and E). Consider the circuit of Figure C-10a, a resistor and capacitor in parallel. From AC circuit theory, the driving point impedance is

$$\begin{aligned} Z_s(\omega) &= R(\omega) + j X(\omega) \\ &= \frac{R_s}{1 + \omega^2 R_s^2 C^2} + j \frac{-R_s \omega C}{1 + \omega^2 R_s^2 C^2} \end{aligned} \quad (4C.11)$$

and Nyquist's theorem states that the incremental mean-square noise generator is:

$$d\overline{V_n^2} = 4kT_s R(\omega) df = 4kT_s \frac{R_s}{1 + \omega^2 R_s^2 C^2} df \quad (4C.12)$$

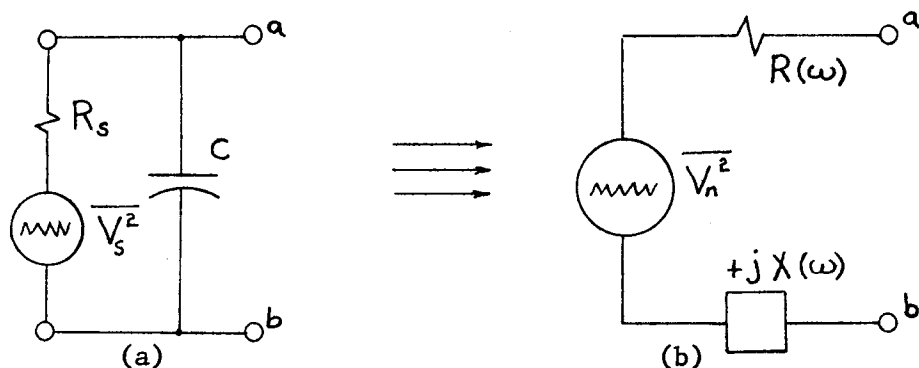


Figure C-10. Nyquist's Theorem Applied to a RC Parallel Network

Comparing the mean-square noise voltage of the original source resistance

$$d\overline{V_s^2} = 4kT_s R_s df$$

gives the result:

$$d\overline{V_n^2} = d\overline{V_s^2} \frac{1}{1 + \omega^2 R_s^2 C^2} \quad (4C.13)$$

Whereas the mean-square noise voltage of the source resistance depends upon T_s , R_s and bandwidth, the equivalent noise voltage is a function also of frequency and capacitance. These results should generally be kept in mind:

- a) The resulting equivalent mean-square voltage obtained by applying Nyquist's theorem is frequency dependent.
- b) The available power is frequency and bandwidth limited.

The mean-square noise voltage available from the source resistance is limited only by the sample bandwidth, Δf

$$\overline{V_s^2} = 4kT_s R_s \Delta f \quad (4C.14)$$

while the mean-square noise voltage from the RC network is limited to (Appendix, Part B, Equation B.16):

$$\overline{V_n^2} = 4kT_s R_s \int_0^{\infty} \frac{1}{1 + \omega^2 R_s^2 C^2} d\omega = 4kT_s R_s \left(\frac{\pi}{2R_s C} \right) \quad (4C.15)$$

By comparison with (4C.14), the effective noise bandwidth is $\frac{\pi}{2R_s C}$

which is in agreement with Part B of the Appendix.

Now consider the parallel tuned circuit of Figure C-11.

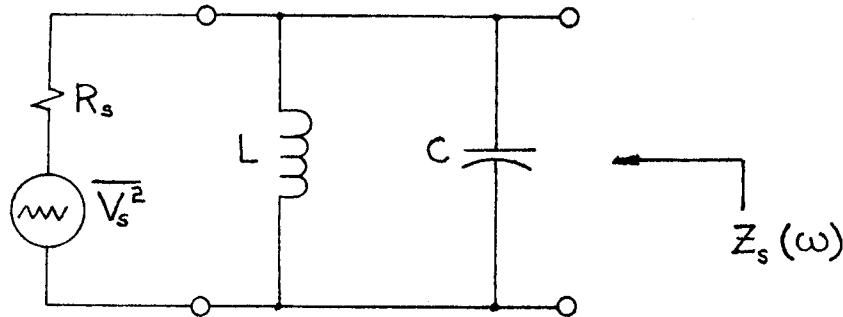


Figure C-11. Nyquist's Theorem Applied to an RLC Parallel Network

From AC circuit theory we get

$$R(\omega) = \frac{R_s}{1 + R_s^2 \left(\omega C - \frac{1}{\omega L} \right)^2} \quad (4C.16)$$

Making the substitution

$$Q_0 = \frac{R_s}{\omega_0 L} = R_s \omega_0 C \quad \omega_0 = \frac{1}{\sqrt{LC}}$$

gives the result in terms of the circuit Q at resonance:

$$R(\omega) = R_s \frac{1}{1 + Q_o^2 \left(\frac{\omega}{\omega_o} - \frac{\omega_o}{\omega} \right)^2} \quad (4C.17)$$

In a manner analogous to that done for the RC network we have:

$$\begin{aligned} d\overline{V_s^2} &= 4kT_s R_s df \\ d\overline{V_n^2} &= d\overline{V_s^2} \frac{1}{1 + Q_o^2 \left(\frac{\omega}{\omega_o} - \frac{\omega_o}{\omega} \right)^2} \end{aligned} \quad (4C.18)$$

Integrating to find the total mean-square noise voltage gives:

$$\overline{V_n^2} = 4kT_s R_s \int_0^{\infty} \frac{df}{1 + Q_o^2 \left(\frac{f}{f_o} - \frac{f_o}{f} \right)^2} = 4kT_s R_s \left(\frac{\pi}{2} \frac{f_o}{Q_o} \right) \quad (4C.19)$$

For the RLC parallel-tuned circuit, the equivalent noise bandwidth is

$$\Delta f = \frac{\pi}{2} \frac{f_o}{Q_o}$$

and since the circuit Q at resonance is equal to the ratio of resonant frequency to 3db bandwidth we get the result,

$$\Delta f = \frac{\pi}{2} BW_{3db} \quad (4C.20)$$

In conclusion, the effective noise bandwidth for a parallel-tuned circuit is $\pi/2$ times the 3db or half-power bandwidth.

At frequencies near resonance, the Nyquist resistance of (4C.17) can be approximated by

$$R(\omega) \cong R_s \quad \text{for} \quad \frac{\Delta\omega_0}{\omega_0} < \frac{.05}{Q_0} \quad (4C.21)$$

where $\Delta\omega_0$ is the frequency increment away from resonant frequency ω_0 . The proof of this can be seen by expanding the denominator of (4C.17) in a power series.

The circuit manipulations that are required to show the noise factor degradation for a lossy tuned circuit will be included to illustrate noise calculations. Figure C-12 shows the schematic representation of the input circuit for an RF amplifier.

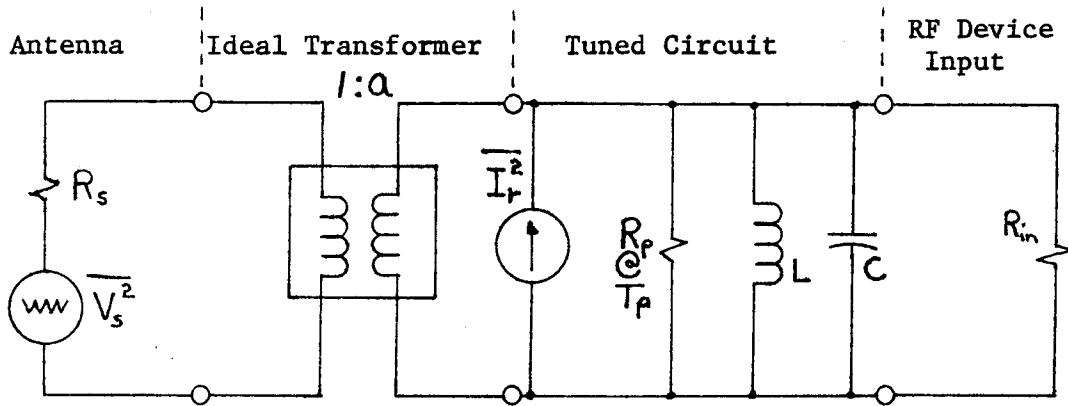


Figure C-12. Equivalent RF Input Circuit for an RF Amplifier

The resistance R_p represents the parallel equivalent resistance of the tuned circuit. The noise current generator $\overline{i_r^2}$ represents the effective noise of the RF device referred to the input. The ideal transformer is used to represent the transformation of R_s that is necessary when R_p is

finite. Now we eliminate the transformer and show all noise sources by noise current generators explicitly in Figure C-13.

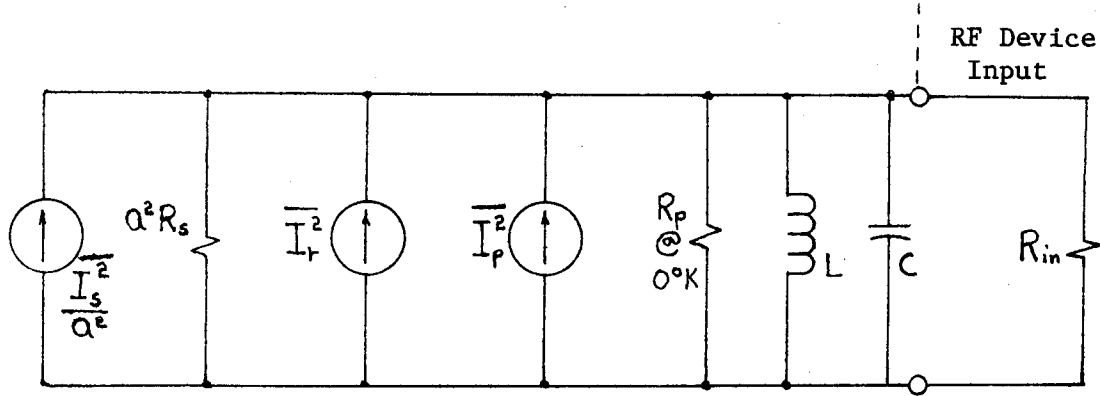


Figure C-13. Parallel Equivalent of RF Input Circuit

The purpose of the transformer is to maintain a constant parallel resistance for the amplifier input. It is only meaningful to compare noise performance when the source resistance is held constant. Under ideal conditions (lossless tuned circuit) the following relationships hold

Ideal conditions

$$a^2 = 1$$

$$R_p = \infty$$

$$\overline{i_p^2} = 0$$

$$\text{Source resistance} = R_s$$

while for a lossy circuit R_p is finite and:

Non-ideal conditions

$$a^2 = \frac{R_p}{R_p - R_s} \quad R_s < R_p \leq \infty, \quad a \gg 1$$

$$\overline{I_p^2} = 4kT_p G_p \Delta f \quad G_p = \frac{1}{R_p}$$

$$\text{Source resistance} = \frac{\alpha^2 R_s R_p}{\alpha^2 R_s + R_p} = R_s$$

For a lossless network the noise factor is (Appendix, Part E)

$$F_o = \frac{\overline{I_s^2} + \overline{I_r^2}}{\overline{I_s^2}} = 1 + \frac{\overline{I_r^2}}{\overline{I_s^2}} \quad (\alpha^2 = 1)$$

while for the lossy network we have:

$$F_L = \frac{\frac{\overline{I_s^2}}{\alpha^2} + \overline{I_p^2} + \overline{I_r^2}}{\frac{\overline{I_s^2}}{\alpha^2}} = 1 + \alpha^2 \frac{\overline{I_p^2} + \overline{I_r^2}}{\overline{I_s^2}} \quad (4C.22)$$

Letting the mean-square noise current generators be represented by their Nyquist equivalents

$$\overline{I_s^2} = 4kT_o G_s \Delta f \quad (T_s \equiv T_o)$$

$$\overline{I_p^2} = 4kT_p G_p \Delta f \quad (4C.23)$$

$$\overline{I_r^2} = 4kT_r G_s \Delta f$$

the noise factor of Equation 4C.22 becomes:

$$F_L = 1 + \alpha^2 \frac{T_p G_p + T_r G_s}{T_o G_s} \quad (4C.24)$$

Upon substitution for α^2 , the final result for the noise factor of an RF amplifier with lossy input network is obtained:

$$F_L = 1 + \frac{T_r}{T_o} \left(\frac{R_p}{R_p - R_s} \right) + \frac{T_p}{T_o} \left(\frac{R_s}{R_p - R_s} \right) \quad (4C.25)$$

Several limiting cases are noted:

- a. For large R_p ($R_p \gg R_s$)

$$F_L = 1 + \frac{T_r}{T_o} + \frac{T_p R_s}{T_o R_p} \quad (4C.26)$$

- b. For Large R_p and $T_p \approx T_o$

$$F_L = 1 + \frac{T_r}{T_o} + \frac{R_s}{R_p} \quad (4C.27)$$

- c. Ideal conditions ($R_p \rightarrow \infty$)

$$F_L = 1 + \frac{T_r}{T_o} \quad (\text{Compare, Appendix, Part E})$$

- d. Noiseless RF amplifier ($T_r = 0$)

$$F_L = 1 + \frac{T_p}{T_o} \left(\frac{R_s}{R_p - R_s} \right)$$

For most low-noise designs Equation 4C.27 is appropriate. Limiting case d can be thought of as the "noise factor of a tuned circuit".

A word of explanation is needed for why the tuned circuit frequency response didn't enter into the problem. The reason it does not is because the device noise is referred past the tuned circuit and the effect is accounted for in the value of i_r^2 . One last example of

the numerous applications and special cases for Equation 4C.24 is that of the case where the parallel equivalent resistance R_p is equal to the transformed resistance $\alpha^2 R_s$. Mathematically we have

$$\alpha^2 R_s = R_p = 2 R_s \quad \therefore R_p // \alpha^2 R_s = R_s, \quad \alpha^2 = 2$$

which upon substitution into Equation 4C.24 gives

$$\tilde{F} = 1 + \frac{T_p}{T_o} + 2 \frac{T_r}{T_o} \quad (4C.28a)$$

If it is assumed that the parallel resistance is near standard temperature ($T_p \approx T_o$) then

$$\tilde{F} = 2 \left(1 + \frac{T_r}{T_o} \right) \quad (4C.28b)$$

which is twice the ideal value (special case c). This is the so-called 3db noise figure degradation point (twice noise factor) and serves as a handy point of reference in measurements.

To discuss transformer noise, two broad categories are considered; narrow-band LC matching networks and the linear-core transformer. For LC matching networks, the techniques developed for RC and RLC networks can be applied. For the linear-core transformer, the losses in the transformer equivalent circuit will be discussed. Figure C-14 shows a transformer equivalent circuit with circuit values referred to the primary.

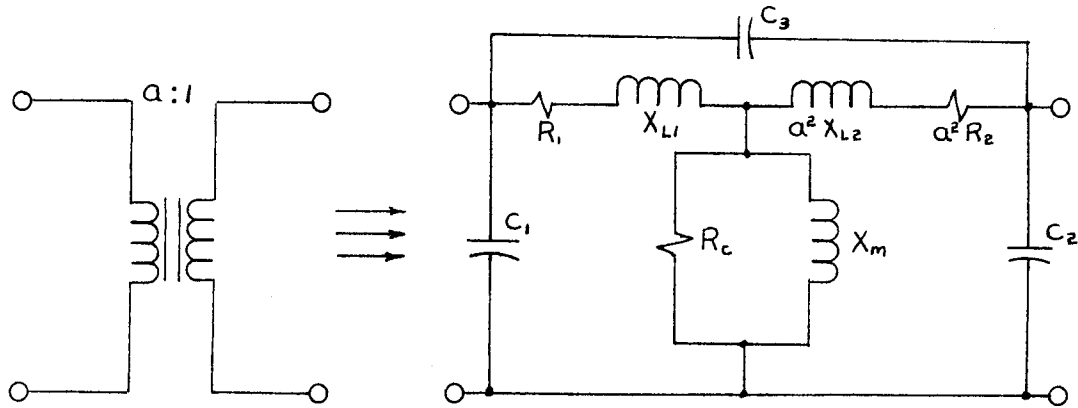


Figure C-14. Transformer Equivalent Circuit

The noise in the transformer comes from the ohmic loss resistances R_1 and $a^2 R_2$ and from the magnetization loss resistance R_c . If the transformer has a ferromagnetic core the noise temperature of R_c might be higher than ambient because of a Barkhausen noise contribution.

For practical applications the transformer is assumed to be at standard temperature ($T_o = 290^\circ\text{K}$). For computations, this author's practical experience has shown that noise factor for a transformer can be calculated from its insertion loss by treating it as a resistive attenuator or a transmission line (Parts 1 and 4 of this Chapter).

3. Filter noise

Filter noise and filter loss have their most important effect in the low-noise portions of a receiver. In particular, the first RF filter directly affects noise factor and noise temperature. The analysis for filter noise is only approximate because the exact analysis of a multistage filter would be extremely difficult. For analysis we will consider the RF bandpass filter as represented in Figure C-15.

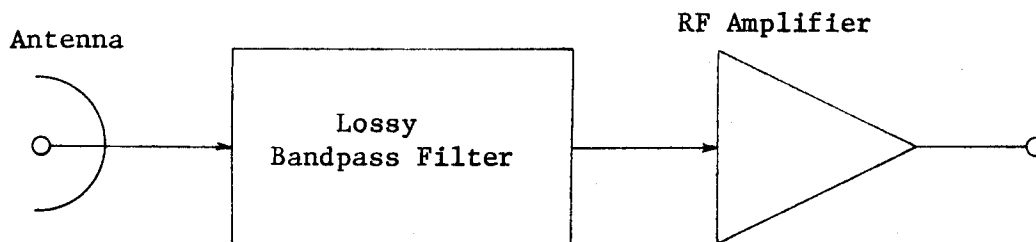


Figure C-15. Block Diagram for RF Filter Noise Analysis

The antenna, filter, and RF amplifier will now be replaced by their equivalent circuits as shown in Figure C-16. It is assumed that the bandpass filter can be represented by a resistive attenuator (Pad) and a lossless filter in cascade. The noise generated by the filter is accounted for with the pad and the attenuation out of the passband with the filter transfer characteristic.

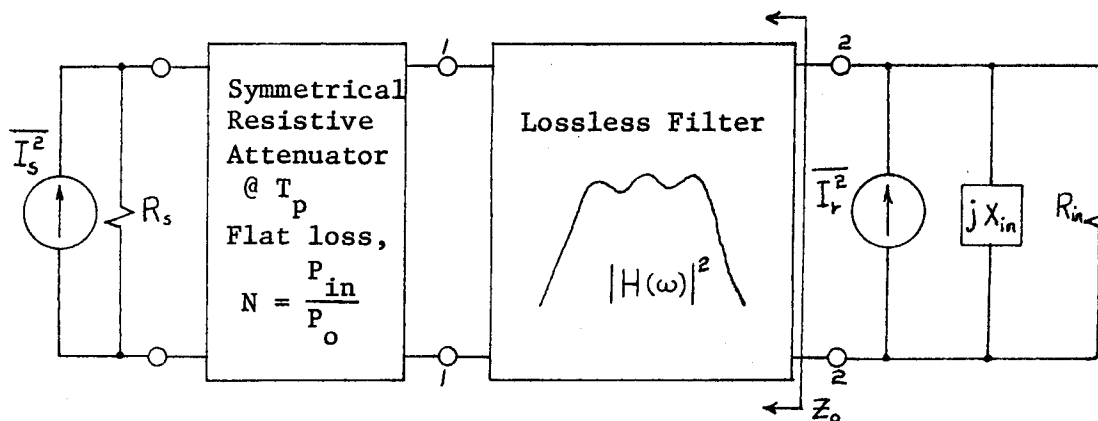


Figure C-16. Equivalent Circuit for RF Filter Noise Analysis

The attenuation of the pad has a value of the flat loss* of the filter. The noise factor of Figure C-16 is obtained by applying the definition of the ratio of input and output signal-to-noise ratios. $|H(\omega)|^2$ is the power attenuation factor for the filter where $H(\omega)$ is the current transfer ratio and represents the attenuation of a noiseless filter (purely reactive elements). $\overline{I_r^2}$ represents the referred noise of the receiver.

Now we proceed to write the noise factor for the circuit of Figure C-16 as the ratio of total mean-square current output to that due only to the source resistance at standard temperature:

$$F_{rt} = \frac{\frac{\overline{I_s^2}}{N} |H(\omega)|^2 + \overline{I_p^2} |H(\omega)|^2 + \overline{I_r^2}}{\frac{\overline{I_s^2}}{N} |H(\omega)|^2} \quad (4C.29)$$

The noise factor equation is further reduced by substituting the following Nyquist equivalents

$$\begin{aligned} \overline{I_s^2} &= 4 k T_o G_s \Delta f \\ \overline{I_p^2} &= 4 k T_p G_p \Delta f \\ \overline{I_r^2} &= 4 k T_r G_s \Delta f \end{aligned} \quad (4C.30)$$

where $\overline{I_p^2}$ is a noise current generator across nodes 1-1 which represents the noise generated by the pad at temperature T_p . This noise

*The flat loss of a filter is defined to be the insertion loss of the filter at the frequency of maximum amplitude.

representation for the resistive attenuator can be better understood if the equivalence between the pad and the transformer/resistor representation of Figure C-12 is shown. Refer to Figure C-17 for definitions.

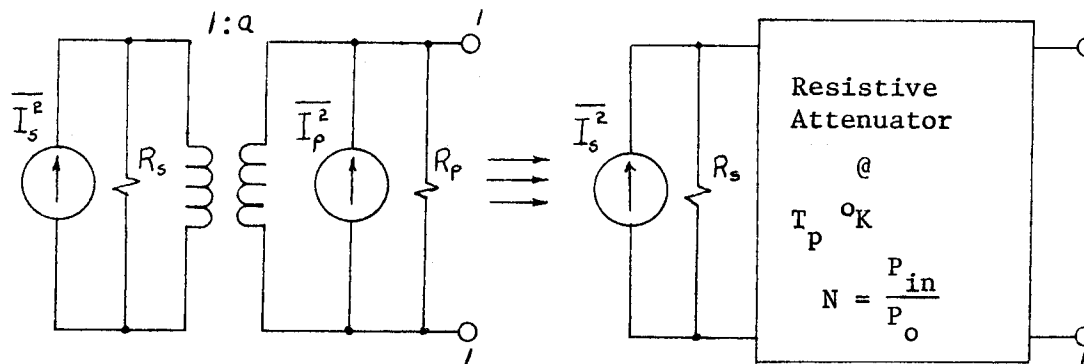


Figure C-17. Equivalence Between Resistive Attenuator and Transformer/Resistor Combination

The mean-square output current $\overline{I_{Th}^2}$ for the transformer circuit is (assume an ideal transformer and any source temperature)

$$\overline{I_{th}^2} = \frac{\overline{I_s^2}}{a^2} + \overline{I_p^2} = 4k R_s \left(\frac{T_s}{Q^2} + T_p \frac{R_s}{R_p} \right) \Delta f \quad (4C.31)$$

while that for the attenuator is (Figure C-9):

$$\overline{I_{th}^2} = 4k R_s \left(\frac{T_s + T_p (N-1)}{N} \right) \Delta f \quad (4C.32)$$

Using the identities

$$a^2 = \frac{R_p}{R_p - R_s} \quad a^2 = N \quad \frac{a^2}{a^2 - 1} = \frac{R_p}{R_s} \quad (4C.33)$$

and substituting into (4C.31) we get:

$$\begin{aligned}\overline{I_{th}^2} &= 4k R_s \left(\frac{T_s}{\alpha^2} + T_p \frac{\alpha^2 - 1}{\alpha^2} \right) \Delta f \\ &= 4k R_s \left(\frac{T_s + T_p (N-1)}{N} \right) \Delta f\end{aligned}\quad (4C.34)$$

The noise factor equation (4C.29) was actually obtained with the resistive attenuation replaced by the transformer equivalent so that the current generator $\overline{I_p^2}$ could be used to represent the filter noise.

Reducing Equation 4C.29 we obtain

$$F_{rt} = 1 + \alpha^2 \frac{T_p}{T_o} \frac{R_s}{R_p} + \frac{\alpha^2}{|H(\omega)|^2} \frac{T_r}{T_o} \quad (\alpha^2 = N) \quad (4C.35a)$$

and since $\frac{R_s}{R_p} = \frac{\alpha^2 - 1}{\alpha^2}$ we get the final form:

$$F_{rt} = 1 + \frac{T_p}{T_o} (N-1) + \frac{T_r}{T_o} \frac{N}{|H(\omega)|^2} \quad (4C.35b)$$

The equivalent noise temperature is:

$$T_{rt} = T_r \frac{N}{|H(\omega)|^2} + T_p (N-1) \quad (4C.35c)$$

This analysis can be applied to the case of the simple parallel tuned circuit of Figure C-12. Equation 4C.25 is simplified by the substitution $\alpha^2 = N$ which yields:

$$F_L = 1 + \frac{T_r}{T_o} N + \frac{T_p}{T_o} (N-1) \quad (4C.36a)$$

$$T_L = T_r N + T_p (N-1) \quad (4C.36b)$$

The results of (4C.25) were derived for the case when the device noise is referred past the tuned circuit. This corresponds to the case $|H(\omega)|^2 = 1$ and Equations 4C.35 and 4C.36 are equivalent. The spot noise factor at all frequencies for the single-tuned-circuit filter of Figure C-12 is (apply Equation 4C.35a and compare to Equation 4C.25):

$$F_L(\omega) = 1 + \frac{T_p}{T_o} (\alpha^2 - 1) + \frac{T_r}{T_o} \alpha^2 \left[1 + Q_o^2 \left(\frac{\omega}{\omega_o} - \frac{\omega_o}{\omega} \right)^2 \right] \quad (4C.37)$$

Application of these techniques to other filters will yield similar results. It should be noted that, for ideal impedance transformations, the available power and noise temperature remain unchanged. The noise bandwidths for some simple RF bandpass filters are compared to their 3db bandwidths in Kraus (1966, p. 265).

It cannot be emphasized enough that the receiver mean-square noise generator and hence receiver noise temperature T_r depends upon the filter output impedance and frequency. The rather simple expressions of Equations 4C.35 cannot relate the complicated dependence of T_r on both Z_o and frequency. The section on two-port noise theory will help explain these complicated dependencies. The noise factor in this

section is a spot noise factor and thus it and the resulting noise temperature are both point functions of frequency.

4. Antenna feedline--transmission line noise

The noise behavior of a transmission line is important because the noise temperature of a noise source as seen through a lossy line and the system noise temperature of a receiving system are both affected. The transmission line will increase noise factor and introduce errors in noise calibrations. Figure C-18 illustrates a noise source and a transmission line as might be used in a noise standard.

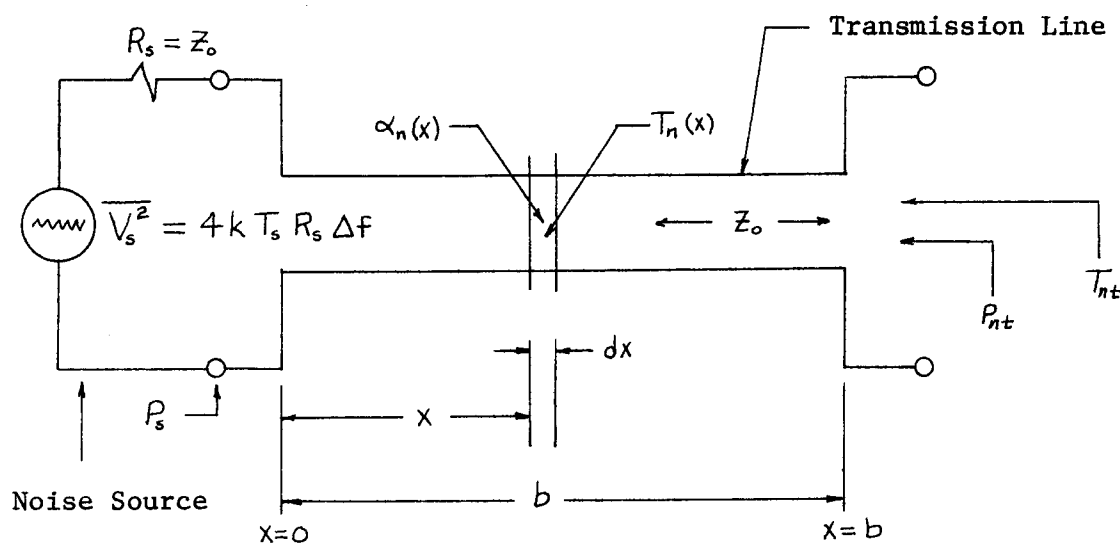


Figure C-18. Noise Source and Transmission Line Noise

The quantities in Figure C-18 are defined as follows:

R_s = The resistance of the noise source.

$\overline{V_s^2}$ = The mean-square noise voltage of the source
in a bandwidth Δf .

P_s = Available power of the noise source.

$\alpha_n(X)$ = Attenuation in nepers per unit-length for an incremental section of line, dx

$T_n(X)$ = Noise temperature of an incremental section of line, dx

b = Total length of line

P_{nt} = Available noise power at the output

T_{nt} = Effective noise temperature at the output.

The following assumptions will be used in deriving an expression for

T_{nt} :

- a. The transmission line is homogeneous
- b. Line losses are small enough that the characteristic impedance is real (distortionless line)
- c. The noise source is impedance matched to the line, $R_s = Z_o$.

The noise power, P_{nt} , available at the output is determined by two different sources; the noise power available from the noise source after it has been attenuated by the line and the noise power contributed by the lossy transmission line.

The available power, P_{nt} , will depend on the power available from the noise source, the noise power available from the line, and the line attenuation factor. From transmission line theory we know that the voltage wave along the line is attenuated by an exponential factor as expressed in the equation

$$\hat{E}_2 = \hat{E}_1 e^{-\alpha x} \quad (\text{Voltages in RMS Values}) \quad (4C.38)$$

and for a distortionless line the power attenuation is proportional to the mean-square voltage attenuation:

$$\frac{E_2^2}{E_1^2} = e^{-2\alpha x} \quad P_2 = P_1 e^{-2\alpha x} \quad (4C.39)$$

The power absorbed in a differential element of length, dx becomes (see Equation 4C.42 for definition of terms):

$$\text{Power absorbed} = -2 \alpha_n(x) P(x) dx \quad (4C.40)$$

When the line is in thermal equilibrium the power absorbed is equal to the power generated (Siegman, 1964, p. 374) so:

$$\text{Emission Power} = 2 \alpha_n(x) P_n(x) dx \quad (4C.41)$$

Since the thermal noise power generated is independent of the total noise power flowing, a differential equation for the change in total power in a line length dx can be written by combining the emission and absorption equations

$$dP(x) = -2 \alpha_n(x) P(x) dx + 2 \alpha_n(x) P_n(x) dx \quad (4C.42)$$

where $P(x)$ = Total power traveling in the transmission line
 $P_n(x)$ = Emission power in the line, due to thermal emission,
generally a function of x
 $\alpha_n(x)$ = Line attenuation in nepers per unit length, also a
function of x .

The conditions of power absorption and emission in a transmission line are analogous to those which exist for the emission and absorption of electromagnetic radiation in a gas cloud. For example if a radio source (noise source) is observed through an emitting and absorbing cloud (transmission line), the source brightness observed (available power) will depend upon the true source brightness and the emission and absorption coefficients which characterize the cloud.

Equation (4C.42) can be rearranged to give a relationship called the "equation of transfer":

$$\frac{dP(x)}{dx} + 2\alpha_n(x)P(x) = 2\alpha_n(x)P_n(x) \quad (4C.43)$$

This differential equation of the first order and first degree is a form of Leibnitz equation and is directly analogous to that obtained by Kraus (1966, p. 95) for external irradiation with internal emission and absorption as applied to radio and optical astronomy. The generalized form of Equation 4C.43 and its solution are given by:

$$\frac{dP(x)}{dx} + QP(x) = R(x) \quad (4C.44)$$

$$P(x) = A \exp\left[-\int Q dx\right] + \exp\left[-\int Q dx\right] \int \exp\left[+\int Q dx\right] R(x) dx$$

By substituting the terms of Equation 4C.43 into 4C.44 and integrating over the length of the transmission line we will evaluate the power available at the output as:

$$P_{nt} = A e^{-\tau_c} + e^{-\tau_c} \int_0^b 2 \alpha_n(x) P_n(x) \exp \left[\int_0^x 2 \alpha_n(x) dx \right] dx \quad (4C.45)$$

where

$$\tau_c = \int_0^b 2 \alpha_n(x) dx \quad (4C.46)$$

Now we will apply the boundary conditions for Equation 4C.45 to solve for the constant A and to determine the physical meaning of the other terms. It should be pointed out that the line attenuation, $\alpha_n(x)$, and the line emission power, $P_n(x)$, are generally functions of position and must be kept under the integral sign. For a line of zero length, $b = 0$, the power available at the output is simply P_s so that:

$$P_{nt} = A = P_s \quad \text{when } b = 0. \quad (4C.47)$$

Total line loss is computed by integrating the attenuation over the total line length

$$N = \exp \left[\int_0^b 2 \alpha_n(x) dx \right] = e^{2 \alpha_o b} = e^{\tau_c} \quad (4C.48)$$

where $\alpha_o = \frac{1}{b} \int_0^b \alpha_n(x) dx$ the average line attenuation in nepers-

per-unit-length

b = Total line length

N = Line loss factor.

For notational simplicity we will let the attenuation of a line of length, x , be:

$$N_x = \exp \left[\int_0^x 2 \alpha_n(x) dx \right] \quad (4C.49)$$

Now Equation 4C.45 can be written in the form:

$$P_{nt} = \frac{1}{N} \left[P_s + \int_0^b 2 \alpha_n(x) P_n(x) N_x dx \right] \quad (4C.50)$$

Since the noise powers are all proportional to a noise temperature (Nyquist representation for thermal noise),

$$P_{nt} = k T_{nt} \Delta f$$

$$P_s = k T_s \Delta f$$

$$P_n(x) = k T_n(x) \Delta f$$

we can obtain the expression for noise temperature at the output by dividing Equation 4C.50 by $k\Delta f$ to give:

$$T_{nt} = \frac{1}{N} \left[T_s + \int_0^b 2 \alpha_n(x) T_n(x) N_x dx \right] \quad (4C.51)$$

For the special case where the line attenuation-per-unit-length and the line temperature are constants we have

$$\alpha_n(x) = \alpha_o, \quad \text{a constant}$$

$$T_n(x) = T_c, \quad \text{a constant}$$

and the integral in Equation 4C.51 becomes:

$$2\alpha_0 T_c \int_0^b N_x dx = 2\alpha_0 T_c \int_0^b e^{2\alpha_0 x} dx = \left[e^{2\alpha_0 b} - 1 \right] T_c \quad (4C.52)$$

Equation 4C.51 may now be written in two forms as

$$T_{nt} = T_s / N + T_c (1 - 1/N) \quad (4C.53)$$

or

$$T_{nt} = T_s e^{-\tau_c} + T_c (1 - e^{-\tau_c}) \quad (4C.54)$$

where $N = e^{\tau_c}$ and $\tau_c = 2\alpha_0 b$.

The nepers attenuation of the line, τ_c , is called the optical depth in astronomy. An optical depth of unity corresponds to a reduction in the source noise power, P_s , of $1/e$. It should be noted that Equation 4C.51 is an exact expression for computing the effective noise temperature for any distribution of line temperature and attenuation factor while Equations 4C.53 and 4C.54 are valid only for attenuation and temperature constant and independent of x .

Equation 4C.53 is often written in any one of the three forms (compare Figure C-9)

$$T_{nt} = \frac{1}{N} \left[T_s + T_c (N-1) \right] \quad (4C.55a)$$

$$T_{nt} = T_c + \frac{1}{N} (T_s - T_c) \quad (4C.55b)$$

$$T_{nt} = \epsilon T_s + (1 - \epsilon) T_c, \quad \left(\epsilon = \frac{1}{N} \right) \quad (4C.55c)$$

where T_s = Source temperature, $^{\circ}\text{K}$
 T_c = Constant line temperature, $^{\circ}\text{K}$
 $N = e^{2\alpha_o b}$, line loss factor
 $\epsilon = 1/N$, Transmission efficiency ($0 \leq \epsilon \leq 1$)
 α_o = Constant line attenuation in nepers per unit length.

For the matched, homogeneous transmission line the total line loss factor is called flat loss and can be computed in db as:

$$\text{Flat loss in db} = 10 \log_{10} N = 20 \alpha_o b \log_{10} e. \quad (4C.56)$$

Noise due to attenuation has also been discussed in Kraus (1966, p. 261). Stelzried (1968) shows an alternate derivation to Equation 4C.53 and also shows solutions to Equation 4C.51 for temperature and attenuation distributions that are not constant.

The second term of Equation 4C.53 can be thought of as additive noise in the system i.e., the noise power added to the noise source by the transmission line. Notice that for the special case where the transmission line and the noise source are at the same temperature ($T_s = T_c$):

$$T_{nt} = T_s \quad \text{and} \quad P_{nt} = P_s. \quad (4C.57)$$

The results for the equivalent noise temperature of a noise source as seen through a lossy transmission line will now be summarized and some useful limiting cases presented. The equation that will be used is

$$T_{nt} = \epsilon T_s + T_c (1 - \epsilon) \quad (4C.55c)$$

where T_{nt} = Noise temperature of a noise source as seen through a lossy transmission line

T_s = Noise temperature of the source

T_c = Uniform noise temperature of the transmission line

$\epsilon = \frac{P_{out}}{P_{in}}$, the transmission efficiency ($0 \leq \epsilon \leq 1$).

The transmission efficiency, $\epsilon = e^{-2\alpha_0 b}$, accounts for the flat loss or insertion loss of the transmission line. A value of $\epsilon = 0$ corresponds to an infinite loss while $\epsilon = 1$ is a lossless line. The following limits are observed:

a. Infinite line

$$\lim_{\epsilon \rightarrow 0} T_{nt} = T_c$$

b. Lossless line

$$\lim_{\epsilon \rightarrow 1} T_{nt} = T_s$$

c. Line temperature equals source temperature

$$\lim_{T_c \rightarrow T_s} T_{nt} = T_s$$

d. Transmission line at cryogenic temperatures

$$\lim_{T_c \rightarrow 0} T_{nt} = \epsilon T_s$$

e. Zero source temperature

$$\lim_{T_s \rightarrow 0} T_{nt} = T_c (1 - \epsilon).$$

Figure C-20 is a plot of Equation 4C.55c normalized with respect to the source temperature, T_s .

$$\frac{T_{nt}}{T_s} = \frac{T_c}{T_s} + \epsilon \left(1 - \frac{T_c}{T_s}\right) \quad (4C.58)$$

The effect of a lossy, noisy transmission line on the noise temperature of a receiving system will now be presented with Figure C-19 defining the terms.

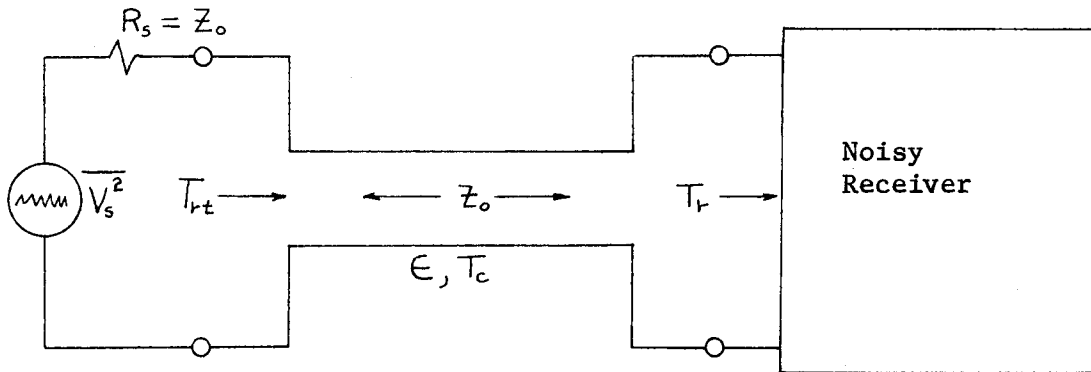


Figure C-19. System Noise Temperature and Transmission Line Noise

The total receiver noise temperature and noise factor at the source terminals can be obtained by considering the transmission line to be a resistive attenuator (unity SWR) and letting $\epsilon = 1/N$. This will allow the use of Equations 4C.35 with $|H(\omega)|^2 = 1$ to give:

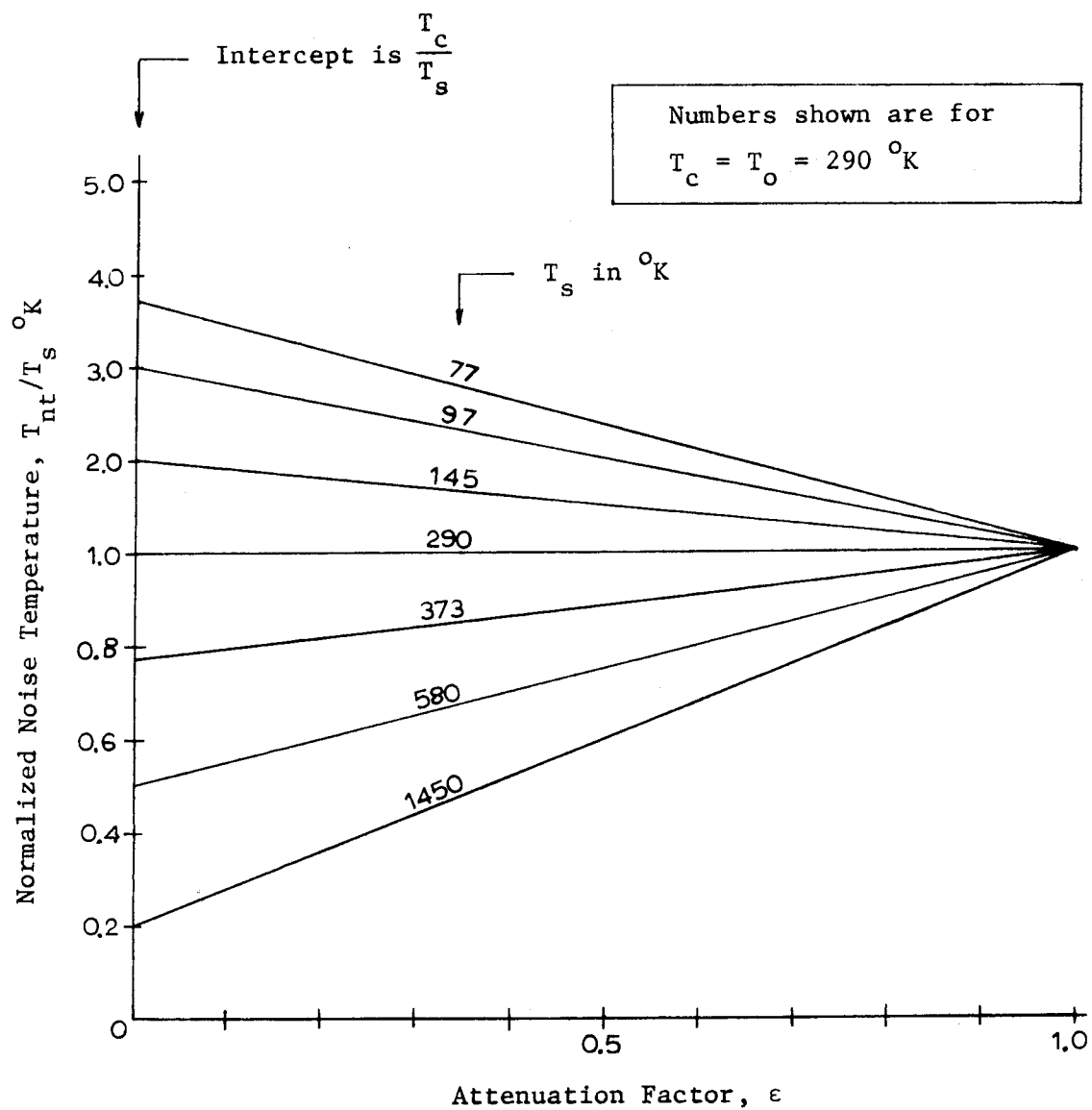


Figure C-20. Noise Temperature of Noise Source Through a Lossy and Noisy Transmission Line

$$F_{rt} = 1 + \frac{T_r}{\epsilon T_o} + \frac{T_c}{T_o} \left(\frac{1}{\epsilon} - 1 \right) \quad (4C.59a)$$

$$T_{rt} = \frac{T_r}{\epsilon} + T_c \left(\frac{1}{\epsilon} - 1 \right) \quad (4C.59b)$$

The noise temperature is also seen in the alternate forms (compare Equations 4C.55 with $\epsilon = 1/N$):

$$T_{rt} = \frac{T_r + T_c (1 - \epsilon)}{\epsilon} \quad (4C.60a)$$

$$= T_r + (T_c + T_r)(N - 1) \quad (4C.60b)$$

$$= N T_r + T_c (N - 1) \quad (4C.60c)$$

The noise that is added by the transmission line is represented by the factor $(T_c + T_r)(N - 1)$. Sometimes the factor $T_c(N - 1)$ is referred to as the noise temperature of an attenuator because it is the additive noise after accounting for the effect of flat loss.

The results for the total receiver noise temperature at the source terminals as seen through a lossy transmission line will now be summarized and some useful limiting cases presented. The equation that will be used is

$$T_{rt} = T_r + (T_c + T_r)(N - 1) \quad (4C.61)$$

where T_{rt} = Total receiver noise temperature as seen through
a lossy transmission line

T_r = Receiver noise temperature at the receiver
terminals

T_c = Uniform noise temperature of the transmission line

$N = 1/\epsilon$, Line loss factor ($1 \leq N \leq \infty$).

The following limits are observed:

a. Large line loss

$$\lim_{N \gg 1} T_{rt} = N (T_c + T_r)$$

b. Lossless line

$$\lim_{N \rightarrow 1} T_{rt} = T_r$$

c. Line at cryogenic temperatures

$$\lim_{T_c \rightarrow 0} T_{rt} = N T_r$$

d. Noiseless receiver

$$\lim_{T_r \rightarrow 0} T_{rt} = T_c (N - 1)$$

e. Low-noise receiver

$$\lim_{T_r \ll T_c} T_{rt} = T_r + T_c (N - 1)$$

f. High-noise receiver

$$\lim_{T_r \gg T_c} T_{rt} = N T_r.$$

Figure C-21 is a plot of Equation 4C.61 normalized with respect to receiver noise temperature, T_r .

$$\frac{T_{rt}}{T_r} = 1 + \left(\frac{T_c}{T_r} + 1 \right) (N - 1) \quad (4C.62)$$

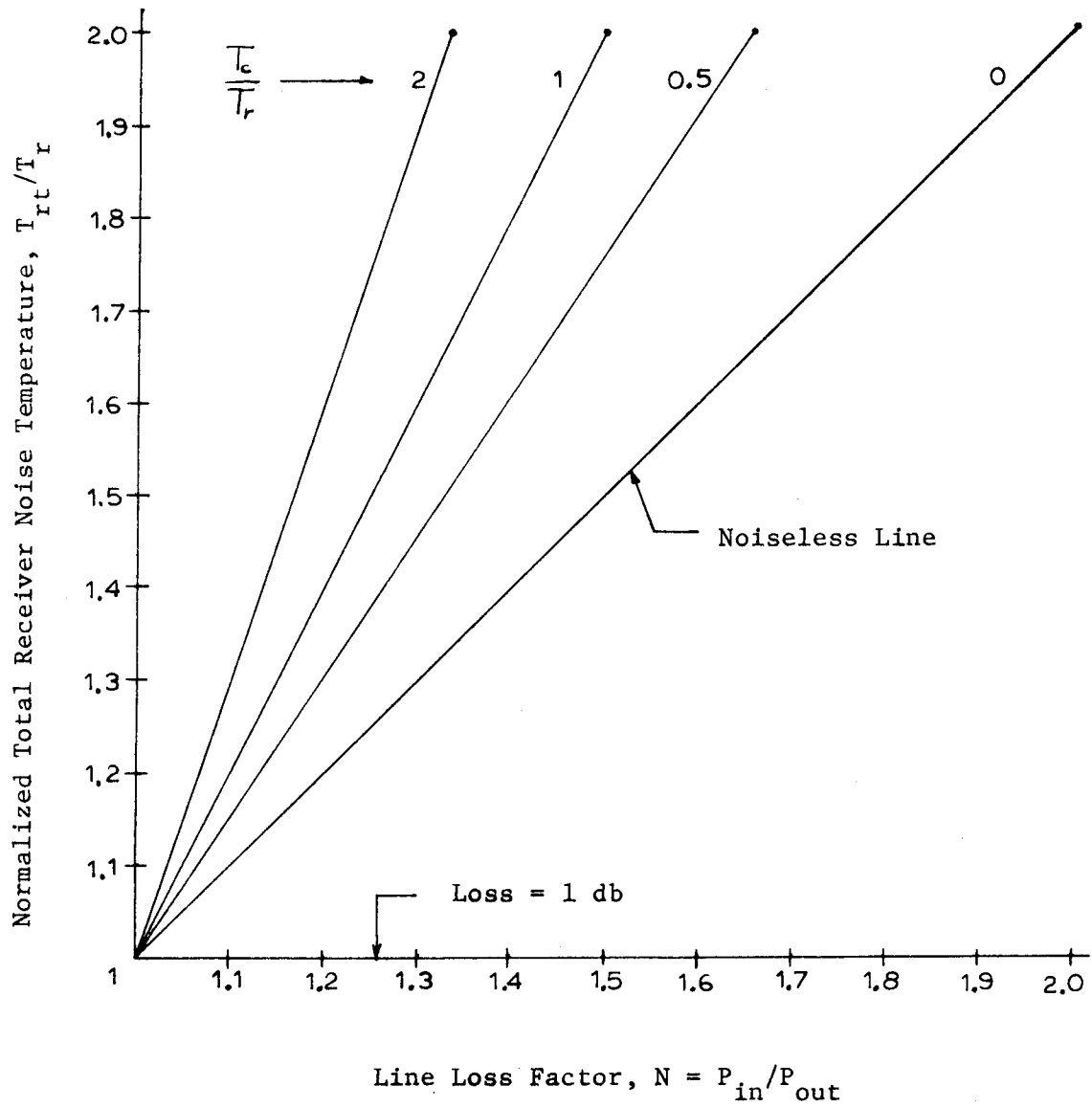


Figure C-21. Total Receiver Noise Temperature, Including Noisy Transmission Line

Figure C-21 shows the effect of any resistive attenuation device, with a flat loss N , on the total receiver noise temperature.

By definition, the total receiver noise figure is:

$$NF_{rt} = 10 \log \left(1 + \frac{T_{rt}}{T_o} \right) = 10 \log \left[1 + \frac{T_r}{T_o} + \frac{T_c + T_r}{T_o} (N-1) \right] \text{ db} \quad (4C.63)$$

For the particular circumstance where the temperature of the transmission line is standard temperature ($T_c = T_o$), the noise figure becomes

$$NF_{rt} = 10 \log \left[N \left(1 + \frac{T_r}{T_o} \right) \right] = NF_r + 10 \log N \text{ db} \quad (4C.64)$$

with NF_r the receiver noise figure.

This leads to the widely used rule-of-thumb that the total receiver noise figure as seen through a lossy transmission line is the sum of the receiver noise figure at the receiver terminals plus the line flat loss in db. Although this rule-of-thumb is valid only when $T_c \approx T_o$, it can generally be used for rough calculations and, for laboratory measurements, is usually adequate.

5. Antenna noise

The noise temperature of a receiving antenna is determined by the noise environment in which the antenna is operating. Under worst conditions this noise comes from man-made and natural sources while under the best conditions the noise temperature is due to only natural sources such as cosmic noise and ground temperature. For theoretical considerations the noise temperature is determined by the integrated noise

brightness distribution from all parts of the antenna's environment while in practice the actual value is approximately calculated by considering only the major sources of noise. For precision work, the noise temperature must be measured (Chapter IX-D).

In the theoretical case of an ideal isotropic antenna in free space, the antenna noise temperature is zero. The isotropic antenna in homogeneous space, where cosmic noise is uniformly distributed, has a noise temperature equal to the space noise temperature. In actual space, the noise is due to a large number of thermal and non-thermal sources and these sources have an almost random distribution. For these conditions the antenna noise temperature is the integrated noise brightness distribution.

When a beam antenna is employed, the noise temperature is determined by the temperature of the noise sources within the main beam. For example, a narrow beam antenna, with 10 db gain, in a uniform noise environment will have a noise temperature the same as that of an isotropic antenna but the received signal from the beam direction will be ten times larger, thus increasing the signal-to-noise ratio. In contrast, a broad beam antenna directed at a point source signal will receive a large noise contribution from noise sources at large angular distances from the signal source. When this happens, a narrower antenna beam can often bring a good improvement in the signal-to-noise ratio.

For radio telescope applications where the main beam is pointed at the sky, the minor lobes will be pointed in undesirable and often noisy directions such as the ground. When the main beam is pointed

toward a cold part of the sky, this noise contribution of the minor lobes becomes very significant. Because of this, it is desirable to reduce the minor lobe response as much as possible or at least when this cannot be done, the antenna should be designed to place the minor lobes in low-temperature directions.

The six major noise sources which contribute to the equivalent noise temperature of an antenna are solar radio noise, cosmic noise*, man-made noise, atmospheric noise (static), ground noise, and antenna conductor noise. Solar radio noise is a result of intense radio emission from the hot sun. Neglecting solar flares, this noise emission is so intense that it may produce several degrees of noise temperature in the antenna. Quite often the intensity is high enough that solar noise coming in on a minor lobe can completely mask the weak, desired signal on the main lobe. Obviously, solar noise is reasonably predictable and can often be avoided (such as night operation). Cosmic noise is the result of powerful thermal and non-thermal radio noise emitters which occur throughout the universe. These sources account for much of the antenna noise in the high HF and low VHF frequencies. Man-made noise is discussed in a previous section. Atmospheric noise or static is a problem at the frequencies below 20 MHz and is the exclusive limit of sensitivity at the frequencies below 5 MHz. This radio noise comes from disturbances in the earth's atmosphere and may be in the form of a steady hiss, a popping noise, whistlers, and lightning discharges.

*The term cosmic noise will be used to denote extraterrestrial noise other than the sun.

Ground noise is a result of the antenna receiving thermal radiation from the ground. This can be minimized by proper antenna directivity and shielding. The thermal noise contributed by the antenna conductor resistivity is usually so small that it can be neglected. This is especially true when the antenna conductor resistance is small compared with the antenna radiation resistance.

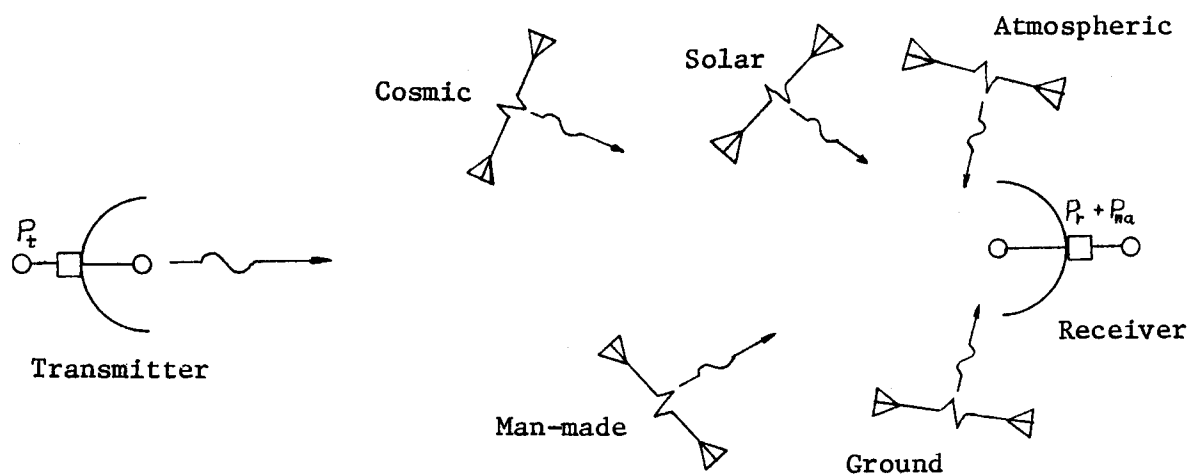


Figure C-22. Schematic Representation of Antenna Environment Showing Signal and Noise Sources

Figure C-22 is a schematic representation of the noise sources that influence the low-noise performance of a receiving antenna. For purposes of discussion, the noise due to extraterrestrial sources (solar and cosmic) and atmospheric sources will be called sky noise. The antenna, as an electromagnetic transducer, will be represented by the two-port equivalent circuit of Figure C-23.

The following terms will be defined:

$$R_{ra} = \text{Antenna radiation resistance, ohms}$$

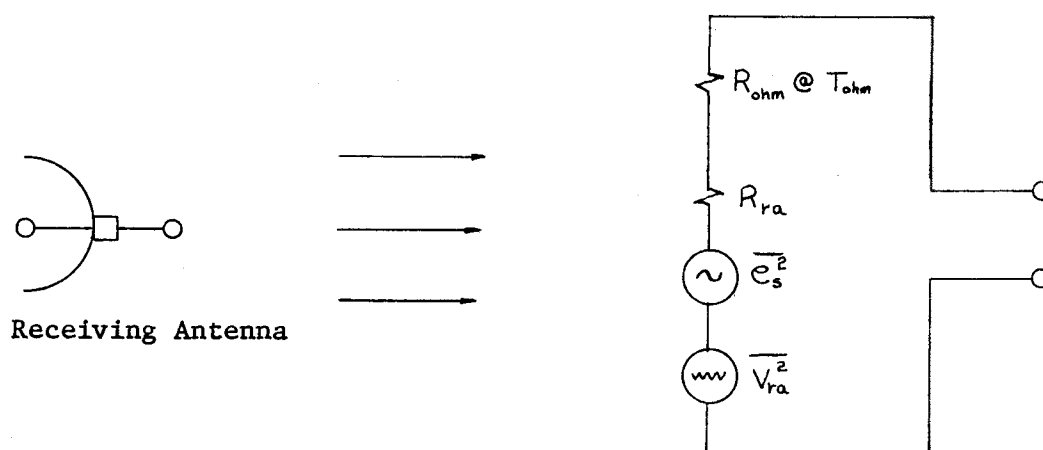


Figure C-23. Two-port Equivalent Circuit for a Receiving Antenna in a Noisy Environment

R_{ohm} = Ohmic loss resistance of the antenna, ohms

T_{ohm} = Physical temperature of the antenna conductors, $^{\circ}\text{K}$

$\overline{e_s^2}$ = Mean-square signal voltage, volts²

$\overline{V_{ra}^2}$ = Mean-square noise voltage due to all noise sources external to the antenna, volts².

The mean-square noise voltage is represented by the Nyquist equivalent

$$\overline{V_{ra}^2} = 4k(T_{sky} + T_g + T_{mm}) R_{ra} \Delta f \quad (4C.65)$$

where

$$T_{sky} = T_{solar} + T_{cosmic} + T_{atmospheric}$$

T_g = Antenna temperature contribution due to ground noise

T_{mm} = Antenna temperature contribution due to man-made noise.

The temperatures in Equation 4C.65 are not the actual temperatures of the various sources but are the equivalent antenna temperatures induced in the antenna by the noise flux from these sources. The physical temperature and the equivalent temperature are related and can be calculated in special cases (Kraus, 1966, Sec. 3-18) but for the most part, the equivalent temperatures must be measured. To do antenna calculations it is convenient to reduce the circuit of Figure C-23 even further and develop an equivalent signal source to represent the antenna. This antenna equivalent is shown in Figure C-24.

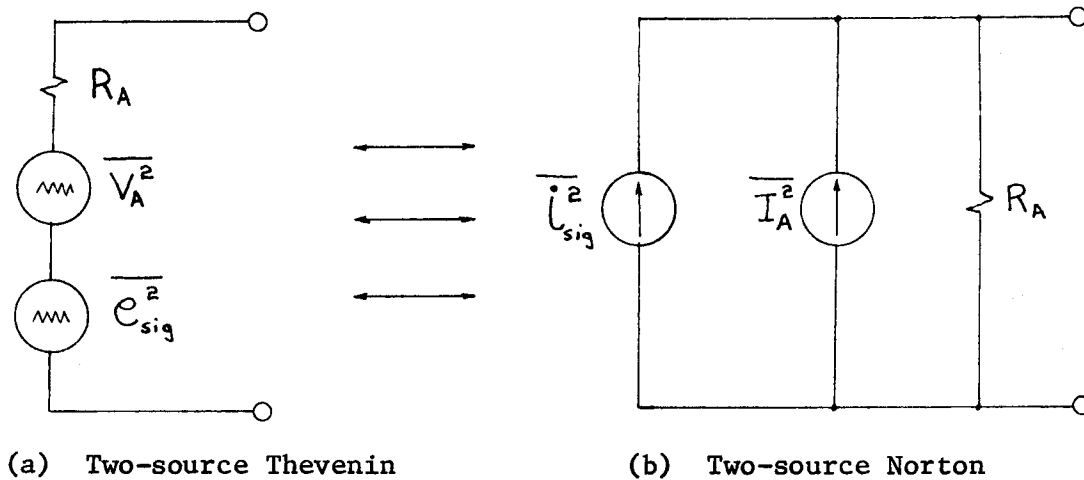


Figure C-24. Signal Source Equivalent Circuit for a Receiving Antenna

The following terms for Figure C-24 are defined:

$$R_A = R_{ra} + R_{ohm}, \text{ the total antenna terminal resistance which is the source resistance for the receiver}$$

$\overline{V_a^2} = 4 k T_A R_A \Delta f$, the total mean-square antenna noise voltage for all antenna noise sources.

The total antenna noise temperature is determined by combining the mean-square noise voltage contributions from $\overline{V_{ra}^2}$ and R_{ohm} . T_A is determined as follows:

$$\overline{V_a^2} = \overline{V_{ra}^2} + \overline{V_{ohm}^2} = 4k (T_{ra} R_{ra} + T_{ohm} R_{ohm}) \Delta f \quad (4C.66)$$

Setting $\overline{V_a^2} = 4 k T_A R_A \Delta f$ and solving for T_A yields

$$T_A = \frac{T_{ra} R_{ra} + T_{ohm} R_{ohm}}{R_{ra} + R_{ohm}} \quad (4C.67)$$

where $T_{ra} = T_{sky} + T_g + T_{mm}$.

If the antenna ohmic loss factor is low (Equation A.20, Chapter III) then the total antenna noise temperature is approximated by ($R_{ohm} \ll R_{ra}$):

$$\begin{aligned} T_A &\approx T_{ra} + T_{ohm} \frac{R_{ohm}}{R_{ra}} \\ &\approx T_{sky} + T_g + T_{mm} + T_{ohm} \frac{R_{ohm}}{R_{ra}} \\ &\approx T_{solar} + T_{cosmic} + T_{atmospheric} + T_g + T_{mm} \\ &\quad + T_{ohm} \frac{R_{ohm}}{R_{ra}} \end{aligned} \quad (4C.68)$$

For most practical applications, Equation 4C.68 will represent the total effective antenna noise temperature for all calculations. It is important to note that, unless all other sources of noise are extremely low, the noise temperature of the antenna conductors have a very small contribution to the effective antenna noise temperature. The antenna noise equivalent circuit of Figure C-24 is used in the derivation of the relationship between blackbody radiation and circuit noise. This relationship is demonstrated in Kraus (1966, Sec. 3-18) and Lawson and Uhlenbeck (1950, Sec. 5-2).

Numerous graphs are available on the amplitude of sky noise for various conditions. While none of these graphs will allow highly accurate calculations, they are useful for obtaining an estimate of the magnitude of sky noise. Figure C-25 is a plot of sky noise temperature as a function of frequency for an idealized antenna. The graph is a composite of data obtained from Skolnik (1970, p. 2-32), Kraus, (1966, p. 237) and International Telephone and Telegraph Corp. (1956, Ch. 25). For data at frequencies below 10 Mhz, consult the curve in Henney (1959, p. 19-16).

In this context, an idealized antenna is a pencil beam antenna with no ohmic losses and zero ground noise. The antenna is pointed toward the sky. The wide variation in sky temperature at any one frequency is caused by the variable factors of beam direction and time of day. Generally the zenith angle affects the atmospheric noise contribution while beam direction affects the galactic noise. Naturally the time of day and level of sunspot activity will affect the sun noise contribution. The noise temperature of an actual receiving antenna can

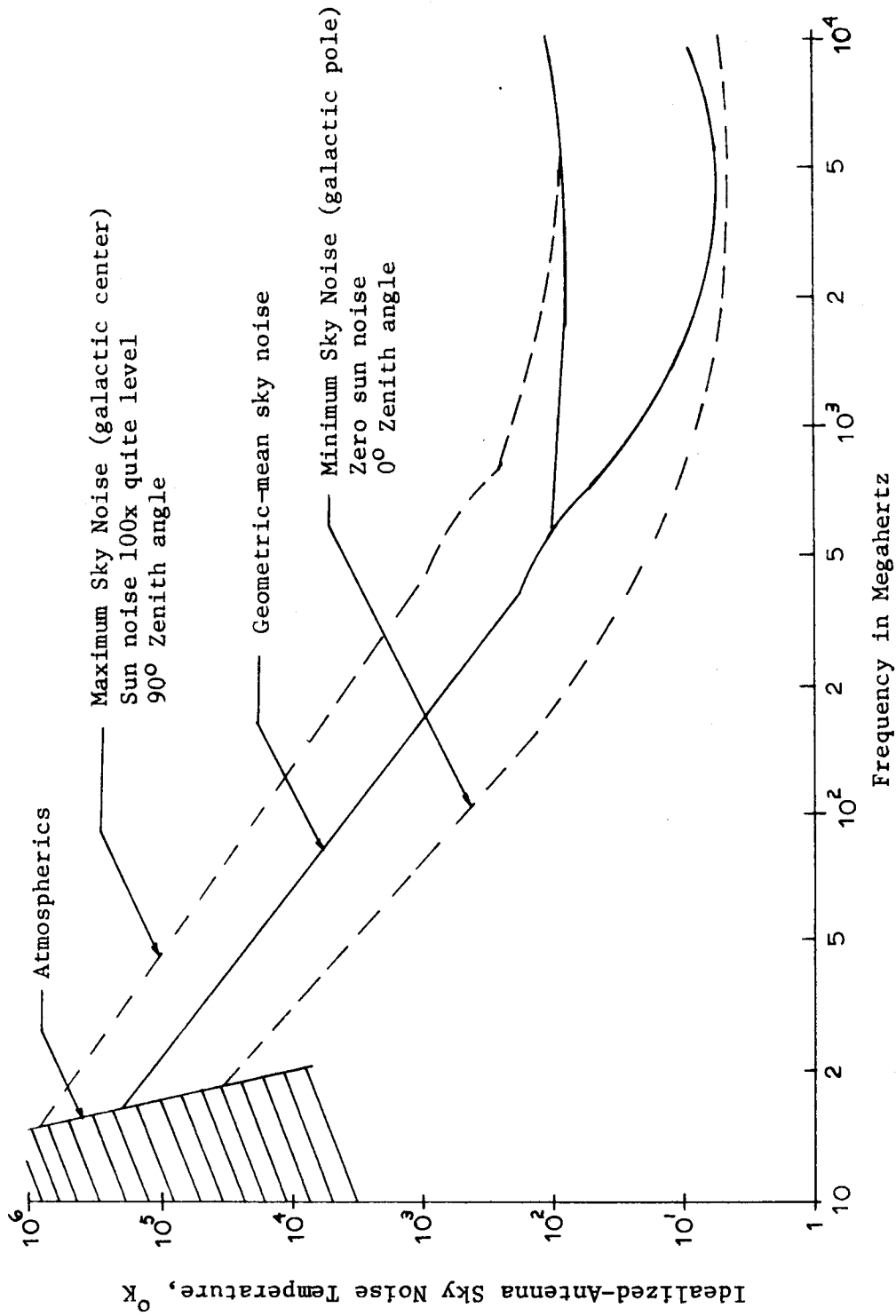


Figure C-25. Antenna Sky Noise Temperature as a Function of Frequency for an Idealized Antenna

be considerably lower than the temperature of Figure C-25 because the main lobe response is not pointed at the sky. The noise temperature of the graph does give a good approximation to the sky noise temperature for a horizontally oriented dipole.

Even if it were possible to have a perfectly noiseless receiver, communication over long distances would still be plagued by antenna noise. By taking into consideration the ideas developed in Chapter III for antennas it is possible to discuss the signal-to-noise ratio for an antenna. The available signal power for a receiving antenna is determined by Equation A.24 in Chapter III

$$\frac{\overline{e_s^2}}{4R_A} = W_r = \frac{\lambda^2}{4\pi} S_r G_r P_r(\theta_r, \phi_r) \quad (4C.69)$$

where λ = Operating wavelength

S_r = Signal power density at the receiving antenna

G_r = Antenna gain

$P_r(\theta_r, \phi_r)$ = Normalized power pattern.

While the available noise power in a bandwidth Δf is,

$$\frac{\overline{V_a^2}}{4R_A} = k T_A \Delta f \quad (4C.70a)$$

We are now assuming that the antenna noise is white for the receiver noise bandwidth Δf . Actually the antenna noise temperature is a function of frequency and the exact expression is:

$$\frac{\overline{V_a^2}}{4 R_A} = k \int_0^{\infty} \frac{G(f)}{T_A(f) G_{\max}} df \quad (4C.70b)$$

where $\frac{G(f)}{G_{\max}}$ is the normalized receiver frequency response (Appendix, Part B).

The maximum signal-to-noise ratio for the antenna is the ratio of the two powers ($P_r(\theta_r, \phi_r) = 1$):

$$\text{Antenna SNR} = \frac{\lambda^2}{4\pi} \frac{S_r G_r}{k T_A \Delta f} \quad (4C.71)$$

In radio astronomy applications, the "signal" is also "white" noise and the antenna SNR can also be written as

$$\text{Antenna SNR} = \frac{T_{ns}}{T_A} \quad (4C.72)$$

where T_{ns} is the antenna noise temperature due only to the signal and T_A is the total antenna noise temperature minus that due to the signal. The antenna SNR is also written with the received power density expressed in terms of the transmitter characteristics and path loss (Equation A.25, Chapter III):

$$\text{Antenna SNR} = \left(\frac{\lambda}{4\pi r_o} \right)^2 \frac{W_t G_t G_r}{k T_A \Delta f} K_s \quad (4C.73)$$

A similiar form of this equation can be found in Blake (1972).

D. Receiving System Noise Temperature

The antenna SNR and antenna noise temperature do not tell the whole story of receiving system sensitivity. It is the system noise temperature, T_{sys} , which is made up of noise from the antenna, feed system, and receiver which will determine the sensitivity and SNR of the communication system. The system noise temperature is all the noise of the system referred to the antenna and referenced with respect to the antenna resistance. Figure D-1 shows an elementary receiving system with the basic components that determine system noise temperature; antenna, feed system, and receiver. We will show in this section how to calculate the system noise temperature and noise factor when the noise characteristics of the basic components are known.

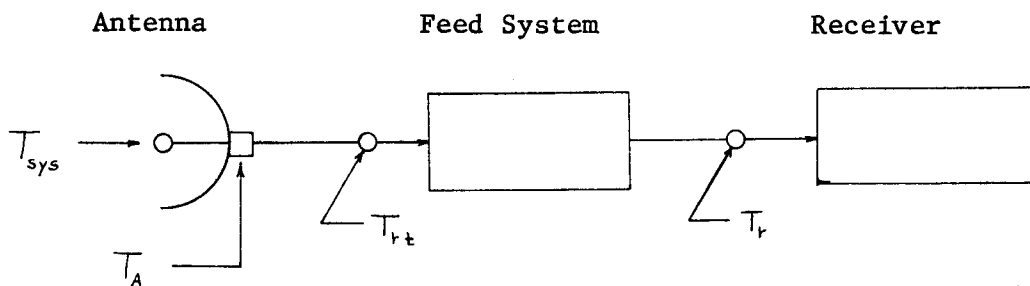


Figure D-1. Elementary Receiving System for System Noise Temperature Calculations

The important factors to be determined are the effective input noise temperature at the receiver terminals T_r , the total receiver noise temperature (which includes the feed system), T_{rt} , and the antenna noise temperature, T_A . The simplest equation for system noise temperature is:

$$T_{sys} = T_A + T_{rt} \quad (4D.1)$$

When T_A and T_{rt} are measured values, we are finished with system noise temperature calculations but usually we have to calculate the value of T_{rt} or in a design problem we make tradeoffs which affect T_A and T_{rt} and we wish to calculate the predicted noise temperature.

As a simple example consider the case when the feed system is a transmission line of flat loss N , connecting receiver and antenna, and the transmission line meets the criteria establish for Equation 4C.60c. The system noise temperature is:

$$T_{sys} = T_A + T_{rt} = T_A + T_r N + T_c (N-1) \quad (N \gg 1) \quad (4D.2)$$

The system noise factor is:

$$F_{sys} = 1 + \frac{T_{sys}}{T_o} \quad (4D.3)$$

For this example it has already been shown that the total receiver noise figure is:

$$NF_{rt} = NF_r + 10 \log N \quad (T_c \equiv T_o) \quad (4C.64)$$

and for noise figure measurements of the receiver it is possible to measure NF_{rt} and simply subtract the cable flat loss. This can be helpful in bench testing receiving systems where it is sometimes desirable to separate the receiver and noise source or when a resistive attenuator (Pad) is inserted between noise source and receiver.

For a receiving system which has more than one lossy element between the basic receiver and the antenna, it is not a simple matter to

compute the total receiver noise temperature, T_{rt} . The lossy elements usually consist of; antenna relays, coax connectors, sections of transmission line, and rf filters. When all the lossy elements are at the same temperature it would be possible to add up all the losses and compute a total attenuation, N_T , and compute the system noise temperature as before. This scheme will not work for the more general case where each lossy element is at a different temperature. The solution to the problem of different temperatures requires the application the theory presented in Chapter IV-C. The exact analysis involves the evaluation of integral equations by digital computer except in a few special cases. The exact approach is not worth the effort for most applications. A much simpler procedure will now be presented which can give the total receiver noise temperature to engineering accuracy. The scheme employed is to use a recursive formula which is valid for a cascade of lossy elements when the SWR is low. The figure below will illustrate this procedure.

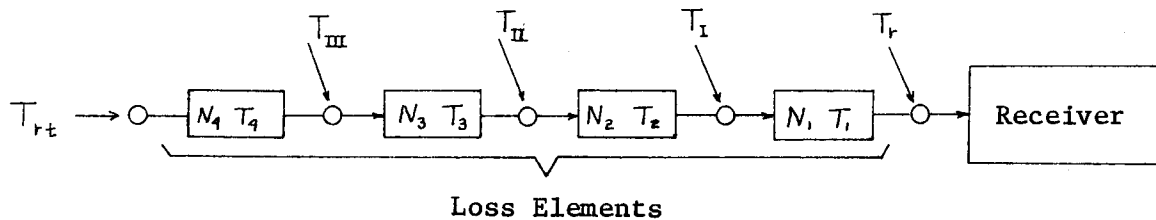


Figure D-2. Total Receiver Noise Temperature Calculations

Now we apply a slightly different form of Equation 4D.2 to get the following recursion formulas:

Example:

$$\begin{aligned}
 T_I &= T_r + (T_1 + T_r)(N_1 - 1) & T_I &= 200 + (290 + 200)(1.1 - 1) \\
 T_{II} &= T_I + (T_2 + T_I)(N_2 - 1) & T_{II} &= 249 + (290 + 249)(1.26 - 1) \\
 T_{III} &= T_{II} + (T_3 + T_{II})(N_3 - 1) & T_{III} &= 389 + (240 + 389)(1.1 - 1) \\
 T_{rt} &= T_{III} + (T_4 + T_{III})(N_4 - 1) & T_{rt} &= 452 + (240 + 452)(1.58 - 1) \\
 & & T_{rt} &= 853 \text{ } ^\circ\text{K} \quad NF_{rt} = 5.86 \text{ db}
 \end{aligned}$$

(4D.4)

The accuracy of the results obtained with the above recursion formulas can be contrasted with the results obtained by a simpler and often used procedure which requires only a knowledge of element losses. For this calculation the loss elements are assumed to be at standard temperature ($T_c = T_o$) and the total loss of the feed system is the product of the individual losses. With these assumptions we get the following equations:

$$\begin{aligned}
 N_T &= N_1 N_2 N_3 N_4 \\
 T_{rt} &= T_r N_T + T_o (N_T - 1) \quad \text{assume } (T_c = T_o) \\
 & & & (4D.5) \\
 T_{rt} &= 200 (2.42) + 290 (1.42) = 484 + 412 = 896 \text{ } ^\circ\text{K} \\
 NF_{rt} &= 6.12 \text{ db} \quad \text{Error} = + 0.26 \text{ db or } 45 \text{ } ^\circ\text{K}
 \end{aligned}$$

It is important to note that the Equations 4D.4 and 4D.5 are valid only assuming that the SWR at each point in the system is essentially unity.

Once the system noise temperature is obtained, it is a simple matter to obtain the system signal-to-noise ratio which is the ratio of antenna signal power to system noise power:

$$\text{System SNR} = \frac{W_r}{k T_{\text{sys}} B}$$

Substitution for signal power, W_r , using Equation A.20 of Chapter III gives

$$\text{System SNR} = \frac{\frac{\lambda^2}{4\pi} S_r G_r}{k T_{\text{sys}} B} \quad (4D.6)$$

where S_r is the average power density at the receiving antenna and G_r is the receiving antenna gain. Also by applying the procedure used for Equation 4C.71 and using Equation A.25 from Chapter III it is possible to express the system SNR in terms of the transmitter and signal path characteristics--when they are known. This substitution gives:

$$\text{System SNR} = \left(\frac{\lambda^2}{4\pi r_o} \right) \frac{W_t G_t G_r}{k T_{\text{sys}} B} \quad (4D.7)$$

Equation 4D.7 is similiar to the radar-transmission equation (Skolnik, 1970, p. 2-4) and may be used to calculate:

- a. System SNR given the antenna gains, distance, path loss, and receiving system temperature and bandwidth
- b. Required transmitter power for a given system SNR and other factors listed in a
- c. Required antenna gains, $G_r G_t$
- d. Required system noise temperature, T_{sys}
- e. Required system noise bandwidth, B .

Solutions to the various problems enumerated above are not as readily obtained as Equation 4D.7 might indicate. One complicating factor is that antenna gain, path loss, and system noise temperature are all functions of frequency and the solutions to (4D.7) are thus also frequency dependent.

Of the various applications for (4D.7), the ones which have practical appeal are the determination of receiver power sensitivity and/or antenna gain. We will define, for purposes of this paper, a measure of receiver sensitivity to be called receiving system power sensitivity, P_{rs} . The receiving system power sensitivity will be defined using the minimum acceptable system signal-to-noise ratio as follows:

$$\left(\frac{S}{N}\right)_{sys, min} = \frac{\overline{e_{sig}^2}/4R_A}{kT_{sys} B} = \frac{P_{rs}}{kT_{sys} B} \quad (4D.8)$$

where R_A is the antenna resistance and e_{sig} is the minimum acceptable open circuit signal voltage on the antenna. The equation is rewritten to show the definition as:

$$P_{rs} \triangleq kT_{sys} B \left(\frac{S}{N}\right)_{sys, min} \quad (4D.9)$$

Receiving system power sensitivity is defined because there is a need to be able to specify the amount of available signal power at the antenna terminals needed to give a specified signal-to-noise ratio. Equation 4D.9 shows that the required P_{rs} can be determined from the required

system signal-to-noise ratio, system noise temperature and system noise band-width.

The actual receiving system SNR must always be greater than the minimum or the system will not perform properly. The actual received power is

$$P_{ac} = k T_{sys} B \left(\frac{S}{N} \right)_{ac} \quad (4D.10)$$

where the subscript "ac" denotes actual values. As a measure of how much the actual ratio exceeds the minimum ratio we define an excess signal-to-noise ratio

$$n_m \triangleq \frac{\text{Actual system SNR}}{\text{Minimum system SNR}}$$

which can now be used to relate P_{ac} and P_{rs} as:

$$P_{ac} = n_m P_{rs} \quad (4D.11)$$

Combining Equation 4D.9 with (4D.6), (4D.7) and (4D.11) gives

$$P_{rs} = \frac{\lambda^2}{4\pi} S_r G_r \frac{1}{n_m} \quad (4D.12a)$$

or

$$P_{rs} = \left(\frac{\lambda}{4\pi r_o} \right)^2 W_t G_t G_r k_s \frac{1}{n_m}. \quad (4D.12b)$$

These equations specify the relationships between receiving system power sensitivity and the external signal parameters that will yield an excess SNR of n_m .

Equation 4D.12b is now manipulated to give the following logarithmic

$$\begin{aligned}
 \text{(db) equation: } 10 \log \eta_m = & + \left[10 \log \left(\frac{1}{P_{rs}} \right) + 10 \log W_t \right] \\
 & + \left[10 \log G_r + 10 \log G_t \right] \\
 & - \left[20 \log \left(\frac{4\pi k}{\lambda} \right) + 10 \log \left(\frac{1}{k_s} \right) \right] \quad (4D.13a)
 \end{aligned}$$

The term on the left hand side is called the system SNR margin, the first term in brackets on the right is the receiver/transmitter factor, the second is the antenna gain factor and the third is the path attenuation factor.

These definitions (all terms in db) are summed up in Equation 4D.13b:

$$\begin{aligned}
 \text{System SNR margin} = & + (\text{Receiver/Transmitter factor}) \\
 & + (\text{Antenna gain factor}) \\
 & - (\text{Path attenuation factor}) \quad (4D.13b)
 \end{aligned}$$

For a given system, these factors can be used to make a graph for predicting system SNR margin. Figure D-3 is an example of such a graph.

This figure is a graphical representation of Equation 4D.13 and has been designed to show the effect of antenna gain on system SNR margin. The curve shown is a plot of path attenuation factor v.s. frequency and corresponds to the minimum acceptable SNR. Any convenient power reference may be chosen for the Receiver/transmitter factor as long as P_{rs} and W_t are consistent. In the example shown, a receiving-plus-transmitting antenna gain of 50 db yields a system SNR margin of

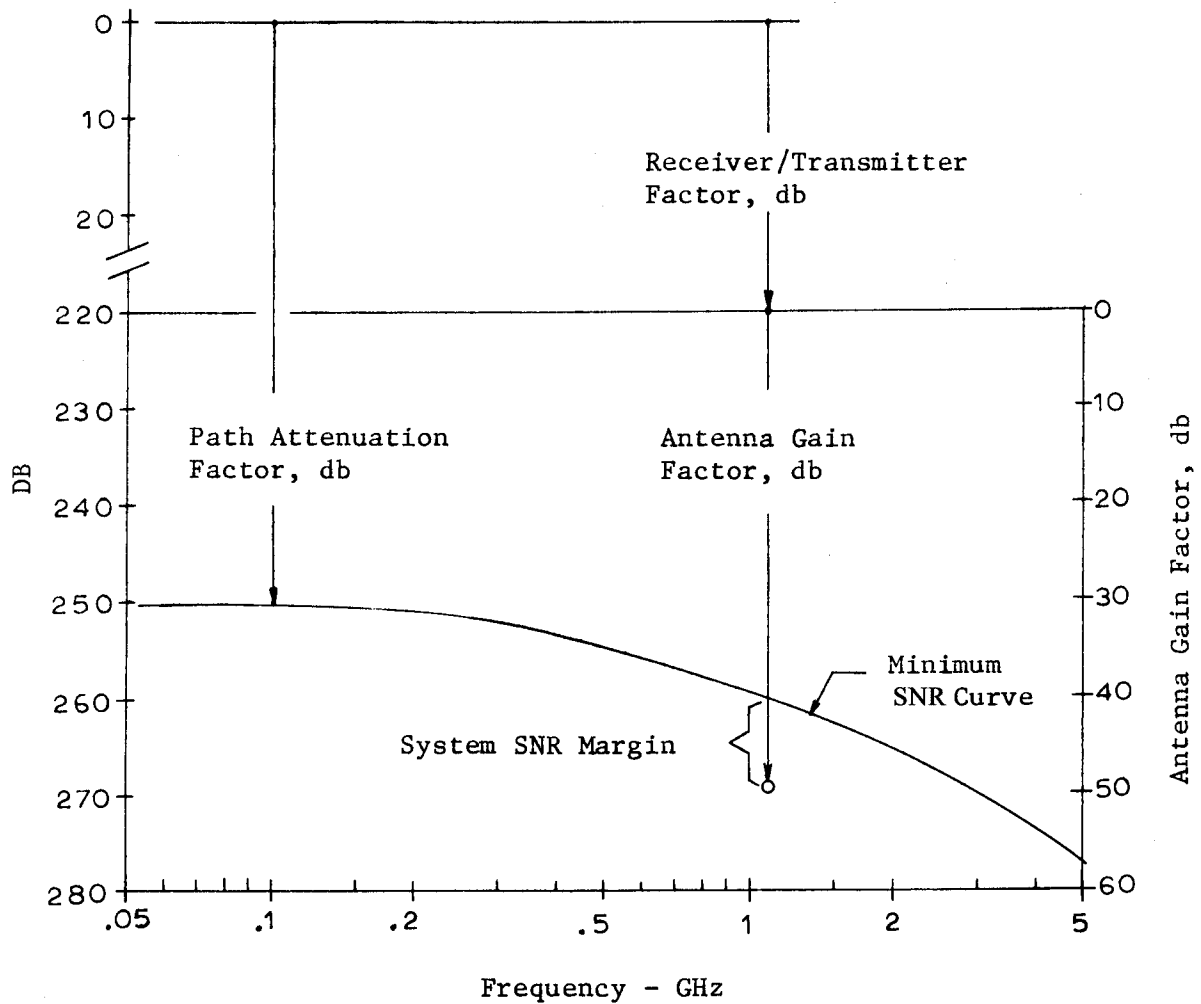


Figure D-3. Graph for Computing System SNR Margin from Antenna Gain

10 db. This graphical technique was first brought to the author's attention in an article by Ashby (1961). In Ashby's article, a graph similar to D-3 is used to determine moon relay requirements for amateur radio.

The received signal does not always have to be deterministic as implied by (4D.8) but may be a noise signal. An example of this would

be a total-power receiver (also called a radiometer) as used in radio astronomy. The signal of a radiometer can be represented by an equivalent signal noise temperature, T_{ns} , which is not included in the antenna noise temperature, T_A . The equivalent circuit of the antenna would still be represented by Figure C-24 but with the signal generator, E_{sig} , replaced with the mean-square noise signal voltage generator $\overline{V_{ns}^2} = 4 k R_A T_{ns} \Delta f$. The system SNR for a radiometer is now written:

$$\text{System SNR} = \frac{\overline{V_{ns}^2}}{\overline{V_{sys}^2}} = \frac{T_{ns}}{T_{sys}} \quad (4D.14)$$

The minimum value of T_{ns} that can be detected is called the minimum detectable noise temperature, T_{min} . The minimum detectable noise temperature, a function of T_{sys} and system SNR, is determined by the dc and ac voltage levels of the integrated detector-output. T_{min} is the value of T_{ns} that will produce a change in the detector dc output that is equal in magnitude to the low-frequency RMS noise level. A discussion of this measure of receiver sensitivity is given in Tiuri (1964) and Kraus (1966, P. 102 and Ch. 7). The minimum detectable noise temperature for a total-power receiver is

$$\Delta T_{min} = K_s T_{sys} \sqrt{\frac{2 B_L}{B_h}} \quad (4D.15)$$

where T_{sys} = Total system noise temperature, $^{\circ}\text{K}$.

B_h = Predetection noise bandwidth, Hz

B_L = Postdetection noise bandwidth, Hz

K_s = System sensitivity constant ($1 \leq K_s \leq 2\sqrt{2}$).

When the postdetection filter is an ideal integrater, Equation 4D.15 becomes

$$\Delta T_{\min} = K_s \frac{T_{\text{sys}}}{\sqrt{B_h t}} \quad (4D.16)$$

where t is the postdetection integration time. A discussion of the derivation of Equation 4D.15 will be presented in the chapter on noise power detectors.

E. Noise Theory for Two-Port Networks

The most convenient and efficient way of describing the noise performance of an active device or system of active devices is by means of a linear two-port circuit model which incorporates external noise generators. The theory to be developed is general enough that it can be applied to any linear system element which may be described by a two-port model. The basis for this approach was first examined by Rothe and Dahlke in 1956 and has since become a popular means of specifying the noise performance of RF amplifiers. What will be done in this section is to review the highlights of their original work and to include additional concepts which have since been developed. It is important that the reader understand the general approach to analyzing noise in a two-port and for this reason, it is presented in more detail than might otherwise be necessary. Although much of what is presented must, of necessity, be a paraphrasing of the original work it is hoped that it

will provide the necessary background for a more detailed study and the interested reader is encouraged to consult the original paper.

Two-port network theory is highly developed and well known for RLC passive networks and active networks which contain controlled sinewave generators. In most treatments of this topic, the noise is neglected because it is assumed to be much smaller than any practical signal. This assumption does not apply to most receiving systems, however, because the signal and the noise are often competing on a nearly equal basis. When this happens, as in the case of a low-noise RF amplifier, it is necessary to account for the noise generated internally. This can be done by applying the two-port parameter definitions (International Telephone and Telegraph Corp., 1956, Ch. 5) and accounting for the internal noise by external generators.

1. Linear two-port noise model

First consider a noisy two-port network as shown in Figure 4E-1 with appropriate conventional notation. The open-circuit and short-circuit parameters which account for both small-signal behavior and noise behavior can be written by including external noise generators as shown in Figure 4E-2. It should be noted that these generators are obtained by the direct application of two-port parameter definitions so that the generators have real physical significance and could be obtained for any network.

The two-port equations which apply are given below:

$$\begin{aligned}
 \mathbf{Z}'s \left\{ \begin{aligned} V_1 &= Z_{11} I_1 + Z_{12} I_2 + V_{n1} \\ V_2 &= Z_{21} I_1 + Z_{22} I_2 + V_{n2} \end{aligned} \right. \quad \mathbf{Y}'s \left\{ \begin{aligned} I_1 &= Y_{11} V_1 + Y_{12} V_2 + I_{n1} \\ I_2 &= Y_{21} V_1 + Y_{22} V_2 + I_{n2} \end{aligned} \right. \quad (4E.1)
 \end{aligned}$$

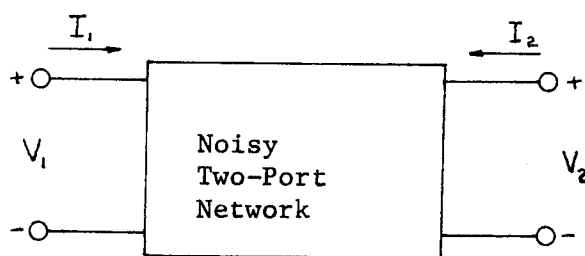


Figure 4E-1. Two-port Network Model with Internal Noise

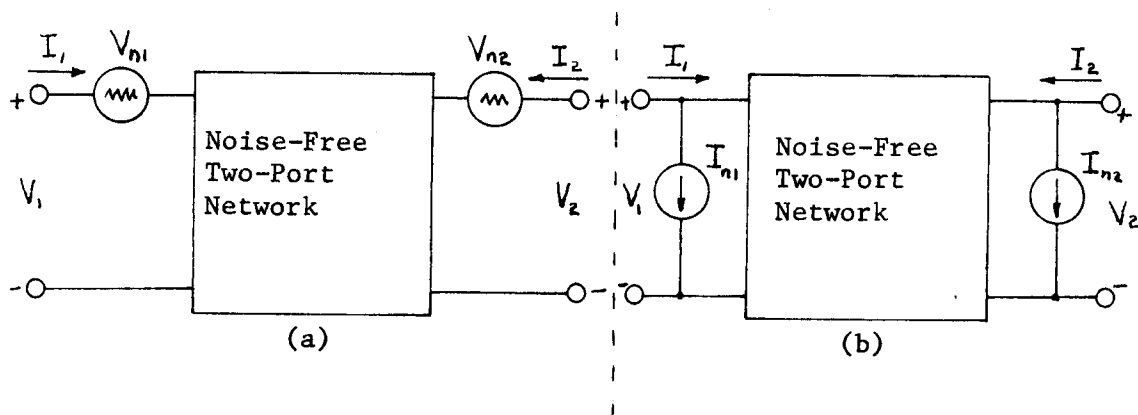


Figure 4E-2. Two-ports with Equivalent External Noise Generators

Perhaps it would be helpful to comment on the significance of the notation used for the noise generators and the mathematical qualifications necessary. The ~~two~~port parameters are, in general, complex and the noise generators are represented by the Nyquist formula:

$$\overline{V_{n1}^2} = 4kT_{n1}R_{n1}\Delta f$$

$$\overline{V_{n2}^2} = 4kT_{n2}R_{n2}\Delta f$$

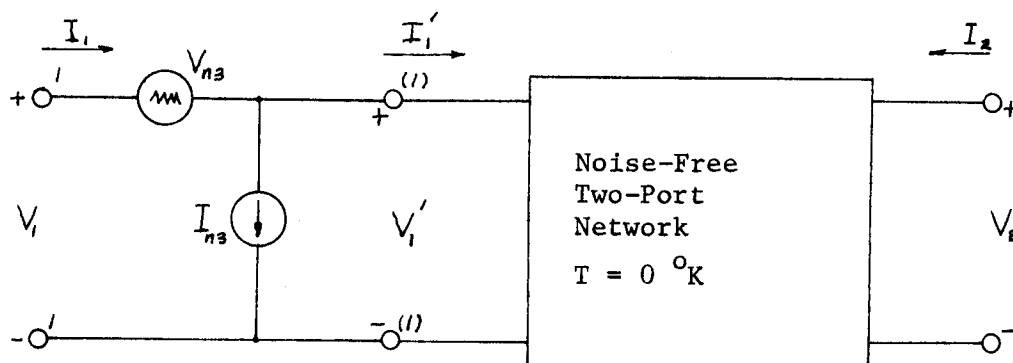
Where Δf is a infinitesimal bandwidth about some operating frequency f . Since the treatment of two-port theory will be done in the frequency domain, this representation is convenient because it allows us to use Fourier analysis techniques. This is the reason why the noise generators can be represented by simply V_{n1} and V_{n2} . The mathematical techniques employed must take into account the random nature of V_{n1} and V_{n2} .

As to the physical interpretation of the external noise generators-- they are used to represent all of the noise inside the network. The most common sources of noise are the thermal noise of the resistances inside the network and any shot noise if the two-port is active. The result of this analysis will be to show that a noisy linear two-port network needs eight parameters to describe its operation. Four of these are the ordinary two-port parameters and the other four are needed to account for noise. Only two noise generators are shown but if they are partly correlated then a complex correlation function is needed which adds two more parameters.

Because the definitions were strictly applied, it is possible that a particular noise element inside the network may contribute some noise to each generator. For this reason, a correlation between the two generators has to be assumed and it is this correlation that complicates the analysis and produces some of the unusual effects such as noise

tuning. It is convenient to transform the effect of the noise generators to the input of the two-port. This is common practice in noise studies because it simplifies the analysis and facilitates the formulation of some useful noise definitions.

The noise generators can be transformed to the input by applying Kirchoffs circuital laws to the networks of Figure 4E-2 and isolating the system into a noise free two-port preceded by a noise voltage and noise current two-port. The equations of transfer are shown below in Figure 4E-3.



$$\begin{aligned} I_i &= I_i' + I_{n3} \\ V_i &= V_i' + V_{n3} \end{aligned} \quad (4E.2)$$

$$\begin{aligned} I_i' &= Y_{11} V_i' + Y_{12} V_2 & V_i' &= Z_{11} I_i' + Z_{12} I_2 \\ I_2 &= Y_{21} V_i' + Y_{22} V_2 & V_2 &= Z_{21} I_i' + Z_{22} I_2 \end{aligned} \quad (4E.3)$$

Figure 4E-3. Two-port Noise Model with Equivalent Noise Referred to the Input

The linear equations can be transformed by substituting (4E.2) for the primed quantities in (4E.3)

$$\begin{aligned} I_1 &= Y_{11} V_1' + Y_{12} V_2 + I_{n3} & V_1 &= Z_{11} I_1' + Z_{12} I_2 + V_{n3} \\ I_2 &= Y_{21} V_1' + Y_{22} V_2 & V_2 &= Z_{21} I_1' + Z_{22} I_2 \end{aligned} \quad (4E.4)$$

substituting again

$$\begin{aligned} I_1 &= Y_{11} (V_1 - V_{n3}) + Y_{12} V_2 + I_{n3} & V_1 &= Z_{11} (I_1 - I_{n3}) + Z_{12} I_2 + V_{n3} \\ I_2 &= Y_{21} (V_1 - V_{n3}) + Y_{22} V_2 & V_2 &= Z_{21} (I_1 - I_{n3}) + Z_{22} I_2 \end{aligned}$$

and separating out the noise terms gives:

$$\begin{aligned} I_1 &= Y_{11} V_1 + Y_{12} V_2 + (I_{n3} - Y_{11} V_{n3}) & V_1 &= Z_{11} I_1 + Z_{12} I_2 + (V_{n3} - Z_{11} I_{n3}) \\ I_2 &= Y_{21} V_1 + Y_{22} V_2 + (-Y_{21} V_{n3}) & V_2 &= Z_{21} I_1 + Z_{22} I_2 + (-Z_{21} I_{n3}) \end{aligned} \quad (4E.5)$$

From these equations we can identify the original noise generator terms by comparing with (4E.1):

$$\begin{aligned} I_{n1} &= I_{n3} - Y_{11} V_{n3} & V_{n1} &= V_{n3} - Z_{11} I_{n3} \\ I_{n2} &= -Y_{21} V_{n3} & V_{n2} &= -Z_{21} I_{n3} \end{aligned} \quad (4E.6)$$

solving (4E.6) for V_{n3} and I_{n3} yields

$$V_{n3} = -\frac{I_{n2}}{Y_{21}} = \frac{I_{n2} - I_{n1}}{Y_{11}} \quad (4E.7a)$$

$$I_{n3} = - \frac{V_{n2}}{Z_{21}} = \frac{V_{n3} - V_{n1}}{Z_{11}} \quad (4E.7b)$$

Finally we get equations relating the noise generators of Figure 4E-2 to those of Figure 4E-3 by solving (4E.7):

$$V_{n3} = V_{n1} - V_{n2} \left(\frac{Z_{11}}{Z_{21}} \right) \quad I_{n3} = I_{n1} - I_{n2} \left(\frac{Y_{11}}{Y_{21}} \right) \quad (4E.8)$$

By these algebraic manipulations we have demonstrated a very important conclusion: any noisy two-port network can be modeled by the circuit of Figure 4E-3 where the parameters of the noise free two-port are those obtained by turning off all internal noise generators (setting $T = 0^\circ\text{K}$). The original noise generators can be related to V_{n3} and I_{n3} by Equations 4E.8.

For most high frequency devices, V_{n3} and I_{n3} have some degree of correlation and to account for this we will define a linear correlation coefficient, γ . Before doing so, however, it will be convenient to split V_{n3} (I_{n3}) into two parts, one which is totally correlated with I_{n3} (V_{n3}) and one which is totally uncorrelated as shown in Equations 4E.9:

$$\begin{aligned} V_{n3} &= Z_{\text{cor}} I_{n3} + V_n \\ I_{n3} &= Y_{\text{cor}} V_{n3} + I_n \end{aligned} \quad (4E.9)$$

Z_{cor} (Y_{cor}) is a multiplying factor called correlation impedance (admittance) and V_n (I_n) is the totally uncorrelated component of V_{n3} (I_{n3}). Since V_n and I_n are totally uncorrelated the average value of the product $V_{n3} I_{n3}$

$$\overline{V_{n3} I_{n3}} = Z_{\text{cor}} \overline{I_{n3}^2} = Y_{\text{cor}} \overline{V_{n3}^2} \quad (4E.10a)$$

is related to both I_{n3} and V_{n3} .

The mean-square value of the sum ($V_{n3} + I_{n3}$) is

$$\begin{aligned} \overline{(V_{n3} + I_{n3})^2} &= \overline{V_{n3}^2} + \overline{I_{n3}^2} + 2 \overline{V_{n3} I_{n3}} \\ &= \overline{V_{n3}^2} + \overline{I_{n3}^2} + 2 \gamma \sqrt{\overline{V_{n3}^2} \cdot \overline{I_{n3}^2}} \end{aligned} \quad (4E.10b)$$

where γ is defined as the ratio of the covariance (Beckmann, 1967, p. 88) of V_{n3} , I_{n3} to the square root of the product of their variances:

$$\gamma = \frac{\overline{V_{n3} I_{n3}}}{\sqrt{\overline{V_{n3}^2} \cdot \overline{I_{n3}^2}}} \quad (4E.11a)$$

The correlation coefficient is, in general, a complex number of magnitude less than or equal to unity:

$$\gamma = |\gamma| e^{j\theta} = |\gamma| (\cos \theta + j \sin \theta) \quad 0 \leq |\gamma| \leq 1 \quad (4E.11b)$$

The correlation coefficient and the correlation impedances are related by combining Equations 4E.11a and 4E.10b to give:

$$Y_{\text{cor}} = \frac{\overline{V_{n3} I_{n3}}}{\overline{V_{n3}^2}} = \gamma \sqrt{\frac{\overline{I_{n3}^2}}{\overline{V_{n3}^2}}} \quad (4E.11c)$$

$$Z_{\text{cor}} = \frac{\overline{V_{n3} I_{n3}}}{\overline{I_{n3}^2}} = \gamma \sqrt{\frac{\overline{V_{n3}^2}}{\overline{I_{n3}^2}}} \quad (4E.11d)$$

Substitution of Equations 4E.11 into Equations 4E.9 and taking the mean square value will give for the totally uncorrelated components:

$$\overline{V_n^2} = \overline{V_{n3}^2} (1 - |\gamma|^2) \quad (4E.12a)$$

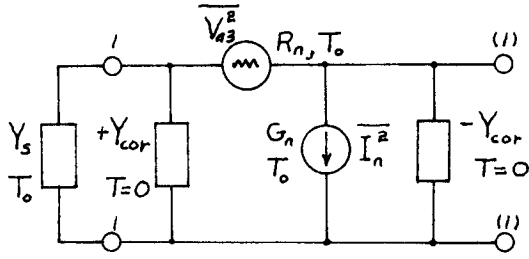
$$\overline{I_n^2} = \overline{I_{n3}^2} (1 - |\gamma|^2) \quad (4E.12b)$$

It is important to note that Equations 4E.9 and 4E.12 are really specifying the same property, cross correlation, but in different ways.

The correlation between V_{n3} and I_{n3} can be incorporated into the equivalent circuit of Figure 4E-3 to produce the complete mathematic and circuit description of a noisy two-port. This is done by substituting the correlation Equations 4E.9 into the equations of transfer (4E.2) for Figure 4E-3:

$$\begin{aligned} I_i &= I_i' + I_n + V_{n3} Y_{\text{cor}} = I_i' + I_n + Y_{\text{cor}} (V_i - V_i') \\ V_i &= V_i' + V_n + I_{n3} Z_{\text{cor}} = V_i' + V_n + Z_{\text{cor}} (I_i - I_i') \end{aligned} \quad (4E.13)$$

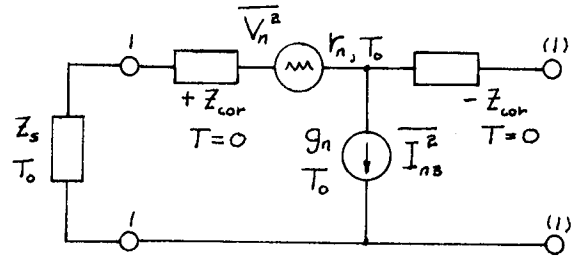
Two network realizations of this transformation are summarized in Figure 4E-4 with noise sources represented by their Nyquist equivalents. The source admittance and impedance are shown for clarification. It should



$$\overline{V_{ns}^2} = 4kT_0 R_n \Delta f$$

$$\overline{I_{ns}^2} = 4kT_0 G_n \Delta f$$

$$Y_{cor} = Y \sqrt{\frac{\overline{I_{ns}^2}}{\overline{V_{ns}^2}}}$$



$$\overline{V_n^2} = 4kT_0 r_n \Delta f$$

$$\overline{I_{ns}^2} = 4kT_0 g_n \Delta f$$

$$Z_{cor} = Z \sqrt{\frac{\overline{V_{ns}^2}}{\overline{I_{ns}^2}}}$$

Figure 4E-4. Input Noise Circuits for a Noisy Two-Port with Correlation Impedances and Source Impedance

be emphasized that Y_{cor} , Z_{cor} ; R_n , G_n ; r_n , g_n are not reciprocals each other and to avoid confusion, reciprocal elements will not be used in this section. This is consistent with generally accepted two-port notation where, for example, Y_{22} is not the reciprocal of Z_{22} .

The circuits of Figure 4E-4 describe completely the noise performance of any linear two-port and it is an important conclusion that only four characteristic noise terms are needed for this description; a noise conductance (G_n or g_n), a noise resistance (R_n or r_n) and a complex immittance (Y_{cor} or Z_{cor}). The description of a noisy two-port is now

$$\overline{I_{in}^2} = \overline{I_s^2} + \overline{I_n^2} + \overline{V_{n3}^2} |Y_s + Y_{cor}|^2 \quad (4E.14)$$

Equation 4E.14 is obtained from a circuit analysis of Figure 4E-5 and its simple form is a result of the fact that none of the noise sources in the circuit are correlated.

This mean-square current is proportional to noise power at the two-port output so we can define noise factor as the ratio of the short circuit mean-square current at terminals (1)(1) when all sources are contributing to that when only the source, $\overline{I_s^2}$ at 290 °K, contributes:

$$F = \frac{\overline{I_s^2} + \overline{I_n^2} + \overline{V_{n3}^2} |Y_s + Y_{cor}|^2}{\overline{I_s^2}} \quad (4E.15)$$

Each noise current can be replaced by its Nyquist equivalent resistance by substituting the following equations into (4E.15)

$$\begin{aligned} \overline{I_s^2} &= 4kT_o G_s \Delta f \\ \overline{I_n^2} &= 4kT_o G_n \Delta f \\ \overline{V_{n3}^2} &= 4kT_o R_n \Delta f \end{aligned} \quad (4E.16)$$

which gives:

$$F = 1 + \frac{1}{G_s} (G_n + R_n |Y_s + Y_{cor}|^2) \quad (4E.17a)$$

The equation above completely specifies the spot noise factor of the terminated two-port. The terms, $Y_s = G_s + j B_s$, characterize the termination at the input and G_n , R_n and $Y_{cor} = G_{cor} + j B_{cor}$, characterize the noise of the two-port. The two-port noise terms are functions of both frequency and source impedance and therefore are valid at only one frequency and one source impedance, for any specific situation.

Equation 4E.17a can be further simplified by separating it into the following factors:

$$F = 1 + A + \frac{1}{G_s} B + G_s R_n \quad (4E.17b)$$

where,

$$A = 2 R_n G_{cor}$$

$$B = G_n + R_n [(B_s + B_{cor})^2 + (G_{cor})^2]$$

There is an optimum value of source conductance which will minimize the noise factor. The adjustment of the source network to obtain this optimum value is called noise matching. The optimum can be found by taking the derivative:

$$\frac{\partial}{\partial G_s} F = R_n - \frac{B}{G_s^2} = 0 \quad G_s = G_{s,opt} = \sqrt{\frac{B}{R_n}} \quad (4E.18)$$

Substituting for G_s we get

$$\begin{aligned} F_{nm} &= 1 + A + \frac{B}{G_{s,opt}} + R_n G_{s,opt} \\ &= 1 + A + 2\sqrt{R_n B} \end{aligned} \quad (4E.19)$$

where the subscript nm refer to the minimum value of noise factor that can be obtained by simply noise matching. By substitution of (4E.18) into (4E.17b) we can write (4E.17b) as:

$$F = 1 + A + \sqrt{R_n B} \left(\frac{G_{s,opt}}{G_s} + \frac{G_s}{G_{s,opt}} \right) \quad (4E.17c)$$

When the input is noise tuned, the condition $B_s + B_{cor} = 0$ is satisfied and the noise factor for a noise-tuned network becomes:

$$F = 1 + 2 R_n G_{cor} + \sqrt{R_n G_n + R_n^2 G_{cor}^2} \left(\frac{G_{s,opt}}{G_s} + \frac{G_s}{G_{s,opt}} \right) \quad (4E.20)$$

Two limiting cases for two-port noise conditions will now be noted from Equation 4E.20:

- a) V_{n3} and I_{n3} are uncorrelated and the input is noise tuned then, $Y_{cor} = 0$, $G_{cor} = B_{cor} = 0$, $B_s = 0$,

$$F = 1 + \sqrt{R_n G_n} \left(\frac{G_{s,opt}}{G_s} + \frac{G_s}{G_{s,opt}} \right) \quad (4E.21)$$

- b) Absolute minimum noise factor, $G_s = G_{sopt}$ (noise matching):

$$F_{min} = 1 + 2 \sqrt{R_n G_n} \quad (4E.22)$$

The basic analysis of noise in two-port networks is now completed and the results can be used to make some important conclusions

and applications. The most general equation for the spot noise factor is (adapted from Equation 4E.17c)

$$F = 1 + A + \sqrt{R_n B} \left(\frac{R_s}{R_{s,opt}} + \frac{R_{s,opt}}{R_s} \right) \quad (4E.23)$$

where

$$A = 2 R_n G_{cor}$$

$$B = G_n + R_n [(B_s + B_{cor})^2 + (G_{cor})^2]$$

and the restriction on reciprocal element notation is now relaxed so that $R_s = 1/G_s$.

The following terms will be defined to aid in properly interpreting (4E.23):

- a) R_s is the source resistance presented to the input of the two-port network. Generally R_s is the antenna or system impedance when working with a system but when working with a single device it is usually the source resistance presented at the device terminals
- b) $R_{s,opt}$ is the optimum value of source resistance, R_s , which gives the minimum value of noise factor. When $R_s = R_{s,opt}$, the two-port is said to be noise matched
- c) R_n is the Nyquist equivalent resistance which represents the uncorrelated component of the equivalent noise generator V_{n3} of Figure 4E-3. R_n is dependent upon device parameters as well as frequency. R_n accounts for the device noise produced when R_s is small

- d) G_n is the Nyquist equivalent conductance which represents the uncorrelated component of the equivalent noise generator I_{n3} of Figure 4F-3. G_n is dependent upon device parameters as well as frequency
- e) B_s is the reactive part of the source admittance Y_s and is used to noise-tune the two-port so that $B_s + B_{cor} = 0$. Generally the source admittance must be capacitive for noise tuning
- f) $Y_{cor} = G_{cor} + j B_{cor}$ is the correlation admittance and is used as a circuit technique to describe the degree of correlation between the noise generators V_{n3} and I_{n3} . The correlation admittance is defined by Equations 4E.9 and 4E.11.

It can be emphasized with the help of (4E.23) that the source resistance for maximum power transfer is not the same as that for minimum noise factor. For maximum power transfer

$$Y_s = Y_{in}^* \quad G_s = G_{in} \quad B_s = -B_{in} \quad (4E.24)$$

while for minimum noise factor where the two-port is both noise watched and noise tuned

$$G_s = G_{s,opt} = \sqrt{\frac{B}{R_n}} \quad B_s = -B_{cor} \quad (4E.25)$$

and it can be clearly seen that maximum power transfer does not occur at minimum noise factor. This is illustrated in Figure N-1 of

Part N of the Appendix. The low-noise circuit designer must resign himself to the fact that maximum device gain and minimum device noise factor do not occur simultaneously for the same source impedance. To obtain the minimum possible two-port noise factor each receiver must have an input matching network capable of transforming the antenna or system source resistance to R_{sopt} for noise (not power) matching.

The losses and noise contribution of such a matching network were discussed in Chapter IV-C and the techniques presented there can be used to compute the increase in noise factor due to a lossy input matching network.

The method used to obtain the noise factor of Equation 4E.15 is a common one in device noise studies. This technique is derived from that definition of noise factor which is the ratio of total noise at the output to that noise due only to the source at standard temperature. Since the noise of the two-port is accounted for by an equivalent noise two-port at the input, the noise factor can be determined by working exclusively with the input. Notice that the two-port noise model of Figure 4E-5 is really two two-ports in cascade, one which is "completely" noisy and one which is noiseless. Thus all the noise properties of the two-port can be developed by looking at the available noise power from terminals (1)(1). It is important to realize that the available noise power and hence noise factor is completely independent of the two-port input admittance, Y_{in} . A reasonable question to ask is why stop at reducing the noise in a two-port network to that which is represented by the generators V_{n3} and I_{n3} when the noise can be completely referred to the input to give an equivalent noise temperature.

In fact, this is commonly done as explained in Part E of the Appendix and we can develop the equivalent from the circuit of Figure 4E-4. Using Equation 4E.23, the effective noise temperature (spot noise temperature) which refers all two-port noise to the receiver input is:

$$\begin{aligned} T_{eff} &= T_o (F - 1) \\ &= T_o A + \sqrt{R_n B} \left(\frac{R_s}{R_{s,opt}} + \frac{R_{s,opt}}{R_s} \right) \end{aligned} \quad (4E.26)$$

It should be noted that effective noise temperature is a function of frequency and source resistance as is noise factor.

The dependence of noise factor on source resistance is demonstrated in plots of noise figure as a function of source resistance normalized by $R_{s,opt}$. Such a plot is illustrated in Figure 4E-6 for the typical noise factor equations:

$$F_a = 1 + \frac{1}{4} + \frac{1}{2} \left(\frac{R_s}{R_{s,opt}} + \frac{R_{s,opt}}{R_s} \right) \quad \begin{matrix} A = \frac{1}{4} \\ \sqrt{R_n B} = \frac{1}{2} \end{matrix}$$

$$F_b = 1 + \frac{1}{2} \left(\frac{R_s}{R_{s,opt}} + \frac{R_{s,opt}}{R_s} \right) \quad \begin{matrix} A = 0 \\ \sqrt{R_n B} = \frac{1}{2} \end{matrix}$$

where two different arbitrary but typical values for A , R_n , and B have been chosen.

Data taken on an actual device (Figure M-1 of the Appendix) shows the typical parabolic shape typical of all high-frequency amplifiers.

In the actual design and tune-up of a low noise amplifier it is helpful to note that the point of optimum noise tuning is independent of source resistance, R_s , but that the optimum source resistance is not independent of the optimum detuning reactance. Another way to say this

is that the point of optimum noise tuning is independent of the point of noise matching but not vice versa. The proof of this statement can be seen by considering (4E.23) and (4E.18).

The noise factor is affected by changes in B_s (noise tuning) and R_s (noise matching) but we see that the condition $B_s + B_{cor} = 0$ is independent of R_s while R_{sopt} is dependent on B in the equation

$$R_{s,opt} = \sqrt{\frac{B}{R_n}}$$

and B is, in turn, dependent on $(B_s + B_{cor})$. This means that in attempting to noise tune the two-port, the necessary value of R_{sopt} will change but once noise tuning is achieved it will not be upset by changes in the source resistance.

A suggested procedure for tune-up based on this fact is as follows:

- a) Tune the input to resonance for maximum gain.
- b) Adjust the input matching network to achieve $R_s = R_{sopt}$ for noise matching.
- c) Adjust B_s , the reactive part of the source admittance, for noise tuning so that $B_s + B_{cor} = 0$.
- d) Tuning the input circuit for a net reactance has changed R_{sopt} so now R_s must once again be adjusted to achieve noise matching, $R_s = R_{sopt}$.
- e) Iterate.

Using this procedure for tune-up of a low-noise amplifier will provide the absolute minimum noise factor as given in Equation 4E.22.

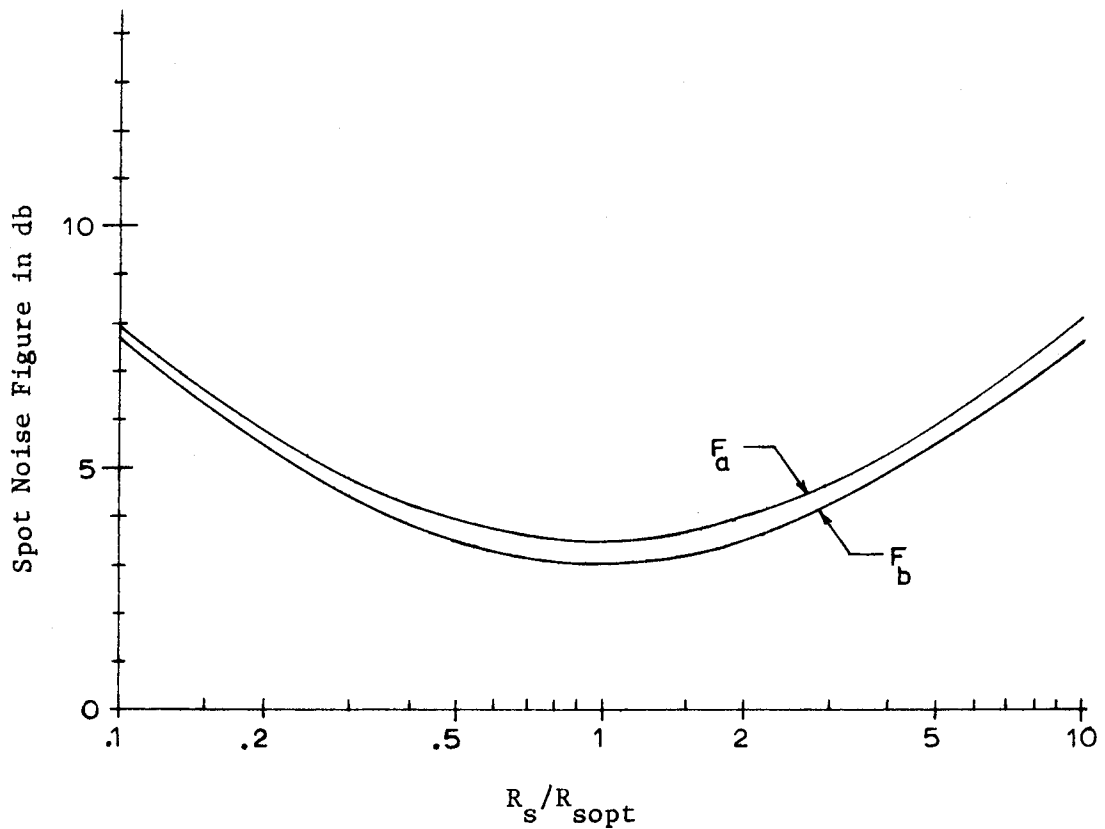


Figure 4E-6. Noise Figure as a Function of Normalized Source Resistance

F. Noise Generation in Electron Devices

The physics of noise generation and how it affects the noise factor of various amplifying and mixing devices needs to be examined because the ultimate sensitivity of a radio receiver is usually dependent upon the noise performance of the first and second active devices. When specifying or designing low-noise receiving systems it is helpful to know the expected noise behavior of the active devices used as RF amplifiers and mixers. The two-port noise model is sufficient to

describe the noise behavior of a two-port device but for a knowledge of the design limitations imposed upon that noise model, the nature of the noise sources in each active device needs to be studied. Noise in most active devices comes from either shot or thermal sources. A study of device noise usually becomes a study of how these two types of noise are generated in device operation and what parameters are used to specify noise factor. The noise mechanisms of the most common devices will now be presented and noise factors based upon the most commonly accepted models will be given.

1. Noise in vacuum tubes

Vacuum tubes are rarely used in low-noise receivers of modern design but the sources of noise encountered in a vacuum tube offer an excellent means of presenting many of the physical mechanisms which cause noise. For this reason, and for completeness, we will look at the sources of noise in vacuum tubes.

The vacuum tube diode is the simplest electronic device that exhibits shot noise. Shot noise, as we discussed in Chapter IV-B, is caused by the discreteness of the electron current and the random arrival of electrons at the plate or anode. First, we will consider the "ideal" vacuum-tube noise diode and develop the full-shot-noise equation which is fundamentally important to the study of all shot-noise mechanisms. The ideal noise diode is represented in Figure 4F-1 and has the following properties:

1. The anode or plate voltage is high enough so that
all the electrons emitted by the cathode reach the

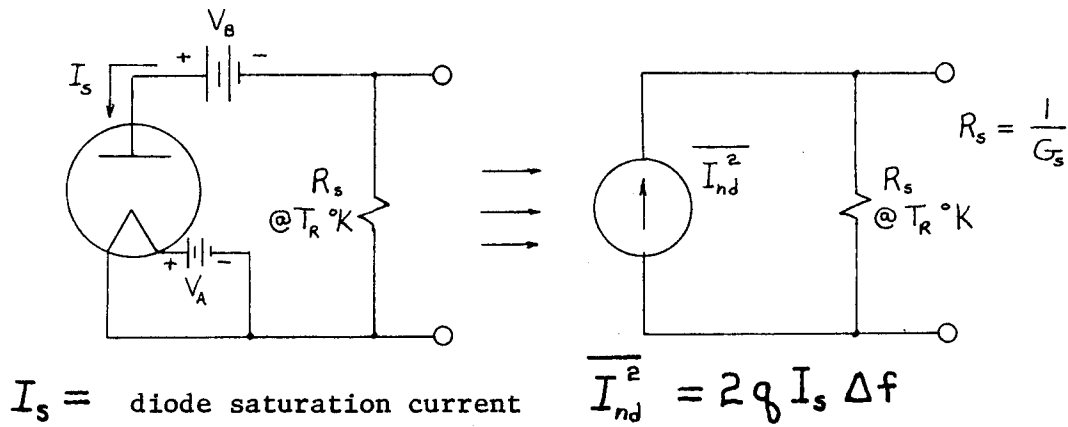


Figure 4F-1. Ideal Vacuum-Tube Noise-Diode

anode. This is called the temperature-limited mode of operation which means the average dc current through the diode is independent of anode voltage and dependent only upon cathode temperature.

2. The electron transit time between anode and cathode is so short that the resulting time lag can be neglected when compared to the period of the frequency of operation.
3. The space charge effect at the cathode is negligible.
4. The electrons are emitted from the cathode at a uniform rate and their arrival at the anode is a random function of time.

The ideal-shot-noise equation is obtained by assuming the electron arrival frequency is large so that the Poisson distribution is replaced with a Gaussian distribution. Then Maxwell-Boltzmann statistics can be applied to one-dimensional current flow in a planar diode. Under these circumstances (Smullin and Haus, 1959, Ch. 1), the power spectral density function is

$$S_{\text{shot}}(\omega) = 2 q I_s \quad (\text{Ideal-shot-noise equation}) \quad (4F.1)$$

where q = Electronic charge, 1.6×10^{-19} coul

I_s = DC diode current (actually, the diode saturation current).

When the spectral power is integrated over the noise bandwidth of the noise diode circuit the mean-square value of shot noise-current is given by:

$$\overline{I_{nd}^2} = 2 q I_s \Delta f \quad (\text{amperes})^2 \quad (4F.2)$$

Taking into consideration the thermal noise of the parallel resistance, as was done in Chapter IV-B, the total mean-square noise current is the sum of the mean-square currents due to the diode and the resistor (see Equations 4B.13 and 4B.14):

$$\overline{I_n^2} = \overline{I_{nd}^2} + \overline{I_{nR}^2} = 2 q I_s \Delta f + 4 k T_R G_s \Delta f \quad (4F.3)$$

The total available noise power is:

$$\begin{aligned} \frac{\overline{I_n^2}}{4G_s} &= \frac{qI_s \Delta f}{2G_s} + kT_R \Delta f \\ &= k \left[\frac{qI_s}{2kG_s} + T_R \right] \Delta f \quad \text{Watts} \end{aligned} \quad (4F.4)$$

Since the noise powers are additive it is possible to consider the shot noise introduced by the diode as having increased the "noise temperature" of the resistor. This noise increase has the same effect as physically heating the resistor to a higher temperature. In this manner, the noise diode can provide a means of obtaining effective noise temperatures of thousands of degrees Kelvin. The factor $qI_s/2kG_s$ in Equation 4F.4 is called the excess noise temperature, T_{ex} , because it represents the additional noise due to the diode. The concept of excess noise is useful for presenting sensitivity measurement theory.

Figure 4F-2 is the Norton equivalent circuit for an ideal noise diode source. When the diode current is zero ($I_s = 0$), the excess noise temperature is zero and the effective temperature of the source ($T_{eff} = T_{ex} + T_R$) becomes the physical temperature of the resistor, T_R . Departure from ideal diode operation and its effect on measurement accuracy will be discussed in Chapter X.

The noise behavior of the vacuum tube triode can be studied by considering the effect of adding a grid to the diode structure. When grids are added, additional sources of shot noise are introduced. These

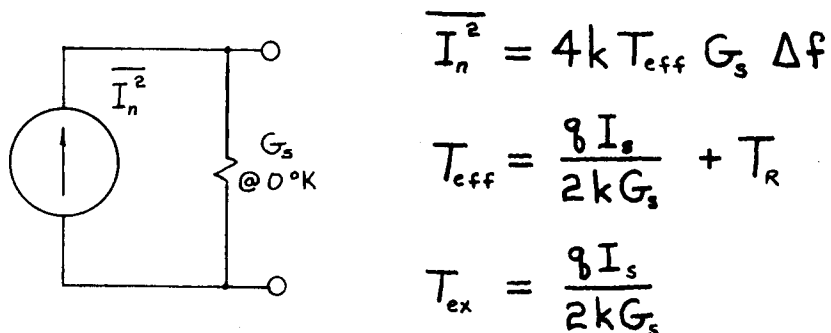


Figure 4F-2. Equivalent Circuit and Equivalent Noise Temperature for an Ideal Noise Diode Source

additional shot noise sources are the result of electrons flowing through and into the grid structures.

For a triode of planar geometry, the mean-square shot noise current in the plate is given by (Smullin and Haus, 1959, Ch. 4)

$$\overline{I_p^2} = 3 \left(1 - \frac{\pi}{4} \right) 4k T_K g_p \Delta f \quad (4F.5)$$

where the triode plate conductance g_p is larger than the diode conductance and is related to the triode transconductance g_m by the factor:

$$g_p = \frac{g_m}{\sigma} \quad (4F.6)$$

The value of σ depends upon tube geometry and electrode potentials but usually lies between one-half and one. T_K is the cathode temperature.

After substituting (4F.6) into (4F.5), the mean-square shot noise current for the plate of a vacuum tube triode becomes:

$$\overline{I_p^2} = 3 \left(1 - \frac{\pi}{4}\right) 4kT_k \frac{g_m}{\pi} \Delta f \quad \left(\frac{1}{2} \leq \sigma \leq 1\right) \quad (4F.7)$$

As more grids are added to the basic diode structure*, more sources of noise are introduced. The electron current must now be shared between two or more electrodes. This sharing causes a randomness that introduces additional noise sources referred to as partition noise. A special category of grid noise is induced grid noise.

Induced grid noise is the result of current pulse doublets induced into the grid circuit when an electron passes through the grid. It's effect is important at HF and VHF because the mean-square value of induced grid current is proportional to the square of space-charge input capacitance and to the square of frequency thus it gets larger as frequency increases. Two equations for induced grid noise are presented for reference

$$\overline{I_g^2} = 4kT_k \left(\frac{G_g}{0.7}\right) \Delta f \quad (4F.8)$$

or

$$\overline{I_g^2} = \left(\frac{B'_g}{g_m}\right)^2 \overline{I_p^2} \quad (4F.9)$$

where T_K = Cathode temperature
 G_g = Grid input conductance due to transit-time effects
 $B'_g = \omega C_e$, the grid input susceptance where C_e is the space-charge input capacitance

*Vacuum tube noise sources are usually diodes or triodes. This comment was intended to inform the reader that, low-noise amplifiers should be kept to a minimum of grid elements.

$$g_m = \text{Transconductance}$$

$$\overline{I_p^2} = \text{Plate mean-square shot noise current}$$

and it is assumed that there is complete correlation between induced grid noise and plate shot noise. Actual data shows a significant component of induced grid noise which is not correlated to plate noise. For this reason it is usually necessary to represent $\overline{I_g^2}$ by a Nyquist equivalent circuit obtained from actual data.

Application of the Nyquist equivalent should be made with care, however because Equation 4F.9 shows that $\overline{I_g^2}$ is not white noise.

It will now be convenient to show how to represent the plate shot noise contribution with a Nyquist equivalent noise voltage generator in the grid circuit. Figure 4F-3 illustrates the transformation.

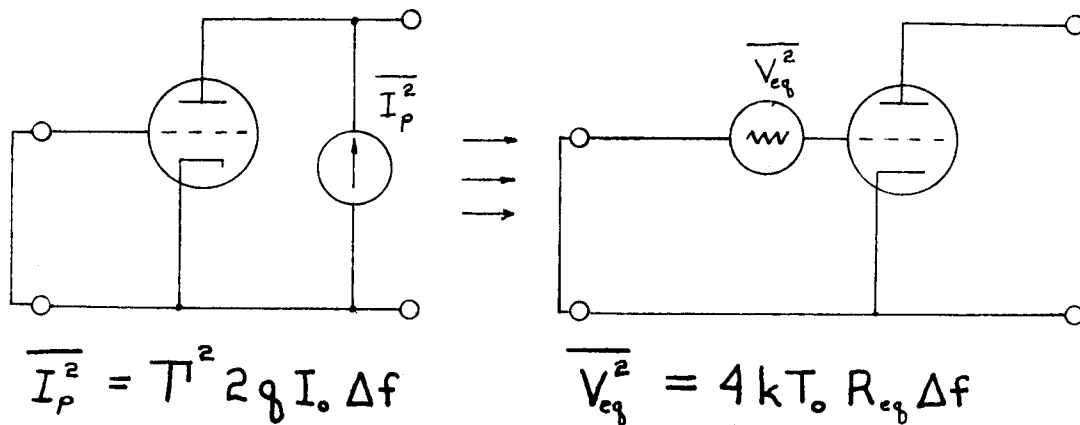


Figure 4F-3. Plate Shot Noise Referred to the Grid Input

The output shot noise current and the series-input noise voltage are related by the tube transconductance:

$$\overline{I_p^2} = g_m^2 \overline{V_{eq}^2} \quad (4F.10)$$

An alternate representation for the mean-square value of plate shot noise current is given by (Smullin and Haus, 1959, p. 178)

$$\overline{I_p^2} = \overline{\gamma}^2 2 q I_o \Delta f \quad (4F.11)$$

where I_o = Plate current

$\overline{\gamma}^2$ = Space charge reduction factor, $0 \leq \overline{\gamma} \leq 1$.

Equating the Nyquist equivalent voltage to plate shot noise current using Equation 4F.10 gives

$$\overline{\gamma}^2 2 q I_o \Delta f = g_m^2 4 k T_o R_{eq} \Delta f$$

which can be solved for the Nyquist equivalent resistance:

$$R_{eq} = \frac{\overline{\gamma}^2}{g_m^2} \frac{q I_o}{2 k T_o} \quad (4F.12)$$

The space-charge reduction factor is given by theory to be (Smullin and Haus, 1959, p. 160):

$$\overline{\gamma}^2 = 6 \left(1 - \frac{\pi}{4}\right) \frac{k T_k}{q I_o} \frac{g_m}{\sigma} \quad (4F.13)$$

* Capitol gamma is the symbol chosen to represent the space-charge reduction factor.

Substituting (4F.13) into (4F.12) gives as the final result:

$$R_{eq} = 3 \left(1 - \frac{\pi}{4}\right) \frac{1}{\sigma g_m} \frac{T_K}{T_o} \quad (4F.14)$$

The equivalent resistance, R_{eq} , can be used as a convenient representation for the shot noise produced in the plate circuit and is called the equivalent noise resistance. Substitution of nominal values for T_K and σ into Equation 4F.14 gives the following approximation of R_{eq} for a vacuum triode that is so often quoted in the literature:

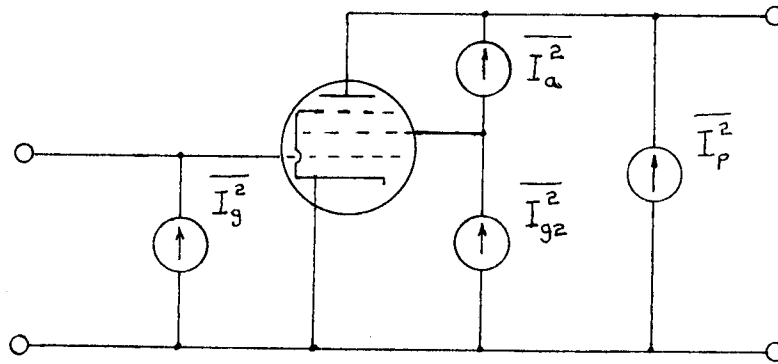
$$R_{eq} \approx \frac{2.5}{g_m} \quad \sigma = 3/4, \quad T_K = 840^\circ K \quad (4F.15)$$

The noise sources for a vacuum tube pentode can be conveniently summarized with Figure 4F-4. These noise sources are usually reduced to just two equivalent sources at the tube grid by referring all sources to the input. When this is done, vacuum tube noise effects can be accounted for by the equivalent circuit of Figure 4F-5. The equations for the equivalent current and voltage are

$$\overline{V_{eq}^2} = 4kT_o R_{eq} \Delta f \quad (4F.16)$$

$$\overline{I_g^2} = 4kT_K \left(\frac{G_g}{0.7}\right) \Delta f \quad (4F.17a)$$

$$\approx 4kT_o (5 G_g) \Delta f \quad (4F.17b)$$



- $\overline{I_p^2}$ = Plate shot noise
 $\overline{I_g^2}$ = Induced grid noise (not white)
 $\overline{I_a^2}$ = Partition noise
 $\overline{I_{g2}^2}$ = Screen-grid shot noise

Figure 4F-4. Vacuum Tube Pentode Circuit Showing Equivalent Shot Noise Current Generators

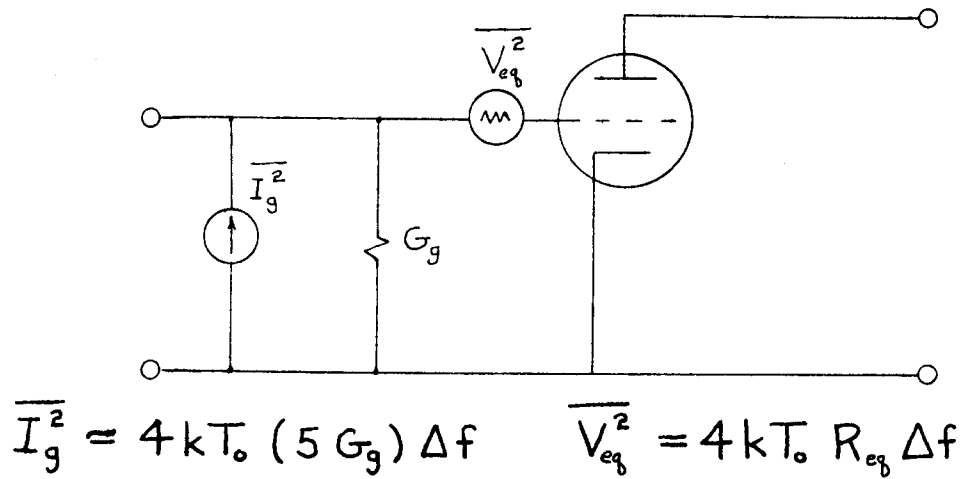


Figure 4F-5. Standard Equivalent Circuit for Vacuum Tube Noise

where R_{eq} = Equivalent noise resistance
 T_K = Cathode temperature
 G_g = Input conductance due to transit-time effects
 $\frac{T_K}{0.7 T_o} \approx 5$ for a typical oxide-coated cathode.

Following the same procedure that was used to obtain the equivalent noise resistance for a vacuum triode we have similar equations for R_{eq} for the following cases (Pappenfus et al., 1964, p. 246):

Triode amplifier,

$$R_{eq} \approx \frac{2.5}{g_m}$$

Pentode amplifier,

$$R_{eq} \approx \frac{I_o}{I_o + I_{g2}} \left(\frac{2.5}{g_m} + \frac{19 I_{g2}}{g_m^2} \right) \quad (4F.18)$$

Triode mixer,

$$R_{eq} \approx \frac{4}{g_c} \quad (4F.19)$$

Pentode mixer,

$$R_{eq} \approx \frac{I_o}{I_o + I_{g2}} \left(\frac{2.5}{g_c} + \frac{19 I_{g2}}{g_c^2} \right) \quad (4F.20)$$

Pentagrid mixer,

$$R_{eq} \approx 20 \frac{I_o (I_k - I_o)}{I_k g_c^2} \quad (4F.21)$$

where

I_o = plate current

I_{g2} = screen current

I_k = cathode current

g_m = amplifier transconductance

g_c = conversion transconductance.

Typical values for R_{eq} range from 200 to 600 ohms while those for G_g range from 9 to 30 micromhos. The fact that there is partial correlation between $\overline{I_g^2}$ and $\overline{V_{eq}^2}$ is taken care of by a correlation coefficient in the same manner as was presented in Chapter IV-E.

Talpey (Smullin and Haus, 1959, p. 200) has given the noise factor of a common-cathode stage as

$$F = 1 + \frac{G_{eq}}{G_s} + \frac{R_{eq}}{G_s} \left[(G_s + G_g)^2 + (B_s + B_g - B'_g)^2 \right] \quad (4F.22)$$

where

$Y_s = G_s + j B_s$, the source admittance

G_g = input conductance

G_{eq} = equivalent noise conductance of the uncorrelated component of $\overline{I_g^2}$

R_{eq} = equivalent noise resistance

B_g = total grid input susceptance

$B_g' = \omega C_e$, grid input susceptance due to the space charge effect.

The optimum value of source conductance (the source conductance which gives minimum noise factor) is obtained by differentiating F with respect to G_s and equating to zero. This gives:

$$G_{s,opt} = \sqrt{\frac{G_{eq}}{R_{eq}} + G_g^2 + (B_s + B_g - B_g')^2} \quad (4F.23)$$

Notice that optimum source conductance is dependent on input tuning through the factor $(B_s + B_g - B_g')^2$. Notice also that optimum source conductance is not equal to the input conductance of the tube, G_g .

The condition for resonance at the input is

$$(B_s + B_g) = 0$$

but the condition for minimum noise factor (4F.22) is:

$$(B_s + B_g - B_g') = 0 \quad (4F.24)$$

The input must be reactively tuned by an amount B_g' to achieve minimum noise factor. This process is called noise tuning (Appendix, Part N).

The fact that $G_{s,opt} \neq G_g$ and $B_s \neq B_g$ for minimum noise factor emphasizes the necessity that the input circuit must be mismatched for lowest noise factor.

The noise factor when the circuit is noise tuned ($B_s + B_g - B_g' = 0$) is, from Equation 4F.22:

$$F_{nt} = 1 + \frac{G_{eq}}{G_s} + \frac{R_{eq}}{G_s} (G_s + G_g)^2 \quad (4F.25a)$$

$$= 1 + 2 R_{eq} G_g + \frac{1}{G_s} (G_{eq} + R_{eq} G_g^2) + G_s R_{eq} \quad (4F.25b)$$

Equation 4F.25b is of the same form as (4E.23) when the following terms are equated:

$$\begin{aligned} R_{eq} &= R_n \\ G_g &= G_{cor} \\ G_{eq} &= G_n \\ B_s + B_{cor} &= 0. \end{aligned}$$

The noise factor of (4F.25a) in the form of (4F.23) becomes:

$$F_{nt} = 1 + 2 R_{eq} G_g + \sqrt{R_{eq} (G_{eq} + R_{eq} G_g^2)} \left(\frac{R_s}{R_{s,opt}} + \frac{R_{s,opt}}{R_s} \right) \quad (4F.26)$$

This equation for the vacuum tube has been derived to illustrate the application of the noise theory of Chapter IV-E.

The absolute minimum noise factor for a vacuum tube that is both noise matched and noise tuned is obtained from Equation 4F.26 by letting $R_s = R_{s,opt}$ to give:

$$F_{min} = 1 + 2 R_{eq} G_g + 2 \sqrt{R_{eq} (G_{eq} + R_{eq} G_g^2)} \quad (4F.27)$$

In most cases the approximation $G_g \ll G_{s,opt}$ is valid so that Equation 4F.25a will reduce to

$$F_{nt} = 1 + \frac{G_{eq}}{G_s} + R_{eq} G_s \quad (4F.28)$$

for $G_s \simeq G_{s,opt}$. This approximation also reduces $G_{s,opt}$ to

$$G_{s,opt} \simeq \sqrt{\frac{G_{eq}}{R_{eq}}}$$

which can be substituted into (4F.28) to give a well known result:

$$F_{nt} \simeq 1 + \sqrt{G_{eq} R_{eq}} \left(\frac{G_{s,opt}}{G_s} + \frac{G_s}{G_{s,opt}} \right) \quad (4F.29)$$

$$F_{min} \simeq 1 + 2 \sqrt{G_{eq} R_{eq}} \quad (4F.30)$$

This treatment of tube noise has been brief because the topic does not warrant more time consideration. Much work has been done on the theory of tube noise that is of historical and theoretical interest. The reader desiring more information about the theory of tube noise is encouraged to consult the following references: Smullin (1959), Bennett (1960), Bell (1951), van der Ziel (1954) and Pappenfus (1964).

2. Noise in semiconductor diodes

The noise behavior of a junction diode has been examined by van der Ziel and Becking (1958), van der Ziel (1958) and many others. Before

presenting this theory, it will be necessary to review some p-n junction theory and obtain the equations that are used to calculate the noise generated. Consider the p-n junction diode represented by Figure 4F-6.

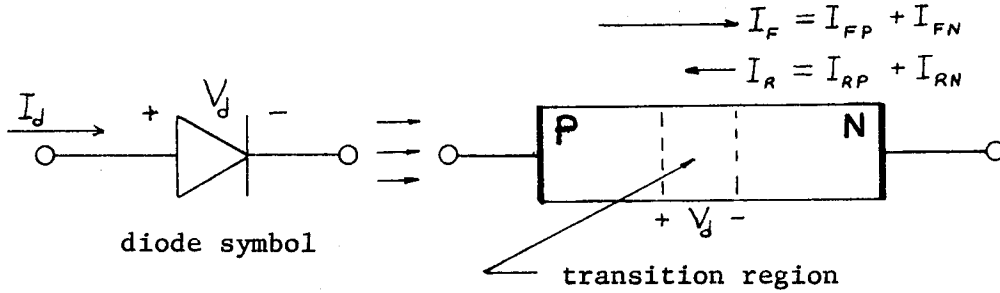


Figure 4F-6. Representation of a P-N Junction Diode

The diode current I_d is actually the sum of four different diode currents which are defined as follows:

I_{FP} = The hole current due to holes in the P region
(majority carriers) diffusing from the P region
to the N region where they recombine. These holes
have sufficient energy to overcome the junction
potential V_d

I_{FN} = The electron current due to electrons in the N
region (majority carriers) diffusing from the
N region to the P region. These electrons must
have sufficient energy to overcome the junction
potential V_d

I_{RP} = The drift current caused by holes in the N region
(minority carriers) diffusing toward the transition

region until they reach it and are swept across by the favorable electric field caused by V_d

I_{RN} = The drift current caused by electrons in the P region (minority carriers) diffusing toward the transition region until they reach it and are swept across by the favorable electric field caused by V_d .

The total forward current in the diode is the sum of the diffusion currents

$$I_F = I_{FP} + I_{FN}$$

while the total reverse current is given by the sum of the drift currents:

$$I_R = I_{RP} + I_{RN}$$

The total diode current is defined as the net dc current flowing in the diode terminals in a direction from P to N:

$$I_d = (I_F - I_R) = (I_{FP} + I_{FN} - I_{RP} - I_{RN})$$

The reverse saturation current, I_s , of the diode is defined as that current that flows when the diode is reversed biased below breakdown. The field produced by reverse bias is large enough to virtually stop any carrier diffusion and only the drift currents remain so:

$$I_s = I_{RP} + I_{RN}$$

The dc diode equation is obtained by solving the equations of carrier motion at the junction which gives the total diode current in terms of saturation current, temperature, and bias voltage

$$I_d = I_s \left[e^{\frac{qV_d}{kT_j}} - 1 \right] \quad (\text{ideal diode equation}) \quad (4F.31)$$

where

- q = electronic charge
- k = Boltzmann's constant
- T_j = diode junction temperature
- V_d = diode junction potential.

The low-frequency diode conductance, g_o , can be obtained from the ideal diode equation by differentiation with respect to diode voltage

$$g_o = \frac{\partial I_d}{\partial V_d} = I_s \frac{q}{kT_j} e^{\frac{qV_d}{kT_j}} = I_s \frac{q}{kT_j} \left[\frac{I_d + I_s}{I_s} \right] \quad (4F.32)$$

which gives:

$$g_o = \frac{q}{kT_j} (I_d + I_s) \quad (4F.33a)$$

This expression is most commonly seen in the inverted form to give the diode resistance as

$$1/g_o = r_o \simeq \frac{26}{I_d(\text{ma})} \quad (I_d \gg I_s) \quad (4F.33b)$$

where I_d is in milliamperes and $T_j \simeq 300^\circ \text{ K}$.

Van der Ziel (1955) has used a transmission-line analogy for the diode structure which modifies the low-frequency conductance to give a high-frequency conductance of

$$g_e = g_o \left[\frac{1}{2} \sqrt{1 + \omega^2 \tau_p^2} + \frac{1}{2} \right]^{1/2} \quad (4F.33c)$$

where ω = operating frequency

τ_p = Carrier lifetime of holes diffusing from P to N.

τ_p is a measure of the recombination rate.

Van der Ziel and Becking (1958) presented a derivation of junction diode noise based on a simple planar diode with the N region much more lightly doped than the P region. Figure 4F-7 is a schematic representation of hole flow under these conditions.

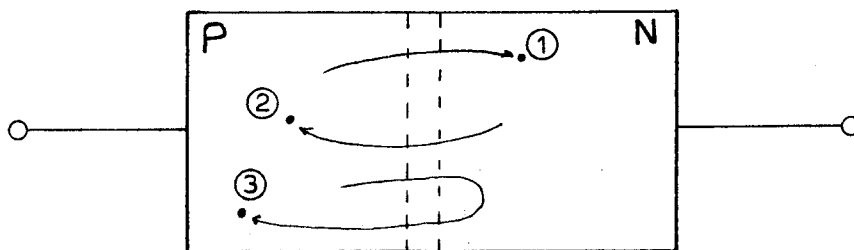


Figure 4F.7. Hole Flow for a Junction Diode with Lightly Doped N Region

If the N region is much more lightly doped than the P region, the diode current is essentially all carried by holes so that I_{FN} and

I_{RN} can be neglected. The charge carriers can then be divided into three groups:

- ① Holes entering the N region and recombining. This is the current I_{FP} .
- ② Drift current of holes from the N region to the P region. This is the current I_{RP} .
- ③ Holes which diffuse to the N region but drift back to the P region before recombining.

Assuming that all three currents are statistically independent, they give rise to full shot noise and the resulting mean-square values of current are:

$$\overline{I_1^2} = 2q I_{FP} \Delta f$$

$$\overline{I_2^2} = 2q I_{RP} \Delta f$$

$$\overline{I_3^2} = 4kT_j (g_e - g_o) \Delta f$$

The carriers of group ③ give no contribution to the net current and therefore generate only a thermal noise term due to their random motion.

The net diode current is $I_d = I_{FP} - I_{RP}$ and the reverse saturation current is $I_s = I_{RP}$ so the equations for noise become:

$$\overline{I_1^2} = 2q (I_d + I_s) \Delta f$$

$$\overline{I_2^2} = 2q I_s \Delta f$$

$$\overline{I_3^2} = 4kT_j (g_e - g_o) \Delta f$$

All of these sources are in parallel so their mean-square values can be added to give the total mean-square value of noise current as

$$\overline{I_n^2} = \left[2q(I_d + I_s) + 2qI_s + 4kT_j(g_e - g_o) \right] \Delta f$$

which is reduced to its well known form by substituting (4F.33a) to give

$$\overline{I_n^2} = 4kT_j g_e \Delta f - 2qI_d \Delta f \quad (4F.34a)$$

where g_e = high frequency diode conductance
 I_d = diode forward bias current
 T_j = diode junction temperature.

Van der Ziel and Becking (1958) have shown that Equation 4F.34a has general validity and does not depend on diode geometry or doping levels. For a derivation of (4F.34a) in more detail, refer to his paper.

Equation 4F.34a can be simplified by using the approximation $I_d \gg I_s$ (normal bias) to reduce Equation 4F.33a to

$$kT_j g_o = qI_d$$

which is substituted into Equation 4F.34a to give:

$$\overline{I_n^2} = 4kT_{eq} g_e \Delta f$$

$$T_{eq} = \frac{T_j}{2} \left(2 - \frac{g_o}{g_e} \right) \quad I_d \gg I_s \quad (4F.34b)$$

Now from (4F.33c) we know that

$$g_e \geq g_o$$

and we get limits on T_{eq} as:

$$T_j/2 \leq T_{eq} \leq T_j \quad (4F.35)$$

This illustrates the important point that noise generated by the "electronic" resistance, g_e , is not simply the thermal noise of an equivalent physical resistor. In this case the electronic resistance produces less equivalent noise. Figure 4F-8 shows the Nyquist equivalent circuit for a forward-biased junction diode.

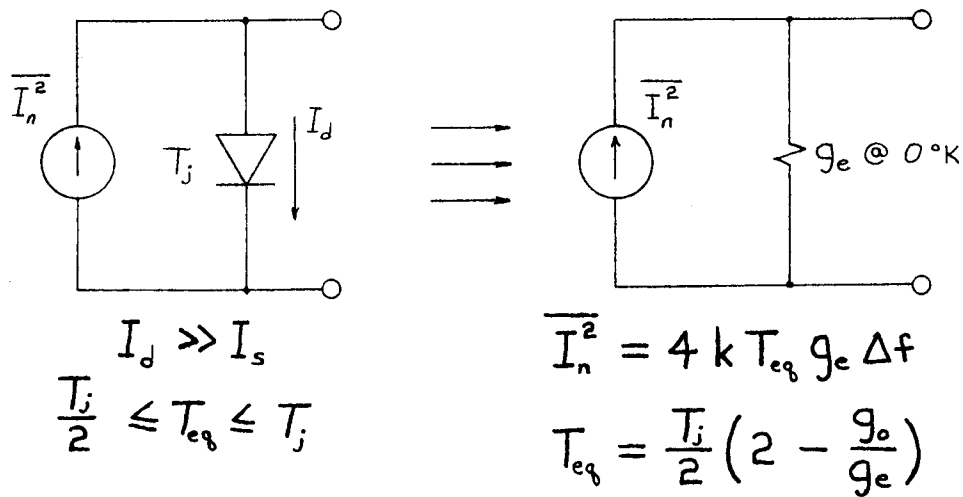


Figure 4F-8. Nyquist Equivalent Circuit for a Forward Biased P-N Junction Diode

The semiconductor diode produces noise other than that of the simple forward-bias case. Other important aspects of diode noise are the noise produced in diodes used as mixers and the noise produced in a reverse-biased diode due to breakdown effects. Also, a significant amount of noise is produced in microwave signal sources using impact avalanche diodes. These topics of noise are too extensive to be included in great detail in this thesis. A brief presentation of diode mixer noise will be given in the section on mixer noise. Noise in impact avalanche diodes is a topic that is being widely discussed in microwave journals. The noise produced when a diode is operated in reverse breakdown is useful for making solid-state noise sources which have high values of excess noise. Commercial sources are claiming excess noise ratios of 25 to 40 db or equivalent noise temperatures of 10^5 to 3×10^6 °K. These sources are used in noise figure meters and for high-power noise sources. The theory of operation of noise diodes operating in the breakdown region will not be presented but the reader is encouraged to consult the literature for more information because these sources will become increasingly important. Two brief references on the topic can be found in Yakutis (1968) and Haitz (1967).

3. Noise in bipolar transistors

The bipolar transistor is the most widely used active device for modern low-noise applications. The field-effect transistor is a close second for HF and VHF applications but the very-low-noise systems still require bipolar designs. Noise temperatures in the range of 50 to 300° K are possible for frequencies from 10 Khz to 1000 Mhz. These

low values make the bipolar transistor very competitive with any device which does not require cryogenic techniques. The physics of noise generation in a bipolar transistor can only be understood by studying the basic mechanisms involved in transistor operation. The ever present noise sources due to electron flow (shot noise) and thermal resistance (thermal noise) will contribute most of the noise as is the case for just about all other active devices.

The noise analysis of bipolar transistors depends upon the manufacturing processes and junction formation because of the effects of doping impurity levels, impurity profiles, and surface contamination. A complete study of the various transistor processes and their associated noise models is beyond the scope of this text but it is necessary to select some process to provide a basis for a noise model which will satisfy most high-frequency criteria. The selection should be based upon the most common technology for low-noise transistors. For these reasons, the planar epitaxial transistor technology was chosen. Figure 4F-9 illustrates the physical construction of a planar transistor and the resulting three-section schematic representations.

As was true in the case of the junction diode, a review of transistor theory will be helpful in understanding the noise representation and eventual calculation of noise factor. The common-base representations will be presented first and then followed by the common-emitter.

One approximate, high-frequency, small-signal, ac model for a common base junction transistor is shown in Figure 4F-10. This circuit was developed (Phillips, 1962, p. 294) from the physical principles of

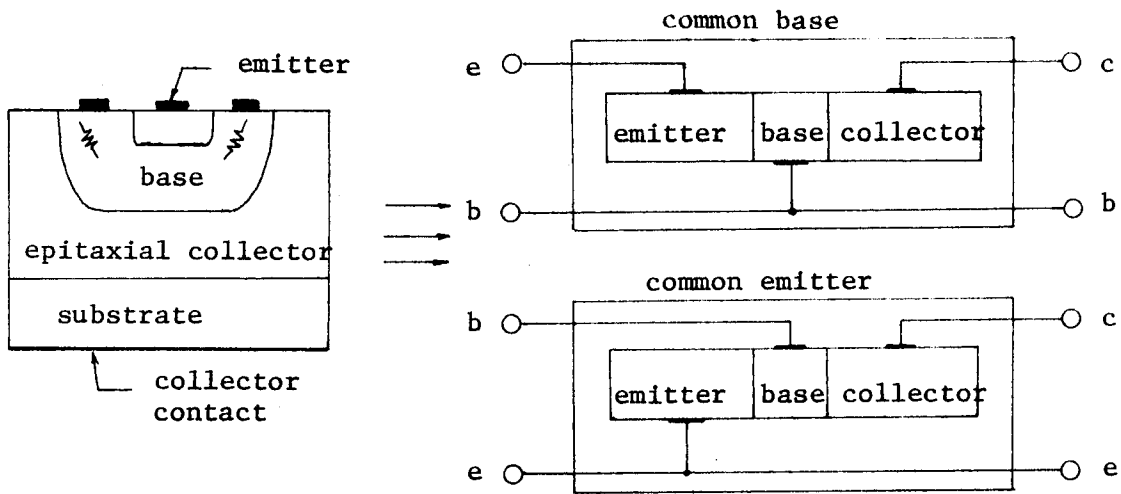


Figure 4F.9. Physical and Schematic Representation of a Bipolar Transistor of Planar Epitaxial Construction

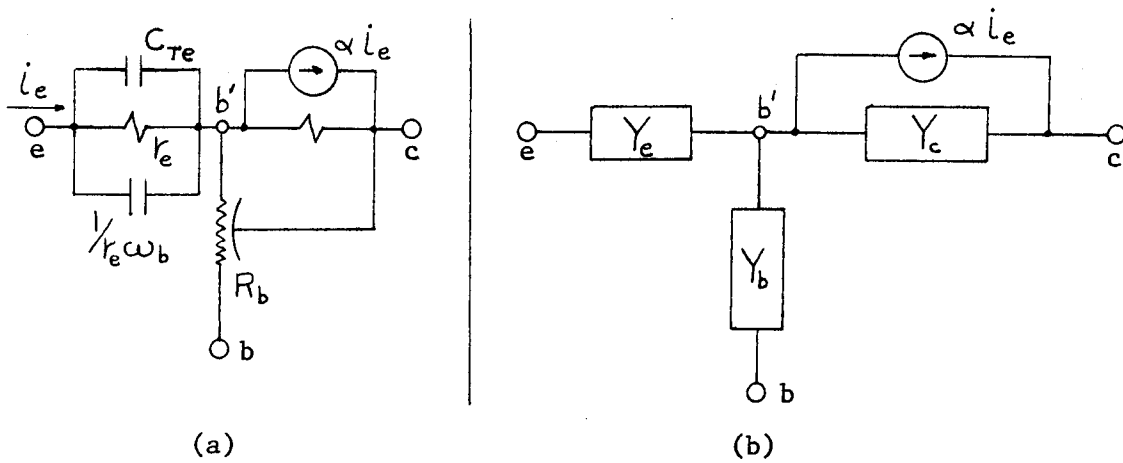


Figure 4F.10. Equivalent Tee Models for the Bipolar Transistor in the Common Base Configuration

transistor operation and is the lumped-circuit model which most closely relates the circuit elements to specific transistor mechanisms.

From theory we can identify the specific admittances in Figure 4F-10b by approximating the distributed RC nature of the base-collector junction with fixed elements. These admittances are:

$$Y_e = \frac{1}{r_e} + j\omega \left(C_{Te} + \frac{1}{r_e \omega_b} \right) \quad \alpha = \frac{\alpha_0}{(1 + j\omega r_e C_{Te})(1 + j\frac{\omega}{\omega_b})}$$

$$Y_c = g_c + \omega_b C_{oc} \left(\frac{\omega}{\omega_a} \right)^2 + j\omega (C_{Tc} + C_{Dc}) \quad Y_b = \frac{1}{r_{bb'}}$$

The equivalent circuit components are now defined:

r_e = The dynamic resistance of the base-emitter diode at low frequencies. This resistance plays the same role as the diode dynamic resistance, $r_o = 1/g_o$ of diode noise theory.

$r_{bb'}$ = The base bulk resistance between the external base contact, b, and the active base region, b'. This is also called the base-spreading resistance.

g_c = The low-frequency base-collector conductance due to base-width modulation.

C_{Te} = Emitter-base transition region capacitance.

$\frac{1}{r_e \omega_b}$ = Emitter-base diffusion capacitance.

C_{Tc} = Collector-base transition region capacitance.

C_{Dc} = Collector-base diffusion capacitance.

$\omega_b C_{Dc} \left(\frac{\omega}{\omega_b}\right)^2$ = Frequency dependent base-collector diffusion conductance.

α_o = Low frequency common-base current gain.

ω = Frequency of operation.

ω_b = Base cutoff frequency (not to be confused with beta-cutoff). The alpha-cutoff frequency and ω_b are related through the equation, $\frac{1}{\omega_b} = \frac{1}{\omega_\alpha} - r_e C_{Te}$.

An approximate high-frequency common-base circuit model has now been defined which will provide the basis for an evaluation of transistor noise performance. The reader desiring a review of transistor operation will find references such as Alley and Atwood (1971), Phillips (1962), or the GE Transistor Manual very helpful.

The noise analysis to be presented will parallel the work done by A. van der Ziel who has developed much of the device noise theory of the past two decades. His work provides the basic core for all solid-state device studies and the reader interested in a detailed study of device noise is encouraged to read the papers written by him.

With the aid of several papers by van der Ziel, the following theory on noise in bipolar transistors is summarized.

The majority of the noise produced in a bipolar transistor comes from three sources:

1. Random fluctuations in the dc emitter current
2. Random fluctuations in the dc collector current
3. Thermal noise due to the bulk base resistance r_{bb}' .

As one would suspect from studying noise in a P-N junction diode, the emitter-base diode in a bipolar transistor will contribute the same kind of noise. The dc current flowing in the collector-base junction will also cause shot noise but its contribution will be different because it is a back-biased diode--not a forward-biased one. An additional complicating factor also arises in the transistor--most of the current which flows in the emitter will flow in the collector. Since the charge carriers are the same, it is reasonable to expect the noise in the collector junction and that in the emitter to be correlated. Finally, the physical resistance in the base is at the temperature of the transistor chip and thus will contribute thermal noise as will any resistor at a finite temperature.

Van der Ziel and Becking (1958) have derived equations for the noise generators which account for these sources of noise (see Figure 4F-11)

$$1. \quad \overline{I_{ne}^2} = 4kT_j g_e \Delta f - 2q I_e \Delta f \quad (4F.36a)$$

$$2. \quad \overline{I_{nc}^2} = 2q I_c \Delta f \quad (4F.36b)$$

$$3. \quad \overline{V_{nb}^2} = 4k T_j R_{bb'} \Delta f \quad (4F.36c)$$

$$4. \quad \overline{I_{ne}^* I_{nc}} = 2k T_j Y_{fb} \Delta f \quad (4F.36d)$$

where $g_e = R_e(Y_e) = 1/r_e$, the real part of the emitter-base junction admittance

I_{ne} = Noise current in the emitter junction (see equation 4F.34a)

I_e = Emitter dc current

I_c = Collector dc current

Y_{fb} = Common-base forward transfer admittance

$\overline{I_{ne}^* I_{nc}}$ = Cross correlation product of emitter and collector shot noise currents

T_j = Temperature of the transistor chip or junction.

Figure 4F-11 shows the common-base circuit with the noise generators added. The model is a simple modification of Figure 4F-10b where the admittances have been changed to equivalent impedances and the shot noise current generator in the emitter has been transformed to a noise voltage generator. These transformations have been done to conform with van der Ziel's (1958b) presentation which simplifies calculation of noise factor.

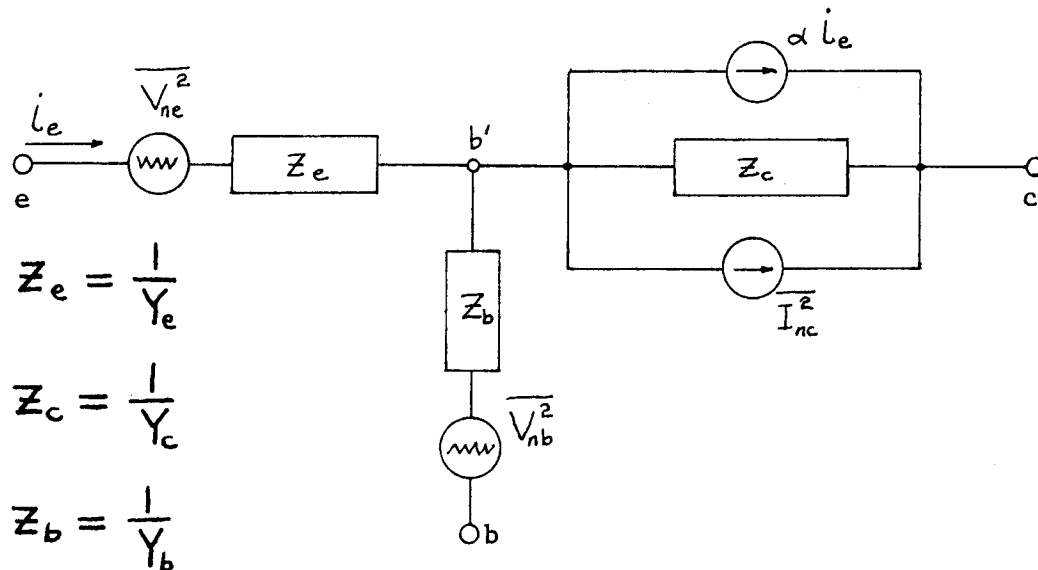


Figure 4F.11. Noise Model for a Bipolar Transistor in the Common-Base Configuration

Equations 4F.36 must be transformed to apply to the modified model.

The first equation is transformed by:

$$\overline{V_{ne}^2} = \overline{I_{ne}^2} |Z_e|^2$$

The second by substituting for the collector current the expression

$$I_c = (\alpha_o - |\alpha|^2) I_e + I_{co}$$

where I_{co} is the collector leakage current. The fourth is transformed by the equation:

$$Y_{fb} = \alpha Y_e$$

If the dc emitter current, I_e , is much larger than the emitter diode saturation current, then the approximations of Equation 4F.34b apply. Also if the relation between emitter noise voltage and noise current, $V_{ne} = Z_e I_{ne}$, is used and if we substitute $Y_e = g_o - Y_e^*$ then Equations 4F.36 become:

$$1. \quad \overline{V_{ne}^2} = 2k T (2g_e - g_o) |Z_e|^2 \Delta f \quad (4F.37a)$$

$$2. \quad \overline{I_{nc}^2} = 2q [(\alpha_o - |\alpha|^2) I_e + I_{co}] \Delta f \quad (4F.37b)$$

$$3. \quad \overline{V_{nb}^2} = 4k T_j R_{bb} \Delta f \quad (4F.37c)$$

$$4. \quad \overline{V_{ne}^* I_{nc}} = 2k T_j \alpha [g_o - Y_e^*] \Delta f \quad (4F.37d)$$

Remember that the noise performance analysis is made more complex because of the correlation between emitter and collector noise currents, i.e. V_{ne} and I_{nc} are not statistically independent. In general the common-base current gain α is complex and thus the correlation factor is complex. Also, the correlation is frequency dependent through both α and Y_e . Notice that for lower frequencies

$$Y_e^* \simeq g_o$$

and the correlation is practically zero.

The noise factor for the common-base model is computed by connecting a source impedance Z_s at temperature T_o to the input and looking at the short-circuit output current. The ratio of the short-circuit output current with internal transistor noise "turned on" to that when only the source Z_s is contributing is the noise factor. The resulting equation has been given by van der Ziel (1958b)

$$F = 1 + \frac{(r_{bb'} + \frac{1}{2g_e})}{R_s} + \frac{g_n}{R_s} |Z_s + Z_e + Z_b + Z_{cor}|^2 \quad (4F.38)$$

where the equivalent noise voltage generator V_{ne} has been split into a part V_{ne}' which is completely correlated with I_{nc} and a part V_{nc}'' which is totally uncorrelated. The noise conductance g_n has been defined from the collector shot noise current as

$$\overline{I_{nc}^2} = 4kT_o |\alpha|^2 g_n \Delta f \quad (4F.39)$$

where:

$$|\alpha|^2 g_n = \frac{g}{2kT_o} \left[(\alpha_o - |\alpha|^2) I_e + I_{co} \right] \quad (4F.40)$$

The Nyquist equivalent for V_n'' is

$$\overline{V_n''^2} = 4kT \frac{1}{2g_e} \Delta f \quad (4F.41)$$

and the correlation impedance is defined as:

$$Z_{cor} = \frac{\alpha V_{ne}'}{I_{nc}} = \frac{\alpha \overline{V_{ne} I_{nc}^*}}{I_{nc}^2} \quad (4F.42)$$

It should be realized now that g_e , g_n and Z_{cor} described the noise characteristics of the transistor. Also the noise factor equation assumes that the transistor is at standard temperature ($T_j = T_o$). The error due to this assumption will be discussed in Chapter X.

The noise factor equation in its most common form is obtained from Equation 4F.38 by expanding the absolute value factor and using $g_e = 1/r_e$ which gives (compare with Equation 4E.17b and with Agouridis, 1967)

$$F = 1 + A + \frac{B}{R_s} + g_n R_s \quad (4F.43)$$

where

$$A = 2g_n (r_e + r_{bb'} + R_{cor})$$

$$B = r_{bb'} + \frac{1}{2} r_e + g_n \cdot \left[(r_e + r_{bb'} + R_{cor})^2 + (x_s + x_e + x_b + x_{cor})^2 \right]$$

$$g_e = 1/r_e$$

with:

$$Z_e = r_e + j x_e$$

$$Z_b = r_{bb'} + j x_b$$

$$Z_{cor} = R_{cor} + j X_{cor}$$

$$Z_s = R_s + j X_s$$

The optimum source resistance for minimum noise factor can be obtained by taking the partial derivative of F with respect to the source resistance and solving for $R_{s,opt}$:

$$\frac{\partial F}{\partial R_s} = 0 \quad R_{s,opt} = \sqrt{\frac{B}{g_n}} \quad (4F.44)$$

Substituting (4F.44) into (4F.43) we get the noise factor obtained when the stage is noise matched:

$$F_{nm} = 1 + A + 2 \sqrt{\frac{B}{g_n}} \quad (4F.45)$$

The condition for noise tuning is to minimize B by adjusting X_s so that:

$$X_s + X_e + X_b + X_{cor} = 0 \quad (4F.46)$$

The frequency dependence of noise factor comes from the frequency dependence of Z_{cor} and g_n . The frequency dependence of g_n is obtained from Equation 4F.40 by substituting the equation for α which was defined with Figure 4F-10

$$\alpha \simeq \frac{\alpha_o}{(1 + j\omega r_e C_{Te})(1 + j\frac{\omega}{\omega_b})} \simeq \frac{\alpha_o}{1 + j\frac{\omega}{\omega_a}}$$

where ω_α is the alpha-cutoff frequency. Substituting this expression for α into Equation 4F.40 and making the approximations $I_{co} \ll I_e$ and $\beta_o \simeq \frac{1}{1-\alpha_o}$ gives

$$g_n \simeq g_e \left[\frac{1}{\beta_o} + \left(\frac{\omega}{\omega_\alpha} \right)^2 \right] \quad (4F.47)$$

where β_o is the low frequency beta of the transistor. Assuming that $\beta_o > 10$ and $R_{cor} \simeq 0$ and the stage is noise tuned, the noise factor of Equation 4F.43 reduces to

$$F_{nt} = 1 + A + \frac{B}{R_s} + g_n R_s \quad (4F.48)$$

where

$$\begin{aligned} A &\simeq 2 \left(1 + \frac{r_{bb'}}{r_e} \right) \left[\frac{1}{\beta_o} + \left(\frac{\omega}{\omega_\alpha} \right)^2 \right] \\ B &\simeq r_{bb'} \left\{ 1 + 2 \left(\frac{\omega}{\omega_\alpha} \right)^2 + \frac{r_{bb'}}{r_e} \left[\frac{1}{\beta_o} + \left(\frac{\omega}{\omega_\alpha} \right)^2 \right] \right\} \\ &\quad + \frac{1}{2} r_e \left[1 + 2 \left(\frac{\omega}{\omega_\alpha} \right)^2 \right]. \end{aligned}$$

For low frequencies $\omega < \frac{1}{10} \omega_\alpha$ the noise factor of Equation 4F.48 is

$$\begin{aligned} F_{nt} (\omega \ll \omega_\alpha) &= 1 + \frac{2}{\beta_o} \left(1 + \frac{r_{bb'}}{r_e} \right) + R_s \left(\frac{1}{\beta_o r_e} \right) \\ &\quad + \frac{1}{R_s} \left[r_{bb'} \left(1 + \frac{r_{bb'}}{\beta_o r_e} + \frac{r_e}{2 r_{bb'}} \right) \right] \end{aligned} \quad (4F.49)$$

where it has been assumed that $1/\beta_o \gg (\omega/\omega_\alpha)^2$. In Equation 4F.49 it becomes possible to see what transistor parameters are actually affecting the lowest value of noise factor. The important parameters are:

1. The base bulk resistance, $r_{bb'}$
2. The ac resistance of the base-emitter diode r_e (which depends directly on emitter current).

The optimum source resistance from Equation 4F.49 is

$$R_{s,opt} = \sqrt{\beta_o r_e r_{bb'} \left(1 + \frac{r_{bb'}}{\beta_o r_e} + \frac{r_e}{2 r_{bb'}} \right)} \quad (4F.50)$$

and the noise factor of Equation 4F.49 in terms of optimum source resistance becomes

$$F_{nt}(\omega \ll \omega_\alpha) = 1 + \frac{2}{\beta_o} \left(1 + \frac{r_{bb'}}{r_e} \right) + \sqrt{\frac{r_{bb'}}{\beta_o r_e} \left(1 + \frac{r_{bb'}}{\beta_o r_e} \right)} \left(\frac{R_s}{R_{s,opt}} + \frac{R_{s,opt}}{R_s} \right) \quad (4F.51)$$

where $R_{s,opt}$ has been factored out of Equation 4F.49. For the low-frequency model, the base-emitter diode ac resistance r_e can also be written in terms of the emitter current, I_e

$$r_e = kT_j / qI_e$$

and the noise factor of a noise tuned common-base amplifier at low frequencies ($\omega \ll \omega_a$) is

$$F_{nt}(\omega \ll \omega_a) = 1 + \frac{2}{\beta_o} \left(1 + r_{bb'} \frac{q}{kT_j} I_e \right) + \sqrt{\frac{r_{bb'} q}{\beta_o kT_j} I_e \left(1 + \frac{r_{bb'} q}{\beta_o kT_j} I_e \right)} \left(\frac{R_s}{R_{s,opt}} + \frac{R_{s,opt}}{R_s} \right) \quad (4F.52)$$

which shows the explicit dependence of noise factor on emitter current.

For high-frequency work with common-emitter configurations, probably the most popular equivalent circuit is the hybrid-pi circuit shown in Figure 4F-12b. The hybrid-pi model is attractive because it can be used to describe transistor operation when considering neutralization and when using Y-parameters. The hybrid-pi model is generated from the common-base equivalent circuit (Figure 4F-10) by interchanging base and emitter terminals and applying superposition and a delta-wye transformation to the base-collector terminals. The results of these transformations are shown schematically in Figure 4F-12.

The resistance shown shunting the output current generator is included to account for the base feedback generator which was neglected in the common-base model. This conductance must be included to account for the frequency dependent output conductance found in neutralized common-emitter stages. To be completely specific about this transformation, the admittance matrix for the hybrid-pi model is related to the equivalent tee impedances by the transformation:

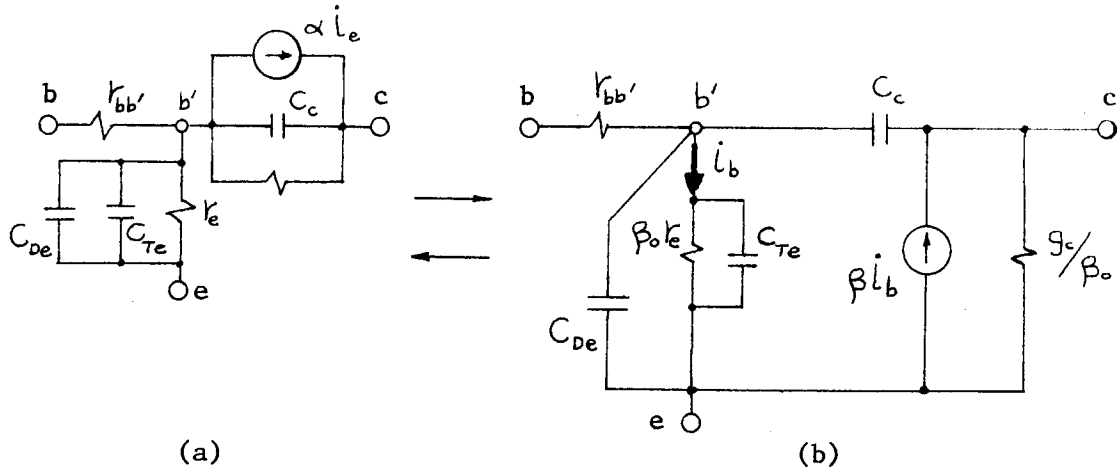


Figure 4F-12a. Generation of the Hybrid-pi Model from the Common-Base Model

$$[Y]_{\text{hybrid-pi}} = \frac{1}{Z_e Z_b + Z_c [Z_e + Z_b (1-\alpha)]} \begin{bmatrix} Z_e + Z_c (1-\alpha) & -Z_e \\ \alpha Z_c - Z_e & Z_e + Z_b \end{bmatrix}$$

where Z_e , Z_b and Z_c are defined by Figure 4F-11.

We know that simply changing the configuration of a transistor stage will not affect the internal noise mechanisms. They remain the same as for the common-base stage. What does change is the noise factor and optimum source resistance and correlation impedance. These change because the noise currents flow through different impedances when the configuration is changed. The noise factor for a common-emitter stage at UHF and microwave frequencies has been given an excellent treatment by Fukui (1966a).

He has taken a hybrid-pi equivalent circuit with header parasitics added and has computed the noise factor of the entire stage. The results of Fukui are based on measurable transistor parameters and show how noise factor varies with frequency and with transistor Q-point. The effect of header parasites is illustrated with measurements. What will be done for this thesis is to take Fukui's results and simplify them to a model without header parasites. Other features of the original presentation will be maintained.

The noise equivalent circuit for a bipolar transistor in the common-emitter configuration without parasites is shown in Figure 4F-13. The noise generators are the same as in the common-base model. The other symbols are defined as follows:

- $C_{Te} \triangleq$ Emitter-base transition region capacitance
- $C_{De} \triangleq$ Emitter diffusion capacitance
- $r_e \triangleq$ Dynamic resistance of the base-emitter diode
- $r_{bb'} \triangleq$ Base bulk resistance (Base-spreading resistance)
- $g_c/\beta_o =$ Output conductance
- $\beta = \beta_o [1 + j\beta_o(\omega/\omega_\alpha)]^{-1}$, high frequency current gain
- $\beta_o \triangleq$ Low-frequency current gain
- $\omega_\alpha \triangleq$ Alpha-cutoff frequency.

The noise factor is obtained as usual by adding a source admittance and looking at the short circuit output current for noisy and noiseless transistor operation. The noise factor as computed by Fukui is:

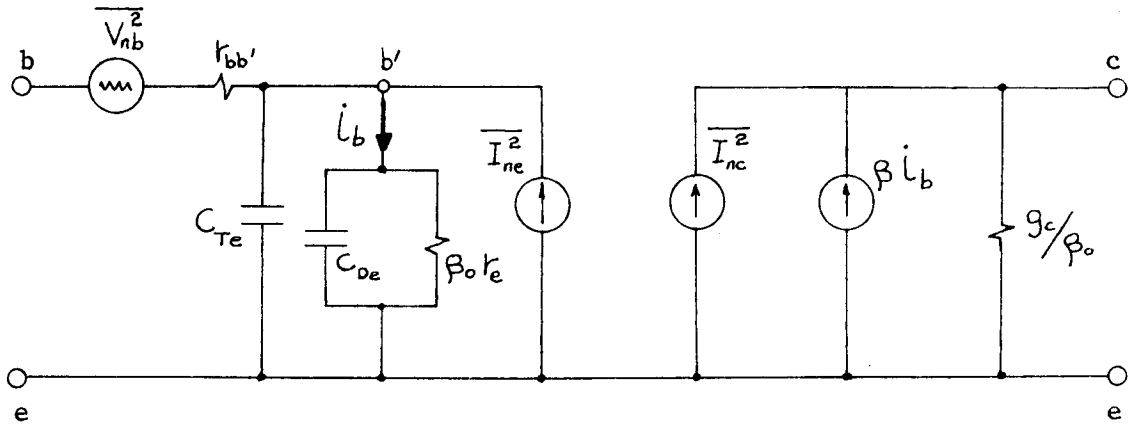


Figure 4F-12b. Noise Equivalent Circuit for a Common-Emitter Stage

$$\begin{aligned}
 F = & 1 + \frac{r_{bb'}}{G_s} |Y_s|^2 \\
 & + \frac{q I_b}{2 k T G_s} |1 + Y_s r_{bb'}|^2 \\
 & + \frac{k T}{2 q I_c G_s} |Y_s + Y_{be} + Y_{be} Y_s r_{bb'}|^2
 \end{aligned} \tag{4F.53}$$

where $Y_s = G_s + j B_s$, the source admittance

$$Y_{be} = \frac{1}{\beta_0 r_e} + j\omega(C_{De} + C_{Te})$$

I_c = Collector dc current

I_b = Base dc current.

Fukui has solved Equation 4F.50 in terms of the transistor operating parameters and has put it into the same form we have used throughout this paper

$$F = 1 + A + B G_s + \frac{1}{G_s} (C + B B_s^2 + D B_s) \quad (4F.54)$$

where

$$\begin{aligned} A &= 1/\beta_o + y \\ B &= r_{bb'} + \frac{1}{2} r_e [1 + y^2] \\ C &= y/r_{bb'} \\ D &= (f/f_T) \end{aligned}$$

and the parameter y accounts for the transistor noise parameters and noise factor frequency dependence. This parameter is defined as

$$y \triangleq \frac{r_{bb'}}{r_e} \left[\frac{1}{\beta_o} + \left(\frac{f}{f_T} \right)^2 \right] = \frac{qI_e}{kT_j} r_{bb'} \left[\frac{1}{\beta_o} + \left(\frac{f}{f_T} \right)^2 \right] \quad (4F.55)$$

where f is the operating frequency and f_T is the unit-gain frequency or the gain-bandwidth product in Mhz.

The minimum noise factor is obtained by noise matching and noise tuning and is computed by Fukui to be

$$F_{\min} = 1 + A + \sqrt{4BC - D^2} \quad (4F.56a)$$

which upon substitution of the parameters A , B , C , D defined in quation 4F.54 gives:

$$F_{\min} = 1 + \frac{1}{\beta_o} + y + \sqrt{1/\beta_o + 2y + y^2} \quad (4F.56b)$$

Fukui has given an alternate expression to (4F.54) for noise factor which incorporates both the minimum noise factor and the optimum source conductance and susceptance. This equation is an alternate way of expressing the noise factor in the form we have used in Equations 4F.52 and 4F.26 and is a clever way of obtaining an equation which expresses the dependence of noise factor on source admittance. The alternate expression is

$$F = F_{\min} + \frac{B}{G_s} \left[(G_s - G_{s,\text{opt}})^2 + (B_s - B_{s,\text{opt}})^2 \right] \quad (4F.57)$$

where: $G_{s,\text{opt}}$ = Optimum source conductance. When $G_s = G_{s,\text{opt}}$,
the stage is noise matched.

$B_{s,\text{opt}}$ = Optimum source susceptance. When $B_s = B_{s,\text{opt}}$,
the stage is noise tuned.

The optimum values of source conductance and susceptance are given as:

$$G_s = \frac{\sqrt{4BC - D^2}}{2B} \quad (4F.58)$$

$$B_{s,\text{opt}} = -\frac{D}{2B} = -\frac{\left(\frac{f}{f_T}\right)}{2B} \quad (4F.59)$$

Equation 4F.57 is used by Baechtold and Strutt (1968) to calculate the transistor noise parameters for microwave transistors in the frequency range 0.6 to 4.2 GHz.

The low-frequency limit on the minimum noise factor is obtained from (4F.56b) where the parameter y becomes

$$y \rightarrow \frac{r_{bb'}}{\beta_o r_e} \quad \text{for} \quad \left(\frac{f}{f_T}\right)^2 \ll \frac{1}{\beta_o}$$

which is substituted into (4F.56b) to give the low-frequency noise factor for a common-emitter transistor amplifier:

$$F_{\min}(\text{low frequency}) = 1 + \frac{2}{\beta_o} \left[\frac{1}{2} + \frac{r_{bb'}}{r_e} \right] + \sqrt{\frac{1}{\beta_o} + \frac{2r_{bb'}}{\beta_o r_e} \left[1 + \frac{r_{bb'}}{2\beta_o r_e} \right]} \quad (4F.60)$$

The high frequency limit is obtained by letting the frequency of operation approach f_T and neglecting the terms $1/\beta_o$ i.e.,

$$y \rightarrow \frac{r_{bb'}}{r_e} \left(\frac{f}{f_T}\right)^2 = h \quad (4F.62a)$$

which is substituted into Equation 4F.56b to give the minimum high-frequency noise factor for a common-emitter transistor amplifier:

$$F_{\min}(\text{high frequency}) = 1 + h \left[1 + \sqrt{1 + \frac{2}{h}} \right] \quad (4F.61)$$

The parameter h can also be written in terms of the transistor emitter current and base bulk resistance as:

$$h = \frac{q}{kT_j} \left(\frac{f}{f_T}\right)^2 I_e r_{bb'} \quad (4F.62b)$$

Equation 4F.61 is valid for frequencies above a cutoff frequency specified by

$$\frac{f}{f_T} \geq \sqrt{\frac{10}{\beta_o}} \quad (4F.63)$$

which for typical values of low-frequency beta is $f > \frac{1}{3} f_T$.

For low-noise transistor amplifiers, the emitter currents are seldom less than 1 ma. and the base bulk resistance is made as small as possible but is generally in the neighborhood of 10-20 ohms. These practical limits place a lower limit on the parameter h of approximately $h_L > 1/20$. The actual lower limit on h is obtained by substituting (4F.62) into (4F.61) which gives:

$$h_L \approx \frac{q}{kT_j} \left(\frac{10}{\beta_o}\right) I_e r_{bb'}, \quad (4F.64a)$$

or

$$h_L \approx \frac{r_{bb'}}{r_e} \left(\frac{10}{\beta_o}\right) \quad (4F.64b)$$

It should be apparent from Equation 4F.61 that the noise factor of a transistor will increase with increasing frequency and this is indeed true as verified by laboratory measurements. Transistors will exhibit an upper-noise-corner frequency at which the noise figure is 3db above the low-frequency value. To obtain the value of h for which the noise factor of Equation 4F.61 has risen by a factor of two (3 db), we consider the minimum noise factor to be that obtained with h_L and solve for h_{3db} where F_{min} is twice that value. Doing this, the value of h corresponding to an increase in low-frequency noise figure of 3db is:

$$h_{3db} = \frac{1}{2} + h_L + \sqrt{2h_L} \quad (4F.65)$$

Equation 4F.65 in terms of the upper-noise-corner frequency, f_A , is obtained by substituting (4F.64b) into (4F.65) as follows:

$$h_{3db} = \frac{r_{bb'}}{r_e} \left(\frac{f_A}{f_T} \right)^2 = \frac{1}{2} + \frac{r_{bb'}}{r_e} \left(\frac{10}{\beta_o} \right) + \sqrt{\frac{2r_{bb'}}{r_e} \left(\frac{10}{\beta_o} \right)}$$

$$f_A = f_T \left[\frac{r_e}{2r_{bb'}} + \frac{10}{\beta_o} + \sqrt{\frac{5r_e}{\beta_o r_{bb'}}} \right]^{1/2} \quad (4F.66)$$

A plot of Equation 4F.61 is shown in Figure 4F-13 and is an adaption of a similar plot given by Fukui (1966a).

Cooke (1961) has presented an equation for the upper-noise-corner frequency which is based on an alternate equation for noise factor and is in terms of the alpha-cutoff frequency. The noise factor equation given by Cooke is

$$F = 1 + \frac{1}{R_s} \left(r_{bb'} + \frac{1}{2} r_e \right) + \frac{(R_s + r_e + r_{bb'})^2}{2R_s r_e} \left[\frac{1}{\beta_o} + \left(\frac{f}{f_a} \right)^2 \right] \quad (4F.67)$$

and the upper-noise-corner frequency that results is:

$$f_A = f_a \left[\frac{1}{\beta_o} + \frac{r_e (2R_s + 2r_{bb'} + r_e)}{(R_s + r_{bb'} + r_e)^2} \right]^{1/2} \quad (4F.68)$$

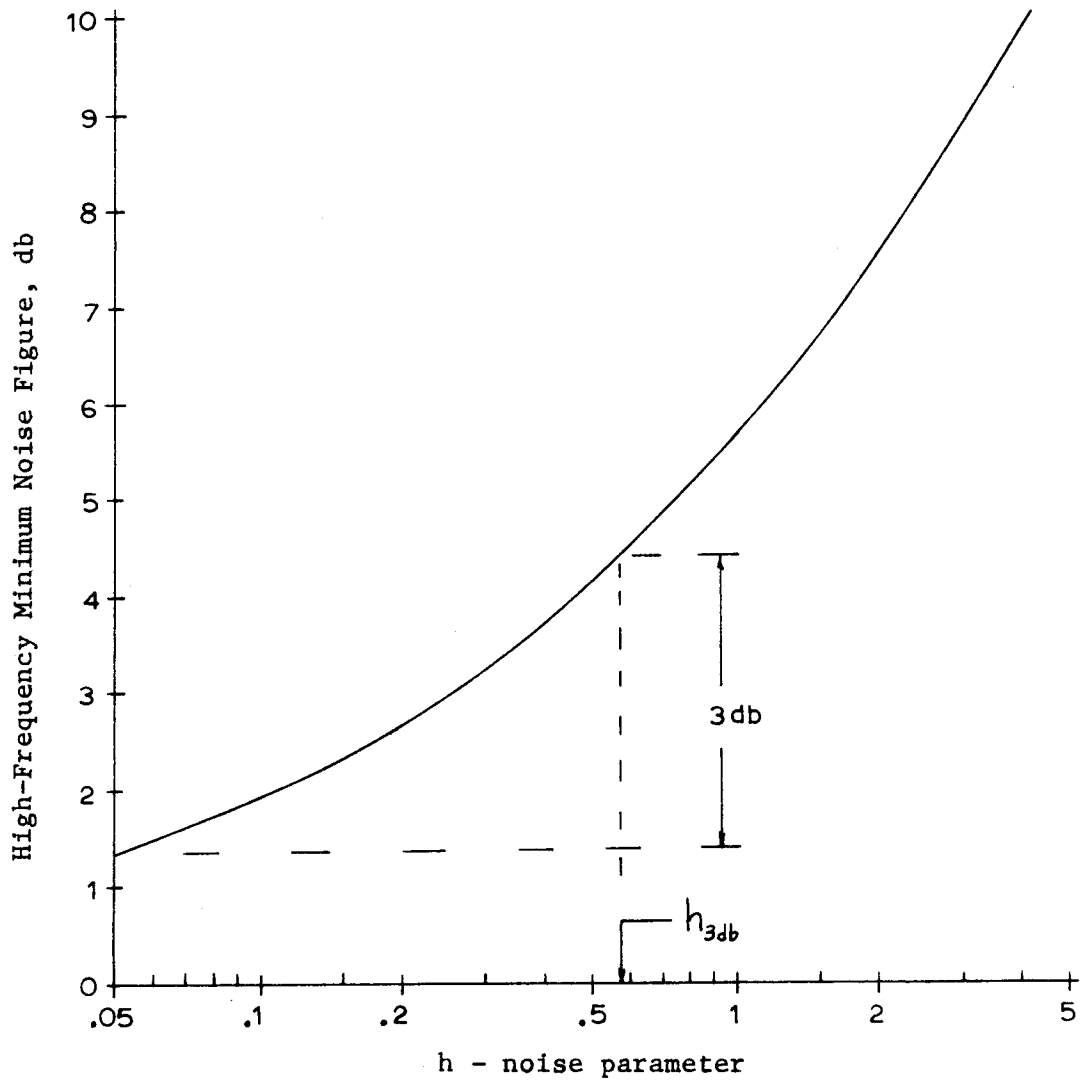


Figure 4F-13. High-Frequency Minimum Noise Figure as a Function of the Noise Parameter h

where f_{α} is the alpha-cutoff frequency. Experimental data by Cooke shows excellent agreement with Equations 4F.67 and 4F.68.

Presentation of data on the noise figure of a transistor presents a problem because the measured noise figure depends upon frequency, emitter current and source resistance which are three parameters under the control of the user. The bulk base resistance cannot be changed by the user. A common technique used to present noise figure data is by use of noise figure contours. These are curves of constant noise figure as a function of frequency or emitter current and source resistance. They are usually minimum noise figures which means the device is noise tuned at each data point and also the emitter current has been adjusted for minimum high-frequency noise figure. If the conditions for minimum noise figure are not met, the graph of contours must contain information about the condition of noise tuning and the value of emitter current. Figures 4F-14a and 4F-14b illustrate two possible techniques for presenting noise figure contours for a common-emitter transistor amplifier. The plot of noise figure as a function of source resistance, such as Figure M-1 in the Appendix, can be obtained for the noise figure contour of Figure 4F-14a by fixing the operating frequency. The contours of Figure 4F-14b are adopted from data obtained in an application note by Brubaker (1968). More information on noise figure contours can be obtained from an application note from Princeton Applied Research Corp. (1969) on how to use noise figure contours and from an article by Sato (1971).

Figure 4F-15 is an appropriate conclusion for this section on noise in bipolar transistors. This figure is a composite of data from a

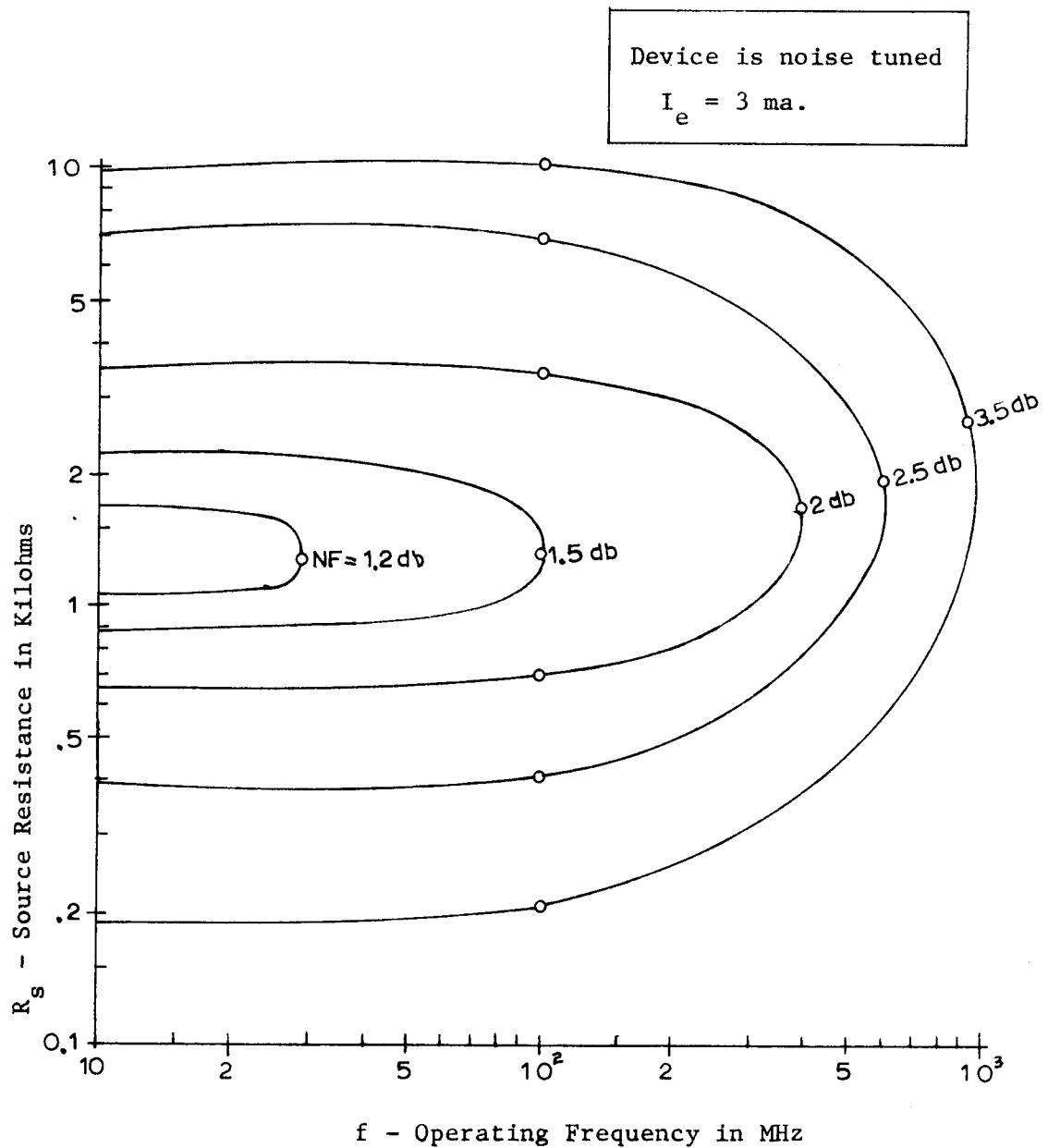


Figure 4F-14a. Typical Noise Figure Contours for a Common-Emitter Transistor Amplifier

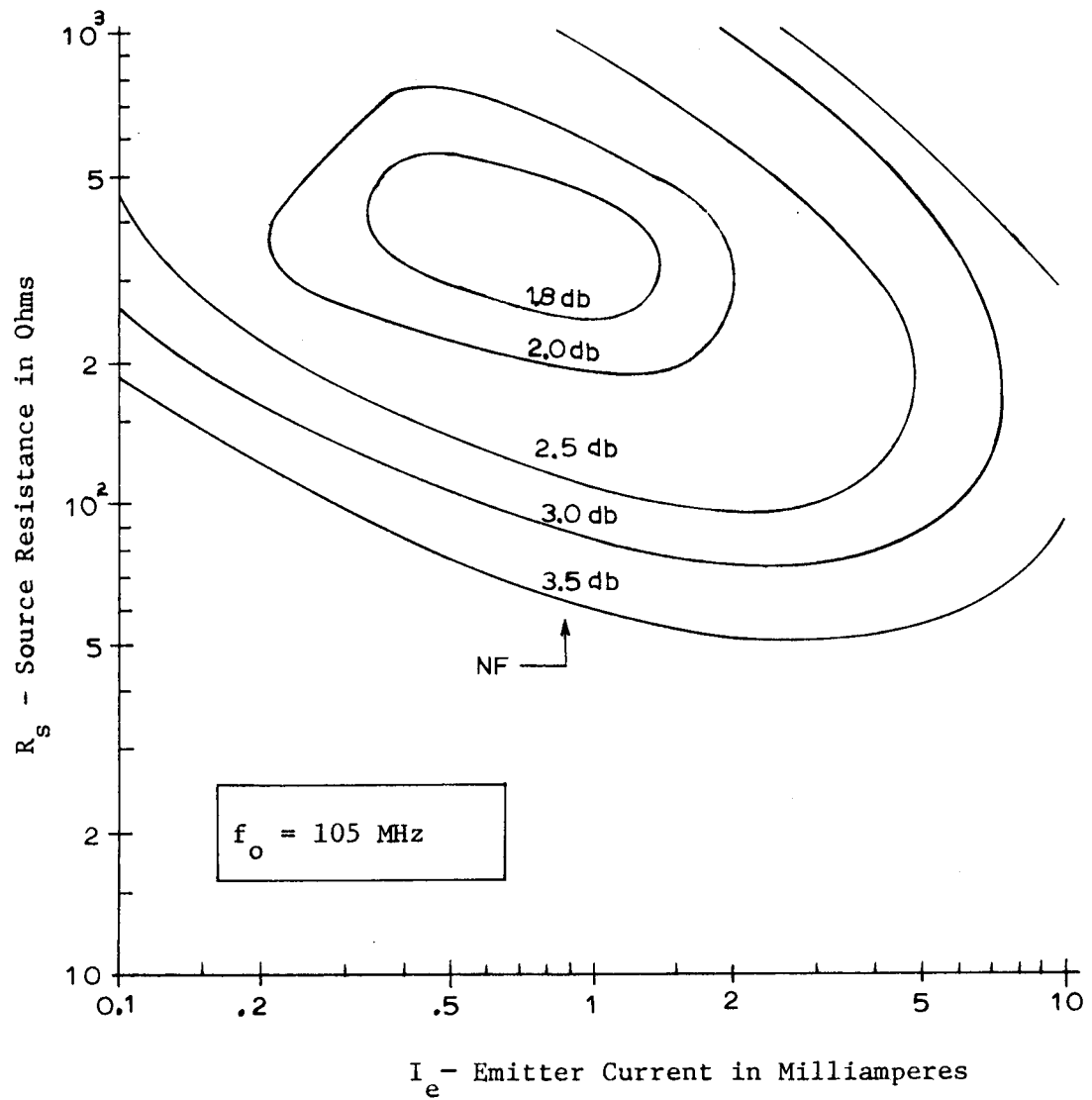


Figure 4F-14b. Typical Noise Figure Contours for a Common-Emitter Transistor Amplifier

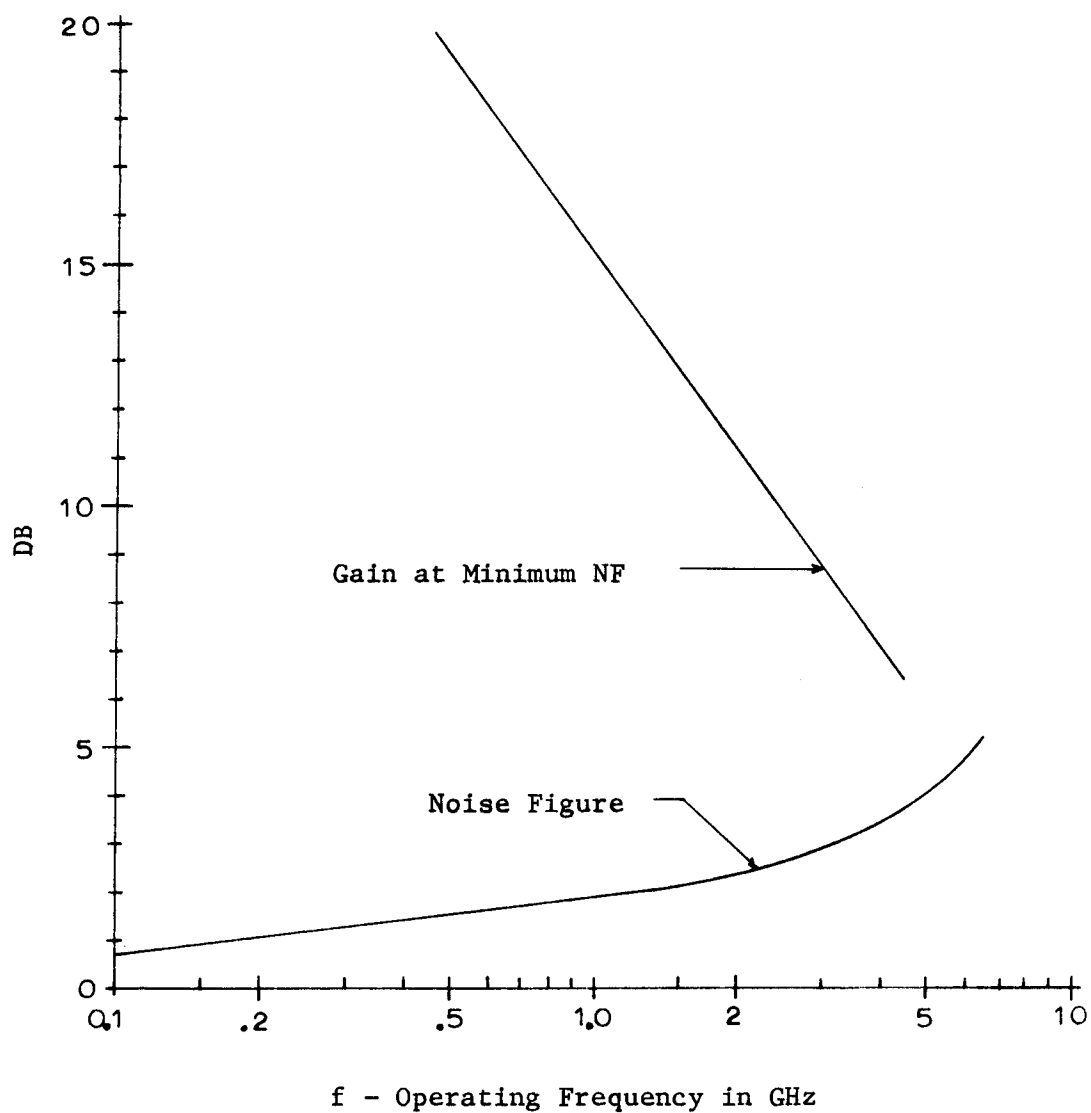


Figure 4F-15. State-of-the-Art Noise Figure and Gain at Minimum Noise Figure for Commercially Available Transistors (December, 1972)

record kept by the author over the year 1972. The data was obtained from advertisements by various manufactures. The gain and noise figures shown are achievable simultaneously.

4. Noise in field-effect transistors

The noise generation mechanisms in field-effect transistors have been studied by Klaassen (1967, 1969), van der Ziel (1962a, 1970) and Bruncke and van der Ziel (1966). These studies have shown that the dominant device noise at medium and high frequencies comes from three sources:

1. Thermal noise in the channel
2. Induced gate noise
3. Thermal noise from the bulk resistance of the chip.

The induced gate noise is caused by capacitive coupling between the active region of the channel and the gate. The capacitance couples noise from the noise voltage distribution along the channel. For the intrinsic FET, the noise factor can be essentially determined by considering the thermal noise of the channel, the induced gate noise, and the correlation between them. For the practical FET, the effects of feedback and bulk resistance noise must also be included.

A summary of FET operation is important because it can be used to establish the important FET parameters. Figure 4F-16 illustrates the physical construction of a junction FET and the equivalent circuit of the intrinsic FET that will be used for noise factor calculations.

The high-frequency admittance parameters are given by Bruncke (1966) and van der Ziel in terms of the equivalent circuit of Figure 4F-16. The conductive and capacitive terms of the admittances are

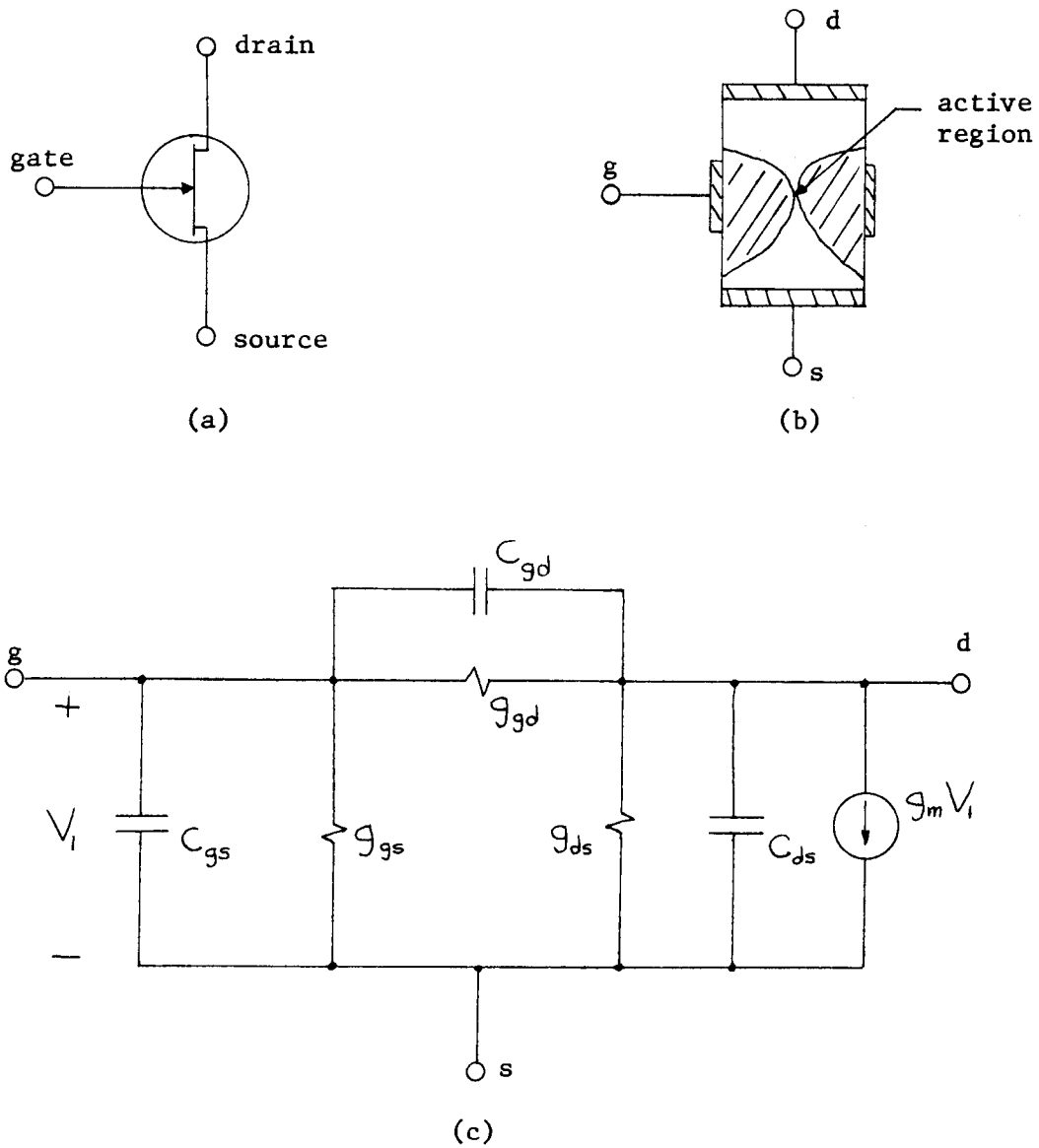


Figure 4F-16. Junction-FET Equivalent Circuit and Physical Construction

$$\begin{aligned} g_{11} &= g_{gs} + g_{gd} & g_{12} &= -g_{gd} \\ & & & (4F.69a) \end{aligned}$$

$$\begin{aligned} g_{21} &= \frac{g_m}{1 + \left(\frac{f}{f_o}\right)^2} - g_{gd} & g_{22} &= g_{ds} + g_{gd} \end{aligned}$$

$$\begin{aligned} c_{11} &= c_{gs} + c_{gd} & c_{12} &= -c_{gd} \\ & & & (4F.69b) \end{aligned}$$

$$\begin{aligned} c_{21} &= -c_{gd} - \frac{g_{mo}}{2\pi f_o \left[1 + \left(\frac{f}{f_o}\right)^2\right]} & c_{22} &= c_{ds} + c_{gd} \end{aligned}$$

where g_m = low frequency value of the intrinsic device
transconductance

f_o = a defined cutoff frequency which is slightly larger
than the gain-bandwidth product.

The noise in the junction FET is represented by a noise current generator I_{nd} in the drain-source circuit which represents the thermal noise of the channel and a noise current generator I_{ng} in the gate-source circuit which represents induced gate noise.

A simple equivalent noise circuit for the junction FET is shown in Figure 4F-17 where the noise current generator I_d at the FET output has been referred to the input by a transformation with the complex transconductance, Y_{21} :

$$I_d = Y_{21} V_{gs}$$

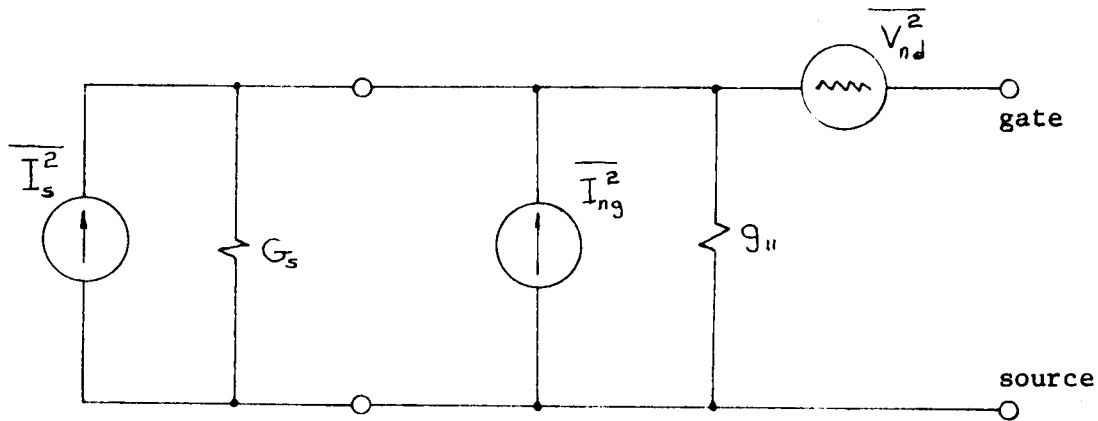


Figure 4F-17. Noise Sources in a Junction-FET where the Thermal Noise of the Channel has been Referred to the Input

For a simple analysis we will ignore the correlation between I_{ng} and V_{nd} to arrive at a simple expression for noise factor. The mean-square values for the noise generators of Figure 4F-17 are:

$$\begin{aligned}\overline{V_{nd}^2} &= 4 k T_o R_n \Delta f \\ \overline{I_{ng}^2} &= 4 k T_o g_{11} \Delta f \\ \overline{I_s^2} &= 4 k T_o G_s \Delta f\end{aligned}\tag{4F.70}$$

The equivalent noise resistance R_n has been given by Bruncke and van der Ziel (1966) to be

$$R_n \approx \frac{1}{\sqrt{2} g_m}$$

where g_m is the apparent transconductance of the device. The conductance g_{11} is the high-frequency, short-circuit input conductance of the device. The noise factor of the circuit of Figure 4F-17 is

$$F = \frac{\overline{I_s^2} + \overline{I_{ng}^2} + \overline{V_{nd}^2} (G_s + g_{11})^2}{\overline{I_s^2}}$$

which upon substitution of the Nyquist equivalents of Equations 4F.70 gives:

$$F = 1 + \frac{g_{11}}{G_s} + \frac{R_n}{G_s} (G_s + g_{11})^2 \quad (4F.71a)$$

$$= 1 + 2 R_n g_{11} + G_s R_n + \frac{g_{11}}{G_s} (1 + R_n g_{11}) \quad (4F.71b)$$

The optimum value of source conductance is obtained by differentiating F with respect to G_s and equating to zero which gives:

$$G_{s,opt} = \sqrt{\frac{g_{11}}{R_n} (1 + R_n g_{11})} \quad (4F.72)$$

The noise factor in terms of $G_{s,opt}$ is

$$F = 1 + 2 R_n g_{11} + \sqrt{R_n g_{11} (1 + R_n g_{11})} \left(\frac{G_s}{G_{s,opt}} + \frac{G_{s,opt}}{G_s} \right) \quad (4F.71c)$$

and the minimum noise factor for $G_s = G_{s,opt}$ is:

$$F_{min} = 1 + 2 R_n g_{11} + 2 \sqrt{R_n g_{11} (1 + R_n g_{11})} \quad (4F.73)$$

Measured data by Bruncke and van der Ziel show that the gate noise can be slightly larger than the thermal noise of g_{11} which will result in a noise factor slightly higher than predicted.

Klaassen and Prins (1969) have presented theory and data on the behavior of FETs at VHF and UHF. They treat the intrinsic FET and then consider the influence of feedback and bulk source resistance on the noise factor.

The equivalent circuit used by Klaassen and Prins to represent FET noise is shown in Figure 4F-18. This equivalent circuit is valid for frequencies up to a few times greater than the gain-bandwidth product, f_T . The quantities in the figure are defined as follows:

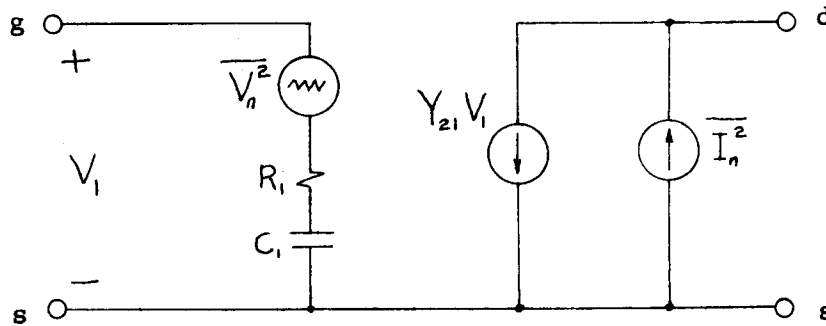


Figure 4F-18. Equivalent Circuit for a Noisy FET at high Frequencies

$$\overline{V_n^2} = 4 k T_O R_1 \Delta f, \text{ Mean-square noise voltage due to the induced gate noise}$$

$$\overline{I_n^2} = 4 k T_O b g_m \Delta f, \text{ Mean-square noise current due to the thermal noise of the channel}$$

$R_1 = a/g_m$, the FET input resistance

$C_1 = 2/3 C_{gs}$ where C_{gs} is the gate to source capacitance

Y_{12} = Forward transfer admittance or the complex transconductance.

Klassen and Prins have included both junction and MOS FET's in their presentation by introducing the empirical factors a and b to account for variations in device parameters. Thus, the noise analysis that will follow is valid for both JFET's and MOSFET's. The factors a and b have the range:

$$\begin{aligned} a &= 1/3 \\ 2/3 \leq b \leq 1 \end{aligned} \quad \text{for the JFET} \quad (4F.74)$$

$$\begin{aligned} a &\leq 1/5 \\ 2/3 \leq b \leq 4 \end{aligned} \quad \text{for the MOSFET}$$

If all the noise of the FET is referred to the input, a simple equivalent circuit such as Figure 4F-19 is the result. The equations which accomplish this transformation are,

$$\begin{aligned} V_{nd} &= -I_n/Y_{21} \\ I_{ng} &= Y_{11} (V_n + V_{nd}) \end{aligned} \quad (4F.75)$$

where Y_{11} is the input admittance and Y_{21} is the transfer admittance.

This circuit is not analogous to that given by Bruncke and van der Ziel (Figure 4F-17) where I_{ng} will account for the induced gate noise and V_{nd} the thermal noise of the channel.

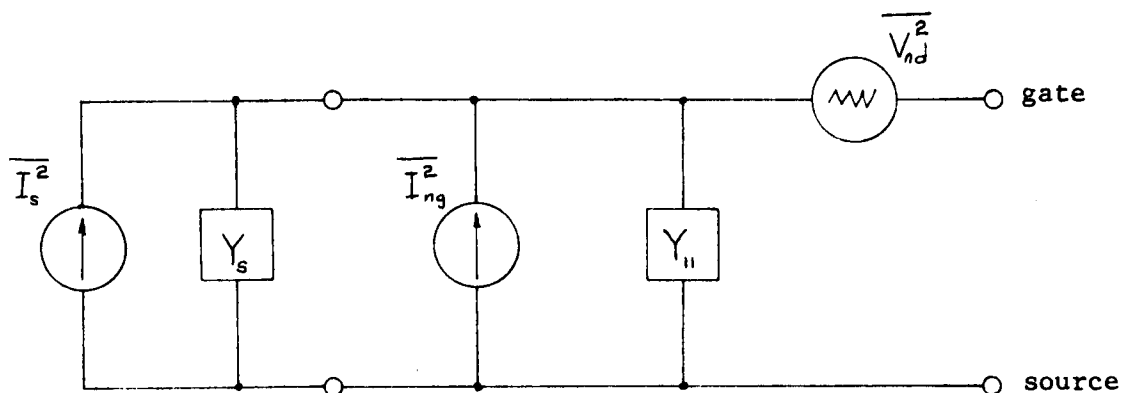


Figure 4F-19. Noise Sources Referred to the Input of the FET

The approximate high-frequency minimum noise factor is determined by Klaassen and Prins to be

$$F_{min} \simeq 1 + 2 \sqrt{\frac{R_i}{R_n} (1 - \gamma_i^2)} \left(b \frac{f}{f_T} \right) + 2 \sqrt{\frac{R_i}{R_n}} \left(\sqrt{\frac{R_i}{R_n}} + \gamma_r \right) \left(b \frac{f}{f_T} \right)^2 \quad (4F.76)$$

valid for frequencies $f < \frac{3}{b} f_T$,

where $R_1 = \frac{a}{g_m}$, the FET input resistance

$R_n \cong b/g_m$, the equivalent noise resistance

$f_T = g_m C_1$, the gain-bandwidth product

$\gamma_c = \gamma_r \left(\frac{bf}{f_T} \right) + j \gamma_i$, a complex correlation coefficient.

The complex correlation coefficient is a measure of the correlation between V_{nd} and I_{ng} and is defined with the equation:

$$\overline{V_n I_n^*} = \gamma_c \sqrt{\frac{R_i}{R_n}} \left(b \frac{f}{f_T} \right) \quad (4F.77)$$

Typical values for γ_r and γ_i are:

$$\begin{aligned} -0.10 < \gamma_r < -0.15 \\ 0.30 < \gamma_i < 0.40 \end{aligned} \quad (4F.78)$$

Finally, the optimum source conductance and susceptance are given by:

$$\begin{aligned} G_{s,opt} &= \sqrt{\frac{R_i}{R_n} (1 - \gamma_i^2)} (\omega C_i) \\ B_{s,opt} &= - \left(1 - \gamma_i \sqrt{\frac{R_i}{R_n}} \right) (\omega C_i) \end{aligned} \quad (4F.79)$$

Klaassen and Prins (1969) have used these equations and others which were obtained by considering feedback effects to arrive at the following conclusions:

1. The thermal noise in the channel is the dominant noise at high frequencies
2. The intrinsic FET has identical noise figures when used in either the common-source or common-gate configuration
3. Feedback has only a small effect on device noise figure
4. $G_{s,opt}$ is generally not equal to the real part of the input admittance (4F.79). Data on minimum noise factor as a function of frequency verifies the quadratic nature of (4F.76).

5. Since $R_n \approx 1/g_m$, the minimum noise factor is a quadratic function of drain current and larger currents give lower minimum noise factor.

Van der Ziel (1970, p. 124) has given an equation for FET noise factor which more closely resembles those obtained in previous sections of this thesis. His equation is

$$F = 1 + \frac{g_n}{G_s} + \frac{R_n}{G_s} \left[(G_s + g_n + G_{cor})^2 + (B_s + B_n + B_{cor})^2 \right] \quad (4F.80)$$

where $R_n = b/g_m$, the equivalent noise resistance
 g_n = equivalent noise conductance
 $Y_{11} = g_{11} + j B_{11}$, the FET input admittance
 $Y_{cor} = G_{cor} + j B_{cor}$, the complex correlation impedances
 used to account for the correlation between induced
 gate noise and channel noise.

The FET at high frequencies behaves in a manner similar to all two-port devices in that it exhibits both noise matching effects and noise tuning effects. This can be seen from Figures M-1 and N-1 in the Appendix.

5. Mixer noise

The problem of analyzing device noise is compounded many-fold when it is used as a mixer. This results from the multifrequency nature of a mixer and the many possible port terminating combinations. Essentially, the noise output is due to internal shot noise and thermal noise which

has been heterodyned from all unshorted frequencies and may include noise from the image frequency.

On a circuit basis, and conceptually, the noise contribution of the mixer stage can be treated like any other noisy two-port (or in terms of frequency spectrums, a multiport). A conceptual artifice which provides a good working model is to consider a mixer as the cascade connection of an ideal frequency translator and an RF amplifier. The block diagram of this representation is shown in Figure 4F.20. The ideal frequency translator obeys the port frequency equation:

$$f_{\text{RF}} = f_{\text{LO}} \pm f_{\text{if}}$$

If the RF amplifier passband is narrow enough so that only one of the two possible RF inputs is amplified, an equivalent noise temperature for the mixer, T_m , can be defined such that the Friis equation is obeyed or:

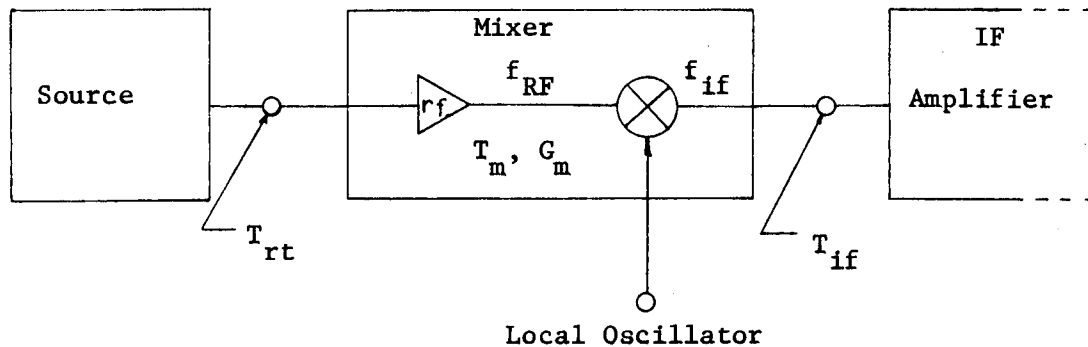


Figure 4F-20. Conceptual Model of an RF Mixer Showing RF Amplifier and Ideal Frequency Translator

$$T_{rt} = T_m + \frac{T_{if}}{G_m} \quad (4F.81)$$

$$F_{rt} = F_m + \frac{(F_{if} - 1)}{G_m} \quad (4F.82)$$

The term G_m is the conversion gain of the mixer defined in the same manner as transducer gain for amplifiers. If the RF amplifier passband is wide enough to let some of the image noise into the mixer, the mixer noise output will increase. When no information is being transmitted on the image frequency, this represents a net increase, of up to 3 db, in the noise figure of the primary channel. This effect is discussed in Section G of Chapter X.

The mixer model of Figure 4F-20 will work well for narrowband receivers employing tuned circuits but for wideband applications more sophisticated models are needed. In particular, resistive switching mixers (double-balanced mixers) and microwave crystal diode mixers may be handled in alternate ways.

First consider the double-balanced diode-quad mixer circuit of Figure 4F-21. The noise contribution of shot noise due to diode current can be essentially ignored when compared to T_o . Because of this, the noise figure of a double-balanced mixer is equal to the conversion loss i.e. the equivalent receiver noise temperature is computed just as though the mixer were a passive two-port network at temperature T_o . The noise temperature equation which applies to double-balanced mixers is widely used. In Chapter IV-C, the effective noise temperatures for receivers

preceded by attenuators or transmission lines was given in Equations 4C.37b and 4C.60c. In Chapter X the noise temperature equation accounting for two-port loss is generalized to account for impedance mismatch errors (10E.3).

This same equation is used in Chapter V (Equation 5.2). For mixers, the noise temperature equation is written as

$$T_{rt} = \mathcal{L}_m T_{if} + (\mathcal{L}_m - 1) T_o \quad (4F.83a)$$

where \mathcal{L}_m is the available conversion ~~S~~ loss of the mixer. The term $\mathcal{L}_m T_{if}$ is the noise due to the IF noise multiplied by the conversion loss. The term $(\mathcal{L}_m - 1) T_o$ is additive noise due just to a passive mixer at a physical temperature of T_o . For transmission line noise (4C.60c) the conversion loss \mathcal{L}_m is replaced by the flat loss N and T_{if} becomes the receiver noise. Equation 4F.83a is really a "prototype" equation which can be applied to many situations.

From (4F.83a) we get the receiver noise factor as

$$F_{rt} = \mathcal{L}_m \left(1 + \frac{T_{if}}{T_o} \right) = \mathcal{L}_m F_{if} \quad (4F.83b)$$

and the noise figure (Equation 4C.64) is:

$$NF_{rt} = NF_{if} + 10 \log \mathcal{L}_m \text{ db} \quad (4F.84)$$

Thus for a double-balanced mixer, the noise figure at the input to the mixer is equal to the IF noise figure added to the available conversion loss in db. The equations assume that the mixer will be used so that

the image noise is suppressed. If the noise figure of a double-balanced mixer is measured with a wideband noise source connected directly at the input, the noise input at both LO sidebands will cause the indicated noise figure to be 3 db lower than the single channel noise figure. By applying the Friis equation to (4F.83) we get the noise figure for the double-balanced mixer as:

$$NF_m \approx 10 \log \mathcal{L}_m \text{ db} \quad (4F.85)$$

The approximation sign denotes the assumption that the shot noise contribution of the diodes is neglected compared to $T_o = 290^\circ\text{K}$.

A third method of specifying the noise in a mixer is by use of a quantity which is called the mixer noise-temperature ratio, t_m (Strum,

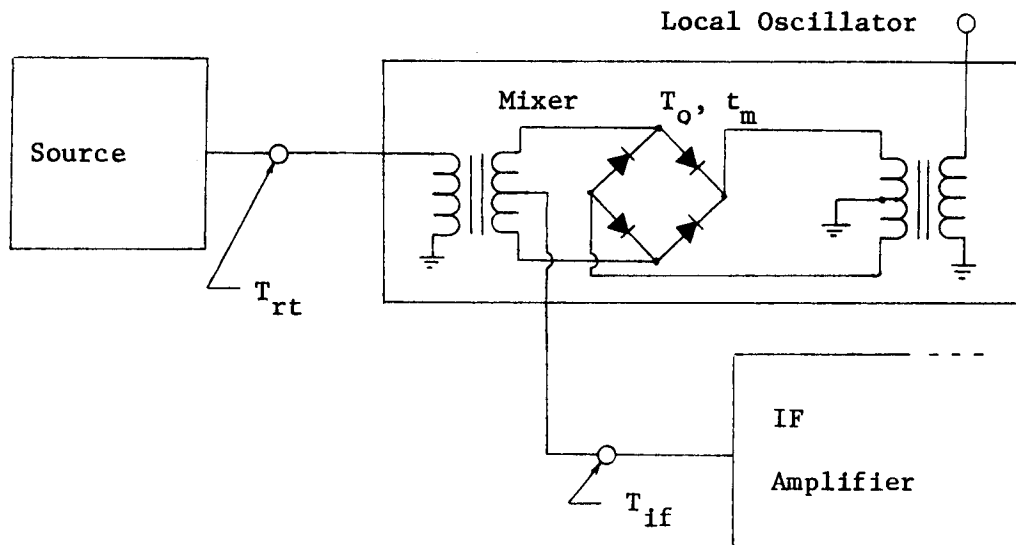


Figure 4F-21. Double-Balanced Diode Mixer

1953; Messenger and McCoy, 1957). The use of this term was initiated when microwave receivers for radar applications used a broadband crystal diode mixer and a method for specifying broadband mixer noise was needed. The term t_m is sometimes referred to as a noise temperature in some older literature but this is really a misnomer as t_m is dimensionless.

The mixer noise-temperature ratio is really a type of noise factor in the sense that it is the ratio of two output powers that compare the excess noise of the mixer. t_m is defined as (Kraus, 1966, p. 265):

"the ratio by which the actual mixer output noise power exceeds its thermal output noise power, assuming both mixer and source are at a temperature T_o ".

If G_m is the conversion gain of the mixer and $\mathcal{L}_m = 1/G_m$ is the conversion loss, this definition is equivalent to taking the ratio of mixer noise factor with excess noise to the noise factor of an ideal mixer (no excess noise). From (4F.83) we know that \mathcal{L}_m is the noise factor of an ideal mixer so:

$$t_m = F_m / \mathcal{L}_m \quad \text{or} \quad F_m = t_m \mathcal{L}_m \quad (4F.86)$$

Thus t_m plays the role of a multiplying factor to account for excess noise. From this definition, t_m has the range $1 \leq t_m \leq \infty$. From (4F.86) the mixer equivalent noise temperature is:

$$T_m = (\mathcal{L}_m t_m - 1) T_o \quad (4F.87)$$

Using (4F.86) and (4F.87) with (4F.81) and (4F.82), we calculate receiver total noise temperature and noise factor as:

$$T_{rt} = \mathcal{L}_m T_{if} + (\mathcal{L}_m t_m - 1) T_o \quad (4F.88)$$

$$F_{rt} = \mathcal{L}_m (t_m + F_{if} - 1) \quad (4F.89)$$

The theory of mixer operation for the various devices will not be discussed because of the complexity of conditions involved. A brief review of mixer noise characteristics will be given and supplemented with literature references. Noise generation in junction transistor mixers is given a very comprehensive treatment by Webster (1961). Webster shows that the noise figure of a junction transistor used as a mixer is always higher than for its corresponding use as an amplifier. The principle cause of this increase is the heterodyning of the base resistance noise from many frequencies to the IF frequency. Also, the common-emitter configuration has lower noise figure than common-base.

Shot noise in p-n diode mixers is discussed by Uhlir (1958). This is an excellent review of diode conduction and noise theory and is highly recommended. Another paper which discusses thermal and shot noise in a pumped diode is given by Dragone (1968). The bibliography contains several additional references. Shot noise in Schottky barrier diodes is discussed by Cowley and Zettler (1968). Noise figure and conversion loss in microwave Schottky barrier mixer diodes is reviewed briefly by Barber (1967).

For microwave "crystal-diode" mixers the important noise factor parameters are conversion loss \mathcal{L}_m and mixer noise-temperature ratio t_m . Values for these two parameters can be determined from theory but are usually measured experimentally. Typical values for conversion losses

run from 4 to 7 db and values for t_m run from 1 to 2, with 1.3 being average. Microwave receivers using "crystal diode" mixers have noise figures ranging from 7 to 13 db (includes IF noise).

As stated previously, the excess noise for a double-balanced diode-quad mixer is usually small compared to $T_o = 290^\circ\text{K}$. The mixer noise temperature ratio is on the order of 1.02 so that Equation 4F.89 can be approximated by (4F.83) or, in logarithmic form, (4F.85). Conversion losses will vary from 5 to 9 db depending upon LO level and frequency.

V. RF TRANSLATOR NOISE

If it can be argued that noise factor or effective noise temperature is the best single specification of the noise performance of a receiver, it follows from the Friis equation that receiver noise performance is determined by the RF translator. In most receiving systems the total receiver noise temperature is determined by the effective noise temperature of the RF translator and the effective noise temperature of the feed system. The study of a low-noise receiving system usually reduces to a study of noise in the RF translator and the effects of coupling to the antenna. Two-port noise theory for active and passive networks is used to determine the noise performance of the RF translator.

When designing a receiving system it is impossible to consider sensitivity specifications completely independent of other performance criteria. The most important receiver specification which must be considered along with sensitivity is that of dynamic range or distortion. There are many important trade-offs between sensitivity and distortion that must be made to achieve the best possible receiving system. This is one of the reasons why such topics as receiving system noise temperature (Chapter IV-D) and antenna sky noise (Figure 4C-25) were included. As a general rule, the intermodulation distortion performance of a receiver can only be improved at the expense of receiver noise figure. One of the many reasons for this is that the active devices must be operated with larger device currents to achieve better distortion performance. This increase in current increases the device noise factor due to increased shot noise. In many designs it is profitable to operate

at the highest possible noise factor consistent with good system performance. This allows the circuit designer to achieve the best possible distortion performance. Another example of a distortion--sensitivity trade-off is that of receiver input mismatch. Consider as an example, the amplifier data of Figure M-1 in the Appendix. If the device is operated at a source resistance lower than optimum, the noise figure increases but the voltage level that causes the distortion decreases. By this technique it is sometimes possible to trade one db of noise figure for several db of distortion improvement. This brief discussion of distortion--sensitivity trade-offs is not intended to be a primer on the subject but is only included to increase the reader's awareness of distortion problems.

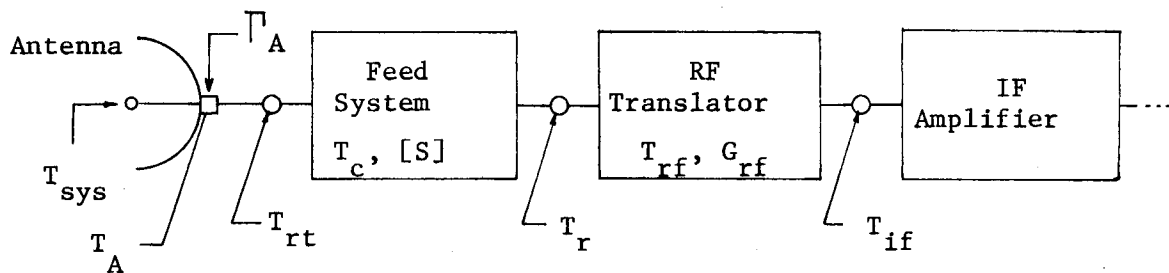


Figure 5-1. Block Diagram of Receiving System Showing the Elements which Are Important in Determining System Noise Temperature

The system that will be discussed in this chapter is shown in block diagram form in Figure 5-1. The following quantities are defined:

- a. $G_{rf} \triangleq$ the transducer gain of the RF translator (see Appendix, Part D)

- b. $T_c \triangleq$ the physical temperature of the feed system, $^{\circ}\text{K}$
- c. $T_{\text{sys}} \triangleq$ the noise temperature of the complete receiving system ($T_{\text{sys}} = T_A + T_{\text{rt}}$), $^{\circ}\text{K}$
- d. $T_{\text{rt}} \triangleq$ the total receiver noise temperature at the input to the feed system, $^{\circ}\text{K}$
- e. $T_r \triangleq$ the receiver noise temperature at the input to the RF translator, $^{\circ}\text{K}$
- f. $T_{\text{if}} \triangleq$ the effective noise temperature at the input to the IF amplifier, $^{\circ}\text{K}$
- g. Γ_A = the reflection coefficient of the antenna.

All noise temperatures can be converted to an equivalent noise factor using the definition:

$$F = 1 + \frac{T}{T_o}$$

The noise temperature of the complete receiving system depends upon the antenna noise temperature and T_{rt} . It is T_{sys} which really specifies the quality of a communication system and not T_A or T_{rt} alone. Antenna noise is discussed in Chapters IV-C, IX-D, and XI-D. The interaction of antenna noise temperature and receiver noise figure is best seen in Figure 11D-1. Notice, for example, that for an antenna temperature of 2000°K , the power sensitivity is changed only one db for noise figures between 0 and 4 db. It is hardly worth reducing receiver noise figure below 4 db. From Figure 4C-25 we see that antenna noise temperature is larger than 2000°K for frequencies below 50 MHz so that noise figures below 4 db are not needed. At frequencies below 20 MHz, atmospheric noise completely dominates the system. In the crowded

HF spectrum where large signals cause interference, it is much better to design for large dynamic range than for low noise figure. The important thing to keep in mind is that antenna noise determines the practical lower limit for receiver noise figure.

There are several noise temperatures to be considered in the system of Figure 5-1. First, there is the system noise temperature which is the sum of antenna and total receiver noise temperatures (see Chapter IV-D):

$$T_{\text{sys}} = T_A + T_{\text{rt}} \quad (5.1)$$

Next, the total receiver noise temperature is determined by the noise temperature at the RF translator input, T_r , the physical temperature of the feed system, T_c , and the available loss of the feed system, \mathcal{L} :

$$T_{\text{rt}} = \mathcal{L} T_r + (\mathcal{L} - 1) T_c \quad (5.2)$$

This equation is analogous to Equations 4C.60c, 4F.83a, and 10E.3. It is widely used to describe the effect of a passive two-port on receiver noise temperature (Kraus, 1966, p. 263; Livingston and Bechtold, 1968).

The available loss, \mathcal{L} , of the feed system is determined by the reflection coefficient of the antenna, Γ_A , and the feed system scattering parameters $[S]$. The equation for the available loss of any passive two-port network was given in Chapter X (10B.4). This equation is:

$$\mathcal{L} = \frac{(|1 - S_{11}\Gamma_A|^2 - |S_{22}(1 - S_{11}\Gamma_A) + S_{12}S_{21}\Gamma_A|^2)}{|S_{21}|^2 (1 - |\Gamma_A|^2)} \quad (5.3)$$

A general discussion on reflection coefficients and scattering parameters is given in Chapter X. The S's in (5.3) are the scattering parameters of the feed system and are convenient for describing the effects of loss and impedance mismatch. The available loss \mathcal{L} is not the same as insertion loss and is much more difficult to measure. In many cases the insertion loss is nearly equal to the available loss if the scattering parameters Γ_A , S_{11} , and S_{22} are small. Approximating the available loss with insertion loss is convenient in many practical situations but one must be careful when doing this.

If the feed system is simply a length of transmission line, the available loss is given by (10B.29)

$$\mathcal{L} = N \frac{\left(1 - \frac{|\Gamma_A|^2}{N^2}\right)}{\left(1 - |\Gamma_A|^2\right)} \quad (5.4)$$

where N is the flat loss. The noise temperature at the input to the RF translator is determined by the translator noise temperature T_{rf} and gain G_{rf} and the noise temperature of the IF amplifier. Its value is determined by the Friis equation as (see Appendix, Part J):

$$T_r = T_{rf} + \frac{T_{if}}{G_{rf}} \quad (5.5)$$

The equivalent noise temperature of the RF translator is much easier to measure than it is to calculate because of the many components within. From Figure 3-1 we see that the translator may contain RF and IF amplifiers and filters as well as RF mixers. The noise contributions

of these devices can be determined by applying the information given in Chapter IV and combining contributions by applying the Friis equation.

The equivalent noise temperature of the RF translator is determined primarily by the noise temperature of the first active device and the RF filtering. This is because most modern devices have sufficient gain to overcome the noise contribution of succeeding stages. The notable exception to this rule is the resistive switching diode mixer (double-balanced mixer) which has a loss of 6-8 db (see Chapter IV-F). The equivalent noise temperature of a device can be written as (Equation 10E.2 or Equation 4F.57)

$$T'_e = T_e + T_o \frac{B}{G_s} \left[(G_s - G_{sopt})^2 + (B_s - B_{sopt})^2 \right] \quad (5.6)$$

where T_e and B are noise parameters of the device, $(Y_s = G_s + j B_s)$ is the source admittance and $(Y_{sopt} = G_{sopt} + j B_{sopt})$ is the optimum source admittance for both noise matching and noise tuning. The minimum noise temperature occurs when $Y_s = Y_{sopt}$ so that $T'_e = T_e$. The effect of an RF filter in the signal path preceding the active device can be accounted for using the techniques discussed in Chapter IV-C. From Figure 4C-16, the equivalent noise temperature at the input to the RF filter was determined to be (see Equation 4C.35c)

$$T_{Filter}(f) = T'_e \frac{N}{|H_n(f)|^2} + T_c (N - 1) \quad (5.7)$$

where N is the numerical flat loss of the filter at peak response and $H_n(f)$ is the normalized transfer function.

The effect of RF filter amplitude response must be considered along with system requirements and IF bandwidth. For the superheterodyne receiver, the IF bandwidth is much smaller than the RF bandwidth. This situation is illustrated in Figure 5-2. Since the RF response is flat over the passband of the IF, the transfer function is a constant i.e., $H(f) \rightarrow H(f_o)$. When this occurs, the Friis equation for the equivalent noise temperature at the RF translator input becomes (see Appendix, Part J)

$$T_r(f_o) = T_{\text{Filter}}(f_o) + \frac{\overline{T}_{\text{if}}}{G_{\text{rf}}(f_o)} \quad (5.8)$$

where f_o is the RF operating frequency and \overline{T}_{if} is the average noise temperature of the IF amplifier. As the local oscillator is tuned and the IF passband is translated inside the RF passband, the spot noise temperature $T_{\text{Filter}}(f_o)$ and translator gain $G_{\text{rf}}(f_o)$ will change. The average noise temperature of the IF amplifier is unchanged by local oscillator tuning.

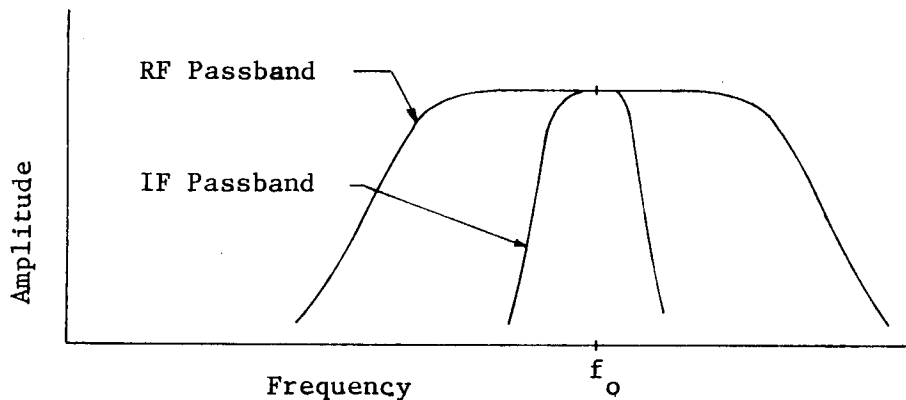


Figure 5-2. Relative RF and IF Passband Widths for a Superheterodyne Receiver

The terminating impedances as well as the output impedance of the RF translator will affect receiver noise temperature. If the RF translator does not present the optimum impedance to the IF amplifier, the IF noise temperature will be seriously degraded. The translator output impedance can be adjusted to give minimum noise temperature by making tradeoffs between G_{rf} and \overline{T}_{if} . Another approach is to make the translator output the optimum impedance for the IF amplifier. This usually results in a 0 to 3 db gain loss for the translator but still may improve the overall noise temperature of the system.

The feed system must supply the RF translator with the optimum source impedance or the translator noise temperature will be degraded. This almost always results in an impedance mismatch between feed system and translator. This mismatch will lower the delivered power but it will improve signal-to-noise ratio (see Chapter IV-E).

Methods for measuring the equivalent noise temperatures of the various RF translator components are given in Chapter IX. The errors that are involved in making these measurements are discussed in Chapter X. It seems unlikely that noise figure uncertainties of better than ± 1 db can be achieved with commonly available laboratory equipment. For more accurate measurements, loss and measurement error corrections must be made. Automatic noise figure meters have a typical accuracy of ± 0.7 to ± 1.5 db depending upon the operating frequency and scale. The best noise source accuracy is obtained from hot-cold noise sources.

Figure 5-3 is an appropriate conclusion for this chapter. This figure shows the noise figures of various commercially available

broadband RF amplifiers. Band endpoints are denoted by squares. State-of-the-art device noise figure is shown for comparison.

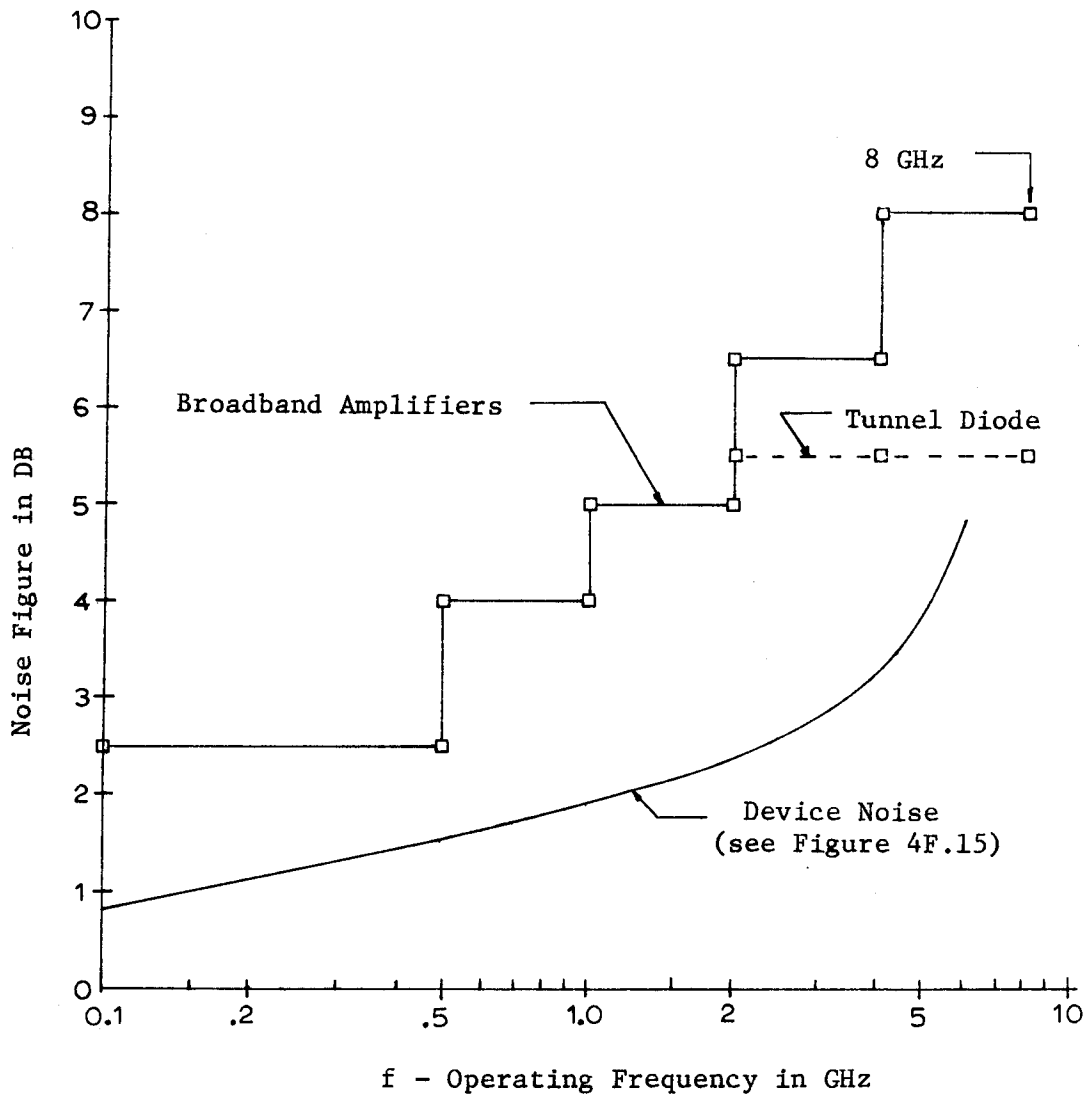


Figure 5-3. Noise Figure of Commercially Available Broadband RF Amplifiers (December, 1972)

VI. NOISE POWER DETECTORS

Sensitivity measurements, and consequently noise voltage measurements, rely on the use of noise power detectors for output indicators. The use of the detector can be classified into one of two important categories: those measurements which require the relative indication of two noise levels and those which require the absolute indication of noise level. In the former category are measurements such as the noise diode determination of noise factor where only the output power ratio is needed. For these measurements it is assumed that the spectral characteristics of both receiver internal noise and injected noise are identical and that the output indicator is capable of indications that are linearly proportional to the different powers. In the latter category are measurements of total output power and measurements of signal-plus-noise-to-noise ratios. In this case, the output power indicator must be capable of determining the absolute output power of either signal or noise or the superposition of the two. For relative measurements, it is possible to use a variety of detectors but for absolute measurements, only detectors that can measure power or true RMS voltages are satisfactory.

The type of output indicator (sensory transducer) and power detector selected for a particular measurement will depend upon the type of measurement and the accuracy desired. This accounts for the variety of sensitivity measurement methods commonly used. For many types of noise measurements it is desirable to have a detector capable of measuring the "true" root-mean-square value of a noise voltage. To emphasize

the strict theoretical relationship between noise power and noise voltage, let us examine the case of thermal noise. Statistically, we can only determine the available noise power in a bandwidth Δf as given by:

$$P_{\text{avail}} = \frac{\overline{V_n^2}}{4R_n} = k T_n \Delta f \quad \text{watts}$$

Now even though the equivalent noise voltage for the resistor is random, and therefore not deterministic, it is common practice to define a thermal noise voltage from the available power as

$$V_n = \sqrt{\overline{V_n^2}} = \sqrt{4 k T_n R_n \Delta f} \quad \text{volts RMS}$$

where this RMS value of voltage is consistent with the value of available power predicted by statistical theory. To be a true-reading RMS voltmeter, it must be capable of measuring thermal noise voltages.

In a strict sense, there are no instruments capable of measuring true RMS voltages for large noise bandwidths but only those which measure average voltage, peak voltage or power. Even the so-called true-reading RMS voltmeters rely on a calorimetric power measurement which is converted into an equivalent RMS voltage.

Typically, a voltmeter will be calibrated using a sinewave. When this same meter is used to measure noise voltages, the reading will have errors caused by the varying meter response between sinewaves and noise. This varying response, which is caused by the way the meter responds to the statistical differences between sinewaves and noise, will affect

measurement accuracy. Detector requirements are much more strict for absolute measurements than for relative ones. The basic properties of output detectors will now be presented and the relative merits of each for noise measurements will be discussed.

Listed below are the output indicators most often used for sensitivity measurements:

- a. Power meter
- b. RMS voltmeter
- c. Average-reading voltmeter
- d. Peak-reading voltmeter.

These indicators can be classified into two different categories according to their principles of operation. In the first category are those instruments which operate on some calorimetric principle whereby the receiver output power is converted into heat. Power meters and RMS voltmeters belong in this category. Generally this type of instrument is superior because, a) it operates over a wide range of frequencies and, b) its output indication does not depend on the signal waveform but only its RMS value.

With these features, the output power of both signals and noise can be measured to give high accuracy for signal-plus-noise-to-noise ratio measurements. Examples of these instruments are the barretter (Montgomery, 1964, p. 156), and bolometers such as thermistors and thermocouples. The capability of the RMS voltmeter to measure complex signal waveforms and/or noise is contrasted with the usual AC voltmeter which is capable of measuring only average or peak values and is calibrated only for sinewaves. In spite of this contrast, the high cost and low

availability of adequate power meters and RMS voltmeters usually forces the user to select a more available instrument and accept the resulting inaccuracies or determine methods of compensation. Typical accuracies for power meters are $\pm 1-2\%$ which is 0.04 - 0.09 db.

A study of average-reading and peak-reading voltmeters is a study of their detector circuits. For this reason we will now analyze commonly used detector circuits and show how their output can be processed to yield noise power measurements. Figure 6-1 shows a block diagram of a generalized power detector circuit which includes predetection filter and amplifier, γ^{th} -law detector device, and low-pass (postdetection) filter.

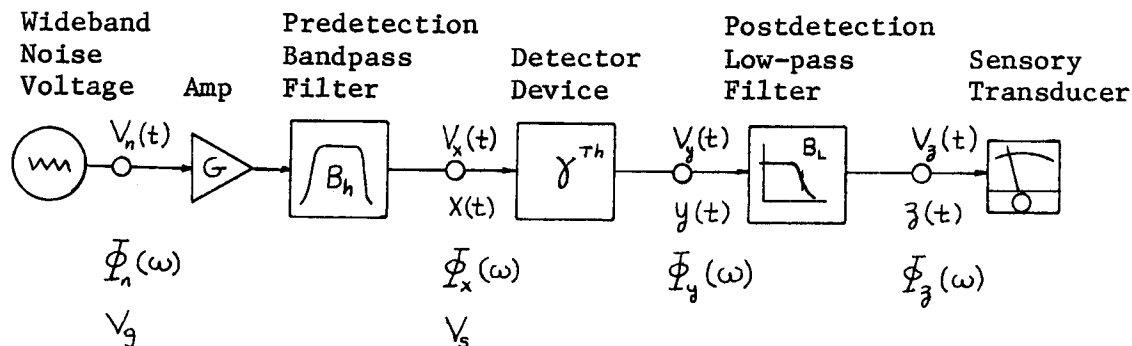


Figure 6-1. Generalized Power Detector Circuit

The detector types that will be considered are:

- a. Envelope
- b. Full-wave square-law

- c. Half-wave linear
- d. Full-wave linear
- e. Phase sensitive (product detector).

Before discussing detector types, the definitions for the average value of a Gaussian noise voltage, the average value of a half-wave and full-wave rectified Gaussian noise voltage, and the average value of the envelope of a Gaussian noise voltage should be presented. These averages are computed from the statistical definition presented in Chapter IV-A. The Gaussian probability density function for a noise voltage is obtained from Equation 4A.18 by setting $X_0 \equiv 0$ to give:

$$P(V_n) = \frac{1}{\sigma_n \sqrt{2\pi}} e^{-\frac{V_n^2}{2\sigma_n^2}}$$

When the noise voltage is a sample function of a process which is both stationary and ergodic, the statistical average and the time average are equal and we can compute the following time averages:

- a. The average value of the noise voltage is zero

$$\overline{V_n(t)} = \frac{1}{\sigma_n \sqrt{2\pi}} \int_{-\infty}^{+\infty} V_n e^{-\frac{V_n^2}{2\sigma_n^2}} dV_n = 0 \quad (6.1)$$

- b. The average value of the full-wave rectified noise voltage is

$$\overline{|V_n(t)|} = 2 \frac{1}{\sigma_n \sqrt{2\pi}} \int_0^{\infty} V_n e^{-\frac{V_n^2}{2\sigma_n^2}} dV_n = \sqrt{\frac{2}{\pi}} \sigma_n \quad (6.2)$$

c. The average value of the half-wave rectified noise voltage is

$$\frac{1}{2} \overline{|V_n(t)|} = \frac{\sigma_n}{\sqrt{2\pi}} \quad (6.3)$$

d. The average magnitude of the envelope of $V_n(t)$ is determined from the Rayleigh distribution (Equation 4A.22) as

$$V_{ave} = \int_0^{\infty} V_n \left(\frac{V_n}{\sigma_n} e^{-\frac{V_n^2}{2\sigma_n^2}} \right) dV_n = \sqrt{\frac{\pi}{2}} \sigma_n \quad (6.4)$$

A. Peak-Reading Voltmeter

It has been known for several years that the envelope of a Gaussian noise voltage has a Rayleigh distribution (Landon, 1942). This is demonstrated with the help of probability theory in Davenport and Root (1958, p. 160). An ideal envelope detector is defined as one in which the output voltage follows the envelope of the input voltage exactly. If we denote RMS noise voltages with E_r ($E_r = \sigma_v$) and measure a Gaussian noise voltage with an ideal envelope detector followed by an average-reading meter, the average voltage will be determined by applying the result of Equation 6.4 to give:

$$V_{ave} = \sqrt{\frac{\pi}{2}} E_r = \sqrt{\frac{\pi}{2}} \sqrt{4kT_n R_n \Delta f} \quad (6.5)$$

The ideal-diode detector is a type of envelope detector (used for AM demodulation) but is not an ideal envelope detector. A peak-reading

voltmeter uses an ideal-diode detector for voltage measurements. The circuit for a simplified peak-reading voltmeter is shown in Figure 6-2. The circuit shows a Nyquist noise source driving a simple peak rectifier (ideal-diode detector).

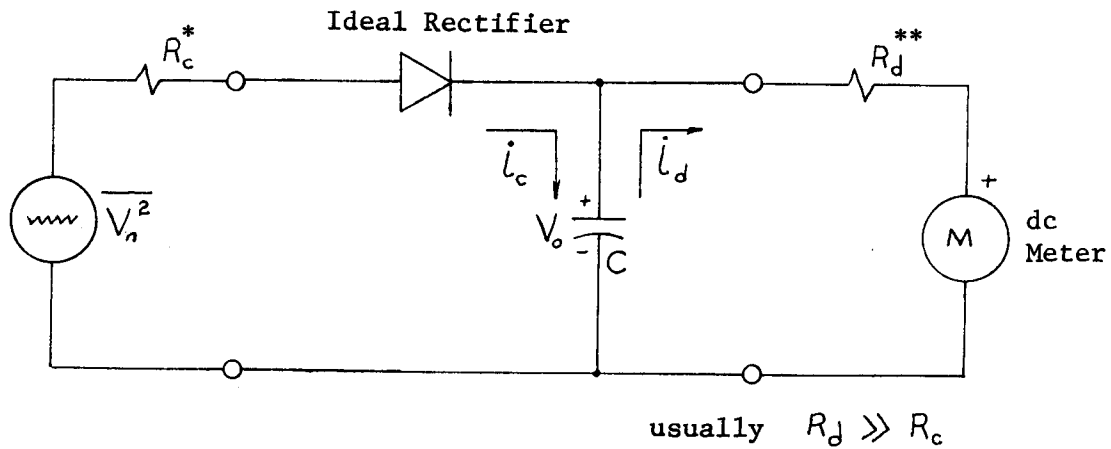


Figure 6-2. Simplified Peak-Reading Voltmeter

* R_c is the equivalent Thevenin Resistance of the diode.

** R_d is the equivalent Thevenin Resistance of the dc meter

When the meter is calibrated to read the RMS value of a sinewave, the peak value V_p and the indicated (RMS) value are related by:

$$V_m = \frac{V_p}{\sqrt{2}}$$

Now when the sinewave voltage is replaced by a Gaussian noise voltage

generator ($E_r = \sqrt{V_n^2} = \sqrt{4kT_n R_n \Delta f}$), the RMS noise voltage, E_r , is

found by analyzing the charge and discharge equations for the circuit.

We know from circuit theory that when the peak rectifier is in the

steady-state condition the average charge and discharge currents are equal:

$$i_{\text{charge}} = i_{\text{discharge}} = \frac{V_o}{R_d}$$

If it is assumed that the reciprocal of the generator noise bandwidth, $1/\Delta f$, is much smaller than either the charge ($R_c C$) or discharge ($R_d C$) time constants, the time average of the charge current and the ensemble average will be equal (the assumption of ergodicity) and the current equation can be written

$$\frac{V_o}{R_d} \simeq \frac{1}{R_c} \int_{V_o}^{\infty} V_n P(V_n) dV_n \quad (6.6)$$

where the integral represents the average value of a half-wave rectified Gaussian noise voltage biased off by a dc voltage of V_o , which is the time average voltage on the capacitor. The assumption of wideband noise is necessary to preserve the ergodicity of the process.

For wideband Gaussian noise the Gaussian probability function is substituted into (6.6) to give:

$$\begin{aligned} \frac{R_c}{R_d} &= \frac{1}{V_o E_r \sqrt{2\pi}} \int_{V_o}^{\infty} V_n e^{\frac{-V_n^2}{2E_r^2}} dV_n \\ &= \frac{E_r}{V_o \sqrt{2\pi}} e^{\frac{-V_o^2}{2E_r^2}} \end{aligned} \quad (6.7)$$

Now since the meter is calibrated to read RMS voltage with a sinewave, the dc voltage V_o and the indicated meter voltage will be related by, $V_o = \sqrt{2} V_m$. Substituting this into (6.7) and letting the factor K be defined as

$$K = \frac{\text{Meter voltage reading}}{\text{True RMS Voltage}} = \frac{V_m}{E_r} = \frac{V_o}{\sqrt{2} E_r}$$

results in the transcendental equation (Oliver, 1955)

$$\frac{R_d}{R_c} = 2 K \sqrt{\pi} e^{K^2} = 2 \left(\frac{V_m}{E_r} \right) \sqrt{\pi} e^{\left(\frac{V_m}{E_r} \right)^2} \quad (6.8)$$

which relates the measured (V_m) and RMS (E_r) values for a wideband Gaussian noise voltage. From this analysis we realize that the ratio R_d/R_c must be accurately known to solve for values of K . A unique value of the ratio R_d/R_c exists for which $K = 1$ and there is no correction necessary i.e., $V_m = E_r$. This occurs when:

$$\frac{R_d}{R_c} = 2\sqrt{\pi} e = 9.636$$

It is possible to construct a peak-reading voltmeter that will read true RMS voltage for both a sinewave and wideband Gaussian noise. One must be careful, however, to be sure that all assumptions are satisfied. Generally, the noise bandwidth, Δf , of the noise source driving the peak rectifier is much larger than the 100 Hz bandwidth found in a typical peak-reading voltmeter. Also, a typical meter will have a ratio R_d/R_c of 10^4 which means that it will indicate a voltage 2-4 times larger than

the true RMS value. The user should check the particular meter he is using to determine what its specific time constants are and also to be able to properly correct any readings by applying Equation 6.8.

The peak-reading voltmeter has limited usefulness in sensitivity measurements because its operation is so dependent upon input voltage waveshape. In fact we have shown it can be accurately used for measurement of either a pure sinewave or a wideband Gaussian noise voltage but not the superposition of the two. Thus, it can be used for noise ratio measurements but is not very useful for measuring signal-plus-noise-to-noise ratios. This is a direct result of the fact that the ratio of indicated RMS value to true RMS value is a function of the voltage waveshape and the charge and discharge time constants of the peak detector (a measure of this dependancy is called the rectification efficiency). Even when measuring the power ratio of two strictly Gaussian white-noise outputs, one must be careful that the noise output does not contain any pulse noise or other non-Gaussian components. An example of this is measuring audio outputs where both thermal and flicker noise are present. When this occurs, the use of a peak-reading voltmeter is not recommended. For the times when one must use a peak-reading voltmeter to measure RMS noise voltages, it is apparent that special care must be taken to interpret the results and apply any needed corrections.

B. Average-Reading Voltmeter

The average-reading voltmeter, which really measures the average value of the full-wave rectified input, may be used for sensitivity

measurements when the user is aware of its inaccuracies and limitations. Figure 6-3 shows a simplified schematic of an average-reading voltmeter.

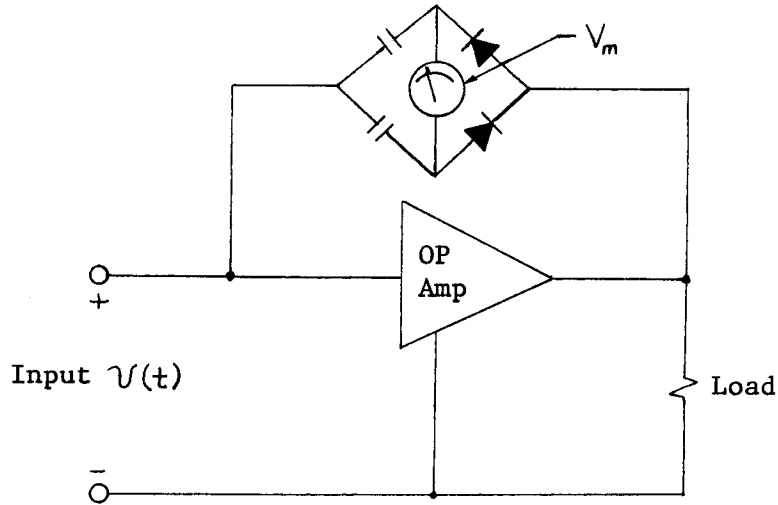


Figure 6-3. Basic Circuit of Average-Reading Voltmeter

In the circuit of Figure 6-3 the diodes maintain a unidirectional current in the meter and the capacitors are used for AC coupling.

When the input noise voltage is Gaussian, the average value of the full-wave rectified signal is obtained by finding the mean absolute value of the input (Landon, 1941). This is done by applying random variable theory to find the mean (or expected) value as the integral of the product of the absolute magnitude of the random variable and its probability density function.

The mean absolute value of the Gaussian input voltage is (Equation 6.2)

$$\overline{|V_n|} = \frac{2}{E_r \sqrt{2\pi}} \int_0^{\infty} V_n e^{-\frac{V_n^2}{2E_r^2}} dV_n \quad (6.2)$$

- where
1. E_r = RMS value of the input noise voltage
 2. The probability density function is for a normally distributed random variable
 3. The factor of 2 accounts for full-wave rectification.

The upper limit of the integral is infinity but we know that the amplifier used in the meter cannot have an infinite dynamic range. This means that some of the high noise peaks will be clipped by the amplifier. This will cause an error in the measured value but this error is very small if the amplifier is capable of handling voltage peaks of $5 E_r$. The value of the integral of (6.2) with an upper limit of $5 E_r$ is very nearly the same as when the upper limit is infinity.

Integration of the above equation yields:

$$V_n = \sqrt{\frac{2}{\pi}} E_r \quad (6.9a)$$

Since the average-reading AC voltmeter is calibrated with a sinewave to read RMS volts, we need to convert from RMS values to average values by the equation:

$$V_{rms} = \frac{\pi}{2\sqrt{2}} V_{ave}$$

The indicated meter reading, V_m , is the RMS voltage and the mean absolute value of the input is the average voltage so:

$$V_m = V_{rms}$$

$$V_{ave} = \overline{|V_n|}$$

Combining the results of the last four equations we can relate the voltage indicated by the meter, V_m , to the RMS value of the input noise voltage, E_r , as:

$$E_r = \frac{2}{\sqrt{\pi}} V_m = 1.128 V_m \quad (6.9b)$$

The ratio of indicated voltage to RMS voltage is

$$\frac{V_m}{E_r} = \frac{\sqrt{\pi}}{2} = 0.886 \quad (6.9c)$$

Which is a ratio of -1.05db. From this it is concluded that the average reading voltmeter will read 1.05 db low when the input is Gaussian noise and will read correctly for a noiseless sinewave. For voltages which are the superposition of sinewaves and noise there is, as yet, no exact error determination method. For noise sources which are not Gaussian, one must apply Equation 6.2 to the appropriate probability density function.

The average-reading voltmeter does give measurements accurate to within 1.05 db and is useful for measurements which do not require accuracies better than this. For noise power ratio measurements, it is the preferred instrument because of its low cost and reasonable availability.

C. Square-Law Detector

The most widely analyzed detector, because of its mathematical tractability and its simplicity and predictability in use, is the square-law detector characterized by a detector device voltage transfer equation

$$V_y(t) = a V_x^2(t) \quad (6.10a)$$

where $V_y(t)$ is the device output voltage, $V_x(t)$ is the device input voltage, and a is an amplitude scaling constant. We will now present the derivation of the probability density functions for the square-law detector and to simplify notation, the voltages of Figure 6-1 will be represented by the functions $x(t)$, $y(t)$ and $z(t)$.

The probability density function for the output of a full-wave square-law device is determined by Equation 6.10a and the theory of functions of a random variable (Beckmann, 1967, Sec. 2.2). The full-wave square law device equation is

$$y = ax^2 \quad (6.10b)$$

or $y = f(x)$ where both x and y are random variables. Denoting the probability densities of x and y by $P_x(x)$ and $P_y(y)$ respectively and the inverse function by $x = f^{-1}(y)$, the probability density of y can be determined by solving (6.10b) for x and using the general formula for functions of a random variable (Beckmann, 1967, p. 63)

$$P_y(y) = P_x(x_1) \left| \frac{dx_1}{dy} \right| + P_x(x_2) \left| \frac{dx_2}{dy} \right| + \dots \quad (6.11)$$

where $x_1, x_2, x_3, \dots, x_n$ are the single-valued branches of the inverse function as given by $x_1 = f_1^{-1}(y)$, $x_2 = f_2^{-1}(y)$, \dots , $x_n = f_n^{-1}(y)$ with n total branches. For (6.10b) there are two branches:

$$x = \pm \left(\frac{y}{a} \right)^{\frac{1}{2}}, \quad x_1 = \left(\frac{y}{a} \right)^{\frac{1}{2}}, \quad x_2 = - \left(\frac{y}{a} \right)^{\frac{1}{2}} \quad (6.12)$$

Applying (6.11) we get:

$$P_y(y) = P_x\left(\sqrt{\frac{y}{a}}\right) \left| \frac{1}{2\sqrt{ay}} \right| + P_x\left(-\sqrt{\frac{y}{a}}\right) \left| -\frac{1}{2\sqrt{ay}} \right|$$

$$P_y(y) = \frac{P_x\left(\sqrt{\frac{y}{a}}\right) + P_x\left(-\sqrt{\frac{y}{a}}\right)}{2\sqrt{ay}} \quad (6.13a)$$

Equation 6.13a relates the probability density function of the output of a square-law device to the probability density function of the input. This can always be done to any probability density by applying (6.11). What we really wanted to obtain is the output probability density

function which can then be used to determine the characteristics of the detector output.

A technical distinction is being made between the detector device and the detector. The word detector is used to include predetection and postdetection filtering as well as the device that actually provides the nonlinear action. Reference to Figure 6-1 should clarify this point.

The n^{th} moment of the output of a square-law device is (Davenport and Root, 1958, p. 253)*:

$$E(y^n) = a^n \int_{-\infty}^{+\infty} x^{2n} p_x(x) dx = a^n E(x^{2n}) \quad (6.13b)$$

while the autocorrelation function is:

$$R_y(t_1, t_2) = a^2 E(x_1^2 x_2^2) \quad (6.13c)$$

The general results of Equations 6.13 summarize the statistical properties of a square-law device. It is not practical to elaborate beyond these forms without specifying the statistical properties of the detector input.

Consider now that the detector device input is a Gaussian noise voltage with probability density function:

* Expected value notation will be used for simplicity. For a discussion on expected value and moments consult Davenport and Root (1958, Sec. 4-2) or any text on probability theory.

$$P(x) = \frac{1}{\sigma_x \sqrt{2\pi}} e^{\frac{-x^2}{2\sigma_x^2}} \quad (6.14a)$$

Applying (6.13a), the probability density function of the output of the square-law device is

$$P(y) = \frac{1}{\sigma_x \sqrt{2\pi a y}} e^{\frac{-y}{2a\sigma_x^2}} \quad (y \geq 0) \quad (6.14b)$$

which is a chi-squared distribution (Equation 4A.27). In itself, the output distribution (6.14b) is not useful for determining the characteristics of the detector output, $z(t)$.

Since the detector device input will always be bandlimited by the predetection filter, (Figure 6-1), the input voltage to the detector device is a sample function of a narrow-band Gaussian process and can be represented by the form (Davenport and Root, 1958)

$$X(t) = V_m(t) \cos [\omega_o t + \theta(t)] \quad (6.15a)$$

where

1. $V_m(t)$ is the envelope of the Gaussian input noise voltage and is a random function, $V_m(t) \geq 0$
2. $\theta(t)$ is the phase of the input noise voltage and is a random function, $0 \leq \theta(t) \leq 2\pi$
3. ω_o is the mean frequency of the narrow-band input spectrum.

For a band-limited Gaussian noise voltage it can be shown (Beckmann, 1967, Sec. 7-3) that the envelope has a Rayleigh probability density function

$$P_R(V_m) = \frac{V_m}{\sigma_x^2} e^{-\frac{V_m^2}{2\sigma_x^2}} \quad (V_m \geq 0) \quad (6.15b)$$

and the phase angle has a uniform distribution between 0 and 2π . The output of the square-law device as a function of time is obtained by substitution of (6.15a) into (6.10a) which gives:

$$y(t) = \frac{a V_m(t)}{2} + \frac{a V_m(t)}{2} \cos [2\omega_0 t + 2\theta(t)] \quad (6.16)$$

The first term of (6.16) is a low-frequency voltage with spectral density centered about zero frequency while the second has a spectral density centered about $2\omega_0$. If the low-pass filter can sufficiently filter out the spectrum at $2\omega_0$ while passing the spectrum at zero frequency, then the filter output is

$$z(t) = b \frac{a V_m^2(t)}{2} \quad (6.17)$$

where b is the low-pass filter amplitude scaling factor.

The form of Equation 6.17 is the same as that of (6.10b) so it is possible to apply a square-law transformation of probability density. Equation 6.13a can be applied to the Rayleigh distribution of Equation 6.15b which is valid for the envelope voltage $V_m(t)$ in Equation 6.17. Solving (6.17) for $V_m(t)$ gives:

$$V_m(t) = \sqrt{\frac{2z(t)}{ab}} \quad V_m(t) \geq 0 \quad (6.18)$$

Applying (6.13a) yields

$$\begin{aligned} P(z) &= P_R\left(\sqrt{\frac{2z}{ab}}\right) \left| \frac{1}{2} \left(\frac{2}{ab}\right)^{1/2} z^{-1/2} \right| \\ &= \frac{1}{ab \sigma_x^2} e^{\frac{-z}{ab \sigma_x^2}} \quad (z \geq 0) \end{aligned} \quad (6.19)$$

which is an exponential density function.

We now have sufficient information to calculate the mean and mean-square noise voltage outputs for both the square-law device and the square-law detector. These values can be obtained by applying the statistical definitions of Equations 6.13b or 4A.1 and 4A.7.

The outputs for the square-law device using the probability density of (6.14b) and (6.13b) are

$$\overline{V_y(t)} = E(y) = a \sigma_x^2 = a E_r^2 \quad (6.20a)$$

$$\overline{V_y^2(t)} = E(y^2) = 3 a^2 \sigma_x^4 = 3 a^2 E_r^4 \quad (6.20b)$$

where $E_r = \sigma_x$ and E_r is the RMS value of the input noise voltage $V_x(t)$. Notice from Figure 6-1 that the predetection filter determines E_r by limiting the spectral width of the voltage $V_n(t)$. In a similar manner the probability density of (6.19) is used to obtain the mean and mean-square noise voltage outputs from the square-law detector (the output is after the postdetection filter):

$$\overline{V_z(t)} = E(z) = ab \sigma_x^2 = ab E_r^2 \quad (6.21a)$$

$$\overline{V_z^2(t)} = E(z^2) = 2a^2b^2 \sigma_x^4 = 2a^2b^2 E_r^4 \quad (6.21b)$$

We now have, from a relatively simple procedure, calculated the mean and mean-square outputs for a square-law device and a square-law detector.

The analysis of a square-law detector using probability density functions has yielded equations for the mean and mean-square noise voltage outputs in terms of the RMS noise voltage input. Unfortunately, these equations do not provide any information about the spectral distribution of energy at the output and it is precisely this information that is needed to determine the useful noise properties of the detector. To get this information it will be necessary to study the system in terms of the various autocorrelation functions and power spectral density functions. Using this technique it will be possible to determine the effects of predetection and postdetection filtering on detector sensitivity, output, and time response. The techniques of Fourier analysis which we will now use are developed in many texts and

papers. The reader is referred to Section IV-A and Part A of the Appendix for definitions. The following texts are also recommended; Davenport and Root (1958), van der Ziel (1954), Brown and Nilsson (1962), Bracewell (1965), Beckmann (1967), Bennett (1960) and Kraus (1966).

The autocorrelation function for the output of a full-wave square-law device (device not detector) is given in terms of the input by the expected value as:

$$R_y(t_1, t_2) = \alpha^2 E(x_1^2 x_2^2) \quad (6.13c)$$

When the input signal has a Gaussian distribution, the autocorrelation function is simplified to (Davenport and Root, 1958, p. 255)

$$R_y(t_1, t_2) = \alpha^2 E^2(x^2) + 2\alpha^2 E^2(x, x_2) \quad (6.22)$$

and if the input is also stationary and ergodic then (6.22) can be further simplified by substituting the following expressions for the expected values in Equation 6.22

$$E(x^2) = \overline{X^2}(t) = R_x(0)$$

$$E(x, x_2) = R_x(\tau)$$

where $\tau = (t_2 - t_1)$ and R_x is the autocorrelation function of the noise voltage input to the square-law device. These substitutions give the important result of Equation 6.23:

$$R_y(\tau) = \alpha^2 R_x^2(0) + 2\alpha^2 R_x^2(\tau) \quad (6.23)$$

Assume that the noise voltage at the input of the detector is Gaussian white noise with a power spectral density of:

$$S_n(\omega) = \frac{\overline{V_n^2}}{4R_n\Delta f} = kT_n \text{ watts/Hz} \quad (6.24)$$

The double-sided power spectral density at the input to the square-law device is found from the product of the detector input spectral density and the transfer function of the amplifier/predetection filter (Figure 6-1)

$$\Phi_x(\omega) = \frac{1}{2} kT_n G |g_h(\omega)|^2 \quad (6.25)$$

where G is the available gain of the amplifier/filter and $g_h(\omega)$ is the normalized transfer function of the predetection filter*. The factor $1/2$ arises in the conversion from single-sided to double-sided power spectra (Appendix, Part R).

* The noise bandwidth of the predetection filter (Appendix, Part B) is:

$$B_h = \frac{1}{2\pi} \int_0^{\infty} |g_h(\omega)|^2 d\omega$$

The power spectral density after the square-law device can be obtained using the autocorrelation function (6.23) and the Fourier transform relationship between power spectral density and autocorrelation (Appendix, Parts A and R):

$$\begin{aligned}\Phi_y(\omega) &= \int_{-\infty}^{+\infty} R_y(\tau) e^{-j\omega\tau} d\tau \\ &= \int_{-\infty}^{+\infty} [\alpha^2 R_x^2(0) + 2\alpha^2 R_x^2(\tau)] e^{-j\omega\tau} d\tau\end{aligned}\quad (6.26)$$

The Fourier transform of a constant is an impulse function (represented by the Dirac-delta symbol, Equation 4A.52b)

$$\int_{-\infty}^{+\infty} \alpha^2 R_x^2(0) e^{-j\omega\tau} d\tau = 2\pi\alpha^2 R_x^2(0) \delta(\omega) \quad (6.27)$$

While the Fourier transform of the product of two autocorrelation functions has the form

$$\int_{-\infty}^{+\infty} R_x(\tau) R_x(\tau) e^{-j\omega\tau} d\tau = \frac{1}{2\pi} \int_{-\infty}^{+\infty} \Phi_x(\omega') \Phi_x(\omega - \omega') d\omega' \quad (6.28)$$

where

$$\Phi(\omega) = \int_{-\infty}^{+\infty} R_x(\tau) e^{-j\omega\tau} d\tau.$$

Substituting these relationships into (6.26) gives the device output spectral density in terms of the input:

$$\Phi_y(\omega) = 2\pi\alpha^2 R_x^2(0) \delta(\omega) + \frac{\alpha^2}{\pi} \int_{-\infty}^{+\infty} \Phi_x(\omega') \Phi_x(\omega - \omega') d\omega' \quad (6.29)$$

The first term, which represents the mean-square dc output of the square-law device, can be written in the alternate forms:

$$2\pi\alpha^2 R_x^2(0) \delta(\omega) = 2\pi\alpha^2 \left[\frac{1}{2\pi} \int_{-\infty}^{+\infty} \Phi_x(\omega) d\omega \right]^2 \delta(\omega) \quad (6.30)$$

The second term represents the noise output in a bandwidth about zero frequency and about $2\omega_0$ where ω_0 is the center frequency of the spectrum of the predetection filter.

The output spectral density function is now determined by
(Appendix, Part B)

$$\Phi_z(\omega) = \Phi_y(\omega) |H(\omega)|^2 \quad (6.31)$$

where $H(\omega)$ is the unnormalized transfer function (even in ω) of the low-pass filter. The output spectral density function for the detector can be expressed in terms of the input spectral density by substituting (6.29) into (6.31):

$$\begin{aligned} \Phi_z(\omega) = & 2\pi\alpha^2 R_x^2(0) \delta(\omega) |H(\omega)|^2 \\ & + \frac{\alpha^2}{\pi} |H(\omega)|^2 \int_{-\infty}^{+\infty} \Phi_x(\omega') \Phi_x(\omega - \omega') d\omega' \end{aligned} \quad (6.32)$$

This equation for the output power spectral density is only valid for Gaussian probability densities because the autocorrelation function of Equation 6.22 was obtained for an input signal with a Gaussian distribution.

The desired goal has now been achieved and we have an equation (6.32) which relates the output and input spectral densities for a square-law detector. In principle, it is possible to solve the convolution integral of (6.32) but, practically, there are a limited number of input spectral density functions which can be solved. Numerical or graphical convolution can be accomplished when curves of input spectra and filter response are available. One must be sure, before applying this method, that the noise input is Gaussian.

The simplest example for demonstrating this method is when the predetection filter is a rectangular bandpass filter with bandwidth B_r (rad/sec) as described by

$$|g_h(\omega)|^2 = \begin{cases} 1 & \text{for } \left(\omega_0 - \frac{B_r}{2}\right) < |\omega| < \left(\omega_0 + \frac{B_r}{2}\right) \\ 0 & \text{otherwise} \end{cases} \quad (6.33)$$

and the detector input spectral intensity becomes (Equation 6.25):

$$\phi_x(\omega) = \begin{cases} \frac{1}{2} k T_n G & \text{for } \left(\omega_0 - \frac{B_r}{2}\right) < |\omega| < \left(\omega_0 + \frac{B_r}{2}\right) \\ 0 & \text{otherwise} \end{cases} \quad (6.34)$$

The "autoconvolution" of this function can be done graphically as shown in Figure 6-4. Figure 6-4b illustrates the resulting convolution which can be used to obtain the power spectral density of the output of a

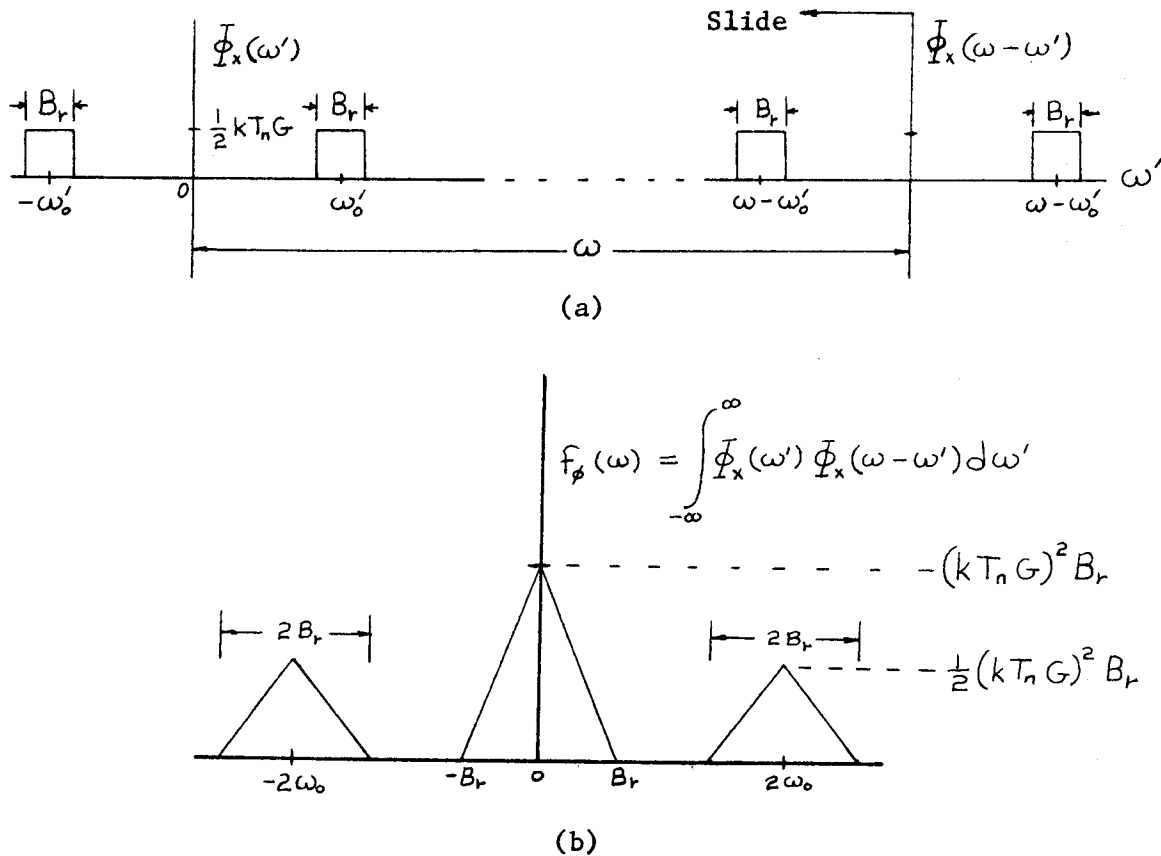


Figure 6-4. Graphical Interpretation of the Autoconvolution Integral of Equation 6.32 for a Rectangular Bandpass Predetection Filter

square-law device where the predetection filter has a rectangular passband.

Another important example for convolution is when the predetection filter has a low-pass characteristic (baseband IF). When the base bandwidth is B_r (corresponding to an audio or video bandwidth) the autoconvolution can be performed as illustrated in Figure 6-5.

Before discussing the interpretation of these results, the equations for device output spectrum and detector output spectrum will be written in the forms (compare Equations 6.29 and 6.32)

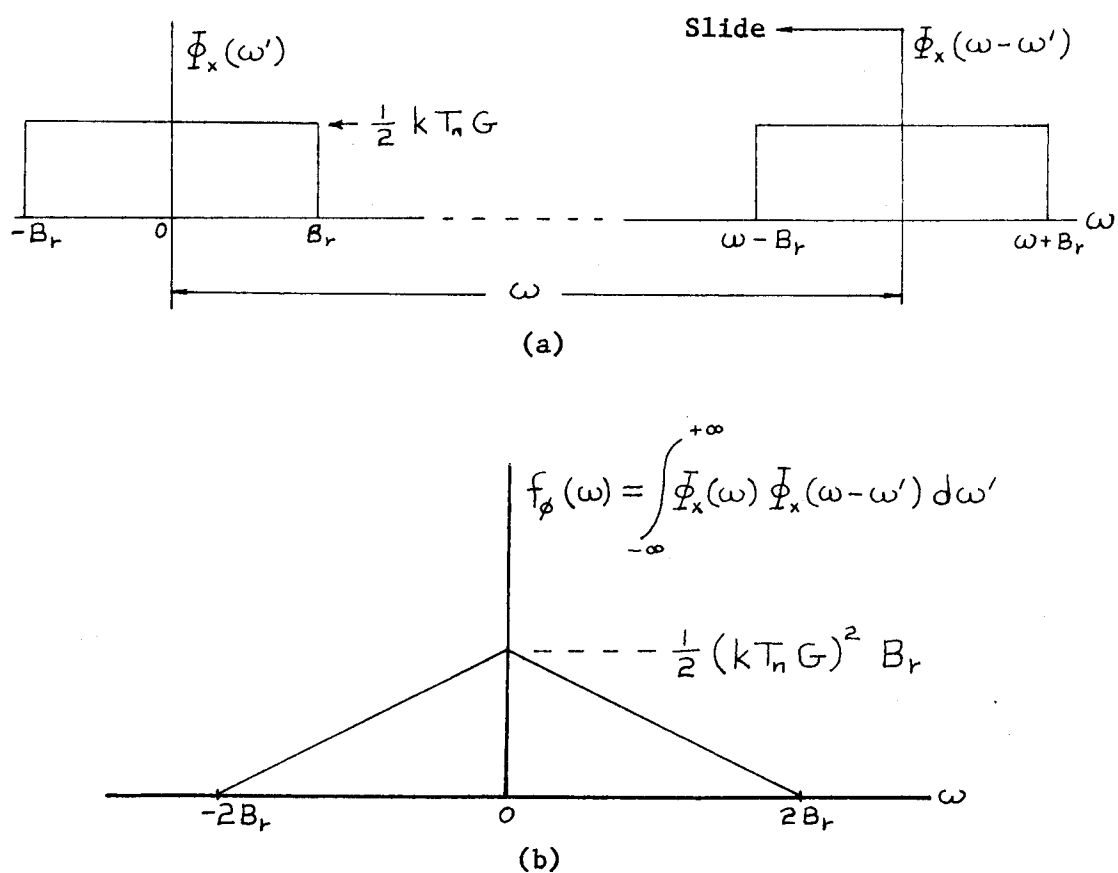


Figure 6-5. Graphical Interpretation of the Autoconvolution Integral of Equation 6.32 for a Rectangular, Low-pass Predetection Filter Passband

$$\Phi_y(\omega) = 2\pi\alpha^2 R_x^2(0) \mathcal{S}(\omega) + \frac{\alpha^2}{\pi} f_\phi(\omega) \quad (6.35)$$

$$\Phi_y(\omega) = 2\pi\alpha^2 R_x^2(0) \mathcal{S}(\omega) |H(\omega)|^2 + \frac{\alpha^2}{\pi} |H(\omega)|^2 f_\phi(\omega) \quad (6.36)$$

where $f_\phi(\omega)$ is the autoconvolution of the input spectrum. With the output power spectral densities expressed in the form of Equations 6.35 and 6.36 it is easier to discuss some simplifying approximations that are used to obtain $f_\phi(\omega)$.

The detector output will be influenced by the steady-state transfer function (impulse response), $H(\omega)$, of the low-pass filter. With this in mind it is possible to distinguish three different cases for the form of $f_{\phi}(\omega)$:

1. The postdetection noise bandwidth, B_L , is much smaller than the predetection noise bandwidth, B_h , so that the autoconvolution function in Equation 6.32 is essentially independent of ω and will assume the value:

$$f_{\phi}(\omega) \approx f_{\phi}(0) \quad \text{when} \quad B_L \ll B_h.$$

This criterion is analogous to the bandwidth assumption made in the section on peak-reading voltmeters.

2. The postdetection filter is a low-pass zonal filter which passes only the noise in the spectrum about zero frequency i.e., referring to Figure 6-4b only that noise in a bandwidth B_r centered about zero frequency. When this is the case;

$$f_{\phi}(\omega) = \begin{cases} f_{\phi}(\omega) & |\omega| < B_h \\ 0 & \text{otherwise} \end{cases}$$

3. Finally, when neither case above will apply, the autoconvolution integral must be performed in detail either by direct integration for a few specialized spectrums or else by graphical or digital techniques so

$$f_{\phi}(\omega) = \int_{-\infty}^{+\infty} \Phi_x(\omega') \Phi_x(\omega - \omega') d\omega'$$

for all ω .

The mean-square output of a full-wave square-law detector can be found by integrating the output power spectral density function over all real frequencies (Appendix, Part R):

$$\sigma_o^2 = R_z(0) = \frac{1}{2\pi} \int_{-\infty}^{+\infty} \Phi_z(\omega) d\omega$$

This is a convenient representation because it will yield ac and dc components for the output. Substituting Equation 6.35 into the equation above gives the general solution for the output as:

$$\sigma_o^2 = \alpha^2 R_x^2(0) |H(0)|^2 + \frac{\alpha^2}{2\pi^2} \int_{-\infty}^{\infty} |H(\omega)|^2 f_{\phi}(\omega) d\omega \quad (6.37)$$

The first term of (6.37) is identified as the mean-square dc output because all the terms are constants evaluated at zero frequency so:

$$\sigma_{dc}^2 = \alpha^2 |H(0)|^2 \left[\frac{1}{2\pi} \int_{-\infty}^{\infty} \Phi_x(\omega) d\omega \right]^2 = \alpha^2 |H(0)|^2 R_x^2(0) \quad (6.38)$$

The second term is the mean-square ac output:

$$\sigma_{ac}^2 = \frac{\alpha^2}{2\pi^2} \int_{-\infty}^{+\infty} |H(\omega)|^2 f_{\phi}(\omega) d\omega \quad (6.39)$$

We now have the important results--the mean-square outputs in terms of the characteristics of the detector components. The terms in Equations 6.37, 6.38, and 6.39 will now be defined for additional clarity:

$\sigma_o^2 = \sigma_{ac}^2 + \sigma_{dc}^2$, the mean-square output voltage for the full-wave square-law detector of Figure 6-1, valid only for a Gaussian noise voltage $V_n(t)$.

σ_{ac}^2 = Mean-square ac output voltage

σ_{dc}^2 = Mean-square dc output voltage

$H(\omega)$ = The steady-state transfer function of the post-detection low-pass filter

$H(0)$ = Transfer function at dc ($\omega = 0$)

$R_x(0)$ = The mean-square value of the noise voltage, $V_x(t)$

$\Phi_x(\omega)$ = Power spectral density function of the noise voltage $V_x(t)$

a = Square-law device amplitude scaling constant

$f_\phi(\omega)$ = Autoconvolution function of the power spectral density $\Phi_x(\omega)$.

It is difficult to determine the ac output, σ_{ac}^2 , for any spectrum, $\Phi_x(\omega)$, because of the difficulty in evaluating the autoconvolution function $f_\phi(\omega)$. Since this cannot be done in general, we will now specialize the analysis to the first case where the postdetection noise bandwidth, B_L , is much smaller than the predetection noise bandwidth, B_h . This is the most important practical case and the criterion

$B_L \ll B_h$ is almost always satisfied when making noise power measurements.

When ($B_L \ll B_h$) the mean-square dc and ac voltage outputs are obtained in the following way. The dc output is determined from (6.38) where the mean-square value of the noise voltage $V_x(t)$ is

$$R_x(0) = \frac{1}{2\pi} \int_{-\infty}^{+\infty} \frac{1}{2} k T_n G |g_h(\omega)|^2 d\omega = k T_n G B_h$$

which gives:

$$\sigma_{dc}^2 = a^2 |H(0)|^2 (k T_n G B_h)^2 \quad (6.40)$$

The ac output is evaluated from (6.39) where

$$f_\phi(\omega) \approx f_\phi(0) \quad \text{for} \quad \omega \ll B_h$$

and:

$$f_\phi(0) = \int_{-\infty}^{+\infty} \Phi_x^2(\omega') d\omega' = \int_{-\infty}^{+\infty} \Phi_x^2(\omega) d\omega$$

If the bandwidth of the low-pass filter is much smaller than the spectrum of the autoconvolution function, the function is essentially constant and is evaluated at zero frequency (6.39) becomes:

$$\sigma_{ac}^2 \approx \frac{a^2}{2\pi^2} f_\phi(0) \int_{-\infty}^{+\infty} |H(\omega)|^2 d\omega \quad (6.41a)$$

The equivalent noise bandwidth of the low-pass filter is (Appendix, Part B):

$$B_L = \frac{1}{2\pi |H(0)|^2} \int_0^{\infty} |H(\omega)|^2 d\omega$$

The equivalent noise bandwidth is used in Equation 6.41a to give:

$$\begin{aligned} \sigma_{ac}^2 &= 2 \frac{a^2}{\pi} |H(0)|^2 B_L f_p(0) \\ &= 2 \frac{a^2}{\pi} |H(0)|^2 B_L \int_{-\infty}^{+\infty} \Phi_x^2(\omega) d\omega \end{aligned} \quad (6.41b)$$

Finally, the equation for the power spectral density (6.25) is used to get the final result using (6.41b):

$$\sigma_{ac}^2 = \frac{a^2}{\pi} |H(0)|^2 B_L (kT_n G)^2 \int_0^{\infty} |g_h(\omega)|^4 d\omega \quad (6.41c)$$

The integral in Equation 6.41c is an interesting result. It is not a noise bandwidth because the normalized transfer function is taken to the fourth power and not the second. To be able to get values for σ_{ac}^2 it will be necessary to compute the value of the integral for several commonly used filter responses. Before doing this, however, it would be interesting to see if anything can be done to the form of Equation 6.41c which would allow us to interpret the integral in terms of a noise bandwidth. In fact, this can be done by defining a correction constant K_F^2 which will be interpreted as a factor which will correct

for the "distortion" of the predetection noise bandwidth caused by the square-law device. The factor may be introduced in the following manner.

The equivalent noise bandwidth of the predetection filter is

$$B_h = \frac{1}{2\pi} \int_0^{\infty} |g_h(\omega)|^2 d\omega \quad (6.42)$$

and a correction constant for the predetection filter noise bandwidth needed to account for various filter amplitude responses is defined as:

$$K_F^2 \triangleq \int_0^{\infty} |g_h(\omega)|^4 d\omega \left[\int_0^{\infty} |g_h(\omega)|^2 d\omega \right]^{-1} \quad (6.43)$$

The correction constant comes from the integration of the squared, filter power-amplitude response and is normalized by the predetection equivalent noise bandwidth by using (6.42) in (6.43) to get:

$$K_F^2 = \frac{1}{2\pi B_h} \int_0^{\infty} \left[|g_h(\omega)|^2 \right]^2 d\omega \quad (6.44a)$$

The correction constant is also used to define another predetection bandwidth, B_{pd} by the following equation:

$$B_{pd} = \frac{B_h}{K_F^2} = \left[\int_{-\infty}^{+\infty} |g_h(\omega)|^2 d\omega \right]^2 \cdot \left[2\pi \int_{-\infty}^{+\infty} |g_h(\omega)|^4 d\omega \right]^{-1} \quad (6.44b)$$

B_{pd} is considered to be an "equivalent" bandwidth of the predetection filter which is different from either the equivalent noise bandwidth or the half-power bandwidth.

Using the bandwidths of Equations 6.44b and 6.42, the ac output of Equation 6.41c can be written in the alternate forms:

$$\begin{aligned}\sigma_{ac}^2 &= 2Q^2 |H(0)|^2 (kT_n G)^2 B_L B_h K_F^2 \\ &= 2Q^2 |H(0)|^2 (kT_n G)^2 B_L B_h \left(\frac{B_h}{B_{pd}}\right)\end{aligned}\quad (6.45)$$

Tables for the actual predetection equivalent noise bandwidth B_h and the defined predetection bandwidth B_{pd} can be found in Kraus (1966, p. 245 and p. 265).

The correction factor is affected by the shape of the filter pass-band but not by the magnitude of the filter bandwidth. This fact makes it convenient to make a table of K_F for various filter amplitude responses as is done in Table 6-1. It is convenient to note that the limits on the correction factor, for the commonly used filters listed in the table, are:

$$\frac{1}{2} \leq K_F^2 \leq 1$$

Since it is the RMS output that is measured and not the mean-square output we now can express the dc and ac output voltage for the detector ($B_L \ll B_h$) as:

$$\sigma_{dc} = Q |H(0)| kT_n G B_h \quad \text{volts, dc} \quad (6.46a)$$

$$\sigma_{ac} = Q |H(0)| kT_n G K_F \sqrt{2 B_L B_h} \quad \text{volts, RMS} \quad (6.46b)$$

Table 6-1. Correction constant for the noise bandwidth of the predetection filter for various filter amplitude responses

Type of Filter	$ g_h(\omega) ^2$	K_F^2	K_F
n cascaded single-tuned stages	$\left[1 + \left(2 \frac{\omega - \omega_0}{\Delta\omega_{3dB}}\right)^2\right]^{-n}$		
n = 1 (single-tuned stage)		1/2	.707
n = 3		.659	.812
n = 5		.685	.828
n = ∞ (Gaussian)		.707	.841
2n-pole Butterworth filters	$\left[1 + \left(2 \frac{\omega - \omega_0}{\Delta\omega_{3dB}}\right)^{2n}\right]^{-1}$		
n = 1 (single-tuned stage)		1/2	.707
n = 2		.749	.865
n = 3		.833	.913
n = ∞ (ideal filter, rectangular passband)		1	1

The voltage signal-to-noise ratio at the output (this indicates the relative deviation of a meter reading the voltage) is:

$$\text{Output VSNR} = \frac{\sigma_{dc}}{\sigma_{ac}} = \frac{1}{K_F} \sqrt{\frac{B_h}{2 B_L}} \quad (6.47)$$

This analysis technique is also very useful in analyzing total power receivers as used in radio astronomy. Suppose that the input noise temperature T_n is the sum of a signal temperature ΔT and the system noise temperature T_{sys} :

$$T_n = T_{sys} + \Delta T \quad (6.48)$$

If the dc voltage caused by the system noise is offset by a fixed dc voltage

$$V_o = a |H(0)| k T_{sys} G B_h$$

then the voltage SNR at the output would be:

$$VSNR = \frac{\sigma_{dc} - V_o}{\sigma_{ac}} = \frac{\Delta T}{T_{sys} + \Delta T} \cdot \frac{1}{K_F} \sqrt{\frac{B_h}{2 B_L}} \quad (6.49)$$

If it can be assumed that the minimum detectable change in noise temperature ΔT occurs when the VSNR is unity then:

$$\Delta T_{min} = \frac{T_{sys}}{\left(\frac{1}{K_F} \sqrt{\frac{B_h}{2 B_L}} - 1 \right)}$$

But the derivation of all these last equations depends on the assumption $B_L \ll B_h$ so we get as a final result

$$\Delta T_{min} = \frac{T_{sys}}{\frac{1}{K_F} \sqrt{\frac{B_h}{2 B_L}}} \quad (6.50a)$$

or substituting (6.44b) gives

$$\Delta T_{min} = \frac{T_{sys}}{\sqrt{\frac{B_{pd}}{2 B_L}}} \quad (6.50b)$$

where B_{pd} was the defined or "equivalent" predetection bandwidth and B_h is the actual noise bandwidth of the predetection filter.

In some receiver applications, the minimum detectable change in input noise temperature, ΔT_{min} , is further modified by receiver designs which switch the receiver between the antenna and a calibrated noise source or other such schemes for improving receiver gain stability. These techniques are discussed in Chapter 7 in Kraus (1966). The use of switching introduces a correction factor into Equations 6.50a and 6.50b so that the final equation for ΔT_{min} becomes

$$\Delta T_{min} = K_s K_F \frac{T_{sys}}{\sqrt{\frac{B_h}{2B_L}}} \quad (6.50c)$$

where ΔT_{min} = Minimum detectable change in input noise temperature, $^{\circ}\text{K}$

T_{sys} = System noise temperature, $^{\circ}\text{K}$

B_h = Equivalent noise bandwidth of the predetection filter, Hz

B_L = Equivalent noise bandwidth of the post-detection low-pass filter, Hz

K_F = Correction constant for the noise bandwidth of the predetection filter, $(.707 \leq K_F \leq 1)$

K_s = Receiver sensitivity constant, $(1 \leq K_s \leq 2\sqrt{2})$.

$K_s = 1$ for unswitched receivers.

and we have assumed a voltage signal-to-noise ratio of unity.

The following summary of minimum detectable noise temperatures for various types of postdetection filters was obtained with the help of Table 6-2 in Kraus (1966, p. 246):

a) Ideal integrator, integrating time t

$$B_L = \frac{1}{2t} \quad |H(\omega)|^2 = \frac{\sin^2\left(\frac{1}{2}\omega t\right)}{\left(\frac{1}{2}\omega t\right)^2}$$

$$\Delta T_{\min} = K_s K_F \frac{T_{\text{sys}}}{\sqrt{B_h t}} \quad (6.51a)$$

b) Single RC filter

$$B_L = \frac{1}{4RC} \quad |H(\omega)|^2 = \frac{1}{1 + \omega^2 R^2 C^2}$$

$$\Delta T_{\min} = K_s K_F \frac{T_{\text{sys}}}{\sqrt{B_h (2RC)}} \quad (6.51b)$$

c) Second-order filter

$$B_L = \frac{\omega_o}{8\delta} \quad |H(\omega)|^2 = \frac{\omega_o^4}{(\omega_o^2 - \omega^2)^2 + (2\delta\omega\omega_o)^2}$$

$$\Delta T_{\min} = K_s K_F \frac{T_{\text{sys}}}{\sqrt{B_h \frac{4\delta}{\omega_o}}} \quad (6.51c)$$

where ω_o is the undamped natural frequency and δ is the damping constant.

The important equations for the noise characteristics of a full-wave square-law detector have been presented and can now be applied to a specific circuit that is widely used in practical applications. A

noise power detector that consists of a square-law device output and RC low-pass filter is shown in Figure 6-6.

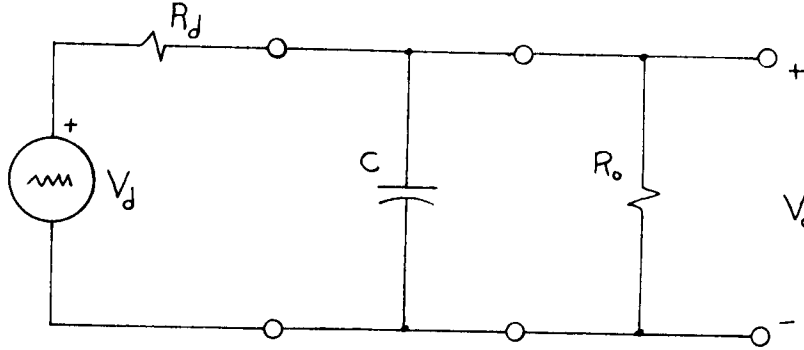


Figure 6-6. Schematic Representation of a Noise Power Detector with RC Low-Pass Filter

The noise voltage output of the square-law device is represented by a Thevenin equivalent circuit where R_d is the output resistance and V_d is a noise voltage generator whose mean-square value, $\overline{V_d^2}$, is determined by (Appendix, Part R)

$$\overline{V_d^2} = 4 R_d \frac{1}{2\pi} \int_{-\infty}^{+\infty} \Phi_y(\omega) d\omega \quad (6.52a)$$

where $\Phi_y(\omega)$ is the output power spectral density function defined by Equations 6.29 or 6.35.

To determine $\overline{V_d^2}$, we substitute Equation 6.35 into (6.52a) to give:

$$\begin{aligned}
\overline{V_d^2} &= \frac{4R_d}{2\pi} \int_{-\infty}^{+\infty} 2\pi \alpha^2 R_x^2(\omega) \delta(\omega) + \frac{\alpha^2}{\pi} f_\phi(\omega) d\omega \\
&= 4R_d \alpha^2 R_x^2(0) \int_{-\infty}^{+\infty} \delta(\omega) d\omega + \frac{4R_d \alpha^2}{2\pi^2} \int_{-\infty}^{\infty} f_\phi(\omega) d\omega \\
&= 4R_d \alpha^2 (kT_n G B_h)^2 + 4R_d \frac{\alpha^2}{2\pi^2} \int_{-\infty}^{\infty} f_\phi(\omega) d\omega \quad (6.52b)
\end{aligned}$$

The detector output voltage, as we have already seen (Equations 6.46), is the sum of a dc voltage and a low-frequency ac voltage:

$$V_o = \sigma_{dc} + \sigma_{ac}$$

$$\sigma_{dc} = \alpha |H(0)| kT_n G B_h \quad \text{volts, dc} \quad (6.53a)$$

$$\sigma_{ac} = \alpha |H(0)| kT_n G K_F \sqrt{2B_L B_h} \quad \text{volts, ac} \quad (6.53b)$$

The dc voltage is proportional to the input noise temperature, predetection gain and noise bandwidth and the dc attenuation of the post-detection filter. The postdetection bandwidth does not affect the dc output. The dc attenuation of the RC filter is simply:

$$|H(0)| = \frac{R_o}{R_d + R_o}$$

On the other hand, the RMS ac output is proportional to the square root of both predetection and postdetection filter noise bandwidths.

Now with

$$B_L = \frac{\pi}{2RC} \quad \text{where} \quad R = \frac{R_o R_d}{R_o + R_d}$$

the ac voltage can be reduced to an arbitrarily low value by increasing the RC time constant. This can be done without affecting the relative dc output level by changing only the capacitance C and leaving R_o and R_d fixed. A change in R_o or R_d will affect $H(0)$ which in turn affects the dc output. Substitution of the dc attenuation and low-pass noise bandwidth give as a final result for the ac and dc outputs:

$$\sigma_{dc} = (a k) T_n G B_h \frac{R_o}{R_o + R_d} \quad (6.54a)$$

$$\sigma_{ac} = (a k) T_n G K_F \sqrt{B_h} \left(\sqrt{\frac{\pi}{RC}} \right) \frac{R_o}{R_o + R_d} \quad (6.54b)$$

As a final topic, we will look at the output of a square-law detector when the input voltage is a Gaussian noise voltage added to a single, unmodulated sinewave. This result will be applied to the problem of measuring noise factor with a sinewave generator. The analysis will proceed in a manner completely analogous to that done previously for a "noise only" input. Because of this analogy, the steps in the following derivations will be abbreviated and the reader is referred to the previous discussion for many of the details.

The input signal for this case is

$$X(t) = S(t) + n(t)$$

where $s(t)$ is an unmodulated sinewave. The autocorrelation function for the output of the square-law device is (Davenport and Root, 1958, p. 258)

$$R_y(t_1, t_2) = a^2 E [(s_1 + n_1)^2 (s_2 + n_2)^2] \quad (6.55)$$

and because the input noise is stationary we get (Davenport and Root, 1958, p. 258)

$$R_y(t) = a^2 [R_{s^2}(\tau) + 4R_s(t)R_n(t) + 2\sigma_s^2\sigma_n^2 + R_{n^2}(t)] \quad (6.56)$$

where $R_s(\tau)$ and $R_n(\tau)$ are the signal and noise autocorrelation functions, σ_s^2 and σ_n^2 are the mean-square signal and noise voltages and:

$$R_{s^2}(t) = E(s_1^2 s_2^2) \quad (6.57)$$

$$R_{n^2}(t) = E(n_1^2 n_2^2)$$

The output of the square-law detector consists of three types of terms:

1. $R_{sxs}(\tau) = a^2 R_{s^2}(\tau)$, which represents the interaction of the sinewave signal with itself,
2. $R_{nxn}(\tau) = a^2 R_{n^2}(\tau)$, which represents the interaction of the noise with itself and,

3. $R_{sxn}(\tau) = 4a^2 R_s(\tau) R_n(\tau) + 2a^2 \sigma_s^2 \sigma_n^2$, which represents the interaction of signal and noise.

The autocorrelation function of the output can be written in the form:

$$R_y(\tau) = [R_{sxs}(\tau) + R_{sxn}(\tau) + R_{nzn}(\tau)] \quad (6.58)$$

Now since the input is Gaussian, the nxn part of the autocorrelation function is just that when the sinewave is absent (Equation 6.23):

$$R_{nzn}(\tau) = \alpha^2 R_x(0) + 2\alpha^2 R_x^2(\tau) \quad (6.59)$$

The autocorrelation function of the input sinewave is determined from Equation 4A.50 in the last section as

$$R_s(\tau) = \frac{V_s^2}{2} \cos \omega_0 \tau, \quad (s(t) = V_s \cos \omega_0 t) \quad (6.60a)$$

which is used to determine the autocorrelation function for the interaction of signal and noise:

$$R_{sxn}(\tau) = 4\alpha^2 R_s(\tau) R_x(\tau) + 2\alpha^2 \sigma_s^2 \sigma_n^2 \quad (6.61a)$$

The mean-square value for the sinewave signal is the available power from the sinewave generator

$$\sigma_s^2 = \frac{V_s^2/2}{4 R_s} \quad (6.60b)$$

but for simplicity we will represent the mean-square value with the autocorrelation function

$$\sigma_s^2 = R_s(0) = \frac{V_s^2}{2}$$

where the factor $4R_s$ in the denominator of (6.60b) is normalized to unity. This factor will be re-introduced in Equations 6.82. The mean-square value of the noise signal is:

$$\sigma_n^2 = R_n(0)$$

Substituting these and (6.60) into (6.61a) gives:

$$R_{sxn}(\tau) = 4\alpha^2 R_s(0)R_x(t)\cos \omega_0\tau + 2\alpha^2 R_s(0)R_x(0) \quad (6.61b)$$

Finally, the autocorrelation function for the square of the input signal is determined using the definition (Appendix, Equation A.3) and $s^2(t) = V_s^2 \cos^2 \omega_0 t$ to give (Davenport and Root, 1958, p. 260):

$$R_{sxs}(\tau) = \alpha^2 R_s^2(0) \left[1 + \frac{1}{2} \cos 2\omega_0\tau \right] \quad (6.62)$$

We now have the three autocorrelation terms of Equation 6.58 and they can be used to determine the output of the square-law device when the input is Gaussian noise and a single, unmodulated sinewave.

The output spectral density function of the square-law device can now be determined by taking the Fourier transform of the output autocorrelation function $R_y(\tau)$. First express $R_y(\tau)$ in terms of $R_{n\lambda n}(\tau)$, $R_{sxn}(\tau)$, and $R_{sxs}(\tau)$ by substituting Equations 6.62, 6.61b and 6.59 into Equation 6.58:

$$\begin{aligned} R_y(\tau) = & +a^2 R_s^2(0) \left[1 + \frac{1}{2} \cos 2\omega_0 \tau \right] \\ & + 4a^2 R_s(0) R_x(\tau) \cos \omega_0 \tau + 2a^2 R_s(0) R_x(0) \\ & + a^2 R_x(0) + 2a^2 R_x^2(\tau) \end{aligned}$$

Now apply the Fourier transform (Appendix, Part A) to get the output power spectral density function (analogous to Equation 6.26):

$$\begin{aligned} \Phi_y(\omega) &= \int_{-\infty}^{+\infty} R_y(\tau) e^{-j\omega\tau} d\tau \\ &= \int_{-\infty}^{+\infty} [R_{sxs}(\tau) + R_{sxn}(\tau) + R_{n\lambda n}(\tau)] e^{-j\omega\tau} d\tau \quad (6.63) \end{aligned}$$

The three separate integrals of Equation 6.63 can be associated with the following output spectral densities:

1. The output spectrum due to the sinewave interacting with itself,

$$\Phi_{sxs}(\omega) = \mathcal{F} [R_{sxs}(\tau)]$$

2. The output spectrum due to the noise interacting with itself,

$$\Phi_{n \times n}(\omega) = \mathcal{F} [R_{n \times n}(\tau)]$$

3. The output spectrum due to the noise and sinewave interacting,

$$\Phi_{s \times n}(\omega) = \mathcal{F} [R_{s \times n}(\tau)]$$

The following spectral densities are obtained

$$\Phi_{s \times s}(\omega) = 2\pi \alpha^2 R_s^2(0) \delta(\omega) + \frac{\pi}{2} \alpha^2 R_s^2(0) [\delta(\omega - 2\omega_0) + \delta(\omega + 2\omega_0)] \quad (6.64a)$$

$$\Phi_{n \times n}(\omega) = 2\pi \alpha^2 R_x^2(0) \delta(\omega) + \frac{\alpha^2}{\pi} f_\phi(\omega) \quad (6.64b)$$

where $f_\phi(\omega) = \mathcal{F}[R_x^2(\tau)]$ and the results are the same as those obtained in Equation 6.35, and finally:

$$\Phi_{s \times n}(\omega) = 2\alpha^2 R_s(0) [\Phi_x(\omega - \omega_0) + \Phi_x(\omega + \omega_0)] + 4\pi \alpha^2 R_s(0) R_x(0) \delta(\omega) \quad (6.64c)$$

The spectral density of the interaction of signal and noise, Equation 6.64c, is obtained by applying the following Fourier transformation equations:

$$\begin{aligned}
\Phi_{sxn}(\omega) &= \int_{-\infty}^{+\infty} R_{sxn}(\tau) e^{-j\omega\tau} d\tau \\
&= \int_{-\infty}^{\infty} [4\alpha^2 R_s(0) R_x(\tau) \cos \omega_0 \tau + 2\alpha^2 R_s(0) R_x(0)] e^{-j\omega\tau} d\tau \quad (6.65a)
\end{aligned}$$

The second term in the brackets will transform to a delta function because it is a constant and the first term in the brackets contains the autocorrelation function of a sinewave (6.60) so the integral can be reduced to:

$$\Phi_{sxn}(\omega) = 4\alpha^2 \int_{-\infty}^{+\infty} R_s(\tau) R_x(\tau) e^{-j\omega\tau} d\tau + 4\pi\alpha^2 R_s(0) R_x(0) \delta(\omega) \quad (6.65b)$$

The Fourier transform of a product (6.28) reduces (6.65b) to:

$$\Phi_{sxn}(\omega) = \frac{2\alpha^2}{\pi} \int_{-\infty}^{+\infty} \Phi_s(\omega') \Phi_x(\omega - \omega') d\omega' + 4\pi\alpha^2 R_s(0) R_x(0) \delta(\omega) \quad (6.65c)$$

Equation 6.65c can be further reduced by substituting the expression for the spectral density of the input sinewave (4A.51):

$$\Phi_s(\omega') = \mathcal{F}[R_s(\tau)] = \pi R_s(0) [\delta(\omega' - \omega_0) + \delta(\omega' + \omega_0)]$$

The autoconvolution integral in (6.65c) becomes

$$\int_{-\infty}^{+\infty} \bar{\Phi}_s(\omega') \bar{\Phi}_x(\omega - \omega') d\omega' = \pi R_s(0) [\bar{\Phi}_x(\omega - \omega_0) + \bar{\Phi}_x(\omega + \omega_0)] \quad (6.66)$$

which is substituted into (6.65c) to give as a final result Equation 6.64c:

$$\bar{\Phi}_{sxn}(\omega) = 2\alpha^2 R_s(0) [\bar{\Phi}_x(\omega - \omega_0) + \bar{\Phi}_x(\omega + \omega_0)] + 4\pi\alpha^2 R_s(0) R_x(0) \delta(\omega)$$

We now have some useful equations for the spectral output of the square-law device. These spectral functions can now be used to obtain the spectral output of the detector by applying the relationship

$$\bar{\Phi}_z(\omega) = \bar{\Phi}_y(\omega) |H(\omega)|^2$$

to give:

$$\bar{\Phi}_z(\omega) = [\bar{\Phi}_{sxs}(\omega) + \bar{\Phi}_{nxs}(\omega) + \bar{\Phi}_{sxn}(\omega)] |H(\omega)|^2 \quad (6.77)$$

The mean-square voltage output of a square-law detector with sinewave plus Gaussian noise input can be found by integrating the output power spectral density (6.77) over all frequencies:

$$\begin{aligned}
\sigma_o^2 &= \frac{1}{2\pi} \int_{-\infty}^{+\infty} \Phi_I(\omega) d\omega \\
&= \frac{1}{2\pi} \int_{-\infty}^{+\infty} \Phi_{sxs}(\omega) |H(\omega)|^2 d\omega \\
&\quad + \frac{1}{2\pi} \int_{-\infty}^{+\infty} \Phi_{hxn}(\omega) |H(\omega)|^2 d\omega + \frac{1}{2\pi} \int_{-\infty}^{\infty} \Phi_{sxn}(\omega) |H(\omega)|^2 d\omega
\end{aligned} \tag{6.78}$$

A partial evaluation of (6.78) can be accomplished by substituting Equations 6.64 into (6.78) and evaluating those parts of the integrals which contain Dirac-delta functions. When this is done, Equation 6.78 is reduced to:

$$\begin{aligned}
\sigma_o^2 &= \alpha^2 R_s^2(0) |H(0)|^2 + \frac{\alpha^2}{2} R_s^2(0) |H(2\omega_o)|^2 + \alpha^2 R_x(0) |H(0)|^2 \\
&\quad + \frac{\alpha^2}{2\pi^2} \int_{-\infty}^{+\infty} |H(\omega)|^2 f_\phi(\omega) d\omega \\
&\quad + \frac{\alpha^2 R_s(0)}{\pi} \int_{-\infty}^{+\infty} [\Phi_x(\omega - \omega_o) + \Phi_x(\omega + \omega_o)] |H(\omega)|^2 d\omega \\
&\quad + 2\alpha^2 R_s(0) R_x(0) |H(0)|^2
\end{aligned} \tag{6.79}$$

This form for the mean-square voltage output is the simplest that can be obtained without any simplifying assumptions about the transfer function of the low-pass filter, $H(\omega)$. Assuming that the low-pass filter has a noise bandwidth much smaller than the predetection noise bandwidth ($B_L \ll B_h$) we can evaluate the integrals in (6.79) using the same technique that was used to get Equation 6.41. The results of the integrations are summarized below

$$\int_{-\infty}^{+\infty} |H(\omega)|^2 f_{\phi}(\omega) d\omega \simeq f_{\phi}(0) 4\pi |H(0)|^2 B_L$$

and

$$\begin{aligned} \int_{-\infty}^{+\infty} [\Phi_x(\omega - \omega_0) + \Phi_x(\omega + \omega_0)] |H(\omega)|^2 d\omega \\ = 8\pi \Phi_x(\omega_0) |H(0)|^2 B_L \end{aligned}$$

These values are substituted into Equation 6.79 to give an equation for the mean-square voltage output for the special case when $B_L \ll B_h$.

$$\begin{aligned} \sigma_o^2 = & \alpha^2 R_s(0) |H(0)|^2 \\ & + \alpha^2 R_x(0) |H(0)|^2 + \frac{2}{\pi} \alpha^2 |H(0)|^2 B_L f_{\phi}(0) \\ & + 8\alpha^2 R_s(0) \Phi_x(\omega_0) |H(0)|^2 B_L + 2\alpha^2 R_s(0) R_x(0) |H(0)|^2 \quad (6.80) \end{aligned}$$

The term containing $H(2\omega_0)$ is dropped because the passband of the low-pass filter is too low to pass a frequency of $2\omega_0$.

The dc terms of the output can be identified from (6.80) as those with no frequency dependence:

$$\begin{aligned}\sigma_{dc}^2 &= \alpha^2 |H(0)|^2 \left[R_s^2(0) + 2R_s(0)R_x(0) + R_x^2(0) \right] \\ &= \alpha^2 |H(0)|^2 \left[R_s(0) + R_x(0) \right]^2\end{aligned}\quad (6.81a)$$

The low-frequency ac terms are actually distributed in a narrow spectrum about zero frequency because $|H(\omega)|^2$ is a narrow bandwidth:

$$\sigma_{ac}^2 = \frac{2}{\pi} \alpha^2 |H(0)|^2 B_L \left[f_\phi(0) + 4\pi R_s(0) \Phi_x(\omega_0) \right] \quad (6.81b)$$

These last two equations can be compared with the results obtained in the previous derivation for a "noise only" input. With $V_s = 0$ ($R_s(0)=0$), Equation 6.81a becomes identical to (6.38) while Equation 6.81b becomes (6.41).

Assuming the noise voltage at the input to the detector is Gaussian and white, the double-sided spectral density function for the input is represented by Equation 6.25. The sinewave voltage at the input to the detector, V_g , is related to the voltage at the input to the square-law device by $V_s = \sqrt{G}V_g$ where both are peak voltages and G is the power gain of the amplifier. The factor in Equation 6.81b which contains $f_\phi(0)$ can be re-written in terms of the input power spectral

density function and noise bandwidth by using the techniques of Equations 6.41 and 6.42.

The power spectral density function, $\Phi_x(\omega_o)$, is simply the amplitude of the power spectrum at ω_o or:

$$\Phi_x(\omega_o) = \frac{1}{2} kT_n G |g_n(\omega_o)|^2 = \frac{1}{2} kT_n G$$

The mean-square value of the sinewave signal, $R_s(0)$, is the available power of the source which can now be written in terms of the peak generator voltage V_g and the source resistance

$$R(0) = \frac{V_g^2/2}{4R_s} = \frac{V_g^2}{8R_s} \cdot G$$

where the factor $4R_s$ un-normalizes the autocorrelation function (see Equation 6.60b).

Equations 6.81 are now written in terms of circuit values by substituting in the following values for the mean-square signal, mean-square noise, the noise power spectral density function and the auto-convolution function:

$$R(0) = \frac{V_g^2}{8R_s} \cdot G$$

$$R(0) = kT_n G B_n$$

$$\Phi_x(\omega_0) = \frac{1}{2} k T_n G$$

$$f_{\phi}(0) = \pi (k T_n G)^2 B_h K_F^2$$

Applying these substitutions, Equations 6.81 become:

$$\sigma_{dc}^2 = a^2 |H(0)|^2 G^2 \left[\frac{V_g^2}{8R_s} + k T_n B_h \right]^2 \quad (6.82a)$$

$$\sigma_{ac}^2 = a^2 |H(0)|^2 B_L \left[2 (k T_n G)^2 B_h K_F^2 + \frac{V_g^2 G^2 k T_n}{2 R_s} \right] \quad (6.82b)$$

The dc and ac RMS voltages for the detector output become:

$$\sigma_{dc} = a |H(0)| G \left(\frac{V_g^2}{8R_s} + k T_n B_h \right) \quad (6.83a)$$

$$\sigma_{ac} = a |H(0)| G \sqrt{(k T_n K_F)^2 2 B_L B_h + k T_n \frac{V_g^2}{2 R_s}} \quad (6.83b)$$

Equations 6.83 can be used to show how the predetection signal-to-noise ratio or average noise factor of a receiver can be determined using an unmodulated CW signal generator and by measuring the dc output voltage of the square-law detector. Let the dc output of the detector

with no sinewave input ($V_g = 0$) be denoted by E_o where from (6.83a):

$$E_o = \alpha |H(0)| G k T_n B_h \quad (6.84)$$

The predetection signal-to-noise ratio is the ratio of the available powers at the input:

$$S_p = \frac{G \frac{V_g^2/2}{4 R_s}}{k T_n B_h G} = \frac{V_g^2/2}{4 R_s k T_n B_h} \quad (6.85)$$

The ratio of dc output voltage with sinewave input to that without is

$$\frac{\sigma_{dc}}{E_o} = \left(1 + \frac{\frac{V_g^2}{8 R_s}}{k T_n B_h} \right) = (1 + S_p) \quad (6.86)$$

obtained from (6.83a) and (6.84). Thus, a measure of σ_{dc}/E_o gives the predetection signal-to-noise ratio using (6.86). For the average noise factor over the predetection noise bandwidth B_h (Appendix, Part H) we have

$$\overline{F} = 1 + \frac{T_r}{T_o} \quad \text{and} \quad T_n = T_r + T_o \quad (6.87)$$

where the noise temperature T_n is the sum of the source noise temperature, which is the standard T_o , and the receiver noise temperature, T_r .

The mean-square value of sinewave voltage at the input is denoted by

$$E_g^2 = \frac{V_g^2}{2} \quad (\text{volts, RMS})^2$$

so that Equation 6.85 can be re-written in the form:

$$E_g^2 = S_p [4k T_n R_s B_h] = S_p [4k (T_r + T_o) R_s B_h] \quad (6.88)$$

Solving (6.88) for the noise temperature of the receiver being tested gives:

$$T_r = \frac{E_g^2}{S_p [4k R_s B_h]} - T_o \quad (6.89)$$

Equations 6.89 and 6.86 are substituted into (6.87) to give the average noise factor of the receiver

$$\overline{F} = \frac{E_g^2}{S_p [4k T_o R_s B_h]} = \frac{E_g^2}{\left(\frac{\sigma_{dc}}{E_o} - 1\right) 4k T_o R_s B_h} \quad (6.90)$$

where E_g = RMS input voltage in hard volts RMS

$\frac{\sigma_{dc}}{E_o}$ = dc output voltage ratio, generator-on to generator-off

R_s = Source resistance

T_o = 290° K

B_h = Predetection noise bandwidth

S_p = Predetection signal-to-noise ratio.

The ac noise voltage of Equation 6.83b will limit the resolution of the measurement and will determine the smallest signal-to-noise ratio that can be measured. This is a result of the fact that both σ_{dc} and E_o must be measured in the presence of a "noise" voltage σ_{ac} that will cause a measurement uncertainty.

D. Linear Diode Detector

The most widely used detector in communication receivers is the linear diode detector. When the input voltage is large enough, the response of the detector is described by the relationships (see Chapter III-E)

$$\begin{aligned} y &= ax & x > 0 \\ y &= 0 & x < 0 \end{aligned} \quad (6.91)$$

where x and y can represent voltages or currents. Actually the diode is really only approximately linear but for large inputs the approximation is valid. The ratio of detector dc output voltage with sinewave input to that without is determined by the predetection signal-to-noise ratio as given by (Blake, 1972)

$$\frac{\sigma_{dc}}{E_o} = e^{-\frac{S_p}{2}} \left[(1+S_p) I_0\left(\frac{S_p}{2}\right) + S_p I_1\left(\frac{S_p}{2}\right) \right] \quad (6.92)$$

where S_p = Predetection signal-to-noise ratio

$E_o = a \frac{\sigma_n}{\sqrt{2\pi}}$, the dc output when the input sinewave is zero

$$\begin{aligned} I_0(x) &= J_0(ix) \\ I_1(x) &= iJ_1(ix) \end{aligned} \quad \text{modified Bessel functions}$$

σ_{dc} = Detector dc output with input sinewave.

Blake (1972) has solved Equation 6.92 and published tables of S_p as a function of σ_{dc}/E_o . Using his results we can determine the average

noise factor in the same manner as was used to obtain Equation 6.90

$$\overline{F} = \frac{E_g^2}{S_p [4 k T_o R_s B_h]} \quad (6.93)$$

where S_p = Predetection signal-to-noise ratio
 E_g = RMS input voltage in hard volts which produces
the dc ratio σ_{dc}/E_o
 B_h = Predetection noise bandwidth, Hz.
 T_o = 290° K
 k = Boltzmann's constant
 R_s = Source resistance.

Table 6-2 shows the predetection signal-to-noise ratio for different values of the detector dc voltage ratio σ_{dc}/E_o .

When the input signal to a half-wave linear detector is another noise voltage, the ratio of the dc outputs is determined by (Blake, 1972)

$$\frac{\sigma_{dc}}{E_o} = \sqrt{\frac{\sigma_n^2 + \Delta \sigma_n^2}{\sigma_n^2}} \quad (6.94a)$$

where $\Delta \sigma_n^2$ represents the increase in mean-square noise at the input due to the noise signal. In terms of noise temperature this becomes:

$$\frac{\sigma_{dc}}{E_o} = \sqrt{\frac{T_{sys} + \Delta T}{T_{sys}}} = \sqrt{1 + \frac{\Delta T}{T_{sys}}} \quad (6.94b)$$

Table 6-2. Solution to Equation 6.92 for use in measuring average noise factor

σ_{dc}/E_o	$20 \log (\sigma_{dc}/E_o)$	S_p
$\frac{\sigma_{dc}}{E_o} > 2$	-	$S_p \approx \frac{1}{2} \left[\frac{\pi}{2} \left(\frac{\sigma_{dc}}{E_o} \right)^2 - 1 \right]$
2.00	6 db	2.60
1.50	-	1.13
1.412	3 db	.915
1.260	2 db	.535
1.123	1 db	.254
$\frac{\sigma_{dc}}{E_o} < 1.123$	-	$S_p \approx 2 \left[\frac{\sigma_{dc}}{E_o} - 1 \right]$

When the linear diode detector is used for measuring noise factors, Equation 6.94b can be solved for the measured noise factor in the following manner. For noise factor measurements the source is at standard temperature so

$$T_{sys} = T_o + T_r \quad (6.95)$$

and substituting T_{sys} into (6.94b) and solving for T_r gives:

$$T_r = \frac{\Delta T}{\left[\left(\frac{\sigma_{dc}}{E_o} \right)^2 - 1 \right]} - T_o \quad (6.96)$$

Using Equation 6.87 gives the average noise factor as:

$$\overline{F} = \frac{\Delta T}{T_o \left[\left(\frac{\sigma_{dc}}{E_o} \right)^2 - 1 \right]} \quad (6.97)$$

It is worth mentioning that the results obtained for the half-wave diode detector are equally valid for the full-wave detector. All outputs are doubled but since we are only concerned with ratios, the equations which use ratios remain valid.

E. Phase-Sensitive Detector (Product Detector)

The phase-sensitive detector is a mixer in which the local oscillator frequency is equal to the input frequency (van der Ziel, 1954, p. 343). This is the type of detector used in direct conversion receivers (also called homodyne or autodyne receivers) and in single-sideband receivers (where it is called a product detector). The transconductance of this type of detector is time dependent as expressed by

$$g_m(t) = g_{ma} + 2 g_{mc} \cos \omega_o t \quad (6.98)$$

where g_{ma} = Average g_m of the mixer device
 g_{mc} = Conversion transconductance of the mixer
 ω_o = Input frequency or local oscillator frequency.

Applying van der Ziel's results and using techniques analogous to those used in the square-law detector analysis, the mean-square dc and ac voltages are:

$$\sigma_{dc} = g_{mc}^2 |H(0)|^2 (kT_n G B_h)^2 \quad (6.99a)$$

$$\sigma_{ac} = 2g_{mc}^2 |H(0)|^2 (kT_n G)^2 B_h B_L K_F^2 \quad (6.99b)$$

The voltage signal-to-noise ratio at the output is

$$\frac{\sigma_{dc}}{\sigma_{ac}} = \frac{1}{K_F} \sqrt{\frac{B_h}{2 B_L}} \quad (6.100)$$

which is identical to that for the square-law detector (Equation 6.47). This means that the results obtained for the square-law detector response to a noise input is equally valid for a phase-sensitive detector.

F. Detector Dynamic Range

As a final topic we will look at the dynamic range needed in an output power detector. In all measurements of noise voltages, the output power indicator must be capable of handling crest factors in excess of 4 to 1. The crest factor, which is a ratio of the peak value of a voltage to its RMS value, is not defined for a noise voltage because theoretically the amplitude is unbounded. Theoretical calculations (Landon, 1941) have shown that the number of crests exceeding four times the RMS value (4σ) have a probability of 3×10^{-5} and, if these peaks are clipped by the measuring instrument, their loss will have little effect on the reading. There are inexpensive meters which do not

meet this specification because their amplifiers saturate on large voltage peaks. Measurements made with meters of inadequate dynamic range will indicate RMS values lower than the true values.

Meter response to high peaks causes needle flicker which makes the meter hard to read. This problem can be minimized by proper adjustment of meter damping.

In concluding this section the reader is again reminded of the differences in instruments used for noise power detection and the errors involved. Each measurement problem should be carefully studied for factors which might affect measurement accuracy.

VII. METHODS OF SENSITIVITY COMPARISON

There are several commonly used methods for comparing the sensitivities of receiving systems. Each method has its relative advantages and disadvantages and no one method is satisfactory, or even meaningful, for every receiving system. The need for several methods arises because there are a variety of modulation techniques and detectors employed in communication systems. The most common specifications for determining the relative merit of noise performance for a receiving system are:

1. Noise figure (Noise factor)
2. Equivalent noise temperature
3. Signal-plus-noise-to-noise ratio (AM sensitivity)
4. Tangential noise sensitivity (Pulse code systems)
5. Noise quieting (FM systems)
6. Receiving system power sensitivity.

The specifications of noise figure or equivalent noise temperature are most often used to specify the noise performance of "linear" systems such as single-sideband, AM, and total power receivers. Also, the "linear" portions of most receivers or at least those circuits closest to the antenna, such as RF amplifiers and mixers can be evaluated for noise performance on the basis of noise figure or noise temperature. In this context, the word "linear" is used to mean that the available power output is linearly proportional to the available power input.

For AM systems, a very common designation of noise performance is the signal-plus-noise-to-noise ratio for a given sinewave input. It is referred to as AM sensitivity but this is really a misnomer as it is the

signal-to-noise ratio that is the ultimate specification for every system. The signal-plus-noise-to-noise ratio specification is meaningful for every system which is linear and which can be measured with a AM modulated sinewave input. Although AM sensitivity is probably the most common specification of noise performance, it is also probably the most abused and confused one. Since AM sensitivity is closely related to the information theory requirement of a specified minimum SNR, it seems to be a most meaningful and desirable specification, but it also can be very nebulous. This problem occurs because the AM sensitivity of a linear receiver depends on 1) antenna impedance, 2) receiver equivalent bandwidth and 3) the type and percentage of amplitude modulation used for the measurement. All of these variables must be stated along with the measured SNR and input level or it will be impossible to make meaningful comparisons among receivers.

When testing receivers used in data transmission links, the specification of tangential noise sensitivity is usually the most meaningful. This specification relates the amount of peak RF signal needed at the input to produce an output pulse of a specified peak amplitude above the receiver noise level. It is desirable to use this specification when the receiver has nonlinear stages of amplification and the desired output is pulse coded.

In the case of FM receivers, and especially when evaluating a complete system, the commonly used specification is noise quieting which relates the amount of RF signal required at the input to produce a specific reduction in audio noise at the output. Noise quieting is caused by the ability of the FM detector to "capture" the largest

signal and to suppress weaker ones. The problems associated with specifying noise quieting are similar to those of specifying AM sensitivity because one also has to give, 1) antenna impedance, 2) FM bandwidth, 3) deviation ratio of the system.

The specification of receiving system power sensitivity relates the amount of available signal power needed at the receiving antenna to achieve a specified signal-to-noise ratio at the output. This specification is valid for linear receivers and is an alternate way of expressing noise figure or equivalent noise temperature. A definition of this quantity is given in Chapter IV-D.

At this point, the importance of a specific signal-to-noise ratio at the output should be discussed and emphasized. In the information theory aspect of this problem, the output must meet certain user defined criteria or the system becomes unusable. This means that a specific minimum signal-to-noise ratio is desirable and must be achieved. Consistent with other requirements, there will always be design variables which allow the designer to maximize signal-to-noise ratio. Receivers having the highest ratio will perform the best for the user. The most basic system requirement is always the signal-to-noise ratio that can be achieved for a given level of input. Since the receiver is usually linear in the first stages of RF, where the noise factor can be meaningfully specified, the system requirement can be determined knowing the noise factor of the RF stages and the type of detector to be used.

The truth is summarized by the following statement:

"System sensitivity is a function of noise figure and detector characteristic,"

i.e., other factors being equal, the system with the lowest noise figure or equivalent noise temperature will always produce the highest output signal-to-noise ratio.

A brief summary of the types of sensitivity specifications which should be applied to a given component will now be given. The theory of sensitivity measurements and how to measure and present data is presented in the following two chapters.

A. Complete Receiving Systems

The sensitivity specification of a complete receiving system must take into account the type of modulation employed and hence the kind of detector used. For "linear" systems such as SSB, AM and total-power receivers (Radiometers), the specifications of noise figure, equivalent noise temperature, AM sensitivity or receiving system power sensitivity are adequate. For systems employing pulse code modulation it is more convenient and meaningful to specify tangential noise sensitivity because it is more closely related to the information theory requirement and because it can be directly measured.

The behavior of the FM detector in marginal signal environments makes the specification of noise quieting the logical choice.

B. Two-Port Devices

The testing and specification of the noise performance of individual stages such as RF amplifiers, RF mixers, IF amplifiers, solid-state devices, filters, attenuators and feed system components is best done with noise figure or equivalent noise temperature. The concepts of

noise generation in amplifying and mixing devices are well suited to being described by these specifications. Individual electron devices such as vacuum tubes, bipolar transistors, field-effect transistors, and diodes are most often specified for their noise performance by noise figure. This is all right if the user will accept the fact that many circuit conditions and requirements must be met before the device will perform in an amplifier or mixer circuit with the stated noise figure. These conditions are discussed in Sections IV-C, IV-D, and IV-E.

The specialized concept of Noise Measure (Appendix, Part K) was developed to overcome the limitations of noise figure in specifying the noise performance of low-gain or negative-resistance amplifiers. Noise measure is useful in choosing between two amplifiers to be connected in cascade but is not applicable to a single amplifier. A technique which helps choose among several amplifiers for a specific application is given in the Appendix, Part L and is called noise merit.

C. Detectors

The analysis of the noise performance of detectors will not be presented in any more detail than the theory that is given in Chapter VI. It has been demonstrated (Fubini and Johnson, 1948) that every type of practical detector will exhibit some kind of nonlinear threshold effect. By "threshold effect" it is meant that; when the predetection SNR falls below a certain level, the output SNR drops by a greater factor. This means that the requirement of linearity of input and output power, that was given at the beginning of this chapter, is not satisfied and this effect will introduce errors into the measurement. For example, in AM

detectors it has been observed that the presence of a low-level carrier will actually increase the noise output and thus make the output SNR worse than the input SNR. In FM detectors, the threshold effect is much more pronounced where predetection signal-to-noise ratio may change from 7 to 5 db and the output signal-to-noise ratio may drop from 15 db to 0 db. More information on this threshold effect will be given in Chapters VIII and X. For more information about the noise performance of detectors, the reader is referred to the following sources: Fubini and Johnson (1948), Middleton (1948, 1960), DeLano (1949), Bridges (1954), Baghdady (1961), Wakeley (1963), Beckmann (1967) and Davenport and Root (1958).

VIII. THEORY OF SENSITIVITY MEASUREMENTS

Sensitivity measurements on receiving systems are made for one purpose--to compare receivers by measuring which receiver will produce the best output signal-to-noise ratio for a given input signal level. This fundamental measurement may be broken up into several sub-measurements such as measuring the noise performance of each component but the fundamental comparison criteria still remain the same. The results of any sensitivity measurement and how to interpret it correctly depends on an understanding of sensitivity measurement theory. It is the purpose of this chapter to present this theory and to develop the theory behind the commonly used measurement techniques which are presented in the next chapter. The essential components that make up a sensitivity measuring system are illustrated in Figure 8-1. This same diagram will be used for discussing the measurements on a complete receiver or any of its sub-components.

Each block in the diagram will now be discussed and the essential characteristics listed. Circled numbers will be used for reference:

- ① The test signal source is a generator connected to the input of the device being tested. The generator has a nominal impedance equal to the impedance of the transmission line which is R_s , the source resistance specified for the device being tested. The generator impedance R_s is at standard temperature, T_o . The generator output will be made up of the noise due to R_s at T_o and a controlled signal E_g which may be:

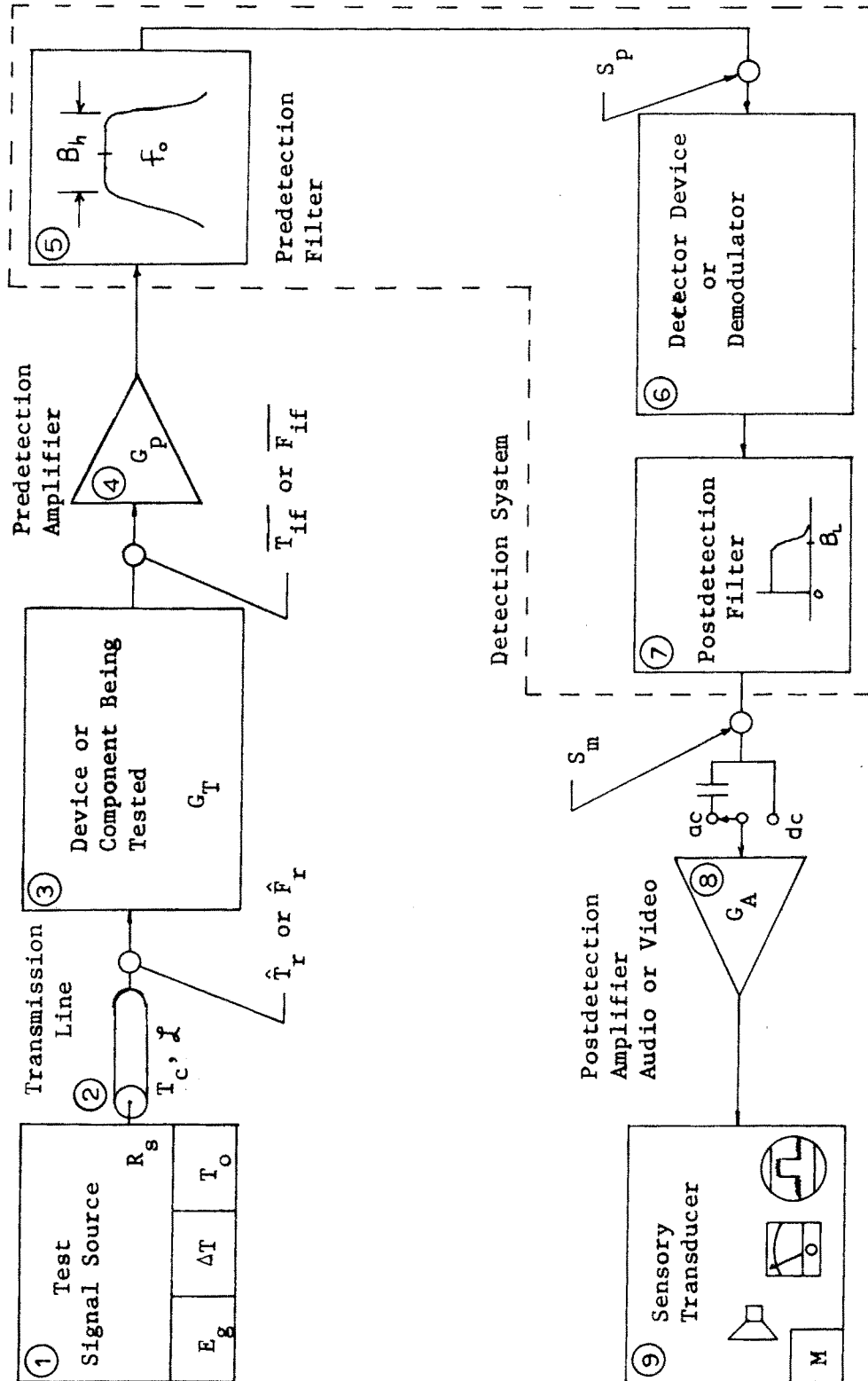


Figure 8-1. Essential Components of a Sensitivity Measuring System

- a. An excess noise signal which has a mean-square value of $E_g^2 = 4 k R_s \Delta T \Delta f$.
- b. An unmodulated sinewave with mean-square value E_g^2 .
- c. An AM modulated sinewave with a mean-square value $m^2 E_g^2$ where m^2 will be used to account for the percentage of modulation.
- d. An exact reproduction of the input signal that will actually be used in the receiving system.

The Thevenin's equivalent circuit for the signal source is the same as that used for the receiving antenna, Figure 4C-23 in Chapter IV.

- ② A transmission line connects the test signal source and the device being tested. The transmission line is characterized by a flat loss N , a physical temperature T_c , and a characteristic impedance $Z_o = R_s$. For the theory presented in this section, the transmission line effects will be omitted by letting it be lossless (see Chapter IV-C). The errors caused by this simplification will be discussed in Chapter X.
- ③ The device or component being tested can be a single device such as a transistor, a subassembly unit such as an amplifier or mixer stage, or a complete receiver.
- ④ The predetection amplifier accounts for the gain preceding the detector or demodulator system and provides

a suitable termination for the device being tested. It also provides a known noise factor so that its noise contribution to the total noise factor, F_r , can be accounted for. The important characteristics of the predetection amplifier are:

- a. Gain, G_p
- b. Equivalent noise temperature, T_{if}
- c. Bandwidth.

It will be assumed that the bandwidth of the predetection amplifier is larger than the predetection noise bandwidth which is determined by ⑤. The predetection amplifier represents the IF amplification in a receiver.

- ⑤ The predetection filter determines the information bandwidth and also the equivalent noise bandwidth for noise factor measurements. It is this filter that regulates the spectrum of signals going into the detector device. The important characteristics of the predetection filter are:

- a. The shape of the passband response
- b. The equivalent noise bandwidth, B_h
- c. The center frequency of the passband, f_o .

The predetection filter is used to represent the IF filtering in a receiver. Typical noise bandwidths range from 1 to 50 KHz for communication receivers and .1 to 1 MHz for radiometers. Typical IF frequencies include .050, .455, 1.6, 4.5, 9.0, 18.0, 30.0, 60.0 and

105 MHz. For more discussion on how to determine the noise bandwidth and the effect of passband shape on measurements, refer to the Appendix, Part B and Chapter VI-C.

- ⑥ The detector device or demodulator is used to recover the information on the input signal in an actual application but in a measurement application it is used to modify the statistical character of the signal in such a way that measurements can be made to determine the nature of the input signal. Usually this is accomplished by rectification to change a signal with a zero mean to one with a nonzero mean. The types of detectors or demodulators that are considered to be the most important for noise measurements are:

- a. Square-law detectors
- b. Linear diode detector
- c. Product detectors (Phase sensitive detector)
- d. Envelope detector (AM demodulator)
- e. Peak-reading voltmeter (Peak rectifier)
- f. Average-reading voltmeter
- g. RMS voltmeter.

For more information on detectors refer to Chapters III, VI, and VII.

- ⑦ The postdetection filter is used to filter and shape the output of the detector device or demodulator. This filter has a low-pass response and an equivalent noise

bandwidth B_L . The postdetection filter in a receiver is the audio filter or video filter and has a bandwidth less than the predetection bandwidth. It also determines the output signal-to-noise ratio, S_m . The important characteristics of the postdetection filter are:

- a. Equivalent noise bandwidth, B_L
- b. DC attenuation, $|H(o)|$
- c. Passband shape.

⑧ The postdetection amplifier is used to amplify the signals from the postdetection filter so that they may be used to drive the desired sensory transducer. This amplifier accounts for the audio or video amplification in a communication receiver. Its important characteristics are:

- a. Gain, G_A
- b. Bandwidth
- c. Output impedance
- d. Flicker noise contribution
- e. DC response
- f. Linearity.

The postdetection amplifier must have a bandwidth low enough so that it will not contribute an appreciable noise signal. It must be linear or it can seriously affect measurement data. It may or may not have a response at dc as illustrated by the switched capacitor at the input.

- ⑨ The sensory transducer is a device used to display the outputs of the measuring system. It can be a meter, oscilloscope, loudspeaker or stripchart recorder. The choice of output display is up to the user but in many applications the choice is obvious. Some of the common choices are: meters for the linear sensitivity measurements such as noise figure, noise temperature, AM sensitivity and power sensitivity, oscilloscope for tangential noise sensitivity and loudspeaker and meter for FM noise quieting.

A. A Theorem for Sensitivity Measurements

All sensitivity measurements are based on the same fundamental truth:

Postdetection information is used to determine predetection RF signal-to-noise ratio.

This fact is used as a basis for the following theorem of sensitivity measurements:

"The sensitivity performance of every receiving system can be specified by the input noise factor (or equivalent noise temperature) and the functional relationship between the predetection and postdetection signal-to-noise ratios."*

The receiver noise factor F_r and the predetection signal-to-noise ratio uniquely determine the predetection noise performance of a receiver and are related by the fundamental equation

$$\hat{F}_r = \frac{E_g^2}{S_p [4 k T_o R_s B_h]} \quad (8A.1)$$

*Predetection SNR is the SNR that exists in the linear portion of the receiver, prior to the detector. Postdetection SNR is the measured SNR after the detection stage. The detector may be either linear or non-linear.

where \hat{F}_r = the average noise factor, over the predetection bandwidth B_h , of the device being tested. This is not the average noise factor for the device (see Appendix, Part H).

E_g^2 = the mean-square value of the generator test signal used to measure the noise factor, F_r . When E_g is a sinewave it is measured in hard volts RMS (Appendix, Part Q).

B_h = the equivalent noise bandwidth of the predetection filter.

S_p = Predetection signal-to-noise power ratio.

R_s = Specified source resistance for the device or component being tested.

k = Boltzmanns constant.

T_o = Standard temperature, 290° K.

The predetection and postdetection signal-to-noise ratios are related by some function:

$$\begin{aligned} S_p &= f_s(S_m) \\ S_m &= f_s^{-1}(S_p) \end{aligned} \tag{8A.2}$$

The study of the noise behavior of a detector is the study of this functional relationship.

In actual measurements, the predetection signal-to-noise ratio is determined by a ratio measurement at the output which is usually the

ratio of two ac or two dc voltages. This relationship is expressed in the function:

$$S_p = f_M(M) \quad (8A.3)$$

where M is the ratio of the measured output when the test signal source is turned on ($E_g \neq 0$) to that when it is turned off ($E_g = 0$). The various forms of $f_M(M)$ will be given later in this chapter. The functional dependence of predetection and postdetection signal-to-noise ratio is best represented in the graphs of Figure 8A-2.

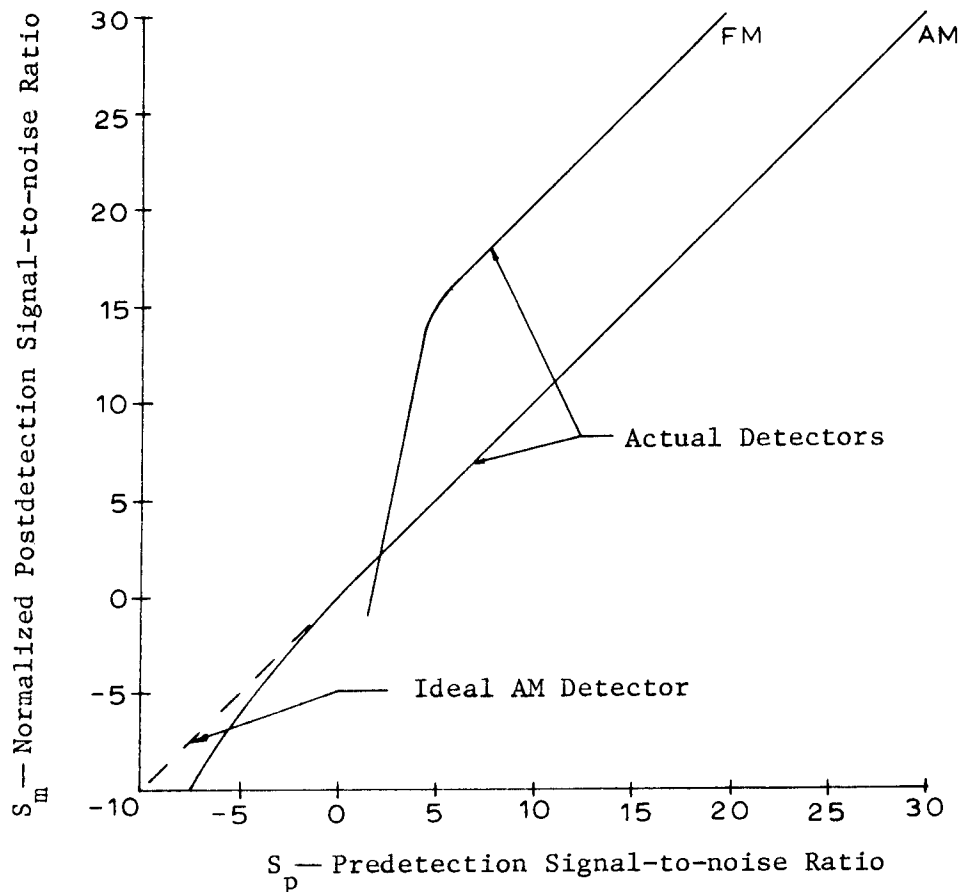


Figure 8A-2. Comparison of Output SNR to Input SNR for Typical Detector Types

The degrading of output signal-to-noise ratio at low input signal-to-noise ratio is illustrated for FM detectors and linear diode detectors. The ideal detector curve represents the response assumed for an ideal "linear" system where the total power at the output is directly related to the power input. Data on the functional dependence of input and output SNR for various types of detectors can be found in the following references; Davenport and Root (1958, p. 266), Fubini and Johnson (1948), Bridges (1954) and Middleton (1948, 1960).

It must be kept in mind that the relationship $S_p = f_s(S_m)$ is not of fundamental importance in sensitivity measurements but is for system specification. What is important is--how does the predetection signal-to-noise ratio depend on the ratio of measured outputs, Equation 8.3? The measured ratio at the output is usually the ratio of two dc voltages or two ac noise voltages. The postdetection SNR will affect the accuracy of the measurement.

This concludes the introductory discussion of sensitivity measurement and the sensitivity measurement theorem. The next three sections will describe the application of sensitivity measurement theory to various systems and how they relate to the block diagram. The order of presentation is for convenience and has no other significance.

B. Noise Quieting (FM Systems)

A meaningful way to measure the relative sensitivity of FM receivers has been developed which takes advantage of the capture effect in an FM receiver. The capture effect is the ability of an FM receiver to favor the strongest signal in the passband and discriminate against the weaker

ones. A difference in input level of only 3-4 db can cause several db of output difference. Because of this effect, when the FM receiver is tuned to an unmodulated carrier, the output noise will decrease. This decrease in noise is called quieting and will be described shortly but first we need to present more information on the FM detector. Figure 8A-2 is only meant to illustrate the threshold effect in FM detectors and does not give absolute information. A more complete story of FM detection can be given with the help of Figure 8B-1. This figure shows the threshold effect and how it varies with the deviation ratio, D , defined as:

$$D = \frac{\text{Maximum instantaneous frequency excursion from the carrier}}{\text{Modulation frequency}}$$

In theory, the signal-to-noise ratio for an FM system compared to an AM system is given by (Cook and Liff, 1968, p. 49)

$$\frac{(S_m)_{FM}}{(S_m)_{AM}} = 3D^2$$

valid when the input SNR is high enough to put the detector above the full FM improvement threshold. Notice from the figure that this threshold depends upon the deviation ratio. The higher the deviation ratio the more FM improvement, but the threshold has to be reached with larger and larger input signal-to-noise ratios. What does one sacrifice for this SNR improvement? The answer is bandwidth. The higher the FM deviation ratio, the larger the FM bandwidth.

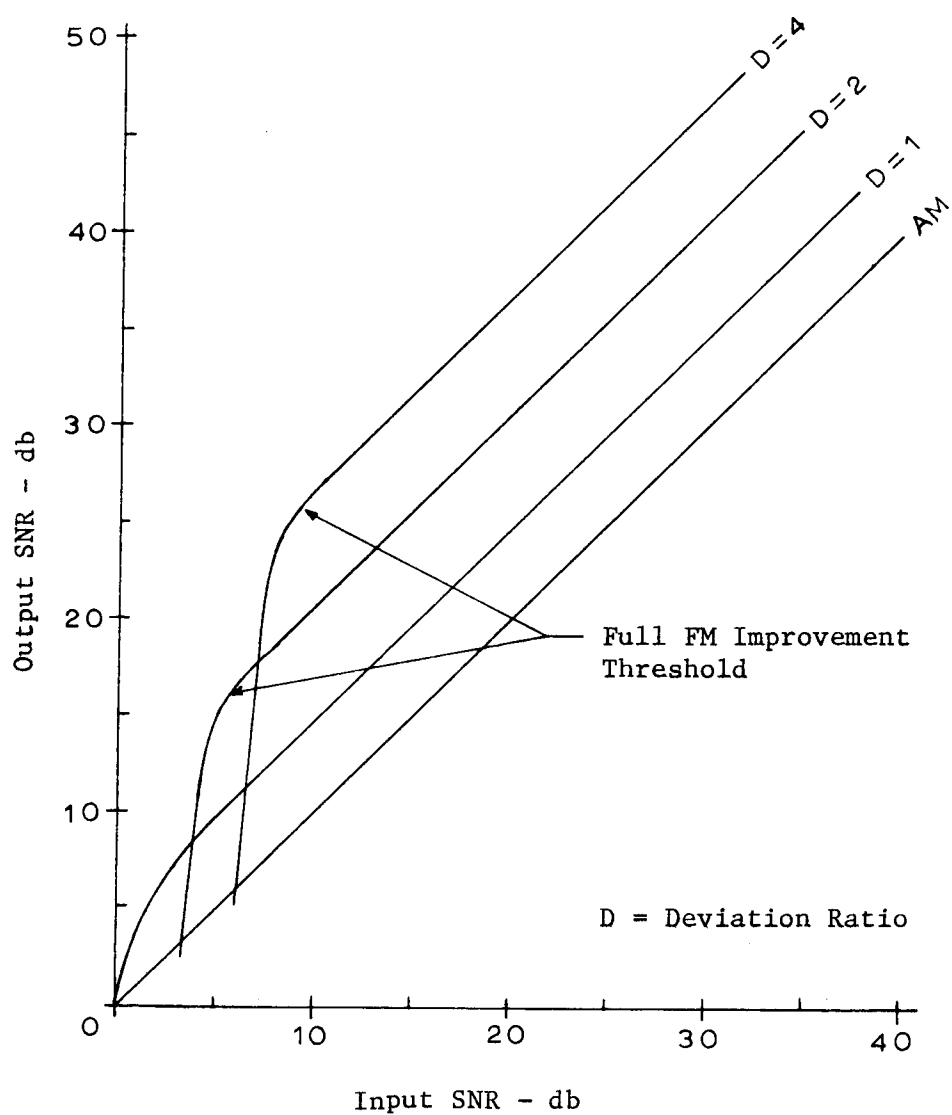


Figure 8B-1. Signal-to-Noise-Ratio Characteristics for an Ideal FM Detector

A study* of FM modulation and bandwidth requirements, based upon Bessel functions and output signal distortion, shows that reasonable bandwidth rules can be obtained for various ranges of deviation ratio. These rules are summarized below:

FM Bandwidth Rules

$0 \leq D \leq 0.25$	$FMBW \approx 2 f_m$	
$0.25 \leq D \leq 1$	$FMBW \approx 4 f_m$	
$1 \leq D$	$FMBW \approx 2(D + 1)f_m$	(Speech)
	$\approx 2(D + 2)f_m$	(music)

where f_m is the maximum audio frequency to be transmitted.

For low deviations ($D < .25$), the FM bandwidth is equal to the required AM bandwidth, but for deviations which will give a signal-to-noise ratio improvement ($D \leq \frac{1}{\sqrt{3}}$), the required FMBW is at least twice that of the AM system. For a deviation ratio of 2, the required FMBW for music transmission is four times that needed for AM. Feldman (1966, p. 27) discusses quieting in an FM receiver. The FM sensitivity of a receiver can be specified by measuring the required input signal level that will give a specified output quieting ratio:

$$QR = \frac{\text{Audio noise output with unmodulated sinewave signal}}{\text{Audio noise output without sinewave signal}}$$

* These rules were developed for presentation in an FM Two-Way Radio Course taught by the author for Engineering Extension at Iowa State University, Ames, Iowa.

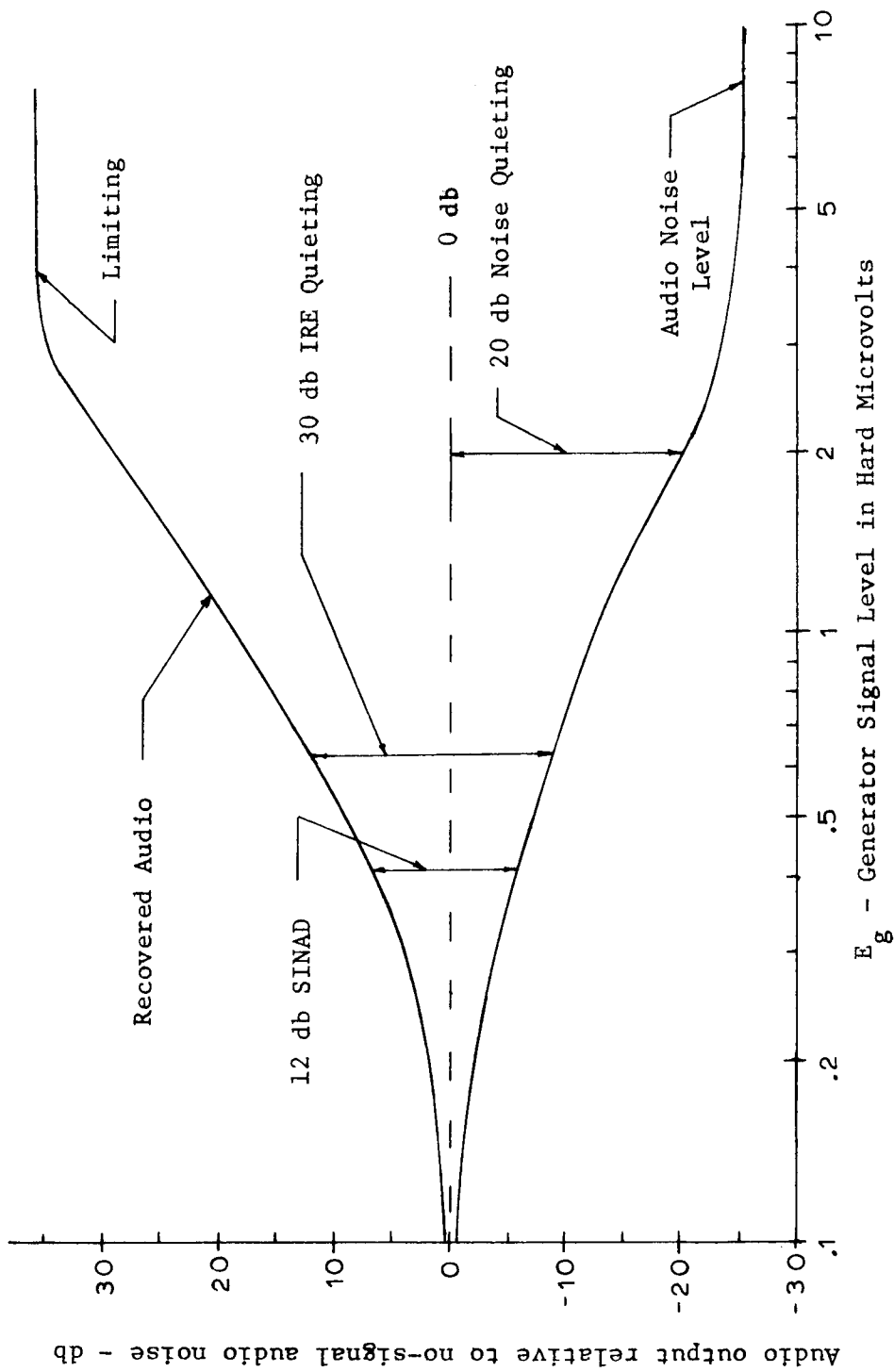


Figure 8B-2. Typical Quieting Curve for a Wideband FM Receiver

A typical quieting curve is shown in Figure 8B-2 (some of the terms shown in the figure will not be defined until Chapter IX). The quieting ratio is specified in db (usually 20 or 30 db) and is high enough to get above the FM threshold.

Besides FM quieting there are methods of specifying FM sensitivity which employ the recovered audio of the system. These methods are designed to test the quality of recovered audio. The additional methods are discussed in Section IX-C.

C. Tangential Noise Sensitivity (PCM Systems)

For systems which employ pulse-code modulation (PCM) such as for radar and data transmission, the pulse receivers are probably best tested with a pulsed test signal source. This is a complete system test and takes into account the affect of the detector on signal-to-noise ratio. The minimum detectable signal is a hard criterion to define for any system and usually requires a knowledge of communication theory and detector operation. The best minimum detectable signal criterion that has been found for pulse receivers is the Tangential Noise Sensitivity measured using a pulse generator and an oscilloscope for a sensory transducer. The measurement is described with the help of Figure 8C-1. The sinewave test generator is pulsed on and off so that the output of the pulse detector is an ac noise signal superimposed on two dc output levels. The output ac noise voltage is described as "grass" because, when the sweep rate of the scope is much slower than the reciprocal bandwidth of the predetection filter, the waveform looks like grass. The output of the pulse generator is adjusted so that the

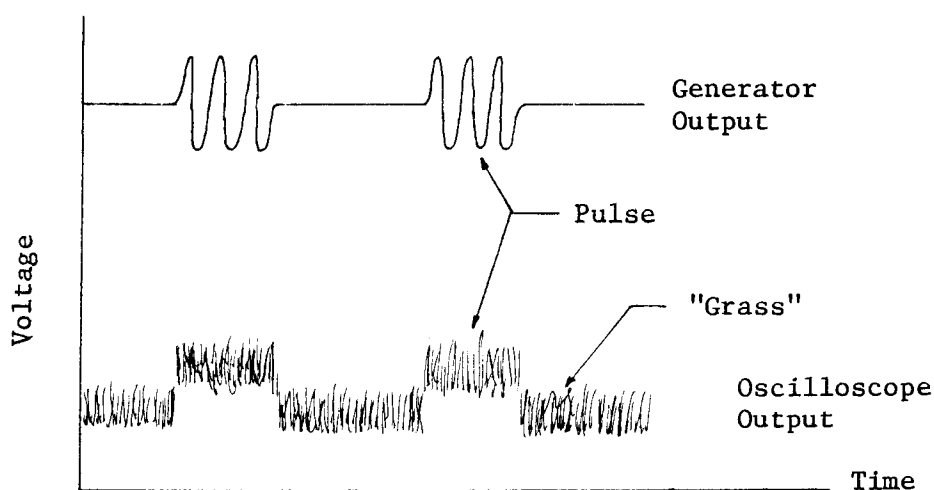


Figure 8C-1. Waveforms Representing Tangential Noise Sensitivity Measurement

bottom of the "grass" during the "pulse on" period is even with, or tangent to, the top of the grass during the "pulse off" period.

Measurements taken by qualified observers showed (Montgomery, 1964, p. 228) that accuracies no better than 1 to 2 db can be expected with this method. Actual data taken showed a 2db standard deviation for the reported mean value for all observers. Repetitive measurements by a single observer showed a deviation from the mean of less than 1 db. The actual value of tangential sensitivity will depend upon the detector type and the subjective evaluation of the observer. The observer tests reported above also determined that the value of peak pulse input power needed to give a tangential signal was 9.2 db above that needed to give an output signal-to-noise ratio of unity. A square-law detector was used in these measurements. A discussion of sensitivity measurements for wideband pulse receivers is given by Klipper (1965). In his paper,

Klipper presents the power sensitivities for square-law and linear detectors based upon several criteria. The criteria of tangential sensitivity and unity output SNR will be summarized here. If the predetection bandwidth is much greater than the postdetection bandwidth ($B_h \gg B_L$), the sensitivity equation given by (8A.1) becomes

$$\hat{F}_r = \frac{E_g^2}{4 k T_o R_s [K_D \sqrt{2 B_h B_L}]} \quad (8C.1)$$

where $S_p B_h = K_D \sqrt{2 B_h B_L}$. The factor K_D is a numerical constant whose value depends upon both the detector type and the measurement criteria. Klipper (1965) has given values of K_D for square-law and linear detectors. The values of K_D for unity SNR ($S_o/N_o = 1$) and tangential sensitivity are given in Table 8C-1. For the purpose of judging when the signals are tangent, Klipper employed a value of $3.5 \sigma_N$ as the practical top of the "grass". When tangential sensitivity and unity SNR are compared on this basis, the input signal required for tangential sensitivity is 8.5 db higher, or equal to the ratio of the respective K_D 's. This number compares favorably with the 9.2 db reported in Montgomery (1964, p. 228).

Table 8C-1. Sensitivity constant, K_D , for square-law and linear diode detectors.

Detector Type	$S_o/N_o = 1$	Tangential Sensitivity	Ratio
Square-law	1	7	~ 8.5 db
Linear diode	1/2	3.5	~ 8.5 db

The power sensitivity of the receiver in terms of available input power in dbm, is from Equation 8C.1

$$\frac{E_g^2}{4R_s} \text{ (dbm)} = S_i \text{ (dbm)} = -114 + 10 \log F + 10 \log K_D + 10 \log \sqrt{2B_h B_L} \quad (8C.2)$$

where B_h and B_L are in MHz. From this equation and the K_D values we see that the linear diode detector is 3-db more sensitive than the square-law detector.

D. Noise Factor and AM Sensitivity

In Chapter VII a special definition of "linear" receiver was used when talking about noise factor and AM sensitivity. Montgomery (1964, p. 233) uses the term "linear-gain receiver" to describe the same property. The linear-gain receiver is defined to be one in which the output power is proportional to the input power. This distinction is important to sensitivity measurement theory. The sensitivity of a linear-gain receiver is completely specified by Equation 8A.1. When this equation is applied to a linear-gain receiver the measured sensitivity can be specified by two factors; the predetection signal-to-noise ratio and the mean-square value of test signal needed to obtain it. Each measurement technique that is presented in the following sections will follow the same procedure; the type of test signal source is specified which determines E_g^2 , then the detector type is specified

which determines the functional relationship between the measured output ratio, M , and the predetection signal-to-noise ratio, S_p .

The special forms of Equation 8A.1 which apply to each measurement will be derived along with information on how to determine the functional relationship between M and S_p (Equation 8A.3). The theory will be discussed by detector type and test generator type. The fundamental quantity of noise factor will be used throughout this section because it is fundamentally related to the actual measurements and because equivalent noise temperature and receiving system power sensitivity are related to noise factor through definitions. To better define the concepts involved, the first two articles of this section will deal with the definition of noise factor and how to specify the test signal generator. Figure 8D-1 is a simplified block diagram for sensitivity measurements.

1. Noise factor measurement theory

The noise factor method of specifying receiver sensitivity is completely independent of the widely variable factors of receiver bandwidth and gain or, as in the case of AM sensitivity, signal generator characteristics such as modulation percentage and distortion. Also, as an added bonus, the noise factor specification is independent of the input impedance of the receiver. The attractiveness of the noise factor specification has resulted in its use to specify not only receivers, but a wide variety of active electronic amplifying devices. Various definitions for noise factor exist and are successfully applied to many devices but one has to be cautious to avoid applying them incorrectly.

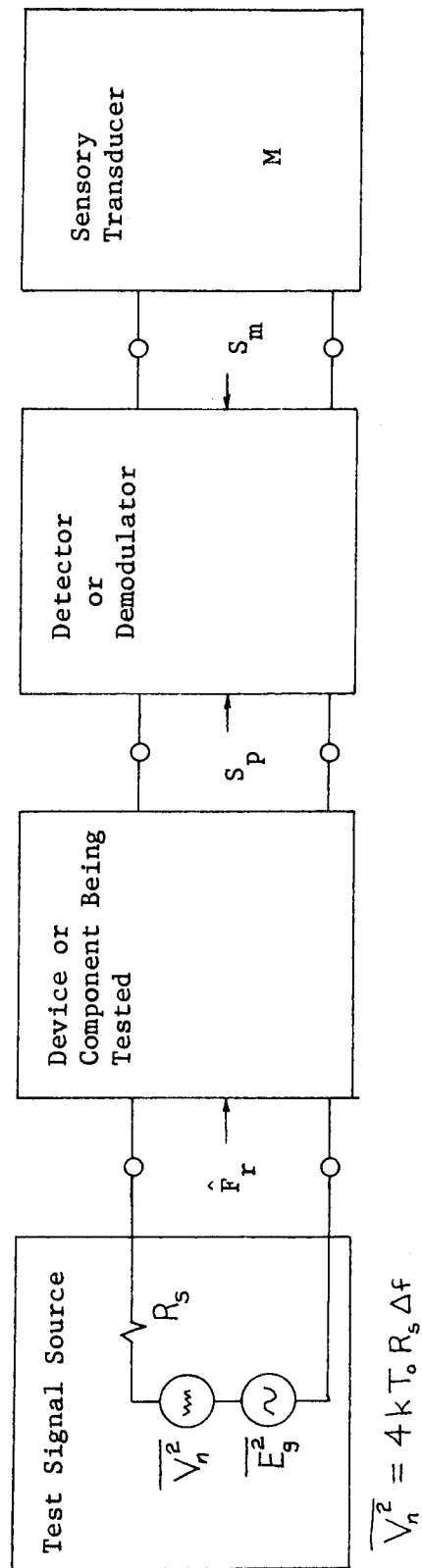


Figure 8D-1. Simplified Block Diagram for Sensitivity Measurements

After becoming familiar with these definitions, it is possible to simplify many calculations by choosing the one most appropriate. It is to this end we now discuss the definitions.

North (1942) defines noise factor as, "the ratio of actual noise power to that developed by an ideal receiver". Taken out of context, the definition sounds nebulous but when the ideas which are presented are correlated, the definition may be stated as:

Noise factor is the ratio of actual noise power output from a noisy receiver connected to an antenna to the noise power output from a noiseless but otherwise indetical receiver connected to the same antenna, or

$$F = \frac{\text{Total noise power at the output}}{\text{Noise power at the output due only to the antenna}} \cdot \quad (8D.1)$$

Applying North's definition exactly was a problem however, because it left too much room for interpretation when trying to define such things as "antenna" and "noiseless receiver". The definition also was dependent upon assigning a particular reference temperature, T_o , to the antenna. This is equivalent to saying that we don't want the denominator of the noise factor definition to go to zero because:

$$\lim_{T_o \rightarrow 0} F = \infty \quad (8D.2)$$

To remedy these difficulties, more strict definitions have been developed, including an IRE(IEEE) standard in 1963b.

The explicit definition of noise factor can be best illustrated by the use of Figure 8D-2 where the source could be an antenna, a noise

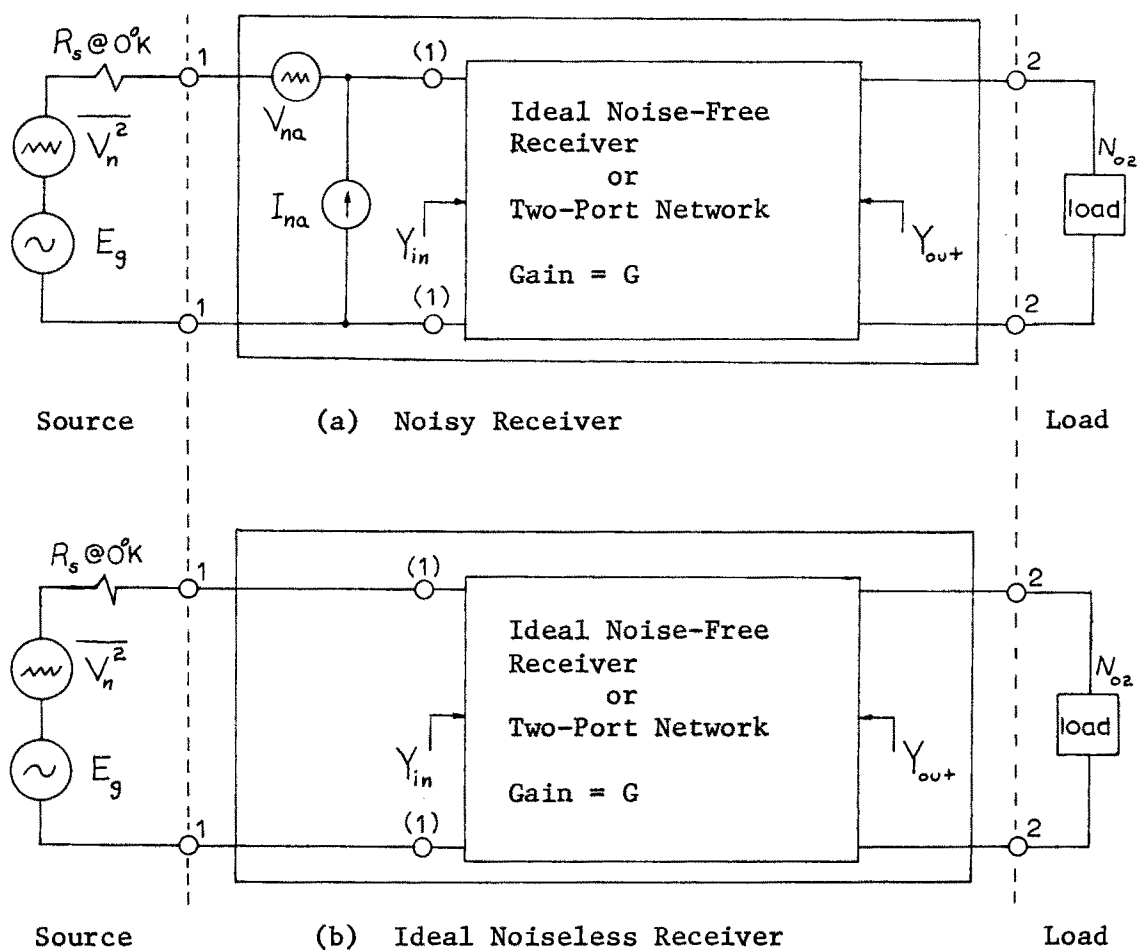


Figure 8D-2. Circuits for Noise Factor Definition

generator, or the Thevenin's equivalent of the output of a previous stage.

Figure 8D-2a shows the noisy receiver with equivalent noise generators referred to the input. Figure 8D-2b is the same circuit except the receiver noise generators have been omitted.

The quantities in the figure are defined as follows:

R_s = Source resistance (may be antenna radiation resistance, test generator resistance, or the Thevenin's equivalent resistance of the previous stage)

E_g = RMS voltage of the test signal generator
 $\frac{V_n^2}{V_n} = 4k R_s T_o \Delta f$, the mean-square value of noise voltage for R_s

V_{na}, I_{na} = Equivalent noise generators for the noisy receiver or amplifier, undesired noise (see Section IV-E)

N_{02} = Noise power output when the noisy receiver is in the circuit

N_{01} = Noise power output when the noisy receiver is replaced by an ideal noiseless receiver.

The noisy receiver is actually any noisy two-port, described by its noise parameters and its noiseless two-port matrix coefficients. The exact definition of noise factor, dependent upon the reference temperature T_o , is (see also the Appendix, Part H):

$$F = \frac{N_{o2}}{N_{o1}} \quad \text{NOISE FACTOR} \quad (8D.3)$$

Several restrictions and definitions subtle to the definition are listed for clarification:

1. The noise factor definition is dependent upon the reference temperature T_o which is now generally accepted to be 290° K^* .

*This value has been adopted by the Institute of Electrical and Electronics Engineers as a standard, so that all receivers can be evaluated and compared to each other based on their noise and sensitivity characteristics.

2. The ideal noiseless receiver is derived from the noisy receiver by letting all internal noise source temperatures go to zero so that $V_{na} = I_{na} = 0$.
3. The result of simply "turning off" the noise sources to obtain the ideal receiver is that all of the noiseless two-port parameters remain the same, so that the receiver gain G and the terminated two-port admittances Y_{in} and Y_{out} are unchanged.
4. The restriction that the entire system remain linear is still needed and it must be emphasized that noise factor is only meaningful for a linear two-port.
5. When specifying the noise factor of a two-port, it is necessary also to specify the source resistance R_s .

An alternate, and very useful definition for noise factor is obtained using the idea of signal-to-noise ratio.

The source in Figure 8D-2 includes a noise voltage, V_n , and a signal voltage, E_g . The ratio of E_g^2 to $\overline{V_n^2}$ defines the signal-to-noise ratio available to the receiver and it is surmised that an ideal receiver would preserve this ratio; certainly we could not expect to improve it! The definition is derived as follows; the signal power output S_o is G times the signal power input S_i , and from the previous definition of noise factor (Equation 8D.3 or 8D.1)

$$F = \frac{G N_i + G N_r}{G N_i} \quad (8D.4)$$

where N_i = Available noise power at the receiver input
 due to $\overline{V_n^2}$
 N_r = Available noise power at the receiver input due
 to the internal noise of the receiver.

Divide the numerator and denominator of (8D.4) by GS_i to get

$$F = \frac{\frac{GN_i + GN_r}{GS_i}}{\frac{GN_i}{GS_i}} = \frac{\frac{GS_i}{GN_i}}{\frac{GS_i}{GN_i + GN_r}} = \frac{(S_i/N_i)}{(S_o/N_o)} \quad (8D.5)$$

which is the ratio of available input SNR to available output SNR. For a noiseless receiver ($F = 1$) the signal-to-noise ratio is preserved. It is impractical to measure noise factor directly using the signal-to-noise ratio definition but we use this definition to obtain measurement techniques which are practical.

The IRE definition of noise factor is taken from two standards published in 1957 and 1963b. To quote the definition, "Noise factor (Noise figure) of a two-port transducer; at a specific input frequency, the ratio of:

1. The total noise power per-unit-bandwidth (at a corresponding output frequency) available at the output port when the Noise Temperature of its input is standard (290° K) at all frequencies (Reference: Definition for average noise factor) to,

2. That portion of 1. engendered at the input frequency by the input termination at the Standard Noise Temperature (290° K).

Note 1: For heterodyne systems there will be, in principle, more than one output frequency corresponding to a single input frequency, and vice versa; for each pair of corresponding frequencies a Noise Factor is defined. 2. includes only that noise from the input termination which appears in the output via the principal-frequency transformation of the system, i.e. via the signal-frequency transformation(s), and does not include spurious contributions such as those from an unused image-frequency or an unused idler-frequency transformation.

Note 2: The phrase "available at the output port" may be replaced by "delivered by system into an output termination."

Note 3: To characterize a system by a Noise Factor is meaningful only when the admittance (or impedance) of the input termination is specified.

The underlined words in the definition were added in the 1963b Standard for increased clarity.

The available input signal-to-noise-ratio is simply the ratio of available powers of E_g and V_n or

$$\frac{S_i}{N_i} = \frac{\frac{E_g^2}{4R_s}}{\frac{V_n^2}{4R_s}} = \frac{E_g^2}{4 k T_o R_s B_h} \quad (8D.6)$$

where B_h is the noise bandwidth of the receiver. The output signal-to-noise ratio is really the predetection SNR, S_p , and is only related to the actual receiver output SNR, S_m . Substituting (8D.6) and S_p into the definition of (8D.5) gives

$$F = \frac{E_g^2}{S_p [4 k T_o R_s B_h]}$$

which is the same as Equation 8A.1.

2. Test signal sources

There will be three types of test signal sources to consider:

1. A noise voltage generator which produces an equivalent mean-square value, $\overline{E_g^2} = 4 k R_s \Delta T B_h$. ΔT is the excess noise temperature of the generator.
2. An unmodulated sinewave voltage generator with mean-square value E_g^2 .
3. An amplitude modulated sinewave generator with modulation index m which produces a mean-square voltage of $m^2 E_g^2$ when only the recovered audio produces an output.

The noise factor equation of the form of (8A.1) is modified by the type of generator employed. The following equations are obtained for noise

factor by substituting in the mean-square values of test signal voltages:

1. Noise Voltage Generator

$$\hat{F}_r = \frac{\Delta T}{S_p T_o} \quad (8D.7a)$$

2. Unmodulated Sinewave

$$\hat{F}_r = \frac{E_g^2}{S_p [4 k T_o R_s B_h]} \quad (8D.7b)$$

3. AM Sinewave

$$\hat{F}_r = \frac{m^2 E_g^2}{S_p [4 k T_o R_s B_h]} \quad (8D.7c)$$

Notice that the measurement of noise factor using a noise source (8D.7a) has eliminated all considerations of effective predetection noise bandwidth. This is the primary reason why noise sources are preferred for test signal sources when very accurate noise factors must be measured.

3. Detectors for noise factor measurements

The following presentation of the characteristics of detectors for noise factor measurements represents the most commonly used techniques. Others which are not presented may be equally valid.

The square-law detector will be presented first. For a measurement where the test signal is a noise voltage generator the ratio of the

output dc voltages with and without noise signal is given by (Chapter VI, Equation 6.86)

$$S_p = f_M(M) = \left(\frac{\sigma_{dc}}{E_o} - 1 \right) = (M_{dc} - 1) \quad (8D.8)$$

where

$$M_{dc} = \frac{\text{Detector dc output with generator "on"}}{\text{Detector dc output with generator "off"}}$$

The measured noise factor then becomes:

$$\hat{F}_r = \frac{\Delta T}{(M_{dc} - 1) T_o} \quad (8D.9)$$

When the test signal is an unmodulated sinewave, the mean-square voltage is E_g^2 and the predetection SNR is still given by Equation 8D.8 and the resulting noise factor becomes:

$$\hat{F}_r = \frac{E_g^2}{(M_{dc} - 1) [4 k T_o R_s B_h]} \quad (8D.10)$$

Since the ac output voltage of a square-law detector is proportional to the input noise temperature (Equation 7.46b), the ratio of ac output voltages also determines the predetection SNR i.e.

$$S_p = (M_{ac} - 1) \quad (8D.11)$$

where

$$M_{ac} = \frac{\text{Detector ac output noise voltage with generator "on"}}{\text{Detector ac output noise voltage with generator "off"}}$$

The measured noise factor then becomes

$$\hat{F}_r = \frac{\Delta T}{(M_{ac}^2 - 1) T_o} \quad (8D.12)$$

which is the same form as Equation 8D.9. The square-law detector with a modulated sinewave input will not be discussed.

The linear-diode detector is the next most useful detector for sensitivity measurements. When the test signal is noise, the predetection SNR is related to the measured dc ratio by (Equation 6.97)

$$S_p = (M_{dc}^2 - 1) \quad (8D.13)$$

which gives a resulting noise factor of:

$$\hat{F}_r = \frac{\Delta T}{(M_{dc}^2 - 1) T_o} \quad (8D.14)$$

When the input is an unmodulated sinewave, the measured output dc ratio is related to the predetection SNR by the transcendental (7.92).

Data for the solution to this equation was given in Table 6-2. For the special case where the measured dc ratio is two ($M_{dc} = 2$), the predetection SNR is 2.60. For larger predetection signal-to-noise ratios, the approximation given below is valid

$$S_p \approx \frac{1}{2} \left(\frac{\pi}{2} M_{dc}^2 - 1 \right) \quad M_{dc} \geq 2 \quad (8D.15)$$

which gives for a measured noise factor:

$$\hat{F}_r = \frac{E_g^2}{\frac{1}{2} \left(\frac{\pi}{2} M_{dc}^2 - 1 \right) [4 k T_o R_s B_h]} \quad (8D.16)$$

The product detector behaves the same as the square-law detector when the test signal is noise. This means Equations 8D.9 and 8D.12 are valid for the product detector. The product detector with a sinewave input will not be discussed.

The peak-reading voltmeter can be used for noise ratio measurements i.e. the ratio of two ac noise voltages but should not be used for measuring sinewaves-plus-noise. The corrections which apply to noise measurements of absolute voltages are discussed in Section VI-A.

The average-reading voltmeter can be used to measure noise voltage ratios and signal-plus-noise-to-noise ratios for large ratios ($\text{SNR} > 6 \text{ db}$). At large SNR's, the 1.05 db correction factor discussed in Section VI-B must be applied.

The true-reading RMS voltmeter or power meter can be used to measure predetection signal-to-noise ratios for either noise voltages alone or sinewaves-plus-noise. This instrument is capable of direct noise factor measurements provided the gain of the system is large enough to produce measurable powers (usually around -20 dbm).

Sensitivity measurements using an AM demodulator can be made using either a noise source or a modulated sinewave generator. When the noise source is used as a test signal, the output SNR of the detector is assumed to be the same as the input SNR. This is valid when both the receiver noise and the noise of the source have the same spectral and statistical properties, hence

$$S_p = S_m$$

or

$$S_p = S_o/N_o \quad (8D.17)$$

where S_o is the power output due to the test signal and N_o is the power output due to receiver noise and source noise. The measurement at the output is the ratio of the noise power output with test signal to that without or the signal-plus-noise-to-noise ratio which is:

$$\frac{S_o + N_o}{N_o} \quad (8D.18)$$

Combining (8D.16) and (8D.15) we get the relationship between input SNR and measured signal-plus-noise-to-noise ratio,

$$S_p = \left[\frac{S_o + N_o}{N_o} - 1 \right] \quad (8D.19)$$

which gives a measured noise factor of:

$$\hat{F}_r = \frac{\Delta T}{\left[\frac{S_o + N_o}{N_o} - 1 \right] T_o} \quad (8D.20)$$

The input excess noise temperature, ΔT is that which produces the ratio $(S_o + N_o)/N_o$.

When the test signal generator is an AM sinewave, the mean-square input voltage which determines the recovered audio is $m^2 E_g^2$ where m is the modulation index. For large predetection signal-to-noise ratios ($\text{SNR} > 6 \text{ db}$) the detector threshold effect can be neglected but the equivalent noise bandwidth must be determined. The noise signal measured at the audio output depends upon both the

predetection and postdetection noise bandwidths. In high quality receivers of modern design, the IF bandwidth determines the information bandwidth of the system and is approximately equal to twice the audio bandwidth. Quite often, however, the audio bandwidth is smaller than one-half the IF bandwidth. When this is the case, the average noise factor is determined by the audio bandwidth. If the noise contribution of the audio stages can be ignored compared to the IF noise output, the effective noise bandwidth for AM sensitivity measurements is determined for three conditions:

1. The audio noise bandwidth is smaller than one-half the predetection or IF noise bandwidth, $B_L < \frac{1}{2} B_h$.
2. The audio noise bandwidth is larger than one-half the predetection noise bandwidth, $B_L > \frac{1}{2} B_h$.
3. The audio noise bandwidth is nearly equal to one-half the predetection noise bandwidth, $B_L \approx \frac{1}{2} B_h$.

The measured noise factor determined by AM sensitivity is

$$\hat{F}_r = \frac{m^2 E_g^2}{\left[\frac{S_o + N_o}{N_o} - 1 \right] [4 k T_o R_s B_c]} \quad (8D.21)$$

where B_c is the effective noise bandwidth of the receiver. The effective noise bandwidth is, for the first two cases above:

1. $B_c = 2B_L$ when $B_L < \frac{1}{2} B_h$
2. $B_c = B_h$ when $B_h > \frac{1}{2} B_h$.

For the case where $B_L \approx \frac{1}{2} B_h$, the composite bandwidth of the predetection and postdetection filters must be used. This composite or effective noise bandwidth can be determined by measuring the total receiver frequency response from RF input to audio output. It usually has a value very close to the predetection noise bandwidth, B_h .

Figure 8D.3 is a summary of the results in this section. The following quantities are defined for additional clarity:

ΔT = Excess noise of the noise source used as a test generator, $^{\circ}\text{K}$.

E_g^2 = Mean-square value of sinewave voltage.

m = Modulation index for amplitude modulation, $0 \leq m \leq 1$.

M_{dc} = Ratio of detector dc output voltage with test source on to that with test source off.

M_{ac} = Ratio of detector ac output voltage with test source on to that with test source off.

$\frac{S_o + N_o}{N_o}$ = Ratio of output signal-power-plus-noise-power to noise power alone.

R_s = Test generator source resistance, ohms.

B_h = Predetection equivalent noise bandwidth of the measurement system, Hz.

B_c = Composite or effective noise bandwidth for an AM receiver. In special circumstances it is equal to either predetection or postdetection noise bandwidths.

T_o = Standard Temperature, 290°K .

Test Signal Type		Detector Type		
		Square-law	Linear-diode	AM Demodulator
Noise $E_g^2 = 4k\Delta TR_{s_h}$	M_{ac} and $\frac{S+N_o}{S_o}$	$\hat{F}_r = \frac{\Delta T}{(M_{ac}-1)T_o}$	—	$\hat{F}_r = \frac{\Delta T}{\frac{S+N_o}{N_o}(-1)T_o}$
	M_{dc}	$\hat{F}_r = \frac{\Delta T}{(M_{dc}-1)T_o}$	$\hat{F}_r = \frac{\Delta T}{(M_{dc}^2-1)T_o}$	Not Meaningful
Unmodulated Sinewave E_g^2	M_{dc}	$\hat{F}_r = \frac{E_g^2}{(M_{dc}-1)[4kTR_{s_h}]}$	$\hat{F}_r = \frac{E_g^2}{\frac{1}{2}(M_{dc}^2-1)[4kTR_{s_h}]}$	Not Meaningful
		—	—	$\hat{F}_r = \frac{E_g^2}{\frac{S+N_o}{N_o}(-1)[4kTR_{s_h}]}$
Modulated Sinewave E_g^2	$\frac{S+N_o}{N_o}$	—	—	—
Notes: $M_{ac}^2 = \frac{S+N_o}{N_o}$, ac output ratio in db = $10 \log \left(\frac{S+N_o}{N_o} \right) = 20 \log (M_{ac})$				

Figure 8D-3. Summary of Measurement Equations

When making sensitivity measurements, one must distinguish between a measured output voltage ratio, M_{ac} and a measured output power ratio, $(S_o + N_o)/N_o$. If the output level change is measured in db, this must be converted to a numerical factor by one of the conversions:

$$\begin{aligned} \text{Ratio in db} &= 10 \log \left(\frac{S_o + N_o}{N_o} \right) \\ &= 20 \log (M_{ac}) \end{aligned} \quad (8D.22)$$

The results of this chapter will now be applied to practical techniques for measuring sensitivities.

IX. SENSITIVITY MEASURING METHODS

The purpose of this chapter is to present the commonly used techniques of measuring sensitivity. It is not possible to enumerate all of the various combinations of measuring systems and specifications so only the most common ones will be presented. Much of the basic theory underlying these techniques is presented in other chapters and will not be repeated. The details of measurement accuracy will not be given here but are reserved for Chapter X. No amount of detailed theory can substitute for good common sense when it comes to making accurate sensitivity measurements. The paramount consideration in all of the techniques that will be discussed is: how can measurement errors be minimized by careful technique? The techniques are grouped according to the type of generator used to make the measurement.

A. Using Noise Generators

The use of a noise generator to measure the noise factor or equivalent noise temperature of a linear-gain receiver or linear two-port network is popular because the noise bandwidth of the system does not have to be known and noise generators are capable of giving the best accuracy. These reasons account for the fact that high accuracy noise factor measurements are made using commercially available noise sources and automatic noise-figure meters. It is recommended that, whenever possible, the sensitivity of "linear" systems should be measured using a calibrated noise source.

1. Noise sources

There are four noise sources which are commonly used to make noise factor measurements. They are:

1. Hot-cold noise source
2. Temperature limited noise diode
3. Gas-discharge noise source
4. Solid-state diode noise source.

The hot-cold noise source is constructed using two calibrated resistive terminations, one at a "hot" temperature and one at a "cold" temperature. This arrangement allows the receiver noise to be measured using two different source temperatures. The schematic representation of a hot-cold noise source is shown in Figure 9A-1 (adapted from Pastori, 1967).

The temperature-limited diode noise source was discussed in Chapters IV-B and IV-F. The deleterious effects of stray reactance and transit time in noise diodes will be discussed in Chapter X.

The gas-discharge noise source produces broadband microwave noise by current flow in a gaseous plasma. The noise produced by the plasma is coupled to a coax or waveguide to be used as a noise source. The construction and operation of gas-discharge noise sources is discussed by Hart (1962), Pastori (1967), and Trembath (in Mumford, 1968, p. 709).

The solid-state diode noise source uses the noise produced in the breakdown of a diode junction. The solid-state noise source can produce much higher levels of noise than the other types of sources. Excess noise ratios of 25-40 db are typical.

The important characteristics of any noise source are:

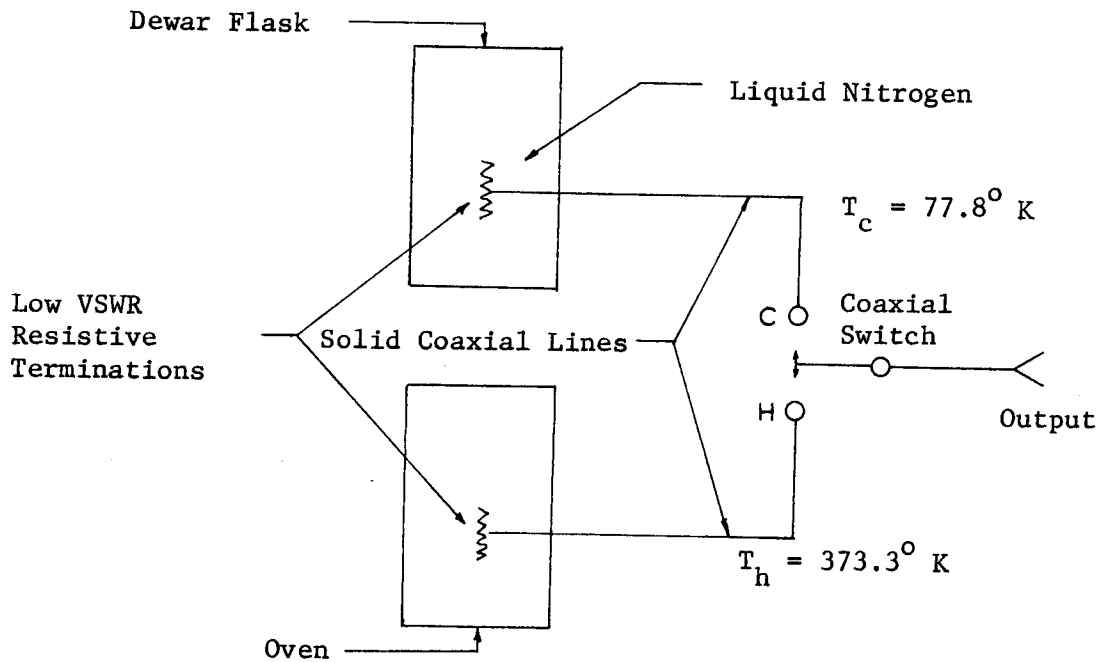


Figure 9A-1. Schematic Representation of a Typical Hot-Cold Noise Source

1. The characteristic impedance, R_s .
2. The value of the two characteristic noise temperatures, T_h and T_c .

For noise diode and gas-discharge noise sources, the "cold" temperature is T_o and the "hot" temperature is the effective noise temperature of source due to the added noise. The added noise is referred to as excess noise (Appendix, Part G). Thus for these types of noise sources,

the important characteristics are impedance, R_s , and excess noise ratio.

The excess noise ratio is defined as

$$\text{ENR} = 10 \log (R_{\text{ex}}) \quad (9A.1)$$

where $R_{\text{ex}} = \frac{T_{\text{ex}}}{T_o} = \frac{T_h - T_o}{T_o}$

$T_c = T_o$, the "cold" temperature

$T_{\text{ex}} = T_h - T_o$, the excess noise of the source

T_h = the "hot" temperature.

Table 9A-1 summarizes the typical characteristics of commercially available noise sources.

Table 9A-1. Typical noise source characteristics

Source Type	R_s , ohms	VSWR	ENR, db	T_h , °K	T_c , °K
Noise diode 10-30 MHz	50	1.2	5.2 (±0.2)	1250 (+46) (-43)	290
Noise diode 600 MHz	50	1.3	6.6 (±0.5)	1616 (+161) (-145)	290
Hot-cold 0-6 GHz	50	1.2	--	373.3 (±2.0)	77.8 (±2.0)
Gas-discharge 0.4-18 GHz	--	1.2 to 3.0	15.6 (±0.6)	10,819 (+1560) (-1358)	290

2. Y-Factor method

The so-called Y-Factor method of measuring effective noise temperature or noise factor is the most general method for linear-gain receivers. It is based on the fact that if the predetection output power is measured at two different levels of input source temperature, the effective noise temperature can be determined from the resulting power ratio. Figure 9A-2 is an idealized schematic representation of the measurement technique.

Y-Factor is the ratio of output noise power with the source at effective temperature T_2 to the noise power output when the source is at temperature T_1 . Y-Factor is essentially a predetection signal-plus-noise-to-noise ratio for two noise sources.

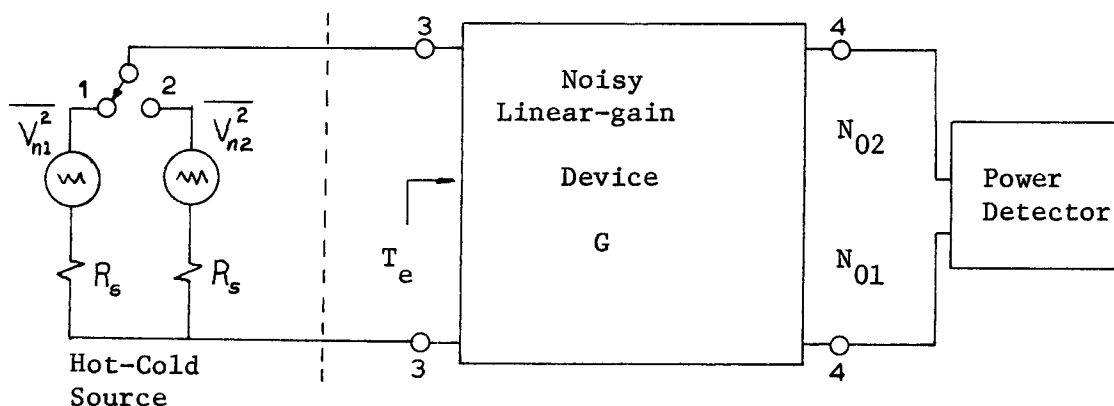


Figure 9A-2. Simple Representation of Y-Factor Method

Applying the definition with the help of Figure 9A-2 we get

$$Y = \frac{N_{02}}{N_{01}} = \frac{k (T_2 + T_e) B_h G}{k (T_1 + T_e) B_h G} = \frac{T_2 + T_e}{T_1 + T_e} \quad (9A.2)$$

where N_{02} = available output noise power when the source at temperature T_2 is connected.

N_{01} = available output noise power when the source at temperature T_1 is connected.

T_e = effective input noise temperature of the device being measured.

B_h = predetection noise bandwidth of the RMS power meter or the equivalent noise bandwidth of the measuring system.

G = Transducer gain of the device being measured.

T_2 = Noise temperature of source #2. This is the "hot" source ($T_2 > T_1$).

T_1 = Noise temperature of source #1. This is the "cold" source ($T_1 < T_2$).

The effective input noise temperature of the device is determined by solving (9A.2) for T_e :

$$T_e = \frac{T_2 - Y T_1}{(Y - 1)} \quad (T_2 > T_1) \quad (9A.3)$$

Noise factor is obtained by substituting T_e into the defining equation,

$T_e = (F - 1) T_o$, to obtain:

$$F = 1 + \frac{\frac{T_2}{T_o} - Y \frac{T_1}{T_o}}{(Y - 1)} \quad (9A.4)$$

When a hot-cold source is used, equations 9A.3 and 9A.4 cannot be simplified but when a noise diode or gas-discharge source is used, the "cold" temperature T_1 becomes standard temperature. For these sources

$$\begin{aligned} T_1 &= T_o \\ T_2 - T_1 &= T_2 - T_o = T_{ex} \end{aligned} \quad (9A.5)$$

where T_{ex} is the excess noise temperature. Substituting these relationships into Equations 9A.3 and 9A.4 gives:

$$T_e = \frac{T_{ex}}{(Y - 1)} - T_o \quad (9A.6)$$

$$F = \frac{\left(\frac{T_2}{T_o} - 1\right)}{(Y - 1)} = \frac{T_{ex}}{(Y - 1) T_o} = \frac{R_{ex}}{(Y - 1)} \quad (9A.7)$$

Equation 9A.7 can be compared to Equation 8D.17. We see that $\Delta T = T_{ex}$ and the measured Y-Factor is simply the measured predetection signal-plus-noise-to-noise ratio.

The simple test setup shown in Figure 9A-2 is usually impractical because it requires a very accurate RMS power detector and a device gain high enough to give usable readings. A more practical test setup is obtained by a modification of Figure 8-1. This scheme is illustrated in Figure 9A-3. The key to this system is a calibrated variable

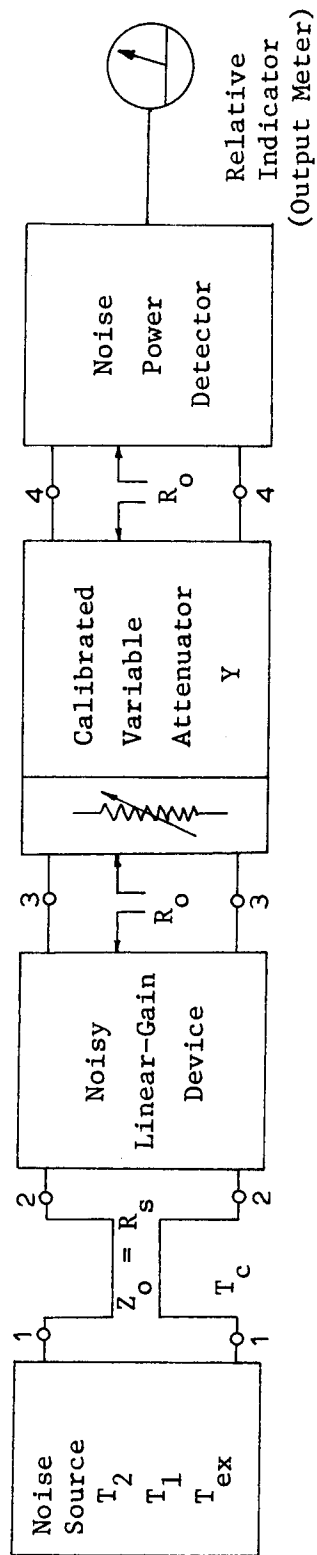


Figure 9A-3. A Practical Test Setup for Measuring Effective Noise Temperature or Noise Factor by the Y-Factor Method

attenuator of high resolution. The measurement procedure is as follows (assume $T_2 > T_1$):

1. The input is connected to source #1 (the "cold" source) and the attenuator is set for a convenient reference power output, N_{01} .
2. Next, the input is switched to source #2 (the "hot" source) and the attenuator is adjusted until the same relative output is again achieved.
3. The attenuator will now indicate the ratio of the two output powers as the Y-Factor:

$$Y = \frac{N_{02}}{N_{01}} \quad (T_2 > T_1)$$

The accuracy of the measurement will depend primarily on the accuracy of the noise source and the attenuator. The detector used does not have to be linear in power because it is used for only relative indications, any type of ac voltmeter is satisfactory. The location of the calibrated Y-Factor attenuator in the actual measurement circuit is not critical as long as the following three criteria are observed:

1. The attenuator must be in a constant impedance circuit and the reflection coefficients of its terminations must be very low.
2. The attenuator must be inserted far enough after the noise factor determining elements so its loss will not affect device noise factor.
3. The attenuator must be inserted before the detector to eliminate detector errors.

In a few special cases, the attenuator can be inserted after the detector but only when the detector is nearly linear in power and when the errors introduced by detector power nonlinearity can be tolerated. Since Y-Factor is really a predetection signal-plus-noise-to-noise ratio, it can be related to the SNR's developed in Chapter VIII-D. With the help of Figure 8D.3 we can relate Y-Factor to the postdetection measured quantities for the following detectors:

Square-law

$$Y = \frac{M_{ac}}{M_{dc}} \quad (9A.8)$$

Linear-diode

$$Y = \frac{M_{dc}^2}{M_{dc}} \quad (9A.9)$$

AM Demodulator

$$Y = \frac{S_o + N_o}{N_o} \quad (9A.10)$$

For the AM detector we must assume a linear power characteristic before (9A.10) is valid.

The noise figure in terms of Y-Factor is obtained by taking the log of both sides of Equation 9A.7 to get:

$$10 \log F = 10 \log \left[\frac{R_{ex}}{Y - 1} \right]$$

$$NF = 10 \log R_{ex} - 10 \log (Y - 1)$$

$$NF = ENR - 10 \log (Y - 1) \quad (9A.11)$$

The excess noise ratio in db is defined by Equation 9A.1 and can be related to excess noise temperature. Figure 9A-4 is a plot of Y-Factor V.S. noise figure as given by Equation 9A.11. The dependence of measured Y-Factor on excess noise ratio is clearly illustrated. These curves also show the steep slope for small values of Y and indicate the poor measurement accuracy for Y_{db} less than one db. The actual error is given by Equation 10E.46a in Chapter X.

When a hot-cold noise source is used in the Y-Factor technique the concept of excess noise ratio is no longer meaningful if the cold source is not at standard temperature. When this is the case, Equation 9A.3 is used to determine effective input noise temperature. The "hot" temperature is limited to values which will not destroy the resistive termination and yet are high enough to give usable Y-Factors. Possible hot temperatures which can be produced with good accuracy are:

1. Steam point at STP, 373.16°K
2. Melting tin, 504.35°K
3. Melting lead, 600.46°K
4. Sulphur point, 717.76°K

Possible cold temperatures are:

1. Water triple-point, 273.16°K
2. Freezing mercury, 234.30°K
3. Dry ice (CO_2), $\sim 195^{\circ}\text{K}$
4. Boiling liquid oxygen, $\sim 90.2^{\circ}\text{K}$
5. Boiling liquid nitrogen, $\sim 77.3^{\circ}\text{K}$
6. Boiling liquid hydrogen, H_2 , $\sim 20.4^{\circ}\text{K}$
7. Liquid helium, $\sim 4.2^{\circ}\text{K}$

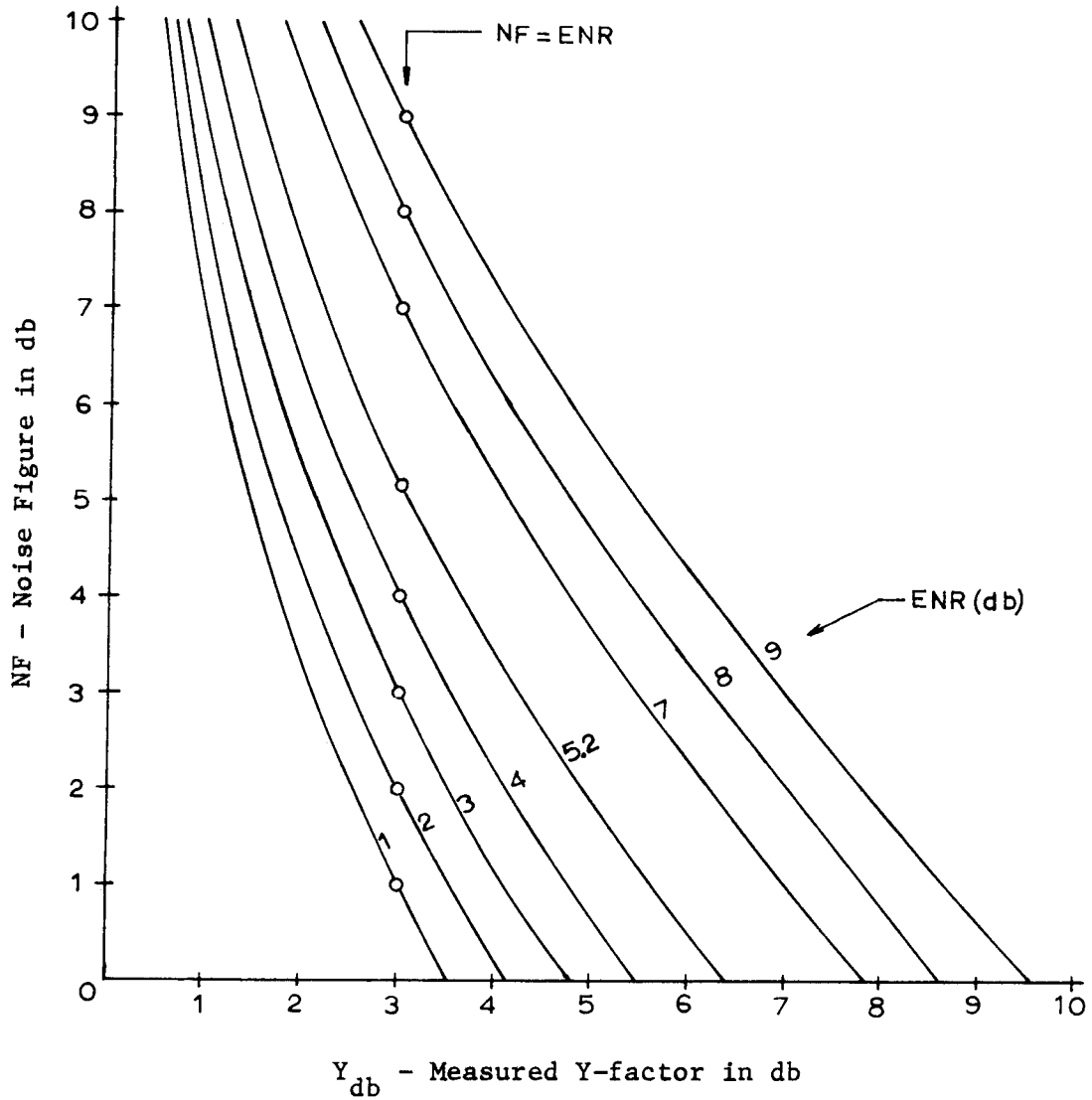


Figure 9A-4. Noise Figure as a Function of Y-Factor for Various Values of the Excess Noise Ratio of the Noise Source

The selection of termination temperatures for Y-Factor measurements depends upon the relative value of T_e to be measured. This can be seen by factoring (9A.3) into the form:

$$T_e = \frac{T_2}{(Y - 1)} \left(1 - Y \frac{T_1}{T_2} \right) \quad (9A.12)$$

Because T_e is always positive we can observe the following limits for (9A.12):

$$\begin{aligned} T_e &> 0 \\ T_2 &> T_1 \\ 1 &\leq Y \leq \frac{T_2}{T_1} \end{aligned} \quad (9A.13)$$

The upper limit for Y and hence the accuracy of the measurement is determined by the ratio of T_2/T_1 . For typical equivalent noise temperatures of 100–500 °K, the ratio T_2/T_1 needs to be greater than about 1.5 to get reasonable accuracy (actually T_2 also affects the accuracy as will be discussed in the next chapter). Based upon these criteria, reasonable choices for hot and cold temperatures are:

$$\begin{aligned} 1. \quad T_2 &= 373 \text{ } ^\circ\text{K} \\ T_1 &= 195 \text{ } ^\circ\text{K} \quad T_2/T_1 = 1.91 \\ 2. \quad T_2 &= 373 \text{ } ^\circ\text{K} \\ T_1 &= 77.3 \text{ } ^\circ\text{K} \quad T_2/T_1 = 4.82 \end{aligned}$$

These temperatures are selected because they are the ones most likely to be available in a lab. Effective noise temperature as a function

of Y-Factor for these two hot-cold sources is given in Figure 9A-5.

3. Noise diode method (3 db method)

A special case of the Y-Factor method that is commonly used to measure noise factor is the noise diode method. This method is probably the simplest and most readily available manual technique for measuring noise factor. The noise source is a diode noise generator terminated with a source resistance, R_s . The excess noise of the source determines the hot temperature T_2 and the cold temperature is the temperature of the source resistance which is at standard temperature. The ratio of noise power output when the diode is on to that when it is off is the Y-Factor and in terms of the excess noise temperature, the noise factor is, from Equation 9A.7

$$F = \frac{T_{ex}}{(Y - 1) T_o} \quad (9A.14)$$

where the excess noise temperature of the diode is (from Figure 4F.2)

$$T_{ex} = \frac{q I_s}{2 k G_s} \quad (9A.15)$$

where

- T_{ex} = excess noise temperature of the noise diode source, $^{\circ}\text{K}$
- Y = measured Y-Factor
- T_o = standard temperature, 290°K
- I_s = diode saturation current, amperes

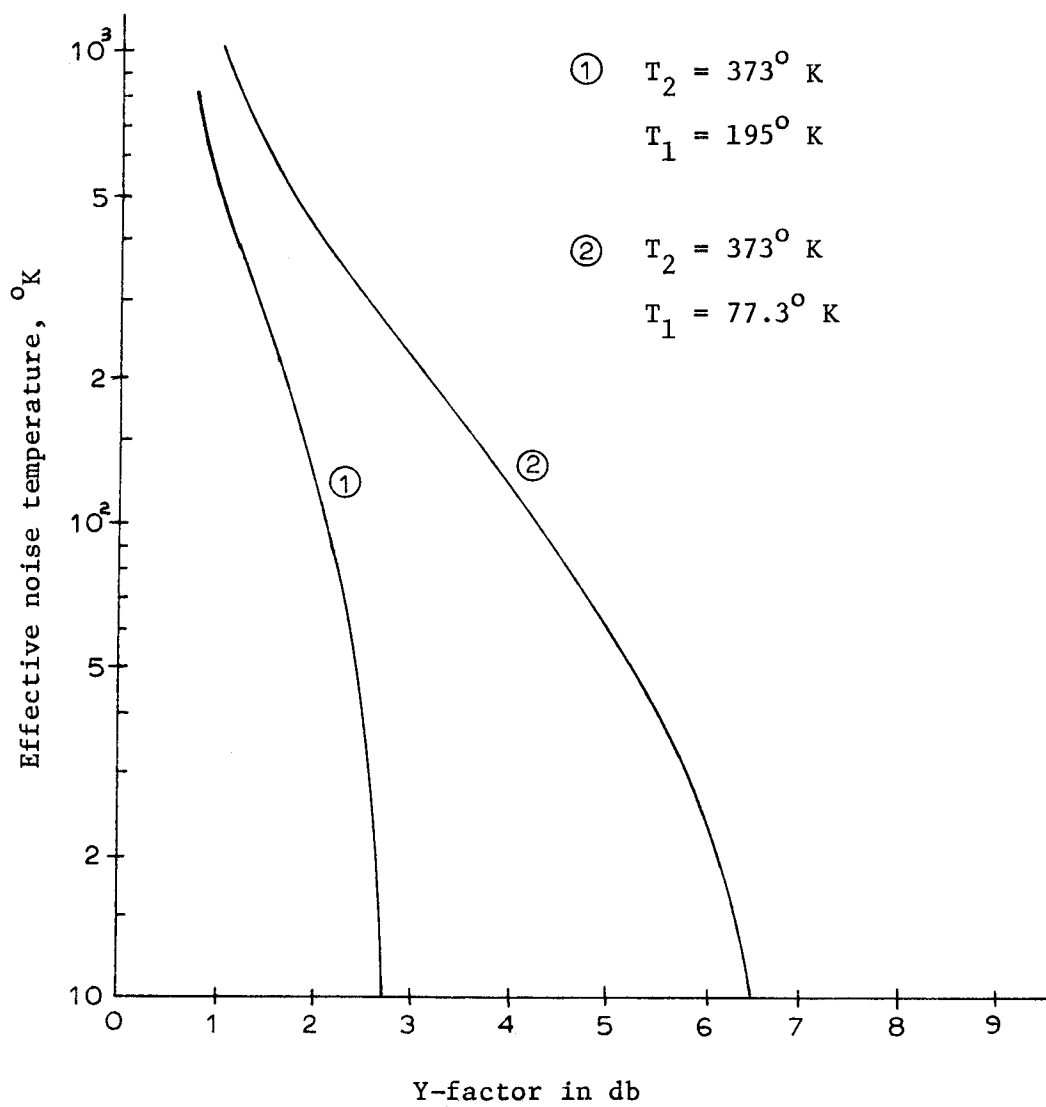


Figure 9A-5. Effective Noise Temperature vs Y-Factor for Two Hot-Cold Noise Sources

G_s = source conductance of the noise source, mhos

k = Boltzmann's constant

q = electronic charge.

The circuit of Figure 9A-6 illustrates two possible techniques for measuring noise factor using a noise diode.

The following measurement procedure is recommended for the circuit of Figure 9A-6a:

1. The noise diode is turned off ($I_s \equiv 0$) and a relative noise power output N_{01} is noted.
2. The noise diode is turned on and the diode current is increased until a reasonable increase in noise power output is obtained. The noise power output is now N_{02} .

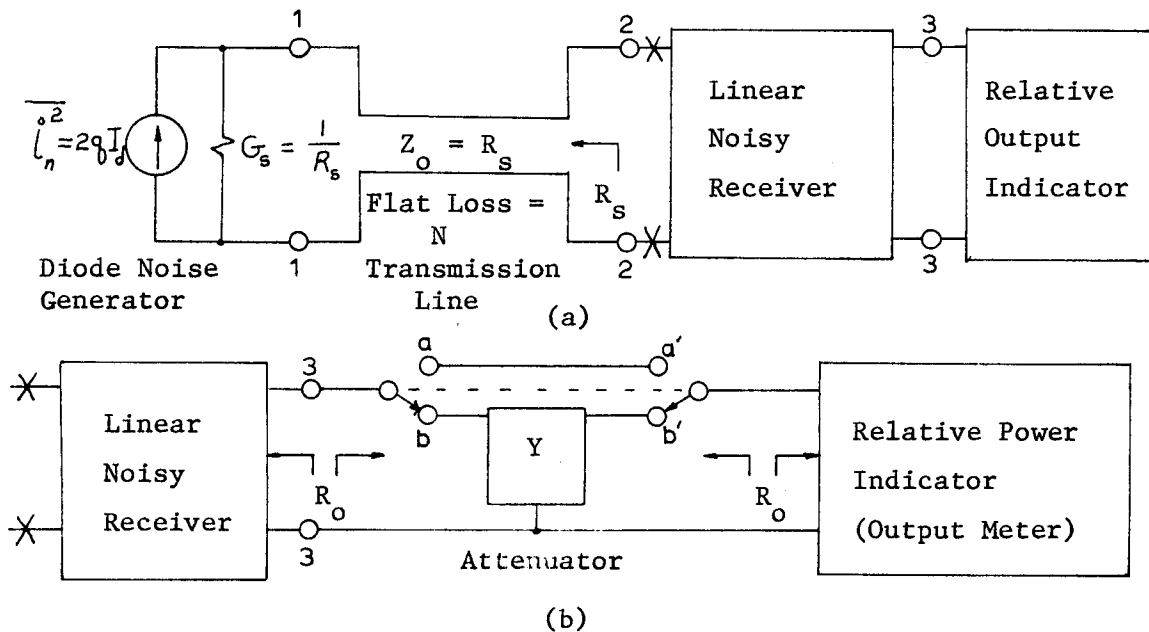


Figure 9A-6. Circuits for Measuring Noise Factor with a Diode Noise Generator

The measured noise factor for both the receiver and transmission line can be computed from the combination of Equations 9A.14 and 9A.15 as

$$F_m = \frac{q R_s}{2 k T_o} \frac{I_s}{(Y - 1)} \quad (9A.16)$$

where R_s is the source resistance and $Y = N_{02}/N_{01}$.

The quantities q , k , and T_o are physical constants. If these constants are substituted into (9A.16) the result is ($T_o = 290^\circ\text{K}$):

$$F_m = 20 R_s \frac{I_s}{(Y - 1)} \quad (9A.17)$$

When the receiver is designed to operate with a source resistance of 50 ohms and the output power level change is predetermined as 2 to 1 (a 3db change), Equation 9A.17 is simplified further by substituting $R_s = 50$ ohms and $Y = 2$. Doing this gives

$$F_m = I_s \text{ (ma.)} \quad [R_s = 50\Omega, Y = 2] \quad (9A.18a)$$

where the measured noise factor, for a Y-Factor of two, is numerically equal to the noise diode d.c. current in milliamperes. Equation 9A.18a is also seen in the alternate form:

$$F_m = 1000 I_s \quad (9A.18b)$$

There are many assumptions which are made to get the simple expressions of Equations 9A.18. These are:

1. The noise diode is ideal so that (9A.15) is valid.
2. The temperature of the source resistance is T_o .
3. The generator source resistance is 50 ohms.
4. The power output increases by a factor of two when the diode is turned on.
5. The diode filament temperature is variable so that the saturation current can be adjusted to give a Y-Factor of exactly two.

It is easy to see from Equation 9A.18b that the minimum diode current is 1 ma. corresponding to an ideal receiver with unity noise factor.

Because the measurement involves the ratio of two noise voltages, the characteristics of the power detector are not critical and practically any ac voltmeter can be used. The circuit of Figure 9A-6b is recommended when the highest possible accuracy is needed. This technique eliminates any nonlinear-gain characteristics the detector may have. This circuit is analogous to Figure 9A-3 where the attenuator is switched in and out instead of being variable. When the diode is off, the attenuator is switched out and a relative power output, N_{01} is noted. Then the attenuator is switched in and the diode current is increased until the same relative output, N_{01} is noted. The noise factor is then computed from Equation 9A.17. For the special case where $R_s = 50$ ohms and Y is 2 (a 3db pad) the noise factor is determined from Equations 9A.18.

The most important assumptions used in obtaining these simple measurement techniques are listed below:

1. The transmission line is assumed to be matched ($R_s \approx Z_o$) to the noise source. For most situations, a VSWR of 1.1 or less is adequate.
2. Assume a linear-gain receiver.
3. The transmission line output impedance at 2-2 presents the receiver with its specified source resistance.
4. The attenuator, Y, is inserted into a constant impedance signal path so that reflection coefficients will not cause an error in the attenuation factor.

The errors caused by source VSWR and attenuator reflection coefficients are discussed in Chapter X.

The precise value of Y greatly affects the measurement accuracy and it is important that Y is neither too large or small. It is recommended that values of Y between 2 and 4 be used. Smaller values cause larger measurement errors and larger values require too much diode current.

The effect of transmission line loss on measured noise temperature was discussed in Chapter IV-C. In terms of the true receiver noise temperature T_r , the measured noise temperature is

$$T_m = T_r N + T_c (N - 1) \quad (9A.19)$$

where T_r = receiver noise temperature
 T_c = physical temperature of the transmission line
 N = flat loss of the line, $= P_{in}/P_{out}$.

Solving 9A.19 for receiver noise temperature gives:

$$T_r = \frac{T_m}{N} - T_c \left(1 - \frac{1}{N}\right), \quad (T_r < T_m) \quad (9A.20)$$

The noise factor of the receiver is obtained by substituting the relation, $T = (F - 1) T_o$, into (9A.20) to give

$$F_r = 1 + \frac{1}{N} (F_m - 1) - \frac{T_c}{T_o} \left(1 - \frac{1}{N}\right) \quad (9A.21)$$

and if the temperature of the transmission line is nearly equal to standard temperature then $T_c \approx T_o$ and the noise factor is reduced to,

$$F_r = \frac{F_m}{N} \quad (9A.22)$$

or in terms of noise figure:

$$NF_r = 10 \log F_m - 10 \log N \quad (9A.23)$$

From this equation we see that when the transmission line is matched to the source ($R_s \approx Z_o$) and is at standard temperature ($T_c \approx T_o$) the line loss in db is simply subtracted from the measured noise figure to obtain the actual noise figure of the receiver.

4. Gas-discharge noise method

The use of a gas-discharge noise generator for measuring noise factor is similar to using a noise diode except that the excess noise temperature (or ENR) of the generator cannot be varied. The measurement setup needed is shown in Figure 9A-3. The noise factor is determined by Equation 9A.7 or the noise figure is determined from the excess

noise ratio and Y-Factor using (9A.11). Figure 9A-7 is a plot of noise figure as a function of Y-Factor for an excess noise ratio of $15.6 \pm .6$ db. The dotted lines show the error limits resulting from the uncertainty in excess noise ratio. The gas discharge noise source is used at microwave frequencies where noise diodes cannot be used because of transit time effects. A problem unique to gas discharge noise sources is that the source impedance changes when the gas is fired (Pastori, 1968b). The error introduced by this effect is discussed in Chapter X.

B. Using an Unmodulated Sinewave Generator

1. Power meter

The use of an unmodulated sinewave generator for measuring noise factor is at best a "tricky business". The threshold effect in detectors is most pronounced when the signal is an unmodulated sinewave and the predetection signal-to-noise ratio is low. This creates a large potential for error because of the detector nonlinear power gain. The test setup of Figure 9A-6a can be used if the noise diode generator is replaced with an unmodulated sinewave generator and if the noise power detector is either a power meter or true-reading RMS voltmeter. For these conditions, the noise factor is computed from Equation 8A.1 where the predetection signal-to-noise ratio, S_p is written in terms of the predetection signal-plus-noise-to-noise ratio, $(S_o + N_o)/N_o$,

$$F_m = \frac{E_g^2}{\left(\frac{S_o + N_o}{N_o} - 1 \right) [4 k T_o R_s B_h]} \quad (9B.1)$$

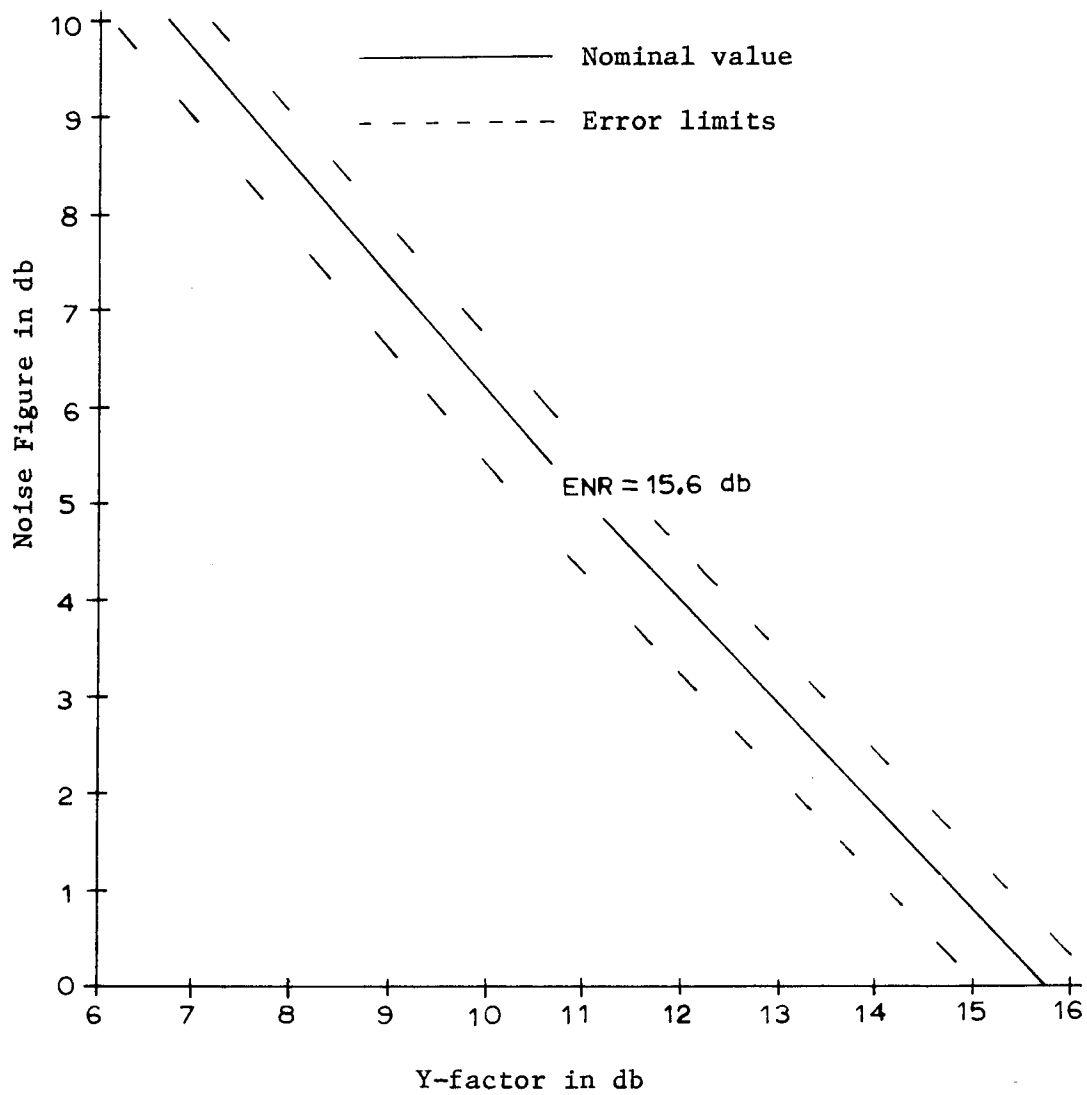


Figure 9A-7. Noise Figure vs Y-Factor for a Typical Gas Discharge Noise Generator

and

B_h = effective noise bandwidth

S_o = measured sinewave signal power

N_o = measured sinewave noise power

$$\frac{S_o + N_o}{N_o} = \frac{\text{Sinewave power plus noise power}}{\text{Noise power}}$$

For a given receiving system, R_s , B_h and F_m are parameters of the system while E_g and the output signal-to-noise ratio are related by Equation 9B.1. The measured noise factor, F_m , of the receiver is treated like a dependent variable in measurement theory equations. Because F_m is a system parameter, the signal E_g and the signal-to-noise ratio cannot be considered as independent variables but rather that E_g determines the SNR. When applying equation 9B.1 it is better to think of E_g as the input voltage that will produce a given output SNR subject to the constraints imposed by F_m .

The predetection signal-plus-noise-to-noise ratio is measured by either turning off the generator or, better yet, tuning it off frequency. If the output ratio is doubled and the source resistance is 50 ohms, Equation 4B.1 can be reduced by making the following substitutions

$$4 k T_o = 1.6 \times 10^{-20} \text{ watt-sec}$$

$$R_s = 50 \text{ ohms}$$

$$\frac{S_o + N_o}{N_o} = 2 \text{ (3 db)}$$

which gives

$$F_m = 1.25 \times 10^6 \frac{E_g^2}{B_h} \quad (9B.2a)$$

where

B_h = predetection equivalent noise bandwidth, Hz.

E_g = RMS sinewave voltage of the generator in hard microvolts.

Typical values of E_g range from .05 to 5 RMS microvolts.

For an output signal-plus-noise-to-noise ratio of 10 db,

$(S_o + N_o)/N_o = 10$, the noise factor is:

$$F_m = 1.39 \times 10^5 \frac{E_g^2}{B_h} \quad (9B.2b)$$

When a power meter cannot be used for the measurement, it is possible to use a square-law detector or a linear-diode detector.

2. Square-law detector

The dc output level of a square-law detector changes when an unmodulated sinewave is applied to the input. The measured noise factor can be determined from these dc ratios by applying Equation 8D.10:

$$F_m = \frac{E_g^2}{(M_{dc} - 1)[4 k T_o R_s B_h]}$$

A typical test setup for measuring noise factor using an unmodulated sinewave generator and a square-law detector is shown in Figure 9B-1.

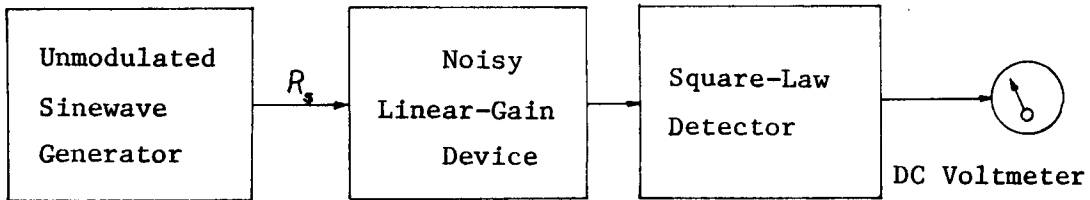


Figure 9B-1. Test Setup for Measuring Noise Factor with a Square-Law Detector

3. Linear-diode detector

The dc output level of a linear diode detector will change when an unmodulated sinewave is applied to the input. The measured noise factor for dc level changes greater than or equal to two ($M_{dc} \geq 2$) is given by Equation 8D.14:

$$F_m = \frac{E_g^2}{\frac{1}{2} \left(\frac{\pi}{2} M_{dc}^2 - 1 \right) [4 k T_o R_s B_h]}$$

The test setup of Figure 8B-1 can also be used for the linear-diode detector.

The technique of putting a calibrated attenuator in the signal path cannot be used for the square-law or linear-diode detector because of nonlinear effects.

C. Using a Modulated Sinewave Generator

The use of a modulated generator implies that the output measurements will be made after some low-frequency amplifier which will amplify

the recovered audio signal. Because of this, the detector and audio amplifiers become an important part of the measurement problem. It will be assumed that the receiver is a linear-gain receiver and that the audio stages are linear for all levels of recovered audio. Sometimes the audio stages are not linear, as for example when crossover distortion occurs, and this will introduce large errors in the measurement. The detector threshold effect must be accounted for or else the measurement must be made at a sufficiently high SNR to insure a linear-gain characteristic. As a general rule, the audio gain should be turned up as high as possible (1/2 to 3/4 of full) to insure that the noise generated in the audio stages will not affect the measurement.

1. AM sensitivity

In the AM sensitivity test, the test signal generator is amplitude modulated by a single audio tone and the output signal-plus-noise-to-noise ratio is measured as a function of input signal level. The actual measured quantity is

$$\frac{S_o + N_o}{N_o} = \frac{\text{Recovered audio power plus noise power}}{\text{Noise power}}$$

because the recovered audio cannot be measured independently from the noise. The level of noise will be determined by the receiver noise factor and the temperature of the generator resistance.

We now consider the test procedure and equipment necessary to make accurate and meaningful signal-plus-noise-to-noise ratio measurements. A typical AM sensitivity test setup is shown in Figure 9C-1.

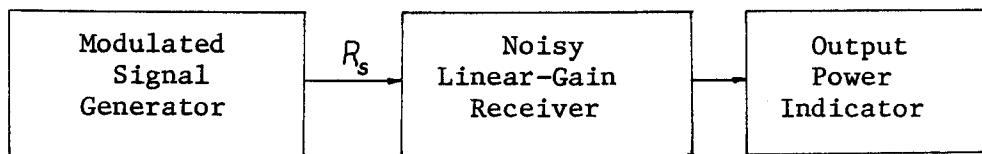


Figure 9C-1. Test Setup for AM Sensitivity

Before discussing the measurement, the minimum performance requirements on the test equipment will now be described.

Signal generator

The AM signal generator must be capable of AM modulation to at least 30% and preferably to 70% while maintaining low distortion and spurious output. In addition, it must have a calibrated RF output that is adjustable in the sub-microvolt region and the output must have a known impedance and VSWR. Finally, the frequency stability must be adequate to allow several measurements to be made without the inconvenience of stopping to reset frequency. Table 9C-1 summarizes some typical values of the important AM generator specifications.

The output level must be accurate because it determines the AM sensitivity measured. Regardless of the optimistic statements made by manufacturers of signal generators, it is very difficult to get accurate output levels much below one microvolt. The cause of this is seldom the attenuator calibration but most often is RF leakage. The high level RF voltages inside the generator leak out of the case and around coax connectors to upset the receiver input. This problem is solved either by very careful generator maintenance and calibration or by receiver and

Table 9C-1. Important AM signal generator specifications

Specification	Typical Values
Output Level:	0.1 microvolts to 0.2 volts \pm 1db
Output Impedance:	50 ohms, VSWR 1.1 - 1.2
Modulation Percentage:	0-30%, 0-50%, 0-95%
Modulation Frequency:	400 and 1000 Hz \pm 5%
Modulation Distortion:	Less than 10%, typical 2% at 30% AM
Spurious AM:	At least 30db down from the carrier and typically 60db down
Drift:	5-50 parts in 10^5 per 10 min.

generator isolation with a shield room. The generator impedance must be compatible with the receiver because the receiver is designed to give the best sensitivity with a specific antenna impedance. Attempts to measure the receiver sensitivity at impedances other than that specified will often result in measured signal-plus-noise-to-noise ratios that are very pessimistic. For more information about the effect of antenna impedance on receiver sensitivity, refer to the sections on RF translator noise and noise theory of two-port networks.

The modulation characteristics of an AM signal generator are very important in determining the reliability and accuracy of AM sensitivity measurements. For example, the percentage of modulation is actually a measure of the AM sideband power in relationship to carrier power. Changes in the modulation percentage directly affect the sideband power which determines the recovered audio level. Because most published data

and methods assume sinewave modulation, it is important to realize that the real criteria is percentage of sideband power and that distortion can cause this power percentage to differ from that obtained assuming an ideal sinewave. When using other types of modulation, it is important to consider a correction factor for correlating the data with that for sinewave modulation. Large ratio measurements require the RF signal to be relatively free from spurious AM output. Hum and incidental AM may degrade the pure RF carrier from the generator and limit the $(S_o + N_o)/N_o$ ratio at the receiver input. In any case, the signal generator should have spurious AM that is 10db better than the $(S_o + N_o)/N_o$ ratio to be measured.

The last specification to be discussed, and often the most frustrating problem, is that of frequency drift. The RF carrier must be stable enough so that the signal and AM sidebands will remain inside the receiver passband long enough to make careful measurements. This means that, in a typical AM receiver with 6 KHz IF bandwidth and a RF carrier with 1 KHz audio sidebands, the carrier frequency must not drift more than ± 2 KHz from center frequency or serious envelope distortion will occur. A good signal generator will remain within 200 Hz of the received frequency for at least one minute which is enough time to get two or three ratio measurements.

Detector

Since all AM detectors will not exhibit the same threshold characteristics it is important that threshold effects be minimized. To insure this, it is necessary that the signal-to-noise ratio for the

measurement be considerably larger than unity. It is recommended that a ratio, at the output, of at least 6 db be used. For more information on AM detector requirements refer to Chapter VIII-D.

Measurement technique

The setup of Figure 9C-1 can be used to make $(S_o + N_o)/N_o$ ratio measurements. Before taking data, the user must check receiver operation to make sure it is operating linearly in power and with sufficient dynamic range to measure the desired ratio. This means that receiver AGC must be disabled and total gain must be low enough to prevent saturation on signal peaks. The procedure is as follows:

- a. Set the signal generator RF to a level well above the threshold response of the receiver, usually a 20db excess.
- b. Modulate the carrier at the desired percentage and frequency. Record the audio output power level.
- c. Turn off the modulation and note the decrease in audio output power.
- d. This measured ratio of modulated carrier audio power to unmodulated is the $(S_o + N_o)/N_o$ ratio.
- e. Adjust the RF carrier level until the desired ratio is achieved. The value of RF input voltage that provides this ratio is called the sensitivity of the receiver in microvolts for a given signal-plus-noise-to-noise ratio at the audio output.

2. Tangential noise sensitivity

The tangential noise sensitivity of a pulse receiver or radar receiver is measured using a pulsed sinewave generator and an oscilloscope for an output transducer. This test is a complete system test and takes into account the threshold effects of the detector. Tangential noise sensitivity can only be related to noise factor by the subjective evaluation of a human observer (Chapter VIII-C). A typical test setup for measuring tangential noise sensitivity is shown in Figure 9C-2.

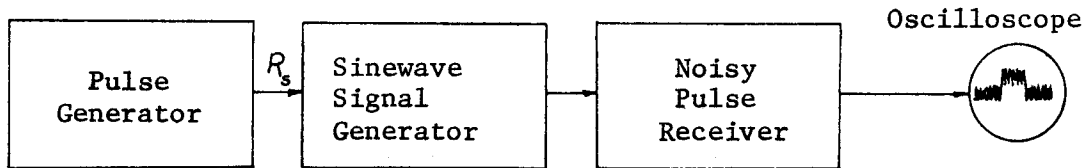


Figure 9C-2. Test Setup for Tangential Noise Sensitivity

The appearance of the noise signal depends upon the sweep rate of the scope relative to the effective noise bandwidth of the receiving system. The ratio of sweep rate to noise bandwidth is important but not the absolute values (Baxendall, 1968a). A reasonably "grassy" appearance can be obtained with a sweep rate that is $1/1000^{\text{th}}$ of the noise bandwidth.

The measurement procedure is as follows:

1. Tune the signal generator off frequency and set the oscilloscope for about $1/8^{\text{th}}$ to $1/3^{\text{rd}}$ vertical deflection on the noise signal. The sweep speed of the scope should be slow enough so that the randomly fluctuating noise voltage looks like grass.
2. Tune the generator on frequency and adjust the peak amplitude so that the bottom of the grass on the pulse is tangent to the top of the grass on the baseline. Figure 9C-3 illustrates the appearance of the noisy pulse on the scope display.
3. The carrier level measured in dbm available power or hard microvolts to achieve a tangential signal is the

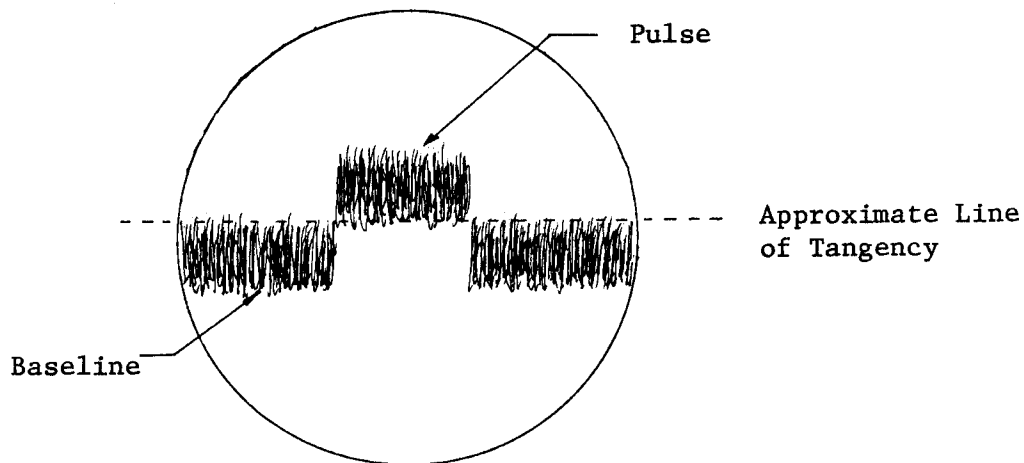


Figure 9C-3. Oscilloscope Display of a Tangential Signal

tangential sensitivity of the receiver. It is unambiguous to report tangential sensitivity in available power but if the sensitivity is reported in microvolts it must also be stated as hard or soft microvolts.

3. FM sensitivity

There are three methods of measuring and specifying FM sensitivity that are in common use. These are:

1. Noise quieting method
2. IRE quieting method
3. 12 db SINAD method.

The last two methods are closely related to the first method which is true noise quieting.

When an unmodulated sinewave generator* is tuned into the passband of an FM receiver, the audio output is observed to decrease (Chapter VIII-B). This audio noise power decrease is used to specify a figure of merit for FM sensitivity called the noise quieting sensitivity.

A typical test setup for measuring noise quieting sensitivity is shown in Figure 9C-4. The loudspeaker is helpful for audio monitoring of the quieting signal to make sure the receiver output does not contain any stray signals.

*Noise quieting was not included in the section on sensitivity measurements using unmodulated sinewave generators because it is desirable to include all FM sensitivity tests in the same section.

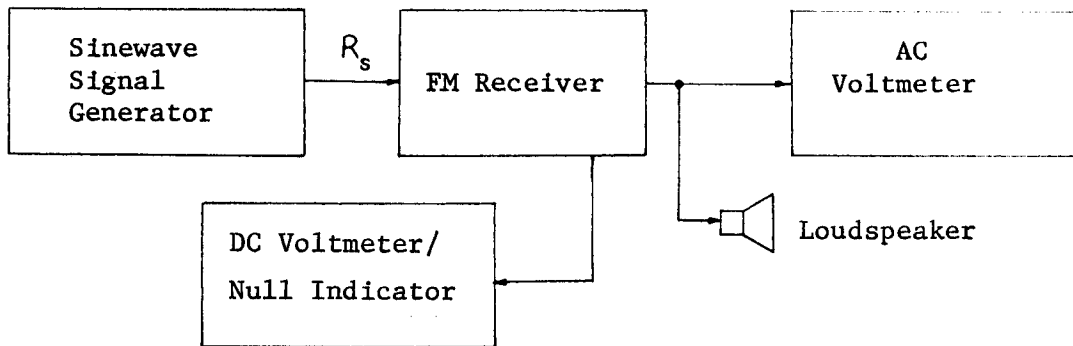


Figure 9C-4. Test Setup for Measuring Noise-Quiting Sensitivity

The test procedure is as follows:

1. Tune the signal generator well off frequency and set the audio output level to near maximum. Note the reading on the AC voltmeter.
2. Tune the signal generator to center frequency by observing a null in the discriminator output.
3. Record data of carrier level VS reduction of audio noise level.
4. The input signal required to give a specified amount of audio noise reduction at the output is referred to as the noise quieting sensitivity.

A widely used quieting ratio for specification purposes is 20 db. Typical 20 db noise quieting sensitivities are 0.3 μV for narrowband FM and 2.0 μV for wideband FM. Since the audio noise output is proportional to predetection noise bandwidth, the measured quieting sensitivity is meaningless unless the FM bandwidth is also specified.

Typical FM bandwidths are 15 KHz for narrowband FM and 210 KHz for wideband FM.

Notice that an AC voltmeter is specified for the output indicator. Any voltmeter that is linear over a 20 db range is satisfactory because a noise ratio is measured, not absolute values. If better accuracy is needed, the test setup of Figure 9A-6b is recommended where Y is the quieting ratio.

The IRE (Institute of Radio Engineers) quieting method is similar to noise quieting except that the signal generator is FM modulated and the ratio of recovered audio to quieting level is measured. This test measures the ability of the FM receiver to supply a given output SNR but it is not as simple to make as noise quieting and requires an FM generator. A typical test setup for measuring IRE quieting is shown in Figure 9C-5.

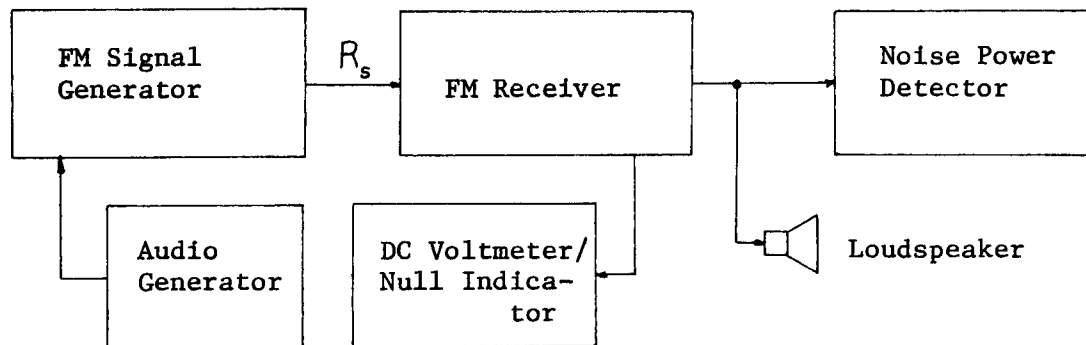


Figure 9C-5. Test Setup for Measuring IRE Quieting Sensitivity

The quality of the FM generator is important to the accuracy of the measurement. Considerations of generator performance are similar to those listed for the AM signal generator except modulation percentage becomes a deviation ratio and incidental AM becomes incidental FM.

The test procedure is as follows:

1. The deviation ratio of the generator is set for 30% of the deviation ratio rating for the system.
2. The generator is tuned to center frequency by nulling the discriminator output.
3. The modulation is switched on and off and the ratio of recovered audio-plus-noise to noise is measured for various levels of input signal.
4. The input level in hard microvolts that gives a specified output ratio (usually 30 db) is called the IRE quieting sensitivity.

Figure 8B-2 shows an IRE quieting sensitivity of 0.62 μ V for a 30 db output ratio.

The 12 db SINAD (signal-plus-noise and distortion) method is used in specifying narrowband FM voice communication systems. This is really the best method for specifying the least usable sensitivity (Feldman, 1966, p. 25) of a two-way FM radio system because it takes into account both background noise limitations and distortion. The 12 db SINAD test is the most difficult to make because it requires both a high quality FM generator and an audio distortion meter for the measurement. A typical test setup for measuring 12 db SINAD sensitivity is shown in Figure 9C-6.

The distortion analyzer is needed because it has a very selective audio notch filter that is used to "notch out" the audio tone when measuring only noise and distortion.

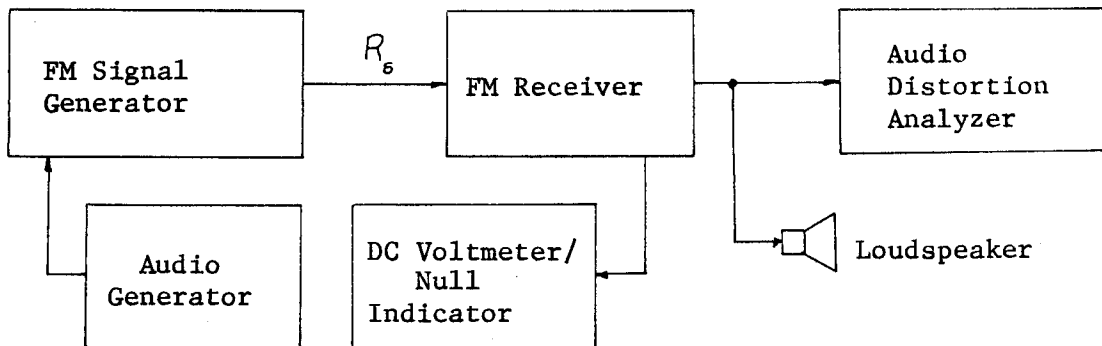


Figure 9C-6. Test Setup for Measuring 12 db SINAD Sensitivity

A recommended test procedure is as follows:

1. The generator modulation is adjusted for a frequency of 1 KHz and a frequency deviation of 2/3 the maximum rated deviation.
2. A large RF signal level is applied (usually 1000 μ V) and the generator is tuned to center frequency. The audio level is adjusted for near maximum output.
3. The 1 KHz notch filter of the distortion analyzer is alternately switched in and out while the RF signal level is decreased. The RF signal level which gives a 12 db ratio at the output is the 12 db SINAD sensitivity of the receiver.

The measured output ratio is:

$$12 \text{ db SINAD Ratio} = \frac{\text{Recovered Audio Plus Noise and Distortion}}{\text{Noise and Distortion}}$$

The audio frequency must be carefully tuned to be exactly in the notch of the audio filter or a measurement error will result. The depth of the audio notch should be at least 20 db when measuring a 12 db ratio. A typical 12 db SINAD sensitivity for a 15 KHz FM bandwidth system is 0.25 μ V.

Figure 8B-2 illustrates the typical quieting ratios and sensitivities which have been presented in this section. From the data on a typical FM receiver one can see the relative values of input level for the different sensitivities. It is usually true that the 12db SINAD sensitivity yields the smallest microvolt level and that true noise-quieting yields the largest.

D. Antenna Noise Measurement

A knowledge of the effective noise temperature of the receiving antenna is helpful in determining the total receiving system performance. There are two simple techniques that can be used to measure the noise temperature of the antenna and both are modifications of the Y-factor technique. Figure 9D-1 illustrates the first technique. This technique employs a receiver with known effective noise temperature and a reference termination of known resistance and temperature.

The receiver input is switched between the antenna and the known reference and the change in output power is measured:

$$M = \frac{N_{02}}{N_{01}}, \text{ the change in output power levels.}$$

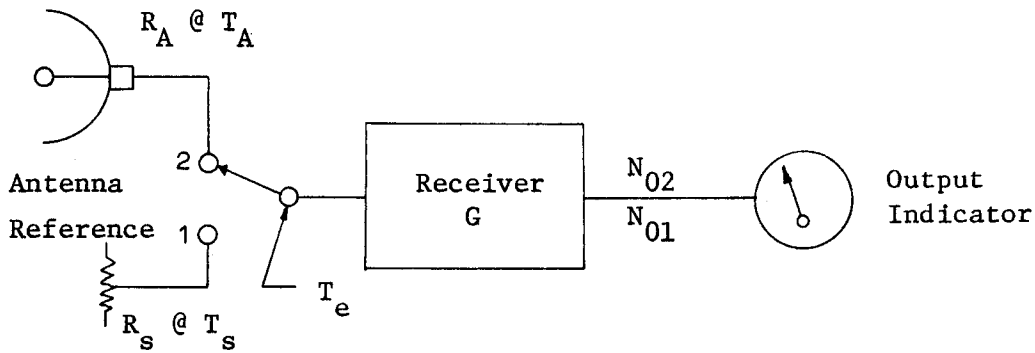


Figure 9D-1. Test Setup* for Measuring Antenna Noise Temperature

*In radio astronomy, this configuration is called a Dicke Radiometer and is used for measuring cosmic radiation noise in low-noise receivers.

The change, M , can be written in terms of the mean-square noise voltages at the input:

$$M = \frac{4 k T_A R_A \Delta f + 4 k T_e R_s \Delta f}{4 k T_s R_s \Delta f + 4 k T_e R_s \Delta f}$$

$$= \frac{T_A R_A + T_e R_s}{T_s R_s + T_e R_s} \quad (9D.1)$$

Solving for the antenna noise temperature gives:

$$T_A = \frac{R_s}{R_A} [M T_s + T_e (m - 1)] \quad (9D.2a)$$

Since the receiver effective noise temperature, T_e , depends upon the source resistance used in the measurement, errors can be minimized if R_A and R_s are equal. This condition reduces (9D.2a) to:

$$T_A = M T_s + T_e (M - 1) \quad (9D.2b)$$

The use of a calibrated noise generator for the reference can be very useful in making precise antenna noise temperature measurements. For this technique, the reference temperature, T_s , is adjusted so that no output level change ($M = 1$) occurs when switching from antenna to reference. When $M = 1$, the antenna temperature and the reference temperature are equal.

When a noise generator is unavailable, the antenna noise can still be measured by using a reference termination which is near standard temperature ($T_s \approx T_o$). For this condition, the antenna temperature (9D.2b) is given by the equation:

$$T_A = M T_o + T_e (M - 1) \quad (9D.3)$$

A plot of Equation 9D-3 for three different values of receiver effective noise temperature is shown in Figure 9D-2. The curves show that, for low values of antenna temperature, the receiver noise temperature must also be low or the measurement accuracy will be very poor. As the slope of the curve increases the measurement error also increases.

A third technique is sometimes used for the measurement of antenna noise temperature whereby the receiver is never disconnected from the antenna during the measurement. When it is important that the receiver be enabled at all times, this technique is very useful. Also the system can perform the useful, and sometimes vital, self-test function for the receiver. If the receiver were to fail or the sensitivity were to be seriously degraded, the measurement would indicate an abnormally high or

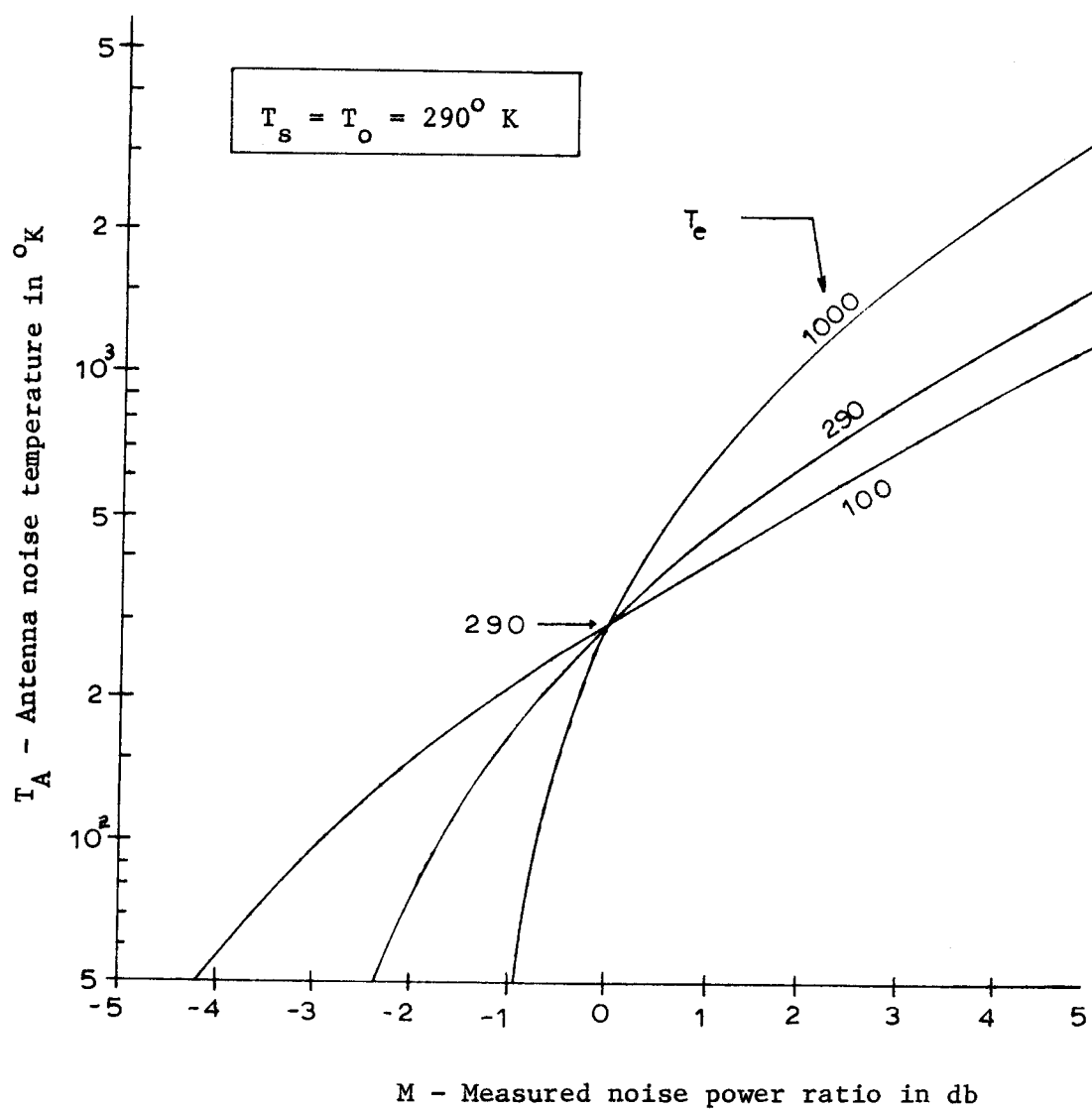


Figure 9D-2. Antenna Noise Temperature vs Output Noise Power Ratio

infinite noise temperature. The measurement system shown in Figure 9D-3 shows a 20 db coupler between the antenna and receiver. This coupler is used to couple in the noise signal from the noise source and yet keep the antenna connected to the receiver at all times. A large coupling ratio such as 20 db is needed so that noise generator loading of the antenna circuit can be neglected.

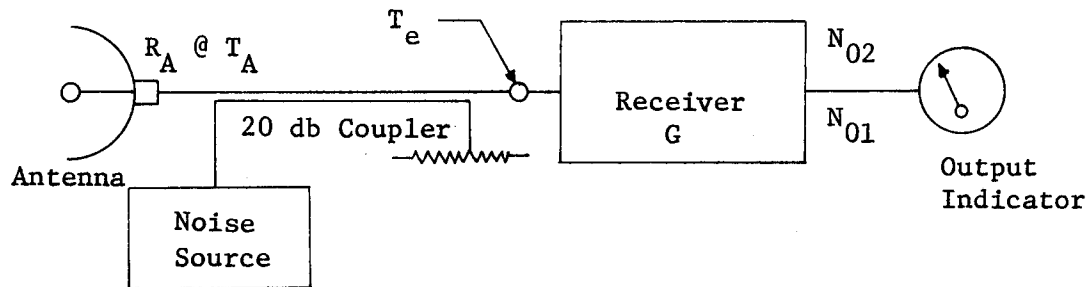


Figure 9D-3. Antenna Noise Measurement Setup Using High-Loss Coupler

The ratio of available noise powers when the noise source is turned on and off is simply the ratio of the noise powers at the input

$$M = \frac{N_{02}}{N_{01}} = \frac{T_A + T_e + (T_o + T_{ex})\alpha}{T_A + T_e} \quad (9D.4)$$

where T_{ex} = excess noise temperature of the noise source

α = the numerical attenuation factor for the coupler

($\alpha = 1/100$ for a 20 db coupler).

Solving Equation 9D.4 for the antenna noise temperature gives:

$$T_A = \frac{(T_o + T_{ex})}{(M - 1)} \alpha - T_e \quad (M \geq 1) \quad (9D.5)$$

This test setup can also be used to measure noise figure if the antenna is replaced with a source resistance at standard temperature.

Letting $T_A = T_o$ and solving Equation 9D.5 for noise factor gives:

$$\begin{aligned} T_o + T_e &= \frac{(T_o + T_{ex})}{(M - 1)} \alpha \\ F = 1 + \frac{T_e}{T_o} &= \frac{(1 + \frac{T_{ex}}{T_o})}{(M - 1)} \alpha \end{aligned} \quad (9D.6)$$

The noise figure in db is

$$\begin{aligned} NF &= 10 \log \left(1 + \frac{T_e}{T_o} \right) \\ &= (ENP - \alpha_{db}) - 10 \log (M - 1) \end{aligned} \quad (9D.7)$$

where

α_{db} = coupler attenuation in db

$ENP = 10 \log (1 + T_{ex}/T_o)$, the excess noise power of the noise source i.e. the noise power above $kT\Delta f$ in db

M = output power ratio, N_{02}/N_{01} .

This equation for noise figure differs only slightly from that of Equation 9A.11 and excess noise ratio (ENR) and excess noise power (ENP) are closely related. Excess noise power is always greater than zero db.

The noise source used for this technique must have an excess noise power greater than the coupler attenuation. A typical excess noise power for commercially available units is 25 db ($T_h = 91,416^\circ\text{K}$) a value that can only be obtained with a solid-state noise source.

Better insight into the results of making an antenna noise measurement can be obtained by examining a different form of Equation 9D.3. The desired equation is obtained by solving (9D.3) for M and introducing noise factor. First, solving for M gives:

$$M = \frac{T_e + T_A}{T_e + T_o} \quad (9D.8)$$

Factor out the equivalent noise temperature in the numerator and the result is:

$$M = \left(\frac{T_A}{T_e} + 1\right) \frac{T_e}{T_e + T_o} \quad (9D.9)$$

Substituting the relationship between noise temperature and noise factor, $T_e = (F_r - 1) T_o$, gives the final result:

$$M = \left(\frac{T_A}{T_e} + 1\right) \left(1 - \frac{1}{F_r}\right) \quad (9D.10)$$

This form for the equation more clearly illustrates the dependence of the measured power ratio, M upon receiver noise factor and the ratio of antenna noise temperature to receiver noise temperature.

A graph of Equation 9D.10 with noise factor expressed as noise figure is shown in Figure 9D-4. The figure shows how a wide range of antenna noise temperature affects the measured power ratio. Generally,

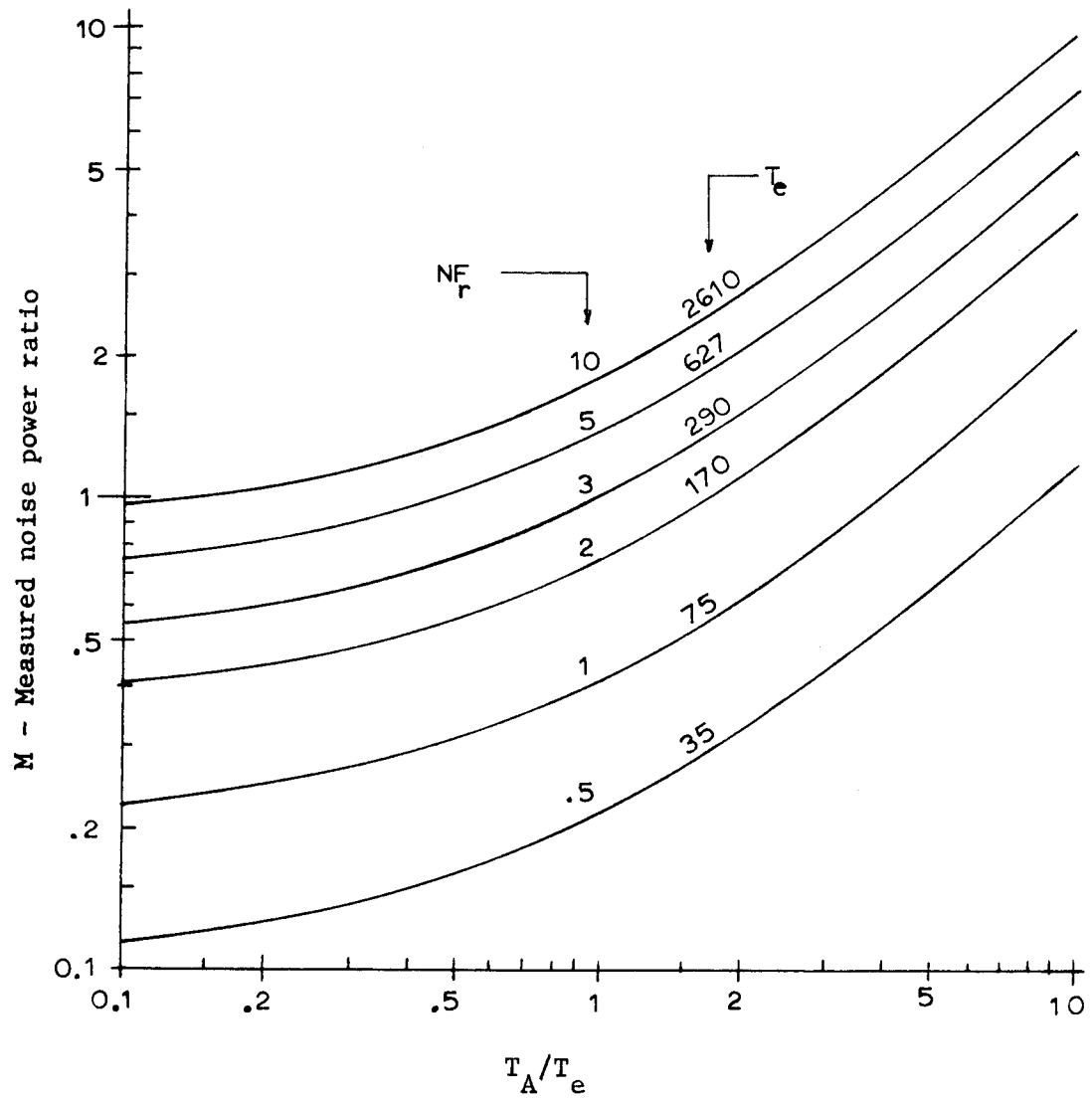


Figure 9D-4. Effect of Antenna Noise Temperature on Measured Output Power Ratio

the smaller the value of M , the better the system noise temperature. Since the system noise temperature is the sum of the antenna noise temperature and the effective noise temperature of the receiver, Equation 9D.8 gives the system noise temperature as:

$$T_{\text{sys}} = M (T_e + T_o) \quad (9D.11)$$

and it is readily apparent that smaller values of M indicate lower values of system noise temperature.

A criterion of good noise performance for the antenna is difficult to obtain and depends a great deal on the needs of the user. If the criterion is adopted that the antenna noise increase the system noise temperature by no more than ten percent, then we have the same requirement that was specified for noise merit (Appendix, Part L).

If this criterion is adopted then

$$T_A \leq \frac{1}{10} T_e$$

and Equation 9D.10 can be used to set the upper limit on M which is determined by receiver noise factor:

$$M \leq 1.1 \left(1 - \frac{1}{F_r}\right) \quad (9D.12)$$

The limits on receiver noise factor and M are (from Equation 9D.12):

$$\begin{aligned} 1 &\leq F_r \leq \infty \\ 0 &\leq M \leq 1.1 \end{aligned} \quad (9D.13)$$

This indicates that the wide range of noise factor is compressed into the measured power ratio range of 0 to 1.1. The accurate measurement of M will determine if the antenna noise is seriously degrading system performance. Other criteria such as $T_A \leq \frac{1}{2} T_e$ and $T_A \leq T_e$ can be adopted if the requirement for low-noise is not severe. A graph of M as a function of receiver noise factor for these three criteria is shown in Figure 9D-5. The measured power ratio must be below the line or the criterion is not met. For convenience, both measured power ratio and receiver noise figure are expressed in db.

Measurements of ratios very nearly 0 db ($M \approx 1$) can be confusing because when the output power does not change it can be interpreted as either a large receiver noise figure or an antenna temperature equal to T_o . In other words: if $M \approx 1$ then,

1. $T_A \approx T_o$, or
2. $T_e \gg T_A$ and $T_e \gg T_o$.

The problem of receiver noise figures so high that they produce noise power ratios of nearly 0 db begins when the noise figure exceeds 10 db.

As a rule, the optimum receiving system design is one in which the antenna noise temperature and receiver noise temperature are nearly equal. This usually results in the simplest design and lowest cost. When the antenna noise temperature is larger than the receiver noise temperature it is better to try to reduce antenna noise than to expend effort on reducing receiver noise. On the other hand, if receiver noise temperature is larger than antenna noise temperature then the effort should be expended to reduce receiver noise. Some discussion of the trade-offs to be made is given in Chapter V.

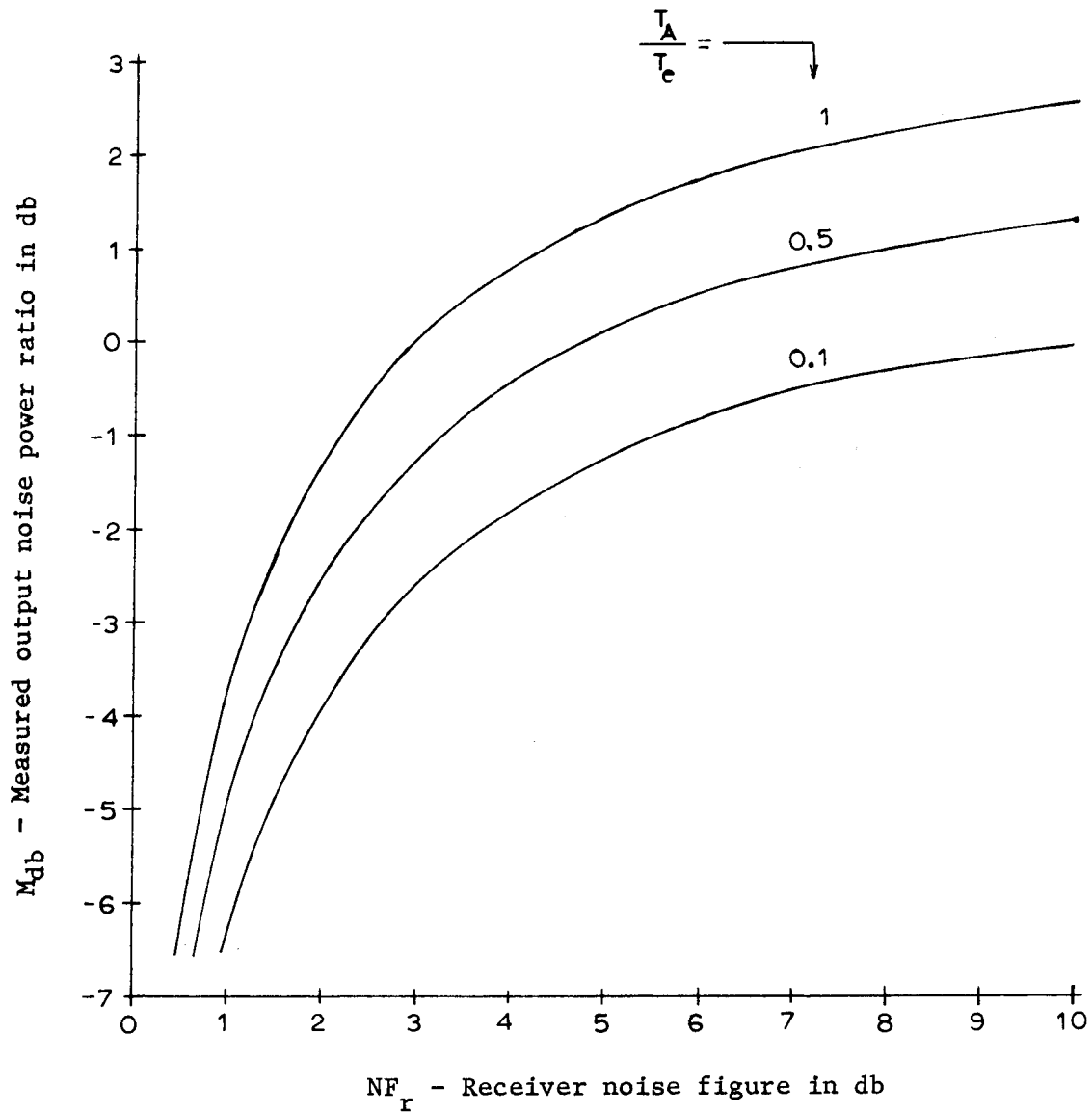


Figure 9D-5. Measured Output Power Ratio as a Function of Receiver Noise Figure for Three Values of Antenna Noise Temperature

X. UNCERTAINTIES IN SENSITIVITY MEASUREMENTS

The sources of error in measuring the sensitivity of a receiving system are legion. It is difficult to get good agreement among various methods and even among various test setups. Typical accuracies for commercial noise figure measuring equipment are 5-10% for noise temperature and ± 0.25 to ± 1 db for noise figure. Accuracies better than ± 0.25 db for noise figure are not possible under ordinary laboratory conditions. For better accuracy one must conduct the tests with extreme care and use only equipment which is laboratory-standards quality. The information given in this chapter is intended to aid in the accurate measurement of receiving system sensitivity. Interrelationships of system parameters make error analysis difficult and preclude all possibility of considering every situation.

Some amusing comments on the frustrations of making accurate noise figure measurements have been given by Cohn (1959), in a technical editorial titled "The Noise Figure Muddle", and by Greene (1961) in a correspondence titled " 'Noisemanship'--the Art of Measuring Noise Figures Nearly Independent of Device Performance". Cohn relates his discovery of image noise errors in noise figure measurements while Greene compiles a partial list of experimental procedures which are designed to produce any noise figure the experimenter desires without regard for the actual device. Although given in a somewhat humorous vein, these papers do illustrate many of the sources of error in the experimental procedures.

The results of measuring noise figure using three different methods is reported by Matthews (1967). His results show variations of 0.2 to 1.2 db at a nominal noise figure of 7.5 db. These variations are typical of what can be expected after taking into account the various system inaccuracies.

The most important sources of error in a sensitivity measuring system are those due to the detector and signal source. These errors are usually caused by detector nonlinearity and reading error and by source SWR and output calibration. Other errors which occur in the system can usually be compensated but errors in sources and detectors are usually of such a fundamental nature that they cannot be easily corrected. The organization of topics on measurement error is difficult because no scheme seems logical. The best approach is to present the essential errors which occur in a measuring system (Figure 8-1) and then consider the errors which occur with various noise sources and measurement techniques.

A. Sensitivity Measuring System

The following is a brief discussion of the possible sources of error and the resulting measurement uncertainties that can occur in each component of a sensitivity measuring system (Figure 8-1). The discussion will be mostly qualitative in this section as the quantitative information will be given in the appropriate sections later in the chapter.

1. Test signal sources

The measurement of sensitivity using a noise source depends upon knowing both the noise temperature and characteristic impedance of the source. When a hot-cold noise source is used, the accuracy problem is compounded because two reference temperatures and two characteristic impedances are involved. The SWR of the source tends to increase the receiver noise factor and temperature errors cause the measured Y-factor to be in error. Also, if the source is connected by a transmission line to the device being measured, the losses in the line will tend to make source temperatures above T_0 appear colder and source temperatures below T_0 appear hotter. If the noise source is a noise diode, the excess noise temperature is changed by stray reactance and transit-time effects. Also, the cold temperature is assumed to be $T_0 = 290^\circ \text{K}$ in most measurement schemes but generally the source resistance temperature is $3\text{--}5^\circ \text{K}$ higher (Appendix, Part 0). A gas-discharge noise source has a characteristic impedance which changes when the source is fired (Pastori, 1968b). This error complicates the measurement problem still further. The accuracy to which the manufacturer has specified excess noise temperature must also be considered in measurement accuracy because the error in excess noise ratio adds directly to the error in measured noise figure (see Equation 9A.11).

When a sinewave test signal source is used to measure sensitivity, the measurement depends upon knowing the impedance of the generator, its output level, and the percentage or index of modulation. Generator VSWR causes the receiver noise figure to increase while the percentage of modulation affects the level of recovered audio. The

generator output level in the sub-microvolt region is difficult to calibrate because of leakage problems. For the highest possible accuracies, the test setup must be carefully calibrated and shielded. It is usually better to measure the percentage of modulation by external means rather than depending upon modulation meter accuracy (usually $\pm 5\%$).

2. Device being tested

When measuring the sensitivity of any device, one must be sure that it is operating properly and that the specified power and terminating impedances are applied. It has been demonstrated several times in previous chapters that the source impedance for lowest noise figure is not the same as that for impedance matching. This must be kept in mind because the designer of the device has specified a certain source impedance for minimum noise figure. Typical source impedances are 50-, 75-, 100-, 200-, 300-, 400-, and 600-ohms but, by far, the most common system impedance is 50 ohms. If the device noise figure is measured with a source impedance other than the one specified, the resulting measured value will be higher than the minimum value.

If the matching network circuits at the device input are mistuned, a serious noise figure degradation can result. Generally the input matching network does not power match or resonate the device input because its function is to provide the optimum source resistance for lowest noise figure and to provide noise tuning. For high-frequency circuits, the input matching network is tuned below resonance for minimum noise figure.

Since it is not possible to tune the input circuits for maximum gain it is usually necessary to have an automatic noise figure meter to tune for minimum noise figure. The point should be emphasized that the noise figure of any device must be measured using the source resistance specified by the designer.

For devices with gains low enough that the noise contribution of the predetection amplifier must be considered, it is necessary to have an accurate measurement of device gain. To be able to accurately apply the Friis equation (Appendix, Part J) the transducer gain must be used but most often it is the insertion gain which is measured. It is shown in Equation D.9 of the Appendix that the transducer gain is always smaller than the insertion gain. When applying the Friis equation, the noise figure calculated using insertion gain is always larger than that obtained using transducer gain and thus will give pessimistic noise figure values for the device.

Problems can occur which are not directly involved in device sensitivity measurement but nevertheless have a deleterious effect on the results. Two of the more common problems are spurious oscillations and power supply noise. A large SWR at either the input or output will cause a marginally stable device to oscillate. If these oscillations occur off frequency they will severely degrade the noise figure of the device. On-frequency oscillations are more obvious. Noise introduced into the signal path from a noisy power supply will also degrade noise figure. This can frequently occur where zener diodes are used for regulation and the zener noise is not adequately bypassed. The solution to these problems is usually better design stability and adequate

bypassing and filtering. Stray RF signals from external sources such as transmitters or grid-dip meters will cause measurement errors.

For many radio-astronomy and radar receivers, the RF filter will pass both the signal and image frequencies. When noise figure measurements are made on this type of receiver, the noise input at the image frequency will add to that at the signal frequency to give noise figure measurements from 0 to 3 db lower than the spot noise figure. Reporting and measuring the sensitivity of multiple-response receivers must be done carefully and full details of the circumstances should be recounted.

3. Predetection amplifier

The predetection amplifier usually has a gain that is high enough to overcome all the noise contributions of succeeding stages and provides the device being tested with a suitable impedance termination and a known noise figure. The bandwidth of the predetection amplifier is assumed to be large enough to give uniform amplification to all signals within the passband of the predetection filter. Inaccuracies in noise figure and bandwidth can have a serious affect on sensitivity measurements.

The noise figure of the predetection amplifier is usually measured from a specified reference impedance but when it is connected to the device output it is usually not operating with the specified source. This will cause the noise figure of the predetection amplifier to increase. The larger noise figure will introduce an error into the Friis equation calculation and cause the calculated noise figure to

be larger than the true value, which will give pessimistic noise figures.

Bandwidth errors, and especially those due to a bandwidth which is too narrow, were discussed in Part J of the Appendix.

4. Predetection filter

The predetection filter bandwidth is used in many noise calculations and sensitivity measurements. Errors in the noise bandwidth used in any of the calculations will cause errors in the measured sensitivity. In some cases the shape of the passband response (see Section VII-C) is important. The bandwidth of the predetection filter determines the bandwidth over which the noise figure is measured. This bandwidth must be smaller than the bandwidth of the device being measured or serious errors can result. The equivalent noise bandwidth for many types of predetection filters is given in Kraus (1966, p. 265). For most practical filters, the noise bandwidth is a factor of 1 to $\pi/2$ times larger than the 3 db bandwidth. For the best precision, the noise bandwidth should be determined graphically. A graphical method for the determination of equivalent noise bandwidth from the filter amplitude response is given by Vigneri et al. (1968).

5. Detector device

Errors in sensitivity measurements which are caused by the detector device are due to threshold effects, nonlinear gain effects, and detector-law disparities. Threshold effects occur in all detectors and cannot be eliminated but are usually compensated for by either direct measurement correction or a clever measurement scheme. If the detector

is nonlinear in gain, the output level will not change db for db with input level change. This introduces errors in the measured-ratio output. Variations in the detector-law characteristics affect the spectral character of the signals and analytical techniques such as were used for a perfect square-law device are extremely difficult to apply.

There is little excuse for letting detector errors limit the accuracy of the sensitivity measurement because there are so many techniques available for eliminating these errors such as operating above threshold or making comparative measurements or using a calibrated attenuator as is done in the Y-factor method. This is not to say, however that detector error is eliminated in every practical measurement. Many times detectors are used in a manner such that their errors do affect accuracy.

6. Postdetection filter

The postdetection filter is most important in determining the measurement resolution limit at the output of the detector. For square-law detectors, the limit is determined by the ratio of predetection and postdetection filter bandwidths as given by Equation 7.47 in Chapter VI. In general, the smaller the noise bandwidth B_L , the more resolution there is in the measurement. This fundamental limitation applies to all dc measuring devices. In AM systems, the postdetection filter determines the audio noise bandwidth and thus affects the noise factor measured by AM sensitivity (Equation 8D.18). The determination of

postdetection noise bandwidth by graphical techniques is the same as discussed previously for the predetection filter.

7. Postdetection amplifier

The postdetection amplifier must amplify the signals from the detector so they may be used to drive the output indicator. If the output is a dc level, the dc stability and linearity of the amplifier must be good or measurement errors will result. DC level changes with temperature or signal level cannot be tolerated. Gain stability is important in both ac and dc measurements because gain changes cause errors in the measured output level change. The bandwidth of the postdetection amplifier may be wide enough to give a significant noise contribution to the output. This noise will tend to "mask" the detector output and introduce a large error.

In many instances, the most critical problem in the postdetection amplifier is the flicker noise output. This limits the resolution of the output indicator because low-pass filtering cannot eliminate the problem. The real-time resolution of the system can never be better than that dictated by flicker noise. Flicker noise error can be minimized by numerically averaging several data points.

8. Sensory transducer (output indicator)

The effect of the output indicator on the accuracy of the sensitivity measurement is determined by the dynamics of the indicator, its relative accuracy, and the bias of the human observer. Such problems as needle flicker and parallax are always present when using a meter indicator. Needle flicker is determined, to a large extent, by the

dynamics of the meter movement. The accuracy of the meter movement is the important factor because most often, relative accuracy is needed and not absolute accuracy. The relative accuracy depends upon scale calibration and meter linearity. The accuracy of a meter can be specified in three ways:

1. Percent of full-scale
2. Percent of reading
3. Percent of reading plus percent of full-scale.

Typical percent of full-scale accuracy is $\pm 2\%$ while percent of reading accuracy is expressed in db and is typically ± 0.2 to ± 0.4 db. These, however, are absolute accuracies and not a true indication of the accuracy of a ratio measurement.

For output ratio measurements, the significant errors are due to scale non-linearity and human observer error. Experience by this author has shown that ratio measurements better than ± 0.05 db for a 3 db ratio are difficult to achieve. Switching scales on the meter to make a large ratio measurement should be discouraged because this introduces an additional error in the measurement that can be as high as the absolute accuracy specification. The crest factor (ratio of peak amplitude to RMS amplitude) capability must be greater than 5 to 1 at full scale or clipping effects will cause the meter to read lower than true value. This tends to make noise ratio measurements smaller than actual measurements which results in pessimistic noise figure values.

When making tangential noise sensitivity measurements with an oscilloscope, the error involved is nearly all due to the subjective evaluation of an observer (see Figure 8C-1). Trying to line up the

"tangencies" of the two noise outputs is difficult. Measurements by qualified observers (Montgomery, 1964, p. 228) show a 2 db standard deviation of the reported sensitivity for all observers and a standard deviation of 1 db for a single observer. These results indicate that measured noise figures using this method would also show the 2 db and 1 db standard deviations.

Strip chart recorders are used primarily for taking data over a long span of time and generally for poor signal-to-noise ratios. The accuracy of a strip chart recorder is really very adequate for sensitivity measurements, especially for measuring noise ratios. The data can be recorded and then averaged to give a very accurate ratio measurement. Scale accuracies are an order of magnitude better than for a meter. Accuracies of $\pm 0.2\%$ of full scale and linearities of $\pm 0.1\%$ are possible.

B. Test Signal Sources

The most fundamental errors occurring in a sensitivity measuring system are those due to the test signal source. In this section, the causes of test signal errors and how they may be calculated are presented. The equivalent circuits approach is used extensively to obtain the error equations and the reader will have to be proficient in the application of Thevenin's theorem, the available power theorem, two-port parameter theory and transmission-line equations. Also it is recommended that many of the referenced papers be read prior to or concurrent with this chapter.

The test signal source of any sensitivity measuring scheme is usually separated from the device being tested by a transmission line. It is of fundamental importance to know the available powers, impedances and reflection coefficients for the combination of transmission line and source. Figure 10B-1 is a schematic representation of the circuit showing the various quantities. For the sake of generality, the transmission line is replaced by a passive two-port described by a flat loss N , a physical temperature T_c and scattering parameters, $[S]$.

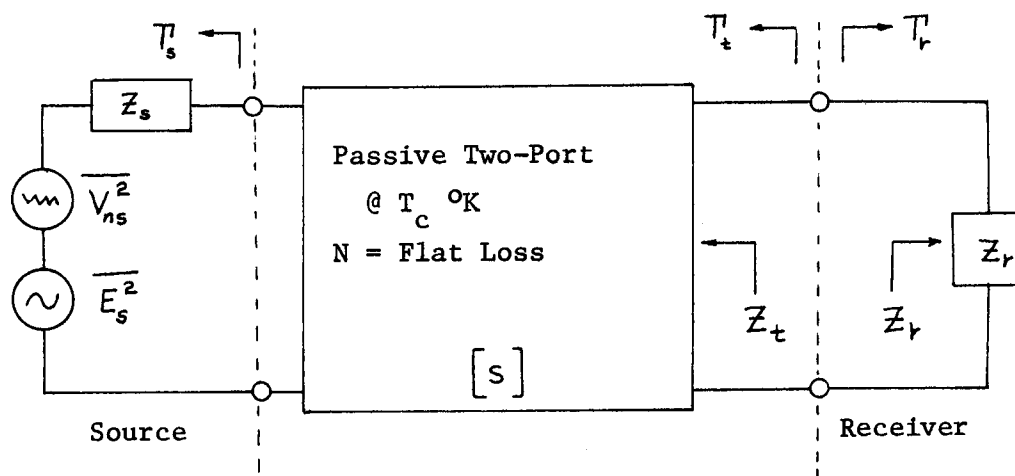


Figure 10B-1. Circuit Used to Illustrate the Effects of a Passive Two-Port between Test Signal Source and Receiver

The following quantities are defined:

$R_o \triangleq$ Reference impedance of the system, usually 50 ohms

$[S] \triangleq \begin{bmatrix} S_{11} & S_{12} \\ S_{21} & S_{22} \end{bmatrix}$, the scattering matrix for the passive two-port measured with respect to R_o

$Z_r \triangleq R_r + jX_r$, the impedance of the load

$Z_t \triangleq R_t + jX_t$, the impedance of the two-port output

$Z_s \triangleq R_s + jX_s$, the impedance of the source

$\overline{V_{ns}^2} \triangleq 4 k T_s \operatorname{Re}(Z_s) \Delta f$, the mean-square noise voltage of the source

$\overline{E_s^2} \triangleq$ the mean-square sinewave signal voltage of the source,
[volts RMS]²

$T_s \triangleq$ noise temperature of the source

$T_c \triangleq$ physical temperature of the two-port

$\Gamma_s \triangleq \frac{Z_s - R_o}{Z_s + R_o}$, the reflection coefficient of the source

$\Gamma_t \triangleq \frac{Z_t - R_o}{Z_t + R_o}$, the reflection coefficient of the output of
the two-port

$\Gamma_r \triangleq \frac{Z_r - R_o}{Z_r + R_o}$, the reflection coefficient of the load

$|a_s|^2 \triangleq \frac{\overline{E_s^2} R_o}{|Z_s + R_o|^2}$, the signal power the source will deliver to

a reference impedance load (see Appendix, Part D)

$|a_{ns}|^2 \triangleq \frac{\overline{V_{ns}^2} R_o}{|Z_s + R_o|^2}$, the noise power the source will deliver to

a reference impedance load.

Livingston and Bechtold (1968) have considered the effect of impedance mismatch on antenna noise temperature and many of their techniques and equations can be applied to this problem. First, the output

reflection coefficient of the two-port network can be written in terms of the source reflection coefficient and the scattering parameters

$$\Gamma_t = \frac{S_{22} + \Gamma_s (S_{12} S_{21} - S_{11} S_{22})}{(1 - \Gamma_s S_{11})} \quad (10B.1)$$

and the output impedance is written in terms of R_o and Γ_t as:

$$Z_t = R_o \frac{1 + \Gamma_t}{1 - \Gamma_t} \quad (10B.2)$$

The signal power delivered to the load is given by Livingston and Bechtold to be:

$$P_s = \frac{|a_s|^2 |S_{21}|^2 (1 - |\Gamma_r|^2)}{|(1 - S_{11} \Gamma_s)(1 - S_{22} \Gamma_r) - S_{12} S_{21} \Gamma_r \Gamma_s|^2} \quad (10B.3)$$

The available loss (defined as the ratio of available input power to available output power) is:

$$\mathcal{L} = \frac{(|1 - S_{11} \Gamma_s|^2 - |S_{22}(1 - S_{11} \Gamma_s) + S_{12} S_{21} \Gamma_s|^2)}{|S_{21}|^2 (1 - |\Gamma_s|^2)} \quad (10B.4)$$

The available loss, \mathcal{L} , is a positive real number greater than or equal to unity ($\mathcal{L} \geq 1$).

In Section IV-C, the noise temperature of a noise source as seen through a lossy transmission line was derived in terms of the flat loss of the line, N , and the physical temperature, T_c . Equation 4C.55a

actually has more general applicability than indicated. It is generally applicable in calculating the two-port output noise temperature for any source temperature and VSWR. To obtain the more general form, the flat loss, N , is replaced by the available loss, \mathcal{L} . This gives the general result (Livingston and Bechtold, 1968)

$$T_s' = \frac{1}{\mathcal{L}} [T_s + (\mathcal{L} - 1) T_c] \quad (10B.5)$$

where T_s' is the effective noise temperature of the real part of Z_t or the available output noise temperature. The equivalent circuit for the two-port output, showing mean-square noise and signal voltages and impedances, is given in Figure 10B-2.

The mean-square noise voltage is obtained by applying Nyquist's Theorem and using the effective noise temperature of (10B.5):

$$\overline{V_{nt}^2} = 4kT_s' \operatorname{Re}(Z_t) \Delta f \quad (10B.6)$$

The two-port output impedance is given by Equation 10B.2. The mean-square signal voltage has to be obtained by considering the signal power delivered to the load.

The power delivered to the load is given by (10B.3) but it is more meaningful to express this power in terms of the available loss and the available signal power at the input (Livingston and Bechtold, 1968):

$$P_s = \frac{1}{\mathcal{L}} \frac{|a_s|^2}{1 - |T_s|^2} \quad (10B.7)$$

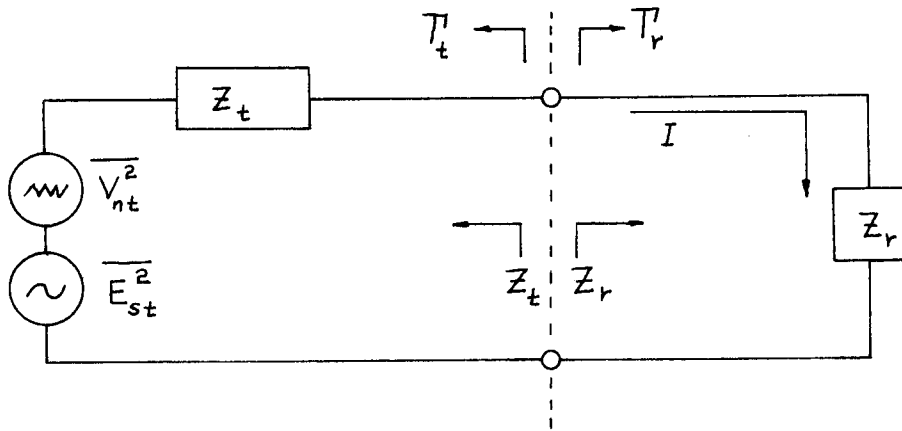


Figure 10B-2. Equivalent Circuit for Two-Port Output and Load

From circuit theory and Figure 10B-2 we know the signal power delivered to the load is (Appendix, Part D):

$$\begin{aligned}
 P_s &= I I^* \operatorname{Re}(Z_r) \\
 &= \frac{\overline{E_{st}^2}}{|Z_t + Z_r|^2} \operatorname{Re}(Z_r)
 \end{aligned} \tag{10B.8}$$

Combining (10B.7) and (10B.8) we get the mean-square signal output voltage as:

$$\overline{E_{st}^2} = \frac{|a_s|^2}{\mathcal{L}} \cdot \frac{|Z_t + Z_r|^2}{(1 - |T_s|^2) \operatorname{Re}(Z_r)} \tag{10B.9}$$

The effects of two-port loss and VSWR on available signal power, noise power and loss have now been described by various equations which will be used later in the chapter.

It is convenient to derive an alternate expression for the signal power, $|a_s|^2$, delivered to R_o . The reflection coefficient for the source is defined as

$$\Gamma_s \triangleq \frac{Z_s - R_o}{Z_s + R_o} \quad (10B.10)$$

and its absolute value is determined by complex algebra to be

$$|\Gamma_s|^2 = \Gamma_s \Gamma_s^* = \left(\frac{Z_s - R_o}{Z_s + R_o} \right) \cdot \left(\frac{Z_s - R_o}{Z_s + R_o} \right)^* \quad (10B.11a)$$

or:

$$1 - |\Gamma_s|^2 = \frac{4 R_o \operatorname{Re}(Z_s)}{|Z_s + R_o|^2} \quad (10B.11b)$$

The signal power delivered to a load R_o from a source impedance Z_s is

$$|a_s|^2 = \frac{\overline{E_s^2} R_o}{|Z_s + R_o|^2} \quad (10B.12)$$

which can be combined with (10B.11) to give the desired result:

$$|a_s|^2 = \frac{\overline{E_s^2}}{4 \operatorname{Re}(Z_s)} (1 - |\Gamma_s|^2) \quad (10B.13)$$

This expresses the signal power delivered to R_o in terms of the available power from the source (Appendix, Part C) and the reflection coefficient, Γ_s . A similar equation can be written for the noise power delivered to R_o :

$$|a_{ns}|^2 = kT_s \Delta f (1 - |\Gamma_s|^2) \quad (10B.14)$$

The ratio of available signal power to available noise power from the source is independent of the reflection coefficient of the source:

$$\frac{\frac{\overline{E_s^2}}{4\text{Re}(Z_s)}}{\frac{\overline{V_{ns}^2}}{4\text{Re}(Z_s)}} = \frac{\overline{E_s^2}}{4kT_s \text{Re}(Z_s) \Delta f} = \frac{|a_s|^2}{|a_{ns}|^2} \quad (10B.15)$$

The ratio of available powers at the output of the two-port is determined by using the delivered power equations for P_s and P_{ns} and a conjugately matched load ($\Gamma_r = \Gamma_t^*$ or $Z_r = Z_t^*$). The available signal power is determined from (10B.3):

$$P_s(\text{avail}) = \frac{|a_s|^2 |S_{21}|^2 (1 - |\Gamma_t|^2)}{|(1 - S_{11}\Gamma_s)(1 - S_{22}\Gamma_t^*) - S_{12}S_{21}\Gamma_t^*\Gamma_s|^2} \quad (10B.16)$$

The available noise power is computed from the circuit of Figure 10B-2 and using Equation 10B.6:

$$\begin{aligned}
 P_{ns}(\text{avail}) &= \frac{\overline{V_{nt}^2}}{|Z_t + Z_L^*|^2} \text{Re}(Z_t^*) \quad (Z_r = Z_t^*) \\
 &= \frac{\overline{V_{nt}^2}}{4 \text{Re}(Z_t)} = k T_s' \Delta f
 \end{aligned} \tag{10B.17}$$

The ratio of available signal-to-noise power at the source to that at the two-port output is the definition of the noise factor of the two-port. The two-port noise factor, F_c , is determined using Equations 10B.17, 10B.16, and 10B.15 as:

$$\begin{aligned}
 F_c &= \frac{|a_s|^2}{|a_{ns}|^2} \cdot \frac{P_{ns}(\text{avail})}{P_s(\text{avail})} \\
 &= \frac{T_s'}{T_s} \cdot \frac{|(1 - S_{11}T_s')(1 - S_{22}T_t^*) - S_{12}S_{21}T_t^*T_s'|^2}{|S_{21}|^2(1 - |T_t|^2)(1 - |T_s|^2)}
 \end{aligned} \tag{10B.18}$$

It should be remembered that T_t and T_s are related through Equation 10B.1.

If the two-port has been designed so that its characteristic impedance (the reference impedance for which the scattering parameters are measured) is the same as the reference impedance R_0 , the input and output scattering parameters will be zero ($S_{11} = S_{22} = 0$). For the condition ($S_{11} = S_{22} = 0$), the equations for the available loss, output reflection coefficient, available signal power, and two-port reflection coefficient can be simplified. Upon simplification of these equations

and applying (10B.19) to get all quantities in terms of T_s , these equations become:

$$1. \quad T_t = S_{12} S_{21} T_s \quad |T_t|^2 = |S_{12}|^2 |S_{21}|^2 |T_s|^2 \quad (10B.19)$$

$$2. \quad \rho = \frac{(1 - |S_{12} S_{21} T_s|^2)}{|S_{21}|^2 (1 - |T_s|^2)} \quad (10B.20)$$

$$3. \quad P_s(\text{avail}) = |a_s|^2 \frac{|S_{21}|^2}{(1 - |S_{12} S_{21} T_s|^2)} \quad (10B.21)$$

$$4. \quad F_c = \frac{T_s'}{T_s} \cdot \frac{(1 - |S_{12} S_{21} T_s|^2)}{|S_{21}|^2 (1 - |T_s|^2)} \quad (10B.22)$$

If we define S_{12} and S_{21} for a transmission line, the above equations can be further specialized in terms of the transmission-line parameters. From transmission-line theory we know that the output impedance is related to the input impedance by the equation

$$Z_t = Z_o \frac{Z_s \cosh \gamma l + Z_o \sinh \gamma l}{Z_o \cosh \gamma l + Z_s \sinh \gamma l} \quad (10B.23a)$$

or in terms of exponentials

$$Z_t = Z_o \frac{e^{\gamma l} + T_s e^{-\gamma l}}{e^{\gamma l} - T_s e^{-\gamma l}} \quad (10B.23b)$$

where Z_0 is the characteristic impedance of the line, $\gamma = \alpha + j\beta$ is the propagation constant, and l is the length of the line.

Equation 10B.23b can be written in an alternate form which is more suitable for this discussion. If the line is distortionless then the characteristic impedance is real ($Z_0 = R_0 + j0$) and multiplying both numerator and denominator by $e^{\gamma l}$ gives:

$$Z_t = R_0 \frac{e^{2\gamma l} + T_s}{e^{2\gamma l} - T_s} \quad (10B.24)$$

For the distortionless line, the scattering matrix for a reference of R_0 is

$$[S] = \begin{bmatrix} 0 & e^{-\gamma l} \\ e^{-\gamma l} & 0 \end{bmatrix} \quad (10B.25)$$

and:

$$S_{12} = S_{21} = e^{-\gamma l} = e^{-\alpha l} e^{-j\beta l} \quad (10B.26a)$$

The absolute magnitude squared of S_{12} or S_{21} is determined from (10B.26a) as:

$$|S_{12}|^2 = S_{12} S_{12}^* = e^{-2\alpha l} \quad (10B.27a)$$

By comparing (10B.26a) with (4C.48) we see that S_{12} and S_{21} can also be written in terms of the line attenuation factor (numerical flat loss), N .

$$S_{12} = S_{21} = \frac{1}{\sqrt{N}} e^{-j\beta l} \quad (10B.26b)$$

$$|S_{12}|^2 = |S_{21}|^2 = \frac{1}{N} \quad (10B.27b)$$

Finally we can use these equations to specialize Equations 10B.19 through 10B.22 for a distortionless transmission line:

$$1. \quad T_t = \frac{1}{N} e^{-j2\beta l} T_s \quad (10B.28)$$

$$2. \quad \mathcal{L} = N \frac{\left(1 - \frac{|T_s|^2}{N^2}\right)}{\left(1 - |T_s|^2\right)} \quad (10B.29)$$

$$3. \quad P_s(\text{avail}) = \frac{|E_s|^2}{4R_s} \cdot \frac{1}{\mathcal{L}} \quad (10B.30)$$

$$4. \quad F_c = \frac{T_s'}{T_s} \mathcal{L} = 1 + (\mathcal{L} - 1) \frac{T_c}{T_s} \quad (10B.31)$$

For a lossless line or one so short that the line attenuation factor is unity ($N = 1$) the available loss becomes unity ($\mathcal{L} = 1$) and the available noise temperature becomes that of the source ($T_s' = T_s$). When the source VSWR is unity, the absolute magnitude of the source reflection coefficient as given by

$$|T_s| = \left| \frac{Z_s - R_o}{Z_s + R_o} \right|$$

or,

$$|T_s| = \frac{VSWR - 1}{VSWR + 1} \quad (10B.32)$$

becomes zero and the available loss becomes N. These limiting cases can be summarized with the expressions:

$$1. \quad \lim_{N \rightarrow 1} L = 1 \quad (10B.33)$$

$$2. \quad \lim_{|T_s|^2 \rightarrow 0} L = N \quad (10B.34)$$

The assumption of unity VSWR was imposed in deriving Equation 4C.55a and if we use the result of (10B.34) in (10B.5) we see that (10B.5) reduces to (4C.55a).

The equations that have been presented in this section will now be applied to the problems of determining the sources of error in sensitivity measuring systems and particularly the available power of test-signal sources.

1. Hot-cold noise source

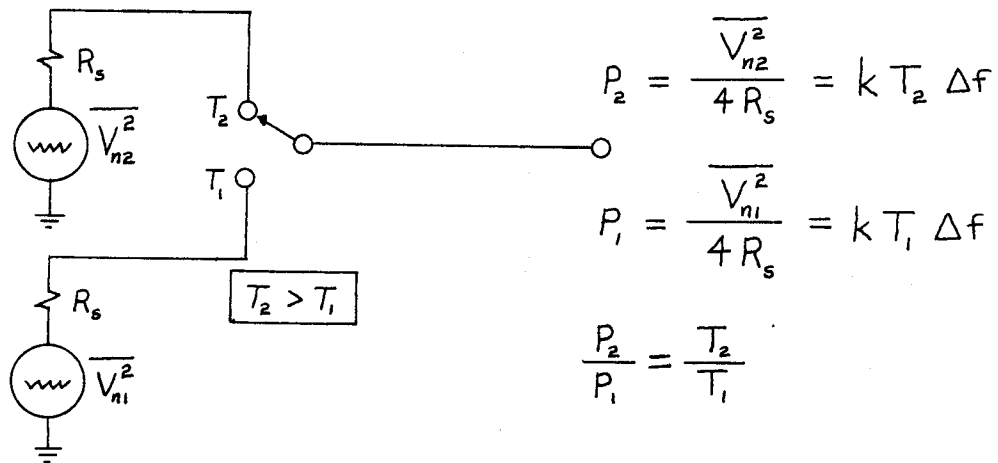
Under ideal conditions, the hot-cold noise source is characterized by two known temperatures, and a single source impedance with unity VSWR. In reality, the source is characterized by two temperatures of

specified accuracy, two source impedances of specified VSWR and a section of transmission line. The line is needed to connect the hot and cold terminations to the device being measured. Figure 10B-3 shows the circuit elements for an ideal and nonideal hot-cold noise source.

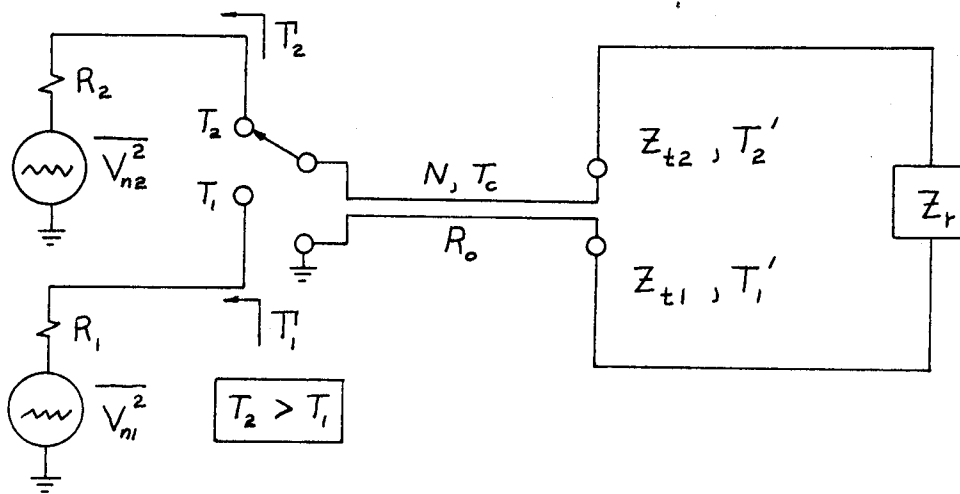
The ideal hot-cold source has unity VSWR for both hot and cold terminations and the transmission line is lossless. For these ideal conditions, the ratio of the available powers for the two sources is simply the ratio of the noise temperatures. For the nonideal source the effects of source VSWR and transmission-line loss must be taken into account. The powers delivered to the load impedance, Z_r , for the T_2 (hot) and T_1 (cold) sources are obtained by applying Equations 10B.6 and 10B.8 to the circuits of Figure 10B-3 to get:

$$\begin{aligned}
 P_2 &= \frac{\overline{V_{t2}^2}}{|Z_r + Z_{t2}|^2} \operatorname{Re}(Z_r) \\
 &= k T_2' \Delta f \frac{4 \operatorname{Re}(Z_r) \operatorname{Re}(Z_{t2})}{|Z_r + Z_{t2}|^2}
 \end{aligned}
 \tag{10B.35}$$

$$\begin{aligned}
 P_1 &= \frac{\overline{V_{t1}^2}}{|Z_r + Z_{t1}|^2} \operatorname{Re}(Z_r) \\
 &= k T_1' \Delta f \frac{4 \operatorname{Re}(Z_r) \operatorname{Re}(Z_{t1})}{|Z_r + Z_{t1}|^2}
 \end{aligned}
 \tag{10B.36}$$



(a) Ideal Hot-Cold Noise Source



(b) Nonideal Hot-Cold Noise Source

Figure 10B-3. Schematic Representations of Ideal and Non-Ideal Hot-Cold Noise Sources

where

$$T_2' = \frac{1}{\mathcal{L}_2} [T_2 + (\mathcal{L}_2 - 1) T_c] \quad (10B.37a)$$

$$T_1' = \frac{1}{\mathcal{L}_1} [T_1 + (\mathcal{L}_1 - 1) T_c] \quad (10B.37b)$$

$$\mathcal{L}_2 = N \frac{\left(1 - \frac{|T_2|^2}{N^2}\right)}{\left(1 - |T_2|^2\right)} \quad (10B.37c)$$

$$\mathcal{L}_1 = N \frac{\left(1 - \frac{|T_1|^2}{N^2}\right)}{\left(1 - |T_1|^2\right)} \quad (10B.37d)$$

The equations for available power, when the line is lossy and the source has a VSWR greater than unity, will reduce to those for the ideal case when $T_2 = T_1 = 0$ and $N = 1$.

The available output noise powers for the T_2 and T_1 sources can be determined from (10B.35) and (10B.36) by impedance matching at the output:

$$P_2(\text{avail}) = k T_2' \Delta f \quad (Z_r = Z_{t2}^*) \quad (10B.38a)$$

$$P_1(\text{avail}) = k T_1' \Delta f \quad (Z_r = Z_{t1}^*) \quad (10B.38b)$$

The error in available noise power is determined by the error in available noise temperature. Letting the subscript on T' be s so

the equations that follow can apply to either T_2' or T_1' , we get

Equation 10B.5:

$$T_s' = \frac{1}{\mathcal{L}} \left[T_s + (\mathcal{L} - 1) T_c \right]$$

which can be factored to give an equation that is suitable for error determination of T_s . Factoring (10B.5) gives

$$T_s' = T_s \left[1 + \left(1 - \frac{1}{\mathcal{L}} \right) \left(\frac{T_c}{T_s} - 1 \right) \right] \quad (10B.39)$$

which is written in an alternate form

$$T_s' = T_s [1 + K_s] \quad (10B.40)$$

with K_s representing the two factors in parentheses. Equation 10B.39 could be used to determine T_s' if all the variables were known exactly but since they are not, (10B.40) is written in a second alternate form

$$\widetilde{T}_s' = \widetilde{T}_s [1 + \widetilde{K}_s] \quad (10B.41a)$$

where the tilde denotes a measured quantity which is known only to a specified accuracy. We will now take Equation 10B.41 and determine the uncertainty in T_s' by looking at the uncertainties in the other parameters. Each variable in (10B.41) can be represented as the sum of a true value and an error value

$$\widetilde{T}'_s = T'_s + \Delta T'_s \quad (10B.42a)$$

$$\widetilde{T}_s = T_s + \Delta T_s \quad (10B.42b)$$

$$\widetilde{K}_s = K_s + \Delta K_s \quad (10B.42c)$$

which are substituted into (10B.41a) to give:

$$T'_s + \Delta T'_s = T_s [1 + K_s] + \Delta K_s T_s + \Delta T_s [1 + K_s + \Delta K_s] \quad (10B.41b)$$

The maximum error or uncertainty in \widetilde{T}'_s is determined from the absolute value of $\Delta T'_s$ (see Appendix, Part S)

$$|\Delta T'_s| \leq |\Delta K_s| T_s + |\Delta T_s| [1 + K_s + |\Delta K_s|] \quad (10B.43)$$

where $|\Delta K_s|$ is the maximum uncertainty in \widetilde{K}_s and $|\Delta T_s|$ is the maximum uncertainty in \widetilde{T}_s . K_s and T_s are nominal values.

The uncertainty in \widetilde{K}_s must now be determined. First let

$$\frac{1}{\widetilde{X}} = \widetilde{Y} \quad (10B.44)$$

and:

$$\widetilde{X} = X + \Delta X \quad (10B.45a)$$

$$\widetilde{Y} = Y + \Delta Y \quad (10B.45b)$$

$$\left(\frac{\widetilde{T}_c}{\widetilde{T}_s} \right) = \frac{T_c}{T_s} + \Delta \frac{T_c}{T_s} \quad (10B.45c)$$

Using (10B.42c) and Equations 10B.45, 10B.39, and 10B.41, we get

$$\widetilde{K}_s = \left[1 - \frac{1}{\widetilde{\mathcal{L}}} \right] \left[\left(\frac{\widetilde{T}_c}{\widetilde{T}_s} \right) - 1 \right] \quad (10B.46a)$$

$$K_s = \left[1 - \frac{1}{\mathcal{L}} \right] \left[\left(\frac{T_c}{T_s} \right) - 1 \right] \quad (10B.46b)$$

$$K_s + \Delta K_s = \left[1 - (\mathcal{E} + \Delta \mathcal{E}) \right] \left[\left(\frac{T_c}{T_s} \right) + \Delta \frac{T_c}{T_s} - 1 \right] \quad (10B.47)$$

and the error in \widetilde{K}_s becomes:

$$\Delta K_s = \Delta \frac{T_c}{T_s} (1 - \mathcal{E}) + \Delta \mathcal{E} \left(1 - \frac{T_c}{T_s} \right) - \Delta \mathcal{E} \Delta \frac{T_c}{T_s} \quad (10B.48)$$

If the uncertainty criteria (Appendix, Part S) are applied to (10B.48) in a term by term manner, the resulting uncertainty is

$$|\Delta K_s| \leq \left| \Delta \frac{T_c}{T_s} \right| + \left| \Delta \frac{T_c}{T_s} \right| \mathcal{E} + |\Delta \mathcal{E}| + \frac{T_c}{T_s} |\Delta \mathcal{E}| + |\Delta \mathcal{E}| \left| \Delta \frac{T_c}{T_s} \right|$$

but this gives a bound which is unrealistically high. A smaller upper bound has been calculated by factorizing (10B.47) into the form of (10B.48) which gives an uncertainty of

$$|\Delta K_s| \leq \left| \Delta \frac{T_c}{T_s} \right| (1 - \mathcal{E}) + |\Delta \mathcal{E}| \left| 1 - \frac{T_c}{T_s} \right| + |\Delta \mathcal{E}| \left| \Delta \frac{T_c}{T_s} \right| \quad (10B.49)$$

which is a smaller value than given by the equation above. What we are striving for is the most realistic value for uncertainty, not the largest.

We have been determining upper bounds on $|\Delta K_s|$ but not a least upper bound. The least upper bound, for small increments, is (see Appendix, Part S)

$$|\Delta K_s| \leq \left| \frac{\partial K_s}{\partial \frac{T_c}{T_s}} \right| \left| \Delta \frac{T_c}{T_s} \right| + \left| \frac{\partial K_s}{\partial \Xi} \right| |\Delta \Xi|$$

which is evaluated using (10B.46b) as:

$$|\Delta K_s| \leq (1 - \Xi) \left| \Delta \frac{T_c}{T_s} \right| + \left| \frac{T_c}{T_s} - 1 \right| |\Delta \Xi| \quad (10B.50)$$

For small errors, (10B.50) and (10B.49) are very nearly equal. The error in Ξ is evaluated from the equation for Ξ which is obtained using (10B.29) and (10B.44):

$$\Xi = \frac{(1 - |T_s|^2)}{N \left(1 - \frac{|T_s|^2}{N^2} \right)} \quad (10B.51)$$

For small errors we can evaluate $|\Delta \Xi|$ from (see Appendix, Part S)

$$\Delta \Xi \leq \left| \frac{\partial \Xi}{\partial |T_s|^2} \right| |\Delta |T_s|^2| + \left| \frac{\partial \Xi}{\partial N} \right| |\Delta N|$$

which gives, using (10B.51):

$$\begin{aligned}
|\Delta \mathfrak{E}| \leq & \frac{N(N^2 - 1)}{(N^2 - |T_s|^2)^2} |\Delta |T_s|^2| \\
& + (1 - |T_s|^2) \frac{N^2 + |T_s|^2}{(N^2 - |T_s|^2)^2} |\Delta N|
\end{aligned} \tag{10B.52}$$

From (10B.52), (10B.50) and (10B.43) it is determined that the uncertainty in \tilde{T}_s' , $|\Delta T_s'|$, is a function of the following variables:

1. $|T_s|^2$, the squared absolute value of the source reflection coefficient
2. N , the line attenuation factor (also called the flat-loss)
3. T_c/T_s , the ratio of transmission line temperature to source temperature
4. T_s , the source temperature
5. and the uncertainties in each of the above variables.

The functional dependence of $|\Delta T_s'|$ is expressed in the equation:

$$|\Delta T_s'| = f\left(T_s, \frac{T_c}{T_s}, N, |T_s|^2, |\Delta T_s|, \left|\Delta \frac{T_c}{T_s}\right|, |\Delta N|, |\Delta |T_s|^2|\right).$$

For source VSWR's less than 1.5, \mathfrak{E} and its uncertainty become:

$$\begin{aligned}
\mathfrak{E} & \approx \frac{1}{N} \\
|\Delta \mathfrak{E}| & \approx \frac{(N^2 - 1)}{N^3} |\Delta |T_s|^2| + \frac{|\Delta N|}{N^2}
\end{aligned}$$

This simplifies Equation 10B.50 to

$$|\Delta K_s| \approx \left(1 - \frac{1}{N}\right) \left| \Delta \frac{T_c}{T_s} \right| + \left| \frac{T_c}{T_s} - 1 \right| \left\{ \frac{(N^2 - 1) |\Delta |T_s|^2| + N |\Delta N|}{N^3} \right\} \quad (10B.53)$$

which can then be used in (10B.43) to determine the uncertainty in T_s' , the available output noise temperature.

For day-to-day work one would like to be able to use equations which are simpler than those just presented. These equations can be simplified by using a low source VSWR approximation which is quite good for practical sources. For low source VSWR

$$\Delta |T_s|^2 \approx 0$$

and if it is assumed that $T_s \gg |\Delta T_s|$ then the following simplified equations may be used:

$$|\Delta K_s| \approx \left(1 - \frac{1}{N}\right) \left| \Delta \frac{T_c}{T_s} \right| + \left| \frac{T_c}{T_s} - 1 \right| \frac{|\Delta N|}{N^2} \quad (10B.54)$$

$$\Xi \approx \frac{1}{N} \quad (10B.55)$$

$$K_s \approx \left(1 - \frac{1}{N}\right) \left(\frac{T_c}{T_s} - 1 \right) \quad (10B.56)$$

$$|\Delta T_s'| \simeq T_s |\Delta K_s| + |\Delta T_s| [1 + K_s] \quad (10B.57)$$

$$\begin{aligned} \widetilde{T}_s' &= T_s (1 + K_s) \pm |\Delta T_s'| \\ &= T_s' \pm |\Delta T_s'| \end{aligned} \quad (10B.58)$$

As a numerical example, consider a noise source of 373°K and a coaxial cable of 1 db loss at 298°K . The actual system specifications are:

$$\widetilde{T}_s = 373 \pm 5^\circ \text{K}$$

$$\widetilde{N} = 1.26 \pm 0.06 \quad (1.0 \pm 0.2 \text{ db})$$

$$\widetilde{T}_c = 298 \pm 5^\circ \text{K}$$

From this data we can compute the following quantities:

$$|\Delta T_s| = 5^\circ \text{K} \quad |\Delta N| = 0.06$$

$$\frac{T_c}{T_s} = 0.80 \quad \left| \Delta \frac{T_c}{T_s} \right| = 0.024$$

Calculating $|\Delta K_s|$ and K_s we get:

$$|\Delta K_s| \simeq \left(1 - \frac{1}{1.26}\right) (0.024) + |-0.2| \frac{0.06}{(1.26)^2} = 0.0125$$

$$K_s \simeq \left(1 - \frac{1}{1.26}\right) (0.80 - 1) = -0.041$$

Finally, using (10B.57) and (10B.58), we can compute $|\Delta T_s'|$ and \tilde{T}_s' :

$$|\Delta T_s'| = 373 (0.0125) + 5 (1 - 0.041) \approx 9.5^\circ \text{K}$$

$$\tilde{T}_s' = 373 (1 - 0.041) \pm |\Delta T_s'|$$

$$\boxed{\tilde{T}_s' = 358 \pm 9.5^\circ \text{K}}$$

The effect of the cable loss has been to reduce the apparent source temperature and increase the absolute error in noise temperature caused by the uncertainty in \tilde{T}_s and \tilde{T}_c . The nominal noise temperature of the source is lowered by 15°K .

2. Noise diode

For many purposes, the errors which occur in a noise diode test source are just simplified versions of those for the hot-cold noise source. The errors that are unique to the noise diode are those associated with diode operation. The errors inherent in the noise diode source are:

1. Space-charge shot-noise reduction
2. Transit-time shot-noise reduction
3. Reactive loading
4. Source VSWR
5. Transmission line loss

The first three error sources result in a net error in the excess noise temperature of the source while the remaining two cause errors in available output noise temperatures.

All noise diodes are operated in the temperature-limited region of operation (Lawson and Uhlenbeck, 1950, p. 83). This means that the electric field between plate and cathode is strong enough to cause every electron emitted from the cathode to be attracted to the plate. If for some reason the electric field drops below a critical value where all electrons are not attracted, the diode current will be limited by the space charge cloud of electrons around the cathode. This space charge suppression lowers the mean-square noise current of the diode. A space-charge-suppression factor \mathcal{T}^2 is used to account for the reduction where:

$$0 \leq \mathcal{T}^2 \leq 1$$

The factor \mathcal{T}^2 is very nearly unity for a good diode noise source. Space charge suppression is discussed by van der Ziel (1954, p. 134) and by Quate (in Smullin and Haus, 1959, Chapter 1) but it is not easy to arrive at a good experimental equation for \mathcal{T}^2 . Hart (1962) discusses the effect of plate voltage on the space-charge-reduction factor and gives experimental values. Data on a typical noise diode indicates less than 1% reduction in shot noise when the plate voltage is greater than 100 V.

Transit-time error has been analyzed by Fraser (1949) and by van der Ziel (1954, p. 126). Fraser derived an equation for the transit-time reduction factor by applying Fourier analysis and statistics to the shot noise current. Fraser's equation is

$$\gamma_{\tau} = \frac{4}{(\omega\tau)^4} \left[(\omega\tau)^2 + 2(1 - \cos\omega\tau - \omega\tau \cos\omega\tau) \right] \quad (10B.59)$$

where ω = operating frequency, rad/sec

τ = electron transit time, sec.

The electron transit time in a planar diode is (van der Ziel, 1954, p. 372)

$$\tau = \frac{2d}{\sqrt{\frac{2q}{m} V_d}} = \frac{3.4 \times 10^{-6} d}{\sqrt{V_d}} \quad (10B.60)$$

where d = plate spacing in meters

q = electronic charge

m = electronic mass

V_d = plate voltage.

For small values of $(\omega\tau)$ the transit-time reduction factor is approximated by expanding the sin and cos terms in (10B.59) in terms of a power series and ignoring higher order terms (van der Ziel, 1954, p. 128):

$$\gamma_\tau \approx 1 - \frac{1}{18} (\omega\tau)^2 \quad (\omega\tau) < \frac{1}{5} \quad (10B.61)$$

After substituting (10B.60) into (10B.61) we get,

$$\gamma_\tau \approx 1 - 7.4 f^2 \frac{d^2}{V_d} \quad (10B.62)$$

as the transit-time reduction factor where f is the operating frequency in MHz.

The third source of error is caused by stray reactances in the noise diode circuits. Figure 10B-4 is a circuit model of a diode noise source showing parallel diode capacitance C_o , series inductance L_o , and termination admittance Y_T .

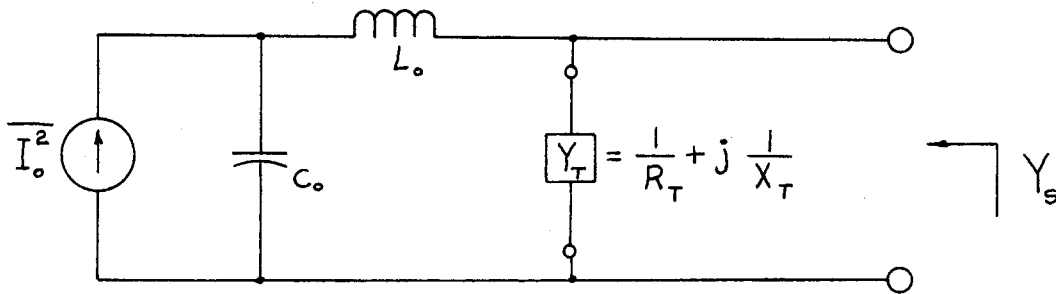


Figure 10B-4. Diode Noise Source Illustrating Noise Current Generator, Stray Reactances, and Termination Admittance

Applying Fourier analysis techniques to the noise generator circuit, and assuming that X_T is adjusted so the source impedance, Y_s , is real, we get the equivalent circuit of Figure 10B-5.

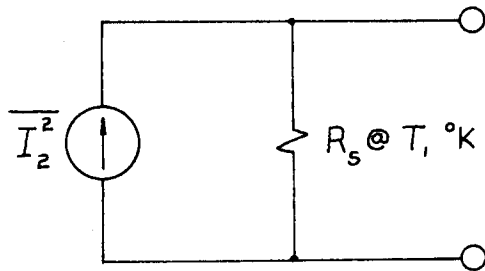


Figure 10B-5. Reduce Equivalent Circuit for Diode Noise Source

The mean-square noise current is

$$\overline{I_2^2} = \frac{1}{\left(1 - \frac{\omega^2}{\omega_o^2}\right)^2} \overline{I_o^2} \quad (10B.63)$$

where $\omega_o^2 = \frac{1}{L_o C_o}$ is the resonant frequency of the series-tuned circuit.

The error due to stray reactance can be accounted for by yet another reduction factor defined as:

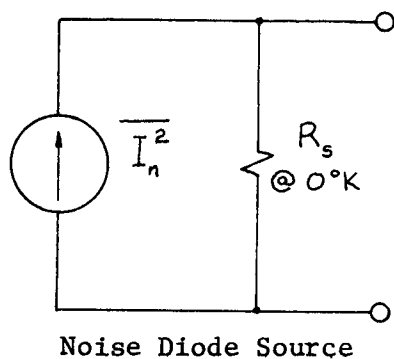
$$\gamma_s = \frac{1}{\left(1 - \frac{\omega^2}{\omega_o^2}\right)^2} \quad \frac{\omega}{\omega_o} < 1 \quad (10B.64)$$

When all three reduction factors are taken into account, the equivalent mean-square noise current for the noise diode becomes:

$$\overline{I_2^2} = 2q I_s \gamma_r \gamma_s T^2 \Delta f \quad (10B.65)$$

A circuit model for the practical noise diode can now be given in terms of the source resistance R_s and the effective noise temperature of the diode. Figure 10B-6 is analogous to Figure 4F.2 in Chapter IV and illustrates how to account for shot noise reduction or modification.

The effects of shot noise reduction and stray reactances are reflected in manufacturers specifications on noise diodes. Figure 10B-8 shows the frequency dependence and error limits on both excess noise ratio and effective noise temperature for a VHF noise diode source. Note the tendency for both the excess noise and the error limits to increase with frequency. The upper frequency limit of 600 MHz is determined by



$$\overline{I_n^2} = 4k T_{\text{eff}} \frac{1}{R_s} \Delta f$$

$$T_{\text{eff}} = \frac{q}{2k} R_s I_s \gamma_s \gamma_r T^2 + T_i$$

$$T_{\text{ex}} = \frac{q}{2k} R_s I_s \gamma_s \gamma_r T^2$$

Figure 10B-6. Circuit Model for a Practical Noise Diode which Accounts for Excess Noise Temperature Errors

transit-time effects. For measuring the noise figure of low-noise amplifiers, the ENR accuracy of ± 0.5 db at the higher frequencies is really not very good and, if better accuracy is desired, one must resort to hot-cold sources or more accurately calibrated diode sources.

The available output noise power for a noise diode source with transmission line is determined the same as it was for a hot-cold noise source. The noise-diode source equivalent circuit used for error determination and measurement of noise figure is shown in Figure 10B-7.

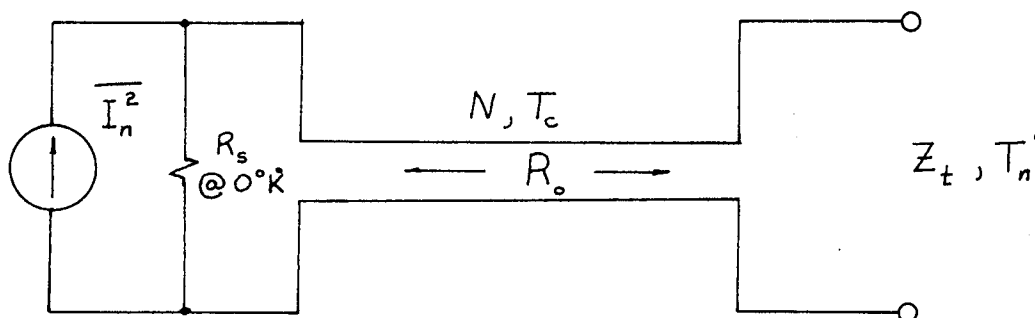


Figure 10B-7. Equivalent Circuit for a Diode Noise Source

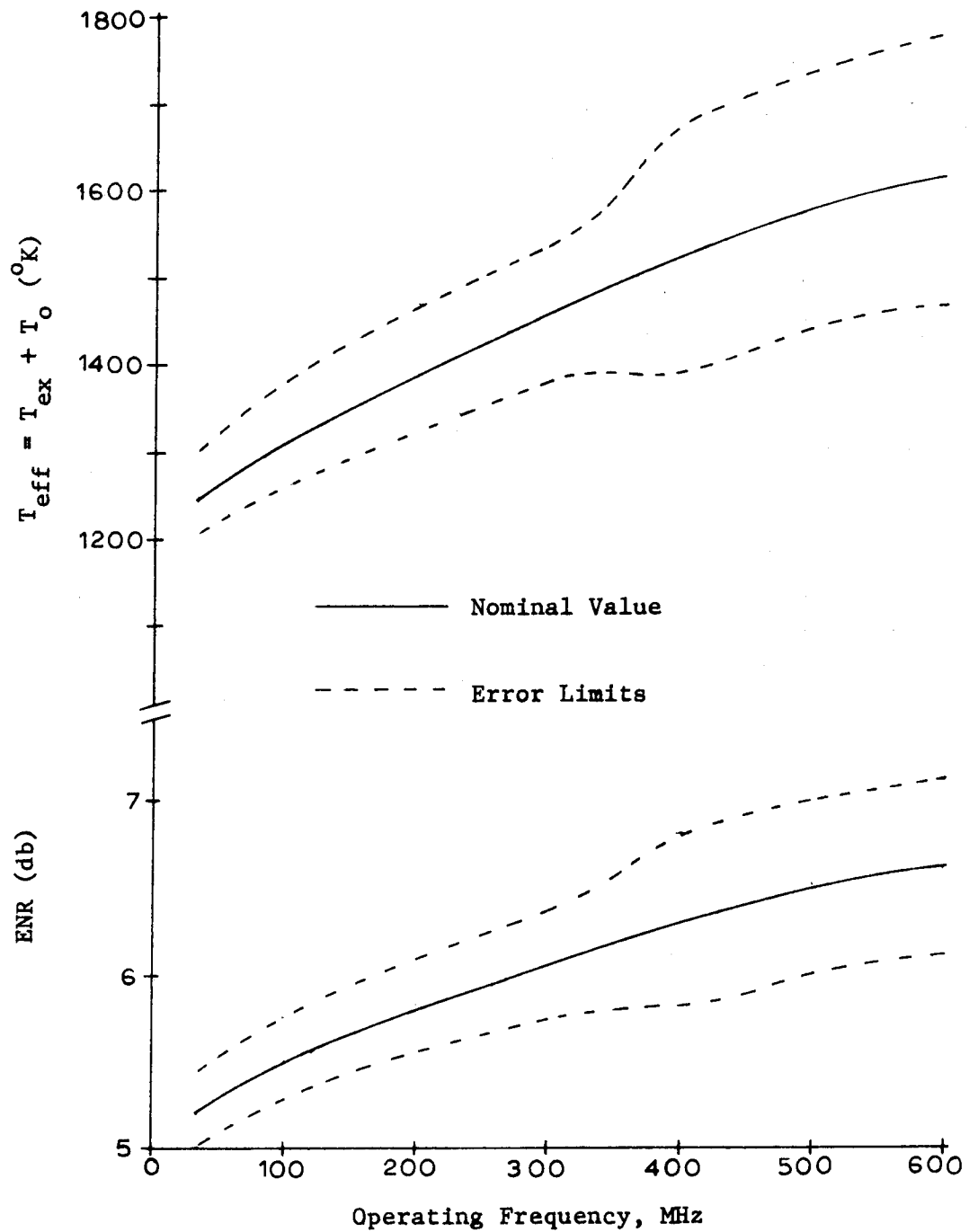


Figure 10B-8. Frequency Dependence of Excess Noise and Error Limits for a Typical VHF Noise Diode Source

The available output noise temperature is (similar to Equations 10B.37 or 10B.39)

$$T_n' = T_{eff} \left[1 + \left(1 - \frac{1}{\rho} \right) \left(\frac{T_c}{T_s} - 1 \right) \right] \quad (10B.66)$$

and the output impedance Z_t is determined by Equation 10B.24. The available loss is computed from (10B.29). The uncertainty in available output noise temperature is given as (similar to Equation 10B.43)

$$|\Delta T_n'| \leq |\Delta K_s| T_{eff} + |\Delta T_{eff}| [1 + K_s + |\Delta K_s|] \quad (10B.67)$$

where K_s is computed from (10B.46b) and $|\Delta K_s|$ is computed from (10B.49). The approximations discussed for the case of low VSWR which resulted in Equations 10B.54 through 10B.58 are also valid for the noise diode source.

3. Gas-discharge

The errors which are inherent in the operation of the gas-discharge noise source are:

1. Output coupling of gas-discharge to transmission line or waveguide
2. Errors in electron temperature of the discharge column caused by variations in pressure, physical size and current (see Olson in Mumford, 1968)
3. Change in output impedance between fired and unfired conditions

4. Transmission line loss.

The situation involved in analyzing the error in the excess noise temperature of a gas-discharge noise source is the same as that for the hot-cold source. The only difference between the two is the mechanism of noise generation. The "hot" or fired noise temperature T_2 is the sum of the excess noise temperature and 290° K. Typical uncertainties in the excess noise ratio of coaxial and waveguide noise sources are ± 0.25 to ± 0.6 db. The uncertainties in measured noise figure associated with VSWR changes and ENR uncertainties will be discussed in Section E of this chapter.

4. Sinewave generator

The errors associated with an AM signal generator were discussed in Section C of Chapter IX but they will now be summarized along with those for FM and Pulse generators. The sources of error common to all generators are:

1. Output level errors caused by attenuator inaccuracy and level detector error
2. Generator VSWR
3. Modulation errors and residual modulation
4. RF leakage
5. Generator excess noise
6. Output indicator interpretation.

The absolute accuracy of the output level is determined by the accuracy of the variable output attenuator and output level detector. The output level detector is some type of rectifier circuit which

samples the RF level input to the output attenuator and feeds a proportional dc level to a meter for accurate level setting. This scheme cannot have a better accuracy than the components used in its construction and usually has a $\pm 5\%$ error caused by resistor and meter errors. The attenuator accuracy depends upon mechanical tolerances used in its construction. These two errors determine the output level accuracy of the generator. The accuracy obtainable in high quality laboratory signal generators is ± 0.25 to ± 1.0 db. Output level specifications should be carefully checked on any signal generator used for sensitivity measurements.

The VSWR of the generator will affect the available output power if a lossy transmission line is used to connect the generator to the receiver. The available signal power from the transmission line can be computed from Equation 10B.7 with $|a_s|^2$ written in terms of the open circuit RMS voltage of the generator, E_s :

$$P_s = \frac{1}{\mathcal{L}} \frac{E_s^2}{4R_s} \quad (10B.68)$$

The available loss, \mathcal{L} , is computed from Equation 10B.29. The uncertainty in P_s is obtained from Equation 10B.52 because P_s is proportional to \mathcal{E} . If we assume VSWR's of less than 1.5, the uncertainty in P_s due to the uncertainty in \mathcal{E} becomes

$$|\Delta P_s| \leq \left[\frac{(N^2 - 1)}{N^3} |\Delta |T_s|^2| + \frac{|\Delta N|}{N^2} \right] \cdot \frac{E_s^2}{4R_s} \quad (10B.69)$$

where N = the line attenuation factor

$|T_s|^2$ = the squared absolute value of the source reflection coefficient

$|\Delta N|$ = uncertainty in N

$|\Delta |T_s|^2|$ = uncertainty in $|T_s|^2$.

The uncertainty in P_s due to an uncertainty in E_s^2 is simply a db for db relationship.

As an example, consider a signal generator with an output level accuracy of ± 1.0 db and a coaxial cable with 1.0 ± 0.2 db loss. The maximum VSWR of the generator is 1.2 at the frequency of consideration. The uncertainty, in db, of the available output noise power is the sum of the generator output level accuracy and the logarithmic uncertainty in P_s

$$1.0 \text{ db} + 10 \log \left[1 \pm \frac{|\Delta P_s|}{P_s} \right] \quad (10B.70)$$

and:

$$\frac{|\Delta P_s|}{P_s} = \frac{(N^2 - 1)}{N^2} |\Delta |T_s|^2| + \frac{|\Delta N|}{N} \quad (10B.71)$$

We compute the following quantities:

$$N = 1.26 \quad |\Delta N| = 0.06$$

$$\left| \Delta \left| T_s \right| \right|^2 = \left| \frac{VSWR - 1}{VSWR + 1} \right|^2 \approx 0.83 \times 10^{-2}$$

$$\frac{|\Delta P_s|}{P_s} = \frac{(1.26)^2 - 1}{(1.26)^2} (0.83 \times 10^{-2}) + \frac{0.06}{1.26} = 0.051$$

The total uncertainty in available output power is computed from (10B.70):

$$\pm (1.0 \text{ db} + 0.22 \text{ db}) = \pm 1.22 \text{ db}$$

Modulation index errors and residual modulation cause errors in the measured level of recovered audio. In AM signal generators, the recovered audio power is proportional to the product of the available input power and the modulation index squared:

$$\text{Audio Power, } P_A \sim m^2 P_s \quad (10B.72)$$

The modulation index is characterized by some actual value plus an error term

$$\tilde{m} = m + \Delta m$$

or squaring \tilde{m} we get:

$$\tilde{m}^2 = m^2 + 2 m \Delta m + (\Delta m)^2$$

If the term $(\Delta m)^2$ is neglected, Equation 10B.72 becomes:

$$(P_A + \Delta P_A) = \tilde{P}_A \sim [m^2 P_s + 2m \Delta m P_s]$$

The relative error is obtained by normalizing the measured value of recovered audio power with the true value:

$$\frac{\tilde{P}_A}{P_A} = 1 + \frac{\Delta P_A}{P_A} = 1 + 2 \frac{\Delta m}{m} \quad (10B.73)$$

The uncertainty in recovered audio power due to an uncertainty in the modulation index can be expressed in db as:

$$\delta m = 10 \log \left[1 \pm 2 \frac{|\Delta m|}{m} \right] \quad (10B.74)$$

The δ -notation will be used to denote uncertainty in db (see Appendix, Part S). For a high quality laboratory generator, a typical modulation accuracy is $\pm 5\%$ at 30% AM. This results in an uncertainty in the recovered audio power of:

$$10 \log \left[1 \pm 2 \frac{1.05}{.30} \right] = \begin{cases} +1.25 \text{ db} \\ -1.60 \text{ db} \end{cases}$$

This error is of considerable significance in any scheme involving the use of a sinewave generator to measure the noise figure of a receiver.

From the FM theory of Chapter VIII, we stated that the input and output signal-to-noise ratios were related to the deviation ratio, D , by the equation:

$$\text{Output SNR} = \text{Input SNR} + 10 \log 3D^2 \quad (10B.75)$$

If the deviation ratio is represented by a nominal value plus error term, the same technique that was used for modulation index can be used for deviation ratio and the uncertainty in output SNR due to the uncertainty in deviation ratio becomes:

$$\delta D = 10 \log \left[1 \pm 2 \frac{|\Delta D|}{D} \right] \quad (10B.76)$$

Typical accuracy for the deviation ratio of an FM signal generator is $\pm 5\%$ for a deviation ratio, $D = 2$. This results in an uncertainty in the output signal to noise ratio or output recovered audio of:

$$10 \log \left[1 \pm 2 \frac{1.05}{2} \right] = \pm 0.22 \text{ db}$$

This magnitude of error is not as important as that for the AM case and is of minor importance when compared to the output level accuracy of ± 1.0 db.

Residual AM and FM must be kept low because they represent modulation on the carrier which is not under control of the user. Their presence will result in low-level audio outputs which interfere with signal-to-noise ratio measurements. These spurious audio outputs must be well below the normal recovered audio for accurate measurements.

Spurious FM should be down at least 40 db and spurious AM down 25 db.

RF leakage from the high level circuits within the generator can couple to the receiver and make the attenuator readings very inaccurate. The amount of RF leakage will vary with test setup and with the physical condition of the generator. Most signal generators designed for general laboratory use have enough RF leakage that they cannot be used for sensitivity measurements below 1 μV . Generators specifically designed for measuring sensitivities can be used down to levels of 0.1 μV . If levels lower than this are required, a special test setup using shield rooms and careful layout is usually required.

In some special cases, the generator may contribute noise to the system which is above the thermal noise of the source impedance. When this occurs, this excess noise will add to the receiver noise temperature so that it will appear to have a higher noise figure. Although this is a rare problem, the possibility of generator excess noise should be examined when making sensitivity measurements.

A very common error which is usually committed by the newcomer to sensitivity measurements is that of misinterpreting the output dial reading. The RF output of most signal generators is not calibrated in open circuit voltage (hard microvolts) but in output voltage across a matched load (soft microvolts). If the open circuit voltage is measured it will be 6 db higher than the output dial reading. Sensitivity measurements are usually stated in open circuit or "hard microvolts" so a measurement using soft microvolts will be 6 db too optimistic. To eliminate this conversion problem, a 6 db pad can be connected at

the generator output and then the output dial will read the open circuit output of the pad. A further discussion of hard and soft microvolts is given in Part Q of the Appendix. A common method of avoiding this problem is to state all sensitivities in available power (usually in DBM).

C. Detectors and Output Indicators

The sensitivity measurement errors which are caused by the detector or output indicator are attributed to:

1. Detector power gain nonlinearity
2. Detector threshold effects
3. Fundamental detection limits
4. Flicker noise in the low-frequency amplifiers.

Quite often the measurement of noise involves the use of two detectors, the detector in the receiver and the detector in the AC voltmeter used to measure the audio noise. When considering the sensitivity measurement problem it is important to account for both detectors. This situation will not receive special treatment because it can be accounted for by the detector theory that is presented in Chapter VI and this chapter.

A nonlinearity exists between the power input and the indicated power output for all detectors. This power gain nonlinearity introduces an error into any ratio measurements.

The effects of power gain nonlinearity are difficult to determine and about the only thing that can be done is to calibrate the detector. Figure 10C-1 shows qualitative data on the linearity of a typical detector.

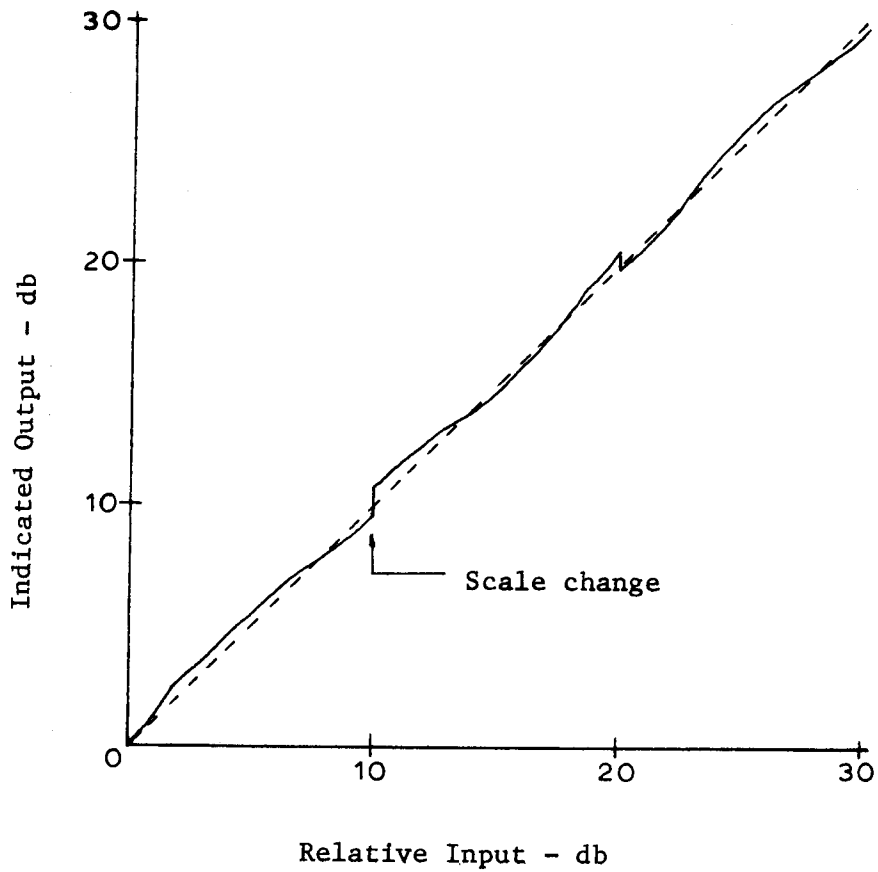


Figure 10C-1. Power-Gain Linearity for a Typical Power Detector

The discontinuities at each 10 db increment are caused by scale changes on the instrument which introduce different components into the signal path. It can be seen from this curve that a given output change in db does not generally correspond to an equal change at the input.

Detector errors due to threshold effects are more obvious and often more detrimental than nonlinearity errors. Threshold effects can occur because of a very nonlinear characteristic such as the diode

detector at low levels or from statistical effects when a sinewave and noise are both present at the diode input. The threshold effect in a diode detector is discussed by Golding (1968) and the reduction in output SNR for low input-SNR is presented by Fubini and Johnson (1948), Middleton (1960) and Davenport and Root (1958, p. 266). The threshold effect for a noise signal is illustrated by Figure 10C-2. The output noise power v.s. input noise power is very nonlinear until a threshold is reached. In the vernacular language of the communications engineer, the detector is said to be "saturated" when the threshold is exceeded. When a diode detector is operated above the threshold it can be characterized by a linear detector. For very small signals, the diode detector behaves like a square-law detector.

The region of linear operation, between threshold and limiting, is not very wide and illustrates that the use of a diode detector should be limited to the known region of linear operation. In many situations the gain of the IF section of a receiver can be adjusted to bring the detector into the linear region. Usually the gain of the receiver is high enough to bring the detector into "saturation" on just the thermal noise of receiver and source.

The reduction of the signal-to-noise ratio for low inputs is illustrated with the help of Figure 10C-3. These are curves for theoretical and experimental data on a square-law detector (Fubini and Johnson, 1948). The carrier-to-noise ratio is defined as:

$$\frac{\text{Available Carrier Power}}{\text{Predetection Noise Power}} = \frac{\frac{E_s^2}{4R_s}}{k(T_o + T_e) B_h}$$

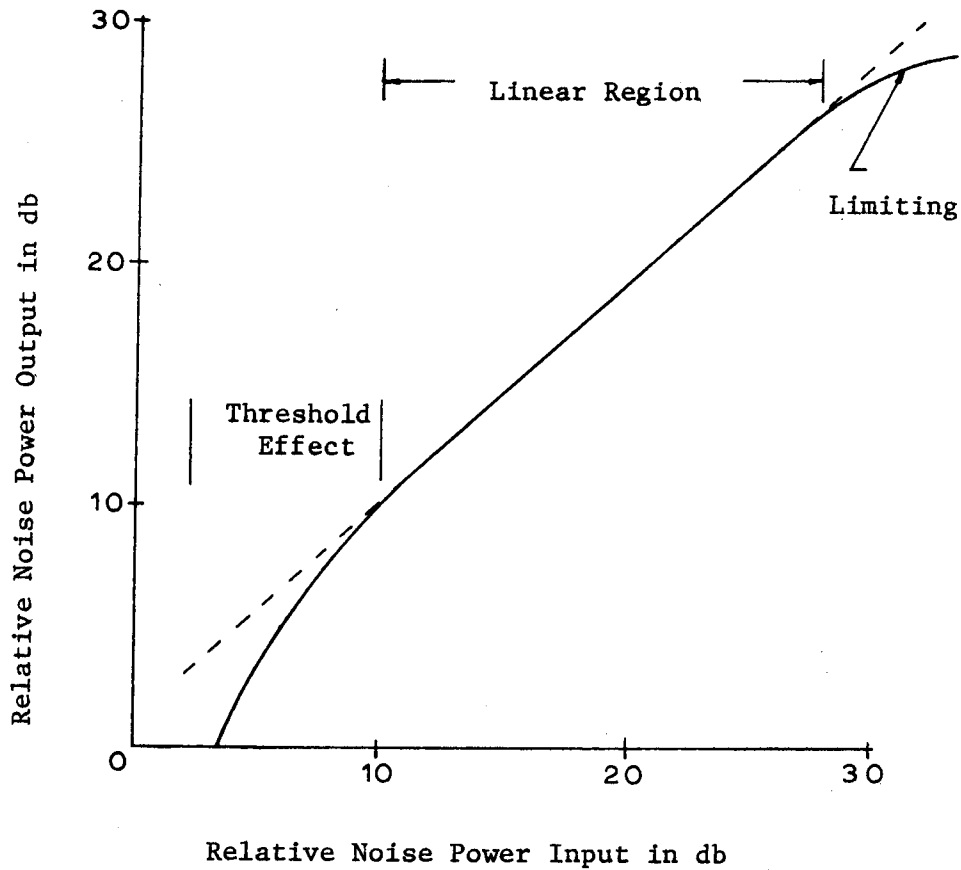


Figure 10C-2. Threshold Effect in a Diode Detector

where

- E_s = Input sinewave signal in hard volts
- R_s = Source resistance
- T_e = Effective noise temperature of the receiver
- B_h = Predetection noise bandwidth

The output signal-to-noise ratio depends on the modulation index, m , and the postdetection noise bandwidth, B_L . The output SNR has been

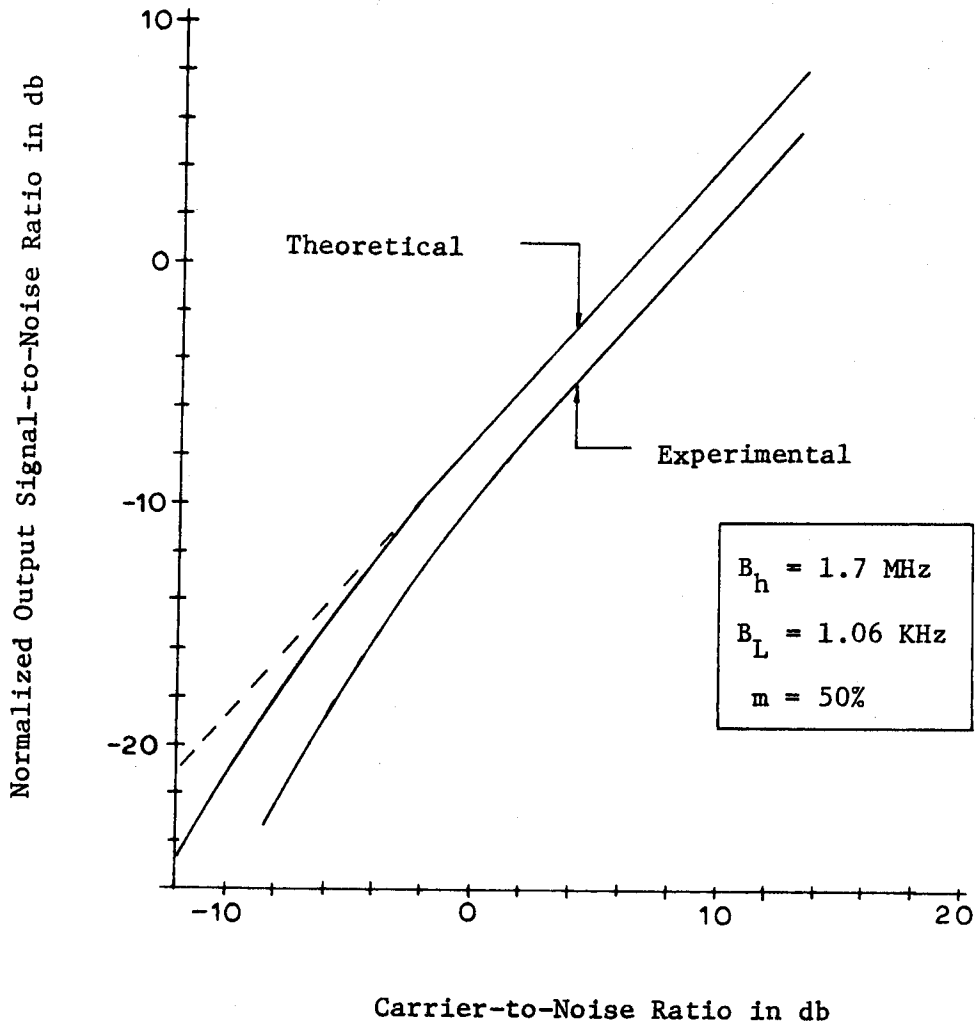


Figure 10C-3. Theoretical and Experimental Curves for Determining Output Signal-to-Noise Ratio of a Square-Law Detector

normalized to account for variations in predetection and postdetection noise bandwidths. To get the true output SNR a factor

$$10 \log \frac{B_h}{2 B_L} \quad (B_h > B_L)$$

must be added to the normalized value given by Figure 10C-3. For the data given in the figure, the carrier was 50% modulated and the IF and AF noise bandwidths were 1.7 MHz and 1.06 KHz respectively. The reader is reminded that all of this discussion is valid only when the post-detection noise bandwidth is much smaller than the predetection noise bandwidth. For an AC voltmeter this criterion is almost always satisfied because the response time is usually larger than $1/10^{\text{th}}$ sec.

A single reading of the output detector will always have an error caused by noise on the DC level being measured. This noise comes from two sources, the low-frequency noise output of the detector and the flicker noise in the audio or DC amplifiers. The RMS deviation due to detector noise can be calculated from the noise bandwidths but the flicker noise cannot. Flicker noise cannot be filtered because it has a spectrum which goes to DC. The simplest method to use in reducing flicker noise effects is to average out the flicker noise contribution. This can be done by numerical signal averaging.

The actual measurement situation is best illustrated with the help of Figure 10C-4. The detector output to a sensory transducer will consist of the following:

1. A nominal dc output voltage level, V_o , determined by the total power input to the detector
2. A change in dc output level, ΔV_o , caused by a change in the input signal
3. A superimposed noise voltage due to flicker noise
4. A superimposed noise voltage due to the low-frequency noise output of the detector.

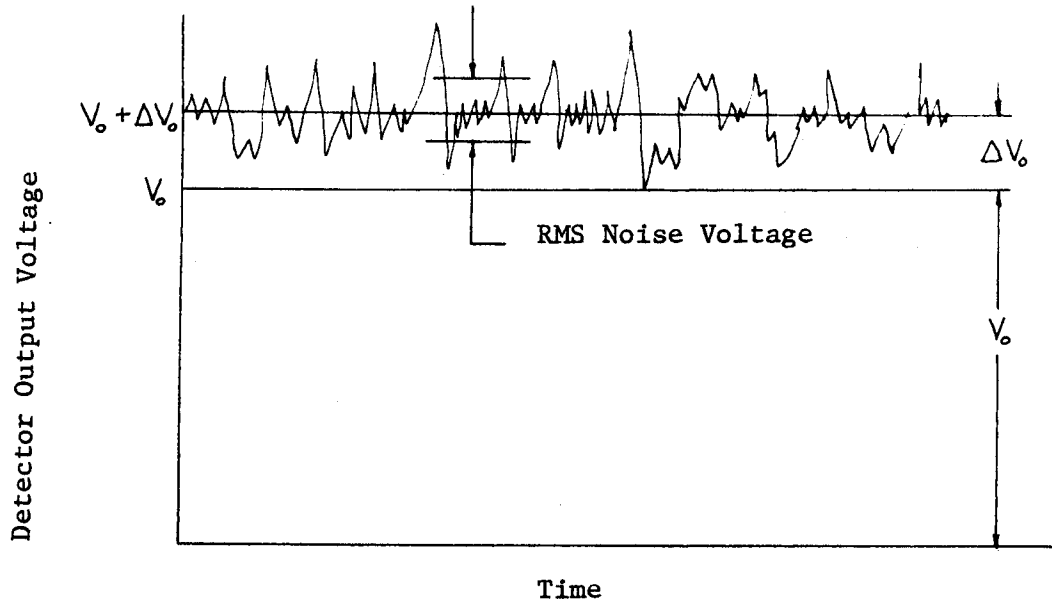


Figure 10C-4. Output Voltage of a Detector Showing DC Levels and Superimposed AC Noise Voltage

The information really needed is the nominal output V_o , the change ΔV_o and the error caused by the noise. In most situations, the nominal value of DC output is known and can be subtracted from any measurement data. In some detector applications, the nominal DC output is subtracted from the total by a DC level shifter so that the recorded output is ΔV_o plus the noise. For these reasons we will not include V_o as part of the explicit output data. The schemes that will be used to determine measurement errors will be concerned with ΔV_o and noise.

The simplest method of determining the average output and probable error is to determine the mean and standard deviation of several data points taken from the output. A commonly adopted technique of reporting error limits is to report the standard deviation. The numerical

techniques for analyzing data can be found in any text on data analysis or statistics. The basic equations for computing the mean and standard deviation will now be given. The following terms are defined where X will represent the measured quantity (in this case ΔV_o):

N = number of data points or voltage measurements taken
at equal time intervals

\bar{X} = mean value of the voltage change

X_i = data point voltage.

Mean Value

$$\bar{X} = \frac{\sum_{i=1}^N X_i}{N} \quad (10C.1)$$

Variance

$$\sigma^2 = \frac{\sum_{i=1}^N (X_i - \bar{X})^2}{N} = \frac{\sum_{i=1}^N X_i^2}{N} - \bar{X}^2 \quad (10C.2)$$

The standard deviation is the square root of the variance or simply σ . This method of reporting the error in a voltage measurement is by no means complete but it does serve as a basis for comparing the relative accuracy of a variety of measurements.

To be more specific on reporting this error, it is convenient to define a quantity called the relative error of a single measurement. This quantity is the ratio of the standard deviation of the noise divided by the mean value:

$$\sqrt{\alpha} \triangleq \frac{\sigma}{\bar{X}} = \frac{\sqrt{\sum_{i=1}^N (x_i - \bar{X})^2}}{\bar{X} \sqrt{N}} \quad (10C.3)$$

The notation $\sqrt{\alpha}$ is used by van der Ziel (1954, p. 338). This relative error is not an absolute one and thus any particular measurement may be in error by more than this amount. The relative error of a single measurement, $\sqrt{\alpha}$, gives the expected RMS deviation between a single reading and the average reading. The concept of relative error and RMS deviation is used in radio astronomy and noise measurement theory to specify the accuracy of a noise temperature measurement.

It is common practice to report the lowest measurable value of a voltage or current as that which gives a voltage signal-to-noise ratio of unity. This gives a value of unity for the relative error, $\sqrt{\alpha}$, and means that the RMS deviation of the noise is equal to the voltage level being measured. This idea was used to determine the minimum detectable noise temperature discussed in Chapter VI-C.

The RMS deviation caused by flicker noise cannot be calculated on a theoretical basis but that caused by low-frequency detector noise can be calculated. The equation for the output VSNR of the square-law detector (6.47) has more general validity than was indicated in Chapter VI. It can be used to calculate the relative error because the VSNR defined in this way is a relative error. Using the reciprocal of (6.47) we get the relative error for a single measurement as:

$$\sqrt{\alpha} = K_F \sqrt{\frac{2 B_L}{B_h}} \quad (10C.4a)$$

where K_F = shape correction factor defined in Chapter VI
 B_h = predetection noise bandwidth
 B_L = postdetection noise bandwidth.

Since the low-pass filter actually performs an integration on the output signal, it is conceptually easier to define an equivalent integration time, τ_o , as

$$\tau_o = \frac{1}{2 B_L} \quad (10C.5)$$

which is substituted into (10C.4a) to give:

$$\sqrt{\alpha} = \frac{K_F}{\sqrt{B_h \tau_o}} \quad (10C.4b)$$

To obtain the relative error for any particular detector is now a matter of finding the predetection and postdetection equivalent noise bandwidths and the shape correction factor, K_F . Kraus (1966, p. 246) has given a table of equivalent integration times for simple low-pass filters and van der Ziel (1954, Ch. 13) has derived expressions for $\sqrt{\alpha}$ for various detector types. For a square-law detector, Table 10-1 gives the equivalent integration times for several filter types.

The relative error computed with (10C.4b) is only that error due to detector noise output and not that due to flicker noise. In a well designed system, the error limit should only depend on detector noise

Table 10-1. Equivalent integration times of several low-pass filters

Type of Filter	Equivalent Integration Time, τ_o
Ideal integrator	τ
Ideal low-pass filter (low-pass zonal filter)	$\frac{1}{2B_L}$
Single RC filter	$2RC$
Two RC filters in cascade	$4RC$
Second-order filter	$\frac{4\delta}{\omega_o}$
Critically damped galvanometer with time constant τ_1	$4\tau_1$

and not on flicker noise but, on the other hand, flicker noise always determines the ultimate limit.

The minimum detectable change in detector output voltage based on the unity VSNR assumption and the RMS deviation is:

$$(\Delta V_o)_{\min} = V_o \sqrt{\alpha} \quad (10C.6)$$

As an example, consider a noise power detector with a single tuned circuit for a predetection filter and a single RC filter for a post-detection filter. The relative error is:

$$\sqrt{\alpha} = \frac{0.707}{\sqrt{B_h(2RC)}}$$

If the relative error is to be less than 1%, $\sqrt{\alpha}$ must be less than 0.01 or by manipulation of the above equation:

$$B_h(2RC) > 5 \times 10^4$$

For a predetection noise bandwidth of 10 KHz, the RC filter time constant must be greater than 2.5 seconds.

D. Attenuators

Variable and fixed attenuators are used in the Y-factor and noise diode methods of measuring noise figure. When an attenuator is inserted into the signal path, the resulting attenuation is generally not equal to the attenuation determined by the flat loss or matched attenuation. This error or uncertainty in insertion loss has a large effect on noise figure measurement accuracy. The uncertainty in insertion loss can be determined with the use of the equations developed in Section B of this chapter. The equivalent circuits for determining insertion loss are shown in Figure 10D-1.

The power delivered to the load when the attenuator is inserted is obtained by combining Equations 10B.3 and 10B.13 to get:

$$P_{s1} = \frac{E_s^2}{4 \operatorname{Re}(z_s)} \cdot \frac{|S_{21}|^2 (1 - |\Gamma_r|^2)(1 - |\Gamma_s|^2)}{\left| (1 - S_{11}\Gamma_s)(1 - S_{22}\Gamma_r) - S_{12}S_{21}\Gamma_r\Gamma_s \right|^2} \quad (10D.1)$$

When the attenuator is removed and the source and load are connected, the power delivered to the load is computed from (10D.1) by substituting

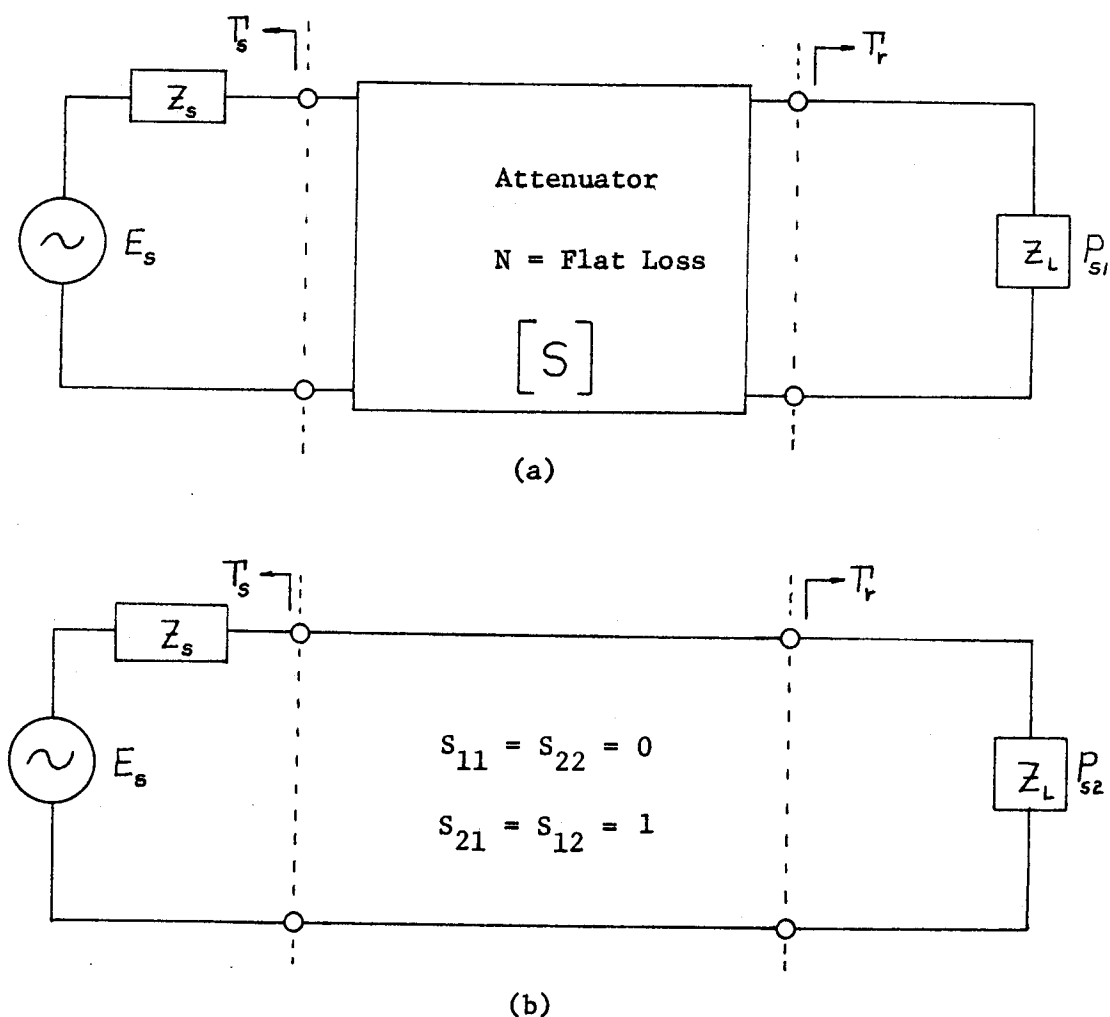


Figure 10D-1. Equivalent Circuits for Computing Insertion Loss and Insertion Loss Error

the scattering matrix for a direct connection ($S_{11} = S_{22} = 0$, $S_{12} = S_{21} = 1$):

$$P_{s2} = \frac{E_s^2}{4 \operatorname{Re}(Z_s)} \cdot \frac{(1 - |P_r|^2)(1 - |P_s|^2)}{|1 - P_r P_s|^2} \quad (10D.2)$$

The insertion loss of the attenuator, L , is determined by the ratio of the power delivered to the load with the attenuator to that without:

$$L = \frac{P_{s1}}{P_{s2}} = \frac{|S_{21}|^2 |1 - \Gamma_r \Gamma_s|^2}{|(1 - S_{11} \Gamma_s)(1 - S_{22} \Gamma_r) - S_{12} S_{21} \Gamma_r \Gamma_s|^2} \quad (10D.3)$$

The flat-loss of the attenuator is the loss measured when the source and load reflection coefficients are zero:

$$\text{Flat loss, } N = \frac{1}{\epsilon} = \frac{1}{|S_{21}|^2} \quad 0 \leq \epsilon \leq 1$$

The insertion loss, L , in terms of the transmission efficiency, ϵ , is

$$L = \epsilon \frac{|1 - \Gamma_r \Gamma_s|^2}{|(1 - S_{11} \Gamma_s)(1 - S_{22} \Gamma_r) - S_{12} S_{21} \Gamma_r \Gamma_s|^2} \quad (10D.4)$$

where both L and ϵ are less than unity.

The terms containing the scattering and reflection coefficients can be grouped together into a single term which will be called the insertion loss error factor, γ_L :

$$\gamma_L = \frac{|1 - \Gamma_r \Gamma_s|^2}{|(1 - S_{11} \Gamma_s)(1 - S_{22} \Gamma_r) - S_{12} S_{21} \Gamma_r \Gamma_s|^2} \quad (10D.5a)$$

The insertion loss error factor is a positive real number which is close to unity but can be either larger or smaller. If all the parameters of (10D.5) are known then the error factor can be computed directly but usually only the magnitudes of the errors are known. Before attempting to derive the uncertainty in insertion loss it will be necessary to make some simplifying assumptions:

1. The VSWR of the attenuator is low so that $S_{11} = S_{22} \approx 0$.
2. The attenuator is symmetric and the transmission coefficient is:

$$S_{12} = S_{21} = \sqrt{\epsilon} e^{j\frac{\theta_s}{2}}$$

Then (10D.5a) becomes:

$$\gamma_L \approx \frac{|1 - T_r T_s|^2}{|1 - S_{12} S_{21} T_r T_s|^2} \quad (10D.5b)$$

The range of values of γ_L can be obtained by using some complex algebra on Equation 10D.5b. First let

$$T_r T_s = |T_r| |T_s| e^{j\theta_r}$$

where θ_r is the sum of the phase angles of T_r and T_s . Substituting this expression into (10D.5b) gives

$$\gamma_L \approx \frac{1 - 2|T_r||T_s|\cos\theta_r + |T_r|^2|T_s|^2}{1 - 2\epsilon|T_r||T_s|\cos(\theta_r + \theta_s) + \epsilon^2|T_r|^2|T_s|^2} \quad (10D.5c)$$

which is in terms of the magnitudes of the parameters and the phase angles of S_{21} , T_s , and T_r . The phase angles are generally unknown so the limits on γ_L are determined by worst case values of the θ 's. The

maximum, minimum and impedance matched values of γ_L are determined from (10D.5c) as follows:

$$1. \cos \theta_r = -1 \quad \cos(\theta_r + \theta_s) = +1$$

$$\gamma_L(\max) = \frac{1 + 2|\Gamma_r||\Gamma_s| + |\Gamma_r|^2|\Gamma_s|^2}{1 - 2\epsilon|\Gamma_r||\Gamma_s| + \epsilon^2|\Gamma_r|^2|\Gamma_s|^2} \quad (10D.6)$$

$$2. \cos \theta_r = +1 \quad \cos(\theta_r + \theta_s) = -1$$

$$\gamma_L(\min) = \frac{1 - 2|\Gamma_r||\Gamma_s| + |\Gamma_r|^2|\Gamma_s|^2}{1 + 2\epsilon|\Gamma_r||\Gamma_s| + \epsilon^2|\Gamma_r|^2|\Gamma_s|^2} \quad (10D.7)$$

$$3. \cos \theta_r = 0 \quad \Gamma_s = \Gamma_r^*$$

$$\gamma_L(\text{match}) = \frac{1 + |\Gamma_r|^2|\Gamma_s|^2}{1 - 2\epsilon|\Gamma_r||\Gamma_s|\cos\theta_s + \epsilon^2|\Gamma_r|^2|\Gamma_s|^2} \quad (10D.8)$$

If the reflection coefficients are small, the factors containing squared terms can be neglected. Applying a binomial expansion to the denominators of (10D.6) and (10D.7) and neglecting higher order terms gives the approximate solutions:

$$\gamma_L (\max) \approx 1 + 2 (1 + \epsilon) |T_r| |T_s| \quad (10D.9)$$

$$\gamma_L (\min) \approx 1 - 2 (1 + \epsilon) |T_r| |T_s| \quad (10D.10)$$

The total uncertainty in insertion loss can be computed by adding the uncertainty due to the accuracy of the specified flat loss with that due to mismatch. The result, in db, is given in the following equation:

$$\delta L = \pm \delta \epsilon + 10 \log [1 \pm 2 (1 + \epsilon) |T_r| |T_s|] \quad (10D.11)$$

The δ -notation is used to denote uncertainty in db (see Appendix, Part S). As an example, consider a typical fixed coaxial attenuator with a flat loss of $3 \pm .3$ db inserted into a circuit where the SWR of both source and load is 1.5. The following values are computed:

$$\delta \epsilon = \pm 0.3 \text{ db} \quad |T_r| = |T_s| = 0.2 \quad \epsilon = 1/2$$

The uncertainty in the insertion loss is:

$$\delta L = \pm 0.3 \text{ db} + 10 \log [1 \pm 2 (1 + 1/2) |.2| |.2|]$$

$$\delta L = \begin{cases} + 0.80 \text{ db} \\ - 0.85 \text{ db} \end{cases}$$

Finally, the insertion loss or change in receiver gain by the insertion of the 3 db attenuator is

$$\tilde{L}_{db} = 3.0 \text{ db } \begin{matrix} +0.80 \\ -0.85 \end{matrix}$$

so that the actual insertion loss or change in gain can range from 2.15 to 3.8 db. This error is very significant when measuring noise figure by the 3 db method.

In many circumstances the VSWR of a source or load can be improved by adding a calibrated attenuation without introducing other deleterious effects. The improvement in VSWR obtained by this method depends upon the flat loss of the attenuator and attenuator VSWR. The attenuator parameters are accounted for by its scattering parameters. The reflection coefficient at the attenuator output, Γ_2 , is related to the reflection coefficient of the generator by Equation 10B.1

$$\Gamma_2 = \frac{S_{22} + \Gamma_1 (S_{12} S_{21} - S_{11} S_{22})}{(1 - \Gamma_1 S_{11})} \quad (10D.12)$$

where Γ_1 = reflection coefficient of the source

Γ_2 = reflection coefficient of the attenuator output or
"improved" coefficient

[S] = scattering parameters of the attenuator.

If we are concerned with just the magnitudes of the reflection coefficients and if S_{11} and S_{22} are sufficiently small then (10D.12) reduces to:

$$|\Gamma_2| = |S_{12} S_{21}| |\Gamma_1| \quad (10D.13)$$

For a symmetrical attenuator, $|S_{12}S_{21}| = \epsilon$ (the attenuator flat loss), and after substituting Equation 10B.32 into (10D.13) and solving for the output VSWR we get:

$$VSWR_2 = \frac{(VSWR_1 + 1) + \epsilon(VSWR_1 - 1)}{(VSWR_1 + 1) - \epsilon(VSWR_1 - 1)} \quad (10D.14)$$

Equation 10D.14 is not valid for low values of VSWR because the output scattering coefficient of the attenuator was neglected in deriving (10D.14) from (10D.12). Practical limits on the output VSWR are:

$$\frac{1 + |S_{22}|}{1 - |S_{22}|} \leq VSWR_2 \leq VSWR_1 \quad (10D.15)$$

where the lower limit is the output VSWR of the attenuator when the source VSWR is unity. For a typical fixed coaxial attenuator the VSWR is less than 1.25.

A useful upper limit on output VSWR for large input VSWR is obtained from (10D.14) by using the approximation $VSWR_1 \gg 1$ to give:

$$VSWR_2 < \frac{1 + \epsilon}{1 - \epsilon} \quad (10D.16)$$

This also is an upper bound for (10D.14) as can be proved by a ratio test. As an example; if a 3 db attenuator ($\epsilon = 1/2$) is used to improve the source VSWR, the upper bound on the output VSWR is 3 regardless of the value of $VSWR_1$.

The effects of attenuator errors on insertion loss uncertainty can be quickly estimated using typical attenuator characteristics. The following typical specifications are included for convenience:

a. Variable attenuator - Flat loss accurate to $\pm 2\%$ of reading in db or ± 0.1 db, whichever is greater. The VSWR is less than 1.2 at both ports.

2. Fixed attenuator - Flat loss accuracies,

3 db \pm 0.3 db

10 db \pm 0.5 db

30 db \pm 1.0 db

The VSWR is less than 1.2 at both ports.

E. Measurement Methods

A groundwork of theory and techniques has been laid in this chapter and many other chapters to be used in this section. The concepts involved in describing errors in sensitivity measurements are difficult because of the large number of variables needed in each equation. The ideas and equations developed in previous chapters will be used extensively in this section. It will be necessary to use many approximations to arrive at reasonable uncertainty equations. The most tangible approach to error analysis will be to develop uncertainty equations with respect to a single variable.

The distinction needs to be made between the effects of circuit losses and errors on the measured sensitivity and the actual sensitivity. For example, a lossy coax cable will degrade the noise temperature of a receiver and will also introduce errors into any attempt to measure the

noise temperature. The equations which describe these two effects are quite different. To distinguish these cases, the following notation will be used:

- a. The use of a tilde, for example \tilde{T}_e , will denote a measured value.
- b. A primed quantity, for example T'_e , will denote a quantity modified by losses or VSWR.
- c. The unprimed variable is used to denote a true value or a value that is known, without error.

1. Y-factor

The equivalent noise factor or noise temperature of a two-port network can be written as (Equation 4F.57 or IRE Subcommittee on Noise, 1960b)

$$F'' = F_{\min} + \frac{B}{G_s} \left[(G_s - G_{s_{opt}})^2 + (B_s - B_{s_{opt}})^2 \right] \quad (10E.1)$$

$$T_e'' = T_e + T_o \frac{B}{G_s} \left[(G_s - G_{s_{opt}})^2 + (B_s - B_{s_{opt}})^2 \right] \quad (10E.2)$$

where F_{\min} and T_e correspond to two-port noise when the input is both noise matched and noise tuned e.g., $Y_s = Y_{s_{opt}}$. Definitions for the terms in these equations are found in Chapter IV. The double-primed notation will be used to indicate the two-port noise is increased by not being noise matched and noise tuned.

When a lossy transmission line (or any lossy two-port) is used to connect the receiver and antenna, a degradation of sensitivity or increase in receiver noise temperature will result. A block diagram illustrating the measurement system is shown in Figure 10E-1. The total receiver noise temperature, T_{rt} , is obtained from Equation 4C.60c where the line loss factor is now replaced by the available loss, (10B.4):

$$T_{rt} = \mathcal{L} T_e'' + (\mathcal{L} - 1) T_c \quad (10E.3)$$

The total receiver noise temperature is expressed in terms of the available loss, \mathcal{L} (which accounts for flat loss and source mismatch), the transmission line noise temperature T_c , and the effective receiver noise temperature T_e'' . The effect of source impedance on receiver noise temperature is accounted for in T_e'' by Equation 10E.2.

When the scattering parameters of the lossy two-port and source VSWR are known, the total receiver noise temperature can be calculated by using Equation 10E.3 but any attempt to measure the noise temperature is hindered by measurement errors. Suppose the Y-factor of the receiver in Figure 10E-1 is measured according to the scheme of Figure 9A-2. The ratio of output powers would be:

$$\tilde{Y} = \frac{N_{o2}}{N_{o1}} = \frac{k [T_2 + (T_{rt})_2] B_h G_2}{k [T_1 + (T_{rt})_1] B_h G_1} \quad (10E.4)$$

If we assume the gain and bandwidth of the system do not change during the measurement, the Y-factor is simplified to:

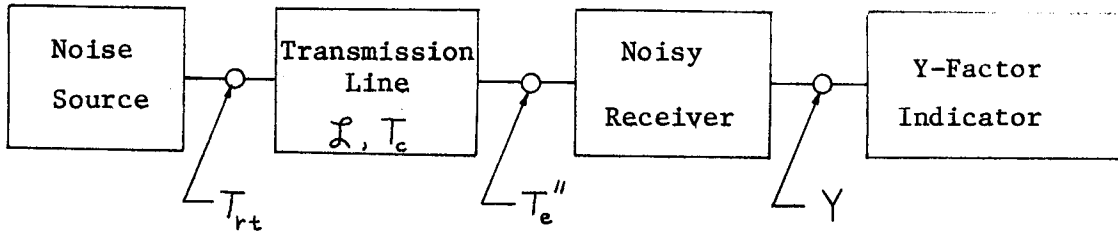


Figure 10E-1. Block Diagram of a Measurement System for Measuring Total Receiver Noise Temperature

$$\tilde{Y} = \frac{T_2 + (T_{rt})_2}{T_1 + (T_{rt})_1} \quad (10E.5)$$

The total receiver noise actually changes from source #2 to source #1 because of the difference in source impedances. For this reason, a unique value of noise temperature cannot be determined by simply measuring the Y-factor. The noise temperature of the receiver can only be specified by specifying a unique value of source reflection coefficient.

The situation is not as dismal as it appears because in many practical situations the total receiver noise temperature does not change significantly for small changes in source impedance. Using Equations 10E.3 and 10E.2, the Y-factor can be expressed as

$$\tilde{Y} = \frac{T_2 + \mathfrak{L}_2 [T_e + (\alpha T_e)_2] + (\mathfrak{L}_2 - 1) T_c}{T_1 + \mathfrak{L}_1 [T_e + (\alpha T_e)_1] + (\mathfrak{L}_1 - 1) T_c} \quad (10E.6)$$

where

$$(T_{rt})_2 = \mathfrak{L}_2 [T_e + (\alpha T_e)_2] + (\mathfrak{L}_2 - 1) T_c \quad (10E.7a)$$

$$(T_{nt})_1 = \mathcal{L}_1 [T_e + (\Delta T_e)_1] + (\mathcal{L}_1 - 1)T_e \quad (10E.7b)$$

$$(\Delta T_e)_2 = T_e \frac{B}{G_2} \left[(G_2 - G_{sopt})^2 + (B_2 - B_{sopt})^2 \right] \quad (10E.8a)$$

$$(\Delta T_e)_1 = T_e \frac{B}{G_1} \left[(G_1 - G_{sopt})^2 + (B_1 - B_{sopt})^2 \right] \quad (10E.8b)$$

The admittances $Y_1 = G_1 + j B_1$ and $Y_2 = G_2 + j B_2$ are the output admittances of the transmission line for sources 1 and 2 respectively.

The fundamental quantity in Equation 10E.6 is the minimum effective noise temperature of the receiver, T_e . If this is known, any total noise temperature can be calculated using (10E.3) and (10E.2) but it is difficult to measure T_e accurately.

Before proceeding with Equation 10E.6 it will be comforting to verify that the complicated expression can be reduced to the more familiar form. If the noise source provides the optimum admittance to the receiver so that noise matching and noise tuning is achieved, $Y_1 = Y_2 = Y_{sopt}$ and $(\Delta T_e)_2 = (\Delta T_e)_1 = 0$. Also if the transmission line is lossless, $\mathcal{L}_1 = \mathcal{L}_2 = 1$ and (10E.6) is reduced to the familiar form of (9A.2):

$$\tilde{Y} = \frac{T_2 + T_e}{T_1 + T_e}$$

The minimum effective receiver noise temperature, T_e , may be obtained by solving Equation 10E.6 and factoring in the following form:

$$T_e = \frac{(T_2 - \tilde{Y} T_1)}{(\mathcal{L}, \tilde{Y} - \mathcal{L}_2)} - T_c \left[1 - \frac{(\tilde{Y} - 1)}{(\mathcal{L}, \tilde{Y} - \mathcal{L}_2)} \right] - \frac{\tilde{Y} \mathcal{L}_1 (\Delta T_e)_1 - \mathcal{L}_2 (\Delta T_e)_2}{(\mathcal{L}, \tilde{Y} - \mathcal{L}_2)} \quad (10E.9)$$

This equation completely describes the functional dependence of T_e on all of the parameters of the circuit but is not very suitable for making error calculations. Generally, one or more approximations can be made which will yield simpler forms of (10E.9).

The most useful approximation is to assume that the reflection coefficients of the hot and cold noise sources are equal i.e. $T_2 = T_1$. Then from (10B.4) we can conclude that $\mathcal{L}_2 = \mathcal{L}_1 = \mathcal{L}$ and from (10B.2), (10B.1) and (10E.8) that $(\Delta T_e)_2 = (\Delta T_e)_1 = \Delta T_e$. These equalities can be substituted into (10E.9) to give:

$$T_e = \frac{T_2 - \tilde{Y} T_1}{\mathcal{L}(\tilde{Y} - 1)} - T_c \frac{\mathcal{L} - 1}{\mathcal{L}} - \Delta T_e \quad (10E.10)$$

From this equation it is possible to get the receiver noise temperature T_e'' , which includes the effect of a nonoptimum source admittance, by simply adding T_e and ΔT_e .

Applying the error and uncertainty criteria discussed in Part S of the Appendix, the following uncertainty components, of the total uncertainty of T_e , are obtained:

a. Uncertainty due to T_2 ,

$$\left| \frac{1}{\mathcal{L}(\tilde{Y} - 1)} \right| |\Delta T_2| \quad (10E.11)$$

b. Uncertainty due to T_1 ,

$$\left| \frac{\tilde{Y}}{\mathcal{L}(\tilde{Y}-1)} \right| |\Delta T_1| \quad (10E.12)$$

c. Uncertainty due to \mathcal{L} ,

$$\left| \frac{T_2 - \tilde{Y} T_1}{\mathcal{L}^2 (\tilde{Y}-1)} \right| |\Delta \mathcal{L}| + \left| T_c \frac{\mathcal{L}^3 - \mathcal{L} + 1}{\mathcal{L}^2} \right| |\Delta \mathcal{L}| \quad (10E.13)$$

d. Uncertainty due to \tilde{Y} ,

$$\left| \frac{T_2 - T_1}{\mathcal{L} (\tilde{Y}-1)^2} \right| |\Delta \tilde{Y}| \quad (10E.14)$$

A different approach has been used by Pastori (1968b) and by Harris (1966) which evaluates the uncertainty, in measured noise factor or noise temperature, caused by mismatch errors. Harris has derived an equation for measured Y-factor in terms of reflection coefficients and total receiver noise temperature. The effective temperature that is used by Harris is different than that used here. Harris works with the effective noise temperature defined when the source reflection coefficient is zero and the receiver is presented with the optimum noise admittance. Using (10E.3) and (10B.29) with $\Gamma_s \equiv 0$ gives:

$$T_H = N T_e + (N-1) T_c \quad (10E.15)$$

where

$T_H = T_{rt}$, when the source VSWR is zero and the receiver
is noise matched and noise tuned

N = flat-loss of the transmission line

T_e = effective noise temperature of the receiver when
it is noise matched and noise tuned

T_c = physical temperature of the transmission line.

For small N , so that the approximation $T_e \simeq T_H$ is valid, the measured
Y-factor is given by Harris (1966) to be

$$\tilde{Y} = \frac{AT_2 + CT_H}{BT_1 + DT_H} \quad (10E.16)$$

where

$$A = \frac{(1 - |\Gamma_2|^2)}{|1 - \Gamma_2 \Gamma_r|^2}$$

$$B = \frac{(1 - |\Gamma_1|^2)}{|1 - \Gamma_1 \Gamma_r|^2}$$

$$C = \frac{(1 + \Gamma_c |\Gamma_2|^2)}{|1 - \Gamma_2 \Gamma_r|^2}$$

$$D = \frac{(1 + \Gamma_c |\Gamma_1|^2)}{|1 - \Gamma_1 \Gamma_r|^2}$$

Γ_2 = reflection coefficient of the hot source.

Γ_1 = reflection coefficient of the cold source

Γ_r = reflection coefficient of the receiver input

Γ_c = reflection coefficient of the receiver input

correlation admittance (see Chapter IV-E).

Equation 10E.16 can be solved for the input noise temperature, T_H :

$$T_H = \frac{AT_2 - \tilde{Y}BT_1}{D\tilde{Y} - C} \quad (10E.17)$$

If $\Gamma_1 = \Gamma_2 = 0$, Equation 10E.17 reduces to Equation 9A.3. The effect of a nonoptimum source admittance on receiver noise temperature is accounted for by Γ_c .

For small Γ_1 and Γ_2 , Harris gives the following approximate expression for \tilde{T}_H

$$\tilde{T}_H \approx \frac{(T_2 - \tilde{Y}T_1) \pm 2|\Gamma_c|(\Gamma_2|\Gamma_2| + \tilde{Y}\Gamma_1|\Gamma_1|)}{(\tilde{Y} - 1) \mp 2|\Gamma_c|(|\Gamma_2| + \tilde{Y}|\Gamma_1|)} \quad (10E.18)$$

which will not be verified here. The reader is referred to the original paper by Harris. Equations 10E.16 and 10E.17 are exact when the transmission line is omitted and T_H is replaced by T_e .

Equations 10E.17 and 10E.3 can be contrasted to illustrate a very important concept. This concept is that the total receiver noise temperature does not depend upon receiver input impedance (10E.3) but that the accuracy of the measured value does depend on it. Conceptually this is very important to an understanding of sensitivity measurements. In the analysis of two-port noise theory, the two-port input impedance does not appear in the noise factor equations. Now we find that receiver input impedance does affect the measurement accuracy. It can be seen from (10E.17) that if the receiver input reflection coefficient is zero,

errors due to source mismatch are eliminated. This condition is rarely achieved in practice.

Pastori (1968b) has derived a noise-figure uncertainty equation based upon Harris' work which gives the uncertainty in measured noise figure due to mismatch errors. Pastori's equation can be derived from (10E.16) by using the approximation,

$$1 + \Gamma_c |\Gamma|^2 \simeq 1$$

which is usually valid for small source VSWR's.

Using this approximation in (10E.16) and writing the equation in terms of the reflection coefficients gives:

$$\tilde{Y} = \frac{|1 - \Gamma_r \Gamma_1|^2}{|1 - \Gamma_r \Gamma_2|^2} \cdot \left[\frac{T_2 (1 - |\Gamma_2|^2) + T_H}{T_1 (1 - |\Gamma_1|^2) + T_H} \right] \quad (10E.19)$$

Solving (10E.19) for T_H and using the substitution

$$M = \frac{|1 - \Gamma_r \Gamma_1|^2}{|1 - \Gamma_r \Gamma_2|^2} \quad (10E.20)$$

gives:

$$T_H = \frac{T_2 (1 - |\Gamma_2|^2) - M \tilde{Y} T_1 (1 - |\Gamma_1|^2)}{M \tilde{Y} - 1} \quad (10E.21)$$

The Y-factor in db is obtained from (10E.19) as:

$$\tilde{Y}_{db} = 10 \log M + 10 \log \left[\frac{T_2 (1 - |\Gamma_2|^2) + T_H}{T_2 (1 - |\Gamma_1|^2) + T_H} \right] \quad (10E.22)$$

The uncertainty in \tilde{Y}_{db} caused by source mismatch is computed from

$$|\delta Y_{db}| = \pm \left| \frac{\partial \tilde{Y}_{db}}{\partial M} \right| |\Delta M|$$

which is applied to (10E.22) to give:

$$|\delta Y_{db}| = \pm 4.34 \left| \frac{\Delta M}{M} \right| \quad (10E.23)$$

The term $\left| \frac{\Delta M}{M} \right|$ is the mismatch uncertainty assuming the nominal value of M is unity. This term is given by the following equation

$$\left| \frac{\Delta M}{M} \right| = \frac{M(\max)}{M} - 1 \quad (10E.24)$$

where M(max) is the maximum value of M determined from the magnitudes of the reflection coefficients. The method for determining M(max) is analogous to that used in Equations 10D.5. This technique gives:

$$M \leq \frac{1 + 2 |\Gamma_H| |\Gamma_1| + |\Gamma_H|^2 |\Gamma_1|^2}{1 - 2 |\Gamma_H| |\Gamma_2| + |\Gamma_H|^2 |\Gamma_2|^2} \quad (10E.25)$$

Substituting (10E.25) into (10E.24) gives the mismatch uncertainty:

$$\left| \frac{\Delta M}{M} \right| = \frac{(1 + |\Gamma_r| |\Gamma_1|)^2}{(1 - |\Gamma_r| |\Gamma_2|)^2} - 1 \quad (10E.26)$$

This mismatch uncertainty is then used in (10E.23) to compute the error in \tilde{Y}_{db} .

In many cases, the error in \tilde{Y}_{db} is used to compute the error in measured noise figure due to mismatch error. The noise factor in terms of Y-factor can usually be written in the form of Equation 9A.7 which gives the following noise figure equation:

$$NF = 10 \log R_{ex} - 10 \log \left(10^{\frac{\tilde{Y}_{db}}{10}} - 1 \right) \quad (10E.27)$$

The uncertainty in NF is computed by:

$$|\delta NF| = \left| \frac{\partial NF}{\partial \tilde{Y}_{db}} \right| |\delta Y_{db}|$$

Performing the differentiation

$$\frac{\partial NF}{\partial \tilde{Y}_{db}} = -10 \frac{d}{dx} \log \left(10^{\frac{\tilde{Y}_{db}}{10}} - 1 \right) = \frac{-1}{\left(1 - 10^{\frac{-\tilde{Y}_{db}}{10}} \right)}$$

and substituting into the equation above gives:

$$|\delta NF| = \frac{|\delta Y_{db}|}{\left(1 - 10^{\frac{-\tilde{Y}_{db}}{10}} \right)} \quad (10E.28)$$

This equation gives the mismatch uncertainty in measured noise figure.

2. Noise diode

The error analysis of the noise diode method of measuring noise factor or equivalent noise temperature is very similar to that for Y-factor because the noise diode method is a special case of the hot-cold Y-factor method. In fact the Y-factor and equivalent noise temperature of Equations 10E.6 and 10E.9 can be simplified by applying the special conditions associated with the noise diode method. First of all, the source impedance is not switched so it stays constant and in almost all cases the diode's internal shunt conductance can be ignored. These conditions mean that the available loss remains a constant during the measurement i.e., $\mathcal{L}_2 = \mathcal{L}_1 = \mathcal{L}$. Secondly, since the source reflection coefficient is a constant, the additive noise temperature caused by a non-optimum source impedance, (10E.8), is constant i.e., $(\alpha T_e)_2 = (\alpha T_e)_1 = \alpha T_e$. Finally, the hot and cold temperatures are related by the excess noise temperature of the diode i.e., $T_2 = T_{ex} + T_1$. If these conditions are applied to Equations 10E.6 and 10E.9, the following equations, valid for noise diode measurements, are

$$\tilde{Y} = 1 + \frac{T_{ex}}{T_1 + \mathcal{L}(T_e + \alpha T_e) + (\mathcal{L} - 1)T_c} \quad (10E.29)$$

$$T_e = \frac{T_2 - \tilde{Y}T_1}{\mathcal{L}(\tilde{Y} - 1)} - T_c \frac{(\mathcal{L} - 1)}{\mathcal{L}} - \alpha T_e \quad (10E.30)$$

where T_{ex} = the excess noise temperature of the diode given in Figure 4F-2

\tilde{Y} = measured Y-factor

\mathcal{L} = available loss of the two-port between the receiver and the noise diode

T_c = physical temperature of the two-port characterized by loss \mathcal{L}

$T_2 = T_{\text{ex}} + T_1$

T_e = minimum receiver noise temperature

αT_e = increase in receiver noise temperature due to a nonoptimum source.

The actual equivalent noise temperature of the two-port, which includes nonoptimum source effects, is the sum of T_e and αT_e as represented by (10E.2) and (10E.8). This value can be measured directly using a noise diode but cannot be measured directly using a hot-cold noise source. In this section we will work with the actual value, T_e'' . The actual effective noise temperature for the receiver is measured by the noise diode to be:

$$T_e'' = \frac{T_2 - \tilde{Y} T_1}{\mathcal{L}(\tilde{Y} - 1)} - T_c \left(\frac{\mathcal{L} - 1}{\mathcal{L}} \right) \quad (10E.31)$$

The corresponding noise factor is obtained from (10E.31) by applying the definition, $T_e'' = (F'' - 1) T_o$, to get:

$$F'' = 1 + \frac{\frac{T_2}{T_o} - \tilde{Y} \frac{T_1}{T_o}}{\mathcal{L}(\tilde{Y}-1)} - \frac{T_c}{T_o} \left(\frac{\mathcal{L}-1}{\mathcal{L}} \right) \quad (10E.32)$$

For convenience of error analysis it will be necessary to obtain an alternate form of Equation 10E.32. First, the cold temperature is the sum of a error temperature and standard temperature i.e., $T_1 = T_o + \Delta T_1$. Second, the hot temperature is the sum of the diode excess noise temperature and the cold temperature i.e., $T_2 = T_{ex} + T_o + \Delta T_1$. Using these relations in (10E.32) gives the more useful form:

$$F'' = \frac{T_{ex}}{\mathcal{L}(\tilde{Y}-1)T_o} - \frac{\Delta T_1}{\mathcal{L}T_o} - \left(\frac{T_c}{T_o} - 1 \right) \left(\frac{\mathcal{L}-1}{\mathcal{L}} \right) \quad (10E.33)$$

This equation is more complicated than (9A.7) because it takes into account the two-port loss between source and receiver, the reference temperature error, and the two-port temperature.

Applying the error and uncertainty criteria to Equation 10E.33 as was done previously in Equations 10E.11 through (10E.14) we get:

- a. Uncertainty due to T_{ex} ,

$$\left| \frac{1}{\mathcal{L}(\tilde{Y}-1)T_o} \right| |\Delta T_{ex}| \quad (10E.34)$$

- b. Uncertainty due to $T_1 \neq T_o$,

$$\frac{|\Delta T_1|}{\mathcal{L}T_o} \quad (T_1 = T_o + \Delta T_1) \quad (10E.35)$$

c. Uncertainty due to \mathfrak{L} ,

$$\left| \frac{T_{ex}}{\mathfrak{L}^2 (\tilde{Y}-1) T_o} \right| |\Delta \mathfrak{L}| + \left| \left(\frac{T_c}{T_o} - 1 \right) \left(\frac{\mathfrak{L}^3 - \mathfrak{L} + 1}{\mathfrak{L}^2} \right) \right| |\Delta \mathfrak{L}| + \frac{|\Delta T_1|}{\mathfrak{L} T_o} |\Delta \mathfrak{L}| \quad (10.36)$$

d. Uncertainty due to \tilde{Y} ,

$$\left| \frac{T_{ex}}{\mathfrak{L} T_o (\tilde{Y}-1)^2} \right| |\Delta \tilde{Y}| \quad (10E.37)$$

The most important sources of error for noise diode measurements are those due to errors in excess noise, reference temperature T_1 , and measured Y-factor. To simplify the error equations we will assume that the noise source is connected directly to the receiver so that the available loss, \mathfrak{L} , is unity. For this case, the noise factor in Equation 10E.32 can be reduced by letting $\mathfrak{L} = 1$ to give

$$F''(\mathfrak{L}=1) = \frac{\left(\frac{T_2}{T_o} - 1 \right) - \tilde{Y} \left(\frac{T_1}{T_o} - 1 \right)}{(\tilde{Y}-1)} \quad (10E.38)$$

which is the most convenient form to use to find the error caused by $T_1 \neq T_o$. This error is computed by assuming that the measured noise factor is determined from \tilde{Y} by assuming $T_1 \equiv T_o$. When this happens the measured value becomes:

$$F_m = \frac{\left(\frac{T_2}{T_0} - 1\right)}{(\tilde{Y} - 1)} \quad (10E.39)$$

The resulting error can be evaluated by taking the ratio of the true value to the measured value which is the ratio of Equations 10E.38 and 10E.39:

$$\frac{F''}{F_m} = 1 - \tilde{Y} \frac{T_1 - T_0}{T_2 - T_0} \quad (10E.40)$$

The ratio is taken instead of the difference because it is more convenient to convert into noise-figure error. The true value of noise figure is determined from (10E.40) as:

$$NF'' = NF_m + 10 \log \left[1 - \tilde{Y} \frac{T_1 - T_0}{T_2 - T_0} \right] \quad (10E.41)$$

The second term is the db error in measured noise figure caused by $T_1 \neq T_0$:

$$\text{db error} = \Delta NF_m = 10 \log \left[1 - \tilde{Y} \frac{\Delta T_1}{T_2 - T_0} \right] \quad (10E.42a)$$

The uncertainty in measured noise figure is simply the maximum error determined by (10E.42). The error equation above has the measured Y-factor as a parameter but the equation can just as well be written in terms of measured noise factor by using (10E.39) to give:

$$SNF_m = 10 \log \left[1 - \frac{\Delta T_1}{T_2 - T_0} - \frac{\Delta T_1}{F_m T_0} \right] \quad (10E.42b)$$

From these error equations we can see that the error in measured noise figure depends upon the value of the hot temperature T_2 , the error in T_1 , and either the measured noise factor F_m or the measured Y-factor \tilde{Y} . This error can be plotted as a function of \tilde{Y} or F_m for any specific noise source with T_1 as a parameter. A curve of error due to termination temperature has been given by Pastori (1967) for a noise source where $T_2 = 10,000^\circ \text{K}$. Figure 10E-2 is a similar curve for a noise diode with an excess noise ratio of 5.2 db ($T_2 = 1250^\circ \text{K}$). It is particularly interesting to note that for a typical laboratory ambient of $294\text{--}300^\circ \text{K}$ (Appendix, Part 0) the error in measured noise figure is -0.05 to -0.12 db for low noise figures. This means that, if this source of error is not accounted for, the resulting reported noise figures will be pessimistic. Figure 10E-2 also conveniently gives the uncertainty in measured noise figure for a given uncertainty in T_1 .

The error in measured noise figure due to an error in Y-factor can be analyzed by starting with Equation 9A.7. The actual noise factor and measured noise factor are respectively

$$F'' = \frac{R_{ex}}{Y-1} \quad (10E.43)$$

and

$$F_m = \frac{R_{ex}}{(\tilde{Y}-1)} = \frac{R_{ex}}{(Y-1) + \Delta Y} \quad (10E.44)$$

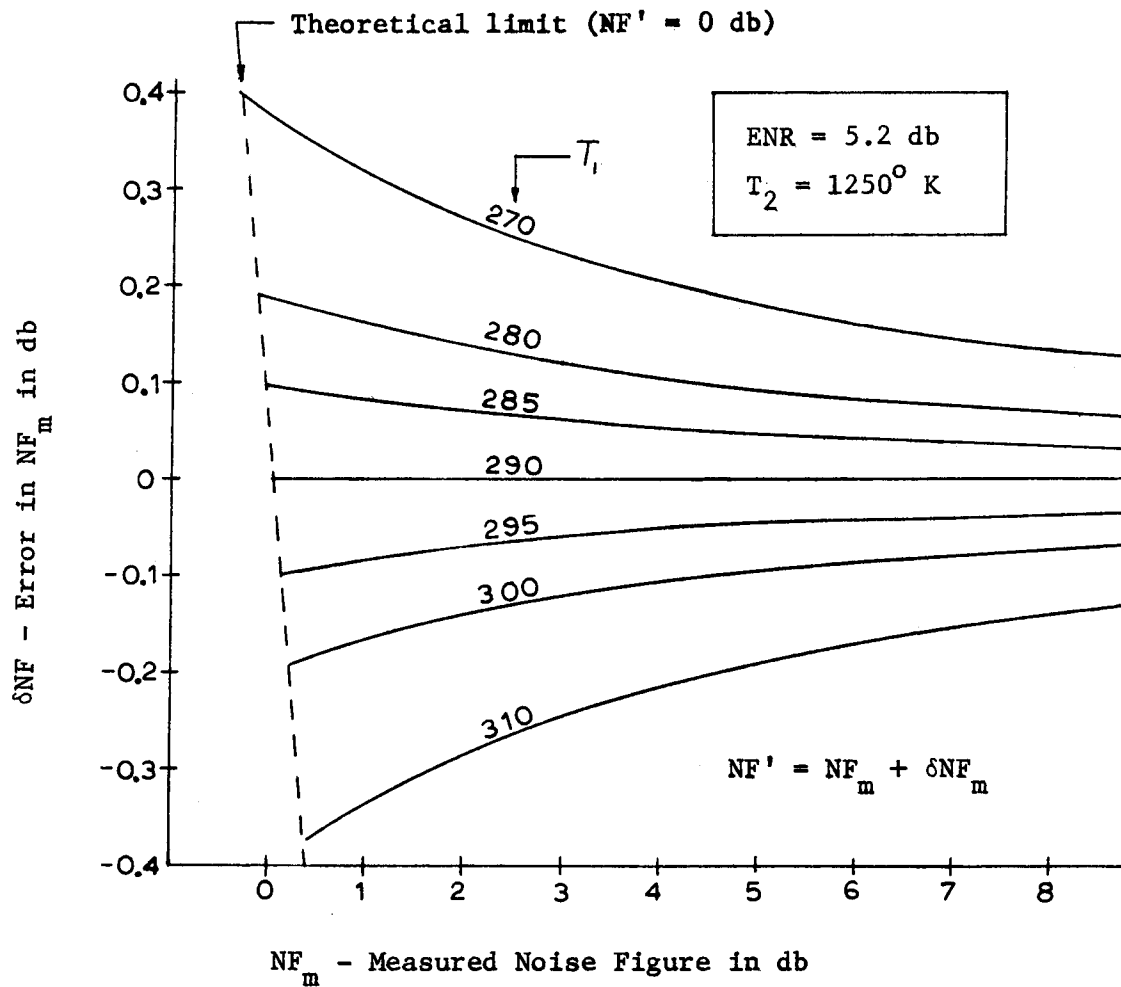


Figure 10E-2. Error in Measured Noise Figure Due to a Termination Temperature which is not Equal to T_0

where, $\tilde{Y} = Y + \Delta Y$, is the measured Y-factor, Y is the true value and ΔY is the error.

These equations can be combined to give

$$F_m = \frac{F''}{1 + F'' \frac{\Delta Y}{R_{ex}}}$$

which is then solved for F'' and (10E.44) is substituted for F_m in the denominator to finally give:

$$F'' = \frac{F_m}{\left[1 - \frac{\Delta Y}{(\tilde{Y}-1)}\right]} \quad (10E.45)$$

This ratio form of expressing the error is convenient for getting the error in db. Using (10E.45), the error equation becomes;

$$NF'' = NF_m - 10 \log \left[1 - \frac{\Delta Y}{(\tilde{Y}-1)}\right] \quad (10E.46)$$

where the error in measured noise figure is

$$\Delta NF_m = -10 \log \left[1 - \frac{\Delta Y}{(\tilde{Y}-1)}\right] \quad (10E.47a)$$

or by using (10E.44) to replace $(\tilde{Y} - 1)$ we can get the error in terms of the excess noise ratio and the measured noise figure:

$$\Delta NF_m = -10 \log \left[1 - \Delta Y \frac{F_m}{R_{ex}}\right] \quad (10E.47b)$$

A plot of Equation 10E.47a is shown in Figure 10E-3. Note how the error in measured noise factor is drastically increased if the measured Y-factor is less than 2 db. The error line for the 3 db method is shown for use with manually operated noise diodes. The error ΔY_{db} is determined in the manner discussed in Part S of the Appendix.

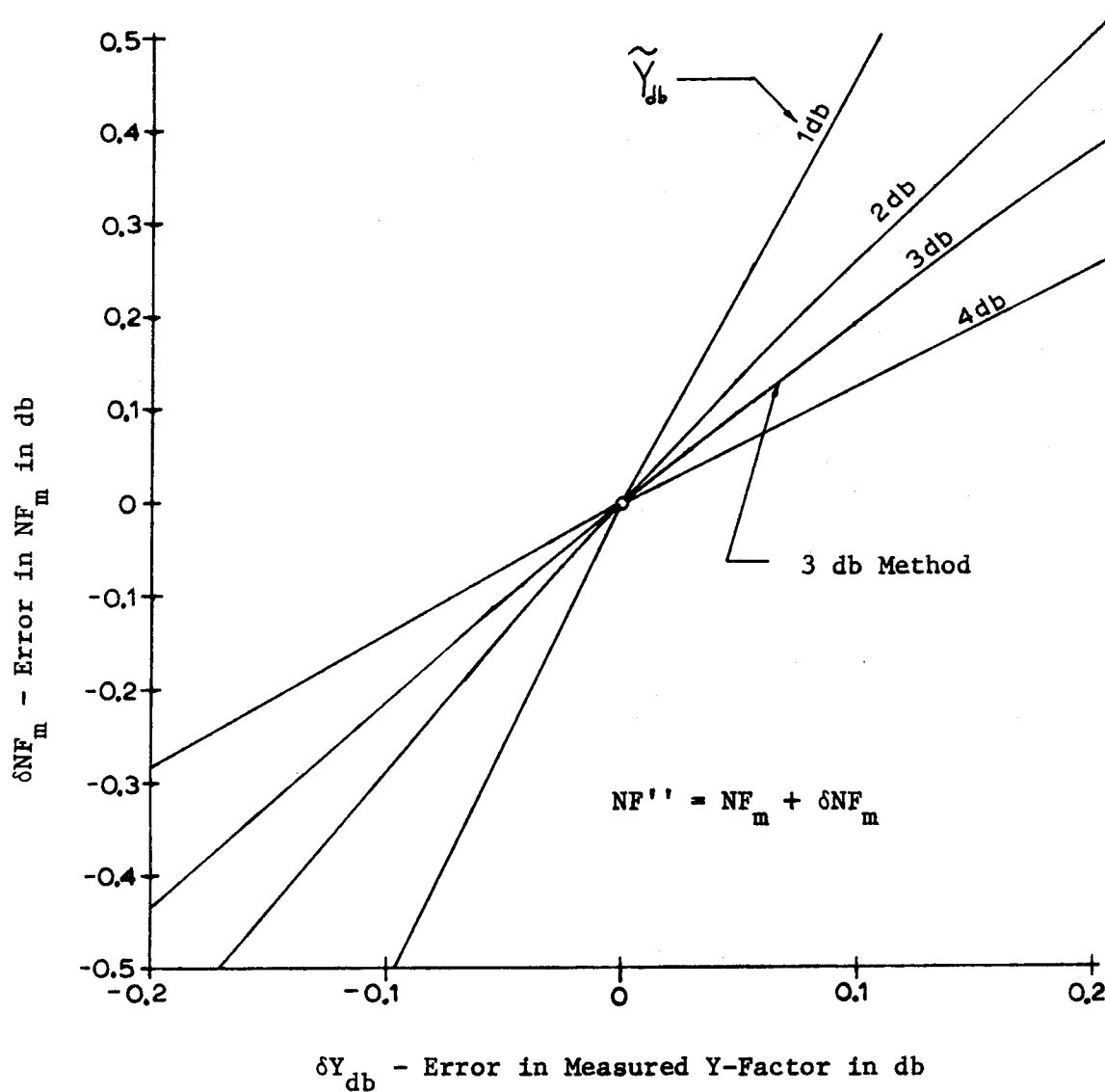


Figure 10E-3. Error in Measured Noise Figure Due to an Error in the measured Y-Factor

The error in measured noise figure caused by an error in excess noise is easily evaluated by using Equations 9A.7 and 9A.11. The measured noise factor is

$$F_m = \frac{\tilde{R}_{ex}}{(\tilde{Y} - 1)}$$

and the true noise factor is

$$F'' = \frac{R_{ex}}{(\tilde{Y} - 1)}$$

where R_{ex} is the actual value of the numerical excess noise ratio. Both equations in terms of noise figure are:

$$NF_m = \widetilde{ENR} - 10 \log (\tilde{Y} - 1) \quad (10E.48)$$

$$NF'' = ENR - 10 \log (\tilde{Y} - 1) \quad (10E.49)$$

If the difference between the measured and true noise figures is taken where, $\widetilde{ENR} = ENR + \delta ENR$ (in db), the noise figure error may be computed from

$$NF'' = NF_m + \delta ENR \quad (10E.50)$$

where δENR is the error, in db, of the excess noise.

The uncertainty in the measured noise figure due to the uncertainty in the excess noise ratio is:

$$\pm |\delta ENR| \quad (10E.51)$$

A low value of ENR will result in a measured noise figure which is pessimistic while a high value gives an optimistic one. For example, a noise diode with a nominal ENR of 5.2 db actually has an ENR of 5.6 db. When this diode is used to measure the noise figure of a 3.4 db receiver, the measured noise figure will be 3.0 db which is 0.4 db below the actual value.

It should be pointed out that the errors given in Figures 10E-2 and 10E-3 are expressed as corrections to the measured value and not as errors on the nominal or true value. Both of the conventions will be used when convenient. Also, the measured value could be plotted against the true value to give the same information as the measured value plotted against the error. The latter scheme was chosen as being a form which allowed a simpler uncertainty estimate.

3. Gas-discharge noise source

The errors involved in using a gas-discharge noise source to measure receiver noise temperature or noise factor have essentially been given in the last two sections. The important sources of error and the applicable equations are now summarized:

- a. Transmission-line loss error, Equation 10E.9
- b. Mismatch error, Equations 10E.16, 10E.26, and 10E.28
- c. Error caused by $T_1 \neq T_0$, Equation 10E.42
- d. Error in measured Y-factor, Equation 10E.47
- e. Error in excess noise ratio, Equation 10E.50.

For a discussion on the magnitude of the mismatch errors to be expected, refer to the article by Pastori (1968b).

4. AM sensitivity

The errors in the measurement of noise factor using the AM sensitivity method are caused by:

- a. Errors in the index of modulation, m
- b. Errors in the open circuit generator voltage, E_g
- c. Errors due to transmission line loss, \mathcal{L}

- d. Errors in the measured output signal-to-noise ratio
(analogous to Y-factor errors)
- e. Errors caused by an incorrect source resistance
- f. Errors in the effective noise bandwidth, B_c .

The measured noise factor when the transmission line loss is unity is given by Equation 8D.18. To obtain an equation for the measured noise factor when the loss is not unity, we combine (8D.18) and (10E.3) with the definition of noise factor to obtain:

$$F'' = \frac{m^2 E_g^2}{\mathfrak{L} \left(\frac{S_o + N_o}{N_o} - 1 \right) [4kT_o R_s B_c]} - \left(\frac{\mathfrak{L}-1}{\mathfrak{L}} \right) \left(\frac{T_c}{T_o} - 1 \right) \quad (10E.52)$$

For the purposes of error analysis we will assume that the generator is connected directly to the receiver so that $\mathfrak{L} \approx 1$. The noise factor of (10E.52) can then be written as

$$F'' = \frac{m^2 E_g^2}{\mathfrak{L} \left(\frac{S_o + N_o}{N_o} - 1 \right) [4kT_o R_s B_c]} \quad (10E.53)$$

where the \mathfrak{L} in the first term has been retained for purposes of showing the effect of very small losses. The noise figure from (10E.53) is:

$$NF'' = 10 \log m^2 + 10 \log E_g^2 - 10 \log \mathfrak{L} \\ - 10 \log \left(\frac{S_o + N_o}{N_o} - 1 \right) - 10 \log [4kT_o R_s B_c] \quad (10E.54)$$

This equation can be used to illustrate the effect of the various errors. The error in the measured receiver noise figure is directly related, db for db, with each of the arguments of the log functions in (10E.54). The error caused by errors in modulation index is:

$$SNF_m = 20 \log \left[1 + \frac{\Delta m}{m} \right] \quad (\tilde{m} = m + \Delta m) \quad (10E.55)$$

A plot of this equation for typical values of m and Δm is shown in Figure 10E-4.

The error in generator voltage is analogous to the error in excess noise ratio (Equation 10E.50) and this error can be computed from:

$$NF'' = NF_m + \mathcal{S}(E_g)_{db} \quad (10E.56)$$

A low value of generator output will result in a measured noise figure which is pessimistic while a high value gives an optimistic one. For more information on generator errors refer to Section C of Chapter IX.

The effects of all the other parameters of Equation 10E.54 on measured noise figure can be evaluated in a similar manner. A few specific comments should be made on receiver noise bandwidth error effects. The error in measured noise figure due to errors in receiver noise bandwidth ($\tilde{B}_c = B_c + \Delta B_c$) is obtained from (10E.54) by separating out the term containing B_c :

$$\begin{aligned} SNF &= - \left[10 \log \tilde{B}_c - 10 \log B_c \right] \\ &= -10 \log \left[1 + \frac{\Delta B_c}{B_c} \right] \end{aligned} \quad (10E.57)$$

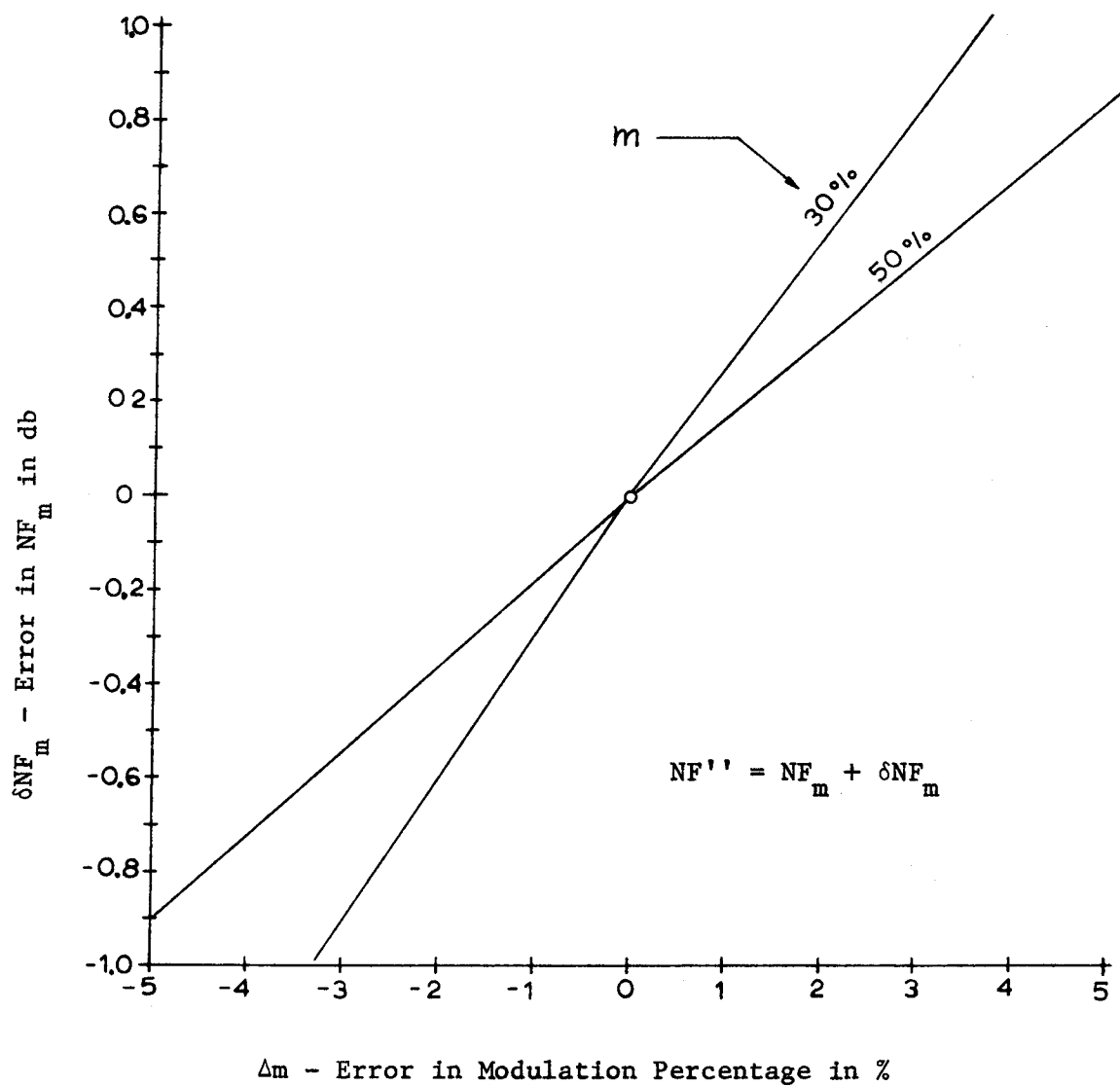


Figure 10E-4. Error in Measured Noise Figure Due to an Error in the Modulation Percentage

When the error is expressed as the number which should be added to the measured value, as in (10E.50) or (10E.56), the sign on δNF_m must be negative for positive errors in noise bandwidth. This reflects the fact that bandwidths too large give pessimistic values for the measured

noise figure. Figure 10E-5 is a plot of the error in measured noise figure as a function of the percentage error in receiver noise bandwidth.

A comparison of Figures 10E-4 and 10E-5 shows that, for a comparative percentage error, the effect on measured noise figure is much more pronounced for modulation percentage. When trying to improve measurement accuracy, it is much more profitable to expend effort on improving modulation accuracy than on improving noise bandwidth accuracy. Errors due to source mismatch and transmission-line loss can be accounted for by applying the analysis of the previous section.

5. FM sensitivity

The errors involved in making FM sensitivity measurements are difficult to analyze because of their extreme dependence on detector characteristics. It is not practical to measure noise figure with an FM system. The error from sources other than the detector can be analyzed by techniques given previously by applying Equation 8A.1. Deviation ratio errors are discussed in Section B of this chapter.

A few comments can be made about FM sensitivity errors in general. First of all, the sensitivity of an FM receiver will always improve with improvements in receiver noise figure. The receiver predetection SNR improves db for db with decreases in RF noise figure. Using this fact and a curve such as given in Figures 8A-2, 8B-1, or 8B-2, it is possible to predict the improvement in output SNR. Likewise, one can predict the effect of a lossy transmission line or noise bandwidth error using these curves and Equation 8A.1. The systems which employ

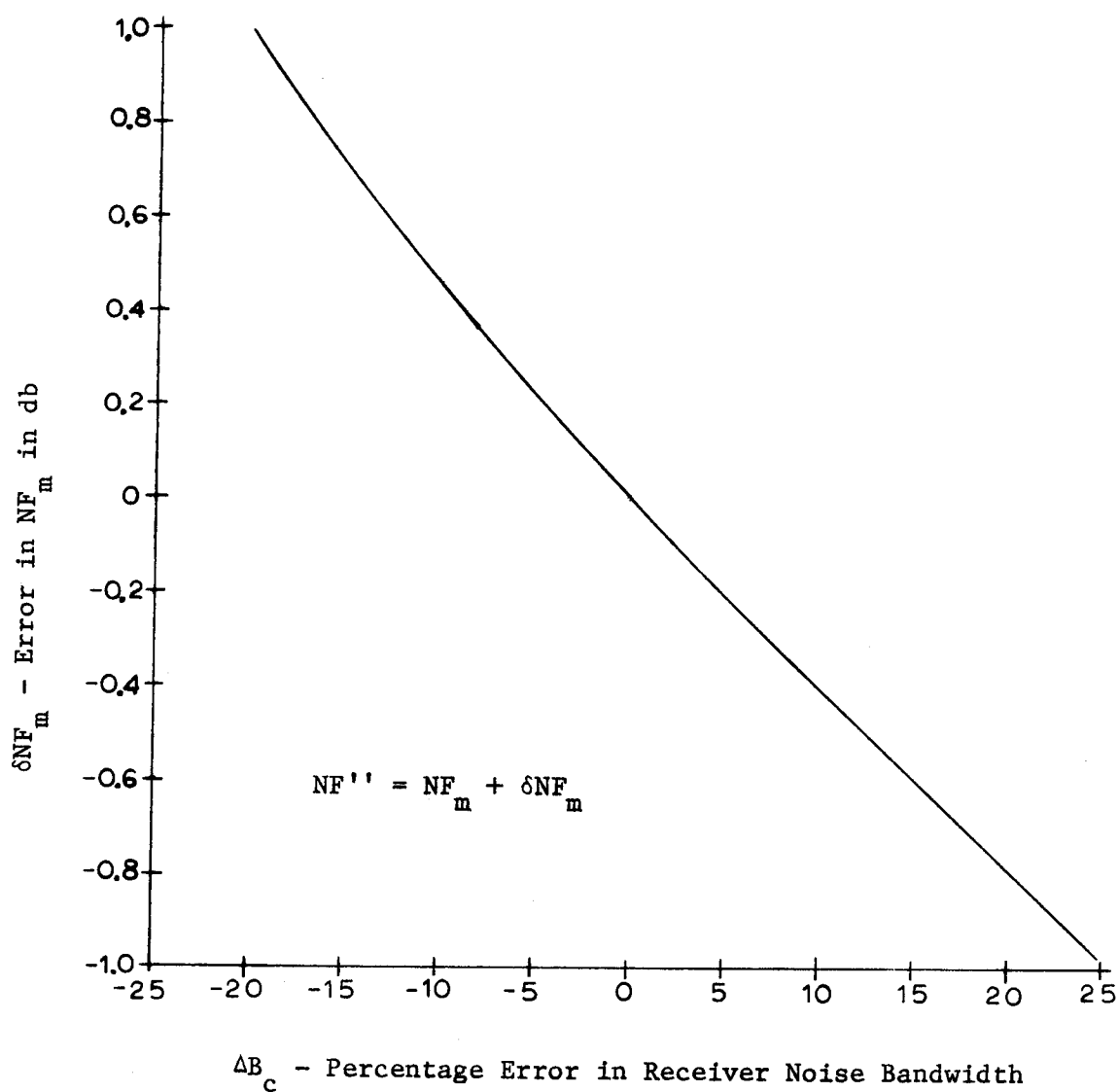


Figure 10E-5. Error in Measured Noise Figure Due to an Error in the Receiver Noise Bandwidth

FM do not usually require accurately known sensitivities thus, for most situations, error analysis becomes a secondary consideration.

6. Tangential noise

The essential theory of tangential noise sensitivity measurements was presented in Chapter VIII. Since Equation 8A.1 is used to determine

noise factor from tangential sensitivity it is used as a basis for error analysis. The principal errors in the measurement of tangential noise are caused by:

- a. Errors in the generator voltage, E_g
- b. Errors due to transmission line loss
- c. Errors caused by incorrect source resistance
- d. Errors in the effective noise bandwidths, B_h and B_L
- e. Observer error.

Observer errors are large in this method, typically ranging from 1-2 db so that errors due to other factors play a minor role in the total error picture. Errors due to the other effects listed above have been discussed in previous sections in this chapter.

7. Antenna noise temperature

The errors involved in measuring antenna noise temperature are directly analogous to those involved in measuring receiver noise temperature by the hot-cold noise-source Y-factor method. Starting with Equation 9D.1 and considering mismatch effects, the change in output power levels is:

$$M = \frac{T_A R_A + T_{eA}'' R_s}{T_s R_s + T_{es}'' R_s} \quad (10E.58)$$

The noise temperatures T_{eA}'' and T_{es}'' are the effective receiver noise temperatures when the receiver is connected to the antenna and to the source. They are different because of mismatch effects caused by the transmission line connecting the receiver to the antenna and to the

source. The equations for T_{eA}'' and T_{es}'' are analogous to Equations 10B.37. The difficulty involved in accounting for changes in receiver noise temperature caused by source mismatch has been amply discussed in the first part of this section. To simplify the equations we will assume that the antenna impedance and the reference source impedance are equal so that Equation 10E.58 can be solved to give

$$T_A = M T_s + T_{rt} (M-1) \quad (10E.59a)$$

where T_{rt} is the total receiver noise temperature given by Equation 10E.3. T_{rt} accounts for the receiver noise temperature modified by the effect of transmission line loss. Substituting (10E.3) into (10E.59a) gives the final result:

$$T_A = M T_s + (M-1) [\alpha T_e'' + (\alpha-1) T_c] \quad (10E.59b)$$

As was done in previous sections, the error involved in the measurement of each quantity in Equation 10E.59 will be expressed as a correction factor to be applied to the measured value i.e.:

$$T_A = \tilde{T}_A + \Delta T_A \quad (10E.60a)$$

$$M = \tilde{M} + \Delta M \quad (10E.60b)$$

$$T_s = \tilde{T}_s + \Delta T_s \quad (10E.60c)$$

$$\mathcal{L} = \tilde{\mathcal{L}} + \Delta \mathcal{L} \quad (10E.60d)$$

$$T_e'' = \tilde{T}_e'' + \Delta T_e'' \quad (10E.60e)$$

The error in \tilde{T}_A due to an error in \tilde{M} is computed from (10E.59) by substituting \tilde{M} to give:

$$\tilde{T}_A = \tilde{M} T_s + (\tilde{M} - 1) [\mathcal{L} T_e'' + (\mathcal{L} - 1) T_c]$$

Solving for nominal values using the correction factor equations above gives:

$$\begin{aligned} T_A - \Delta T_A &= (M - \Delta M) T_s + (M - \Delta M - 1) [\mathcal{L} T_e'' + (\mathcal{L} - 1) T_c] \\ &= M T_s + (M - 1) [\mathcal{L} T_e'' + (\mathcal{L} - 1) T_c] \\ &\quad - \Delta M \{ T_s + [\mathcal{L} T_e'' + (\mathcal{L} - 1) T_c] \} \end{aligned}$$

From this equation, the error in measured antenna noise temperature is identified as:

$$\Delta T_A = \Delta M \{ T_s + [\mathcal{L} T_e'' + (\mathcal{L} - 1) T_c] \} \quad (10E.61)$$

From this equation and (10E.60a) we see that when ΔM is positive, meaning the measured value of M is smaller than the true value, the measured antenna noise temperature is smaller than the true value. In a similar manner we can calculate the errors due to the other parameters.

The following error equations can be computed using (10E.59) and (10E.60):

a. Error due to \tilde{T}_s ,

$$\Delta T_A = M \Delta T_s \quad (10E.62)$$

b. Error due to $\tilde{\mathcal{L}}$,

$$\Delta T_A = (M-1) [T_e' + T_c] \Delta \mathcal{L} \quad (10E.63)$$

c. Error due to \tilde{T}_e''

$$\Delta T_A = \mathcal{L} (M-1) \Delta T_e'' \quad (10E.64)$$

The maximum uncertainty in \tilde{T}_A is obtained by adding the absolute magnitudes of the errors:

$$\begin{aligned} |\Delta T_A| &= |\Delta M| \left\{ T_s + [\mathcal{L} T_e'' + (\mathcal{L}-1) T_c] \right\} \\ &+ |M| |\Delta T_s| + [T_e'' + T_c] |M-1| |\Delta \mathcal{L}| \\ &+ \mathcal{L} |M-1| |\Delta T_e''| \end{aligned} \quad (10E.65)$$

The accuracy of the measured value of antenna noise temperature then becomes:

$$T_A = \tilde{T}_A \pm |\Delta T_A| \quad (10E.66)$$

The following numerical example is included to help clarify the error equations. The system data obtained are

$$\tilde{M} = 1.26 \pm 0.03 \quad (1 \pm 0.1 \text{ db})$$

$$\tilde{T}_s = 295 \pm 5^\circ \text{ K}$$

$$\tilde{\mathcal{L}} = 1.023 \pm 0.023 \quad (0.1 \pm 0.1 \text{ db})$$

$$\tilde{T}_e'' = 220 \pm 20^\circ \text{ K}$$

$$T_c = 295^\circ \text{ K}$$

\tilde{T}_A and the total uncertainty in \tilde{T}_A are computed from (10E.59) and (10E.65) as:

$$\begin{aligned} \tilde{T}_A &= 1.26 (295) + (1.26 - 1) [(1.023) (220) - (1.023 - 1) (295)] \\ &= 429^\circ \text{ K} \end{aligned}$$

$$\begin{aligned} |\Delta T_A| &= (0.03) \{295 + [(1.023) (220) - (1.023 - 1) (295)]\} \\ &\quad + (1.26) (5) + [220 + 295] (.26) (0.023) \\ &\quad + (1.023) (.26) (20) \\ &= 15.4 + 6.3 + 3.1 + 5.3 = 30.1^\circ \text{ K} \end{aligned}$$

The value of antenna noise temperature must then be reported as:

$$T_A = 429 \pm 30.1^\circ \text{ K}$$

Notice that the largest error term is due to the error in \tilde{M} . It is most often true that the largest error is caused by the uncertainty in \tilde{M} .

It should be remembered that the largest possible error does not necessarily reflect system capability i.e., self-compensation of the various errors tends to reduce the total error. Also the maximum error bounds are seldom achieved simultaneously.

When using a comparison technique where the reference temperature is adjusted to equal the antenna temperature, measurement errors are caused by reference temperature errors and mismatch errors.

The antenna noise measurement technique shown in Figure 9D-3 has additional errors associated with the coupler and excess noise temperature. Equation 9D.5 is used to analyze measurement errors. The measured antenna noise temperature is:

$$\tilde{T}_A = \frac{\alpha (T_o + T_{ex})}{(\tilde{M} - 1)} - T_e'' \quad (10E.67)$$

Using the same techniques applied to the other antenna noise measurement system, the errors due to the parameters of Equation 10E.67 are:

a. Error due to \tilde{T}_e''

$$\Delta T_A = - \Delta T_e'' \quad (10E.68)$$

b. Error due to \tilde{T}_{ex}

$$\Delta T_A = \alpha \Delta T_{ex} \quad (10E.69)$$

c. Error due to $\tilde{\alpha}$

$$\Delta T_A = \frac{T_o + T_{ex}}{(\tilde{M} - 1)} \Delta \alpha \quad (10E.70)$$

d. Error due to \tilde{M}

$$\Delta T_A = \frac{-\alpha (T_o + T_{ex})}{(M - 1)^2} \Delta M \quad (10E.71)$$

F. Gain Variations

If the total gain of the receiver changes during a sensitivity measurement, errors are introduced into the ratio measurement. The effect of gain changes can be analyzed by considering Equation 10E.4. Since G_2 and G_1 can be factored out as a ratio, it is possible to define a modified Y-factor such that

$$\tilde{Y} \triangleq \tilde{Y} \frac{G_1}{G_2} \quad (10F.1)$$

and the error due to gain instability can be treated as an error in the measured Y-factor or:

$$Y - \text{factor error in db} = 10 \log \left(\frac{G_1}{G_2} \right) \quad (10F.2)$$

Output fluctuations due to gain changes are interpreted as additional input noise fluctuations by the measurement device and degrade the

minimum receiver sensitivity. For a radiometer as used in radio astronomy, the minimum detectable noise temperature of the system is given by Equation 6.50c.

To account for gain fluctuations, this equation is modified to (Kraus, 1966, p. 248)

$$\Delta T_{\min} = K_s K_F T_{\text{sys}} \sqrt{\frac{2 B_L}{B_h} + \left(\frac{\Delta G}{G}\right)^2} \quad (10F.3)$$

where G is the average power gain and ΔG is the RMS value of the gain variation during the measurement.

For most sensitivity measurements, gain variations are rarely a problem because the measurements are taken over a time interval too short for significant gain fluctuations.

G. Image Response

When measuring the noise figure of a superhetrodyne receiver or any receiver with more than one RF input frequency, care must be taken as to how to report the noise figure. Generally the safest technique is to report the measurement conditions in detail and let the reader interpret the result. For a mixer stage there are two distinct responses, the signal response and the image response. If a noise source is used, noise power can come in on both channels and cause the measured noise figure to be as much as 3 db lower than the actual single-channel noise figure.

The measured noise figure which results from a multiple-input receiver has been variously termed the "two-channel" noise figure,

the "radio astronomy" noise figure or the "radar" noise figure. The reason for this is that these systems usually employ both responses to get the best possible SNR.

The "radio astronomy" noise factor can be computed from the single-channel noise factor by the following formula (Mumford and Scheibe, 1968, p. 53 or Kraus, 1966, p. 266)

$$F_{RA} = \left(1 + \frac{T_e}{T_o}\right) \left[1 + \frac{G_2 B_2}{G_1 B_1} + \dots + \frac{G_n B_n}{G_1 B_1}\right]^{-1} \quad (10G.1)$$

where G_n and B_n are the gain and bandwidth respectively of the n^{th} image channel and G_1 and B_1 are the respective gain and bandwidth of the primary channel.

For example, a noise figure measurement of a wideband mixer will indicate a value 3 db lower than the single-channel value. A wideband mixer with an effective noise temperature of 290° K at both channels will indicate a 0 db noise figure instead of 3 db. More complicated schemes can be analyzed using Equation 10G.1.

A detailed discussion of the noise in a multiple-response receiver is given by the IRE Subcommittee 7.9 on Noise (1963b).

H. Two-Port Devices

The noise factor of a two-port device depends upon the operating temperature because of the internal thermal sources. If the Friis equation (Appendix, Part J) is applied to a passive two-port, the result is

$$F_{rt} = F_c + \frac{(F_r - 1)}{G} \quad (10H.1)$$

where F_{rt} is the total receiver noise factor, F_r is the receiver noise factor without the two-port, F_c is the noise factor of the two-port, and $G = 1/\mathcal{L}$ is the available gain of the two-port. The total receiver noise factor is determined from (10E.3) as

$$F_{rt} = 1 + \frac{T_{rt}}{T_o} = 1 + \mathcal{L} \frac{T_e''}{T_o} + (\mathcal{L} - 1) \frac{T_c}{T_o} \quad (10H.2)$$

and the receiver noise factor is:

$$F_r = 1 + \frac{T_e''}{T_o} \quad (10H.3)$$

Substituting (10H.2) and (10H.3) into (10H.1) and solving for the noise factor of the passive two-port gives

$$F_c = 1 + (\mathcal{L} - 1) \frac{T_c}{T_o} \quad (10H.4)$$

which clearly indicates the dependence of passive two-port noise factor on operating temperature.

The effect of ambient temperature on active two-port noise temperature is much more complicated because the thermal noise sources interact with shot noise sources to give a net effective noise temperature. The noise factor of Equation 4F.57 should be written as:

$$F(T) = F_{min}(T) + \frac{B(T)}{G_s} \left[(G_s - G_{s_{opt}})^2 + (B_s - B_{s_{opt}})^2 \right] \quad (10H.5)$$

to illustrate the temperature dependence. By applying the Nyquist Theorem to the internal thermal noise sources, it is discovered that the temperature effects can be accounted for by simple temperature scaling. In other words, the equivalent noise resistances in the model can be scaled as:

$$r' = r \frac{T_d}{T_o} \quad (10H.6)$$

where r is the equivalent noise resistance at T_o and T_d is the operating noise temperature of the device. This scaling technique is not to be applied to any noise resistance representing shot noise. As an example, consider the noise factor of a junction transistor as represented by Equation 4F.67. The temperature dependance can be accounted for by scaling the base spreading resistance $r_{bb'}$:

$$r'_{bb'} = r_{bb'} \frac{T_d}{T_o} \quad (10H.7)$$

This is substituted into the noise factor Equation 4F.67 to give:

$$F(T_d) = 1 + \frac{1}{R_s} \left(r_{bb'} \frac{T_d}{T_o} + \frac{1}{2} r_e \right) + \frac{\left(R_s + r_e + r_{bb'} \frac{T_d}{T_o} \right)^2}{2 R_s r_e} \left[\frac{1}{\beta_o} + \left(\frac{f}{f_d} \right)^2 \right] \quad (10H.8)$$

The resistance r_e is not scaled because it represents shot noise. A similar procedure can be applied to all the noise factor equations in Chapter IV.

XI. INTERRELATIONSHIPS OF MEASUREMENT METHODS

This chapter is a summary of the important equations relating the various measures of receiver sensitivity. To keep the summary brief, the important equations will be listed but the detailed algebraic manipulations will not be shown. Several graphs will also be included to illustrate more clearly the features of some of the more useful equations.

The important relationships are now summarized (definitions follow the equations):

- a. Relationship between noise factor and effective noise temperature (Appendix, Part E):

$$F = 1 + \frac{T_e}{T_o} \quad \text{or} \quad T_e = (F - 1) T_o \quad (11.1)$$

- b. Relationship between noise factor and AM sensitivity (Equation 8D.7b):

$$F = \frac{m^2 E_{AM}^2}{S_p [4 k T_o R_s B_c]} \quad (11.2)$$

- c. Relationship between noise factor and tangential noise sensitivity (Chapter VIII-C):

$$F = \frac{E_{TN}^2}{4 k T_o R_s [K_D \sqrt{2 B_h B_L}]} \quad (11.3)$$

- d. Relationship between receiving system power sensitivity and effective noise temperature (Equation 4D.9):

$$P_{rs} = k [T_A + T_e] B_c S_{min} \quad (11.4)$$

The following quantities are defined:

- $B_c \triangleq$ The effective noise bandwidth of the receiving system, Hz
(see Equation 8D.18).
- $B_h \triangleq$ Predetection noise bandwidth, Hz.
- $B_L \triangleq$ Postdetection noise bandwidth, Hz.
- $E_{AM} \triangleq$ AM sensitivity in hard volts RMS. Value depends upon receiver noise bandwidth and desired predetection signal-to-noise ratio.
- $E_{TN} \triangleq$ Tangential noise sensitivity in hard volts RMS. Value depends upon K_D , B_h and B_L (see Equation 8C.1).
- $F \triangleq$ The noise factor of the total receiving system.
- $k \triangleq$ Boltzmann's constant, $1.38 \times 10^{-23} \frac{\text{watt-sec}}{^\circ\text{K}}$.
- $K_D \triangleq$ Sensitivity constant for tangential sensitivity.
- $m \triangleq$ Modulation index for amplitude modulation ($0 \leq m \leq 1$).
- $P_{rs} \triangleq$ Receiving system power sensitivity, watts.
- $R_s \triangleq$ Source or antenna resistance for which the sensitivity is measured, ohms.
- $S_p \triangleq$ Predetection signal-to-noise power ratio.
- $S_{min} \triangleq$ The minimum acceptable predetection signal-to-noise power ratio. Quite often arbitrarily chosen as unity.

$T_A \triangleq$ Effective noise temperature of the receiving antenna, $^{\circ}\text{K}$
(see Equation 4C.68).

$T_e \triangleq$ The effective noise temperature of the total receiving
system, $^{\circ}\text{K}$.

$T_o \triangleq$ Standard temperature, 290°K .

The notation for the equations above has been made as simple as possible and may not agree with various equations listed elsewhere. This compromise was considered necessary to achieve definitional simplicity. For more exact notation refer to the appropriate section elsewhere in the text.

A. Noise Factor (Noise Figure)

The following equations relate noise factor to the various other sensitivity parameters:

a. Effective noise temperature, T_e

$$F = 1 + \frac{T_e}{T_o} \quad (11A.1)$$

b. AM sensitivity, E_{AM}

$$F = \frac{m^2 E_{AM}^2}{S_p [4 k T_o R_s B_c]} \quad (11A.2)$$

c. Receiving system power sensitivity, P_{rs}

$$F = 1 + \left[\frac{P_{rs}}{k T_o B_c S_{\min}} - \frac{T_A}{T_o} \right] \quad (11A.3)$$

d. Tangential noise sensitivity, E_{TN}

$$F = \frac{E_{TN}^2}{4 k T_o R_s [K_D \sqrt{2 B_h B_L}]} \quad (11A.4)$$

A plot of noise factor and noise figure as a function of effective noise temperature is shown in Figure 11A-1. The graph is accurate enough to be used for most noise calculations.

Equation 11A.2, which describes the relationship between noise figure and AM sensitivity, can be specialized to a more convenient form by specifying some of the receiver parameters. It is common practice to fix the values of antenna impedance, signal-to-noise ratio, and modulation index when specifying the AM sensitivity of a variety of receivers. Nominally, the predetection SNR is related to the audio output signal-plus-noise-to-noise ratio as (see Equation 8D.18):

$$S_p = \left[\frac{S_o + N_o}{N_o} - 1 \right]$$

The following values are commonly used standards for AM sensitivity measurements:

$$\frac{S_o + N_o}{N_o} = 10 \text{ (Corresponding to a 10 db ratio)}$$

$$R_s = 50 \text{ ohms}$$

$$m = 0.30 \text{ (corresponding to 30\% modulation)}$$

In the normal AM system, the predetection noise bandwidth is twice the audio bandwidth. If B_A is the audio bandwidth, then $B_c = 2 B_A$ and if

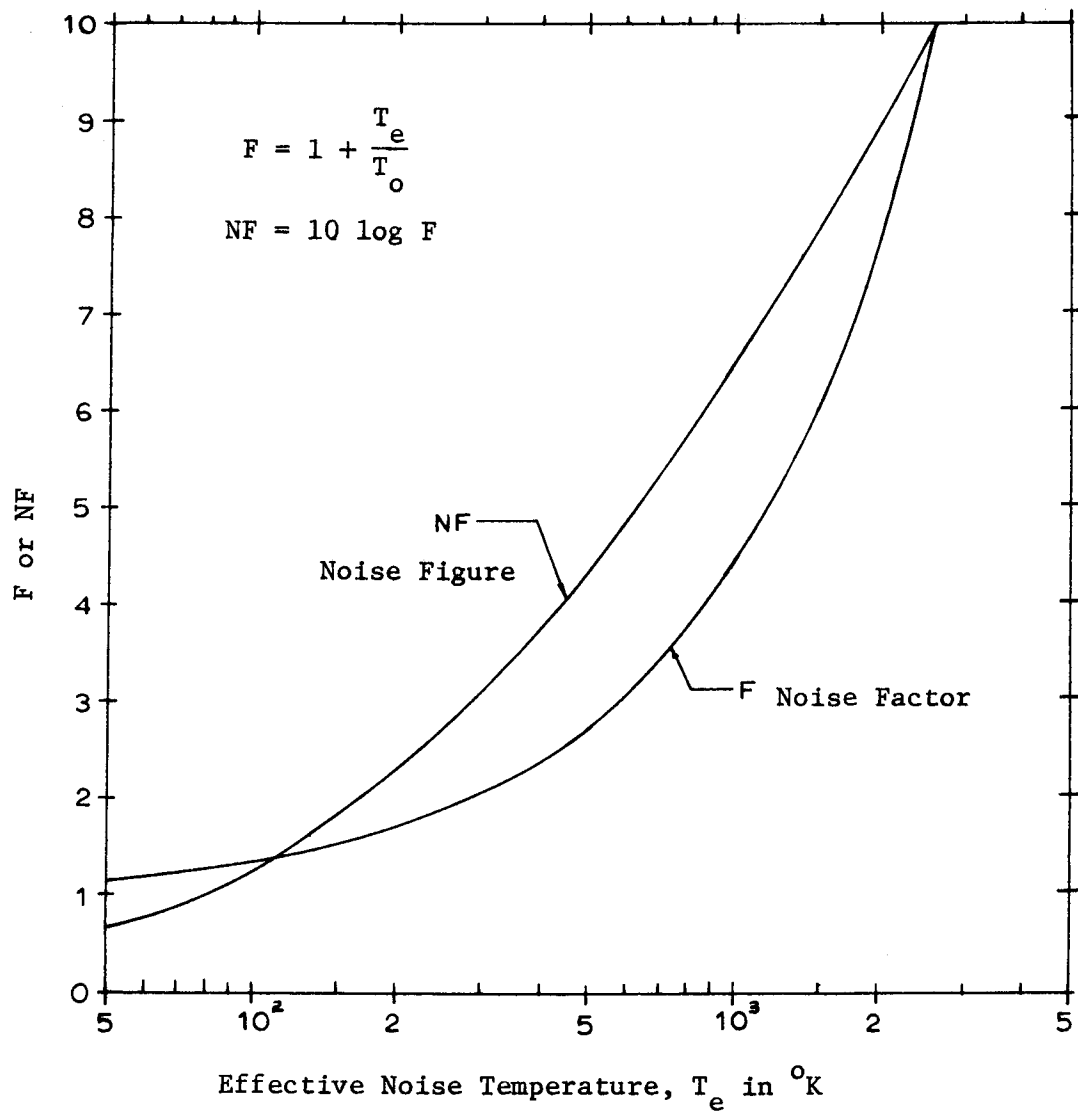


Figure 11A-1. Noise Factor and Noise Figure as a Function of Effective Noise Temperature

this and the constants above are substituted into Equation 11A.2 the result is*

$$F = 6250 \frac{E_{AM}^2}{B_A} \quad (11A.5)$$

where E_{AM} = the receiver AM sensitivity in hard microvolts

RMS (see Appendix, Part Q)

B_A = receiver audio noise bandwidth in Hz.

A very useful plot of Equation 11A.5 is given in Figure 11A-2. This graph can be used to compare receiver AM sensitivity specifications against equivalent noise figure. For example, a receiver with an audio bandwidth of 3 KHz is measured with a 1 KHz tone modulated 50-ohm signal generator. The required input in available signal power is, -111.4 DBM or 1.2 μ V hard, for an audio output signal-plus-noise-to-noise ratio of 10 db. The corresponding noise figure, from Figure 11A-2, is 4.4 db. For any receiver with these characteristics it would be meaningless to report a sensitivity of less than 0.7 μ V hard as this would require a noise figure less than 0 db. A scale of available signal power in DBM with a 50 ohm reference is given at the top of the figure while that for signal level in hard microvolts is given at the bottom.

One must be careful to specify whether the sensitivity is in hard microvolts or soft because of the 6 db difference. For example, an AM sensitivity of -113 DBM corresponds to 1.0 μ V hard and 0.5 μ V soft.

*The convenience and simplicity of this equation was first brought to the author's attention in a private communication from D. B. Hallock of Collins Radio Company, Cedar Rapids, Iowa.

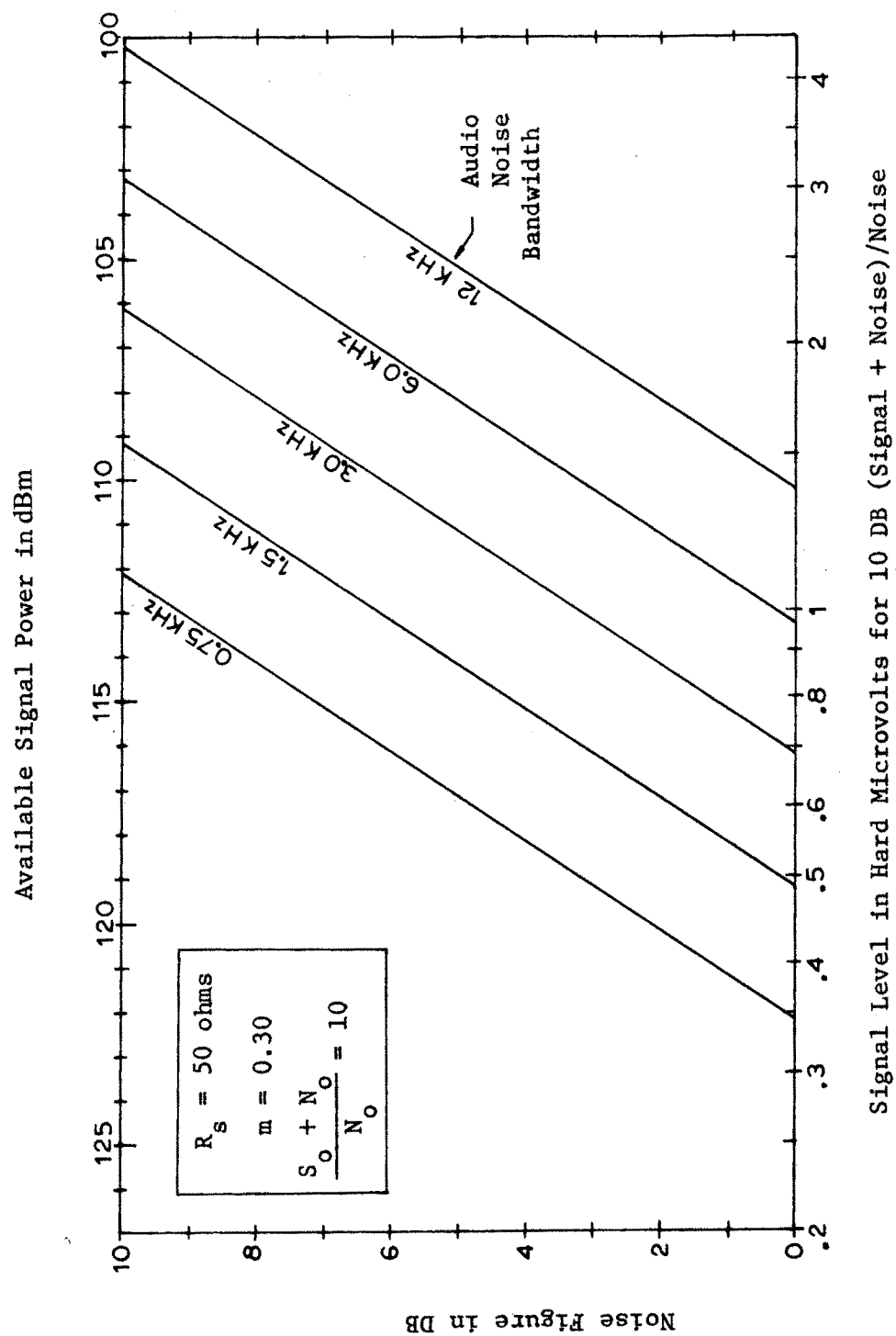


Figure 11A-2. Correspondence between Noise Figure and AM Sensitivity for a 50-ohm System at Standard Temperature. Carrier is modulated 30% and the signal-plus-noise-to-noise ratio is 10 DB.

Typically a signal generator will be calibrated in DBM and soft microvolts. If the sensitivity is read directly off the dial of such an instrument, the reading must be doubled before it is reported as a hard microvolt sensitivity.

B. Effective Noise Temperature

The following equations relate effective noise temperature to the various other sensitivity parameters:

- a. Noise factor, F

$$T_e = (F - 1) T_o \quad (11B.1)$$

- b. AM sensitivity, E_{AM}

$$T_e = T_o \left[\frac{m^2 E_{AM}^2}{S_p [4 k T_o R_s B_c]} - 1 \right] \quad (11B.2)$$

- c. Receiving system power sensitivity, P_{rs}

$$T_e = \frac{P_{rs}}{k B_c S_{min}} - T_A \quad (11B.3)$$

- d. Tangential noise sensitivity, E_{TN}

$$T_e = T_o \left[\frac{E_{TN}^2}{4 k T_o R_s [K_D \sqrt{2 B_h B_L}]} - 1 \right] \quad (11B.4)$$

C. AM Sensitivity

The following equations relate AM sensitivity to the various other sensitivity parameters:

- a. Noise factor, F

$$E_{AM} = \frac{1}{m} \sqrt{F S_p [4 k T_o R_s B_c]} \quad (11C.1)$$

- b. Effective noise temperature, T_e

$$E_{AM} = \frac{1}{m} \sqrt{S_p [4 k (T_e + T_o) R_s B_c]} \quad (11C.2)$$

- c. Receiving system power sensitivity, P_{rs}

$$E_{AM} = \frac{2}{m} \sqrt{R_s \left[\frac{P_{rs}}{S_{min}} - k (T_o - T_A) B_c \right]} \quad (11C.3)$$

- d. Tangential noise sensitivity, E_{TN}

$$E_{AM} = \frac{E_{TN}}{m} \sqrt{\frac{S_p B_c}{K_D \sqrt{2 B_h B_L}}} \quad (11C.4)$$

D. Receiving System Power Sensitivity

The following equations relate receiving system power sensitivity to the various other sensitivity parameters:

- a. Noise factor, F

$$P_{rs} = k \left[T_A + (F - 1) T_o \right] B_c S_{min} \quad (11D.1)$$

b. Effective noise temperature, T_e

$$P_{rs} = k [T_A + T_e] B_c S_{min} \quad (11D.2)$$

c. AM sensitivity, E_{AM}

$$P_{rs} = k B_c S_{min} \left[T_A + T_o \left\{ \frac{m^2 E_{AM}^2}{S_p [4 k T_o R_s B_c]} - 1 \right\} \right] \quad (11D.3)$$

d. Tangential noise sensitivity, E_{TN}

$$P_{rs} = k B_c S_{min} \left[T_A + T_o \left\{ \frac{E_{TN}^2}{4 k T_o R_s [K_D \sqrt{2 B_h B_L}]} - 1 \right\} \right] \quad (11D.4)$$

A special form of Equation 11D.2 is used to describe the power sensitivity of a receiving system. First it is necessary to introduce the concept of absolute sensitivity (Saad, 1966). Take the log of both sides of Equation 11D.2 and write in terms of db:

$$P_{rs}(db) = 10 \log P_{rs} = 10 \log [k (T_A + T_e)] + 10 \log B_c + 10 \log S_{min} \quad (11D.5)$$

The factor,

$$S = 10 \log [k (T_A + T_e)] \quad (11D.6)$$

is referred to as the absolute sensitivity. It is the power sensitivity of a receiver which has a 1 Hz bandwidth and a minimum acceptable

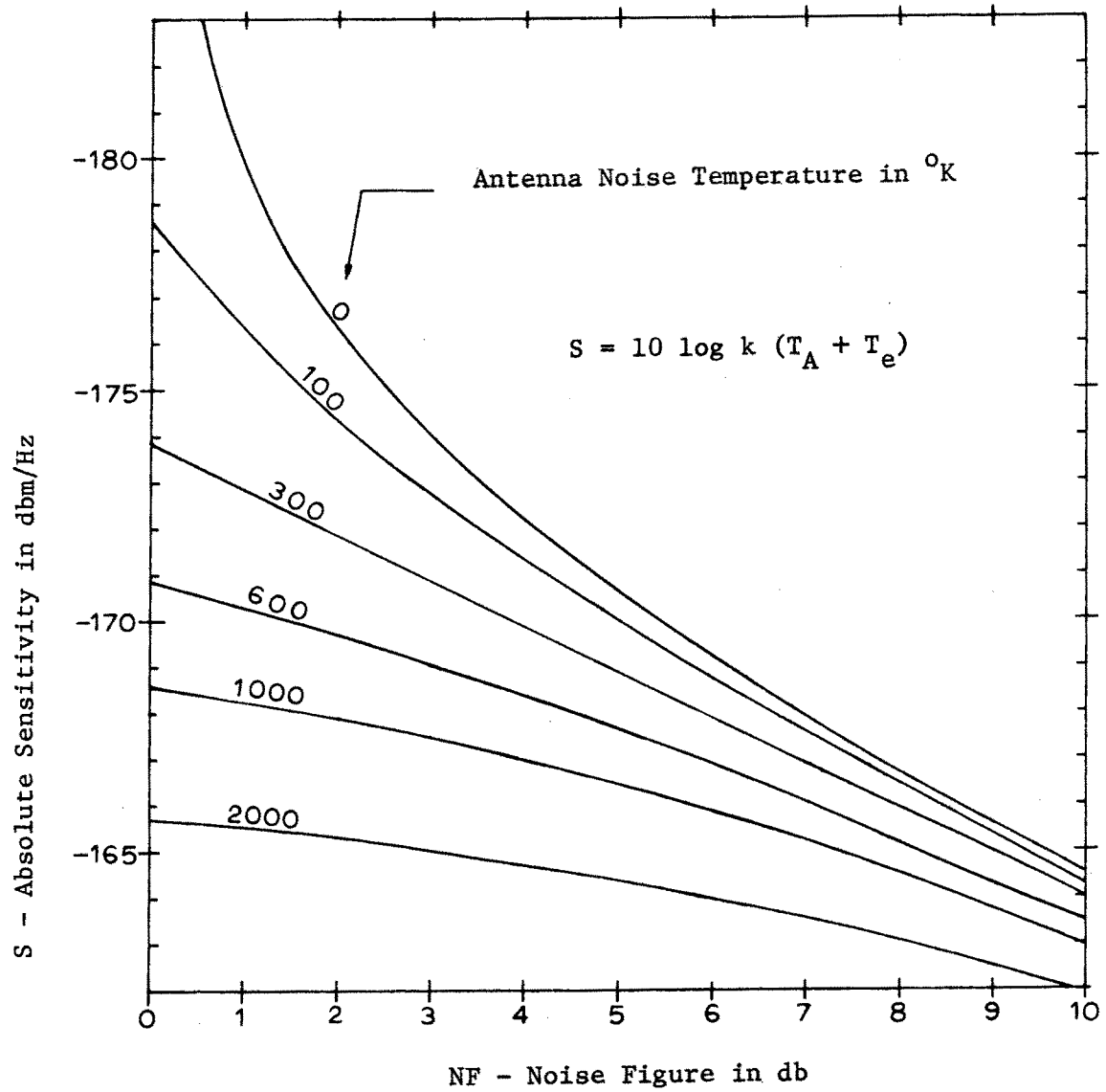


Figure 11D-1. Absolute Sensitivity as a Function of Noise Factor for Various Antenna Noise Temperatures

predetection SNR of unity. For any B_c and S_{min} , the receiving system power sensitivity can be written as:

$$P_{rs}(db) = S + 10 \log B_c + 10 \log S_{min} \quad (11D.7)$$

A plot of absolute sensitivity as a function of receiver noise figure for various values of antenna noise temperature is shown in Figure 11D-1. This figure illustrates several of the interesting features involved in the trade-offs between receiver noise figure and antenna noise temperature. As an example, consider a receiver with a noise bandwidth of 1 KHz, a noise figure of 2 db, and a required minimum SNR of 10 db. When the antenna noise temperature is 100° K, the available signal power at the antenna must be greater than P_{rs} . Using Equation 11D.7 and Figure 11D-1 we calculate:

$$P_{rs}(dbm) = -174.2 + 10 \log 1000 + 10 = -134.2 \text{ dbm}$$

An increase in the antenna noise temperature from 100° K to 1000° K results in a $P_{rs}(dbm)$ of -127.8 dbm. Calculations of this type can be used to determine where improvements in sensitivity can be most economically made.

E. Tangential Noise Sensitivity (Pulse Code Systems)

The following equations relate tangential noise sensitivity to the various other sensitivity parameters:

a. Noise factor, F

$$E_{TN} = \sqrt{F \left[4 k T_o R_s K_D \sqrt{2 B_h B_L} \right]} \quad (11E.1)$$

b. Effective noise temperature, T_e

$$E_{TN} = \sqrt{4 k (T_o + T_e) R_s K_D \sqrt{2 B_h B_L}} \quad (11E.2)$$

c. AM sensitivity, E_{AM}

$$E_{TN} = m E_{AM} \left[\frac{S_p B_c}{K_D \sqrt{2 B_h B_L}} \right]^{-\frac{1}{2}} \quad (11E.3)$$

d. Receiving system power sensitivity, P_{rs}

$$E_{TN} = 2 \sqrt{k R_s K_D \sqrt{2 B_h B_L} \left[\frac{P_{rs}}{k B_c S_{min}} - T_A + T_o \right]} \quad (11E.4)$$

For a 50-ohm system, the constants k and T_o can be substituted into Equation 11A.4 to give

$$F = 1.25 \frac{E_{TN}^2}{K_D \sqrt{2 B_h B_L}} \quad (11E.5)$$

where E_{TN} is in hard microvolts RMS and the bandwidths are in MHz. Another convenient representation is to express the tangential sensitivity in available power at the input. The power sensitivity of the receiver is (from Equation 8C.2)

$$\begin{aligned} S_i(\text{dbm}) &= -114 + 10 \log F + 10 \log K_D + 10 \log \sqrt{2 B_h B_L} \\ &= -114 + NF + 10 \log K_D + 10 \log \sqrt{2 B_h B_L} \end{aligned} \quad (11E.6)$$

where values of K_D are given in Table 8C-1. The quantity $\sqrt{2 B_h B_L}$ is sometimes defined as an effective receiver bandwidth (Klipper, 1965):

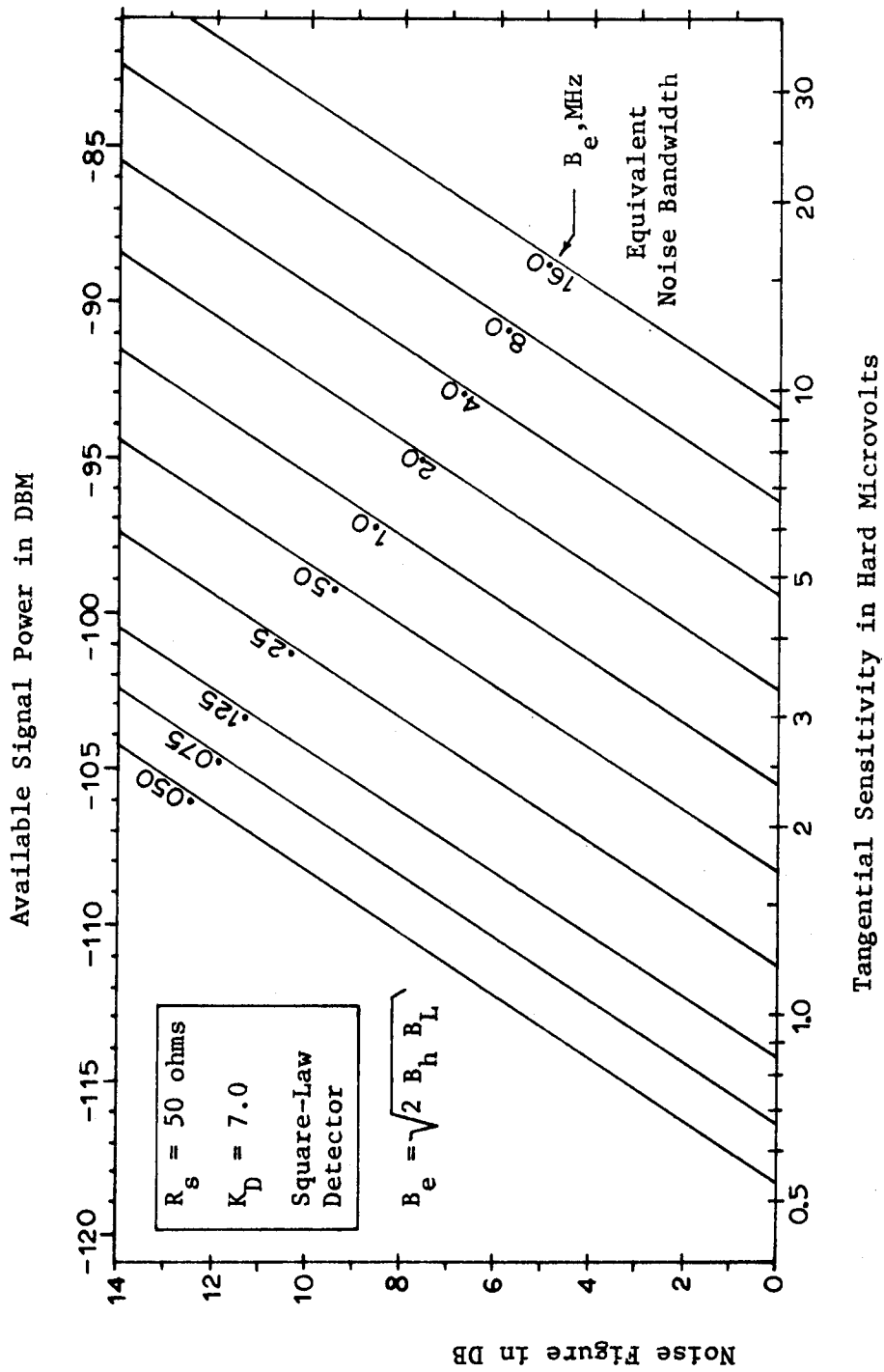


Figure 11E-1. Correspondence between Noise Figure and Tangential Sensitivity for a 50-ohm System at Standard Temperature

$$B_e = \sqrt{2 B_h B_L} \quad (11E.7)$$

For a square-law detector ($K_D = 7$), Equation 11E.6 can be simplified to:

$$S_i(\text{dbm}) = -105.5 + \text{NF} + 10 \log B_e \quad (11E.8)$$

Equation 11E.8 is used to generate the graph of Figure 11E-1. Since the value of the sensitivity constant, K_D , depends on an observer evaluation which is no better than 1-2 db, the accuracy of the graph is limited to the same error.

As an example, consider a pulse receiver with predetection bandwidth of 20 Mhz, a postdetection bandwidth of 0.1 Mhz, a noise figure of 8 db, and a square-law detector. From Equation 11E.7, the effective receiver bandwidth is 2.0 Mhz. From Figure 11E-1, the tangential sensitivity is -94.5 DBM. This is a voltage sensitivity (in a 50-ohm system) of 8.3 μV hard or 4.15 μV soft.

F. Noise Quieting (FM Sensitivity)

A relationship between FM sensitivity and the other sensitivity parameters given in this chapter was not established in Chapters VIII or IX. The reason for this is that the comparisons are too dependent on detector and signal properties. It is because of this that comparisons among the various FM sensitivities were not made. No literature reference that treats these problems was found. Further investigations are needed to provide information about these comparisons.

XII. SUMMARY

Noise theory and sensitivity-measurement theory have been discussed for receiving systems and circuits. The topics were presented from the viewpoint of a design engineer working with high-frequency systems and circuits. Emphasis has been given to the circuit analysis of noise problems in each basic block of a complete receiving system. The main goal of this work has been to provide a self-study guide in these areas for engineers and scientists with very little background on noise theory.

The basic questions: 1) what is receiving system sensitivity, 2) how does it relate to signal-to-noise ratio, and 3) how is it measured, were answered. The functional blocks of a receiving system were described in detail as to their operation and effect on sensitivity. The physics of noise generation, how it is characterized and the physical sources of noise were presented in great detail. The fundamentals of two-port noise theory were emphasized throughout the text.

The overall picture of a communication system was discussed in Chapter II. Each component of the system was described and the reasons for studying the noise in receivers and antennas were stated. In Chapter III, the receiving system was presented and each component of the system was related to the overall performance. A detailed block diagram of the receiver was presented.

A large part of the writing and research was concentrated in Chapter IV on noise in electronic circuits. The physical properties and physical sources of noise were discussed in detail to provide the user with as much background information as possible. This background

was then used to discuss the topics of system and circuit noise and noise theory for two-port networks. Many of the more important equations were derived in this chapter. The last part of the chapter dealt with noise in electron devices. The most important device noise information was condensed so it could be used for self-study.

The discussion on RF translator noise in Chapter V was a summary of information scattered throughout the text. Translator noise was discussed separately because the RF translator is the most important sensitivity determining component in a receiver. The chapter was concluded with an interesting graph showing state-of-the-art noise figures for commercially available broadband RF amplifiers.

The most technically demanding topic was the discussion of noise power detectors in Chapter VI. Detector theory was heavily involved in determining the resolution accuracy of a noise measurement. The different types of detectors were analyzed and the relationship between predetection signal-to-noise ratio and output measurement was presented.

Chapters VII through X dealt with the theory of sensitivity measurements. The common measuring methods and the errors associated with those methods were given in detail.

The relationships among the various sensitivity specifications were presented in Chapter XI. Of special importance were the graphs comparing; noise figure and noise factor with effective temperature, noise figure with AM sensitivity, noise figure with absolute sensitivity, and noise figure with tangential sensitivity.

An extensive appendix was given to provide the fundamental definitions of many of the quantities used in the study of noise theory in electronic circuits.

XIII. BIBLIOGRAPHY

Aarons, Jules

- 1954 Antenna and Receiver Measurements by Solar and Cosmic Noise.
Proceedings of the IRE 42: 810-815. May.

Adler, R. B. and Haus, H. A.

- 1958 Network Realization of Optimum Amplifier Noise Performance.
IRE Transactions on Circuit Theory CT-5: 156-161. September.

Agouridis, Dimitrios C. and van der Ziel, A.

- 1967 Noise Figure of UHF Transistors as a Function of Frequency
and Bias Conditions. IEEE Transaction on Electron Devices
ED-14: 808-816. December.

Alley, Charles L. and Atwood, Kenneth W.

- 1971 Semiconductor Devices and Circuits. New York, N.Y., John
Wiley and Sons, Inc.

Anouchi, A. Y.

- 1958 Measuring Noise Figures of Transistor Amplifiers. Proceedings
of the IRE, Correspondence 46: 619. March.

Antman, Herbert S.

- 1967 Mismatching for Low Noise. Electronic Design 14: 86. July.

Ashby, Bill

- 1961 Moon Relay Requirements. 73 Magazine 1: 31. May.

Baechtold, W. and Strutt, M.J.O.

- 1968 Noise in Microwave Transistors. IEEE Transactions on Micro-
wave Theory and Techniques MTT-16: 578-585. September.

Baghdady, Elie J.

- 1961 A Technique for Lowering the Noise Threshold of Conventional
Frequency, Phase, and Envelope Demodulators. IRE Transactions
on Communication Systems CS-9: 194-206. September.

Baker, William

- 1969 Obtain the Correct Dope on Receiver Sensitivity. Microwaves
8: 50-51. February.

Ballantine, Stuart

- 1930 Fluctuation Noise in Radio Receivers. Proceedings of the IRE
18: 1377-1387. August.

Barber, Mark R.

- 1967 Noise Figure and Conversion Loss of the Schottky Barrier
Mixer Diode. IEEE Transactions on Microwave Theory and
Techniques MTT-15: 629-635. November.

- Baxendall, P. J.
 1968a Noise in Transistor Circuits, Part 1. Wireless World 74: 388-392. November.
- Baxendall, P. J.
 1968b Noise in Transistor Circuits, Part 2. Wireless World 74: 454-459. December.
- Beckmann, Petr
 1967 Probability in Communication Engineering. New York, N.Y., Harcourt, Brace and World, Inc.
- Bell, R. L.
 1951 Induced Grid Noise and Noise Factor. Proceedings of the IRE 39: 1059-1063. September.
- Bendat, Julius S.
 1958 Principles and Applications of Random Noise Theory. New York, N.Y., John Wiley and Sons, Inc.
- Bennett, William R.
 1956 Methods of Solving Noise Problems. Proceedings of the IRE 44: 609-638. May.
- Bennett, William R.
 1960 Electrical Noise. New York, N.Y., McGraw-Hill Book Co., Inc.
- Bevensee, R. M.
 1963 The Fundamental Noise Limit of Linear Amplifiers. Proceedings of the IEEE, correspondence 51: 245. January.
- Blachman, Nelson M.
 1966 Noise and its Effect on Communication. New York, N.Y., McGraw-Hill Book Co., Inc.
- Blackman, R. B. and Tukey, J. W.
 1958 The Measurement of Power Spectra. New York, N.Y., Dover Publications, Inc.
- Blake, Lamont V.
 1972 A Postdetection Method of Measuring Predetection RF Signal-to-Noise Ratio. IEEE Transactions on Aerospace and Electronic Systems AES-8: 168-173. March.
- Bracewell, Ron.
 1965 The Fourier Transform and Its Applications. New York, N.Y., McGraw-Hill Book Company, Inc.
- Brady, M. Michael
 1964 The Influence of Mismatch Error in Noise Performance Measurements. Proceedings of the IEEE 52: 1075-1076. September.

Breazeale, William M.

- 1947 A Note on Noise and Conversion Gain Measurements. Proceedings of the IRE 35: 31-34. January.

Bridges, J. E.

- 1954 Detection of Television Signals in Thermal Noise. Proceedings of the IRE 42: 1396-1405. September.

Brodzinsky, A. and Macpherson, A. C.

- 1959 Noise Measurement of Negative Resistance Amplifiers. IRE Transactions on Instrumentation I-8: 44-46. September.

Brown, R. G. and Nilsson, J. W.

- 1962 Introduction to Linear Systems Analysis. New York, N.Y., John Wiley and Sons, Inc.

Brubaker, Richard

- 1968 Semiconductor Noise Figure Considerations. Motorola Application Note AN-421. Motorola Semiconductor Products, Inc., Phoenix, Arizona. August.

Bruncke, W. C.

- 1963 Noise Measurements in Field-Effect Transistors. Proceedings of the IEEE 51: 378-379. February.

Bruncke, W. C. and van der Ziel, A.

- 1966 Thermal Noise in Junction-Gate Field Effect Transistors. IEEE Transaction on Electron Devices ED-13: 323-328. March.

Buckmaster, H. A.

- 1965 An Alternate Derivation of Fundamental Noise Limit of Linear Amplifiers. Proceedings of the IEEE 53: 194. February.

Burrill, Charles M.

- 1941 Progress in the Development of Instruments for Measuring Radio Noise. Proceedings of the IRE 29: 433-441. August.

Case, Nelson P.

- 1931 Receiver Design for Minimum Fluctuation Noise. Proceedings of the IRE 19: 963-970. June.

Champlin, Keith S.

- 1958 Bridge Method of Measuring Noise in Low Noise Devices at Radio Frequencies. Proceedings of the IRE, correspondence 46: 779. April.

Chemical Rubber Co.

- 1971 Standard Mathematical Tables. Cleveland, Ohio, Chemical Rubber Company.

- Chessin, P. L.
1955 A Bibliography on Noise. IRE Transactions on Information Theory IT-1: 15-31. September.
- Chirlian, Paul M.
1965 Analysis and Design of Electronic Circuits. New York, N.Y., McGraw-Hill Book Co., Inc.
- Cohn, Seymour B.
1959 The Noise Figure Muddle. Microwave Journal: 7-11. March.
- Cook, A. B. and Liff, A. A.
1968 Frequency Modulation Receivers. Englewood Cliffs, N.J., Prentice-Hall, Inc.
- Cooke, Harry F.
1961 Transistor Upper Noise Corner Frequency. Proceedings of the IRE, correspondence 49: 648. March.
- Cooke, Harry F.
1962 On the Two-Generator Method ($e_{n,i}$) of Noise Characterization. Proceedings of the IRE, correspondence 50: 2520-2521. December.
- Cottony, H. V. and Johler, J. R.
1952 Cosmic Radio Noise Intensities in the VHF Band. Proceedings of the IRE 40: 1053-1060. September.
- Cowley, A. Michael and Zettler, Robert A.
1968 Shot Noise in Silicon Schottky Barrier Diodes. IEEE Transactions on Electron Devices ED-15: 761-769. October.
- Crosby, Murray G.
1937 Frequency Modulation Noise Characteristics. Proceedings of the IRE 25: 472-514. April.
- Cushman, Robert H.
1971 Make the Most of Noise: Correlate IT. Electronic Design News 16: 29-35. March.
- Davenport, Wilbur B., Jr. and Root, William L.
1958 An Introduction to the Theory of Random Signals and Noise. New York, N.Y., McGraw-Hill Book Co., Inc.
- DeLano, R. H.
1949 Signal-to-Noise Ratio of Linear Detectors. Proceedings of the IRE 37: 1120-1126. October.
- Dinger, Harold E. and Paine, Harold G.
1947 Factors Affecting the Accuracy of Radio Noise Meters. Proceedings of the IRE 35: 75-81. January.

Dragone, Corrado

- 1968 Analysis of Thermal and Shot Noise in Pumped Resistive Diodes. Bell System Technical Journal 47: 1883-1902. November.

Dyke, Edwin

- 1961 Corrections and Coordination of Some Papers on Noise Temperature. Proceedings of the IRE, correspondence 49: 814-815. April.

Edson, W. A.

- 1960 Noise in Oscillators. Proceedings of the IRE 48: 1454-1466. August.

Eisele, Konrad M.

- 1964 Refrigerated Microwave Noise Sources. IEEE Transactions on Instrumentation and Measurement IM-13: 336-342. December.

Ekiss, J. A. and Halligan, J. W.

- 1961 A Theoretical Comparison of Average and Spot-Noise Figure in Transistor Amplifiers. Proceedings of the IRE, correspondence 49: 1216-1217. July.

Espenschied, Lloyd

- 1931 Methods for Measuring Interfering Noises. Proceedings of the IRE 19: 1951-1954. November.

Feldman, Leonard

- 1966 F-M Multiplexing for Stereo. New York, N.Y., Howard W. Sams and Co., Inc.

Finnegan, P. J.

- 1967 Noise Analysis of Feedback Amplifiers. Electronic Engineering 39: 612-616. October.

Fisher, Sydney T.

- 1962 A Completely Consistent Definition of Temperature Sensitivity Including Negative Conductance Devices. Proceedings of the IRE, correspondence 50: 204. February.

Fraser, B. E.

- 1949 Noise Spectrum of Temperature Limited Diodes. Wireless Engineer 26: 129-131. April.

Freeman, J. J.

- 1958 Principles of Noise. New York, N.Y., John Wiley and Sons, Inc.

Friis, H. T.

- 1944 Noise Figures of Radio Receivers. Proceedings of the IRE 32: 419-422. July.

Fry, Thornton C.

- 1925 The Theory of the Schroteffekt. Journal of the Franklin Institute 199: 203-220. February.

Fubini, Eugene G. and Johnson, Donald C.

- 1948 Signal to Noise Ratios in AM Receivers. Proceedings of the IRE 36: 1461-1466. December.

Fukui, H.

- 1966a The Noise Performance of Microwave Transistors. IEEE Transactions on Electron Devices ED-13: 329-341. March.

Fukui, H.

- 1966b Available Power Gain, Noise Figure, and Noise Measure of Two-Ports and their Graphical Representations. IEEE Transactions on Circuit Theory CT-13: 137-142. June.

Goldberg, Harold

- 1948 Some Notes on Noise Figures. Proceedings of the IRE 36: 1205-1214. October.

- 1949 Correction, Proceedings of the IRE 37: 40. January.

Golding, J. F.

- 1968 AM Receiver Noise Factor Measurements Using Sinewave Test Signals. Electronic Engineering 40: 420-422. August.

Goldner, R. B.

- 1962 An Interesting Black Box Problem Solved by a Noise Measurement. Proceedings of the IRE, correspondence 50: 2509. December.

Goldsmith, A. N. et al., Editors.

- 1948 Frequency Modulation, Volume I. Princeton, N.J., RCA Review, Radio Corporation of America, RCA Laboratories Division.

Gordon, J. P.

- 1962 Quantum Effects in Communication Systems. Proceedings of the IRE 50: 1898-1908. September.

Greene, J. C.

- 1961 "Noisemanship"--The Art of Measuring Noise Figures Nearly Independent of Device Performance. Proceedings of the IRE, correspondence 49: 1223-1224. July.

Grimm, Henry H.

- 1959 Fundamental Limitations of External Noise. IRE Transactions on Instrumentation I-8: 97-103. December.

- Haitz, Roland H.
 1967 Noise of a Self-sustaining Avalanche Discharge in Silicon: Low-Frequency Noise Studies. Journal of Applied Physics 38: 2935-2946. June.
- Hanson, G. H. and van der Ziel, A.
 1957 Shot Noise in Transistors. Proceedings of the IRE 45: 1538-1542. November.
- Harris, I. A.
 1966 Dependence of Receiver Noise-Temperature Measurement on Source Impedance. Electronics Letters 2: 130-131. April.
- Hart, P.A.H.
 1962 Standard Noise Sources. Phillips Technical Review 23: 293-309. July.
- Harvard University, Electronics Training Staff of the Cruft Laboratory
 1947 Electronic Circuits and Tubes. New York, N.Y., McGraw-Hill Book Co., Inc.
- Haus, H. A.
 1962 Noise Figure for Negative Source Resistance. Proceedings of the IRE, correspondence 50: 2135-2136. October.
- Haus, H. A. and Adler, R. B.
 1957 An Extension of the Noise Figure Definition. Proceedings of the IRE, correspondence 45: 690-691. May.
- Haus, H. A. and Adler, R. B.
 1958a Optimum Noise Performance of Linear Amplifiers. Proceedings of the IRE 46: 1517-1533. August.
- Haus, H. A. and Adler, R. B.
 1958b Canonical Form of Linear Noisy Networks. IRE Transactions on Circuit Theory CT-5: 161-167. September.
- Haus, H. A. and Adler, R. B.
 1959 Circuit Theory of Linear Noisy Networks. New York, N.Y., John Wiley and Sons, Inc.
- Henney, Keith
 1959 Radio Engineering Handbook. New York, N.Y., McGraw-Hill Book Company, Inc.
- Heffner, H.
 1962 The Fundamental Noise Limit of Linear Amplifiers. Proceedings of the IRE 50: 1604-1608. July.

Hooper, Wendell P.

- 1970 Noise Temperature Summary. Frequency Technology 8: 22-25. March.

Hudson, A. C.

- 1955 Noise Factor Measurement. Proceedings of the IRE 43: 1974. December.

International Telephone and Telegraph Corp.

- 1956 Reference Data for Radio Engineers, 4th ed. New York, N.Y., American Book-Stratford Press, Inc.

IRE Standards Committee

- 1952 "Standards on Receivers: Definition of Terms, 1952." Proceedings of the IRE 40: 1681-1685. December.

IRE Standards Committee

- 1953 "Standards on Electron Devices: Methods of Measuring Noise." Proceedings of the IRE 41: 890-896. July.

IRE Subcommittee on Noise

- 1960a "IRE Standards on Methods of Measuring Noise in Linear Two-ports, 1959." Proceedings of the IRE 48: 60-68. January.

IRE Subcommittee on Noise

- 1960b "Representation of Noise in Linear Twoports." Proceedings of the IRE 48: 69-74. January.

IRE Subcommittee 7.9 on Noise

- 1963a "IRE Standards on Electron Tubes: Definitions of Terms, 1962 (62 IRE 7.52)." Proceedings of the IEEE 51: 434-435. March.

IRE Subcommittee 7.9 on Noise

- 1963b "Description of the Noise Performance of Amplifiers and Receiving Systems." Proceedings of the IEEE 51: 436-442. March.

Jakobschuk, A.

- 1968 Amplifier Noise Figure Optimization. Proceedings of the IEEE 56: 1631-1632. September.

Jansky, Karl G.

- 1932 Directional Studies of Atmospherics at High Frequencies. Proceedings of the IRE 20: 1920-1932. December.

Jansky, Karl G.

- 1937 Minimum Noise Levels Obtained on Short-Wave Radio Receiving Systems. Proceedings of the IRE 25: 1517-1530. December.

- Jansky, Karl G.
 1939 An Experimental Investigation of the Characteristics of Certain Types of Noise. Proceedings of the IRE 27: 763-768. December.
- Johnson, J. B.
 1925 The Schottky Effect in Low Frequency Circuits. Physical Review 26: 71-85. July.
- Johnson, J. B.
 1928 Thermal Agitation of Electricity in Conductors. Physical Review 26: 97-109.
- Johnson, George D.
 1966 Design Amplifiers for Low Noise. Electronic Design 25: 54-63. November.
- Jolly, W. P.
 1967 Low Noise Electronics. New York, N.Y., American Elsevier Publishing Co., Inc.
- Jones, R. Clark
 1959 Noise in Radiation Detectors. Proceedings of the IRE 47: 1481-1486. September.
- Karni, Shlomo
 1966 Network Theory: Analysis and Synthesis. Boston, Mass., Allyn and Bacon, Inc.
- Klaassen, Francois M.
 1967 High-Frequency Noise in the Junction Field-Effect Transistor. IEEE Transactions on Electron Devices ED-14: 368-373. July.
- Klaassen, Francois M. and Prins, Jan
 1969 Noise of Field-Effect Transistors at Very High Frequencies. IEEE Transactions on Electron Devices ED-16: 952-957. November.
- Klipper, Harold
 1965 Sensitivity of Crystal Video Receivers with RF Pre-Amplification. Microwave Journal 8: 85-92. August.
- Kraus, John D.
 1966 Radio Astronomy. New York, N.Y., McGraw-Hill Book Co., Inc.
- Kurokawa, K.
 1961 Actual Noise Measure of Linear Amplifiers. Proceedings of the IRE 49: 1391-1397. September.

Landon, Vernon D.

- 1936 A Study of the Characteristics of Noise. Proceedings of the IRE 24: 1514-1521. November.

Landon, Vernon D. and Reid, J. D.

- 1939 A New Antenna System for Noise Reduction. Proceedings of the IRE 27: 188-191. March.

Landon, Vernon D.

- 1941 The Distribution of Amplitude with Time in Fluctuation Noise. Proceedings of the IRE 29: 50-55. February.
- 1942 Discussion on Landon Paper. Proceedings of the IRE 30: 425-429. September.
- 1942 Corrections. Proceedings of the IRE 30: 526. November.

Lavoo, Norman T.

- 1949 Measured Noise Characteristics at Long Transit Angles. Proceedings of the IRE 37: 383-386. April.

Lawson, J. L. and Uhlenbeck, George E.

1950. Threshold Signals. New York, N.Y., McGraw-Hill Book Co., Inc.

Lebenbaum, Matthew T.

- 1950 Design Factors in Low-Noise Figure Input Circuits. Proceedings of the IRE 38: 75-80. January.

Livingston, Marvin L. and Bechtold, William C.

- 1968 Effect of Impedance Mismatch on Antenna Noise Temperature. Microwave Journal 11: 79-82. April.

Llewellyn, F. B.

- 1930 A Study of Noise in Vacuum Tubes and Attached Circuits. Proceedings of the IRE 18: 243-265. February.

Llewellyn, F. B.

- 1931 A Rapid Method of Estimating the Signal-to-Noise Ratio of a High Gain Receiver. Proceedings of the IRE 19: 416-420. March.

Matthews, C.N.G.

- 1967 Noise Figure Measurement. Wireless World 73: 393-394. August.

Meissner, Hans

- 1965 Correction of the Reading of Average Reading VTVM for Noise. Proceedings of the IEEE 53: 412. April.

- Menzel, Donald H., Editor
 1960 The Radio Noise Spectrum. Cambridge, Massachusetts, Harvard University Press.
- Messenger, G. C. and McCoy, C. T.
 1957 Theory and Operation of Crystal Diodes as Mixers. Proceedings of the IRE 45: 1269-1283. September.
- Middleton, David
 1948 Rectification of a Sinusoidally Modulated Carrier in the Presence of Noise. Proceedings of the IRE 36: 1467-1477. December.
- Middleton, David
 1960 An Introduction to Statistical Communication Theory. New York, N.Y., McGraw-Hill Book Co., Inc.
- Miller, C.K.S., Daywitt, W. C. and Arthur, M. G.
 1967 Noise Standards, Measurements, and Receiver Noise Definitions. Proceedings of the IEEE 55: 865-877. June.
- Montgomery, Carol G.
 1964 Technique of Microwave Measurements. Lexington, Mass., Boston Technical Publishers, Inc.
- Moxon, Leslie A.
 1949 The Application of IF Noise Sources to the Measurement of Over-all Noise Figure and Conversion Loss in Microwave Receivers. Proceedings of the IRE 37: 1433-1437. December.
- Mumford, W. W. and E. H. Scheibe
 1968 Noise Performance Factors in Communication Systems. Dedham, Mass., Horizon House-Microwave, Inc.
- Mumford, W. W., Guest Editor
 1968 Special Issue on Noise. IEEE Transactions on Microwave Theory and Techniques MTT-16: 575-812. September.
- North, D. O.
 1942 The Absolute Sensitivity of Radio Receivers. RCA Review 6: 332-343. January.
- Nyquist, H.
 1928 Thermal Agitation of Electric Charge in Conductors. Physical Review 26: 110-113. July.
- Oliver, B. M.
 1955 Some Effects of Waveform on VTVM Readings. Hewlett-Packard Journal 6: April, May, June.

- Oliver, B. M.
 1965 Thermal and Quantum Noise. Proceedings of the IEEE 53: 436-454. May.
- Otoshi, Tom Y.
 1968 The Effect of Mismatched Components on Microwave Noise-Temperature Calibrations. IEEE Transactions on Microwave Theory and Techniques MTT-16: 675-691. September.
- Papoulis, Athanasios.
 1965 Probability, Random Variables and Stochastic Processes. New York, N.Y., McGraw-Hill Book Co., Inc.
- Pappenfus, E. W., Bruene, Warren B. and Schoenike, E. O.
 1964 Single Sideband Principles and Circuits. New York, N.Y., McGraw-Hill Book Co., Inc.
- Pastori, William E.
 1967 Measuring Microwave Noise - A Series of Notes. Application Note from Airborn Instruments Laboratory, Division of Cutler-Hammer, Inc., Dear Park, N.Y.
- Pastori, William E.
 1968a Measurement of the Noise Performance of Amplifiers and Receiving Systems. Application Note from Airborn Instruments Laboratory, Division of Cutler-Hammer, Inc., Dear Park, N.Y.
- Pastori, William E.
 1968b New Equation Analyzes Mismatch Errors in Noise Measurements. Microwaves 7: 58-63. April.
- Pastori, William E.
 1971 Simplify Methods for Measuring Noise. Microwaves 10: 55. September.
- dePazzis, O.
 1969 Shot Noise in Antennas. Radio Science 4: 91-92. January.
- Pettit, Joseph M.
 1947 Specification and Measurement of Receiver Sensitivity at the Higher Frequencies. Proceedings of the IRE 35: 302-306. March.
- Phillips, Alvin B.
 1962 Transistor Engineering. New York, N.Y., McGraw-Hill Book Co., Inc.
- Pierce, J. R.
 1956 Physical Sources of Noise. Proceedings of the IRE 44: 601-608. May.

Pietrzak, Walter

- 1967 Nomograph Finds Thermal Noise Voltage. Electronic Design News: L62. May.

Price, Robert

- 1955 A Note on the Envelope and Phase-Modulated Components of Narrow-Band Gaussian Noise. IRE Transactions on Information Theory IT-1: 9-13. September.

Princeton Applied Research Corp.

- 1969 How to Use Noise Figure Contours. Application Note from Princeton Applied Research Corp., Princeton, N.J.

Rheinfelder, William A.

- 1964 Design of Low-Noise Transistor Input Circuits. New York, N.Y., Hayden Book Company, Inc.

Rhodes, D. R.

- 1961 On the Definition of Noise Performance. Proceedings of the IRE, correspondence 49: 376. January.

Robinson, F.N.H.

- 1962 Noise in Electrical Circuits. London, England, Oxford University Press.

Robinson, F.N.H.

- 1969 Noise in Common Source FET Amplifiers at Moderately High Frequencies. Electronic Engineering 41: 77-79. May.

Rothe, H. and Dahlke, W.

- 1956 Theory of Noisy Fourpoles. Proceedings of the IRE 44: 811-818. June.

Rotholz, Ersch L.

- 1962 Noise Figure Calculation Based on the Admittance Matrix of the Network. Proceedings of the IRE, correspondence 50: 477-478. April.

Saad, Ted, Editor.

- 1966 Microwave Engineer's Technical and Buyer's Guide. Dedham, Mass., Horizon House-Microwave, Inc. December.

Sato, Takayuki

- 1971 Probing Transistor Noise. Electronic Design News 16: 21-26. May.

Schneider, B. and Strutt, M.J.O.

- 1959 Theory and Experiments on Shot Noise in Silicon P-N Junction Diodes and Transistors. Proceedings of the IRE 47: 546-554. April.

- Schuster, D. L., Stelzried, C. T. and Levy, G. S.
1962 The Determination of the Noise Temperatures of Large Paraboloidal Antennas. IRE Transactions on Antennas and Propagation AP-10: 286-291. May.
- Sears, Francis Weston
1953 An Introduction to Thermodynamics, the Kinetic Theory of Gases, and Statistical Mechanics. Reading, Massachusetts, Addison-Wesley Publishing Co., Inc.
- Sevin, Leonce J., Jr.
1965 Field Effect Transistors. New York, N.Y., McGraw-Hill Book Co., Inc.
- Shea, Richard F., Editor-in-chief
1966 Amplifier Handbook. New York, N.Y., McGraw-Hill Book Co., Inc.
- Siegman, A. E.
1961 Zero-point Energy as the Source of Amplifier Noise. Proceedings of the IRE, correspondence 49: 633. March.
- Siegman, A. E.
1964 Microwave Solid State Masers. New York, N.Y., McGraw-Hill Book Co., Inc.
- Skolnik, Merrill I.
1970 Radar Handbook. New York, N.Y., McGraw-Hill Book Co., Inc.
- Smullin, Louis D. and Haus, H. A.
1959 Noise in Electron Devices. New York, N.Y., John Wiley and Sons, Inc.
- Staelin, D. H., Boston, Mass.
1966 Detection and Measurement of Radio Astronomy Signals. Private Communication.
- Stelzried, Charles T.
1961 A Liquid-Helium-Cooled Coaxial Termination. Proceedings of the IRE 49: 1224. July.
- Stelzried, Charles T.
1964 Post-Amplifier Noise Temperature Contribution in a Low-Noise Receiving System. Proceedings of the IEEE 52: 76-77. January.
- Stelzried, Charles T.
1968 Microwave Thermal Noise Standards. IEEE Transactions on Microwave Theory and Techniques MTT-16: 646-655. September.

- Strum, P.
1953 Some Aspects of Crystal Mixer Performance. Proceedings of the IRE 41: 875-889. July.
- Strutt, M.J.O. and van der Ziel, A.
1948 Application of Velocity-Modulation Tubes for Reception at UHF and SHF. Proceedings of the IRE 36: 19-23. January.
- Talpey, T. E.
1961 Comment on "On Definition of Noise Performance". Proceedings of the IRE, correspondence 49: 376-377. January.
- Tiuri, M. E.
1964 Radio Astronomy Receivers. IEEE Transactions on Antennas and Propagation AP-12: 930-938. December.
- Uhlir, A., Jr.
1956 High-Frequency Shot Noise in P-N Junctions. Proceedings of the IRE, correspondence 44: 557-558. April.
- Uhlir, A., Jr.
1958 Shot Noise in P-N Junction Frequency Converters. Bell System Technical Journal 37: 951-988. July.
- Vigneri, R., Gulbenkian, G. G. and Diepeveen, N.
1968 Graphical Method for the Determination of Equivalent Noise Bandwidth. Microwave Journal 11: 49-52. June.
- Waggener, William N.
1969 Quickly Compute RMS Noise. Electronic Design News 2: 53-55. March.
- Wait, David F. and Nemoto, Toshio
1968 Measurement of the Noise Temperature of a Mismatched Noise Source. IEEE Transactions on Microwave Theory and Techniques MTT-16: 670-675. September.
- Wakeley, Joseph, Jr.
1963 Sensitivity Improvements from Threshold Extension Techniques. Proceedings of the IEEE, correspondence 51: 1770. December.
- Wallman, Henry, Macnee, Alan B., and Gadsden, C. P.
1948 A Low Noise Amplifier. Proceedings of the IRE 36: 700-708. June.
- Wanselow, Robert D.
1963 Investigation of RF Noise Generation from Space Vehicles. IEEE Transactions on Communication Systems CS-11: 346-351. September.

- Watt, A. D., Coon, R. M., Maxwell, E. L., and Plush, R. W.
 1958 Performance of Some Radio Systems in the Presence of Thermal and Atmospheric Noise. Proceedings of the IRE 46: 1914-1923. December.
- Wax, Nelson
 1954 Selected Papers on Noise and Stochastic Processes. New York, N.Y., Dover Publications, Inc.
- Webster, Roger R.
 1961 The Noise Figure of Transistor Converters. IRE Transactions on Broadcast and Television Receivers BTR-7: 50-65. November.
- Wells, J. S., Daywitt, W. C., and Miller, C.K.S.
 1964 Measurement of Effective Temperatures of Microwave Noise Sources. IEEE Transactions on Instrumentation and Measurement IM-13: 17-28. March.
- White, W. D. and Green, J. G.
 1956 On the Effective Noise Temperature of Gas Discharge Noise Generators. Proceedings of the IRE, correspondence 44: 939. July.
- Wildhack, W. A., Mason, H. L. and Powers, Robert S., Jr.
 1967 Accuracy Charts for RF Measurements. Proceedings of the IEEE 55: 1056-1063. June.
- Yakutis, A. J.
 1968 Solid-State RF Noise Source. Proceedings of the IEEE, correspondence 56: 228. February.
- Young, Hugo D.
 1962 Statistical Treatment of Experimental Data. New York, N.Y., McGraw-Hill Book Co., Inc.
- van der Ziel, Aldert
 1954 Noise. New York, N.Y., Prentice-Hall, Inc.
- van der Ziel, Aldert
 1955 Theory of Shot Noise in Junction Diodes and Junction Transistors. Proceedings of the IRE 43: 1639-1646. November.
- van der Ziel, Aldert
 1957 Theory of Shot Noise in Junction Diodes and Junction Transistors. Proceedings of the IRE 45: 1011. July.
- van der Ziel, Aldert
 1958 Noise in Junction Transistors. Proceedings of the IRE 46: 1019-1038. June.

van der Ziel, Aldert

- 1962a Thermal Noise in Field-Effect Transistors. Proceedings of the IRE 50: 1808-1812. August.

van der Ziel, Aldert

- 1962b On 'The Noise Figure of Negative Conductance Amplifiers'. Proceedings of the IRE, correspondence 50: 2122-2123. October.

van der Ziel, Aldert

- 1970 Noise: Sources, Characterization, Measurement. Englewood Cliffs, N.J., Prentice-Hall, Inc.

van der Ziel, A. and Becking, A.G.T.

- 1958 Theory of Junction Diode and Junction Transistor Noise. Proceedings of the IRE 46: 589-594. March.

XIV. APPENDIX

A. Power Spectral-Density Function, $\Phi(\omega)$

The power per-unit-bandwidth (watts-per-hz) of the frequency distribution of a random signal, $X(t)$, is called the spectral power because its variation with frequency produces a power spectrum. The concept of a spectral density is particularly useful for noise studies because it provides a means of describing the noise behavior of a network using linear system theory. This function is discussed in textbooks on communication theory (Beckmann, 1967) and linear circuit theory (Brown and Nilsson, 1962).

Before defining spectral density it is necessary to define the Fourier Transform Pair to be used in this report:

$$\begin{aligned} g(\omega) &= \int_{-\infty}^{+\infty} f(\tau) e^{-j\omega\tau} d\tau = \mathcal{F}[f(\tau)] \\ f(\tau) &= \frac{1}{2\pi} \int_{-\infty}^{+\infty} g(\omega) e^{+j\omega\tau} d\omega = \mathcal{F}^{-1}[g(\omega)] \end{aligned} \quad (\text{A.1})$$

Other equally valid definitions are sometimes used which distribute the 2π factor in a different manner but the above seems to be the most common.

The definition for the power spectral-density function of a random signal $X(t)$ is that it is the Fourier transform of the autocorrelation function of $X(t)$:

$$\Phi(\omega) = \int_{-\infty}^{+\infty} R(\tau) e^{-j\omega\tau} d\tau \quad \Phi(\omega) \text{ is real.} \quad (\text{A.2})$$

The autocorrelation function of $X(t)$ is a measure of how well the function $X(t)$ is correlated with itself after an elapsed time, τ . This function is obtained by the average of the product, $X(t)X(t-\tau)$, over a time period, T , as T goes to infinity;

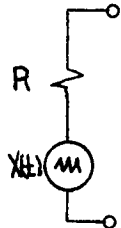
$$R_x(\tau) = \lim_{T \rightarrow \infty} \frac{1}{T} \int_{-T/2}^{T/2} X(t)X(t-\tau) dt. \quad (\text{A.3})$$

If Fourier analysis is to be used, the random signal $X(t)$ must be time stationary, i.e. its statistical properties must not vary with time. This requirement is satisfied by the Gaussian white noise produced in a linear resistor (thermal noise) but not by a noise source with a time varying mean-square value. This is the usual assumption made in receiver noise studies and when Fourier techniques are applied to noise problems.

For the thermal noise produced by a resistor, the power spectral-density function is obtained from the quantum view of radiation. Nyquist (1928) produced a theoretical basis for resistive noise power using thermodynamic and statistical mechanics. He assumed thermal equilibrium and applied the equipartition theorem to obtain the available power-per-unit-bandwidth as:

$$\phi_R(f) = k T \text{ watts/hz.}$$

When Planck derived the black-body-radiation law he found that the kT product in the equipartition law must be replaced by the Planck factor (van der Ziel, 1954) defined by Equation A.4 which is also the power spectral-density for a resistor



$$\Phi(f) = \frac{hf}{\left[e^{\left(\frac{hf}{kT_R} \right)} - 1 \right]} \quad \text{watts/hz.} \quad (\text{A.4})$$

where h = Planck's Constant, 6.63×10^{-34} joule-sec.
 k = Boltzmann's Constant, 1.38×10^{-23} joule/ $^{\circ}\text{K}$.
 T_R = Thermal temperature of the resistor, $^{\circ}\text{K}$.
 f = Frequency, Hz.
 $X(t)$ = Thermal noise voltage, Volts.

Equation A.4 is valid over all frequencies and temperatures but is seldom used in that form at radio frequencies. The Rayleigh-Jeans approximation to Planck's radiation law is used at radio frequencies. This approximation can be obtained by expanding the denominator of (A.4) in a power series to obtain:

$$\left[e^{\frac{hf}{kT_R}} - 1 \right] \approx \frac{hf}{kT_R}, \quad \text{for } \frac{f}{T_R} < 400 \text{ Hz}/^{\circ}\text{K}. \quad (\text{A.5})$$

The power spectral-density function for a noisy resistor can now be written in its simplest and most commonly used form by substitution of (A.5) into (A.4) to get:

$$\bar{\phi}_R(f) = k T_R \text{ watts/hz} \quad (\text{A.6})$$

It is interesting to compute the total power available (Appendix, Part C) from a noisy resistor by integrating Equation A.4 over all frequencies:

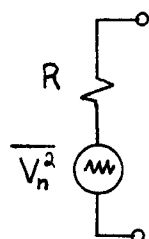
$$\text{Total noise power} = \int_0^{\infty} \bar{\phi}_R(f) df \text{ watts.} \quad (\text{A.7})$$

By using the substitutions, $z = \frac{hf}{kT_R}$ and $dz = \frac{h}{kT_R} df$, equation A.4 becomes:

$$\begin{aligned} \text{Total Power} &= \frac{(k T_R)^2}{h} \int_0^{\infty} \frac{z dz}{e^z - 1} = \frac{(k T_R)^2}{h} \left(\frac{\pi^2}{6} \right) \\ &= \left[\frac{k^2}{h} \frac{\pi^2}{6} \right] T_R^2 = 4.72 \times 10^{-11} T_R^2 \text{ watts.} \end{aligned} \quad (\text{A.8})$$

In the real physical sense, this power is not available to the user because one never has an infinite bandwidth. At standard temperature, $T_0 = 290^\circ\text{K}$, Equation A.8 tells us that the total noise power available from any resistor is about 4 microwatts. With this equation we can set the upper bound on available power for a noisy resistor.

For a finite bandwidth, and using the Rayleigh-Jeans approximation, ($hf \ll kT$), the available power for a noisy resistor can be computed by



$$\frac{\overline{V_n^2}}{4R} = \int_{f - \frac{\Delta f}{2}}^{f + \frac{\Delta f}{2}} \Phi_{I_R}(f) df = kT \Delta f \text{ watts} \quad (\text{A.9})$$

where Δf is a small bandwidth about the frequency f . From this representation the mean-square noise voltage for the bandwidth, Δf , and the Nyquist equation are:

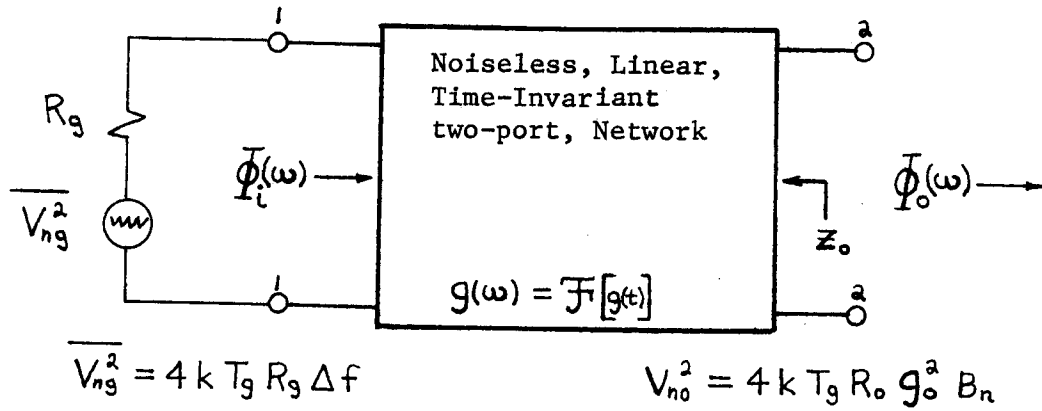
$$\overline{V_n^2} = 4kTR\Delta f \quad (\text{Volts})^2. \quad (\text{A.10})$$

The ideas of power spectral density and Nyquist's equation are useful for many of the derivations that will be presented in this appendix.

B. Noise Bandwidth

The noise bandwidth of a linear, noiseless two-port network is defined in terms of the noise power available (see Appendix, Part C) at the two-port output due to a noise source of constant spectral intensity at the input. The concept of an equivalent noise bandwidth is a convenient one for noise studies because it eliminates the integral equations that result from applying Fourier techniques. The circuit of Figure B-1 illustrates the basic elements needed to derive an expression for equivalent noise bandwidth.

For a time-stationary input such as white Gaussian-noise, we can apply steady-state Fourier analysis which relates the input and output spectral functions:



$\Phi_i(\omega)$ = Power-spectral-density function of the noise
input to the filter $\approx kT_g$.

$\Phi_o(\omega)$ = Power-spectral-density function of the noise
output from the filter.

$g(\omega)$ = Steady-state transfer function (complex).

Z_o = Two-port output impedance, $R_o = \text{Re}(Z_o)$.

Figure B-1. Noise Bandwidth Determination

$$\Phi_o(\omega) = \Phi_i(\omega) |g(\omega)|^2 \text{ watts/hz.} \quad (\text{B.1})$$

The available power in an incremental bandwidth df at both input and output is obtained from the power spectral densities:

$$\text{input} \quad d\left(\frac{\overline{V_{ng}^2}}{4R_g}\right) = dN_g = \Phi_i(f) df \text{ watts,} \quad (\text{B.2})$$

output

$$d\left(\frac{\overline{V_{no}^2}}{4R_o}\right) = dN_o = \overline{\mathcal{F}_i(f)} |g(f)|^2 df. \quad (B.3)$$

Integration of (B.3) gives the total output power

$$N_o = \int_0^\infty \overline{\mathcal{F}_i(f)} |g(f)|^2 df = k T_g \int_0^\infty |g(f)|^2 df, \quad (B.4)$$

where T_g = Noise temperature of R_g
 $g(f)$ = Steady-state transfer function.

From Equation B.4, the effective noise bandwidth for a two-port network can be determined by examining the integral:

$$\int_0^\infty |g(f)|^2 df. \quad (B.5)$$

If we let the amplifier response $|g(f)|^2$ be normalized to unity, at a convenient reference frequency f_o , by dividing by the amplitude g_o^2 , at f_o , the integral of (B.5) becomes

$$\int_0^\infty |g(f)|^2 df = g_o^2 B_n \quad (B.6)$$

where the effective noise bandwidth or normalized noise bandwidth is

$$B_n = \frac{1}{g_o^2} \int_0^\infty |g(f)|^2 df. \quad (B.7)$$

Effective noise bandwidth can also be written in terms of transducer gain, $G(f) = |g(f)|^2$, as (IRE Subcommittee on Noise, 1960a):

$$B_n = \frac{1}{G_n} \int_0^{\infty} G(f) df \quad (\text{B.8})$$

Part (a) of Figure B-2 illustrates the concept of effective noise bandwidth for a smooth passband. Notice that the 3db bandwidth is not the same as the noise bandwidth.

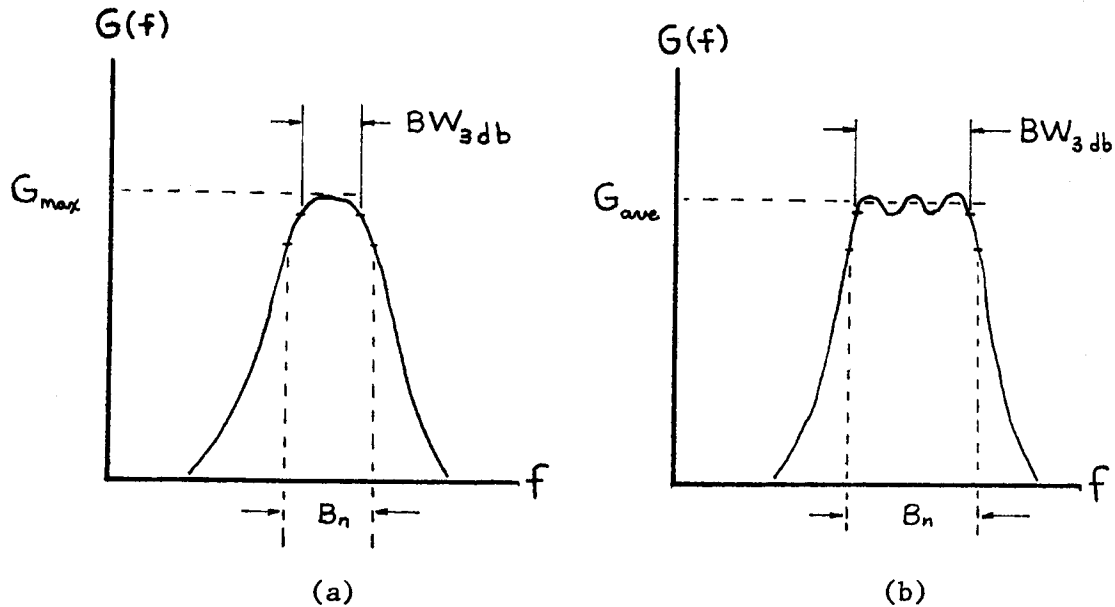


Figure B-2. Effective Noise Bandwidth, B_n

Part (b) of Figure B-2 illustrates a passband shape which is not smooth. For a smooth passband, the peak amplitude is usually chosen for normalization but for passbands with ripple, it may be convenient to choose some other reference. B_n could just as well be normalized around the

average gain while still keeping the total output power constant. Comparing the two methods we get:

$$\begin{aligned} \text{Max, } G_n &= G_{\max} \\ N_o &= k T_g G_{\max} B_n \end{aligned} \quad B_n = \frac{1}{G_{\max}} \int_0^{\infty} G(f) df \quad . \quad (\text{B.9})$$

$$\begin{aligned} \text{Ave, } G_n &= G_{\text{Ave}} \\ N_o &= k T_g G_{\text{ave}} B'_n \end{aligned} \quad B'_n = \frac{1}{G_{\text{ave}}} \int_0^{\infty} G(f) df \quad . \quad (\text{B.10})$$

The factor of normalization does not alter the fundamental meaning or the value of the integral of Equation B.5; however, most authors use the definition of Equation B.9.

Whenever any difficulty arises due to the definition of effective noise bandwidth, the user should resort to the fundamental definition of output power:

$$N_o = k T \int_0^{\infty} |g(f)|^2 df \quad . \quad (\text{B.11})$$

It is convenient for purposes of calculation to normalize the effective noise bandwidth with respect to the 3db bandwidth. Numerical integration can be used to compile tables of the ratio K:

$$K = \frac{B_n}{BW_{3\text{db}}} \quad . \quad (\text{B.12})$$

Tables for passband responses that have well defined maxima, such as a Butterworth response, can be found in Kraus (1966, p. 265) and Lawson and Uhlenbeck (1950, p. 177). For more discussion on the computation of integrals such as Equation B.5 refer to Bennett (1960, p. 18).

A simple noise bandwidth calculation will now be made to illustrate the technique. Figure B-3 shows an RC filter for which the noise bandwidth will be calculated.

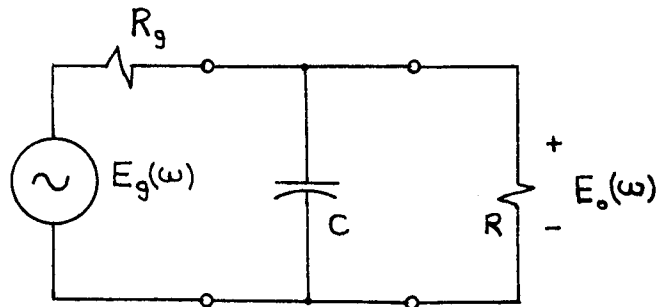


Figure B-3. RC Filter

The transfer function is:

$$\frac{E_o(\omega)}{E_g(\omega)} = g(\omega) = \frac{\frac{1}{R_g}}{\left(\frac{R+R_g}{R R_g}\right) + j\omega C} \quad (B.13)$$

The maximum value of $g(\omega)$ occurs at $\omega = 0$, so

$$g_{\max} = \frac{R}{R + R_g}$$

and normalizing $g(\omega)$ we get

$$\frac{g(\omega)}{g_{\max}} = g_n(\omega) = \frac{1}{1 + j\omega C \frac{R R_g}{R + R_g}} \quad (\text{B.14})$$

Substitute, $T = C \frac{R R_g}{R + R_g}$, and obtain the effective noise bandwidth by

the integral:

$$B_n = \lim_{W \rightarrow \infty} \int_0^W |g_n(\omega)|^2 d\omega. \quad (\text{B.15})$$

Squaring $g_n(\omega)$, integrating over zero to W

$$\int_0^\infty \frac{1}{1 + \omega^2 T^2} d\omega = \frac{1}{T} \tan^{-1}(\omega T)$$

and taking the limit gives:

$$B_n = \lim_{W \rightarrow \infty} \frac{1}{T} \tan^{-1}(\omega T) = \frac{1}{T} \left(\frac{\pi}{2} \right) \quad (\text{B.16})$$

The 3db bandwidth is evaluated from the condition

$$|g_n(\omega)|^2 = \frac{1}{2} = \frac{1}{1 + \omega^2 T^2} \quad (\text{B.17})$$

and we conclude that:

$$BW_{3db} = \frac{1}{T} \text{ rad/sec} \quad (\text{B.18})$$

Finally, the ratio of effective noise bandwidth to 3db bandwidth is taken:

$$\frac{B_n}{BW_{3db}} = \frac{\pi}{2} = 1.57 \quad (B.19)$$

From modern filter theory (Karni, 1966, p. 345) the rational function approximation for a transfer function is of the form

$$|g_n(\omega)|^2 = \frac{1}{1 + Q(\omega^2)}$$

where $Q(\omega^2)$ may be any of a whole class of orthogonal polynomials (Karni, 1966, p. 360).

To the best of this author's knowledge, no tables comparing normalized noise bandwidths with the 3db bandwidths exists for the common functions of modern network theory.

It is suggested that further investigations into the topic of effective noise bandwidth be made.

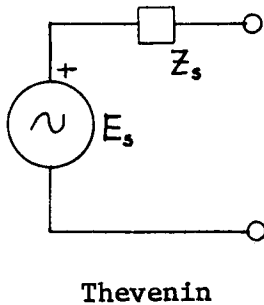
C. Available Power

The concept of the power available from a Thevenin's voltage source or Norton's current source is useful for communication engineering, especially noise factor studies. This idea is used in many papers on noise theory and is presented here to familiarize the reader with this concept. By definition, the available power is independent of the load and is the maximum power that can be drawn from the source by arbitrary variation of the load,

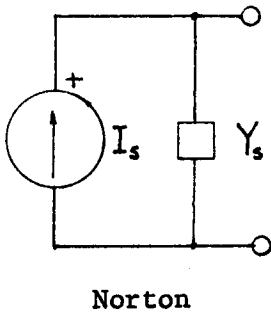
Actual Power Delivered \leq Available Power.

The definition of available power is a direct result of the maximum power transfer theorem and is illustrated with the help of Figure C-1.

E_s and I_s are RMS generators with internal impedance Z_s .



$$\text{Available Power} = \frac{|E_s|^2}{4 R_e(Z_s)} \quad (\text{C.1})$$

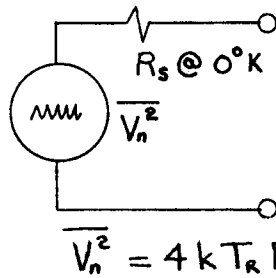


$$\text{Available Power} = \frac{|I_s|^2}{4 R_e(Y_s)} \quad (\text{C.2})$$

Figure C-1. Available Power Network Theorems

Since Z_s and Y_s are functions of frequency, it is necessary to include frequency variation effects if the source, E_s or I_s , contains more than a single frequency.

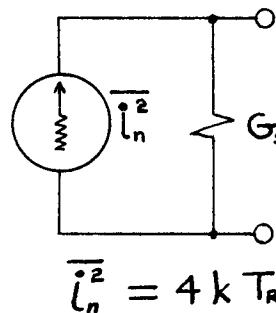
For noisy resistors, the available power is defined with the help of Figure C-2, where $\overline{V_n^2}$ and $\overline{i_n^2}$ are mean square noise voltages and currents.



Available Power (in bandwidth Δf) = $\frac{\overline{V_n^2}}{4R_s} = \int_f^{f+\Delta f} k T_R df$ (C.3)

$$\overline{V_n^2} = 4kT_R R_s \Delta f$$

kT_R = Power Spectral density



Available Power (in bandwidth Δf) = $\frac{\overline{i_n^2}}{4G_s} = \int_f^{f+\Delta f} k T_R df$ (C.4)

$$\overline{i_n^2} = 4kT_R R_s \Delta f$$

Figure C-2. Available Power Theorem for Noisy Resistors

The bandwidth Δf is an incremental bandwidth which actually represents the noise bandwidth over which the available noise power is being measured. When the noisy resistor is connected to a noiseless two-port network, the available noise power at the output can be obtained by combining Equations B.4 and B.6

$$P_{\text{out}} = k T_R B_n g_{\text{max}}^2 \quad (\text{C.5})$$

where T_R = Temperature of the noisy resistor, $^{\circ}\text{K}$.

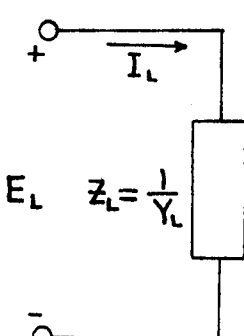
g_{max} = Peak amplitude of the steady-state transfer function.

B_n = The effective noise bandwidth defined as;

$$B_n = \frac{1}{2\pi} \int_0^{\infty} |g_n(\omega)|^2 d\omega \quad (\text{C.6})$$

$g_n(\omega)$ = Steady-state transfer function normalized to its maximum value, g_{max} .

The power delivered to a complex (RLC) load should also be defined. The real power delivered is determined by taking the magnitude of the current, squaring, and multiplying by the real part of the load impedance. Figure C-3 illustrates the derivation of the power equations.



$$P_L = |I_L|^2 R_e(Z_L) = \frac{|E_L|^2}{|Z_L|^2} R_e(Z_L) \quad (\text{C.7})$$

$$P_L = |E_L|^2 R_e(Y_L) = \frac{|I_L|^2}{|Y_L|^2} R_e(Y_L) \quad (\text{C.8})$$

Figure C-3. Power Delivered to a Complex Load

D. Insertion Gain (or Loss)

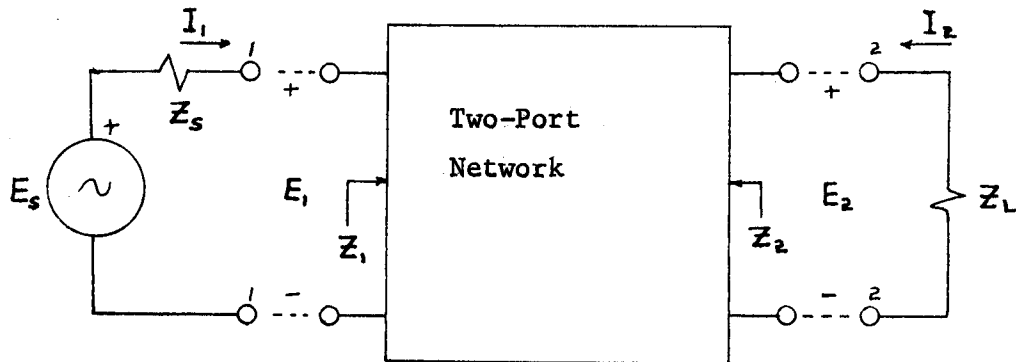


Figure D-1. Insertion Gain - Defining Quantities

When a two-port network is inserted between a source and a load, the degree of impedance match between them may or may not improve. Also, if the two-port is active it may introduce a power gain or if it is passive, a power loss due to resistive dissipation in the network. Finally, the two-port may modify the bandwidth of power transfer between the source and load. This could result in a reduction in the total power available at the source due to an attenuation of some parts of the spectrum. This is particularly true if the input is noise because the output power would then be directly proportional to bandwidth. In any case, the net effect of the insertion will be to increase or decrease the power delivered to the load.

If the power delivered is larger after insertion, we call it an insertion gain. If the power decreases, it is an insertion loss. Taking the ratio of power output after insertion to that before insertion, a

ratio greater than unity denotes a gain while one less than unity denotes a loss. The effect of inserting the two-port can be described in terms of the network's voltage or current gains as will now be shown.

The voltage across Z_L when the two-port is removed and terminals 2-2 are connected to terminals 1-1 is

$$E'_2 = E_s \frac{Z_L}{Z_s + Z_L} \quad (D.1)$$

and when the two-port is inserted it becomes

$$E_2 = A_v E_s \frac{Z_1}{Z_1 + Z_2} \quad (D.2)$$

where A_v is the terminated voltage gain (E_2/E_1) of the network. The terminated gain of a two-port is the gain which actually exists between terminals 1-1 and 2-2 when the two-port is terminated with the desired source and load. A_v can be written in terms of the two-port parameters as will be shown later.

The insertion gain is now computed by taking the ratio of powers delivered to the load under these two conditions as

$$\text{INSERTION GAIN} = \frac{P_o}{P_o'} = \frac{|E_2|^2 \frac{R_e(Z_L)}{|Z_L|^2}}{|E'_2|^2 \frac{R_e(Z_L)}{|Z_L|^2}} = \frac{|E_2|^2}{|E'_2|^2}$$

and from (D.1) and (D.2)

$$= |A_v|^2 \left| \frac{Z_1}{Z_L} \right|^2 \frac{|Z_s + Z_L|^2}{|Z_s + Z_1|^2} \quad (D.3)$$

Insertion gain can also be described by taking the current ratios before and after insertion. The corresponding equations are

$$I_2' = \frac{E_s}{Z_s + Z_L}, \quad I_2 = A_t \frac{E_s}{Z_s + Z_1}, \quad A_t = \frac{I_2}{I_1} \quad (D.4)$$

$$\text{INSERTION GAIN} = \frac{P_o}{P_o'} = \frac{|I_2|^2 R_e(Z_L)}{|I_2'|^2 R_e(Z_L)} = \frac{|I_2|^2}{|I_2'|^2}$$

$$\text{and from (D.4)} \quad = |A_t|^2 \frac{|Z_s + Z_L|^2}{|Z_s + Z_1|^2} \quad (D.5)$$

For a value of insertion gain less than unity, we say the insertion of the two-port has caused a power loss while values greater than unity mean a net power gain. We conclude that gain or loss is only differentiated by the magnitude of the ratio P_o/P_o' being greater or less than unity.

Insertion gain is often expressed in db as determined by (D.6):

$$(\text{INSERTION GAIN})_{\text{db}} = 10 \log \left(\frac{P_o}{P_o'} \right). \quad (D.6)$$

Insertion gain is closely related to another measure of two-port gain called transducer gain defined as:

Transducer Gain = The ratio of the actual power delivered at the output of a two-port to the available power at the source.

Using Figure D-1 and output power in terms of the current gain A_i

$$\begin{aligned} \text{TRANSDUCER GAIN} &= \frac{\text{Actual power at } Z_L}{\text{Available power from the source}} \\ &= \frac{\frac{|I_2|^2 R_e(z_L)}{\frac{|E_s|^2}{4 R_e(z_s)}}}{\frac{|E_s|^2}{4 R_e(z_s)}} = 4 \frac{|I_2|^2}{|E_s|^2} R_e(z_L) R_e(z_s) \end{aligned}$$

and substituting for I_2 from (D.4)

$$= 4 \frac{|A_i|^2 \frac{|E_s|^2}{|z_s + z_i|^2}}{|E_s|^2} R_e(z_L) R_e(z_s) = \frac{4 |A_i|^2}{|z_s + z_i|^2} R_e(z_L) R_e(z_s). \quad (\text{D.7})$$

In terms of voltage gain A_v :

$$\begin{aligned} \text{TRANSDUCER GAIN} &= \frac{\frac{|E_z|^2 \frac{R_e(z_L)}{|z_L|^2}}{\frac{|E_s|^2}{4 R_e(z_s)}}}{\frac{|E_s|^2}{4 R_e(z_s)}} \\ &= |A_v|^2 \left| \frac{z_i}{z_L} \right|^2 \frac{4 R_e(z_L) R_e(z_s)}{|z_s + z_i|^2}. \quad (\text{D.8}) \end{aligned}$$

It is worthwhile to compare transducer and insertion gains. Seldom is the input circuit of a low-noise amplifier power matched to the source impedance so that transducer gain has less practical meaning than insertion gain. Also, insertion gain is easier to measure but the fundamental definition of noise factor as first presented by

Friis (1944) requires the use of transducer gain (see part H of this section). The equivalence between these two gains can be obtained by taking the ratio of (D.8) to (D.3)

$$\frac{\text{TRANSDUCER GAIN}}{\text{INSERTION GAIN}} = 4 \frac{R_e(z_s) R_e(z_L)}{|z_s + z_L|^2} \leq \frac{4 R_s R_L}{(R_s + R_L)^2} \leq 1 \quad (\text{D.9})$$

and it can be concluded that the transducer gain is always less than the insertion gain.

Other gain specifications are often used in two-port discussions and these will now be briefly mentioned. The Available Gain of the two-port is the ratio of power available from the two-port output to the power available from the source:

$$\begin{aligned} \text{AVAILABLE GAIN} &= \frac{\frac{|E_2|^2}{4 R_e(z_2)}}{\frac{|E_s|^2}{4 R_e(z_s)}} = \frac{|E_2|^2}{|E_s|^2} \frac{R_e(z_s)}{R_e(z_2)} \\ &= |A_v|^2 \frac{|z_L|^2}{|z_s + z_L|^2} \frac{R_e(z_s)}{R_e(z_2)} \quad (\text{D.10}) \end{aligned}$$

The Maximum Available Gain (MAG) is determined by conjugate impedance matching the two-port after it has been unilateralized.

From network theory (ITT, 1956, p. 504) the gains and impedances needed to compute insertion gain can be described in terms of the chain

matrix (ABCD matrix) and the admittance matrix elements. The following equations are included for convenience:

$$\begin{pmatrix} E_1 \\ I_1 \end{pmatrix} = \begin{pmatrix} A & B \\ C & D \end{pmatrix} \begin{pmatrix} E_2 \\ -I_2 \end{pmatrix} \quad \begin{pmatrix} I_1 \\ I_2 \end{pmatrix} = \begin{pmatrix} Y_{11} & Y_{12} \\ Y_{21} & Y_{22} \end{pmatrix} \begin{pmatrix} E_1 \\ E_2 \end{pmatrix}$$

Chain or ABCD

Admittance

$$\Delta^y = Y_{11}Y_{22} - Y_{21}Y_{12}$$

Input impedance, Z_1 ;

$$Z_1 = \frac{A Z_L + B}{C Z_L + D}$$

$$Z_1 = \frac{Y_{22} + Y_L}{\Delta^y + Y_{11} Y_L}$$

Output impedance, Z_2 ;

$$Z_2 = \frac{A Z_g + B}{C Z_g + A}$$

$$Z_2 = \frac{Y_{11} + Y_g}{\Delta^y + Y_{22} Y_g}$$

Voltage gain, A_v ;

$$A_v = \frac{Z_L}{B + A Z_L}$$

$$A_v = \frac{-Y_{21}}{Y_{22} + Y_L}$$

Current gain, A_i ;

$$A_i = \frac{1}{C Z_L + D}$$

$$A_i = \frac{-Y_{21} Y_L}{\Delta^y + Y_{11} Y_L}$$

E. Equivalent Noise Temperature

Nyquist's Theorem states that the noise power available at two nodes of an RLC network at uniform temperature, T_r , is simply the noise power available from the real part of the driving point impedance Z_{dp} . This theorem defines the equivalent noise temperature of a one-port network. Any impedance, Z_{dp} , can be represented by a Nyquist equivalent noise source as shown in Figure E-1.

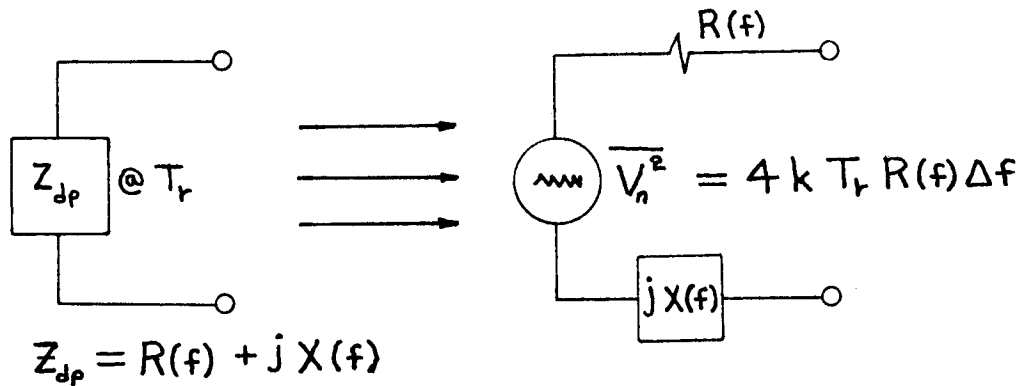


Figure E-1. Nyquist Equivalent Circuit for an RLC Network

Since the real part of the driving point impedance will generally be a function of frequency, it will be necessary to represent the noise quantities by their Fourier coefficients (Smullin and Haus, 1959, p. 190). For this representation, the thermal noise generated by the network can be represented by a mean-square noise voltage generator $\overline{V_n^2}$, and we consider $R(f)$ to be constant over a narrow frequency range f to $f+\Delta f$ and at a temperature T_r . For these conditions, the temperature T_r properly depicts the available noise-power-per-unit-bandwidth,

kT_r , from the network and is therefore called the Equivalent Noise Temperature or sometimes the one-port noise temperature.

In some applications it is necessary to consider the output terminals of a two-port network as a one-port; however, for a two-port network, the equivalent noise temperature is a more difficult concept. For this case, all of the noise at the output due to the internal noise of the two-port is accounted for by adding an additional noise generator to the input resistive termination. Figure E-2 shows the terminated two-port with all the two-port noise referred to the input and represented by the noise voltage generator $\overline{V_{nr}^2}$.

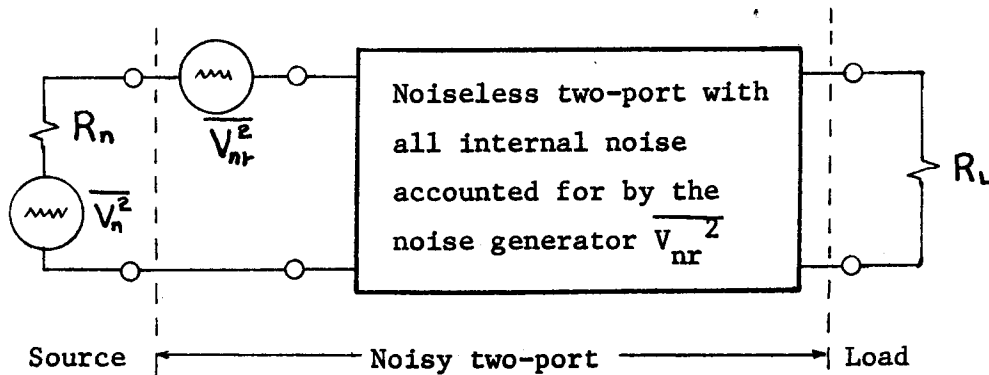


Figure E-2. Two-port Equivalent Noise Temperature

The definition for equivalent noise temperature can be derived in terms of noise factor by applying the basic definition obtained in section IV-E on two-port noise theory. It must be kept in mind that noise factor (and hence effective noise temperature) is a function of the source resistance R_n . For this reason, the equivalent noise voltage source $\overline{V_{nr}^2}$ is over simplified and cannot be used indiscriminately for

noise calculations. For a complete discussion, refer to the two-port noise theory section.

The noise factor for the system of Figure D-2 becomes

$$F = \frac{\overline{V_n^2} + \overline{V_{nr}^2}}{\overline{V_n^2}} = 1 + \frac{\overline{V_{nr}^2}}{\overline{V_n^2}} \quad (\text{E.1})$$

and if we let these mean-square noise voltage generators be represented by their Nyquist equivalent sources (Section IV-B) we have

$$\begin{aligned} \overline{V_n^2} &= 4kT_o R_n \Delta f \\ \overline{V_{nr}^2} &= 4kT_r R_n \Delta f \end{aligned} \quad (\text{E.2})$$

which upon substitution into the noise factor equation gives the final expression relating two-port effective noise temperature and noise factor:

$$F = 1 + \frac{T_r}{T_o} \quad \text{or} \quad T_r = (F - 1) T_o \quad (\text{E.3})$$

The single noise generator, $\overline{V_{nr}^2}$, and equivalent noise temperature, T_r , account for all the noise generated in the two-port without regard for the generating mechanism(s). The deceiving aspect of simply stating an equivalent noise temperature is that T_r is actually a function of all four noise parameters of the two-port as well as R_n so that;

$$T_r = \text{Function of } (R_n, \overline{V_n^2}, \overline{I_n^2}, \overline{V_n I_n^*})$$

When specifying the equivalent noise temperature (or noise factor) of a two-port network it is always necessary to also specify the source resistance.

F. Equivalent Noise Resistance

The equivalent noise resistance is another means of specifying the noise performance of a two-port. The idea of an equivalent noise resistance is used because of its notational convenience and conceptual simplicity. Actually, the equivalent noise resistance is obtained in the same manner as equivalent noise temperature. Referring to Part E of this section we have the noise factor of the two-port as:

$$F = 1 + \frac{\overline{V_{nr}^2}}{\overline{V_n^2}} \quad (F.1)$$

Now instead of defining the Nyquist equivalent sources in terms of an effective noise temperature we can consider the referred amplifier noise source, $\overline{V_{nr}^2}$, as being represented by a resistance R_{eq} at standard temperature T_0 . Doing this gives

$$\begin{aligned} \overline{V_n^2} &= 4kT_0 R_n \Delta f \\ \overline{V_{nr}^2} &= 4kT_0 R_{eq} \Delta f \end{aligned}$$

which upon substitution into F.1 yields

$$F = 1 + \frac{R_{eq}}{R_n} \quad (F.2)$$

Any Nyquist generator can be represented by an equivalent noise resistance at standard temperature. This concept is used extensively in analyzing vacuum tube circuits (Pappenfus, Bruene, and Schoenike, 1964, p. 251) and for specifying two-port noise parameters (van der Ziel, 1970, p. 32).

G. Excess Noise Ratio (Excess Noise)

The excess noise ratio of a noise source is a measure of the amount of additional noise a source contributes in excess of what it would if the source resistance were at standard temperature. The increase in available noise-power-per-unit-bandwidth that is caused by thermal heating or by the addition of a shot noise can be accounted for by an increase in the effective noise temperature. When the source is at standard temperature, the power spectral density is kT_o . When the effective power is increased, the spectral power becomes $k(T_o + T_{ex})$. T_{ex} is the increase in effective temperature above standard temperature and is called the excess noise temperature.

The excess noise ratio is the ratio of excess noise temperature to standard temperature:

$$R_{ex} = \frac{T_{ex}}{T_o} , \quad (G.1)$$

or expressed in decibels,

$$ENR(db) = 10 \log (R_{ex}). \quad (G.2)$$

The excess noise temperature for a resistor heated above standard temperature is illustrated in Figure G-1. The rise might also be caused by the addition of shot noise by a noise diode. The effective noise temperature of the source, T_n , is composed of two parts, the standard temperature, T_o , and the excess noise temperature, T_{ex} .

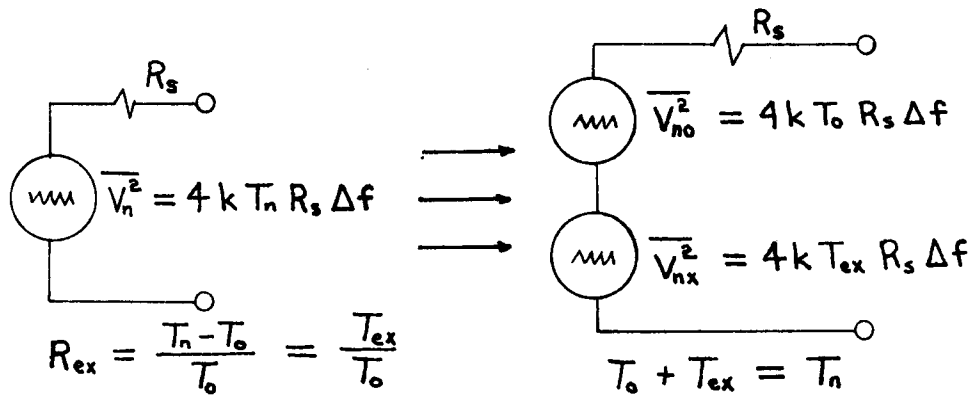


Figure G-1. Excess Noise Ratio Conversion

The idea of excess noise is also used in discussing the noise output of a two-port network. The noise output above that which is due only to the source resistance is called excess noise. All the noise output caused by the noisy two-port is accounted for by an equivalent noise temperature T_r or by the excess noise factor ($F_r - 1$). Figure G-2 will help illustrate the concept.

The noise power output is:

$$N_o = F_r k T_o G B, \quad (G.3)$$

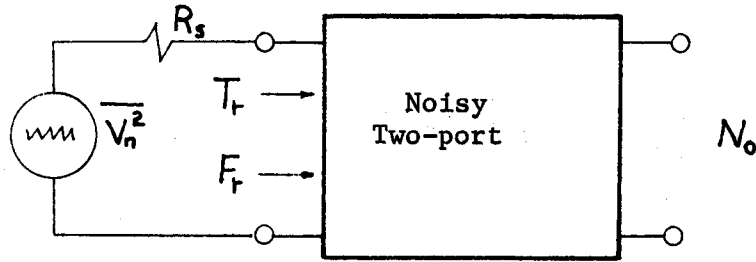


Figure G-2. Two-port Excess Noise Factor

which is the sum of the noise of the source multiplied by the gain and the internal noise of the two-port referred to the input

$$N_o = kT_o GB + kT_r GB \quad (G.4)$$

$$= k (T_o + T_r) GB, \quad (G.5)$$

and we see that T_r is the excess noise contributed by the source.

Equation G.4 can also be written in terms of noise factor using the substitution $(F_r - 1) T_o = T_r$;

$$N_o = kT_o GB + (F_r - 1) kT_o GB. \quad (G.6)$$

The factor $(F_r - 1)$ is called the excess noise factor.

H. Noise Factor (Noise Figure)

D. O. North wrote his famous paper on the Absolute Sensitivity of Radio Receivers in January, 1942, fourteen years after Johnson (1928) and Nyquist (1928) had first experimentally and theoretically verified

noise voltage fluxuations in conductors. It was fourteen years after Johnson had reported a "disturbance which is called 'tube noise' in vacuum tube amplifiers" before a quantitative and absolute method of comparing receiver sensitivities was developed. Many qualitative descriptions of amplifier noise had been given in those intervening years but the definitions depended on various circuit variables and this made it difficult to directly compare receivers. North's proposed method of specifying the internal noise of a receiver was attractive because it depended only upon the antenna or source resistance to which the receiver was connected.

Two years after North had defined the fundamental noise properties of an amplifier with a measure called "noise factor", H. T. Friis (1944) published his classical paper on the Noise Figures of Radio Receivers in which he derived a rigorous definition for noise factor in terms of a terminated two-port network and developed the famous Friis Equation (see Part J of this section) which determines the total noise factor of a cascade of noisy two-port networks.

These two papers formed the foundation for the study of noise in two-port networks and the concepts they developed are still important and very useful in receiver noise studies. To fully appreciate the simplicity of the idea of an absolute sensitivity and to illustrate its utility for amplifiers we will present the noise factor definition much the same as did North and Friis.

Before showing the basic derivation of noise factor, it is appropriate to discuss a disagreement in terminology. The problem is that the quantity which North called noise factor, Friis called noise figure.

Quite often the two terms are used interchangeably as they were in the beginning but it is now common practice in industry to distinguish between the two and we shall do so in the following way:

1. The numerical factor, F , which North called noise factor and Friis called noise figure we shall call Noise factor.
2. The noise factor in db as is commonly specified in the literature we shall call noise figure (NF) thus; $NF(db) = 10 \log F$.

The reader should be cautioned that these definitions are not universally accepted and therefore one must determine a particular author's usage when reading in the literature. As a general rule most formulas and calculations use the numerical noise factor, F . The following derivation of noise factor is based on the simple presentations of North and Friis. Modern definitions and terms are used but we will avoid a rigorous presentation in the hope that a better intuitive idea of the concept of absolute sensitivity may be developed.

Suppose it were possible to build two receivers identical in every respect except that one contained internal noise sources and the other was noiseless. Furthermore we must stipulate that the receivers are linear and that we can describe them with two-port circuit theory. Since they are identical, they will exhibit identical gain and port impedances under identical terminating conditions. Figure H-1 will illustrate the following definition of noise factor.

First, the noiseless receiver is inserted between the source and the load and the output noise due only to the source noise amplified

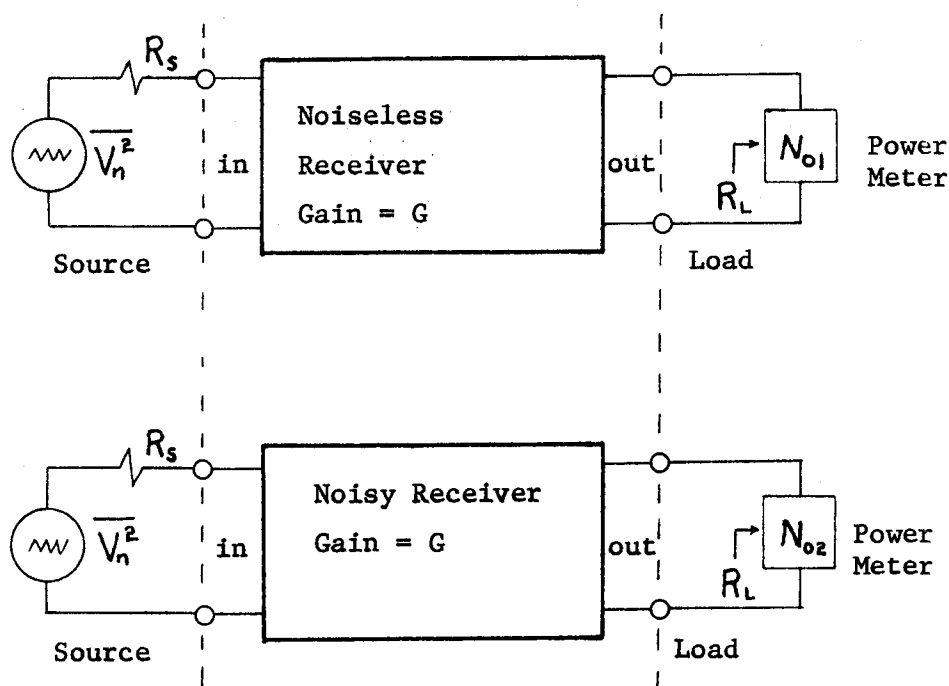


Figure H-1. Noise Figure Definition

by the transducer gain, G , is measured to be N_{01} watts. Then the noiseless receiver is replaced by the noisy one and the noise power output N_{02} , the sum of the noise due to the source and the noise generated internally in the receiver, is measured. North (1942) defined noise factor as the ratio of the noise power output of a noisy receiver to that of a noiseless receiver when the terminating conditions are identical;

$$\text{Noise Factor, } F = \frac{N_{02}}{N_{01}}. \quad (\text{H.1})$$

We know that the output power for the noisy receiver is the sum of receiver noise and source noise which may be separated to obtain

$$N_{02} = N_{01} + N_R \quad (\text{H.2})$$

and the equation for noise factor becomes:

$$F = 1 + \frac{N_R}{N_{01}} \quad (\text{H.3})$$

Equation H.3 for noise factor illustrates the important ideas that a noiseless receiver ($N_R = 0$) has a noise factor of unity and a noise figure of 0db.

Friis presented noise factor by a different method which helped workers already familiar with AM sensitivity measurements of signal-to-noise ratio to better understand the new concept. We recognize the need for the highest possible signal-to-noise ratio at the output of a receiver from considerations of communication theory. By intuition, it seems that the ideal noiseless receiver will preserve the signal-to-noise ratio from input to output and the noisy receiver would degrade it. Also we realize that any definition of noise factor must account for the fact that receiver terminations will affect the receiver noise performance. Friis accounted for both of these by defining noise factor as:

$$F = \frac{\text{Available signal-to-noise ratio at the source}}{\text{Available signal-to-noise ratio at the output}}$$

$$= \frac{(S_i/N_i)}{(S_o/N_o)} . \quad (H.4)$$

The available ratio accounts for variations in terminations by defining the maximum signal-to-noise ratio under any terminating conditions.

Friis' definition can be compared to North's by simply adding a signal voltage generator in series with the noise generator $\overline{V_n^2}$ of the source.

Then we can define the signal and noise terms as:

S_i = Signal Power available from the source.

N_i = Noise power available from the source.

$S_o = G S_i$ (G is the receiver transducer gain).

$N_o = G N_i + N_R = N_{01} + N_R$.

Taking the ratio defined in Equation H.4 we get by substitution of the noise and signal terms

$$F = \left(\frac{S_i}{S_o}\right) \left(\frac{N_o}{N_i}\right) = \frac{N_o}{G N_i} = \frac{N_{01} + N_R}{N_{01}} , \quad (H.5)$$

and finally:

$$F = 1 + \frac{N_R}{N_{01}} . \quad (H.6)$$

This is a form identical to that which was developed in Equation H.3, thus we see that the definitions are consistent.

The actual computation and measurement of noise factor is difficult without developing the concept with more mathematical rigor. In doing this we will look at the meanings of average and spot noise factor and

develop two useful noise relationships. The concept of a Nyquist equivalent for the noise power of the source will be used. The incremental noise power output in a differential bandwidth, df , at a frequency f in the passband of a noiseless receiver, would be

$$d N_{01} = G(f) k T_o df \text{ watts,} \quad (H.7)$$

which is simply the product of the transducer gain, $G(f)$, at frequency f and the noise power available from the source in bandwidth df and at standard temperature. If the noiseless receiver is replaced by a noisy one, that has the same two-port characteristics, the internal noise will be added to that produced by the source to increase the output noise. The multiplication factor used to account for this increase is the spot noise factor, $F(f)$. The total incremental noise output due to both receiver and source becomes:

$$d N_o = F(f) G(f) k T_o df. \quad (H.8)$$

The incremental noise power at the output due only to receiver internal noise is obtained by subtracting (H.7) from (H.8)

$$d N_R = [F(f) - 1] G(f) k T_o df \quad (H.9)$$

and is often referred to as excess noise.

The spot noise factor, $F(f)$, at a frequency f , will be defined as the ratio of total incremental power output to that due only to the source:

$$\text{Spot Noise Factor, } F(f) = \frac{dN_o}{dN_{01}} = 1 + \frac{dN_R}{dN_{01}}. \quad (\text{H.10})$$

The relationships of (H.8) and (H.9) are useful in device noise calculations and will be used in deriving noise factor formulas.

Another definition of noise output leads to the concept of average noise factor, \bar{F} . It is defined as the ratio of total noise power output to that due only to the source. Average noise factor is obtained by integration of (H.7) and (H.8) over all frequencies. Because of this, the average noise factor, \bar{F} , can be thought of as an average over the entire amplifier bandwidth

$$\bar{F} = \frac{N_o}{N_{o1}} = \frac{k T_o \int_0^{\infty} F(f) G(f) df}{k T_o \int_0^{\infty} G(f) df} \quad (\text{H.11})$$

which leads to the definition for average noise factor as given by the IRE Subcommittee 7.9 on Noise (1963b):

$$\bar{F} = \frac{\int_0^{\infty} F(f) G(f) df}{\int_0^{\infty} G(f) df} \quad (\text{H.12})$$

It will now be shown that (H.12) is consistent with the concept of effective noise bandwidth and that the noise factor definitions of North and Friis are valid for average noise factor, \bar{F} .

Integration of Equation H.8 gives a relationship between noise output and noise factor that is widely used (Friis, 1944) and

(Pappenfus, Bruene, Schoenike, 1964, p. 343). It is necessary, however, to know the conditions for which it can be applied. The total noise output is

$$N_o = kT_o \int_0^{\infty} F(f)G(f)df \quad (H.13)$$

which leads to,

$$N_o = \bar{F} kT_o G_n B_n \quad (H.14)$$

where \bar{F} = Average Noise Factor

G_n = Value of $|g(f)|^2$ with which B_n is normalized.

Also G_n is the transducer gain at the frequency of normalization (see Appendix, Part B).

B_n = Effective noise bandwidth.

To show the validity of Equation H.14 we remember that noise bandwidth is defined from the equation (see Equation B.8):

$$\int_0^{\infty} G(f)df = G_n B_n \quad (H.15)$$

On brief examination, Equation H.12 appears to be just a convenient way of defining a product which will lead to Equation H.14. A more satisfying way to define "average" noise factor, and at the same time time verify (H.12), is to obtain the mean (or expected) value of the function $F(f)$ as in the probabilistic sense. Because average noise

factor is obtained by integration over the total amplifier bandwidth, this author chose a probability density function, $P(f)$, which is defined using the equivalent noise bandwidth in the following way;

$$\int_0^{\infty} P(f) df = \int_0^{\infty} G(f) \frac{1}{G_n B_n} df = 1 \quad (\text{H.16})$$

The mean value of the spot noise factor, $F(f)$, is found by integrating the product of $F(f)$ and the probability density function of (H.16), (Beckmann, 1967, p. 80)

$$\overline{F} = \int_0^{\infty} F(f) P(f) df = \int_0^{\infty} F(f) G(f) \frac{1}{G_n B_n} df \quad (\text{H.17})$$

and upon factoring out $G_n B_n$ and substituting (H.15) we get:

$$\overline{F} = \frac{\int_0^{\infty} F(f) G(f) df}{\int_0^{\infty} G(f) df} \quad (\text{H.18})$$

It is important to note that the average value of $F(f)$ was determined for the entire receiver bandwidth by averaging with a probability density determined by the transfer function, $G(f) = |g(f)|^2$.

In certain applications, such as in the Friis equation, it is necessary to use still another concept for average noise factor--the average over a small bandwidth Δf . This average is used in the computation of noise factor for a superheterodyne receiver. By direct

application of the Law of the Mean for Integrals we obtain the average noise factor \hat{F} over a small bandwidth Δf .

$$\hat{F} = \frac{1}{\Delta f} \int_{f - \frac{\Delta f}{2}}^{f + \frac{\Delta f}{2}} F(f) df \quad (\text{H.19})$$

The difference in \bar{F} and \hat{F} is that the former is a weighted average using the bandpass characteristic B_n while the latter is an average over a small bandwidth.

Each of the three types of noise factor have a definite role in noise calculations and they have been presented in this section to acquaint the reader with their differences. In closing, we note that the average noise factor, \hat{F} , and spot noise factor are related by the following limiting process:

$$\lim_{\Delta f \rightarrow 0} \hat{F} = F(f) \quad (\text{H.20})$$

I. Spot and Average Noise Factor

A distinction needs to be made between two different types of noise factor measurement and specification. When the noise factor of a complete receiver or a narrowband RF amplifier is measured, the noise contribution over the entire bandwidth is averaged to give a net noise power output which, when used in the noise factor definition, will give a value referred to as the average noise factor. On the other hand, for a wideband amplifier the noise factor is usually measured over a

narrow portion of the total bandwidth and if we consider the bandwidth infinitesimally small at a specific frequency we have the spot noise factor. The term spot noise factor will be represented by the symbol

$$\text{Spot Noise Factor} = F(f)$$

and is used in emphasizing that the noise factor is a point function of frequency. Usually the distinction is not made when the context of the application makes it clear which noise factor is being used.

The quantitative relation between average and spot noise factor is

$$\text{Average Noise Factor, } \bar{F} = \frac{\int_0^{\infty} F(f) G(f) df}{\int_0^{\infty} G(f) df} \quad (\text{I.1})$$

where f is the receiver input frequency and $G(f)$ is the receiver transducer gain. Refer to the Noise Figure section of this appendix for detailed derivations of the concepts.

Noise factor and noise temperature are related by the equation

$$T = (F - 1) T_0 \quad (\text{I.2})$$

and it follows that noise temperatures must also have spot and average values. This distinction is not made in many papers on noise but it is important to realize that spot and average noise temperatures have the same application as their noise factor counterparts.

J. Friis Equation

The Friis equation (Friis, 1944) relates the noise factor at the input of a cascade of two-port networks to the noise factors and gains of each individual stage. Figure J-1 illustrates the connection for a series of n cascaded stages.

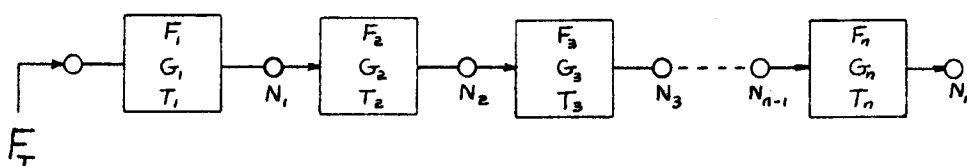


Figure J-1. Cascade of n two-port networks with noise factor, F_n , transducer gain, G_n , and equivalent noise temperature, T_n .

To derive the Friis equation one needs to determine the available noise power output for each two-port and solve for the total input noise factor, F_T . The available output noise power for the first two-port, assuming an optimum source resistance at standard temperature, is

$$N_1 = F_1 k T_0 G_1 B_n \quad (\text{J.1a})$$

or in terms of noise temperature,

$$N_1 = k(T_0 + T_1) G_1 B_n \quad (\text{J.1b})$$

where F_1 = Noise factor of the first two-port

G_1 = Transducer gain

B_n = Effective noise bandwidth normalized at G_1

T_1 = Noise temperature of the first two-port.

To be able to derive the Friis equation in its original form, it is necessary to assume that all two-ports in the cascade have the same equivalent noise bandwidth. We now let this common bandwidth be denoted by B and continue the derivation. Also, to be completely correct, the noise factors and noise temperatures in Equations J.1 through J.5 must be average values. The super-bar denoting average has been left out to make the equations look like those commonly seen in the literature and because, for some special circumstances (Equation J.8), the equations are valid for both spot and average values.

The noise power output from the second two-port can be obtained by multiplying the noise output of the first by G_2 and adding the excess noise (Appendix, Part G and Equation H.9) power output of the second two-port. Doing this we get

$$\begin{aligned} N_2 &= G_2 N_1 + (F_2 - 1) k T_0 G_2 B \\ &= F_1 k T_0 G_1 G_2 B + (F_2 - 1) k T_0 G_2 B \end{aligned} \quad (\text{J.2a})$$

or,

$$N_2 = k (T_0 + T_1) G_1 G_2 B + k T_2 G_2 B_n \quad (\text{J.2b})$$

To obtain the total noise factor of the cascade, the noise factor definition as: the ratio of total noise power output to that due only to the source, is applied to give

$$F_T = \frac{N_2}{k T_0 G_1 G_2 B} = F_1 + \frac{(F_2 - 1)}{G_1} \quad (J.3)$$

where N_2 is obtained from (J.2a) and the output power when the two-ports are noiseless is found from (J.2a) by letting F_1 and F_2 be unity or from (J.2b) by letting T_1 and T_2 be zero.

Continuing this procedure leads to the generalized Friis equation which applies to a cascade of n two-ports:

$$F_T = F_1 + \frac{F_2 - 1}{G_1} + \frac{F_3 - 1}{G_1 G_2} + \dots + \frac{F_n - 1}{G_1 \dots G_{n-1}} \quad (J.4)$$

For additional information on the Friis equation refer to Kraus (1966, p. 262) and for a discussion on the applicability of the Friis equation and its analog for noise measure, refer to van der Ziel (1970, p. 33).

The Friis equation in terms of the noise temperatures in the cascade can be obtained by substitution of the relationship between noise temperature and noise factor (Equation E.3), $T_n = (F_n - 1)T_0$, into Equation J.4:

$$T_T = T_1 + \frac{T_2}{G_1} + \frac{T_3}{G_1 G_2} + \dots + \frac{T_n}{G_1 \dots G_{n-1}} \quad (J.5)$$

The Friis equation in the form of (J.4) is useful for computing the total effective noise temperature of a cascade of linear two-port networks when they have nearly identical passband characteristics. It may also be applied to an RF mixer if the mixer model can be represented by an ideal unity-gain frequency translator followed by a noisy amplifier of similar gain, bandpass, and distortion characteristics.

When the two-ports have dissimilar passband characteristics the actual integrations over gain and noise factor must be carried out. In an incremental bandwidth, df , at frequency f , the incremental power output of the first two-port is

$$dN_1 = kT_o F_1(f) G_1(f) df \quad (J.6)$$

where $F_1(f)$ = Spot noise factor at frequency f
 $G_1(f)$ = Transducer gain or the absolute value of the transfer function squared, $|g_1(f)|^2$.

The incremental noise power output from the second stage would become;

$$dN_2 = G_2(f) dN_1 + kT_o (F_2(f) - 1) G_2(f) df \quad (J.7)$$

The ratio of,

- 1) the incremental noise power output due to amplifiers and source to,
- 2) that noise due only to the source, will give the Friis equation for the spot noise factor at frequency, f

$$F_T(f) = F_1(f) + \frac{F_2(f) - 1}{G_1(f)} \quad (\text{J.8})$$

which is of the same form as Equation J.3. From this we conclude that, for spot noise factor, the Friis equation in the form of (J.4) is valid even if the bandpasses are not identical.

When the average noise factor is measured, the error caused by dissimilar bandwidths may be considerable and the only way to compensate for it is by direct integration. The average noise factor is obtained by taking the ratios of the total powers--not the incremental powers. The total noise power output from the second stage is found by integrating Equation J.7 after substitution of (J.6):

$$N_2 = kT_o \int_0^{\infty} F_1(f) G_1(f) G_2(f) df + kT_o \int_0^{\infty} (F_2(f) - 1) G_2(f) df \quad (\text{J.9})$$

The total noise power output due only to the source is:

$$kT_o \int_0^{\infty} G_1(f) G_2(f) df \quad (\text{J.10})$$

The ratio of Equations J.9 and J.10 defines the average noise factor for the two two-ports in cascade:

$$\overline{F_T} = \frac{\int_0^{\infty} F_1(f) G_1(f) G_2(f) df + \int_0^{\infty} [F_2(f) - 1] G_2(f) df}{\int_0^{\infty} G_1(f) G_2(f) df} \quad (\text{J.11})$$

This equation can be extended to more two-ports in cascade but performing the integrations would not be practical. There are two simplifications that can be made to Equation J.11 which will simplify it to make calculations easier. First, assume that the bandwidth of the first two-port is much wider than the second and that the equivalent noise bandwidth of the second is completely contained in the bandwidth of the first. The integrations will simplify as

$$\begin{aligned} \int_0^{\infty} F_1(f) G_1(f) G_2(f) df &= F_1(f_0) G_1(f_0) \int_0^{\infty} G_2(f) df \\ \int_0^{\infty} G_1(f) G_2(f) df &= G_1(f_0) \int_0^{\infty} G_2(f) df \\ \frac{\int_0^{\infty} (F_2(f) - 1) G_2(f) df}{\int_0^{\infty} G_2(f) df} &= (\overline{F_2} - 1) \end{aligned} \quad (J.12)$$

where it has been assumed that the noise factor and gain of the first stage is essentially constant over the noise bandwidth of the second and that f_0 is the center frequency.

Substitution of these simplifications into (J.11) yields

$$F_T = F_1(f_0) + \frac{(\overline{F_2} - 1)}{G_1(f_0)} \quad (J.13)$$

where $F_1(f_0)$ and $G_1(f_0)$ represent the spot noise factor and gain of the first stage at frequency f_0 , and $\overline{F_2}$ is the average noise factor of the second stage.

Now we assume that the bandwidth of the second stage is much larger than that of the first. For this case the integrations will simplify to:

$$\int_0^{\infty} F_1(f) G_1(f) G_2(f) df = G_2(f_0) \int_0^{\infty} F_1(f) G_1(f) df \quad (\text{J.14})$$

$$\int_0^{\infty} G_1(f) G_2(f) df = G_2(f_0) \int_0^{\infty} G_1(f) df = G_2(f_0) G_1(f_0) B_1$$

Substitution into (J.11) gives

$$\begin{aligned} \overline{F_T} &= \frac{G_2(f_0) \int_0^{\infty} F_1(f) G_1(f) df}{G_2(f_0) \int_0^{\infty} G_1(f) df} + \frac{\int_0^{\infty} (F_2(f) - 1) G_2(f) df}{G_2(f_0) \int_0^{\infty} G_1(f) df} \\ &= \overline{F_1} + \frac{\int_0^{\infty} (F_2(f) - 1) G_2(f) df}{\int_0^{\infty} G_2(f) df} \cdot \frac{\int_0^{\infty} G_2(f) df}{G_2(f_0) \int_0^{\infty} G_1(f) df} \\ &= \overline{F_1} + (\overline{F_2} - 1) \frac{G_2(f_0) B_2}{G_2(f_0) G_1(f_0) B_1} \end{aligned}$$

$$\overline{F_T} = \overline{F_1} + \frac{(\overline{F_2} - 1)}{G_1(f_0)} \cdot \frac{B_2}{B_1}, \text{ for } \frac{B_2}{B_1} \geq 1 \quad (\text{J.15})$$

where B_1 and B_2 are the effective noise bandwidths of the first and second stages. The results of Equation J.15 illustrate the increase in noise factor caused by the wide noise bandwidth of the second stage.

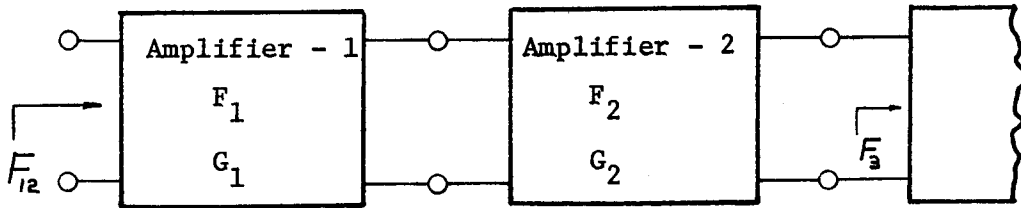
Equation J.13 is representative of the results obtained with a superhetrodyne receiver where the IF bandwidth is much smaller than the RF bandwidth. Equation J.15 illustrates the error in noise figure that can be caused by using a postamplifier with a noise bandwidth larger than the preamplifier noise bandwidth.

K. Noise Measure

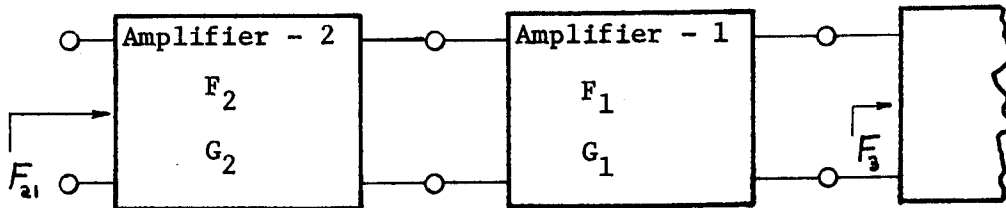
Although the specification of noise factor has remained adequate as a criterion for specifying the low-noise performance of a complete receiver as originally envisioned by North and Friis (see part H of this section), it has limited usefulness for individual amplifier stages. The principle difficulty is that, in trying to eliminate gain as a variable, North eliminated an important functional property of the amplifier--to provide gain. Intuition tells us that a low-noise amplifier with low gain is not as useful as one with a slightly higher noise factor but a much larger gain. This intuitive feeling can be quantitatively verified by using the Friis equation to evaluate the noise performance of an amplifier stage. Haus and Adler (1958a) were the first to formulate a measure of noise performance which accounted for both noise figure and gain. The theory of noise measure as developed by Haus and Adler will be presented here to illustrate the

concept and to demonstrate a useful application of the Friis equation.

Suppose that two amplifiers are to be used in cascade and that a choice has to be made, on the basis of lowest noise factor, as to which will come first. Figure K-1 shows the two different ways of connecting the amplifiers.



(a) Amplifier No. 1 is First



(b) Amplifier No. 2 is First

Figure K-1. Noise Measure Definition

Writing the Friis equation for both connections:

$$F_{12} = F_1 + \frac{F_2 - 1}{G_1} + \frac{F_3 - 1}{G_1 G_2} \quad (\text{K.1})$$

$$F_{21} = F_2 + \frac{F_1 - 1}{G_2} + \frac{F_3 - 1}{G_1 G_2} \quad (\text{K.2})$$

To compare the two connections and determine the best amplifier to be inserted as the first stage we can specify a criterion such as $F_{21} > F_{12}$ and obtain:

$$F_2 + \frac{F_1 - 1}{G_2} > F_1 + \frac{F_2 - 1}{G_1}. \quad (\text{K.3})$$

Rearranging to get amplifier 1 and amplifier 2 terms separated gives

$$\frac{F_1 - 1}{1 - \frac{1}{G_1}} < \frac{F_2 - 1}{1 - \frac{1}{G_2}}, \quad (\text{K.4})$$

and we conclude that the amplifier that should be inserted as the first stage is not the one with the lowest noise factor but the one with the lowest Noise Measure as defined by:

$$\text{Noise Measure, } M = \frac{F - 1}{1 - \frac{1}{G}} \quad (\text{K.5})$$

In summary, the specification of noise measure is best applied to the situation where two amplifiers are to be connected in cascade and the choice as to which connection will be made is one of choosing the amplifier with the lowest noise measure to be first.

L. Noise Merit

After a careful analysis of the problem of choosing between two amplifiers for a particular low-noise application it is the conclusion of this author that there is no single factor of noise merit which can

be specified in advance that will indicate the best choice. Noise factor as a single specification is inadequate because it does not account for the gain which may be needed to overcome the noise of succeeding stages. Noise measure is adequate for specifying which of two amplifiers, that are to be connected in cascade, should come first but it will not indicate the best single amplifier for an application. The only way to make the proper choice is by a direct application of the Friis equation. To compare two amplifiers for a specific application it is necessary to solve the Friis equation for each one and then select the one that yields the lowest total noise factor. Figure L-1 is used to demonstrate how to compare two amplifiers.

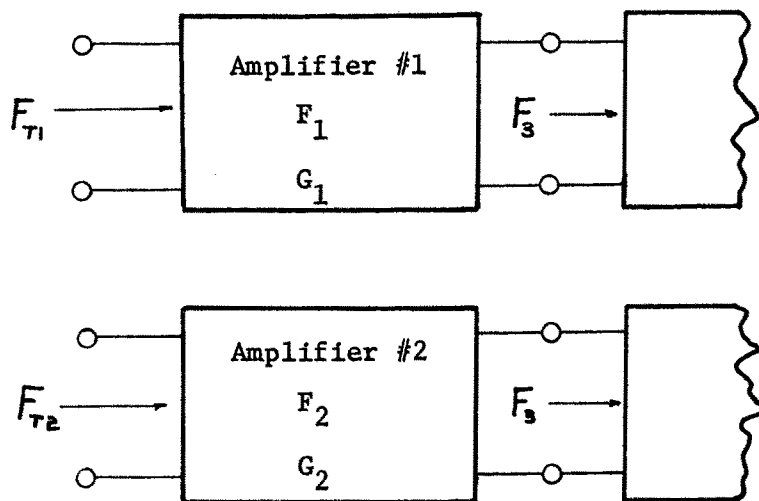


Figure L-1. Total Noise Comparison

The respective total noise factor equations are:

$$F_{T1} = F_1 + \frac{F_3 - 1}{G_1} \quad (L.1)$$

$$F_{T2} = F_2 + \frac{F_3 - 1}{G_2} .$$

These equations have been manipulated to try and develop a single factor of noise merit but all attempts were fruitless. Any expression comparing the amplifiers always contains the noise factor, F_3 , of the succeeding stage which makes any choice depend on three variables; amplifier gain, amplifier noise factor, and the noise factor of the succeeding stage.

It was discovered in the investigation of this problem that it is possible to set reasonable criteria on the selection of system variables to produce the best possible noise factor. The following scheme was developed which can graphically illustrate the trade-offs that exist in amplifier selection. Figure L-2 shows the system to be analyzed and defines the system variables.

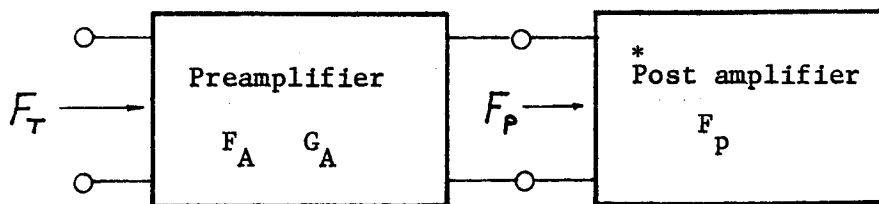


Figure L-2. Circuit Connection for Amplifier Selection

*In a superhetrodyne receiver, the post amplifier is called the Intermediate Frequency (IF) amplifier, or simply the "IF."

The approach used is to select the values of preamplifier gain, G_A , and postamplifier noise factor, F_p , which will degrade the preamplifier noise factor, F_A , by a fixed amount. Setting fixed percentage increases in noise factor or fixed db increases in noise figure were not reasonable because they tend to degrade the lower noise preamplifiers more than practically necessary. To set a reasonable level of degradation it was discovered that a fixed percentage of noise temperature gave the best results.

With this scheme, amplifiers of all levels of noise output receive the same degradation. A ten percent noise temperature degrading scale was devised. The derivation of the applicable equations will now be given.

If the noise temperature of the amplifier is to be degraded by ten percent, the Friis equation written in terms of noise temperature must be determined

$$T_T = T_A + T_P/G_A \quad (L.2)$$

where for ten percent,

$$T_P/G_A = 0.1 T_A \quad (L.3)$$

and

$$T_T = 1.1 T_A. \quad (L.4)$$

Substituting the relationships between noise factor and noise temperature, $T_T = T_O (F_T - 1)$ and $T_A = T_O (F_A - 1)$ yields:

$$F_T = 1.1 F_A - 0.1. \quad (L.5)$$

Using the Friis equation in terms of noise factor and equating with (L.5) gives:

$$F_T = 1.1 F_A - 0.1 = F_A + \frac{F_P - 1}{G_A} \quad (L.6)$$

Solving for F_A and F_T we get

$$F_A = 1 + 10 \frac{F_P - 1}{G_A}$$

and

(L.7)

$$F_T = 1 + 11 \frac{F_P - 1}{G_A}$$

For less than ten percent degrading of noise temperature, Equations L.7 can be solved to give the following conditions;

$$\text{specify } F_A \text{ and } G_A, \text{ then: } F_P \leq 1 + G_A \frac{F_A - 1}{10} \quad (L.8)$$

or

$$\text{specify } F_A \text{ and } F_P, \text{ then: } G_A \geq 10 \frac{F_P - 1}{F_A - 1} \quad (L.9)$$

A plot of equation L.8 for the condition of equality is given in the graph of Figure L-3. Noise figure in db is given for convenience. The

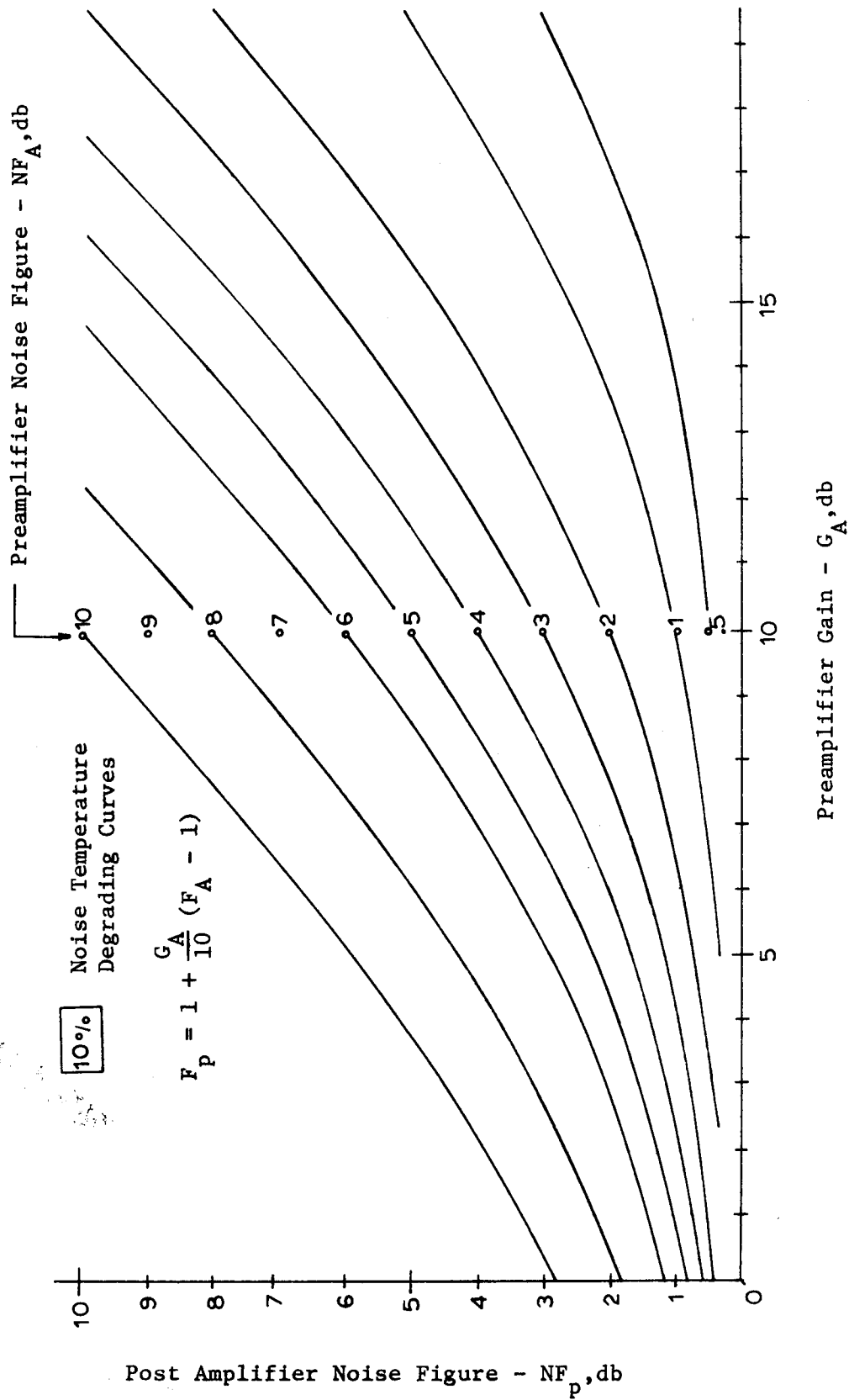


Figure L-3. Trade-off Curves of Gain and Noise Figure in a Low Noise Amplifier

selection of either NF_A and G_A or NF_A and NF_p will specify a point from which the necessary condition on either NF_p or G_A may be read directly. As an example suppose a preamplifier has a noise figure of 6db and a gain of 6 db. Then a postamplifier noise figure of less than 3.4 db will degrade NF_A by less than 0.3 db (the noise temperature is degraded by less than ten percent) and the total noise figure will be less than 6.3 db.

M. Noise Matching

From two-port noise theory (Chapter IV-E) we know that noise factor depends upon the source resistance, R_s , for the two-port input. Also it is known that there exists some optimum value of source resistance, R_{sopt} , which will give a minimum noise factor. We also discovered the condition for maximum power transfer, $R_s = R_{in}$, was not generally the condition for minimum noise factor, i.e. the optimum source resistance, R_{sopt} , is not equal to the two-port input resistance, R_{in} .

In high-frequency amplifier circuits that are used for low-noise applications, an adjustable matching network is usually provided as a means of adjusting for R_{sopt} . When this network has been adjusted so that $R_s = R_{sopt}$ the noise factor is a minimum and the amplifier is said to be noise matched. To illustrate the importance of noise matching, refer to Figure M-1 which is a plot of noise figure as a function of normalized source resistance. It should be emphasized that minimum noise factor does not occur at maximum power transfer, $R_{sopt} \neq R_{in}$. For the example in the figure, $R_{in} = 2.8 R_{sopt}$.

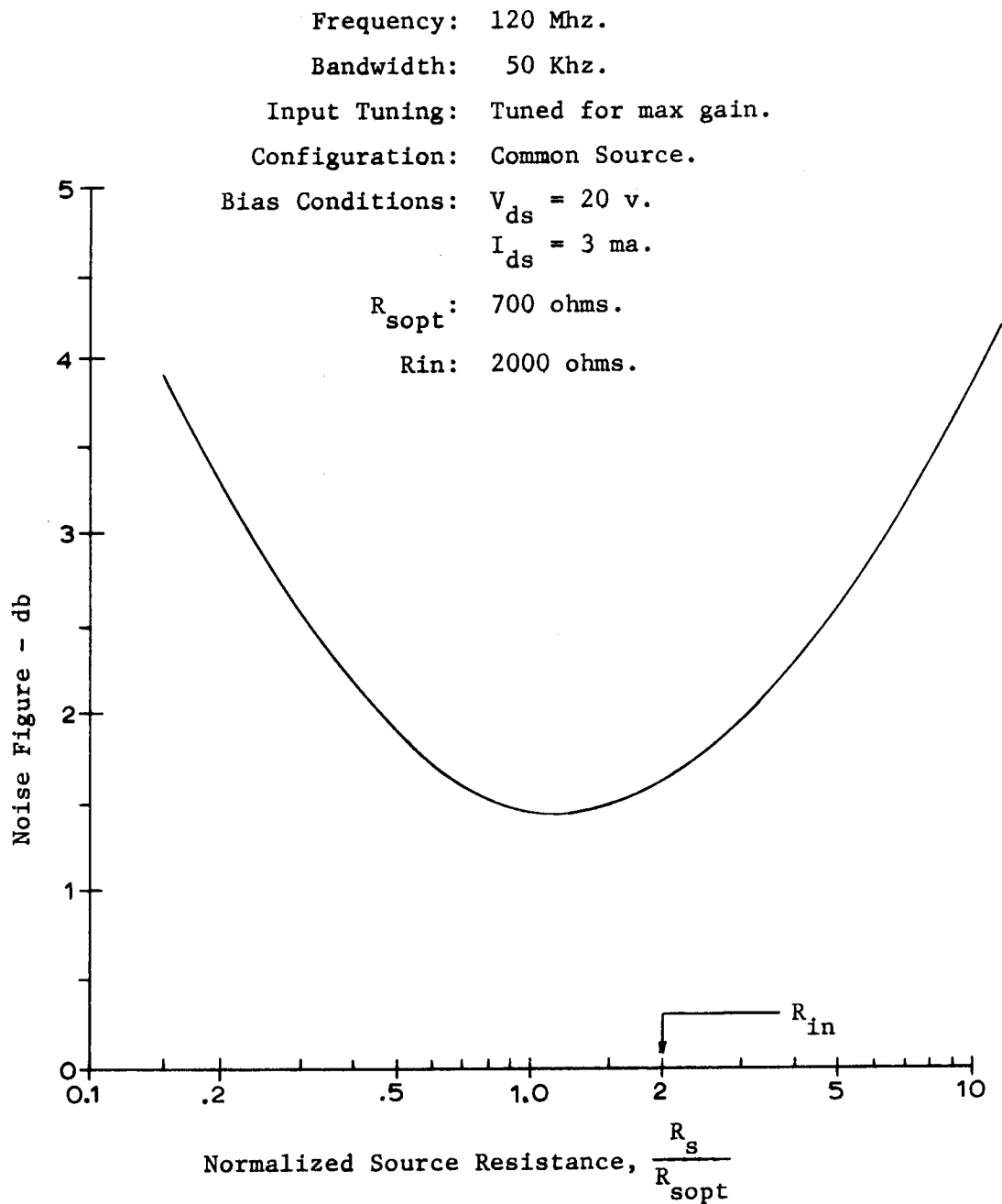


Figure M-1. Noise Figure as a Function of Normalized Source Resistance for a VHF FET Amplifier

N. Noise Tuning

It was shown in the section on two-port noise theory that, in general, the characteristic noise generators are partially correlated (Section IV-E). Because of this correlation it is possible to provide a reactive termination at the input and actually effect a reduction in noise factor. In high-frequency amplifiers this is accomplished by tuning the input tank circuit off resonance. When using an automatic noise figure meter it is possible to tune for a noise factor minimum. This process is referred to as noise tuning. This author's experience has shown that, for low-noise transistor amplifiers, the tank should be tuned below resonance so that the input is presented with a capacitive reactance.

Figure N-1 shows typical NF contours for an amplifier which first, has the input tuned for maximum gain and then, capacitively noise tuned for minimum noise figure. These numbers are typical and illustrate the improvement which can be obtained by noise tuning.

The improvement in noise figure of 1/2 db represents a decrease in the effective noise temperature from 148°K to 101°K . In low-noise applications, the improvement in noise temperature is worth the effort of noise tuning. For both noise matching and noise tuning, an automatic noise figure meter greatly reduces the labor by allowing direct observation of noise figure when adjustments are being made.

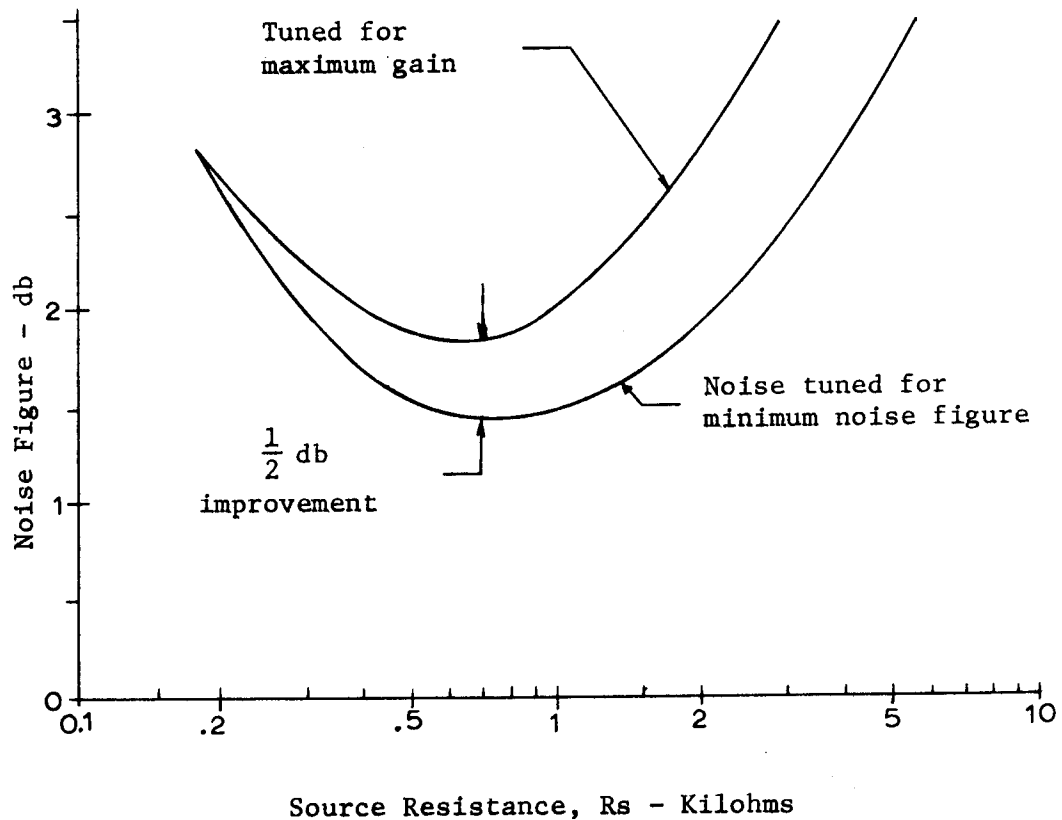


Figure N-1. Effect of Noise Tuning for a Two-Port Network

0. Reference Temperature, T_0

A standard reference temperature needs to be defined when discussing noise theory in communication circuits. Concepts such as Noise Factor and Equivalent Noise Resistance are formulated on the basis of a specific reference temperature. $T_0 = 290^\circ\text{K}$ is the reference temperature which will be used in this report because it is the one most commonly used today.

Table O-1. "Standard" Temperatures

Source	$^{\circ}\text{K}$ (Approx)	$^{\circ}\text{F}$ (Approx)
IRE Subcommittee 7.9 on Noise (1963b), the most accepted standard for noise studies	290	62.6
Earth's average surface temperature, (Kraus, 1966, p. 342).	290	62.6
Healthful room temperature	293-295	68-72
Typical laboratory ambient	294-300	70-80
Smullin and Haus (1959, p. 189)	293	68
Lawson and Uhlenbeck (1950, p. 99)	292	66
Phillips ^a (1962, p. 68)	300	80
Alley and Atwood ^a (1971, p. 19)	300	80

^aTransistor theory texts.

When reading literature on noise theory it is important that the reader know what the author means when he says "standard temperature". Table O-1 lists some commonly used "standard" temperatures for the reader to compare. An argument for retaining 290°K as a standard could be based on the fact that the earth's average temperature is about 290°K , (Kraus, 1966, p. 342). It is difficult to maintain a constant temperature in the laboratory where sensitivity measurements are being conducted. When necessary, the few percent error introduced by making measurements at temperatures other than 290°K can be compensated. Experience by this author has shown that the error involved is

usually within measurement accuracy and therefore is not accounted for in most practical situations.

To this author's knowledge, the first author to adopt a 290°K standard was Friis (1944).

P. Sky Temperature

The solar system and the galaxy are filled with radio noise sources much the same as they are filled with optical sources. It is possible, at times, to have a receiving antenna oriented such that it will receive enough energy from these noise sources to cause an important increase in effective antenna noise temperature. These sources of noise can cause a reduction in signal-to-noise ratio and should be considered in a low-noise receiver installation.

All the noise that is induced in an antenna and caused by extra-terrestrial noise sources will be termed sky noise and its contribution to the effective antenna noise temperature will be called sky temperature. This definition is not universally agreed upon and when reading any article on antenna noise it is advisable that the reader determine the author's usage of the term. The major sources of sky noise are the sun and the galaxy (notably from Cassiopeia A). Other sources which are weaker but may cause interference under certain circumstances of antenna orientation and gain are Jupiter bursts and extragalactic noise from Cygnus A.

The discovery of galactic noise by Jansky in 1932 was the birth of radio astronomy and also signaled the beginning of an awareness that this noise could ultimately limit the sensitivity of a receiving system.

Sky noise contributions from solar radiation are most noticeable during high sunspot activity because solar flares can cause high intensity radio noise (Kraus, 1966, p. 8).

The calculation of sky temperature for a particular antenna installation would be very difficult. One would have to specify the antenna orientation and directive gain $D(\theta, \phi)$, (see Section III-A). The calculation would also depend on time of day and year. Even after all of these are specified, the noise power at the antenna can only be obtained by integration, over the entire visible sky, of the antenna beam power pattern and the flux density of all the sky noise sources. For these reasons it appears that one must measure, not calculate, this contribution for each individual antenna installation.

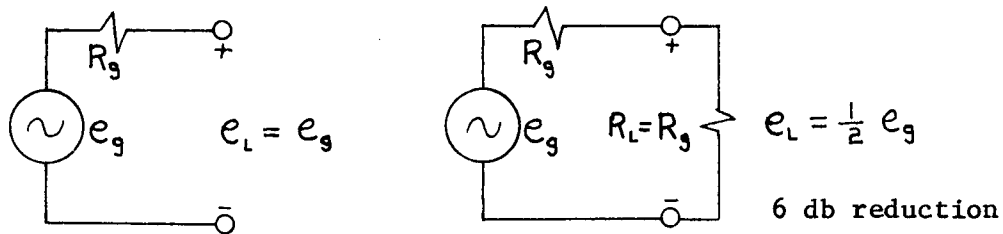
Q. "Hard" and "Soft" Microvolts

When measuring the AM sensitivity of a receiving system, the magnitude of the voltage from the sinewave generator must be determined. Since there are several ways that the voltage level may be reported it is necessary that a standard be adopted. This will help avoid any confusion as to how to report the generator level. There are three meaningful voltages which may be used:

1. The open-circuit or Thevenin voltage of the generator.
This is the so-called "hard" microvolts output.
2. The output voltage when the generator is power matched by the load. This is the actual receiver input terminal voltage under power matched conditions and is the so-called "soft" microvolts output.

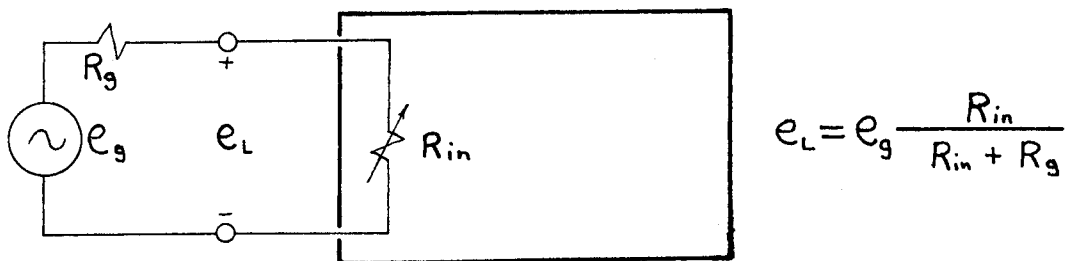
3. The actual terminal voltage at the input to the receiver under test conditions. This voltage may differ considerably among different receivers of the same sensitivity and also from either the "hard" or "soft" voltage.

Figure Q-1 is used to illustrate these three different specifications.



(a) Hard microvolts, e_g

(b) Soft microvolts, $\frac{1}{2} e_g$



(c) Variable R_{in} , variable e_L

Figure Q-1. Microvolt Specification in Receiver Sensitivity Measurements

For most cases, the hard-microvolt specification is the one that should be used. Its advantages are that:

1. It is equivalent to the Thevenin voltage.
2. It is a measure of the available power and hence closely related to the noise voltage generator of the Nyquist equivalent.
3. It is the open circuit voltage of a receiving antenna.
4. It remains constant for variations in the receiver input impedance.

Comparing receivers with different input impedances may seem inconsistent but, as shown by two-port noise theory in Part E of Chapter IV, each receiver should be optimized to provide minimum sensitivity from the same specified source impedance.

R. Single and Double-Sided Power Spectra

The use of Fourier transform theory in the study of noise in communication systems is a very valuable technique but to properly apply this theory one must be careful to distinguish the mathematical tools from the physical concepts. For the most general applications we know that the double-sided power spectral density function and the autocorrelation function are a Fourier transform pair:

$$\Phi_x(\omega) = \int_{-\infty}^{\infty} R_x(\tau) e^{-j\omega\tau} d\tau \quad (\text{R.1a})$$

$$R_x(\omega) = \frac{1}{2\pi} \int_{-\infty}^{\infty} \mathcal{F}_x(\omega) e^{j\omega\tau} d\omega \quad (\text{R.1b})$$

For general transform theory it is necessary to work with the complex transform but when dealing with random processes that are real, both the autocorrelation function and power spectral density function are real and even (Papoulis, 1965, p. 388). Since the random processes for noise in communication systems are real, we can take advantage of the properties of even functions to reduce the integrals to the form

$$\mathcal{F}_x(\omega) = \int_{-\infty}^{\infty} R_x(\tau) \cos \omega \tau d\tau \quad (\text{R.2a})$$

$$R_x(\omega) = \frac{1}{2\pi} \int_{-\infty}^{\infty} \mathcal{F}_x(\omega) \cos \omega \tau d\tau \quad (\text{R.2b})$$

where the exponential is reduced using Eulers relation and the $j\sin\omega\tau$ part of the integral is zero because the sin function is odd. The double-sided power spectral density function is even so

$$\mathcal{F}_x(\omega) = \mathcal{F}_x(-\omega)$$

and it has amplitude for both positive and negative frequencies. Of course the spectra that we deal with in the real world are only defined for positive frequencies so how are the real spectra and the double-sided spectra related? To represent a real spectrum we will define a

"real" or single-sided spectrum to be that either measured or defined for positive frequencies only. The symbol, $S(\omega)$, will be used to represent the power spectral density function of a single-sided spectrum.

The double-sided or "mathematical" power spectral density function is obtained from the single-sided or "real" one by the amplitude-scaling and even-function transformations of:

$$\phi_x(\omega) = \begin{cases} \frac{1}{2} S_x(\omega) & \text{for } \omega \geq 0 \\ \frac{1}{2} S_x(-\omega) & \text{for } \omega < 0 \end{cases} \quad (\text{R.3a})$$

$$S_x(\omega) = \begin{cases} 2 \phi_x(\omega) & \text{for } \omega \geq 0 \\ 0 & \text{for } \omega < 0 \end{cases} \quad (\text{R.3b})$$

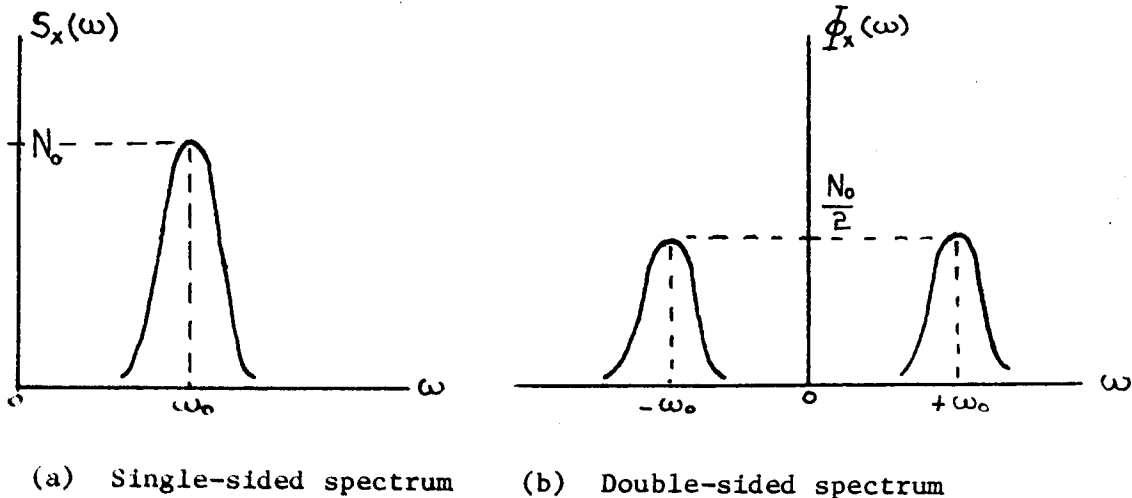


Figure R-1. Spectrum plots for both single and double-sided power spectral density functions

This transformation is obtained from the requirements that the function be even and that the mean-square value computed using either $\phi_x(\omega)$ or $S_x(\omega)$ be the same. Figure R-1 represents the spectrum plots for both the single and double-sided spectra of a real process. Note from the figure that the double-sided power spectral density function is even and that the spectral amplitudes are scaled so both spectra yield the same mean-square value (equal areas) for the variable they represent.

Because the transforms are even functions, the transform pair of Equations R.2 can be reduced to just positive frequencies to give:

$$\bar{\phi}_x(\omega) = \int_0^{\infty} 2 R_x(\tau) \cos \omega \tau \, d\tau \quad (\text{R.4a})$$

$$R_x(\omega) = \frac{1}{\pi} \int_0^{\infty} \bar{\phi}_x(\omega) \cos \omega \tau \, d\omega \quad (\text{R.4b})$$

Now that we are exclusively in the positive frequency domain it follows that the single-sided power spectral density function can now be substituted for the double-sided one to give the single-sided or "real" transform pair:

$$S_x(\omega) = 4 \int_0^{\infty} R_x(\tau) \cos \omega \tau \, d\tau \quad (\text{R.5a})$$

$$R_x(\tau) = \frac{1}{2\pi} \int_0^{\infty} S_x(\omega) \cos \omega \tau \, d\omega \quad (\text{R.5b})$$

Equation R.5a is the common form of the famous Wiener-Khintchine theorem (van der Ziel, 1954, p. 316) which relates the real power spectral density function to the corresponding autocorrelation function.

We now see that there is a choice, when one works with power spectra and transform theory, of dealing with only positive frequencies or extending the analysis technique to negative frequencies. The choice of which transform pair to use is strictly up to the user. As a general rule it seems more appropriate to work with the single-sided spectra since then we only deal with real frequencies but sometimes it is easier to do the integration of the complex form. The user should decide which equations are the most appropriate, in terms of simplicity, for his particular application.

Both single and double-sided power spectral density functions must give the same mean-square value of the time function they represent. Knowing this, we can obtain the following formulas for the mean-square value:

Double-sided

$$\begin{aligned}\overline{X^2(t)} &= R_x(0) \\ &= \frac{1}{2\pi} \int_{-\infty}^{\infty} \Phi_x(\omega) d\omega \\ &= \frac{1}{\pi} \int_0^{\infty} \Phi_x(\omega) d\omega\end{aligned}$$

Single-sided

$$\begin{aligned}\overline{X^2(t)} &= R_x(0) \\ &= \frac{1}{2\pi} \int_0^{\infty} S_x(\omega) d\omega\end{aligned}$$

where a particular value of X_1 is used to determine the slope at that point.

The total error in the function due to incremental errors in the measured variables is the sum of the products of the slopes and the incremental errors (by the chain rule of partial differentiation):

$$\Delta Y = \frac{\partial Y}{\partial X_1} \Delta X_1 + \frac{\partial Y}{\partial X_2} \Delta X_2 + \dots \frac{\partial Y}{\partial X_n} \Delta X_n \quad (S.5)$$

The total uncertainty of the measured variable Y is the absolute magnitude of Equation S.5. From the triangle inequality, we know that the absolute value of the sum of n variables is less than or equal to the sum of their absolute values

$$\left| \sum_{k=1}^n z_k \right| \leq \sum_{k=1}^n |z_k|$$

which is applied to Equation S.5 to give:

$$|\Delta Y| \leq \left| \frac{\partial Y}{\partial X_1} \right| |\Delta X_1| + \left| \frac{\partial Y}{\partial X_2} \right| |\Delta X_2| + \dots \left| \frac{\partial Y}{\partial X_n} \right| |\Delta X_n| \quad (S.6)$$

Larger upper bounds may be found for $|\Delta Y|$ by applying algebraic methods to (S.1) but (S.6) is the smallest of the upper bounds so it is referred to as a least upper bound. The slopes in (S.6) are evaluated at the nominal value of each of the variables while the error values are the maximum possible error. In this respect, the uncertainty is defined as the maximum possible error.

In actual circumstances, the measurement error is seldom as large as the uncertainty so reporting the uncertainty of a measurement gives the most pessimistic estimate. When the variance, $\sigma_{X_i}^2$, is known for each of the variables X_i , the variance for Y of Equation S.1 becomes (Young, 1962):

$$\sigma_Y^2 = \left(\frac{\partial Y}{\partial X_1}\right)^2 \sigma_{X_1}^2 + \left(\frac{\partial Y}{\partial X_2}\right)^2 \sigma_{X_2}^2 + \left(\frac{\partial Y}{\partial X_3}\right)^2 \sigma_{X_3}^2 + \dots \quad (S.7)$$

Reporting both the uncertainty and the variance for Y is better than reporting either alone. The variance gives information about the most common magnitude of error and the uncertainty gives the maximum possible error. More sophisticated techniques of error reporting such as determining confidence levels will not be discussed.

Consider as a simple example, the two variable function of Equation S.7:

$$Y(x,z) = 1 + z(1+x) + x^2 \quad (S.7)$$

The slope of Y for each corresponding variable is:

$$\frac{\partial Y}{\partial x} = z + 2x \qquad \frac{\partial Y}{\partial z} = 1 + x$$

The error in $Y(x,z)$ at the nominal values of X_0 and Z_0 becomes

$$\Delta Y(x_0, z_0) = (z_0 + 2x_0) \Delta x + (1 + x_0) \Delta z \quad (S.8)$$

and the corresponding uncertainty is:

$$|\Delta Y| = |z_0 + 2x_0| |\Delta x| + |1 + x_0| |\Delta z| \quad (S.9)$$

These results could also have been obtained from (S.7) by letting $x_0 = x + \Delta x$, $z_0 = z + \Delta z$, ignoring higher order terms and solving algebraically. This method may be preferred when higher order effects must be accounted for but care must be taken to avoid obtaining too large an upper bound.

Sometimes it is necessary or more desirable to express the error or uncertainty in decibels rather than numerically. This is accomplished by taking the difference of the logarithms of the measured and true values. For the measured variable $\tilde{X} = X + \Delta X$, the true value is X and the numerical error is ΔX . The error in decibels is determined as:

$$\begin{aligned} \delta X &= 10 \log(x + \Delta x) - 10 \log x \\ &= 10 \log \left(1 + \frac{\Delta x}{x} \right) \end{aligned} \quad (S.10)$$

In terms of the uncertainty in X this becomes:

$$\delta X = 10 \log \left(1 \pm \frac{|\Delta x|}{x} \right) \quad (S.11)$$

The δ -notation will be used to denote error and uncertainty values in decibels.

T. Recommended Reference List

1. General reading

Baxendall (1968a, 1968b)

Bennett (1960)

Davenport and Root (1958)

Henney (1959)

Kraus (1966)

Lawson and Uhlenbeck (1950)

Mumford and Scheibe (1968)

Mumford (1968, Special issue on noise)

Pappenfus et al. (1964)

Robinson (1962)

Shea (1966)

Skolnik (1970)

van der Ziel (1954, 1970)

2. Noise factor (Noise figure) and two-port noise theory

Cooke (1962)

Friis (1944)

North (1942)

Rothe and Dalke (1956)

3. Device noise and physical sources of noise

Agouridis and van der Ziel (1967)

Bell (1951)

Brubaker (1968)

Bruncke (1966)

Cooke (1961)

Fukui (1966)

Hanson and van der Ziel (1957)

Klaassen (1967)

Klaassen and Prins (1969)

Messinger and McCoy (1957)

Oliver (1965)

Pierce (1956)

Smullin and Haus (1959)

Uhlir (1958)

Webster (1961)

van der Ziel (1955, 1957, 1958a, 1962a)

van der Ziel and Becking (1958a)

4. Detector theory

Blake (1972)

DeLano (1949)

Fubini (1948)

Klipper (1965)

Middleton (1948, 1960)

5. Probability theory, statistics, random variables, transform theory

Beckmann (1967)

Bracewell (1965)

Brown and Nilsson (1962)